

**Some pages of this thesis may have been removed for copyright restrictions.**

If you have discovered material in AURA which is unlawful e.g. breaches copyright, (either yours or that of a third party) or any other law, including but not limited to those relating to patent, trademark, confidentiality, data protection, obscenity, defamation, libel, then please read our [Takedown Policy](#) and [contact the service](#) immediately

**INVESTIGATION OF THE OXIDATIVE DEGRADATION MECHANISMS  
AND MELT STABILISATION OF A NEW GENERATION  
METALLOCENE POLYETHYLENE**

**UMAR DARAZ**

**Doctor of Philosophy**

**THE UNIVERSITY OF ASTON IN BIRMINGHAM**

**June 2002**

This copy of the thesis has been supplied on condition that anyone who consults it is understood to recognise that its copyright rests with its author and no quotation from the thesis and no information derived from it may be published without proper acknowledgement

ASTON UNIVERSITY

INVESTIGATION OF THE OXIDATIVE DEGRADATION MECHANISMS AND MELT  
STABILISATION OF A NEW GENERATION METALLOCENE  
POLYETHYLENE

UMAR DARAZ

Doctor of Philosophy  
June 2002

SUMMARY

The two main objectives of the research work conducted were firstly, to investigate the processing and rheological characteristics of a new generation metallocene catalysed linear low density polyethylene (m-LLDPE), in order to establish the thermal oxidative degradation mechanism, and secondly, to examine the role of selected commercial stabilisers on the melt stability of the polymers.

The unstabilised m-LLDPE polymer was extruded (pass 1) using a twin screw extruder, at different temperatures (210-285°C) and screw speeds (50-200rpm) and was subjected to multiple extrusions (passes, 2-5) carried out under the same processing conditions used in the first pass. A traditional Ziegler/Natta catalysed linear low density polyethylene (z-LLDPE) produced by the same manufacturer was also subjected to a similar processing regime in order to compare the processability and the oxidative degradation mechanism (s) of the new m-LLDPE with that of the more traditional z-LLDPE. The effect of some of the main extrusion characteristics of the polymers (m-LLDPE and z-LLDPE) on their melt rheological behaviour was investigated by examining their melt flow performance monitored at two fixed low shear rate values, and their rheological behaviour investigated over the entire shear rates experienced during extrusion using a twin-bore capillary rheometer. Capillary rheometric measurements, which determine the viscous and elastic properties of polymers, have shown that both polymers are shear thinning but the m-LLDPE has a higher viscosity than z-LLDPE and the extent of reduction in viscosity of the former when the extrusion temperature was increased from 210°C to 285°C was much higher than in the case of the z-LLDPE polymer. This was supported by the findings that the m-LLDPE polymer required higher power consumption under all extrusion conditions examined. It was further revealed that the m-LLDPE undergoes a higher extent of melt fracture, the onset of which occurs under much lower shear rates than the Ziegler-based polymer and this was attributed to its higher shear viscosity and narrower molecular weight distribution (MWD). Melt flow measurements and GPC have shown that after the first extrusion pass, the initial narrower MWD of m-LLDPE is retained (compared to z-LLDPE), but upon further multiple extrusion passes it undergoes much faster broadening of its MWD which shifts to higher Mw polymer fractions, particularly at the high screw speeds. The MWD of z-LLDPE polymer on the other hand shifts towards the lower Mw end. All the evidence suggest therefore the m-LLDPE undergoes predominantly cross-linking reactions under all processing conditions whereas z-LLDPE undergoes both cross-linking and chain scission reactions with the latter occurring predominantly under more severe processing conditions (higher temperatures and screw speeds, 285°C/200rpm).

The stabilisation of both polymers with synergistic combinations of a hindered phenol (Irganox 1076) and a phosphite (Weston 399) at low concentrations has shown a high extent of melt stabilisation in both polymers (extrusion temperatures 210-285°C and screw speeds 50-200rpm). The best Irganox 1076/Weston 399 system was found to be at an optimum 1:4 w/w ratio, respectively and was found to be most effective in the z-LLDPE polymer. The melt stabilising effectiveness of a Vitamin E/Ultrinox 626 system used at a fraction of the total concentration of Irganox 1076/Weston 399 system was found to be higher in both polymers (under all extrusion conditions). It was found that AOs which operate primarily as alkyl (R•) radical scavengers are the most effective in inhibiting the thermal oxidative degradation of m-LLDPE in the melt; this polymer was shown to degrade in the melt primarily via alkyl radicals resulting in crosslinking. Metallocene polymers stabilised with single antioxidants of Irganox HP136 (a lactone) and Irganox E201 (vitamin E) produced the highest extent of melt stability and the least discolouration during processing (260°C/100rpm). Furthermore, synergistic combinations of Irganox HP136/Ultrinox 626 (XP-60) system produced very high levels of melt and colour stability (comparable to the Vitamin E based systems) in the m-LLDPE polymer. The addition of Irganox 1076 to an Irganox HP136/Ultrinox 626 system was found not to result in increasing melt stability but gave rise to increasing discolouration of the m-LLDPE polymer. The blending of a hydroxylamine (Irgastab FS042) with a lactone and Vitamin E (in combination with a phosphite) did not increase melt stability but induced severe discolouration of resultant polymer samples.

## ACKNOWLEDGEMENTS

I wish to acknowledge with gratitude the guidance, advice and encouragement by my supervisor, Dr. Sahar Al-Malaika.

My thanks are also for Dr. H. Sheena, Prof. M. Khayat and Dr. S. Issenhuth for their help and countless discussions and to all other postgraduate students, Mr. Wei Kong, Mr. Xi Peng and Mr. Eddiyanto in the Polymer Processing and Performance Research (PPP) 'family' as well as project (UG) students of the PPP unit for useful discussions and comradeship during the period of this research work. I am also very grateful to Mr. Roger Wheeler and Mr S. Ludlow for all their help and technical assistance.

I am indebted to the sponsors of this work at Exxon-Mobil Chemical (Baytown, Texas, USA) and in particular to Mr. J. Schemig and Dr. A. Van Loon for their valuable support and discussions during the course of this work.

I would like to dedicate this work to the memory of my beloved grandparents. Last but not least, I owe a great debt of thanks to my beloved mother and all my wonderful family; Noor Daraz, Nisar Begum, Shukura Begum, Mohammed, Ismail and little Eisah, for their love, immense patience and moral support through all these years. Special thanks also to Elisabet Ecenarro for her unwavering support without whom this thesis would still be in progress.



## LIST OF CONTENT

	Page
THESIS TITLE	1
SUMMARY	2
ACKNOWLEDGEMENTS	3
LIST OF CONTENT	4
LIST OF SCHEMES	9
LIST OF TABLES	10
LIST OF FIGURES	16
<b>CHAPTER ONE</b>	<b>30</b>
<b>INTRODUCTION</b>	
1.1 Introduction	30
1.2 The Metallocene Technology and its Application in Polymers.	30
1.3 Polyethylene Polymers	34
1.3.1 Molecular Structure	34
1.3.2 Melt Rheology	37
1.3.3 Physical Properties	38
1.4 Thermal Oxidative behaviour of PE during Melt processing	41
1.5 Stabilisation of PE Polymers during processing and Stabilisation Mechanisms.	48
1.5.1 Performance Criterion	49
1.5.2 Hindered Phenols	52
a. Synthetic Hindered Phenols	52
b. Biological hindered phenols.	55
1.5.3 Lactones	59
1.5.4 Hydroxylamine.	63
1.5.5 Phosphites	66
1.5.6 Synergism and Antagonism effect on the melt and colour stability during processing.	68
1.6 Aims and Objectives of the Study.	70

<b>CHAPTER TWO</b>	<b>EXPERIMENTAL AND ANALYTICAL TECHNIQUES</b>	<b>72</b>
2.1	Materials.	72
2.2	Polymer Processing	77
2.2.1	Twin-screw extrusion of virgin polymers.	78
2.2.2	Twin-screw extrusion of LLDPE in the presence of AO.	79
a.	Compounding	79
b.	Multi-pass Extrusion (P1 to P5).	81
2.3	Sample Preparation and Analysis	96
2.4	Rheology	97
a.	MFI	97
b.	Twin Bore Capillary Rheometry	98
2.5	Gel Permeation Chromatography (GPC)	103
<b>CHAPTER THREE</b>	<b>RHEOLOGICAL AND STRUCTURAL CHARACTERISTICS OF UNSTABILISED, VIRGIN AND EXTRUDED METALLOCENE AND ZIEGLER POLYMERS.</b>	<b>119</b>
3.1	Objective and Methodology	119
3.2	Results and Discussion	120
3.2.1	Molecular and Rheological Characteristics of Virgin m-LLDPE and z-LLDPE polymers	120
3.2.2	Effect of Multiple Extrusion on Changes in Molecular and Rheological Characteristics of Unstabilised m-LLDPE and z-LLDPE polymers	122
3.2.3	Twin Bore Capillary rheometry of stabilised m-LLDPE polymer samples.	127
3.2.4	Thermal Oxidative Degradation mechanism of LLDPE	128
<b>CHAPTER FOUR</b>	<b>MELT AND COLOUR STABILISATION OF m-LLDPE DURING PROCESSING USING DIFFERENT CLASSES OF ANTIOXIDANTS USED SINGLY.</b>	<b>172</b>

4.1	Objective and Methodology	172
4.2	Results.	
4.2.1	Extrusion characteristics of Pass-zero (Po) and Multiple extrusion (P1, P3 and P5) of stabilised (using single antioxidants) Metallocene polymers.	176
4.2.2	Effect of Po and Multiple Extrusions (P1, P3 and P5) on the Melt stability of m-LLDPE.	177
(i).	Synthetic/Biological hindered phenols, Lactones, hydroxylamines and Phosphite.	178
(ii).	Alkyl hydroxyl hindered amine light stabilisers (R-HALS).	179
4.3	Discussion	179
4.3.1	Twin-screw extrusion characteristics of Pass zero (Po) and Multi-pass (P1, P3 and P5) stabilised Metallocene polymers.	180
4.3.2	Effect of a Lactone, Hydroxylamine and Synthetic/Biological hindered phenols and a phosphite on the melt and colour stability of m-LLDPE during processing.	182
4.3.3	Effect of Alkyl Hydroxylamine Antioxidants (R-HALS) on the melt and colour stability of m-LLDPE during processing.	187
4.4	Overall Perspective of Stabilisation Work Using Single AOs.	191
<b>CHAPTER FIVE STABILISATION OF m-LLDPE AND z-LLDPE DURING PROCESSING USING COMBINATIONS OF DIFFERENT CLASSES OF ANTIOXIDANTS.</b>		<b>208</b>
5.1	Objectives and Methodology	208
5.2	Results	214
5.2.1	Extrusion characteristics of homogenised (Pass zero, Po) and Multiply extruded (Pass 1-5) m-LLDPE and z-LLDPE polymer samples.	214
5.2.2	Effect of the compounding step (Po) on the stability of m-LLDPE and z-LLDPE.	216

5.2.3	Effects of Two Antioxidant Combinations on the Melt and Colour Stability of m-LLDPE and z-LLDPE during Multiple extrusion (P1, P3 and P5).	217
A.	Multiple Extrusions of Stabilised m-LLDPE and z-LLDPE polymers at 285°C under Variable speeds.	217
(a).	Blends of Irganox 1076 and Weston 399.	217
(b).	Blends of Irganox E201 and different phosphites with TMP.	218
B.	Multiple Extrusions of Stabilised m-LLDPE polymers at 260°C at 100rpm.	219
(a).	Blends of Lactone and different Phosphites	219
5.2.4	Effects of Three Antioxidant Combinations on the Melt and Colour Stability of m-LLDPE during Multiple extrusion (P1, P3 and P5) at 260°C/100rpm.	220
(a).	Blends of Lactone, Irganox 1076 and different Phosphites.	220
(b).	Blends of Hydroxylamine, Irganox E201 and Ultrinox 626 with TMP.	220
(c).	Blends of Hydroxylamine, Irganox 1076 and Weston 399.	221
(d).	Blends of Lactone, Irganox E201 and different phosphites with/without Zinc Stearate.	222
5.2.5	Effects of Four Antioxidant Combinations on the Melt and Colour Stability of m-LLDPE during Multiple extrusion (P1, P3 and P5) at 260°C/100rpm.	222
(a).	Blends of Hydroxylamine, Irganox 1076, Weston 399 and different R-HALS	222
5.3	DISCUSSION	223
5.3.1	Extrusion characteristics of stabilised Metallocene and Ziegler polymers and the effect of the Compounding step (Po) Process on their Melt Stability.	

	223
5.3.2 Effect of Two Antioxidant Combinations on the melt and colour stabilisation of m-LLDPE and z-LLDPE during multiple extrusion.	224
(a). Blends of Irganox 1076 and Weston 399 (285°C/variable speeds).	224
(b). Blends of Irganox E201 and different Phosphites with TMP (285°C/variable speeds).	226
(c). Blends of Lactone and different phosphites (260°C/100rpm).	229
5.3.3 Effect of Three Antioxidant Combinations on the melt and colour stabilisation of m-LLDPE during multiple extrusion at 260°C at 100rpm.	232
(a). Effect of Phosphites on blends containing Irganox 1076 and Irganox HP136.	232
(b). Effect of Hydroxylamine and Lactone blends containing Hindered Phenols; Irganox E201 or Irganox 1076, and phosphites in the presence or absence of hindered amine stabilisers.	234
5.3.4 Effect of Four Antioxidant Combinations on the melt and colour stability of m-LLDPE during multiple extrusion at 260°C/100rpm.	237
(a). Effect of Hindered Amine stabilisers (HAS) on blends of hydroxylamine, Irganox 1076 and Weston 399.	237
 CHAPTER SIX CONCLUSIONS	 324
6.1 Conclusions	324
6.2 Suggestions for future work	329
 <b>References</b>	 <b>332</b>
<b>Appendices</b>	<b>342</b>

## LIST OF SCHEMES

	Page
Scheme 1.1	Milestones in metallocene chemistry. 31
Scheme 1.2.	Some of the active companies, which are developing and applying metallocene technology in the production of polymers. 32
Scheme 1.3.	Basic autoxidation mechanism 42
Scheme 1.4.	Thermal oxidation of hydrocarbon polymers, RH is the polymer. 44
Scheme 1.5	Highlights the reactions of the alkyl radical in oxygen deficient conditions. 45
Scheme 1.6:	Oxidative degradation processes and antioxidant mechanism. CB-A, Chain breaking acceptor mechanism; CB-D, Chain breaking donor mechanism; PD, peroxide decomposer mechanism (stoichiometric or catalytic). 49
Scheme 1.7.	Transition state in the formation of phenoxy radicals. 54
Scheme 1.8.	Mechanism of oxidation of propionate-type phenolic antioxidants with peroxy radicals. 56
Scheme 1.9.	Complementary chain breaking mechanism of hydroquinone. 63
Scheme 1.10	Stabilisation mechanism of HALS. 64
Scheme 2.1	Method used for the multi-pass extrusion of m-LLDPE at 100rpm, extrusion temperature 210°C, output rate 4.0kg.h <sup>-1</sup> . 85
Scheme 3.1	Proposed thermal oxidative mechanism of LLDPE. 171
Scheme 3.2	Formation of carbonyl groups during the extrusion of m-LLDPE and z-LLDPE groups. 172
Scheme 3.3	Formation of unsaturated groups and crosslinking reactions during the extrusion of m-LLDPE and z-LLDPE under oxygen deficient conditions. 173
Scheme 4.1.	Overview of the methodology used in the stabilisation of m-LLDPE using single antioxidants. 173
Scheme 4.2	Proposed chain breaking and preventive activity of an aromatic phosphite Weston 399 during the melt extrusion of m-LLDPE. 186
Scheme 4.3	Chain breaking activity (CB-A) and redox reactions of R-HALS during the melt extrusion of m-LLDPE. 189

Scheme 5.1.	Overview of the methodology used in the stabilisation of m-LLDPE using two, three and four based AO based systems.	210
Scheme 5.2	Co-operative interactions between Irganox 1076 and Weston 399 under melt processing conditions.	226
Scheme 5.3	Co-operative interactions between Tocopherol and Ultrinox 626 under melt extrusion conditions.	228
Scheme 5.4	Co-operative interactions between a lactone and Ultrinox 626 under melt processing conditions.	231
Scheme 5.5	CB-A activity of a lactone under melt processing conditions.	232

### LIST OF TABLES

Table 2.1:	Typical characteristics of unstabilised m-LLDPE and z-LLDPE resins (measured at Aston University, except for <sup>1</sup> H-NMR and GPC results which were measured at Exxon, Machelen) (Numbers in parenthesis are the original data provided by Exxon).	73
Table 2.2	Chemical structures of antioxidants used.	74
Table 2.3	Temperature (°C) profile for the twin screw extrusions of m-LLDPE and z-LLDPE. Pass-zero, (Po) and multipass extrusion (P1 to P5).	82
Table 2.4	Flow feeding rates (ml/min) used for the addition of the Weston 399 (phosphite) and Irganox E201 (at 100rpm only) during Po stabilisation of <u>m-LLDPE and z-LLDPE</u> at various screw speeds (rpm); 50,100, 150 and 200 and concentrations (ppm).	86
Table 2.5	Flow feeding rates (ml/min) used for the addition of liquid antioxidants during Po stabilisation of <u>m-LLDPE only</u> at a screw speed of 100rpm and an extrusion temperature of 210°C; <u>see tables 4.1 and 5.1-5.2 for identification of codes.</u>	87
Table 2.6:	Flow feeding rates (ml/min) used for the addition of liquid antioxidants during Po stabilisation of <u>m-LLDPE only</u> at a screw speed of 100rpm and an extrusion temperature of 210°C; <u>see table 5.2 for identification of codes.</u>	88
Table 2.7	<u>Preliminary stabilisation work using formulations s1 to s12.</u> Sample codes and conditions used for twin-screw multi-pass extrusion experiment (extrusion temperatures 210 and 285°C, screw speed of 50-200rpm under atmospheric conditions) of <u>Pass-zero stabilised m-LLDPE.</u> Initially compounded (Po) the polymer under nitrogen at 210°C at 100rpm.	89

Table 2.8	<u>Preliminary stabilisation work using formulations s1 to s12. Sample codes and conditions used for twin-screw multi-pass extrusion experiment (extrusion temperatures 210 and 285°C, screw speed of 50-200rpm under atmospheric conditions) of Pass-zero stabilised z-LLDPE. Initially compounded (Po) the polymer under nitrogen at 210°C at 100rpm.</u>	90
Table 2.9	<u>Preliminary stabilisation work using formulations s4 to s13. Sample codes and conditions used for twin-screw multi-pass extrusion experiment (extrusion temperatures 285°C, screw speed of 50-200rpm under atmospheric conditions) of Pass-zero stabilised m-LLDPE and z-LLDPE. Initially compounded (Po) the polymer under nitrogen at 210°C at 100rpm.</u>	91
Table 2.10.	<u>Sample codes and conditions used for twin-screw multi-pass extrusion experiment (extrusion temperatures 260°C, screw speed of 100rpm under atmospheric conditions) of Pass-zero stabilised m-LLDPE containing single antioxidant formulations – s14 to s21. Initially compounded (Po) the polymer under nitrogen at 210°C at 100rpm.</u>	92
Table 2.11.	<u>Sample codes and conditions used for twin-screw multi-pass extrusion experiment (extrusion temperatures 260°C, screw speed of 100rpm under atmospheric conditions) of Pass-zero stabilised m-LLDPE containing combination antioxidant formulations – s22 to s32. These were initially compounded (Po) in the polymer under nitrogen at 210°C at 100rpm.</u>	93
Table 2.12.	<u>Sample codes and conditions used for twin-screw multi-pass extrusion experiment (extrusion temperatures 260°C, screw speed of 100rpm under atmospheric conditions) of Pass-zero stabilised m-LLDPE containing combinations of antioxidant formulationd based on XP-60 and XP-490 systems (s33 to s42). These were initially compounded (Po) in the polymer under nitrogen at 210°C at 100rpm.</u>	94
Table 2.13.	<u>Sample codes and conditions used for twin-screw multi-pass extrusion experiment (extrusion temperatures 260°C, screw speed of 100rpm under atmospheric conditions) of Pass-zero stabilised m-LLDPE containing combinations of antioxidant formulationd based on Vtamin E systems (s43 to s49). These were initially compounded (Po) in the polymer under nitrogen at 210°C at 100rpm.</u>	95
Table 2.14.	<u>Sample and codes of unstabilised m-LLDPE polymer samples sent for GPC analysis; processed under varying extrusion conditions using a twin-screw extruder, under atmospheric conditions.</u>	104
Table 2.15.	<u>Sample and codes of unstabilised z-LLDPE polymer samples sent for GPC analysis; processed under varying extrusion conditions using a twin-screw extruder, under atmospheric conditions.</u>	105
Table 3.1.	<u>Molecular weight characteristics of Virgin m-LLDPE and z-LLDPE polymers.</u>	130



Table 3.2	Effect of Processing parameters on unstabilised extruded <u>z-LLDPE</u> polymer samples. The subscript 's' in the code denotes the addition of Irganox 1076 (0.2%w/w) to the unstabilised extruded polymer samples prior to MI measurements.	166
Table 3.3	Effect of Processing parameters on unstabilised extruded <u>m-LLDPE</u> polymer samples. The subscript 's' in the code denotes the addition of Irganox 1076 (0.2%w/w) to the unstabilised extruded polymer samples prior to MI measurements.	167
Table 3.4	GPC results (provided by Exxon) of virgin and extruded m-LLDPE and z-LLDPE samples (50-200rpm, 210-285°C, atmospheric conditions, 4mm diameter, die).	168
Table 3.5	GPC results (provided by Exxon) of virgin and extruded m-LLDPE and z-LLDPE samples (50-200rpm, 210-285°C, atmospheric conditions, 4mm diameter, die).	169
Table 3.6	Changes in the % Mw and % MWD characteristics (calculated from GPC measurements, provided by Exxon) of virgin and extruded m-LLDPE and z-LLDPE samples; 285°C/50-200rpm).	170
Table 3.7	Effect of screw speeds on the observed and melt temperature of unstabilised multi-extruded (passes 1, 3 and 5) m-LLDPE and z-LLDPE polymer samples.	171
Table 4.1	Metallocene catalysed LLDPE polymer samples containing different antioxidant formulations compounded (Po) in a TSE at 210°C/100rpm under nitrogen.	174
Table 4.2	Metallocene catalysed Polyethylene (m-LLDPE) samples containing antioxidants received from Exxon Chemicals Baytown (USA) in May 2000; Irganox 1076, Irganox HP 136 and Irgastab FS042.	175
Table 4.3	Processing characteristics for <u>Pass-zero stabilisation of m-LLDPE</u> at an extrusion temperature of 210°C and a screw speed of 100rpm (in a Betol TSE under nitrogenous conditions, 4mm die) using <u>single antioxidants</u> (see s14-s22 in table 4.1).	193
Table 4.4	The <u>multiple extrusion characteristics</u> of stabilised <u>m-LLDPE</u> samples containing <u>single antioxidants</u> (see table 4.1) carried out at 260°C/100rpm under atmospheric conditions, P1, P3 and P5. Values for an unstabilised m-LLDPE polymer is shown for comparative purposes.	194
Table 4.5	Effect of Pass zero (Po) stabilised <u>single antioxidants</u> (see s14-s21 in table 4.1); processed at 210°C/100rpm/under nitrogen on the melt stability of <u>m-LLDPE</u> samples Unstabilised polymers extruded under similar conditions are shown for comparison.	198
Table 4.6.	Effect of processing parameters on the melt stability of Po stabilised <u>m-LLDPE</u> polymer samples using <u>single antioxidants</u> (see s14 to s21, in table 4.1) during	

Pass-zero (Po) and multi-pass extrusion. Unstabilised m-LLDPE extruded under similar conditions is shown for comparison.

		201
Table 4.7.	Effect of processing parameters (260°C/100rpm, atmospheric conditions) on the <u>Colour Stability</u> of Po stabilised <u>m-LLDPE</u> polymer samples using <u>single antioxidants</u> (see s14 to s21, in table 4.1) during Pass-zero (Po) and multi-pass extrusion (260°C/100rpm, under atmospheric conditions, P1, P3 and P5). Unstabilised m-LLDPE extruded under similar conditions is shown for comparison.	
		203
Table 5.1	Metallocene and Ziegler/Natta catalysed LLDPE polymer samples containing different antioxidant formulations compounded (Po) in a TSE at 210°C/100rpm under nitrogen.	
		211
Table 5.2	Metallocene catalysed polyethylene (m-LLDPE) samples containing XP-60, XP-490 and Irganox E201 based systems; each combination comprised of a constant 0.6% Phosphite content and 1:2.3 ratio w/w (phosphite:lactone); compounded (Po) in a twin screw extruder at 210°C/100rpm under nitrogen	
		212
Table 5.3	Metallocene catalysed Polyethylene (m-LLDPE) samples containing antioxidants received from Exxon Chemicals Baytown (USA) in May 2000; Irganox 1076, Irganox HP 136 and Irgastab FS042.	
		213
Table 5.4	Processing characteristics for Pass-zero stabilisation of m-LLDPE and z-LLDPE at an extrusion temperature of 210°C and a screw speed of 100rpm (under nitrogenous conditions, 4mm die) using two and three antioxidant based systems.	
		293
Table 5.5	Multiple extrusion characteristics of stabilised m-LLDPE and z-LLDPE polymer samples under an extrusion temperature of 285°C and a screw speed of 50rpm (under nitrogenous conditions, 4mm die) using a two antioxidant based systems. Unstabilised values are shown for comparative purposes.	
		294
Table 5.6:	Melt stability characteristics of Pass-zero (Po) stabilised <u>m-LLDPE</u> samples processed at 210°C/100rpm/under nitrogen; containing 'combinations' s1-s49 (see table 5.1&5.2).	
		295
Table 5.7:	Melt stability characteristics of Pass-zero (Po) stabilised <u>z-LLDPE</u> samples processed at 210°C/100rpm/under nitrogen; containing 'combinations' s1-s13 (see table 5.1). Unstabilised values are shown for comparison.	
		298
Table 5.8	Effect of <u>Irganox 1076:Weston 399 AO systems</u> (at varying concentrations, see s1 to s12, in table 5.1) on the melt stability of <u>m-LLDPE</u> during Pass zero (Po) and Multi-pass extrusion conditions. Unstabilised polymers extruded under similar conditions are shown for comparison.	
		299
Table 5.9	Effect of <u>Irganox 1076:Weston 399 AO systems</u> (at varying concentrations, see s1 to s12, in table 5.1) on the melt stability of <u>z-LLDPE</u> during Pass zero (Po) and	

	Multi-pass extrusion conditions. Unstabilised polymers extruded under similar conditions are shown for comparison.	301
Table 5.10	Effect of <u>Synthetic and Biological hindered phenol in combination with different phosphites</u> on the melt stability of stabilised <u>z-LLDPE</u> polymer samples; (see s4 to s13, in table 5.1), during Pass zero (Po) and Multi-pass extrusion conditions. Unstabilised z-LLDPE extruded under similar conditions is shown for comparison.	303
Table 5.11	Effect of <u>Synthetic and Biological hindered phenol in combination with different phosphites</u> on the melt stability of stabilised <u>m-LLDPE</u> polymer samples; (see s4 to s13, in table 5.1), during Pass zero (Po) and Multi-pass extrusion conditions. Unstabilised z-LLDPE extruded under similar conditions is shown for comparison.	304
Table 5.12	Effect of <u>Synthetic and Biological hindered phenols in combination with different phosphites</u> on the Colour stability of stabilised <u>m-LLDPE</u> polymer samples; (see s4 to s13, in table 5.1), during Pass zero (Po) and Multi-pass extrusion conditions. Unstabilised z-LLDPE extruded under similar conditions is shown for comparison.	305
Table 5.13	Effect of <u>Synthetic and Biological hindered phenols in combination with different phosphites</u> on the Colour stability of stabilised <u>z-LLDPE</u> polymer samples; (see s4 to s13, in table 5.1), during Pass zero (Po) and Multi-pass extrusion conditions. Unstabilised z-LLDPE extruded under similar conditions is shown for comparison.	307
Table 5.14.	Effect of processing parameters on the melt stability of stabilised <u>XP-60 Two antioxidant based systems</u> (s33 to s37, see table 5.2) <u>m-LLDPE</u> samples during Pass-zero (Po) and multi-pass extrusion (260°C/100rpm, under atmospheric conditions, P1, P3 and P5). Unstabilised m-LLDPE extruded under similar conditions is shown for comparison. All formulations with a constant; 0.6% P content and 1:2.3 ratio (lactone :Phosphite)	308
Table 5.15.	Effect of processing parameters (260 <sup>0</sup> C/100rpm, atmospheric conditions) on the <u>Colour Stability of XP antioxidant based systems</u> (s33 to s37, see table 5.2) <u>m-LLDPE</u> samples containing antioxidant combinations during Po and multi-pass extrusion (P1, P3 and P5). Unstabilised m-LLDPE extruded under similar conditions is shown for comparison.	310
Table 5.16	Effect of processing parameters on the melt stability of stabilised <u>Three antioxidant based systems</u> (s22 to s25, see table 5.1) <u>m-LLDPE</u> samples during Pass-zero (Po) and multi-pass extrusion (260°C/100rpm, under atmospheric conditions, P1, P3 and P5). Unstabilised m-LLDPE extruded under similar conditions is shown for comparison. All formulations with a constant lactone content and varying concentrations of Irganox 1076/Weston 399.	311

Table 5.17.	Effect of processing parameters (260 <sup>0</sup> C/100rpm, atmospheric conditions) on the <u>Colour Stability of Three antioxidant based systems (s22 to s25, see table 5.1) m-LLDPE samples containing antioxidant combinations during Po and multi-pass extrusion (P1, P3 and P5). Unstabilised m-LLDPE extruded under similar conditions is shown for comparison.</u>	312
Table 5.18.	Effect of processing parameters on the melt stability of stabilised <u>XP-490 Three antioxidant based systems (s38 to s42, see table 5.2) m-LLDPE samples during Pass-zero (Po) and multi-pass extrusion (260<sup>0</sup>C/100rpm, under atmospheric conditions, P1, P3 and P5). Unstabilised m-LLDPE extruded under similar conditions is shown for comparison. All formulations with a constant; 0.6% P content and 1:2.3:3.3 w/w ratio (lactone :Phosphite:1076)</u>	313
Table 5.19.	Effect of processing parameters (260 <sup>0</sup> C/100rpm, atmospheric conditions) on the <u>Colour Stability of XP 490 antioxidant based systems (s38 to s42, see table 5.2) m-LLDPE samples containing antioxidant combinations during Po and multi-pass extrusion (P1, P3 and P5). Unstabilised m-LLDPE extruded under similar conditions is shown for comparison.</u>	314
Table 5.20	Effect of processing parameters on the melt stability of stabilised <u>Three antioxidant based systems (s26 to s27, see table 5.1) m-LLDPE samples during Pass-zero (Po) and multi-pass extrusion (260<sup>0</sup>C/100rpm, under atmospheric conditions, P1, P3 and P5). Unstabilised m-LLDPE extruded under similar conditions is shown for comparison. All formulations with a constant Vitamin E, Ultrinox 626 and TMP content in the presence and absence of Irgastab FS042.</u>	315
Table 5.21	Effect of processing parameters (260 <sup>0</sup> C/100rpm, atmospheric conditions) on the <u>Colour Stability of Three antioxidant based systems (s26-27, see table 5.1) m-LLDPE samples containing antioxidant combinations during Po and multi-pass extrusion (P1, P3 and P5). Unstabilised m-LLDPE extruded under similar conditions is shown for comparison. All formulations with a constant Vitamin E, Ultrinox 626 and TMP content in the presence and absence of Irgastab FS042.</u>	316
Table 5.22	Effect of processing parameters on the melt stability of stabilised <u>Three antioxidant based systems (s28 to s29, see table 5.1) m-LLDPE samples during Pass-zero (Po) and multi-pass extrusion (260<sup>0</sup>C/100rpm, under atmospheric conditions, P1, P3 and P5). Unstabilised m-LLDPE extruded under similar conditions is shown for comparison. All formulations with a constant 1:4 w/w ratio of Irg. 1076 and Weston 399 respectively.</u>	317
Table 5.23	Effect of processing parameters (260 <sup>0</sup> C/100rpm, atmospheric conditions) on the <u>Colour Stability of Three antioxidant based systems (s28-29, see table 5.1) m-LLDPE samples containing antioxidant combinations during Po and multi-pass extrusion (P1, P3 and P5). Unstabilised m-LLDPE extruded under similar conditions is shown for comparison. All formulations with a constant 1:4 w/w ratio of Irg. 1076 and Weston 399 respectively.</u>	318

Table 5.24.	Effect of processing parameters on the melt stability of stabilised <u>Vitamin E (Irganox E201) Three antioxidant based systems (s43 to s49, see table 5.2) m-LLDPE</u> samples during Pass-zero (Po) and multi-pass extrusion (260°C/100rpm, under atmospheric conditions, P1, P3 and P5). Unstabilised m-LLDPE extruded under similar conditions is shown for comparison.	319
Table 5.25.	Effect of processing parameters (260°C/100rpm, atmospheric conditions) on the <u>Colour Stability of Vitamin E, antioxidant based systems (s43 to s49, see table 5.2) m-LLDPE</u> samples containing antioxidant combinations during Po and multi-pass extrusion (P1, P3 and P5). Unstabilised m-LLDPE extruded under similar conditions is shown for comparison.	320
Table 5.26	Effect of processing parameters on the melt stability of stabilised <u>four antioxidant based systems (s30 to s32, see table 5.2) m-LLDPE</u> samples during Pass-zero (Po) and multi-pass extrusion (260°C/100rpm, under atmospheric conditions, P1, P3 and P5). Unstabilised m-LLDPE extruded under similar conditions is shown for comparison. All formulations with a constant 1:1:4:2 w/w ratio of Irg. 1076/Irgastab FS042/Weston 399/HALS respectively.	322
Table 5.27	Effect of processing parameters (260°C/100rpm, atmospheric conditions) on the <u>Colour Stability of Four antioxidant based systems (s30-32, see table 5.2) m-LLDPE</u> samples containing antioxidant combinations during Po and multi-pass extrusion (P1, P3 and P5). Unstabilised m-LLDPE extruded under similar conditions is shown for comparison. All formulations with a constant 1:1:4:2 w/w ratio of Irg. 1076/Irgastab FS042/Weston 399/HALS respectively.	323

## LIST OF FIGURES

Figure 1.1	Some classes of metallocene catalysts used for olefin polymerisation.	32
Figure 1.2	Approximate location of Mw averages on a MWD curve.	35
Figure 1.3	SCB and MWD; Schematic representation of molecular structure of Metallocene and Ziegler-Natta catalysed LLDPE.	36
Figure 1.4.	Extensional viscosity vs extensional stress for LDPE and HDPE.	38
Figure 1.5.	Representation of the mutual relationship among molecular structure, solid structure and properties of LLDPE produced by metallocene and Ziegler-Natta catalysts.	40
Figure 1.6.	Autocatalytic curve: typical kinetic curves of molecular mass, oxygen uptake, mass change and formation of intermediates and products in the oxidation of PE.	43
Figure 1.7.	Competing reactions of cross-linking and chain scission of LDPE under varying processing conditions.	46

Figure 1.8.	The effect of processing at 150°C on the MFI of LDPE. (1) Open mixer, (2) Closed mixer (limited amount of air) and (3) In argon.	48
Figure.1.9.	Stereochemical structures of natural Vitamin E.	55
Figure 1.10.	CB-D Antioxidant activity of $\alpha$ -tocopherol	57
Figure 1.11	Chemical structures of analogous $\alpha$ -tocopherol derivative antioxidants.	58
Figure 1.12.	Some of the transformation products formed from $\alpha$ -tocopherol during extrusion experiments of LDPE.	59
Figure 1.13.	Stabilisation mechanism of arylbenzofuranone (lactone HP-136).	61
Figure 1.14.	Model trapping reactions with arylbenzofuranone (lactone).	62
Figure 1.15.	Hydroxylamines function as primary antioxidants as free radical.	64
Figure 1.16.	The CB-A/CB-D radical scavenging activity of the nitron oxidation products of hydroxylamines.	65
Figure 1.17.	The peroxidolytic function of hydroxylamines.	65
Figure 2.1.	The screw configurations of the co-rotating screw in the BETOL 30 mm TSE.	83
Figure 2.2	Twin-screw extrusion line and arrangements shown for Po stabilisation (under nitrogen) and multi-pass extrusion (under atmospheric conditions).	84
Figure 2.3.	Schematic diagram of the Davenport melt flow indexer.	99
Figure 2.4	Schematic diagram of the Rosand RH2000 Twin bore capillary rheometer.	101
Figure 2.5	Outline of the material degradation test of stabilised m-LLDPE polymer samples. Five degradation cycles. Each cycle entailed ascending shear rates from 200-1600s <sup>-1</sup> , followed by a 5 minute waiting time. Change in shear viscosity of the stabilised polymer was recorded.	102
Figure 2.6.	Infrared spectrum of a virgin m-LLDPE film (0.18mm thickness).	106
Figure 2.7	Infrared spectrum of a virgin z-LLDPE thin film (0.17mm thickness).	106
Figure 2.8a	UV spectrum of Irg.1076 in hexane.	107
Figure 2.8b	IR spectrum of Irganox 1076, kBr windows.	107
Figure 2.9	IR spectrum of Irg.FS042, kBr windows.	108
Figure 2.10a	UV spectrum of HP136 in a hexane.	109

Figure 2.10b	IR spectrum of HP136, kBr windows.	109
Figure 2.11a	UV spectrum of Irganox E201 in hexane.	110
Figure 2.11b	IR spectrum of Irganox E201, kBr windows.	111
Figure 2.12a	UV spectrum of Irgafos P-EPQ in hexane. Peak at 275nm.	111
Figure 2.12b	IR spectrum of Irgafos P-EPQ, kBr windows.	112
Figure 2.13a	UV spectrum of Weston 399 in hexane.	112
Figure 2.13b	IR spectrum of Weston 399, kBr windows.	112
Figure 2.14a	UV spectrum of Ultrinox 626 in hexane.	113
Figure 2.14b	IR spectrum of Ultrinox 626, kBr windows.	113
Figure 2.15a	UV spectrum of Doverphos S-9228 in hexane.	114
Figure 2.15b	IR spectrum of Doverphos S-9228, kBr windows.	114
Figure 2.16	IR spectrum of Tinuvin 765, kBr windows.	115
Figure 2.17	IR spectrum of XP-60, kBr windows.	116
Figure 2.18	IR spectrum of XP-490, kBr windows.	116
Figure 2.19	IR spectrum of Tinuvin 622LD, kBr windows.	117
Figure 2.20	IR spectrum of Chimassorb 119D, kBr windows.	117
Figure 2.21	IR spectrum of TMP, kBr windows.	118
Figure 3.1	Differences in molecular weight characteristics of Virgin m-LLDPE and z-LLDPE polymers; a. molecular weight features, b. Polydispersity, c.MWD.	131
Figure 3.2	Shear viscosity functions of virgin unstabilised m-LLDPE and z-LLDPE extruded in a capillary rheometer at 210°C and 285°C, 1mm diameter dies (long die of 16mm length and short die of zero length) were used.	132
Figure 3.3	Effect of temperature on the shear viscosity functions of virgin unstabilised m-LLDPE and z-LLDPE, extruded in a capillary rheometry, 1mm diameter dies (long die of 16mm length and short die of zero length) were used.	133

Figure 3.4	% Change in shear viscosity (calculated from the difference in viscosities at 210 and 285°C at a given shear rate) with shear rate of virgin unstabilised m-LLDPE and z-LLDPE, extruded in a capillary rheometry, 1mm diameter dies (long die of 16mm length and short die of zero length) were used.	134
Figure 3.5	Melt fracture of virgin unstabilised m-LLDPE, extruded in a capillary rheometry at 210, 260 and 285°C, 1mm diameter dies (long die of 16mm length and short die of zero length) were used.	135
Figure 3.6	Melt fracture of unstabilised virgin z-LLDPE, extruded in a capillary rheometry at 210, 260 and 285°C, 1mm diameter dies (long die of 16mm length and short die of zero length) were used.	136
Figure 3.7	Critical shear rates at which melt fracture of unstabilised virgin m-LLDPE and z-LLDPE occurs, in function of the extrusion temperature, determined by capillary rheometry using 1mm diameter dies (long die of 16mm length and a short die of zero length) (z-LLDPE only shows melt fracture at 210°C).	137
Figure 3.8	Elongational viscosity functions of unstabilised virgin m-LLDPE and z-LLDPE at 210°C determined by capillary rheometry using 1mm diameter dies (long die of 16mm length and short die of zero length)	138
Figure 3.9	Elongational viscosity functions of unstabilised virgin m-LLDPE and z-LLDPE at 260°C, extruded in a capillary rheometry, 1mm diameter dies (long die of 16mm length and short die of zero length) were used.	138
Figure 3.10	Comparison of log shear viscosity against log shear rate for unstabilised m-LLDPE and z-LLDPE after processing in an extruder at 210°C/200rpm Pass 1.	139
Figure. 3.11.	Comparison of severity of melt fracture between unstabilised m-LLDPE and z-LLDPE after processing in an extruder at 285°C and 200rpm for Pass 1.	140
Figure 3.12.	Comparison of severity of melt fracture between unstabilised m-LLDPE after processing in an extruder at 210oC and 50rpm for Pass 1,3 and 5.	141
Figure 3.13.	Comparison of severity of melt fracture between unstabilised m-LLDPE after processing in an extruder at 210°C and 50rpm for Pass 1,3 and 5.	142
Figure 3.14.	Comparison of severity of melt fracture between unstabilised m-LLDPE after processing in an extruder at 285°C and 50rpm for Pass 1, 3 and 5.	143
Figure 3.15.	Comparison of severity of melt fracture between unstabilised m-LLDPE after processing in an extruder at 285°C and 50rpm for Pass 1, 3 and 5.	144
Figure 3.16.	Comparison of severity of melt fracture between unstabilised z-LLDPE after processing in an extruder at 210 C and 200rpm for Pass 1, 3 and 5.	145



Figure 3.17.	Comparison of severity of melt fracture between unstabilised m-LLDPE after processing in an extruder at 285 C and 200rpm for Pass 1, 3 and 5.	146
Figure 3.18	Comparison of elongational viscosity against extensional stress for unstabilised z-LLDPE and m-LLDPE after processing in an extruder at 210oC/200rpm for passes 1,3 and 5.	147
Figure 3.19.	Effect of processing severity at fixed temperatures; a. 210°C, b. 285°C, and varying screw speeds (50-200rpm) on the MI and HLMI for unstabilised m-LLDPE and z-LLDPE polymer samples.	148
Figure 3.20	Changes in MI and HLMI for multiple extruded m-LLDPE and z-LLDPE polymers at <u>285°C</u> at various screw speeds (50-200rpm).	149
Figure 3.21	Changes in MI and HLMI for multiple extruded m-LLDPE and z-LLDPE polymers at <u>210°C</u> at various screw speeds (50-200rpm).	150
Figure 3.22.	Effect of shear rate (screw speed); 50-200rpm at extrusion temperatures of 210-285°C upon the Mw (as measured by GPC) of extruded m-LLDPE and z-LLDPE polymer samples.	151
Figure 3.23.	Effect of extrusion temperature (210-285°C) at a screw speed of 200rpm upon the Mw (as measured by GPC) of extruded m-LLDPE and z-LLDPE polymer samples.	152
Figure 3.24	Effect of extrusion speed (50-200rpm) at an extrusion temperature of 285°C upon the MWD (PD, as measured by GPC) of multiply extruded m-LLDPE and z-LLDPE polymer samples.	153
Figure 3.25	Effect of extrusion speed (50-200rpm) at an extrusion temperature of 285°C upon the % change in Mw and MWD (as measured by GPC) of multiply extruded m-LLDPE and z-LLDPE polymer samples.	154
Figure 3.26.	Shifts in MWD of virgin m-LLDPE and z-LLDPE polymers relative to their multi-extruded Pass 5 analogues (285°C/200rpm).	155
Figure 3.27	Effect of extrusion temperature 285°C (at screw speeds 50-200rpm) upon the % changes in Mw and MWD of Pass 1 multiple extruded m-LLDPE and z-LLDPE polymer samples.	156
Figure 3.28	Effect of extrusion temperature 285°C (at screw speeds 50-200rpm) upon the % changes in Mw and MWD of Pass 5 multiple extruded m-LLDPE and z-LLDPE polymer samples.	157
Figure 3.29	Shifts in MWD of virgin m-LLDPE and z-LLDPE polymers relative to their multi-extruded Pass 1 analogues (285°C/50-200rpm).	158

Figure 3.30	Shifts in MWD of virgin m-LLDPE and z-LLDPE polymers relative to their multi-extruded Pass 5 analogues (285°C/50-200rpm).	159
Figure 3.31	Shifts in MWD of virgin m-LLDPE and z-LLDPE polymers relative to their multi-extruded Pass 1 and 5 analogues (285°C/50-200rpm).	160
Figure 3.32	Outline of 1 degradation cycle during the material degradation cycle of m-LLDPE polymer samples. Cycle entailed ascending shear rates from 200 to 1600s <sup>-1</sup> followed by a 5 minute waiting before the start of another cycle (5 total cycles).	161
Figure 3.33.	Change in PL of <u>pass 1</u> ; unstabilised, stabilised and virgin m-LLDPE polymer samples during the <u>material degradation test</u> (a shear rate; 1600s <sup>-1</sup> and temperature; 260°C, 5 degradation cycles, 5 minute waiting intervals).	161
Figure 3.34.	Change in PL of <u>pass 3</u> ; unstabilised, stabilised and virgin m-LLDPE polymer samples during the <u>material degradation test</u> (a shear rate; 1600s <sup>-1</sup> and temperature; 260°C, 5 degradation cycles, 5 minute waiting intervals).	162
Figure 3.35.	Change in PL of <u>pass 5</u> ; unstabilised, stabilised and virgin m-LLDPE polymer samples during the <u>material degradation test</u> (a shear rate; 1600s <sup>-1</sup> and temperature; 260°C, 5 degradation cycles, 5 minute waiting intervals).	163
Figure 3.36.	Change in PL of <u>unstabilised and virgin m-LLDPE polymer</u> samples during the material degradation test (a shear rate; 1600s <sup>-1</sup> and temperature; 260°C, 5 degradation cycles, 5 minute waiting intervals).	163
Figure 3.37.	Change in PL of multi-processed (P1, P3 and P5), Po stabilised m-LLDPE polymer samples (using formulations s24 and s26, see table 5.1) during the material degradation test (a shear rate; 1600s <sup>-1</sup> and temperature; 260°C, 5 degradation cycles, 5 minute waiting intervals).	164
Figure 3.38.	Change in Shear viscosity of multi-processed (P1, P3 and P5), Po stabilised m-LLDPE polymer samples (using formulations s24 and s26) during the material degradation test (at a shear rate of 600s <sup>-1</sup> and temperature; 260°C, 5 degradation cycles, 5 minute waiting intervals).	164
Figure 3.39.	<u>Extensional viscosity functions</u> of unstabilised, stabilised and virgin multi-processed m-LLDPE polymer samples during the material degradation test (a shear rate; 600s <sup>-1</sup> and temperature; 260°C, 5 degradation cycles, 5 minute waiting intervals).	165
Figure 4.1.	Change in power consumption during twin screw extrusion of stabilised m-LLDPE (Po, formulation numbers s14-s21 see tables 4.3); N <sub>2</sub> , 210°C, 100rpm. Changes in unstabilised polymers extruded under similar conditions is shown for comparison. Values for unstabilised z-LLDPE polymers shown for comparison.	195

- Figure 4.2 Effect of processing of stabilised polymers on the appearance of the extruded laces (4mm die) of m-LLDPE melt fracture is shown in the case of the metallocene polymer. 195
- Figure 4.3 A comparison of  $\Delta T$  (defined as the temperature difference between the die and melt) stabilised (P<sub>0</sub>, formulation number s14-s21, see table 4.1) and unstabilised (P<sub>1</sub>) m-LLDPE. Values for unstabilised z-LLDPE polymers shown for comparison 196
- Figure 4.4 Changes in melt pressure during processing of stabilised (P<sub>0</sub>, formulation number s14-s21, see table 4.1) and unstabilised (P<sub>1</sub>) m-LLDPE. Values for unstabilised z-LLDPE polymers shown for comparison. 196
- Figure 4.5 Changes in (a). power Consumption, (b). melt Pressure, (c).  $\Delta T$  (difference between the die and actual melt temperature) of unstabilised and stabilised stabilised (Irganox 1076, s14) m-LLDPE polymer samples during multi-pass extrusion; passes 1,3 and 5 (260°C, 100rpm under atmospheric conditions). 197
- Figure 4.6 Melt stability characteristics; a. MI, b. HLMI and c. MFR; of stabilised (see s14-s21, in table 4.1) during the P<sub>0</sub> compounding step (210°C, 100rpm, N<sub>2</sub>). Unstabilised extruded (P<sub>1</sub>) m-LLDPE polymer samples are shown for comparison 199
- Figure 4.7 Changes in the melt stability characteristics; a. %MI, b. %HLMI and c. %MFR; of stabilised (see s14-s21, in table 4.1) during the P<sub>0</sub> compounding step (210°C, 100rpm, N<sub>2</sub>). Unstabilised extruded (P<sub>1</sub>) m-LLDPE polymer samples are shown for comparison. 200
- Figure 4.8 Melt stability characteristics a. MI, b. % MI and c. % MFR; of stabilised m-LLDPE containing Irganox 1076 (s14), Irganox HP136 (s15), Irgastab FS042 (s16), Irganox E201 (s19) and Weston 399 (s20) during multiple extrusion. 204
- Figure 4.9 Colour stability characteristics of P<sub>0</sub> stabilised m-LLDPE containing Irganox 1076 (s14), Irganox HP136 (s15), Irgastab FS042 (s16), Irganox E201 (s19) and Weston 399 (s20) during multiple extrusion. 205
- Figure 4.10 Melt stability characteristics a. MI, b. % MI and c. % MFR; of stabilised m-LLDPE containing Tinuvin 765 (s17), Tinuvin 622LD (s18), and Chimassorb 119D (s21) during multiple extrusion. 206
- Figure 4.11 Colour stability characteristics of P<sub>0</sub> stabilised m-LLDPE containing Tinuvin 765 (s17), Tinuvin 622LD (s18) and Chimassorb 119D (s21) during multiple extrusion. 207
- Figure 5.1. Change in power consumption during twin screw extrusion of stabilised m-LLDPE (P<sub>0</sub>, formulation numbers s4 to s43, see tables 5.1-5.2) and z-LLDPE (P<sub>0</sub>, formulation numbers s1 to s12, see tables 5.1-5.2). Changes in unstabilised polymers extruded (atmospheric conditions, 210°C, 100rpm, P<sub>1</sub>) under similar conditions are shown for comparison. 238

- Figure 5.2 Effect of processing of stabilised polymers on the appearance of the extruded laces (4mm die) of m-LLDPE and z-LLDPE polymers extruded under the same conditions (using formulation s-4, see table 5.1). Clear melt fracture is shown in the case of the metallocene polymer. 239
- Figure 5.3: A comparison of  $\Delta T$  during twin screw extrusion of stabilised m-LLDPE (s4 to s43, see tables 5.1-5.2) and z-LLDPE (s1 to s12, see tables 5.1-5.2). Changes in unstabilised polymers extruded (atmospheric conditions, 210°C, 100rpm, P<sub>1</sub>) under similar conditions are shown for comparison. 240
- Figure 5.4: Changes in melt pressure during of stabilised m-LLDPE (s4 to s43, see tables 5.1-5.2) and z-LLDPE (s1 to s12, see tables 5.1-5.2). Changes in unstabilised polymers extruded (atmospheric conditions, 210°C, 100rpm, P<sub>1</sub>) under similar conditions are shown for comparison. 240
- Figure 5.5. Changes in power consumption of stabilised (Po, formulation S-4, see table m-LLDPE and z-LLDPE during multi-pass extrusion; Passes 1,3 and 5 (285°C, 50rpm under atmospheric conditions). Unstabilised multi-pass extruded m-LLDPE and z-LLDPE samples are shown for comparison. 241
- Figure 5.6 Changes in melt pressure of stabilised (Po, formulation S-4, see table 5.1, nitrogen) m-LLDPE and z-LLDPE during multi-pass extrusion; Passes 1,3 and 5 (285°C, 50rpm under atmospheric conditions). Unstabilised multipass extruded m-LLDPE and z-LLDPE samples (using same conditions) are shown for comparison. 241
- Figure 5.7 Changes in  $\Delta T$  (difference between the die and actual melt temperature) of stabilised (Po, formulation S-4, nitrogen) m-LLDPE and z-LLDPE samples during multi-pass extrusion; Passes 1,3 and 5 (285°C, 50rpm under atmospheric conditions). Unstabilised multipass extruded m-LLDPE and z-LLDPE samples (using same conditions) are shown for comparison. 242
- Figure 5.8 The melt characteristics of Po m-LLDPE and z-LLDPE stabilised samples (see tables 5.1 & 5.2). Unstabilised m-LLDPE and z-LLDPE polymer samples are shown for comparison. 243
- Figure 5.9 % Changes in the melt characteristics of Po m-LLDPE and z-LLDPE stabilised samples (see tables 5.1 & 5.2). Unstabilised m-LLDPE and z-LLDPE polymer samples are shown for comparison. 244
- Figure 5.10. Effect of on the melt stability characteristics; MI, %MI change, HLMI, % HLMI change, MFR and %MFR change of stabilised m-LLDPE polymer samples; using Synthetic hindered Phenol/Phosphite combinations (see s2 and s3 in table 5.1); during multi-pass extrusion at 210°C/50rpm (P<sub>1</sub>, P<sub>3</sub> and P<sub>5</sub> under atmospheric conditions). Unstabilised m-LLDPE polymers processed under the same conditions are shown here for comparison. 245

- Figure 5.11. Effect of on the melt stability characteristics; MI, %MI change, HLMI, % HLMI change, MFR and %MFR change of stabilised z-LLDPE polymer samples, using Synthetic hindered Phenol/Phosphite combinations (see s2 and s3 in table 5.1); during multi-pass extrusion at 210°C/50rpm (P1, P3 and P5 under atmospheric conditions). Unstabilised z-LLDPE polymers processed under the same conditions are shown here for comparison. 246
- Figure 5.12. Effect of processing severity (P1, P3 and P5); multi-pass extrusion at 285°C/50rpm on the melt stability characteristics; MI, %MI change and % MFR change; of unstabilised and stabilised m-LLDPE and z-LLDPE polymer samples containing different combinations of Irganox 1076:Weston 399 blend (see s2 and s4, in table 5.1). 247
- Figure 5.13. Effect on the melt stability, %HLMI change, of stabilised m-LLDPE and z-LLDPE (using s2 and s4, in table 5.1) during multi-pass extrusion at 285°C/50rpm (P1, P3 and P5 under atmospheric conditions). Unstabilised samples processed under the same conditions are shown here for comparison. 248
- Figure 5.14. Effect of processing severity (P1, P3 and P5); multi-pass extrusion at 285°C/200rpm on the melt stability characteristics; MI, % MI change and % MFR change of stabilised m-LLDPE and z-LLDPE polymer samples containing different combinations of a Irganox 1076:Weston 399 AO blend (see s2 and s4 in table 5.1). Unstabilised m-LLDPE and z-LLDPE values are shown here for comparison. 249
- Figure 5.15. Effect on the melt stability, %HLMI change, of stabilised m-LLDPE and z-LLDPE (using s2 and s4, in table 5.1) during multi-pass extrusion at 285°C/200rpm (P1, P3 and P5 under atmospheric conditions). Unstabilised samples processed under the same conditions are shown here for comparison. 250
- Figure 5.17 The effect of phosphite concentration (Weston 399) concentration (formulations containing 500ppm Irganox 1076) during multi-pass extrusion (285°C/50rpm) on MI, %MI change and % MFR change of stabilised m-LLDPE and z-LLDPE polymers under atmospheric conditions. 252
- Figure 5.18 The effect of phosphite concentration (Weston 399) concentration (formulations containing 500ppm Irganox 1076) during multi-pass extrusion (285°C/50rpm) on % HLMI change of stabilised m-LLDPE polymers under atmospheric conditions. 253
- Figure 5.19 The effect of phosphite concentration (Weston 399) concentration (formulations containing 500ppm Irganox 1076) during multi-pass extrusion at 285°C/200rpm on MI, %MI change and % MFR change of stabilised m-LLDPE and z-LLDPE polymers under atmospheric conditions. 254
- Figure 5.20 The effect of phosphite concentration (Weston 399) concentration (formulations containing 500ppm Irganox 1076) during multi-pass extrusion at 285°C/200rpm on % HLMI change of stabilised m-LLDPE and z-LLDPE polymers under atmospheric conditions. 255

- Figure 5.21. Compares the effect on melt stability, MI, of increasing Weston 399 concentrations (fixed Irganox [1076] of 500ppm on each successive pass (1, 3 and 5) during multi-pass extrusion at 285°C at 50 and 200rpm under atmospheric conditions of stabilised m-LLDPE and z-LLDPE polymer samples. 256
- Figure 5.22. Compares the effect of processing severity on the melt stability characteristics of m-LLDPE and z-LLDPE polymers containing a 1:4 w/w ratio of Irganox 1076:Weston 399 (see s-4 in table 5.1) during multi-pass extrusion conditions with an extrusion temperature of 285°C at screw speeds of 50 and 200rpm under atmospheric conditions. 257
- Figure 5.23. Effect of different screw speeds (50, 100 and 200rpm) at a fixed extrusion temperature of 285°C (under atmospheric conditions) on the melt stability, MI, characteristics of stabilised m-LLDPE and z-LLDPE polymer sample, using a 1:4 w/w ratio of Irganox 1076:Weston 399. 258
- Figure 5.24. Compares the effect of different screw speeds (50, 100 and 200rpm) at a fixed temperature (285°C, under atmospheric conditions) with increasing processing severity on the melt stability; using a 1:4 ww/w ratio of a Irganox 1076:Weston 399 (500:2000ppm); of stabilised m-LLDPE and z-LLDPE polymer samples. The stability of the stabilised m-LLDPE polymer (with the same AO blend ratio) extruded at 285°C/100rpm is shown for comparison. 259
- Figure 5.25. Effect of screw speed (50, 100 and 200rpm) with multi-pass extrusion at a fixed extrusion temperature (285°C under atmospheric conditions) on the colour stability of stabilised of m-LLDPE and z-LLDPE polymer samples using a 1:4 w/w ratio of Irganox 1076:Weston 399 stabiliser package. 260
- Figure 5.26. Comparison of the effect of screw speed (50, 100 and 200rpm) with increasing processing severity at a fixed extrusion temperature (285°C under atmospheric conditions) on the colour stability of stabilised of m-LLDPE and z-LLDPE polymer samples using a 1:4 w/w ratio of Irganox 1076:Weston 399 stabiliser package. 261
- Figure 5.27. Comparison of at the effect of AOs on the melt stability, MI, %MI change and % MFR change, in stabilised m-LLDPE; using a Irganox 1076:Weston 399 in combination with phosphites (see s4, s11 and s13 in table 5.1) during multi-pass extrusion (285°C with two different screw speeds, 50 and 200rpm). 262
- Figure 5.28. Comparison of the effect of AOs on the melt stability, HLMI and %HLMI change, of m-LLDPE; using Irganox 1076:Weston 399 in combination with phosphites (see s4, s11 and s13 in table 5.1) during multi-pass extrusion (285°C with two different screw speeds, 50 and 200rpm). 263
- Figure 5.29. Comparison of the effect of AOs on the melt stability, MI, %MI change and % MFR change, of stabilised m-LLDPE and z-LLDPE; using Irganox 1076 and

- Irganox E201 in combination with phosphites (see s4, s11 and s13 in table 5.1) during multi-pass extrusion (285°C at a screw speed of 100rpm). 264
- Figure 5.30. Comparison of the effect of AOs on the melt stability, HLMI and %HLMI change, of m-LLDPE and z-LLDPE; using a Irganox 1076 and Irganox E201 in combination with phosphites (see s4, s11 and s13 in table 5.1) during multi-pass extrusion (285°C at a screw speed of 100rpm). 265
- Figure 5.32 Comparison of the colour stability of stabilised m-LLDPE polymers; using Irganox 1076 and Irganox E201 in combination with different phosphites (see s4 and s11 (see table 5.1) during multi-pass extrusion at an extrusion temperature of 285°C with screw speeds of 50 and 200rpm (under atmospheric conditions). 267
- Figure 5.33 Comparison of the colour stability of stabilised m-LLDPE polymers; using Irganox 1076 and Irganox E201 in combination with different phosphites; s11 and s13 (see table 5.1) during multi-pass extrusion at an extrusion temperature of 285°C with screw speeds of 50 and 200rpm (under atmospheric conditions). 268
- Figure 5.34 Comparison of the colour stability of stabilised m-LLDPE and z-LLDPE polymers; using Irganox 1076 and Irganox E201 in combination phosphites (see s4 and s11 in table 5.1); during multi-pass extrusion at an extrusion temperature of 285°C with a screw speed of 100rpm (under atmospheric conditions). 269
- Figure 5.35 Comparison the colour stability of stabilised m-LLDPE and z-LLDPE polymers; using Irganox E201 in combination with different phosphites (see s4 and s11 in table 5.1); during multi-pass extrusion at an extrusion temperature of 285°C with a screw speed of 100rpm (under atmospheric conditions). 270
- Figure 5.36. Comparison of a. Melt stability b. % MI Changes of m-LLDPE containing Irganox HP136 in combination with different Phosphites; U626 (s33 & s34), PEPQ (s35), Doverphos S9228 (s36) and W.399 (s37); see table 5.1; multi-extruded at 260°C/100rpm. 271
- Figure 5.37. Colour Stability of m-LLDPE containing Irganox HP136 and different phosphites (PEPQ, U.626, D.S9228, W.399) in a 2.3 ratio; stabilised formulations s34-s37, see table 5.1; multi-extruded at 260°C/100rpm. 272
- Figure 5.38. Cost effectiveness of Irganox HP136:phosphite combinations. Cost for the concentration used. 272
- Figure 5.39 Comparison of melt stability characteristics of m-LLDPE containing a fixed lactone content (0.03%w/w) and varying concentrations of Irganox 1076/weston 399 combinations in the presence/absence of TMP; stabilised formulations (see s22-s-25 in table 5.1); multi-extruded at 260°C/100rpm under atmospheric conditions. 273
- Figure 5.40 Colour stability characteristics of m-LLDPE containing a fixed lactone content (0.03%w/w) and varying concentrations of Irganox 1076/weston 399

- combinations in the presence/absence of TMP; stabilised formulations (see s22-s-25 in table 5.1); multi-extruded at 260°C/100rpm under atmospheric conditions. 274
- Figure 5.41 Comparison of melt stability characteristics of m-LLDPE containing Irganox 1076:Irganox HP136 in combination with different phosphites (P-EPQ, U626, Doverphos S9228 and W.399); stabilised formulations (see s39-s-42 in table 5.1); multi-extruded at 260°C/100rpm. 275
- Figure 5.42. Comparative melt stability characteristics of a m-LLDPE polymer containing a commercial, s38 (XP-490) package and a blend of similar composition prepared at Aston, s39, based on a Irganox 1076:Irganox HP136 and PEP-Q system; multi-extruded at 260°C/100rpm under atmospheric conditions. 276
- Figure 5.43 Colour stability characteristics of m-LLDPE containing Irganox 1076:Irganox HP136 in combination with different phosphites (P-EPQ, U626, D. S9228 and W.399) in a 1:2.3 ratio of lactone:phosphite; P0 stabilised formulations s39-s42 see table 5.1; multi-extruded at 260°C/100rpm under atmospheric conditions; XP-490 a commercial package is also shown for comparison (s38). 277
- Figure 5.44. Cost effectiveness of a Irganox 1076:Irganox HP136 in combination with different phosphites. Cost for the concentration used. Note that s-23 expresses cost excluding price of TMP. 277
- Figure 5.45 Comparison of melt stability of m-LLDPE containing a fixed Vitamin E and Ultrinox 626 content (0.03 and 0.06 % w/w respectively) in the presence/absence of dialkyhydroxylamine and co-additive TMP; stabilised formulations (see s11 and s26-s27 in table 5.1); multi-extruded at 260°C/100rpm. 278
- Figure 5.46 The effect of increasing hydroxylamine concentration (Irgastab FS042); formulations containing fixed levels of Vitamin E and Ultrinox 626 (0.03 and 0.06 % w/w respectively) in the presence of TMP during multi-pass extrusion at 260°C/100rpm on MI, %MI change and % MFR change of stabilised m-LLDPE polymers. 279
- Figure 5.47 Colour stability of m-LLDPE containing a fixed Vitamin E and Ultrinox 626 content (0.03 and 0.06 % w/w respectively) in the presence/absence of dialkyhydroxylamine and co-additive TMP; stabilised formulations (see s11 and s26-s27 in table 5.1); multi-extruded at 260°C/100rpm. 280
- Figure 5.48 Comparison of melt stability of m-LLDPE containing a fixed Irganox 1076 and Weston 399 content (0.05 and 0.2 % w/w respectively) in the presence/absence of dialkyhydroxylamine; stabilised formulations (see s4 and s28-s29 in table 5.1); multi-extruded at 260°C/100rpm. 280
- Figure 5.49 The effect of increasing hydroxylamine concentration (Irgastab FS042); formulations containing a constant of Irganox 1076/Weston 399 (0.05 and 0.2 % w/w respectively) during multi-pass extrusion at 260°C/100rpm on MI, %MI change and % MFR change of stabilised m-LLDPE polymers. 281



- Figure 5.50 Colour stability of m-LLDPE containing a fixed Irganox 1076 and Weston 399 content (0.05 and 0.2 % w/w respectively) in the presence/absence of dialkyhydroxylamine; stabilised formulations (see s4 and s28-s29 in table 5.1); multi-extruded at 260°C/100rpm. 281
- Figure 5.51 Comparison of melt stability of m-LLDPE in the presence and absence of co-additives containing Irganox HP136 in combination with different phosphites (P-EPQ, U626, Doverphos S9228 and W.399); in a 1:2.3 w/w ratio with a fixed concentration of Irganox E201 (see s43-s-49 in table 5.1); multi-extruded at 260°C/100rpm. Formulation ms-11 contains no Irg. HP136 shown for comparison. 282
- Figure 5.52 Comparison of melt stability of m-LLDPE in the presence and absence of co-additive, ZnSt, containing Irganox HP136 in combination with phosphite Ultrinox 626; stabilised formulations in a 1:2.3 w/w ratio with a fixed concentration of Irganox E201 (see s43-s-49 in table 5.1); multi-extruded at 260°C/100rpm. 283
- Figure 5.53 Comparison of melt stability characteristics of m-LLDPE in the presence and absence of co-additive, ZnSt, containing Irganox HP136 in combination with phosphite Weston 399; stabilised formulations in a 1:2.3 w/w ratio with a fixed concentration of Irganox E201 (see s43-s-49 in table 5.1); multi-extruded at 260°C/100rpm. 284
- Figure 5.54 Colour stability of m-LLDPE containing Irganox HP136 in combination with different phosphites; in the presence/absence of co-additives; stabilised formulations in a 1:2.3 w/w ratio with a fixed concentration of Irganox E201 (see s43-s11 see in table 5.1); multi-extruded at 260°C/100rpm under atmospheric conditions. 285
- Figure 5.55 Colour stability of m-LLDPE containing Irganox HP136 in combination with different phosphites; a. U626 b. W.399; in the presence/absence of co-additive ZnSt; stabilised formulations in a 1:2.3 ratio with a fixed concentration of Irganox E201 (see s44, s45, s47 and s48 in table 5.1); multi-extruded at 260°C/100rpm under atmospheric conditions. 286
- Figure 5.56 Comparative Colour stability of m-LLDPE containing Irganox E201 in combination with Ultrinox 626 in the presence of co-additives ZnSt and TMP ; stabilised formulations in a 1:2.3 ratio with a fixed concentration of Irganox E201 (see s49 and s11 in table 5.1); multi-extruded at 260°C/100rpm under atmospheric conditions. 287
- Figure 5.57. Cost effectiveness of Irganox HP136:Irganox E201:Phosphite combinations. Cost for the concentration used. 287
- Figure 5.58 Comparison of melt stability of m-LLDPE containing a fixed Irganox 1076/Weston 399/Irgastab FS042 content respectively) in the presence/absence of HALS; stabilised formulations (s30-s32 in table 5.2); multi-extruded at

260°C/100rpm under atmospheric conditions. For comparison a Irganox 1076/Weston 399 blend is shown (s4). 288

- Figure 5.59 Colour stability characteristics of m-LLDPE containing a fixed Irganox 1076/Weston 399/Irgastab FS042 content respectively) in the presence/absence of HALS; PO stabilised formulations (s30-s32 in table 5.2); multi-extruded at 260°C/100rpm under atmospheric conditions. 289
- Figure 5.60 % Changes in MI of m-LLDPE and z-LLDPE stabilised with Irganox 1076:Weston 399 at 1:2 and 1:4 w/w at 285°C and different screw speeds. 290
- Figure 5.61 % Changes in HLMI of m-LLDPE and z-LLDPE stabilised with Irganox 1076:Weston 399 at 1:2 and 1:4 w/w at 285°C and different screw speeds. 291
- Figure 5.62 % Changes in MI of m-LLDPE stabilised with a 1:4 w/w ratio of Irganox 1076 :Weston 399; extruded at 260-285°C/100rpm. Unstabilised m-LLDPE extruded at different temperatures but the same screw speed shown for comparison. 291
- Figure 5.63 % Changes in MI of m-LLDPE and z-LLDPE stabilised with Irganox 1076 :Weston 399 at 1:2 and 1:4 w/w at 285°C/100rpm. 291

## 1.1 General Introduction

Polyolefins represent a commercially important class of bulk thermoplastics due to their low price, versatility, ease of processing and low weight to volume ratio. Metallocene catalysed linear low-density polyethylene, m-LLDPE, is produced by the co-polymerisation of small amounts of  $\alpha$ -olefins, e.g. 1-hexene, with ethylene in the presence of an organometallic catalyst, metallocene (polymerisation activity increased with a cocatalyst) [1,2]. LLDPE has been traditionally polymerised using Ziegler/Natta catalysts (z-LLDPE). The structural characteristics, e.g. narrow molecular weight distribution (MWD), of these new generation metallocene catalysed polymers impart properties which are far superior to those offered by Ziegler/Natta catalysed polymers [1]. However, these advantages of the metallocene catalysed polyolefins can be compromised by thermal oxidative degradation during processing e.g. extrusion. The use of stabilising packages in m-LLDPE during processing would inhibit or minimise their thermal oxidative degradation in the melt.

## 1.2. The Metallocene 'Technology' and its Applications in Polymers.

Metallocene catalysts have been used commercially to produce polyolefins since 1991 although their existence has been known since the 1950s (see scheme 1.1) [1]. The commercial interest centres on their use in making Polyethylene (PE) and Polypropylene (PP). This accounts for 45 per cent of the whole production of plastics and this tendency is growing. It is estimated that in the year 2005, metallocene catalysts will be used to produce about 65 million tons of plastics such as PE and PP [2,3]. More than 50 large companies world-wide are currently involved in a level of industrial research which seeks to exploit the large potential applications of metallocene technology [4-5]. Companies such as Exxon, Mitsui Petrochemicals, Indemitsu, Mitsui Toatsu, Hoechst, Asahi chemical and DOW chemicals are at the forefront of applying these organometallic catalysts to the polymerisation of polyolefins (see scheme 1.2) [6-11].

The name 'Metallocene' was coined in the early 1950s as a more elegant replacement for the term 'iron sandwich' describing dicyclopentadienyliron, a compound of iron and cyclopentadiene,  $(C_2H_5)_2 Fe$  or  $Cp_2Fe$ . Its structure was first elucidated by Fischer and Wilkinson, as an iron atom sandwiched between parallel planar cyclopentadienyl groups [1]. Soon after the discovery of the Ziegler-Natta catalysts, metallocenes were used as transition

metal compounds in combination with aluminium alkyls such as *tris*-methylaluminium (TMA), triethyl aluminium and diethyl aluminium chloride for the polymerisation of olefins [1,2]. The activities of these metallocene catalysts were poor. This situation was changed dramatically in 1975 when Kaminsky [1] at the University of Hamburg discovered accidentally, that significant additions of water greatly increased the metallocene catalysts' activity when TMA was used as the co-catalyst. It was shown that this activity resulted from the formation of Methylaluminoxane (MAO) by the hydrolysis of TMA [1].

#### Scheme 1.1 Milestones in Metallocene chemistry [1,2].

- 1952 Structure of Metallocenes elucidated.
  - 1955 Metallocenes were used as components in Ziegler-Natta catalysis, but showed only limited catalytic activity.
  - 1973 The addition of small amounts of water increased the activity of titanocene/alkylaluminium chloride systems.
  - 1975 Unexpected sharp increases in catalyst activity were noticed after the addition of significant quantities of water ( $\text{Al}:\text{H}_2\text{O}\approx 1:2$ ) to 'halogen' free titanocene and TMA.
  - 1977 Highly active catalysts (for olefin polymerisation) were synthesised by the use of titanocenes and separately synthesised MAO.
  - 1984 The synthesis of chiral titanocenes with  $C_2$  symmetry and the polymerisation of propene with chiral titanocene led to isotactic polypropylene.
  - 1988 The synthesis of syndiotactic polypropylene with  $C_s$  symmetrical zirconocenes.
- Since then, there has been a rapid development in the application of Metallocene technology to polyolefin polymerisation.

Even though the exact structure of MAO is still a matter of controversy, they supposedly exist as a mixture of different cyclic or linear oligomers [1]. Experimental evidence [1] seems to indicate that besides acting as an alkylating agent, MAO is involved in the formation of an active site and prevents deactivation of this site *via* a bimolecular process that stabilises the active species. The active catalytic site formed is an ion pair, a metallocene cation that is unsaturated and is stabilised by a bulky non-co-ordinating MAO anion.

Scheme 1.2. Some of the Active companies, which are developing and applying metallocene technology in the production of Polymers [Courtesy of D. Rotman, A. Wood, "Dow and Exxon jostle in race Metallocene products to the Market", *Chem. Week.*, Sept. 15<sup>th</sup> (1993) [10]].

Youngs Modulus/ MPa



If metallocenes especially with Zirconocenes are combined with MAO, the resulting catalyst can polymerise olefins 10-100 times faster than most active Ziegler-Natta catalysts [1,12]. Some classes of Metallocene catalysts used for olefin polymerisation are shown in figure 1.1.

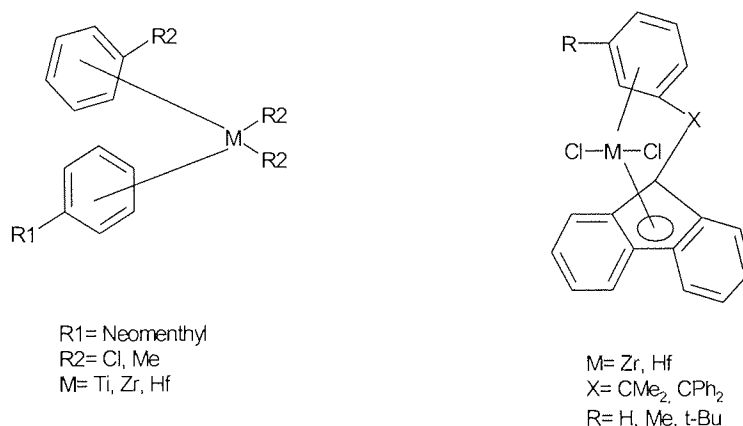


Figure 1.1 Some classes of Metallocene catalysts used for olefin polymerisation [1].

The high degree of control exerted by metallocene catalysts (also known as single-site catalysts, 'SSC') during the polymerisation of a PE polymer such as, low density polyethylene (LDPE), linear low density polyethylene (LLDPE) and high density polyethylene (HDPE), results in property advantages over the traditional Ziegler-Natta catalysts (multi-site catalysts, 'MSC') [1]. There are four main features that distinguish metallocene catalysts from the conventional Ziegler-Natta catalysts used in the polyolefin industry [1].

Metallocene catalysts can: -

1. Polymerise almost any vinyl monomer irrespective of its molecular weight or steric hindrance [1,13-16].
2. Produce uniform polymers and co-polymers of narrow molecular weight distributions (MWD) [16].
3. Control the level of vinyl unsaturation in the polymer produced [17].
4. Polymerise  $\alpha$ -olefins with very high stereoregularity to give isotactic or syndiotactic polymers [2,10].

A marked difference between the two technologies is that Ziegler-Natta technology gives rise to non-uniformity within the polymeric matrix whereas the metallocene technology furnishes high uniformity of the polymer since it permits polymerisation at only a single site [1,18].

The metallocene catalyst systems are poised to make great steps forward in industrial scale production [4]. In addition to the range of polyolefins produced such as PE, LDPE, LLDPE, syndiotactic polypropylene, there is a variety of further materials, which can be easily produced by metallocene technology [4]. For instance syndiotactic polystyrene, copolymerisation with higher proportions (5-30%) of longer chain  $\alpha$ -olefins, elastomers made of ethylene, propene and dienes (EPDM), homopolymerisation and copolymerisation of cyclo-olefins [1].

Metallocene catalysed PE polymers, utilising both homopolymers and random copolymers, may be used in a variety of end applications, many of them consumer oriented, such as highly flexible and tenacious films, one of the top-tier end use markets [4]. Metallocene LLDPE films can be manufactured, bi-axially oriented (BOPP) or non-oriented (NOPP) [4]. BOPP films, with their high clarity, moisture barrier (low water vapour transmission rate, WVTR) and high stiffness, are widely used in tape and food packaging. NOPP films are used in the packaging of textile products, stationary products and food packaging [4]. The first commercially available (1991) metallocene catalysed ethylene polymers were positioned between traditional LLDPE plastics and elastomers. Generally, they were referred to as Plastomers, as they possessed many of the characteristics of both plastics and elastomers [19]. These novel materials are used in wire and cable coating, flooring and medical applications. Metallocene based resins offer improved

strength and toughness, enhanced optical and sealing properties, increased elasticity and cling performance. Flexible plastics based on metallocene polyolefins can also replace plasticised PVC in many applications without requiring the addition of environmentally damaging phthalate plasticisers [19]. Metallocene catalysed polymers may also be used in geo-membrane and rotational moulding applications [20].

### 1.3 Polyethylene Polymers

Polyethylene (PE) is a versatile polymeric material, having a major share of almost all areas of application of commodity plastics. The development and implementation of metallocene catalysts has greatly expanded the range of PE (see section 1.2) [1]. Metallocene catalysed LLDPE, is produced by the co-polymerisation of small amounts of  $\alpha$ -olefin such as 1-hexene and 1-octene [1,2]. The types of catalyst, manufacturing process, reaction conditions are the controlling factors for the molecular structure of the PE polymers [1]. The primary molecular parameters affecting the processing and ultimate properties of LLDPE are molecular weight distribution (MWD), molecular weight (MW), and chain branching [21-22].

#### 1.3.1 Molecular Structure

##### a. Molecular Weight Distribution

Polymerisation reactions lead to polymer heterogeneity in molecular weight, i.e. a polymer has a distribution of chain lengths, thus having different molecular weight. The molecular weight of a polymer is expressed as an average value with different averages being important, e.g.  $\bar{M}_w$ ,  $\bar{M}_n$ , and  $\bar{M}_z$  (see figure 1.2). The ratio of  $\bar{M}_w$  over  $\bar{M}_n$  describes the breadth of the MWD curve. For typical polymers, the  $\bar{M}_n$  lies close to the peak of the weight distribution curve with the next higher average molecular weight that can be measured experimentally is  $\bar{M}_w$ , see figure 1.2. Heavier molecules contribute more to  $\bar{M}_w$  than higher ones, thus  $\bar{M}_w$  is always greater than  $\bar{M}_n$ . The value of  $\bar{M}_w$  is therefore greatly influenced by the presence of high molecular weight species, whereas  $\bar{M}_n$  is affected by species at the low end of the MWD curve. It was shown that  $\bar{M}_w$  and the breadth of the MWD curve or polydispersity ( $\bar{M}_w/\bar{M}_n$ ) are highly significant in determining the end use of PE polymers [7]. In general, copolymerisation initiated by ordinary Ziegler-Natta catalysts gives rise to z-LLDPE with a wide co-monomer distribution and broad MWD curve,

whereas the homogeneous metallocene catalysts lead to m-LLDPE with a narrow molecular weight distribution curve and short chain branches (SCB), distribution [1]. The molecular weight averages and SCB distribution can be characterised using techniques such as gel permeation chromatography (GPC) and temperature rising elution fractionation (TREF), respectively [23]. The narrow molecular weight distribution curve of m-LLDPE, leads not only to good physical properties such as increased toughness, impact strength and less solvent extractables but also to poor melt processability [2,23,25].

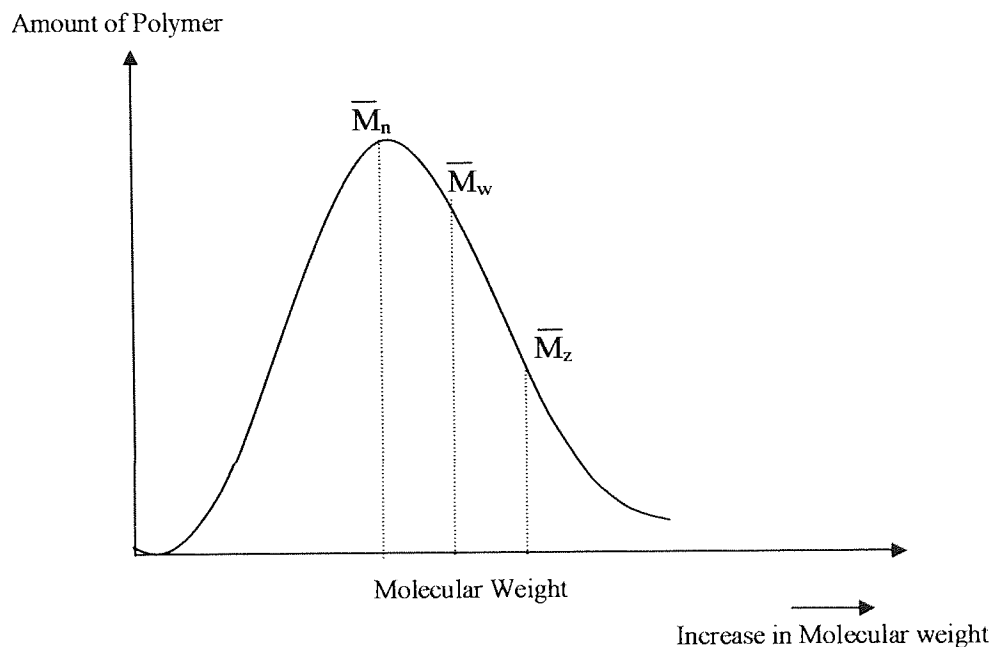


Figure 1.2 Typical distribution of Molar Mass of a Polymer [1a].

### b. Chain Branching

The controlled addition of an  $\alpha$ -olefin co-monomer, (e.g. 1-butene, 1-hexene, 1-octene) to ethylene during polymerisation produces a linear polymer with SCB. The type of  $\alpha$ -olefin added during polymerisation determines the length of the SCB [1,23]. The homogeneous nature of the metallocene catalyst provides even distribution of SCB in LLDPE (compared to non-uniform distribution in SCB exhibited by Ziegler-Natta catalysed LLDPE) (see figure 1.3) [23]. SCB controls mainly the morphology and solid-state properties of LLDPE, i.e. crystallinity and tensile strength [23].



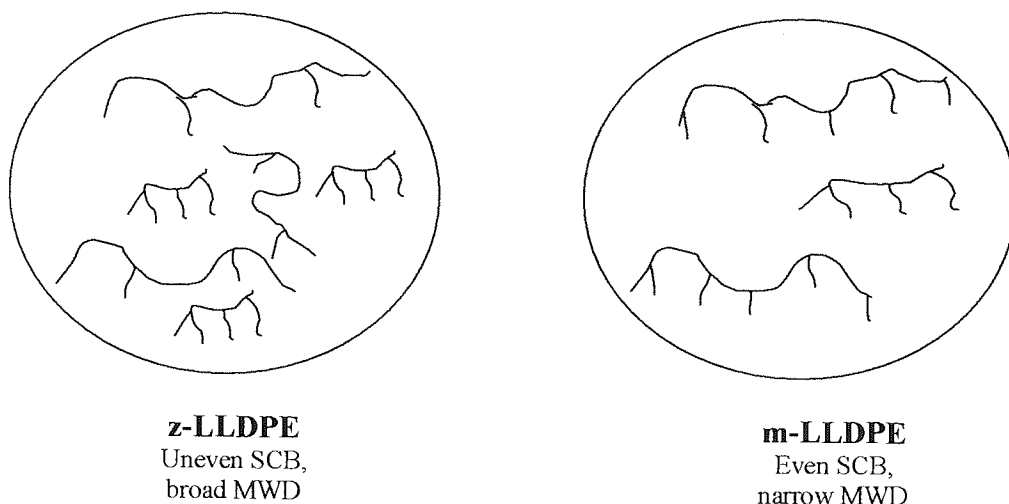


Figure 1.3 SCB and MWD; Schematic representation of molecular structure of Metallocene and Ziegler-Natta catalysed LLDPE.

### c. Crystallinity

The crystallisation of polymers is of enormous technological importance. Many thermoplastic polymers, i.e. LLDPE, will crystallise to some extent when the molten polymer is cooled below its melting point [11,16,23]. There are many factors, which can affect crystal morphology and crystallinity for a particular polymer, i.e. the amount and size of the co-monomer  $\alpha$ -olefin (chain branching), MWD and crystallisation conditions of the polymer [23].

The crystal morphology of LLDPE develops from lamellae formed from the ordering of folded chains [11,23]. The rate of folding is interrupted significantly by the presence of SCB, especially with high molecular weight  $\alpha$ -olefins (e.g. 1-hexene, 1-octene). The SCB (the co-polymer) cannot be incorporated into the crystal core and, is therefore, excluded from crystallising with the rest of the chain [23]. For this reason, a major part of the regular chain close to the short branch cannot be incorporated into the crystal core. This results in significant lowering of the overall crystallinity (thin lamellae) and the crystal size of the polymer. In m-LLDPE (with a narrow MWD and SCB distribution), crystallisation (growth and nucleation) proceeds at a similar rate throughout the polymer (as the chains are of similar size with even SCB along the main polymer backbone). On the other hand, in the heterogeneous z-LLDPE polymer, which has a broad MWD and co-monomer (SCB) distribution, crystallisation progresses steadily at two distinctly different rates [11,23]. A larger portion of SCB are found in the low molecular weight fraction of the

Ziegler-Natta catalysed polymer, thus nucleation and crystal growth continues at a much slower rate than in the higher molecular weight fraction (lower co-monomer content) [11]. This gives rise to a thicker lamella and explains the broader melting points associated with z-LLDPE [11].

### 1.3.2 Melt Rheology

The melt rheology during processing and ultimate properties of polyethylenes is also affected, primarily by molecular weight characteristics such as chain branching, MWD, and molecular weight. Several workers have studied the effect of these important characteristics on the melt processing of PE [22-26].

The effect of chain branching on the rheology of PE can be demonstrated by comparing the melt flow of high-density polyethylene (HDPE) a linear polymer, and low-density polyethylene (LDPE), a highly branched polymer. Extensional viscosity, essentially a tensile deformation is highly sensitive to molecular architecture, e.g. chain branching and MWD. HDPE and LDPE have similar shear flow behaviour, but differ significantly in the level of extensional stress flow [27,28]. This dramatic difference is related to molecular orientation during extensional flow (see figure 1.4). In the case of HDPE, polymer chains are forced to line up and slide smoothly past each other with decreasing resistance (no side branches) [29]. However, in the case of LDPE, the increase in molecular orientation causes an increase in entanglement of the side chain branches, which prevents the polymer chains sliding past each other [29]. Hence, the chain branch points act as 'hooks' to inhibit the flow ability during extensional flow. Therefore, the branched LDPE tends to increase its extensional viscosity with stress, causing tension stiffening whereas linear HDPE thins down under tension, hence shear thinning [28].

The effect of branching can vary with temperature, as viscosity is temperature dependent [29]. A linear polymer such as HDPE is less sensitive to temperature whilst branched LDPE has viscosity which is twice as sensitive to temperature. Moreover, the viscosity of branched LDPE is much more sensitive to mechanical history than that of HDPE [29].

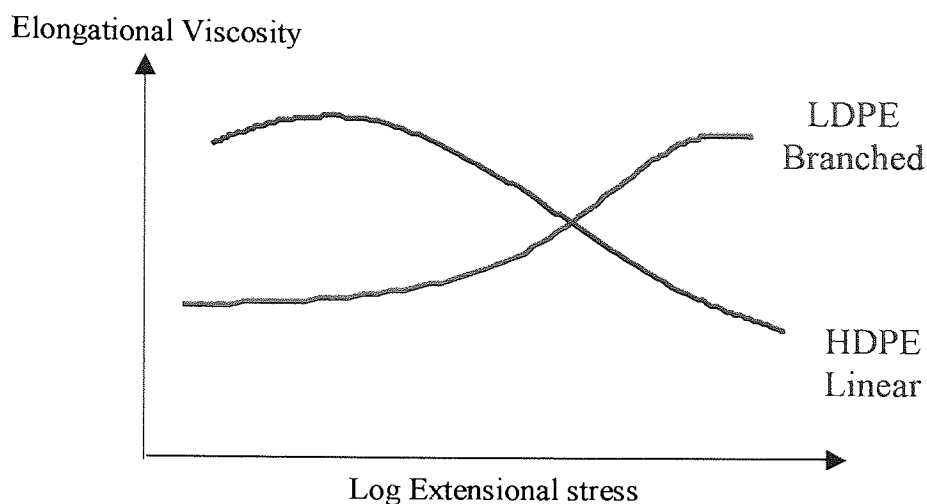


Figure 1.4: Extensional viscosity vs Extensional stress for LDPE and HDPE.

The poor melt flow exhibited by m-LLDPE, is related to the high degree of entanglement and uniform shear stresses incurred by the majority of m-LLDPE polymer chains (with evenly distributed SCB along the main backbone) during extrusion [28]. The narrow Mw and SCB distribution of m-LLDPE results in poor melt processability; low melt strength, high-extruded backpressure and high-energy power consumption during extrusion [28]. Whilst, the good melt flow exhibited by z-LLDPE during high temperature extrusion has been attributed to the low degree of entanglement between the high and low molecular weight chains [28]. The high molecular weight chains (containing a small fraction of SCB) suffer a disproportionately high degree of shear stress, and form a 'protective' network around the low molecular weight polymer chains [28,29]. The low molecular weight chains lubricate the flow of the higher molecular weight chains, thus enhancing the flow of polymer material during high temperature extrusion [28,29].

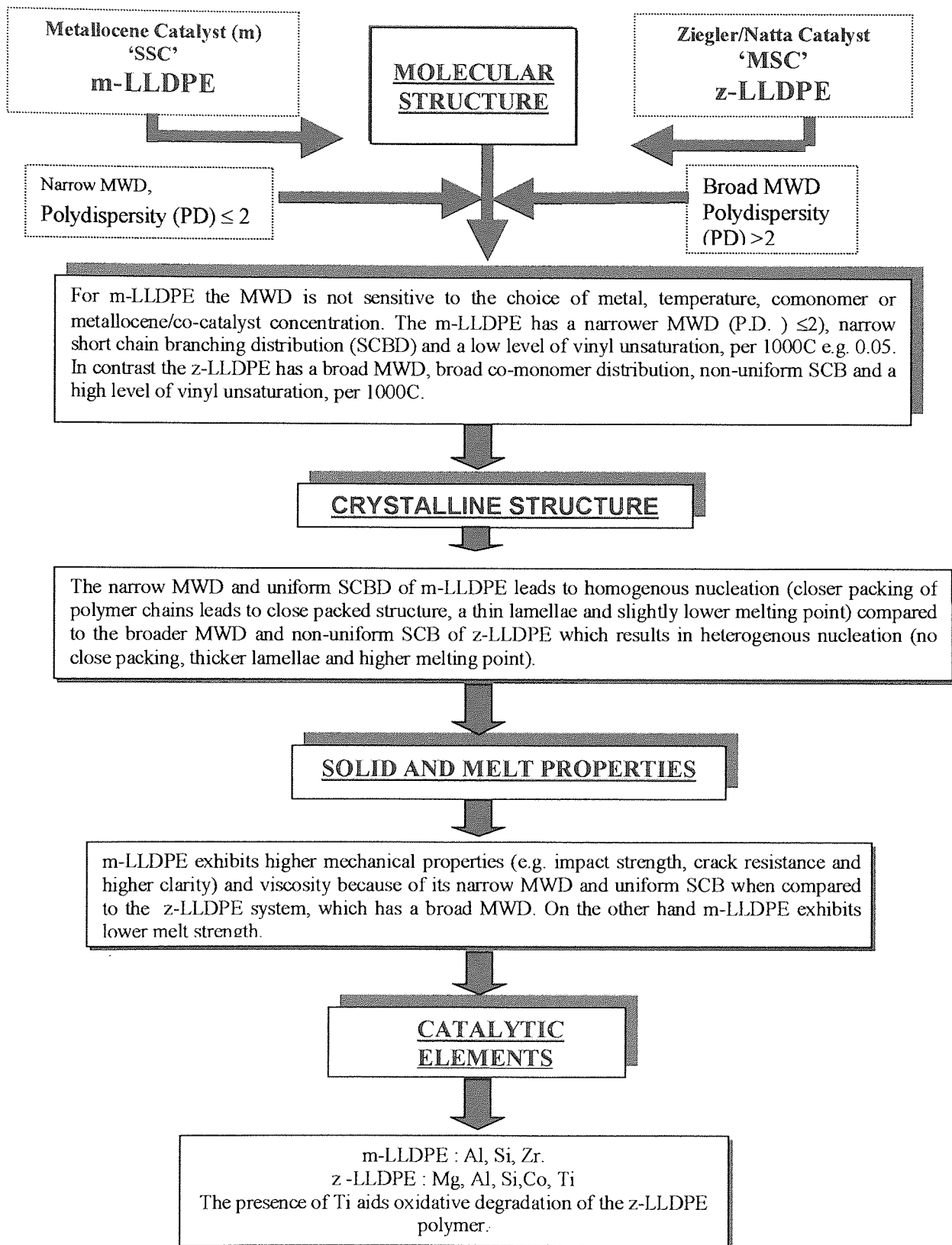
### 1.3.3 Physical Properties

Metallocene catalysed LLDPE exhibits far superior physical properties i.e. tensile strength, optical clarity, dart impact strength, crack resistance and lower melting properties, compared to the conventional Ziegler-Natta based LLDPE [5-6]. The high degree of control exerted by metallocene catalysts during polymerisation provide, opportunities to tailor make polymers to specific applications, i.e. film (blown and cast) and medical [4,19]. Film applications seek to maximise the exceptional physical, optical and heat-sealing attributes of m-LLDPE. Film

manufacturers have incorporated this unique set of properties into a variety of film making applications [4]. For instance, the narrow MWD and a uniform stereoregularity exhibited by metallocene catalysed BOPP and NOPP films are distinguished in general by their high tensile strength, stiffness, gloss and barrier along with good optical clarity [4]. Both tensile strength and stiffness are important properties in the conversion of films to final products. Improved stiffness offers the opportunity for down gauging, an industry demand, to reduce the cost and volume of packaging material. Improved barrier properties mean better flavour preservation and therefore longer shelf life of the final packaging goods [19]. Other segments of the BOPP film market where metallocene catalysed polymers show potential are shrink and heat-sealing film. In the shrink market, improved shrinkage performance, low heat sealing temperature and good hot tack properties accompanied by balanced BOPP physical properties are desired. In the heat-sealing market, easy sealability and high hot tack strength are desired [4,19].

Some of the key attributes of elastomers, derived from metallocene catalysis of ethylene and EPDM, which make them of interest as alternatives to plasticised polyvinylchloride (pPVC) are clarity (especially in thick sections), softness, low modulus, flexibility, superior low temperature toughness, and a low level of extractables (no extractable plasticisers) [19]. This culmination of properties have made elastomers ideal for medical applications e.g. intravenous tubes, caps (made *via* injection moulding), fittings and connectors to large articles such as face-masks. For many of these applications, clarity is essential. Elastomers with densities below about  $0.95\text{g/cm}^3$  are usually clear enough even in thick sections to meet the requirements for the product [19]. The true value of metallocene based PE is not derived from one characteristic but from a superior group of properties (see figure 1.5).

Figure 1.5. Representation of the mutual relationship among molecular structure, solid structure and properties of LLDPE produced by Metallocene and Ziegler-Natta catalysts [4,13].



## **1.4. Thermal – Oxidative Degradation of PE during processing.**

PE is one of the largest volume thermoplastic polymers yet structurally one of the simplest. Thus understanding and controlling degradation during melt processing has been the object of considerable effort in both industry and academia [30-36]. PE grades are differentiated on the basis of MW, MWD, density, co-monomer, co-monomer content and SCB [1,32]. This variation in PE composition produces wide variations in performance, including variations in susceptibility to degradation [32].

Manufacturing PE into useful products such as films, fibres, wire and cable coating require the use of high shear mixing machinery (e.g. extrusion, injection moulding, blow moulding, internal mixing) at elevated temperatures [30,32]. A combination of high shearing, processing temperatures and small residual concentrations of oxygen result in a number of considerable changes in the chemical and morphological structure of PE [30] which drastically affect its physical and mechanical performance 'in-service'.

PE degradation may occur at any stage from manufacture to final disposal but for most PE applications the stage where degradation occurs most rapidly is during melt processing which has a direct effect on the polymer performance under service conditions. Typical PE melt-processing operations consist of extrusion at 175-325°C [34] followed by shaping in a die. The extrudate is typically moulded, cast or blown and then cooled to solidify the plastic into the desired shape [34]. PE is a semi-crystalline polymer, thus contains domains of crystallinity and areas amorphous in nature. Oxidation has been shown in PE to occur only in the amorphous regions due to the impermeability of the crystalline phases to oxygen [35-37].

Degradation may be regarded as any type of modification of PE involving the main chain backbone and/or side groups [30]. The modifications are chemical in nature as it requires the breakdown of primary valence bonds which lead to undesirable reactions such as cross-linking (molecular enlargement), chain scission (lowering of molecular weight) and to the formation of detrimental oxygen containing functional groups (carbonyls, peroxides and unsaturation), which ultimately lead to changes in physical properties [30,32-33]. A change in molecular weight is



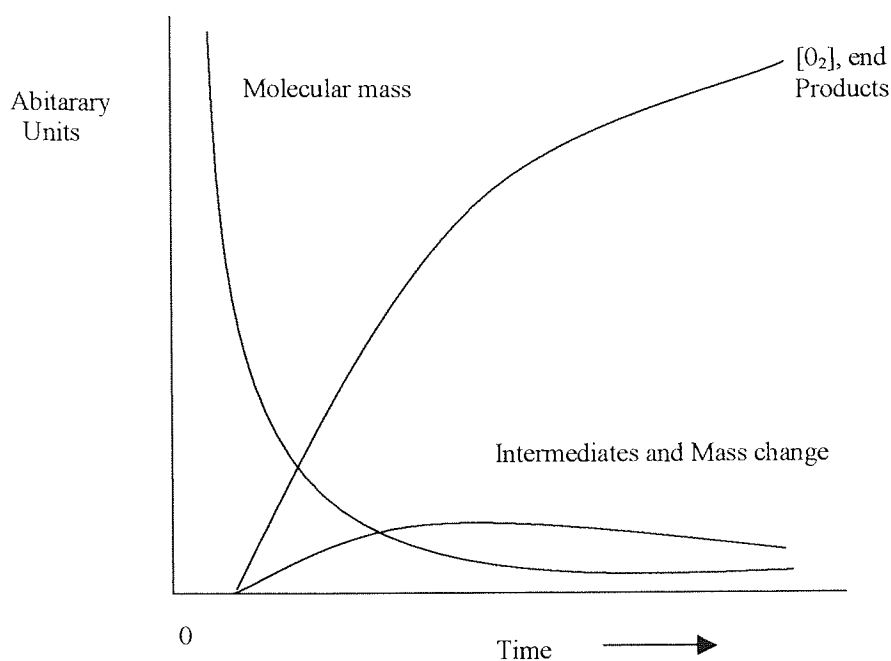


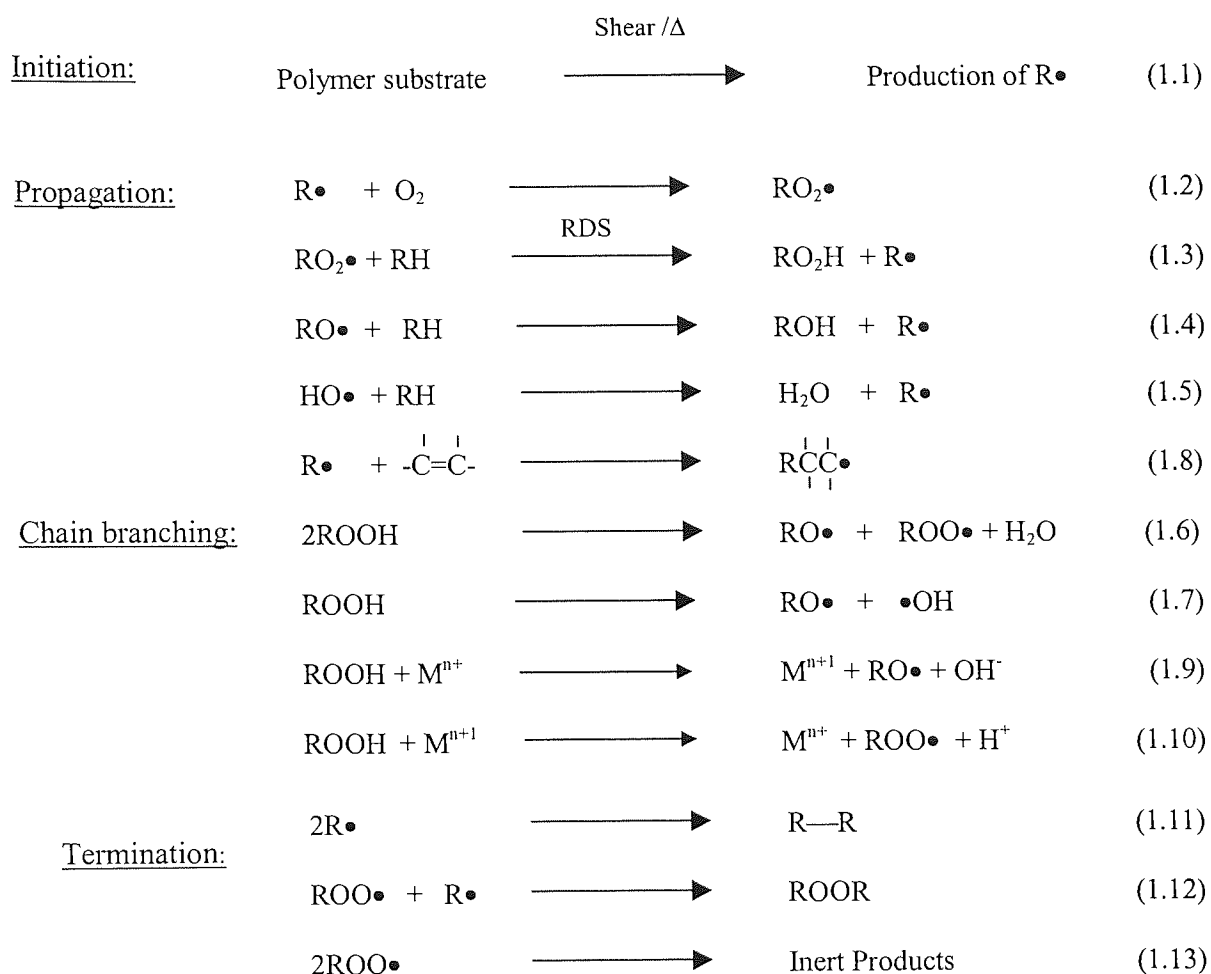
Fig 1.6. Autocatalytic curve: typical kinetic curves of molecular mass, oxygen uptake, mass change and formation of intermediates and products in the oxidation of PE [45].

**Initiation:** the nature of the primary initiation reaction of molecular oxygen with PE, which is responsible for the production of the first free radicals in the chain sequence is complicated and depends upon the nature of the polymer, the impurities (e.g. catalyst residues, reactions 1.9 and 1.10 in scheme 1.4), and the processing conditions (e.g. extent of shear stress, temperature and residual oxygen concentration) [32, 45].

**Propagation:** Alkyl radicals,  $R\bullet$ , which are formed in the initiation step, react immediately (with little or no activation energy) with small residual concentrations of oxygen available (a bi-radical) within the polymer matrix in a fast radical-radical coupling reaction to produce alkylperoxy radicals,  $ROO\bullet$ , (reaction 1.2 in scheme 1.4) [46]. At elevated temperatures during processing under oxygen deficient conditions not all the alkyl radicals,  $R\bullet$ , can be transformed to  $ROO\bullet$  radicals, thus the concentration of  $[R\bullet] > [ROO\bullet]$ . Under these oxygen deficient conditions, depending on the type of polymer and even the catalyst used to produce it, the alkyl radical may undergo many radical reactions [45, 46] (see scheme 1.4).

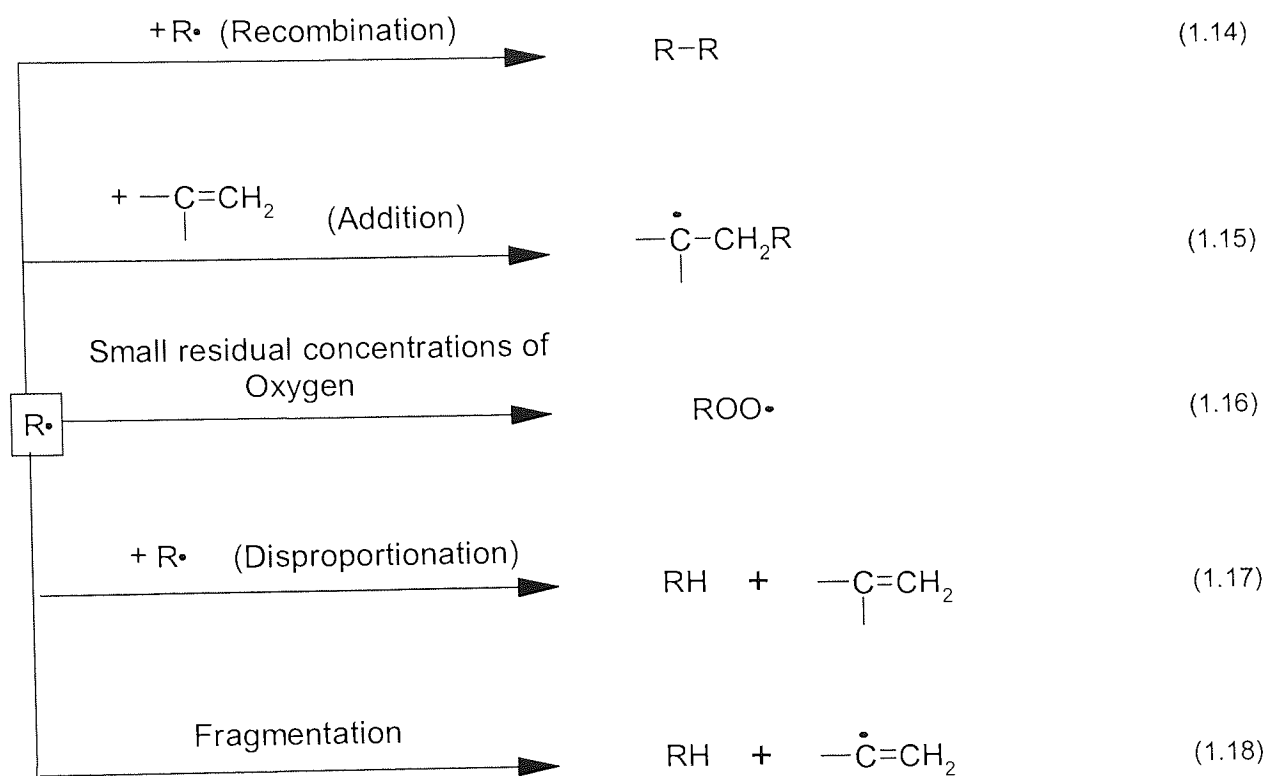


Scheme 1.4. Thermal Oxidation of hydrocarbon polymers, RH is the polymer [45].



Radical coupling (reaction 1.14, scheme 1.5) leads to cross-linking, an increase in the molecular weight, for PE under thermal oxidative melt processing conditions (below 250°C). However, alkyl radical coupling is recognised to be of minor importance compared to the addition reaction of alkyl radicals to olefinic unsaturated groups (reaction 1.15, scheme 1.5) [31,32]. The addition of radicals to a carbon double bond is energetically favoured by the formation of a  $\sigma$ -bond at the expense of a  $\pi$ -bond [32,45].

Scheme 1.5 highlights the reactions of the alkyl radical in oxygen deficient conditions.



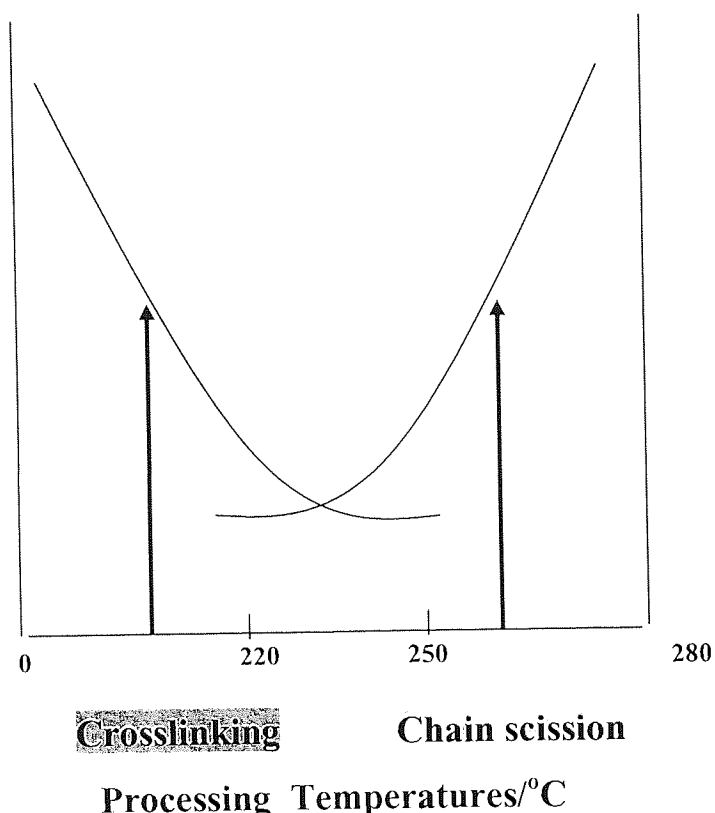
The distribution of unsaturated groups such as vinyls and vinylidenes is dependent on PE polymerisation conditions [30,32,45]. The addition of alkyl radicals to vinyl groups along the polymer backbone contributes to vinyl group disappearance and an increase in crosslinking (long chain branching formation) during melt processing [32]. An addition reaction of vinylidene groups with alkyl radicals does not appear to occur to the same extent as vinyl groups [32].

The primary mechanisms for chain scission which occur by  $\beta$ -cleavage of oxygen centred alkyperoxy radicals, include oxidative and thermal scissions. Oxidative scission is the dominant reaction at moderate temperatures under conditions of high oxygen pressures [32]. Thermal scission involves  $\beta$ -cleavage of secondary alkyl radicals thereby giving rise to vinyl groups ( $\text{CH}_2=\text{CH-R}$ ) whilst tertiary alkyl radicals give rise to vinylidene groups ( $\text{CH}_2=\text{CR}^1\text{-R}^2$ ). Thermal scission does not require high oxygen pressures, hence becoming increasingly important as processing temperatures increase (above 250°C) [32,45]. Many studies of PE degradation have shown the tendency for crosslinking to dominate at lower processing temperatures (< 250°C) and

chain scission to dominate at higher processing temperatures ( $> 250^{\circ}\text{C}$ ) in oxygen deficient conditions (figure 1.7) [32,47]. In oxygen excess conditions, chain scission is the dominant reaction (see figure 1.8).

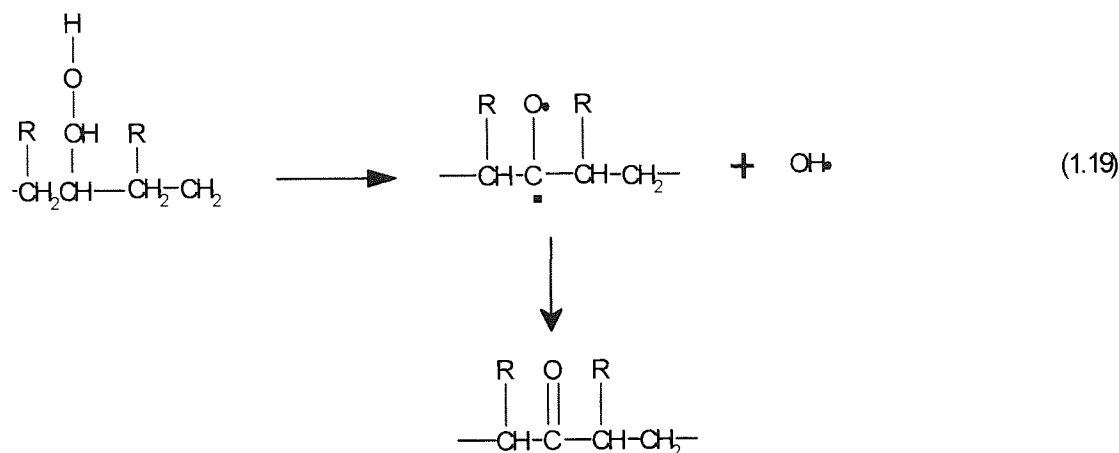
Figure 1.7. Competing reactions of cross-linking and chain scission of LDPE under varying processing conditions [48].

Melt Flow Index (MFI)/g.10min



The formation of hydroperoxides results from the alkylperoxy radicals reacting with the polymer backbone by hydrogen abstraction forming more alkyl radicals (reaction 1.3, scheme 1.4) [32,45]. This is the most important reaction in autoxidation and is the *rate-determining step* (RDS). Increasing the rate constant for this reaction increases the rate of oxidation and the hydroperoxide concentration, which results in the propagating chain reaction becoming longer [45,46]. At the elevated temperatures characteristic of PE melt processing, hydroperoxides rapidly cleave to form alkoxy and hydroxyl radicals (reaction 1.6, scheme 1.5), which in turn cleave rapidly to form more alkyl radicals. Hydroperoxide decomposition also leads to further radical reactions, which yields various degradation products containing carbonyl groups [45]. For example, highly

reactive hydroxyl radicals from the decomposition of hydroperoxide may abstract labile hydrogen at the tertiary carbon atom, forming a bi-radical that subsequently leads to carbonyl formation (see reaction 1.19).

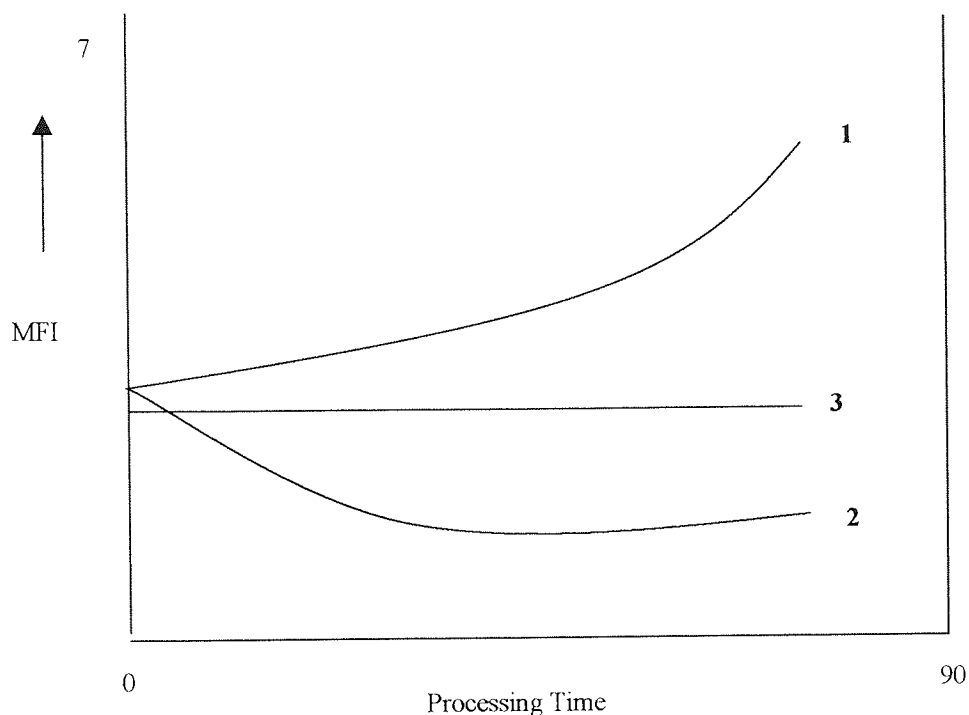


Thermal oxidation generally occurs in the accessible regions of PE and is initiated rapidly in branched PE systems due to the unhindered access to tertiary carbon atoms.

A technique which has been used to give a quick indication of the type of chemical change which occurs during PE processing is that of melt flow index (MFI). The MFI is defined as the mass (in grams) of the molten polymer extruded through a standard die in a given time (normally 10 minutes) and the measurement of the MFI of the polymer is inversely related to its molecular weight [34,48]. An increase in MFI is associated with chain scission whereas a decrease in MFI reflects crosslinking and an increase in molecular weight (see figure 1.8).

**Termination:** termination reactions can occur via alkyl radical coupling (reaction 1.11, scheme 1.4, leading to crosslinking of the polymer) and cross coupling of  $\text{R}\cdot$  with  $\text{ROO}\cdot$  (reaction 1.12, scheme 1.4) [32]. However, at very low oxygen pressures, alkyl radical termination reactions are prevalent [32].

Figure 1.8. The effect of processing at 150°C on the MFI of LDPE. (1) Open mixer, (2) Closed mixer (limited amount of air) and (3) In argon [48].

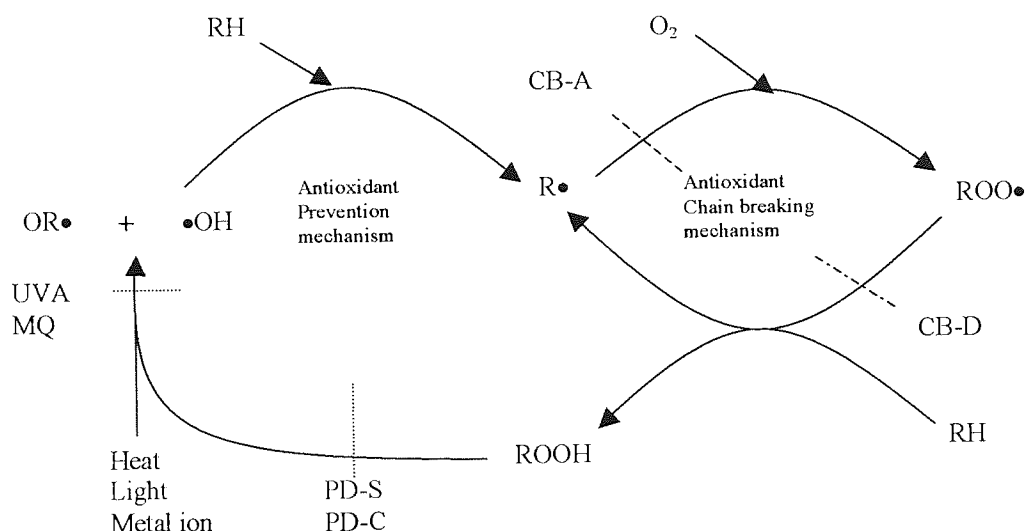


## 1.5 Stabilisation of PE Polymers during Processing and Stabilisation Mechanisms

### 1.5.1. General Mechanisms of Antioxidant Action.

The inhibition of thermal oxidative degradation of PE is a key issue for the plastics processing industry. The susceptibility of PE to oxidative degradation at high temperatures through the propagating alkyl ( $R\bullet$ ) and alkylperoxyl ( $ROO\bullet$ ) radicals and the hydroperoxides which decompose producing further radicals (see section 1.4) has led to the development of antioxidant 'technology'. Without the development of antioxidants, which interfere at specific stages of the auto-oxidative chain cycles, optimum physical property and desired performance after production and in end-use of PE articles would not have been possible. The inhibition of PE oxidation can be achieved by incorporating antioxidants into the polymer matrix before or during the processing stage. Antioxidants may be classified according to their mechanism of action as outlined in scheme 1.6 [49-53]. The primary cycle can be interrupted by antioxidants, which operates by a chain breaking mechanism (CB) by removing the main chain-propagating radicals  $R\bullet$  (CB-A)

and  $\text{ROO}\cdot$  (CB-D), examples include hindered phenols, lactones and aromatic amines. Preventive antioxidants, on the other hand, act by preventing the introduction of the chain-initiating radicals into the polymer system in the secondary cycle [49-53]. The most important preventive mechanism, both theoretically and practically is hydroperoxide decomposition by peroxidolytic antioxidants (PD), which act by producing non-radical products from the decomposition of hydroperoxide. Examples of PD antioxidants are phosphite and sulphur containing compounds.



Scheme 1.6: Oxidative degradation processes and antioxidant mechanism. CB-A, Chain breaking acceptor mechanism; CB-D, Chain breaking donor mechanism; PD, peroxide decomposer mechanism (stoichiometric or catalytic).

### 1.5.2 Criteria for the selection of Antioxidants

The commercial success of antioxidants depends not only on their inherent chemical effectiveness and physical persistence in the polymer but also on their toxicological behaviour and cost considerations. Under aggressive service conditions, the performance of an antioxidant can be dominated by its physical characteristics [37, 51]. Stringent regulations exist, in most countries, on the use of antioxidants in applications involving the human environment, e.g. food packaging.

The physical loss of antioxidants into the contact media i.e. leaching, not only has severe toxicological consequences but also presents risks associated with the premature failure of the polymer product [51]. The effectiveness of antioxidants is a product of a complex relationship

between all the chemical and physical factors; chemical structure of the antioxidant, thermal stability of both the parent antioxidant and of its transformation products, and their physical behaviour e.g. solubility and their interactions with the polymer substrate with due account to chemical and morphological features [51].

#### **a. Chemical effects**

The intrinsic chemical activity of antioxidants is a function of their molecular structure. However, use of the chemical activity alone as an indicator can lead to unreliable predictions of the efficiency of antioxidants in polymers under practical conditions owing to the dominating influence of physical factors under certain conditions [51]. For example, the hindered phenol BHT is amongst the most efficient antioxidants known for liquid hydrocarbons but is ineffective in protecting thermoplastic polymers because of its rapid depletion through volatilisation from the polymer [51].

##### **(i). Effect of transformation products.**

It is known that many antioxidants are converted to higher molecular weight transformation products during their function as antioxidants [50,51,54]. In the case of aromatic amines, intensely coloured poly-conjugated products of high molecular weight and low volatility are produced [51]. Many of these transformation products are themselves antioxidants that contribute to the high efficiency of aromatic amines as heat stabilisers for polymers. However, most are also very highly coloured and result in discolouration of polymers, hence, aromatic amines are not used in polyolefins. Similarly, hindered phenols subjected to high temperature conditions result in transformations to poly-phenols and derived quinones, which are themselves effective antioxidants [50,51]. Antioxidants that deactivate hydroperoxides such as alkyl phosphites have generally poor hydrolytic stability [55]. The hydrolysis of phosphorous stabilisers in polyolefins leads to a loss in effectiveness as a processing stabiliser and presents difficulties in handling the additive. The loss of an effective phosphite processing stabiliser is not cost effective.

#### **b. Physical effects**

The physical behaviour of antioxidants is a major factor affecting their durability, efficiency and acceptability. Physical factors, which control the effectiveness and permanence of antioxidants, include distribution, solubility, diffusivity, volatility and leachability [37, 50-51].

### **(i) Distribution of Antioxidants and Polymer Morphology**

To inhibit the oxidation of polymers, antioxidants have to be present in sufficient concentrations at the various oxidation sites. Thus, both the distribution of antioxidants and the morphology of the host polymer are important. For example, the distribution and concentration of photo-antioxidants in some polyolefins has been shown to be mainly present in the amorphous region, (on the boundaries of the spherulites), which is most susceptible to oxidation (the crystalline phase is normally impermeable to oxygen) [50]. However, in the case of polymer blends, a non-uniform distribution of antioxidants can undermine the overall stability of the blend, especially if it does not occur in favour of the more oxidisable component of the blend.

### **(ii) Compatibility of Antioxidants with Polymers.**

Antioxidants are generally less soluble in polymers than in lower molar mass liquid models. Although antioxidants are usually highly soluble at the elevated processing temperatures (present in the polymer as homogenous solution), they come out of solution on cooling and the solid polymer becomes supersaturated with the antioxidant. In turn, the antioxidant may precipitate as a separate phase, and exude to the polymer surface (this is called blooming) leading to a build up of a concentration gradient near the surface forcing further migration of antioxidant from the bulk [50,51]. Consequently, an antioxidant with low solubility and diffusion rate is prone to blooming and to loss to the surrounding medium by evaporation or through leaching leaving behind an unprotected polymer surface. The compatibility of antioxidants in polymers is improved when the antioxidant and the host polymer have similar characteristics. Compatibility of antioxidants in non-polar hydrocarbon polymers therefore decreases with increasing antioxidant polarity and increases with the number, length, and branching of the inert alkyl substituents attached to the antioxidant function [50].

### **(iii) Antioxidant Diffusion, Volatility and Leachability by Contact Media**

The permanency of antioxidants is affected by diffusion characteristics of the antioxidant and polymer, and the external physical conditions i.e. temperature. Generally, the diffusion coefficient of antioxidants decreases with increasing polar interactions with the polymer, increasing molar mass of antioxidants and branching in their alkyl side chain [50,51]. An increase in molar mass results in an increase in intermolecular dispersion forces, which brings about a decrease in volatility of the antioxidants from the polymers.



### c. Cost-effectiveness of stabiliser packages.

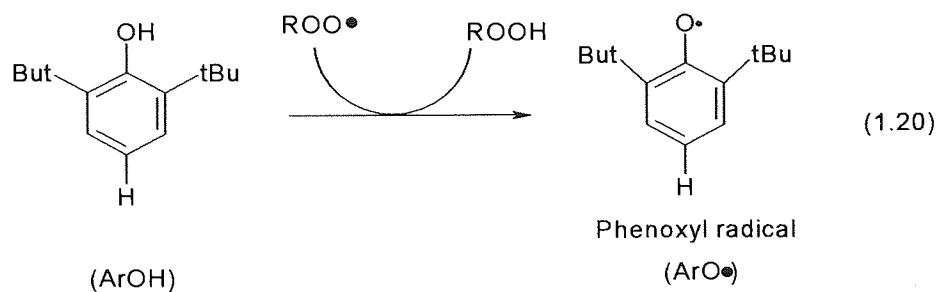
Effective stabilising packages, for readily oxidisable polymers such as polyolefins, may contain several expensive antioxidants, acting by different mechanisms. It is increasingly important in modern polymer-additive technology to develop cost effective multi-component stabiliser packages. Hence the cost, an important consideration, must also be taken into account when developing effective stabiliser systems.

### 1.5.3. Hindered Phenols

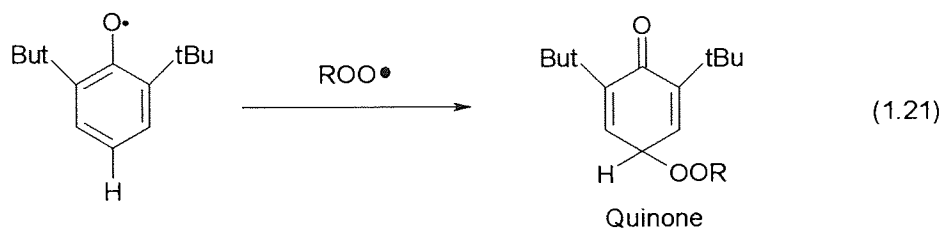
The CB-D mechanism operates under ambient oxygen pressures, where large concentrations of alkylperoxyl radicals,  $\text{ROO}\bullet$ , are present [50-52]. Antioxidants that operate *via* a CB-D action reduce alkylperoxyl radicals,  $\text{ROO}\bullet$ , to hydroperoxides, (ROOH) and alkoxy radicals,  $\text{RO}\bullet$  to alcohols (ROH). A large number of antioxidants, which act by this mechanism, have been studied and the most important are the hindered phenols synthetic and biological, such as Octadecyl-3,5-di-tert-4hydroxy hydrocinnamate, (Irganox 1076), and 6-hydroxy-2,5-dimethyl-2-phytyl-7,8-benzochroman, (Irganox E201) respectively (see in table 2.2, chapter 2) [50-52,56]. Transformation products formed from hindered phenols have been shown to have a great influence on the stabilising function of the antioxidants [49]. With either, an overall antioxidant or prooxidant effect [49]. Hindered phenols such as Irganox 1076 and Irganox E201 are good melt stabilisers for PE whereby quite low concentrations give effective stabilisation [53,56].

#### a. Synthetic Hindered Phenols

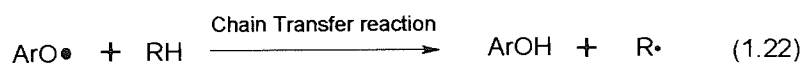
Synthetic hindered phenols are an important class of CB-D antioxidants for polyolefins due to their effective processing and long-term heat stabilising action. The first antioxidant step of all synthetic hindered phenols is to trap alkylperoxyl radicals,  $\text{ROO}\bullet$ , forming phenoxyl radicals (see reaction 1.20).



The phenoxyl radical formed is able to react with an additional  $\text{ROO}\cdot$ , to form a quinonoid based structure (see reaction 1.21) [57].



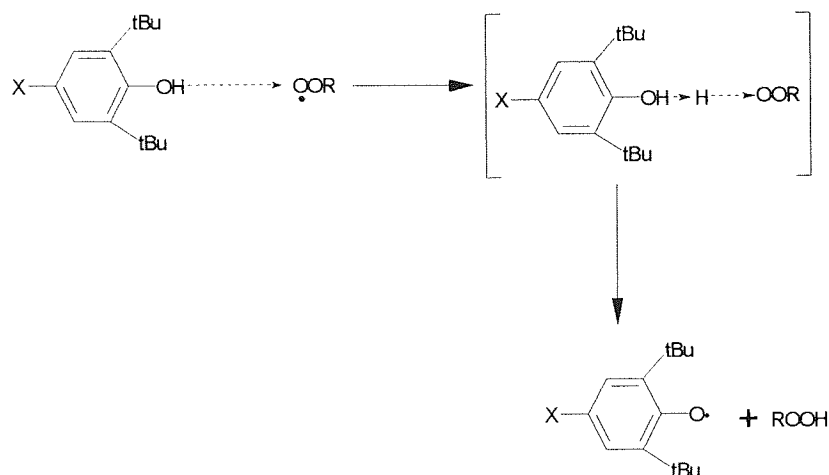
However, the formed phenoxyl radical can also undergo a chain transfer reaction thereby producing further propagating radicals (see reaction 1.22).



The main stabilising action of synthetic phenolic antioxidants (as radical scavengers) is strongly dependent on their structure, their ability to form stable phenoxyl radicals and the nature of their transformation products [52, 57]. In general, the transition state for the formation of a stable phenoxyl radical involves both electron delocalisation and charge separation (see scheme 1.7) [58]. Consequently, groups in the 2, 4 and 6 positions that extend the delocalisation of the unpaired electron (e.g. phenyl or methyl) increase activity. In the para position, electron-releasing groups (e.g.  $\text{R}_2\text{N}$ ,  $\text{RNH}$ ,  $\text{RO}$ ,  $\text{R}$ ) decrease the energy of the transition state and consequently increase antioxidant activity, whereas electron-attracting groups (e.g.  $\text{CN}$ ,  $\text{COOH}$ ,  $\text{NO}_2$ ) decrease activity [57-59]. The presence of at least one tertiary alkyl group in the ortho position is necessary for antioxidant activity. This steric enhancement is due to the increased stability of the derived phenoxyl radical, which reduces the chain transfer reaction.

One of the most widely used and studied synthetic hindered phenols is BHT, this is a highly volatile antioxidant, and is therefore very susceptible to physical loss [51]. To overcome, this problem a variety of higher molecular weight hindered phenols have been developed commercially such as Irganox 1076 and Irganox 1010 (see in table 2.1) [59].

Scheme 1.7. Transition state in the formation of phenoxyl radicals.



The main chemistry of the transformation products of synthetic phenolic antioxidants starts with the formation of stable phenoxyl radicals ( $\text{ArO}\bullet$ ) [58-60]. The nature of further reactions of the phenoxyl radical is complicated and depends upon the structure of the parent-hindered phenol, but in all cases, it has been shown to go through various quinoid type structures [58-60]. In the case of Irganox 1076, it has been shown that the free radical reaction of the Irganox 1076 phenoxyl radical (in its mesomeric cyclohexadienonyl or rearranged hydroxybenzyl form) with  $\text{ROO}\bullet$  radical leads to aryloxy cyclohexadienone (reaction 1.23, scheme 1.8) [58]. Bimolecular disproportionation of the stable phenoxyl radical leads to the initial formation of a quinone methide (QM), which has CB-A chain breaking activity properties (reaction 1.25, scheme 1.8) [58,61-62]. Quinone methides are generally unstable and disproportionates to give mixtures of highly conjugated systems [59]. Molecular rearrangement and dimerisation of QM leads to the formation of products such as cinnamate (C) (reaction 1.26, scheme 1.8) and *bis*-cinnamate (BC) (reaction 1.27, scheme 1.8) which themselves have been shown to have a chain-breaking activity [58-60]. The high efficiency of systems containing a 4-hydroxyphenyl propionate moiety (e.g. Irganox 1076 and Irganox 1010 in table 1.1) has been attributed to this initial formation of quinone methide (QM) [58]. The main drawback in using hindered phenol antioxidants stems from the formation of highly conjugated quinoidal-conversion based structures (e.g. D and E), which lead to severe discolouration of the polymer [58]. This discolouration may be reduced by using the hindered phenols in combination with phosphite (see section 1.5.7). A number of

transformation products of Irganox 1076 and Irganox 1010 are formed during processing and thermal ageing of PP and PE and have been characterised, e.g. Irganox 1076, cinnamate-1076 and *bis*-cinnamate-1076 (see in section 1.10) [64-65].

### b. Biological Hindered Phenol.

Vitamin E, a well known biological antioxidant in living systems [66,67], is a mixture of closely related tocopherols, which differ from one another only in the number and positions of the methyl groups in the aromatic ring (see figure 1.9), and it is mainly found in vegetable oil [66]. In living systems, vitamin E, present in cell membranes, protects polyunsaturated lipids and fatty acids from the damaging effects of peroxidation.

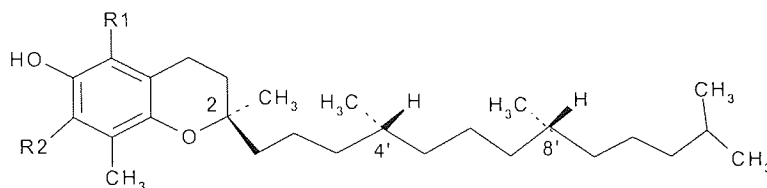


Figure.1.9. Stereochemical structures of natural Vitamin E.

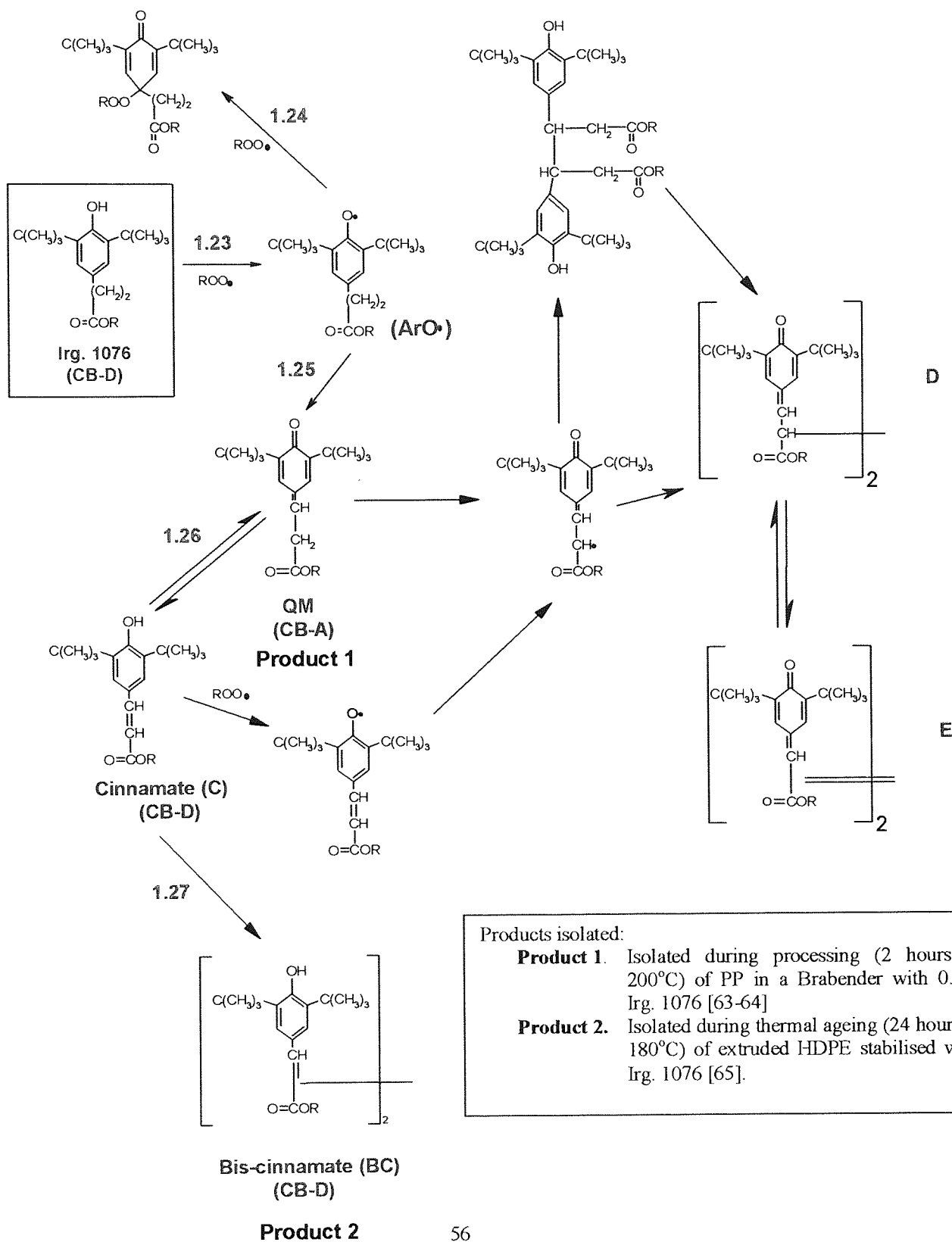
The biological activity of  $\alpha$ -tocopherol is known to be the highest. The four stereochemical diastomeric enantiomers structures of natural Vitamin E are:-

1. *R,R,R* - $\alpha$ -tocopherol: with  $R_1 = \text{CH}_3$ ,  $R_2 = \text{CH}_3$
2. *R,R,R*- $\beta$ - tocopherol: with  $R_1 = \text{CH}_3$ ,  $R_2 = \text{H}$
3. *R,R,R*- $\gamma$ -tocopherol: with  $R_1 = \text{H}$ ,  $R_2 = \text{CH}_3$
4. *R,R,R*-  $\delta$ -tocopherol: with  $R_1 = \text{H}$ ,  $R_2 = \text{H}$

On the other hand, synthetic Vitamin E, also called all-rac- $\alpha$ -tocopherol or dl- $\alpha$ -tocopherol, exists as a mixture of equal amounts of all eight possible optical isomers of  $\alpha$ -tocopherol [56]. The synthesis is based on the acid-catalysed condensation of 2,3,6-trimethyl-hydroquinone with all-rec-isophytol [68]. The isomers are four pairs of diastomeric enantiomers with the following structures:

- 1) *2R, 4'R, 8'R*- and *2S, 4'S, 8'S*- $\alpha$ -tocopherol
- 2) *2R, 4'R, 8'S*- and *2S, 4'S, 8'R*- $\alpha$ -tocopherol
- 3) *2R, 4'S, 8'R*- and *2S, 4'R, 8'S*- $\alpha$ -tocopherol
- 4) *2R, 4'S, 8'R*- and *2S, 4'R, 8'S*- $\alpha$ -tocopherol

Scheme 1.8: Mechanism of oxidation of propionate-type phenolic antioxidants with peroxy radicals [58].



In living systems, lipid peroxidation is a phenomenon of liquid phase oxidation, which involves the same elementary reaction steps as hydrocarbon oxidation, i.e. initiation, propagation and termination [66,70]. The initial free radicals are produced from a precursor molecule, e.g. a metal ion catalysed decomposition of a lipid hydroperoxide [66]. Rate constants, of antioxidant activity for  $\alpha$ -tocopherol has shown [66,70] to be a far better alkylperoxyl radical,  $\text{ROO}\bullet$ , scavenger, (producing a stable tocopheroxyl radical) compared to many commercial antioxidants, e.g. BHT (see figure 1.10).

On the basis, of X-ray structural determinations carried out on the  $\alpha$ -tocopherol model, 2,2,5,7,8-pentamethyl-6-chromanol, the high reactivity of  $\alpha$ -tocopherol for trapping peroxyl radicals was attributed to stereo-electronic effects [71-73]. The heterocyclic ring ensures that the 2p-type lone pair of electrons on the ring oxygen adopts an orientation more or less perpendicular to the plane of the aromatic ring, stabilising the tocopheroxyl radical (see figure 1.10A).

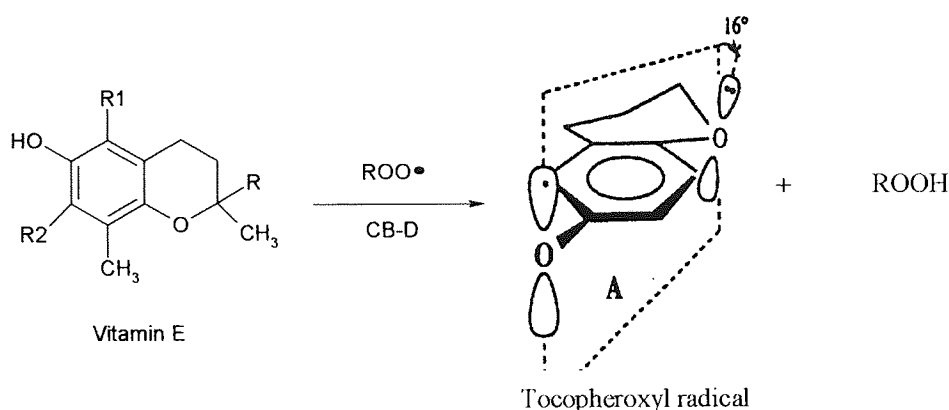


Figure 1.10. CB-D Antioxidant activity of  $\alpha$ -tocopherol

This effect is enhanced with the five membered ring in 2, 3-dihydro-2, 2, 4, 6-pentamethylbenzofuran where the nearly flat ring provides better overlap of the ring oxygen p orbital with the aromatic system [56]. X-ray analysis has shown that the deviation from perfect co-planarity in the phenoxyl was only  $6^\circ$  as opposed to  $16^\circ$  in the  $\alpha$ -tocopherol model.

Furthermore, vitamin K<sub>1</sub> chromanol, 6-hydroxy-2,5-dimethyl-2-phytyl-7,8-benzochroman (see figure 1.10 for structure), was found to be 4 times more active than  $\alpha$ -tocopherol [56]. It was suggested that the fused aromatic ring further delocalises the unpaired electron of the aryloxy

radical and hence raises the antioxidant activity. Finally the antioxidant activity of the five membered analogous  $\alpha$ -tocopherol derivative with a fused aromatic ring, 2,3-dihydro-5-hydroxy-2,4-dimethyl-2-phytylnaphthol [1,2-*b*] furan (see figure 1.11 for structure), was found to be 2.5 times better than the vitamin K<sub>1</sub> chromanol and 10 times better than  $\alpha$ -tocopherol [66].

The higher reactivity of  $\alpha$ -tocopherol compared to  $\beta$ ,  $\gamma$ ,  $\delta$ -tocopherol was attributed to the aromatic *o*-methyl groups, which stabilise the phenoxyl radical [66]. The antioxidant activity was found to decrease in the order  $\alpha$ -> $\beta$ ->  $\gamma$ -> $\delta$ -tocopherol. The antioxidant role of  $\alpha$ -tocopherol (vitamin E) in low-density polyethylene (LDPE) and the nature of its transformation products formed during extrusion of the polymer have been investigated recently [56, 74-76].

The melt stabilising effectiveness of  $\alpha$ -tocopherol has been reported [61,77] to be very high, in fact higher than that of the commercial hindered phenol antioxidants, Irganox 1076 and 1010 [56,74], after single and multiple extrusion at a particularly low concentration (lower than those of the commercial synthetic hindered phenols) [56].

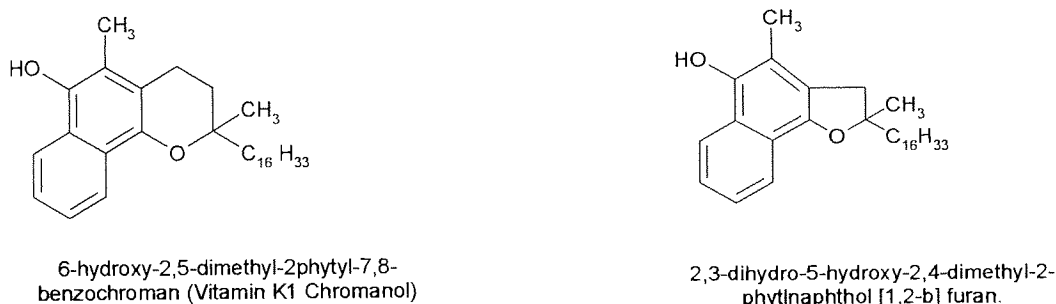
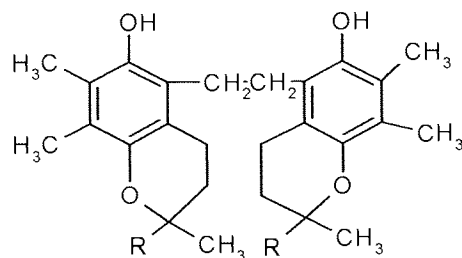


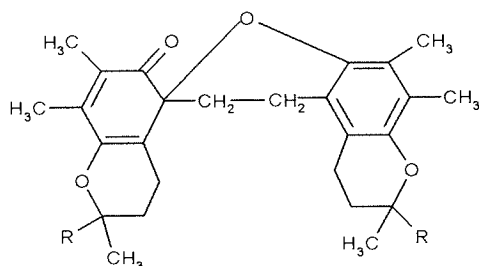
Figure 1.11: Chemical structures of analogous  $\alpha$ -tocopherol derivative antioxidants.

Vitamin E therefore, can be used cost effectively at only a quarter of the concentration typically required for the stabilisation of polyolefins by commercial synthetic hindered phenols, such as Irganox 1010 [56,74]. Unlike the commercial hindered phenols, synthetic Vitamin E can be considered a safe and non-toxic stabiliser and is therefore ideally suitable for use in food packaging plastics [56]. The high antioxidant activity of  $\alpha$ -tocopherol as a melt stabiliser is due in part to its transformation products [56]. These highly coloured transformation products are generally reported to be dimeric, trimeric and aldehydic in nature [56,74-76] (see figure 1.12). The synergistic use of polyhydric alcohols, i.e. Trimethylolpropane (TMP), and phosphites i.e.

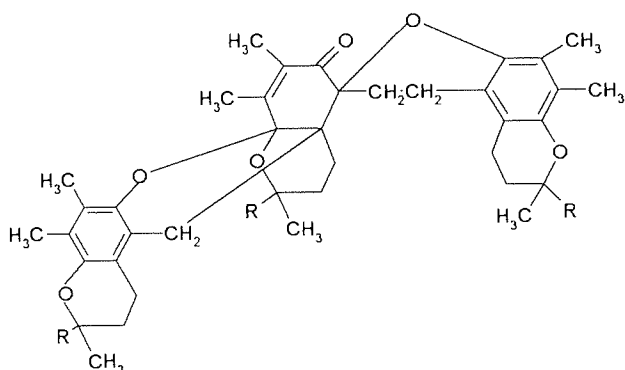
*tris*-(2,4-di-*t*-butylphenyl) pentaerythrityl diphosphite with  $\alpha$ -tocopherol enhances the colour stability of a polymer [56,74-76].



**Dihydroxydimer**



**Spirodimer**



**Trimer**

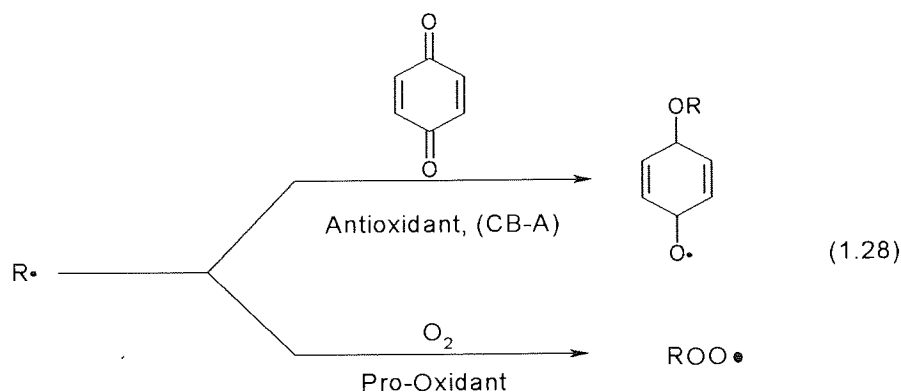
Figure 1.12. Some of the Transformation products formed from  $\alpha$ -tocopherol during extrusion experiments of LDPE [56].

#### 1.5.4. Lactones

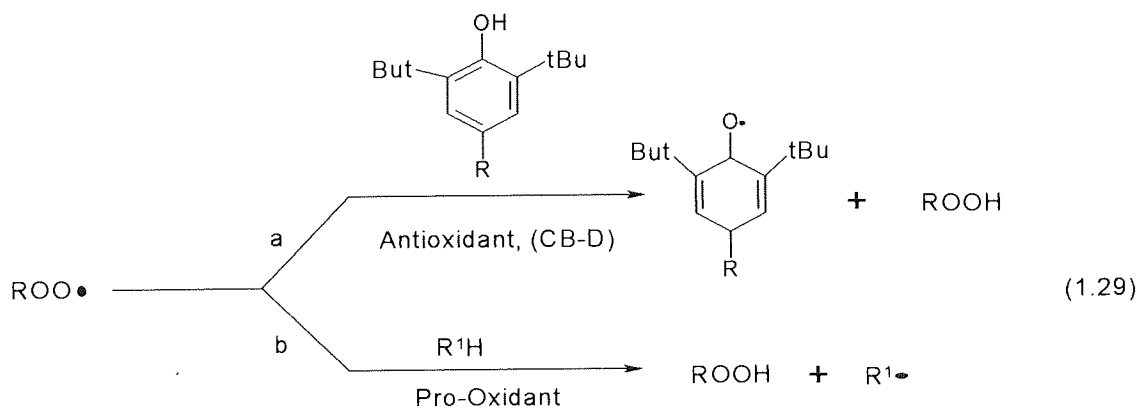
The CB-A mechanism operates under oxygen deficient conditions where alkyl radical concentration,  $R\bullet$ , is high in the polymer substrate [77]. CB-A antioxidants are therefore in direct



competition with residual oxygen (present in the polymer), in reaction with the polymer substrate radical. Examples of CB-A antioxidants include the quinones (see reaction 1.28) and stable radicals such as nitroxyls [61,65].



The CB-D mechanism, on the other hand operates under ambient oxygen pressures (under atmospheric conditions), where high concentrations of alkylperoxyl radicals,  $\text{ROO}\cdot$ , are present (see reaction 1.29a) [61,65].



Therefore, antioxidants that can operate by both complementary mechanisms (i.e. CB-D and CB-A) are effective in inhibiting oxidation under conditions where both alkyl,  $\text{R}\cdot$ , and alkyl peroxy,  $\text{ROO}\cdot$ , radicals are present in the system [57,61,65]. The lactone, 3-arylbenzofuran-2-one, (Irganox HP 136) is a particularly effective chain breaking complementary antioxidant [78-80], operating effectively mainly as an alkyl radical trap,  $\text{R}\cdot$  (CB-A) (see figure 1.13) [78-80]. Irganox HP136 may also function as an alkylperoxyl,  $\text{ROO}\cdot$  (CB-D) radical scavenger (see figure 1.14) [78-80]. It has been shown that the lactone [78] is a very effective melt stabiliser at high

processing temperatures (up to 340°C) in polyolefins, especially when used synergistically (known as an XP system) in combination with synthetic hindered phenol and phosphite antioxidants [78,81]. In the combination, the synthetic hindered phenolic antioxidants function mainly as scavengers of alkylperoxyl radicals, ROO•, and, contributes to the long-term thermal stability of the polymer [60], whereas the phosphite functions as a hydroperoxide decomposer providing processing stability and colour control (see section 1.5.6).

It has been proposed that the high antioxidant activity of Irganox HP 136 is due to the formation of a highly stabilised benzofuranonyl radical **1** by the facile donation of the weakly bonded benzylic hydrogen atom to an alkyl radical, R• (see figure 1.13) [78-80].

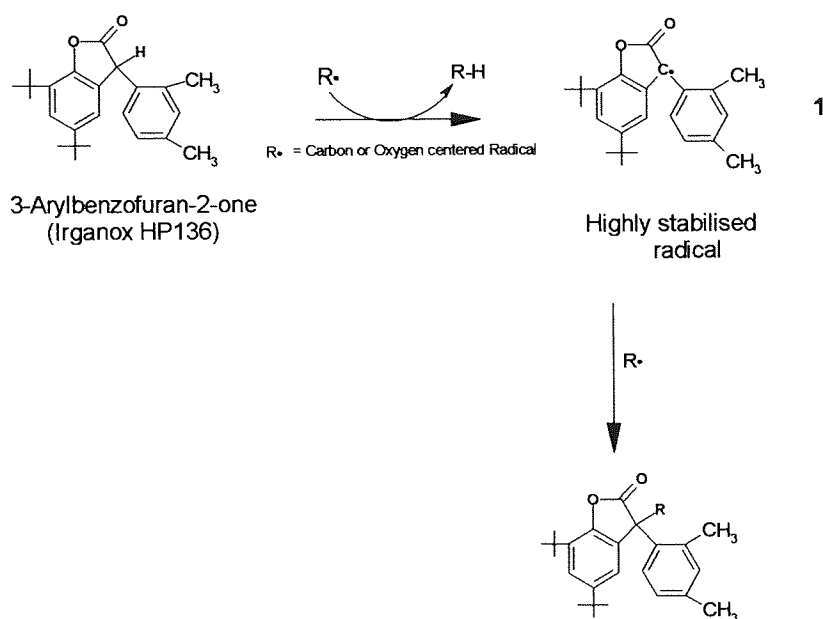


Figure 1.13. Stabilisation mechanism of Arylbenzofuranone (Lactone HP-136) [78].

Model experiments have indicated that the arylbenzofuranone is a highly effective hydrogen atom donor (see figure reactions a, b and c in figure 1.14) [78].

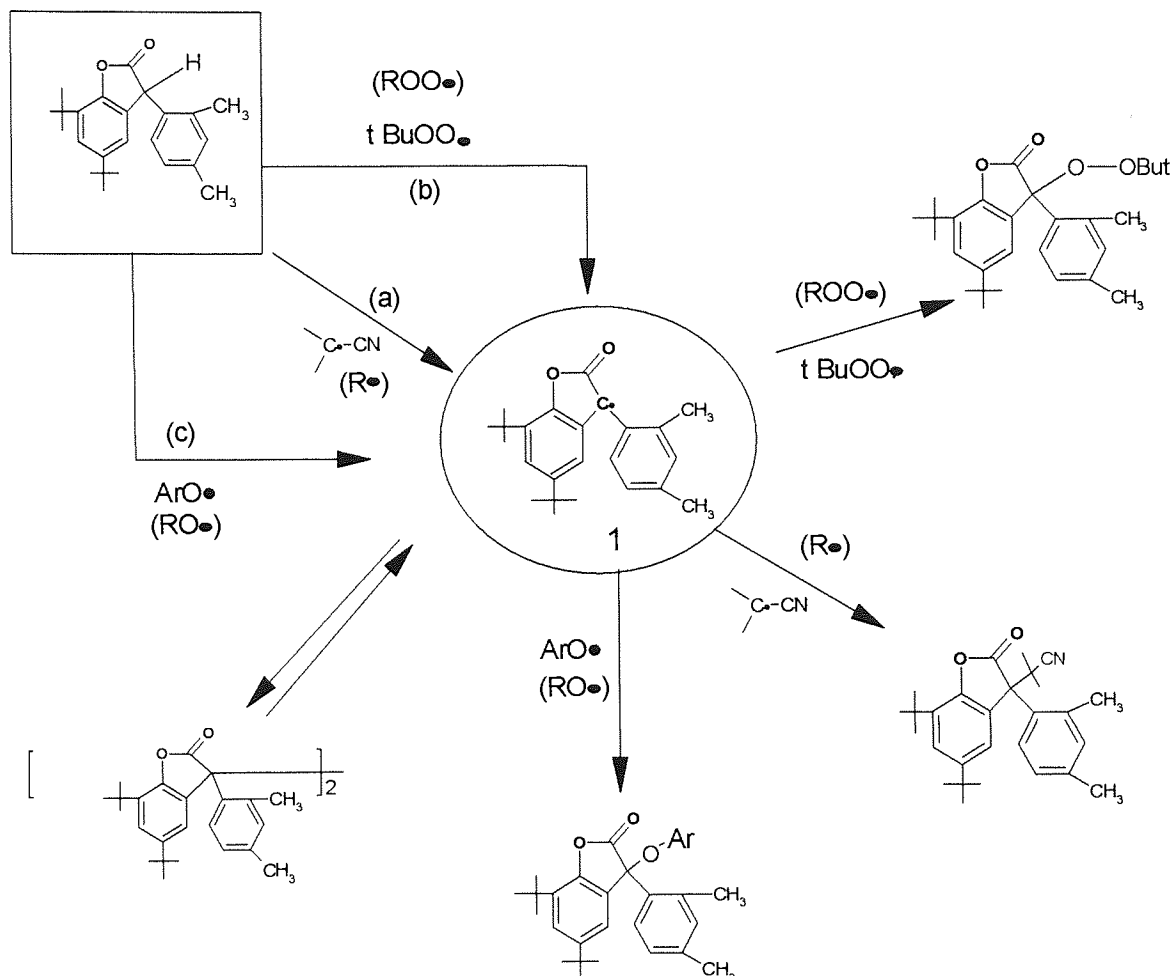
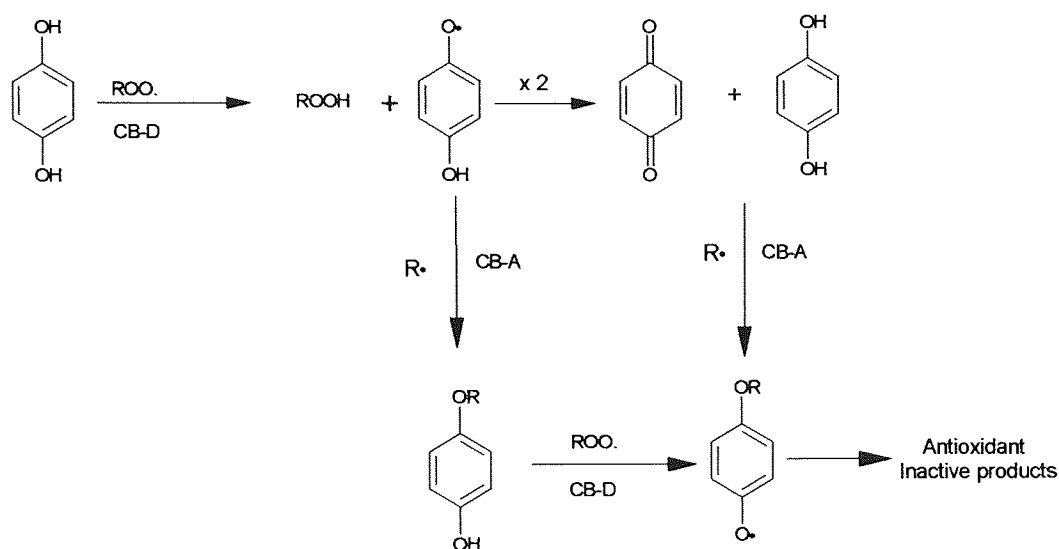


Figure 1.14. Model trapping reactions with Arylbenzofuranone (Lactone) [78].

It has also been proposed [78] that the donation of an hydrogen atom from the benzofuranonyl radical 1 to sterically hindered phenoxyls (generated from a hindered phenol) may lead to effective regeneration of the parent phenolic antioxidant, hence increasing the efficiency of the lactone antioxidant radicals (e.g. reaction c, figure 1.14).

It has been shown that the lactone can be used at a significantly lower concentration to achieve similar melt flow retention to that of the traditional phenol/phosphite blend [80]. High levels of colour retention of polymers after multiple extrusion has been reported to be seen when the lactone stabiliser is combined with high performance phosphites such as Ultrinox 626 [80].

Hydroquinones are also antioxidants, which operate *via* a complementary CBD/CBA mechanism. The Hydroquinone is converted to benzoquinone via a CB-D process (see scheme 1.9) [61]. The latter is a very effective radical trap, it removes R• via a CB-A mechanism. Thus, a large number of radicals are removed from the system before the antioxidant becomes inactive (see scheme 1.9). The hydroquinones and quinones are effective melt stabilisers for polyolefins in conditions of low oxygen concentration [61].



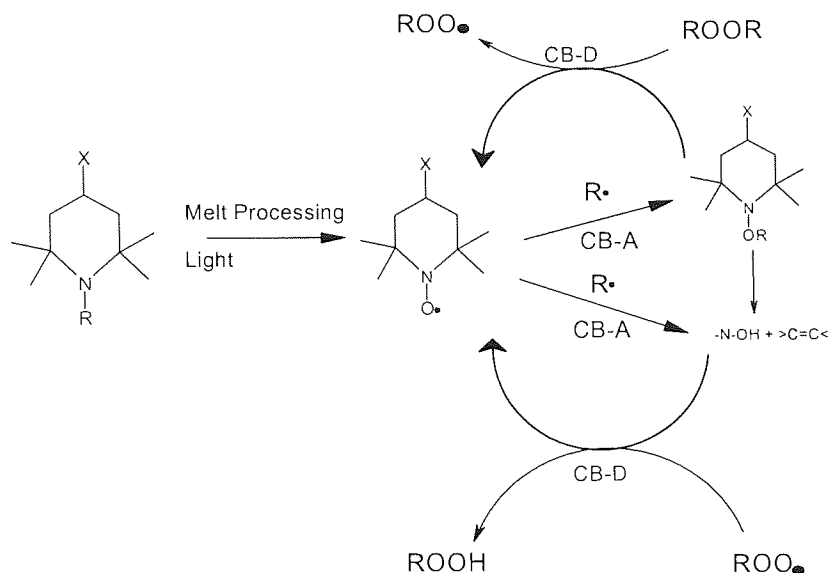
Scheme 1.9. Complementary chain breaking mechanism of hydroquinone [61].

Hindered amine derivatives (often referred to as hindered amine light stabiliser, HALS) also act by a complementary chain breaking mechanism and through their transformation products are able to trap both R• and ROO• in a cyclical regenerative mechanism [61] (Scheme 1.10).

### 1.5.5. DialkylHydroxylamine

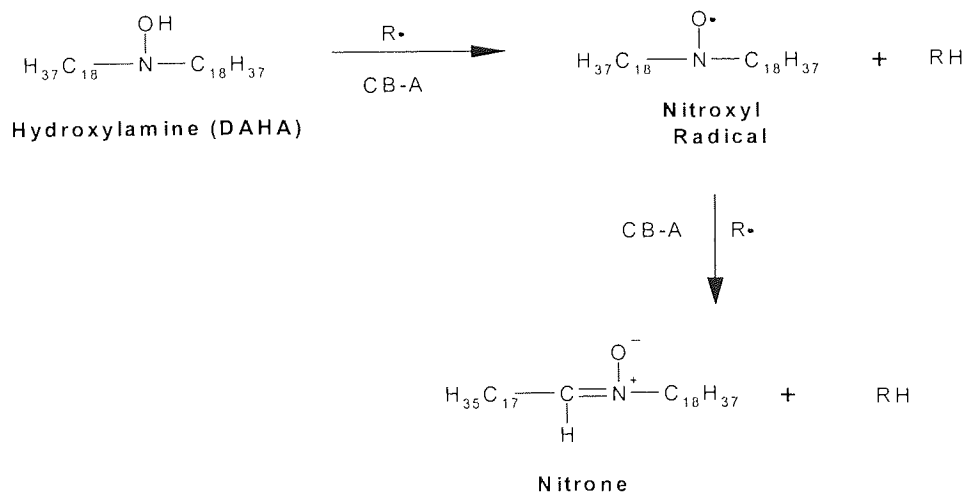
A recently commercialised antioxidant, Irgastab FSO42 [79,82], based on a dialkylhydroxylamine [DAHA, see figure 1.15 for structure] has emerged as part of a possible new class processing stabilisers. It has been proposed that the chemistry of DAHA is not too different from that of the more traditional stabilisers.

Scheme 1.10 . Stabilisation mechanism of HALS [77].

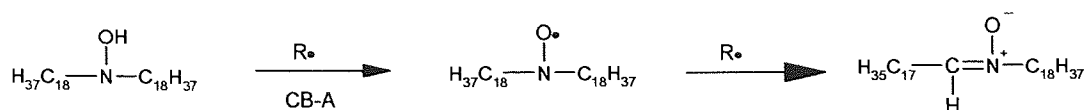


They can act *via* CB-A mechanism, providing effective antioxidant scavenging in conditions where alkyl radicals,  $R\bullet$ , are present in high concentrations (see figure 1.15) [82]. The nitrones produced by the CB-A mechanism have been suggested to be themselves active radical traps (see figure 1.16) [82] as well as peroxide decomposers (see figure 1.17).

Figure 1.15. Hydroxylamines function as primary antioxidants as free radical.



Each nitrone radical is able to scavenge numerous free radicals by repeated conversion to the nitroxide and subsequent  $\alpha$ -hydrogen abstraction.



Hydroxylamine (DAHA)

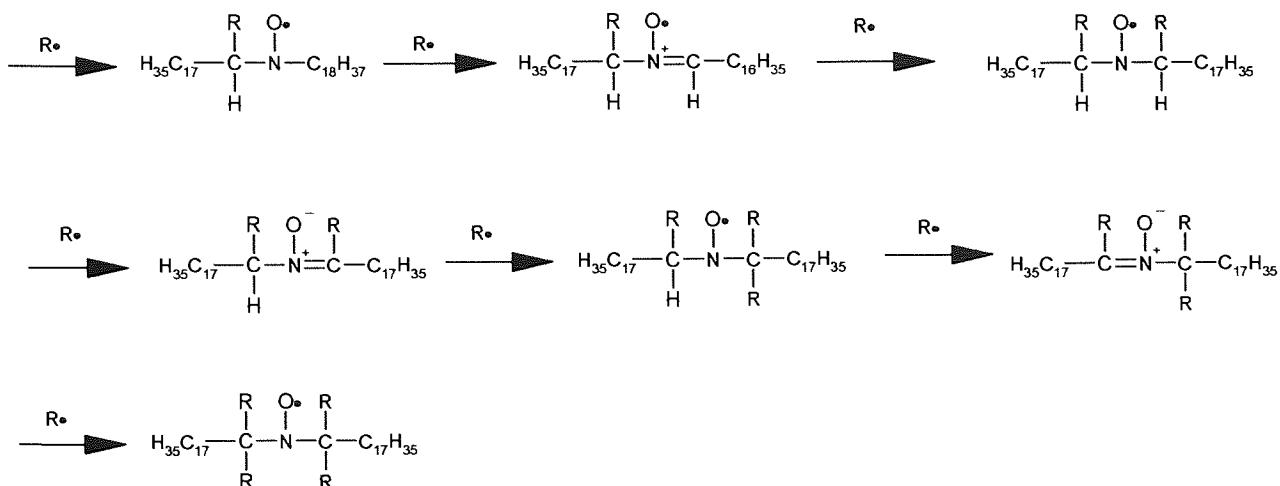


Figure 1.16. The CB-A/CB-D radical scavenging activity of the nitron oxidation products of hydroxylamines.

Using DAHA in combination with sterically hindered amine stabilisers (HALS) rather than with hindered phenols has led to high melt processing stability, high colour retention and long term thermal as well as UV stability [82]. It has been reported that initial trials on PE have shown very high melt processing and colour stability [82].

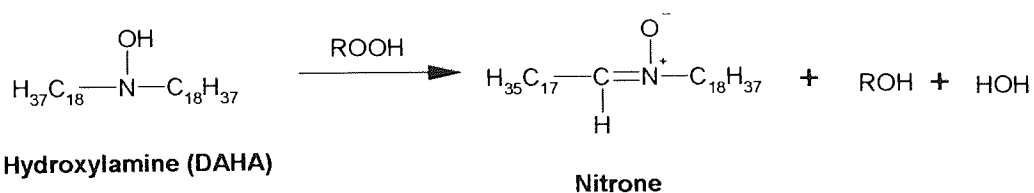
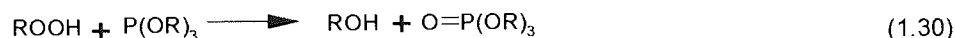


Figure 1.17. The peroxidolytic function of hydroxylamines.

### 1.5.6. Phosphites

Preventive antioxidants, e.g. phosphites, act by preventing the introduction of chain initiating radicals into the polymer system. The most important preventive mechanism is hydroperoxide decomposition by peroxidolytic antioxidant which do not result in the formation of free radicals. Peroxidolytic antioxidants fall into two main classes: stoichiometric peroxide decomposers (PD-S), and catalytic peroxide decomposers (PD-C) [83,85].

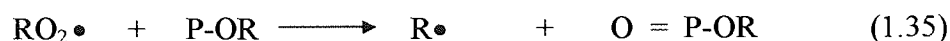
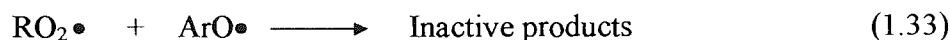
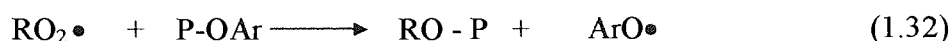
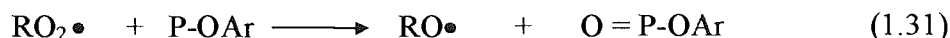
Organic Phosphites are peroxidolytic antioxidants, which decompose hydroperoxides stoichiometrically (PD-S) in a non-radical process [62], suppressing the chain-branching step in the familiar radical chain mechanism to give alcohols and the corresponding phosphate (see reaction 1.30). Organic phosphites are used on a large scale for the stabilisation of polymers against degradation during processing and long-term applications, with the ability to preserve the original colour of the polymer. Generally, phosphorus antioxidants are used in combination with hindered phenols and other stabilisers (resulting in a synergistic effect), but the sterically hindered aryl phosphites are, under some conditions active by themselves since they have chain-breaking activity in addition to their peroxidolytic function. [83-85].



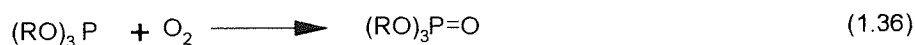
The reactivity of the phosphites towards peroxides is governed mainly by polar and steric effects of the groups bound to phosphorus [83-84], decreasing with increasing electron acceptor ability and bulk of substituent group in the order: alkyl phosphites > aryl phosphites > hindered aryl phosphites. Depending on their structure, aryl phosphites may also act as chain-breaking antioxidants, effective by trapping  $\text{RO}_2\bullet$  and  $\text{RO}\bullet$  radicals, hence terminating the oxidative chain reaction [83-84].

The antioxidant action of phosphites has been studied extensively [83-86]. Phosphites with open-chain sterically hindered aryl groups can act as chain-breaking antioxidants [83] by reducing alkyl peroxy radicals,  $\text{ROO}\bullet$ , to alkoxy radicals,  $\text{RO}\bullet$  (reaction 1.31) which reacts further with the phosphites by substitution, releasing aryloxy radicals (reaction 1.32), which terminates the oxidation chain reaction (reaction 1.33). Alkyl phosphites, on the other hand, are not able to react

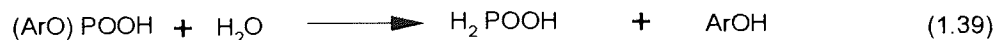
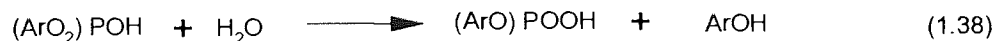
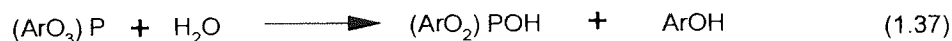
in that way because they are oxidised by alkoxy radicals, RO•, giving alkyl radicals, R•, which propagate the chain reaction (reaction 1.34-1.35).



Phosphites can also react with oxygen at high temperatures as shown in reaction 1.36 [85].



However, one of the main drawbacks of phosphites is their hydrolytic instability reactions with water and much work has been carried out to improve their performance [86,87]. The hydrolysis of a phosphite additive leads to the formation of phosphonate (reaction 1.37), hydrophosphate (reaction 1.38) and phosphorus acid (reaction 1.39) [86,87]. Formation of such compounds has been shown to render the antioxidant activity of the phosphorus additive ineffective and can lead to the corrosion of expensive high shear mixing extrusion machinery (reflected in undesirable black specks in the extrudate) [88]. Hence, hydrolysis should be minimised by appropriate storage (under nitrogen) of phosphite antioxidants



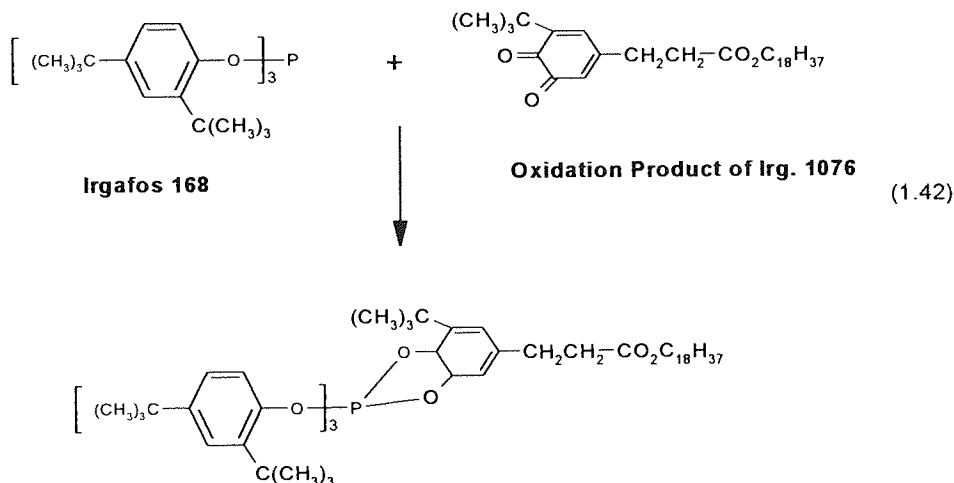
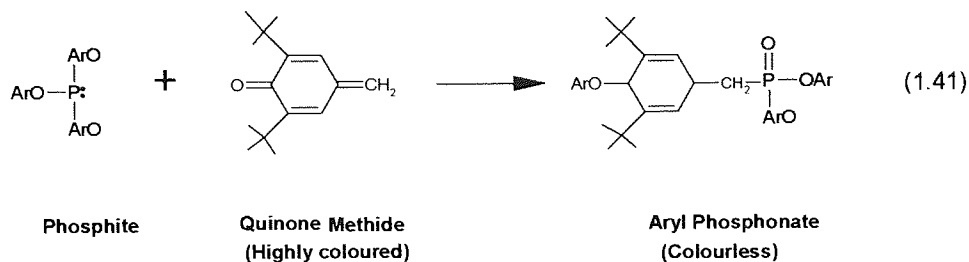
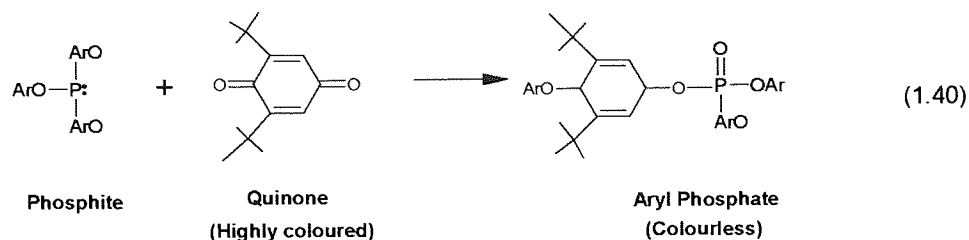
Amongst the high activity commercial phosphite additives on the market today, is *bis* (2, 4-di-*t*-butylphenyl) pentaerythritol di-phosphite (Ultranox 626). Ultranox 626 has very high phosphorus content compared to other common commercial phosphite or phosphonite antioxidants [87].



### 1.5.6 Synergism and Antagonism

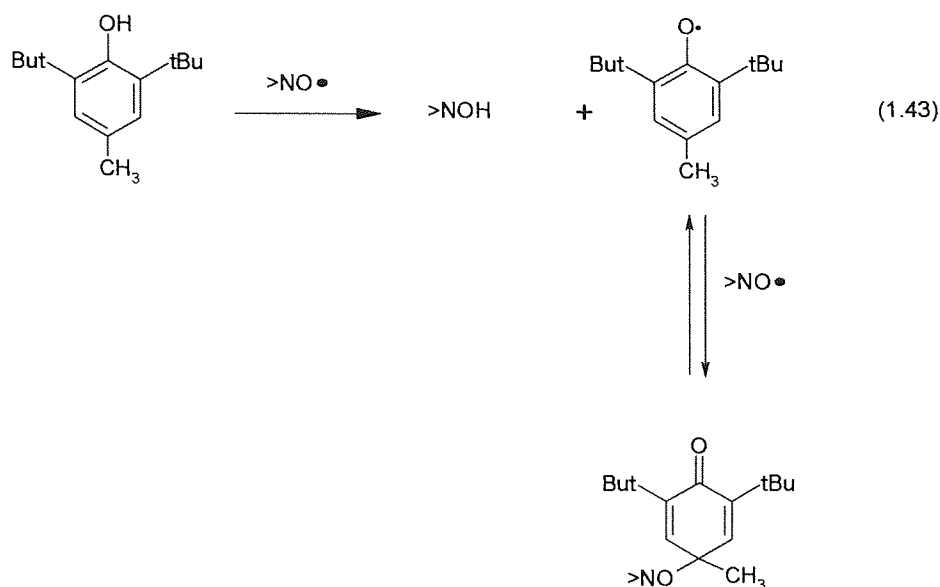
In practice, to enhance the activity of a stabilization system, more than one type of antioxidant, which can act by different mechanisms can be employed in order to reinforce their action. If the overall effect adds to more than the sum of the effect of the individual antioxidants, then this is referred to as 'synergism' [89]. The mechanism by which synergistic mixtures function depends upon the original mechanism of each of the antioxidants in the mixture. Organic phosphites enhance the antioxidant effect of phenols and reduce discolouration of polymers caused by phenol transformation products (generally by reactions with a quinonoidal structure). The phosphites disrupt the conjugated  $\pi$ -electron systems of the quinone derivatives rendering them colourless [55]. Reactions 1.40 and 1.41 show the reactions of an aromatic phosphite with quinone and quinone methide (both of which are highly coloured) to produce the colourless aryl phosphate and colourless phosphonate, respectively [55]. Reaction 1.42 shows the reaction of Irgafos 168 with an oxidation product of Irganox 1076 formed during thermal ageing of PP at 150°C [88]. It has also been suggested that the phosphite stabilisers can react with unsaturated groups and thus disrupt the polyene sequences in the backbone of oxidised PE and hence minimise colour [55].

It was reported [88] that the optimum ratio of a phenolic antioxidant like Irg. 1076 (see table 2.2 for structure) to *tris*-(2,4-di-*tert*-butylphenyl)-phosphite (Irgafos 168) in melt stabilisation was 1:4 in HDPE and LDPE. It was shown [88] that during processing of HDPE with an added phenolic antioxidant at 220 °C in the absence of a phosphite stabiliser, as much as 45% of the phenolic antioxidant was consumed after one extrusion pass. In contrast, in the presence of a phosphite stabiliser, only 20% of the antioxidant was consumed after the first extrusion pass [88]. Therefore, one of the major roles of the phosphite is the preservation of the hindered phenol. The synergistic combination of organic phosphites with phenolic antioxidants can also result in a more cost-effective system for the melt stabilization of polyolefins than a phenolic antioxidant alone.



Unlike synergism, antagonism reduces the overall effectiveness of combinations of antioxidants. For example, it has been reported that under photo-oxidation conditions hindered amine light stabilizers (HALS)/hindered phenol systems in polyolefins showed such antagonistic effects [89]. One reason for this antagonistic effect was suggested to be deactivation of the hindered phenolic moiety when used in combination with HALS due to its oxidation by the  $>\text{NO}\bullet$  radical [89]. The hindered phenol is easily oxidised by nitroxyl radicals to form phenoxyl radical, which is followed by the formation of a benzoquinone (see reaction 1.43). Sulphur containing antioxidants were shown to antagonise the photo-stabilising action of HALS in polyolefins. The antagonistic effect is explained by a mechanism in which sulphur-containing compounds decompose hydroperoxides in the polymer matrix, resulting in retardation or prevention of the formation of

nitroxyl-derived from HALS, since the nitroxyl is considered essential for photo-stabilisation [89].



## 1.6 Aims and Objectives of the Study

The main aim of this research work was two fold; firstly to develop a fundamental understanding of the relationship between molecular structure-performance characteristics of m-LLDPE and z-LLDPE polymers during processing and to compare thermal melt oxidative degradation mechanisms of both sets of polymers (was done in collaboration with a second research worker). Secondly, to investigate the role of different antioxidants on the melt and colour stability of the polymer and to develop a cost effective antioxidant package, which leads to good melt and colour stability of the polymer.

The objectives of the work were as follows:

1. To investigate the thermal oxidative degradation mechanisms of both Metallocene and Ziegler-Natta LLDPE (this part of the work was done in collaboration with a second research worker), which occur in the melt under different extrusion processing conditions. Part of this investigation concerned the changes in viscous and elastic properties of the two polymers under different processing conditions by examining their rheological characteristics.

2. To examine the effect of molecular parameters (viscosity, MW, MWD, type of catalyst) of m-LLDPE and z-LLDPE on processing characteristics.
3. To compound under pre-defined conditions m-LLDPE and z-LLDPE polymers with varying concentrations of solid and liquid antioxidants.
4. To examine the effect of single antioxidants and synergistic combinations, which operate by different mechanisms, on the melt and colour stability of m-LLDPE and z-LLDPE polymers during multi-pass extrusion processing.
5. To determine the best antioxidant systems for m-LLDPE based upon cost, safety, melt and colour stability.

## Chapter 2. Experimental and Analytical Techniques

### 2.1 Materials

Unstabilised metallocene-catalysed linear low-density polyethylene (m-LLDPE) and unstabilised Ziegler catalysed linear low-density polyethylene (z-LLDPE) were supplied as granules by Exxon, Baytown, Texas, USA, (see table 2.1 for their characteristics). The polymers were flushed with nitrogen, vacuum sealed and stored in a freezer room at  $-20^{\circ}\text{C}$  until required; when required the polymers were allowed to thaw while vacuum sealed to room temperature before use.

Commercial antioxidants, Irganox 1076, n-Octadecyl-3-(3',5'-di-t-butyl-4'-hydroxy- phenyl) propionate; Irgastab FS042, *bis*-alkylated hydroxylamine; Irganox HP136, 3-Aryl benzofuran-2-one; Irganox E201, 6-hydroxy-2,5-dimethyl-2-phytl-7,8-benzochroman (stored under nitrogen); Irganox XP-60 (1:2.3, a w/w ratio of Irganox HP136:Ultranox 626 respectively, as given by the manufacturer); Irganox XP-490 (3.3:1:2.3, a w/w ratio of Irganox 1076:Irganox HP136:Irgafos P-EPQ respectively, as given by the manufacturer) and Irgafos P-EPQ, Phosphonous acid, [1,1'-biphenyl]-4,4'-diyl*bis*-tertarkis-[2,4-*bis*(1,1-dimethylethyl) phenyl] ester which were supplied ex. Ciba Specialty (Switzerland) and supplied by Exxon, Baytown (USA) and were used without further purification (see in table 2.2 for structures and characteristics).

Some commercial phosphite melt stabilisers, Weston 399, *tris* (nonylphenyl) phosphite (stored under nitrogen) and Ultranox 626, *bis*-(2,4-di-t-butylphenyl) pentaerythrityl diphosphite were donated by GE specialty chemicals (the Netherlands). Dover Chemicals (USA) supplied Doverphos S9228, *bis*-(2,4-dicumylphenyl) pentaerythritol diphosphite. All phosphite melt stabilisers were used without further purification (see in table 2.2 for structures and characteristics).

Trimethylolpropane (TMP) and Zinc Stearate (ZnSt) were supplied by Aldrich and Witco Corporation, (USA), respectively. HPLC grade, dichloromethane, n-hexane and 1,4-dioxane were supplied by Fisons, and were used without further purification.

The starting materials were characterised using FT-IR and UV-VIS spectroscopy and the results are displayed in figures 2.6-2.21 at the end of this chapter.

Table 2.1: Typical characteristics of unstabilised m-LLDPE and z-LLDPE resins (measured at Aston University [90], except for  $^1\text{H-NMR}$  and GPC results which were measured at Exxon, Machelen) (Numbers in parenthesis are the original data provided by Exxon).

Parameter	m-LLDPE	z-LLDPE	Comments
Melt index, $\text{g.10min}^{-1}$ (MI)	<b>1.00</b> (1.0)	<b>1.00</b> (1.0)	2.16kg, 190°C
High load melt index, $\text{g.10min}^{-1}$ (HLMI)	<b>17.0</b> (16.0)	<b>32.0</b> (29.0)	21.6kg, 190°C
Melt flow ratio (MFR)	<b>17.0</b> (16.0)	<b>32.0</b> (29.0)	
$\bar{M}_w$	101 146	112 720	GPC
$\bar{M}_n$	49 171	32 008	Calculated (Aston)
$\bar{M}_z$	173 087	333 159	Calculated (Aston)
Polydispersity, $\bar{M}_w/\bar{M}_n$	2.06	3.52	GPC
$\bar{M}_z/\bar{M}_w$	1.71	2.96	GPC
Co-monomer type	Hexene-1	Hexene-1	
Co-monomer level, weight %	<b>6.1</b> (8-10)	<b>8.3</b> (8-10)	$^{13}\text{C-NMR}$
Vinyl, $-\text{CH}=\text{CH}_2$ , $908\text{cm}^{-1}$	<b>0.075</b> (0.05)	<b>0.11</b> (0.08)	FTIR/ $^1\text{H-NMR}$ , no. of groups/1000C
Vinylidene, $894\text{cm}^{-1}$ $\diagup\text{C}=\text{CH}_2$	<b>0.026</b> (0.03)	<b>0.039</b> (0.04)	FTIR/ $^1\text{H-NMR}$ , no. of groups/1000C
trans-vinylene, $-\text{CH}=\text{CH}-$ , $965\text{cm}^{-1}$	<b>0.051</b> (0.03)	<b>0.013</b> (0.05)	FTIR/ $^1\text{H-NMR}$ , no. of groups/1000C
Trisubstituted Olefin $\diagdown\text{C}=\text{CH}-$	(0.16)	(0.045)	$^1\text{H-NMR}$ , no. of groups/1000C
Total number of double bonds/1000C	<b>0.31</b>	<b>0.21</b>	$^1\text{H-NMR}$
Hydroperoxide level, $\text{mol.kg}^{-1}$	$(1.1 \pm 0.2) \times 10^{-4}$	$(1.1 \pm 0.2) \times 10^{-4}$	Chemical analysis

Table 2.2 Chemical structures of antioxidants used.

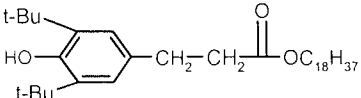
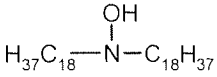
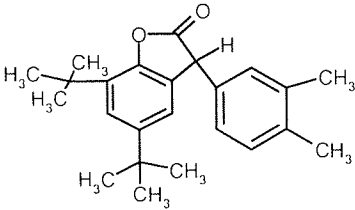
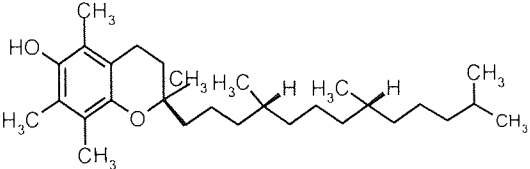
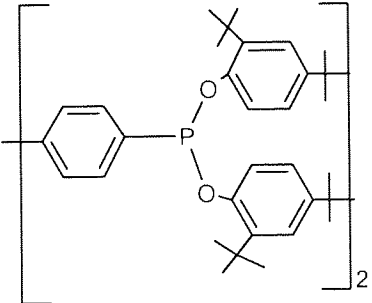
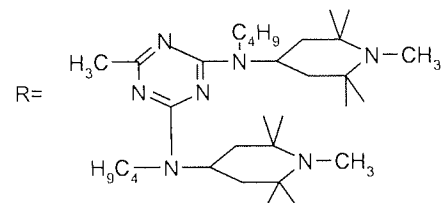
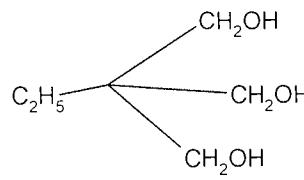
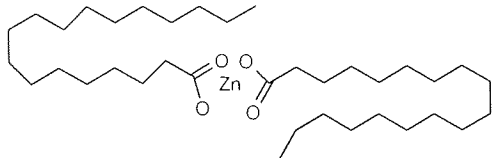
Chemical structure and Commercial Name	Code name (MM/g, State, m.p./°C) UV-Wavelength $\lambda_{\max}$	Origin
 <p>n-Octadecyl-3-(3',5'-di-t-butyl-4' hydroxyphenyl) propionate</p> <p><b>Irganox 1076</b></p>	<p>Irg. 1076 ( 531, white powder, 51.6-52 )</p> <p>276-282nm</p>	<p>Ciba Specialty</p>
 <p>Bis-alkylated hydroxylamine amines</p> <p><b>Irgastab FS042</b></p>	<p>Irg. FS042 ( 537, yellowish powder )</p> <p>270-272nm</p>	<p>Ciba Specialty</p>
 <p>3-aryl benzo furan-2-one</p> <p><b>Irganox HP 136</b></p>	<p>Irg. HP 136 ( 351, white powder, 97-130 ).</p> <p>275, 285nm</p>	<p>Ciba Specialty</p>
 <p>6-hydroxy-2,5-dimethyl-2-phytyl-7,8-benzochroman</p> <p><b>Irganox E201</b></p>	<p>Irg. E201 ( 431, orange-brown viscous oil ).</p> <p>298nm</p>	<p>Ciba Specialty</p>
 <p>Phosphonous acid, [1,1'-biphenyl]-4,4'-diylbis-tetrakis[2,4-bis (1,1-dimethylethyl) phenyl] ester</p> <p><b>Irgafos P-EPQ</b></p>	<p>Irg. P-EPQ ( 991, Yellow crystalline powder, 85 -110 )</p> <p>275nm</p>	<p>Ciba Specialty</p>

Table 2.2; continued.....

Chemical structure and Commercial Name	Code name (MM/g, State, m.p./°C) UV-Wavelength/ $\lambda_{max}$	Origin
$R-NH-\left[CH_2\right]_3-N\left(\begin{array}{c} R \\   \\ \text{---} \end{array}\right)-\left[CH_2\right]_2-N\left(\begin{array}{c} R \\   \\ \text{---} \end{array}\right)-\left[CH_2\right]_3-N-R$  <p>1,3,5-triazine-2,4,6-triamine-N',N''-[1,2-ethane diylbis [[4,6-bis(butyl[1,2,2,6,6-pentamethyl(4-piperidyl) amino]-1,3,5-triazin-2-yl] imino]-3,1-propanediyl]]-bis[N', N''-dibutyl-N',N''-bis(1,2,2,6,6-pentamethyl-4-piperidyl]</p> <p><b>Chimassorb 119D</b></p>	<p>Chim.119D ( <b>2286</b>, Light Yellow granules, 115-150 )</p>	<p>Ciba Specialty</p>
 <p>Trimethylolpropane</p> <p><b>TMP</b></p>	<p>TMP ( <b>134</b>, white crystalline granules )</p>	<p>Aldrich</p>
 <p>Octadecanoic Acid zinc salt</p> <p>Zn (C<sub>18</sub>H<sub>35</sub>O<sub>2</sub>)<sub>2</sub></p> <p><b>Zinc Stearate</b></p>	<p>Zinc Stearate ( <b>632</b>, white pellets, 119 )</p>	<p>Witco</p>
<p>Irganox HP136: Ultrinox 626 1:2.3 w/w ratio <b>XP-60</b> Commercial Blend</p>	<p><b>XP-60</b>, white Powder</p>	<p>Ciba Specialty</p>
<p>Irganox HP136: Ultrinox 626:Irganox 1076 1:2.3:3.3 w/w ratio <b>XP-490</b> Commercial Blend</p>	<p><b>XP-490</b>, white Powder</p>	<p>Ciba Specialty</p>



## 2.2 Polymer Processing

All polymer samples used in this work were processed in a Betol 30mm co-rotating intermeshing twin-screw extruder (TSE). The twin-screw extrusion line and the screw configurations are shown in figures 2.1 and 2.2 respectively. The Betol TSE extruder consisted of a barrel equipped with the two co-rotating intermeshing screws ( $l/d = 33:1$ ) rotating at a fixed speed which can be varied between 50 to 200rpm, capable of running at a high torque rating, divided into eight zones and a die head set at fixed temperatures. Thermocouples assembled in the barrel and die were connected to gauges on the control panel and switched the heaters on and off as necessary to control the temperature of each zone. The barrel heaters were also equipped with a water-cooling circulatory system to control the temperature of each zone. The extruder was equipped with two material feeders (equipped with agitators or stirrers, preventing polymer sticking) above the hopper; a Churchill Auger Single screw feeder (pellets) and a K-Tron twin-screw feeder (granules) respectively, each delivering the required amounts of polymer material, granules or pellets, directly into the hopper. The feeders were electrically driven by a Churchill control console, which controlled the flow rate of material flow into the hopper above the TSE barrel. The close fit screw, made of high-grade steel rotated within the barrel (see figure 2.2). Any gases liberated during extrusion, i.e. steam or volatile solvents (during the compounding step) were removed from the extruder with the aid of a vent connected to a vacuum pump (see figure 2.2). The vent zone was positioned along the barrel where the polymer experienced least pressure (otherwise the melt would simply discharge out). The power to rotate the screw was controlled by a variable speed electric motor. The die, which determines the shape of the extrudate, was simply a circular shaped hole, made of hardened steel.

Twin screw extrusion was carried out at a given temperature profile and the extrudates were cooled on-line, dried and pelletised. The temperature (die and melt), output rate (determined by weighing an extruded sample after one minute intervals), melt pressure, current and the appearance of the polymer lace were recorded for each sample. Any melt fracture, a processing problem, evident on the surface of polymer extrudates as sharkskin or wavy distortions was also noted.

The actual melt temperature of the polymer at the die exit was measured using an infrared THI-500 thermometer. The polymer was extruded into a thin lace through a single hole die with a 4mm internal diameter. This was followed by quenching the lace in cold water ( $\approx 5^{\circ}\text{C}$ ), using an on-line Prism water bath (1metre in length), drying with two air guns and pelletisation on a Prism pelletiser operating at a fixed speed, for samples that needed to be collected for further extrusion passes. During the compounding step, liquid antioxidants were fed drop-wise with the polymer at the appropriate flow rate during the extrusion using a Philips PU4100 Beckham high pressure liquid chromatographic pump (HPLC) into the port under the hopper (under nitrogenous conditions). The power consumption per kg of polymer extruded was calculated according to equation 2.1 (a scaling equation):

$$P = P_m \times (I / I_{\max}) \times (S / S_{\max}) \times 1/F \quad (2.1)$$

Where:-

P is the power consumption hour per kg of polymer extruded (kW.h/kg)

$P_m$  is the maximum power of the motor (7.5 kW)

I is the current of the polymer during extrusion (A)

$I_{\max}$  is the maximum current (28A)

S is the screw speed (rpm)

$S_{\max}$  is the maximum screw speed during extrusion (220rpm)

F is the output rate ( $\text{kg.h}^{-1}$ )

### **2.2.1 Twin-screw extrusion of virgin Polymers.**

Unstabilised m-LLDPE and z-LLDPE polymer granules were processed in the absence of any stabilisers using the method outlined above at varying temperature profiles (see table 2.3, temperature profiles 1 to 4) and screw speeds (50 to 200rpm) under atmospheric conditions (referred to as pass 1). The extruded unstabilised polymer pellets were collected and re-processed for four times (multi-pass extrusion, passes 2 to 5, see scheme 2.1) using the same extrusion conditions. Processing of these unstabilised m-LLDPE and z-LLDPE polymers was carried out by another researcher in the polymer processing group (PPP), whereas the testing for their colour (see section 2.3), melt flow (see section 2.4) and molecular weight characteristics using Gel permeation chromatography (see section 2.6) was carried out in collaboration with this work.

The % experimental error based on processing of an unstabilised polymer sample in triplicate (under the same conditions) followed by measuring the melt flow (low melt index, MI using a load of 2.16kg) was carried out. For example for the first processed sample,  $MI_1 = 0.80$ , for the second processed sample,  $MI_2 = 0.83$  and third processed sample,  $MI_3 = 0.87$ , hence the average MI for the three samples was taken as  $0.83 \pm 0.04$  (g/10min). Thus, the % processing experimental error was found to be between 4-5%. It is important to note here that the MI values of each of the processed samples corresponded to three MI values per sample.

## 2.2.2 Twin-screw extrusion of LLDPE in the presence of Antioxidants

### a. Compounding (Po)

A compounding step in which the antioxidants were homogenised with the polymer will be referred to as extrusion pass zero (Po). Both virgin m-LLDPE and z-LLDPE polymer samples were stabilised by adding low concentrations of various antioxidants to the virgin polymer granules during extrusion in the TSE, under nitrogen using temperature profile 1 (see table 2.3, page 82) at a screw speed of 100rpm. The solid antioxidants, i.e. Irganox 1076, were added to the unstabilised polymer granules and tumble mixed on a roll mill for 24 hours prior to processing. For example, to calculate the amount of solid AO, i.e. 500ppm, to add to 3kg of polymer (see equation 2.2):-

$$\text{Amount of AO to be added to polymer (g)} = \frac{\text{Target Concentration(ppm)} \times \text{Polymer amount (g)}}{1 \times 10^6} \quad (2.2)$$

$$(500/1 \times 10^6) \times 3000 = 1.5\text{g}$$

The solid antioxidants, were added together with the polymer powder granules (after tumble mixing) *via* the K-Tron twin-screw feeder (see figure 2.2).

The viscosity of the liquid phosphites, i.e. Weston 399, were first reduced by a factor of 10, by dilution in dry HPLC grade dichloromethane (99% purity). In the case, of combinations of a biological hindered phenol and polyhydric alcohol (Irganox E201:TMP) ethanol was used. Liquid phosphites antioxidants are hydrolytically unstable hence special precautions were taken to avoid any contact with moisture in the air (the phosphite antioxidants being stored and sealed under nitrogen). Furthermore, liquid phosphites and Irganox E201 were continuously purged with

nitrogen in a sealed container, during its use in the extrusion process and were fed with the polymer, drop-wise at the required flow rate using a HPLC pump through a port under the hopper (with an additional continuous nitrogen purging of the port), directly into the extruder. For example, to add a liquid antioxidant, e.g. 2000ppm, Weston 399 (density, 0.980g/ml<sup>-3</sup>), to m-LLDPE at a screw speed of 100rpm, with an extrusion temperature of 260°C (under nitrogen conditions) and output rate of 4.0kg.h<sup>-1</sup> (66.7g/min); the following calculation was carried out (see equations 2.2-2.3);

$$\text{Amount of AO to be added to polymer} = \frac{\text{Target Concentration(ppm)}}{1 \times 10^6} \times \text{Polymer amount extruded in 1 minute (g/min)} \quad (2.2)$$

$$(2000/1 \times 10^6) \times 66.7 = 0.13 \text{ g in 1 minute}$$

Hence, to determine the volume to be added to the polymer during extrusion;

$$\text{Density} = \text{Mass} / \text{Volume} \quad (2.3)$$

$$0.980 = 0.13 / \text{Volume}$$

$$\text{Volume} = 0.13 \text{ ml/min}$$

Therefore, to add 2000ppm of a liquid antioxidant (diluted by a factor of 10) to 66.7g/min of m-LLDPE, the HPLC pump was set at 1.3ml/min. Tables 2.4-2.6 show all flow feeding rates used for the addition of liquid antioxidants during Po stabilisation.

All stabilised extruded polymer samples were stored in a freezer (-20°C) until required for further analysis. Tables 2.7– 2.13 show the sample codes and extrusion conditions used for all the twin-screw multi-pass extrusion of Po stabilised m-LLDPE.

Initial stabilisation work on both virgin m-LLDPE and z-LLDPE polymers was conducted using an antioxidant package, at various initial concentrations (0.05-0.2%, w/w) based on combinations of a solid synthetic hindered phenol (Irganox 1076) and a liquid phosphite (Weston 399)

antioxidants. For comparative purposes, a combination of Irganox E201/Ultrinox 626/TMP (0.03-0.06%, w/w) was also examined in both polymers

Further stabilisation work was carried out on virgin m-LLDPE only, using single and combinations of varying initial concentrations (0.03-0.19%, w/w) of synthetic and biological hindered phenols (solid and liquid); Irganox 1076, and Irganox E201; Irganox HP 136 (lactone); Irgastab FS042 (hydroxylamine); Phosphites; Weston 399, PEPQ, Doverphos S9228 and Ultrinox 626; and different HALS; Tinuvin 765, Tinuvin 622LD and Chimassorb 119D. Commercially available antioxidant combinations, Irganox XP-60 (an approximate 1:2.3, w/w ratio of Irganox HP136:Ultrinox 626, respectively) and Irganox XP-490 (3.3:1:2.3, w/w ratio of Irganox 1076, Irganox HP136 and Irgafos PEPQ, respectively) were also examined (at initial concentrations of 0.03-1.4%, w/w).

The % experimental error for Po stabilisation was established by processing a Po stabilised polymer four times, under the same conditions, followed by measuring the MI (see tables A1-A2 in appendix 1). For example, for a polymer stabilised with a solid antioxidant and extruded three times the MI values for the four extruded samples were,  $MI_1 = 1.11$ ,  $MI_2 = 1.10$ ,  $MI_3 = 1.07$  and  $MI_4 = 1.08$ , giving an average MI as  $1.09 \pm 0.02$  (g/10min). Thus, the experimental error was found to be 2% for a polymer stabilised with a single solid antioxidant. For a polymer stabilised with a solid/liquid antioxidant the same procedure was repeated giving an experimental error between 1-2%.

#### **b. Multi-Pass Extrusion (P1 to P5)**

All stabilised polymers after the compounding step were then subjected to multiple extrusion using different temperature profiles. Tables 2.7-2.13 shows the samples codes and extrusion conditions used for all multi-pass extrusion experiments throughout this work. These stabilised polymers were then characterised by examining their colour stability (see section 2.3) and melt flow characteristics (see section 2.4), after each passes 1, 3 and 5. It is important to point out here that as each sample was collected and re-processed for four times (multi-pass extrusion, passes 2 to 5, see scheme 2.1) using the same extrusion conditions, the extruder was 'washed' with 650g of the sample in between each pass. The % experimental error was determined by multi-processing the compounded (stabilised) polymer four times, under the same conditions, followed by measuring the MI. For example, for a polymer stabilised with a solid antioxidant and extruded

four times the MI of each extruded sample were,  $MI_1 = 1.02$ ,  $MI_2 = 1.10$ ,  $MI_3 = 1.11$  and  $MI_4 = 1.08$ , the average MI was taken as  $1.08 \pm 0.05$  (g/10min). Thus, the experimental error was found to be 4% for a polymer stabilised with a single solid antioxidant. In a similar experiment for a polymer stabilised with a solid/liquid antioxidant the experimental error was found to be between 3-4%.

Table 2.3: Temperature ( $^{\circ}\text{C}$ ) profile for the twin screw extrusions of m-LLDPE and z-LLDPE. Same temperature profile was used for each extrudate for its  $P_0$  and P1 to P5.

Profile	Die Temp. ( $^{\circ}\text{C}$ )	Zone Temperature/ $^{\circ}\text{C}$								Atmosphere
	Die	8	7	6	5	4	3	2	1	
<b>Profile for Pass-zero (<math>P_0</math>) stabilisation</b>										
A	210	210	205	200	195	190	185	180	175	Nitrogen
<b>Profile for Multipass extrusion</b>										
B	210	210	205	200	195	190	185	180	175	Air
C	235	235	225	215	210	200	190	180	175	Air
D	260	260	245	230	220	210	200	190	175	Air
E	285	285	270	255	240	225	210	190	175	Air



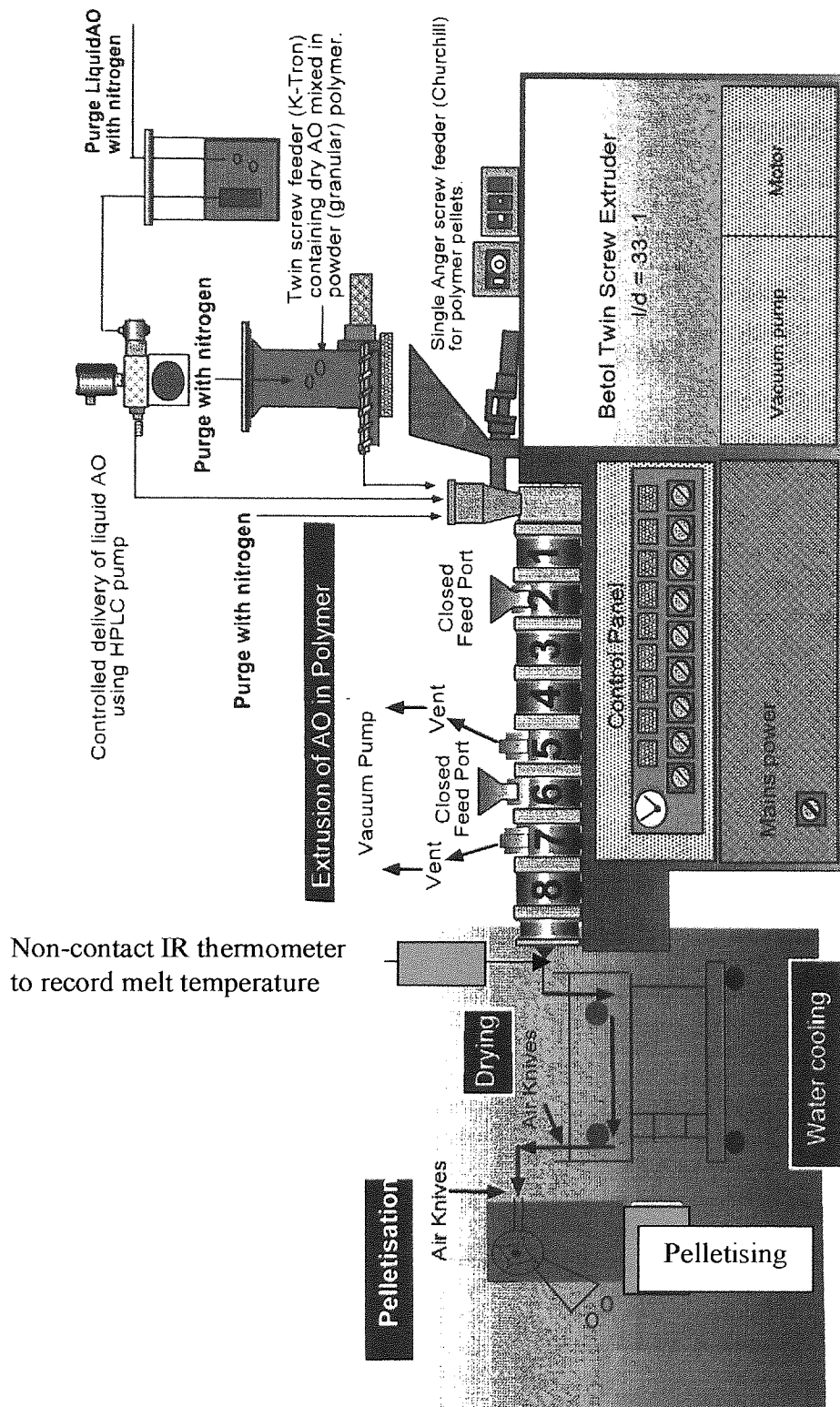
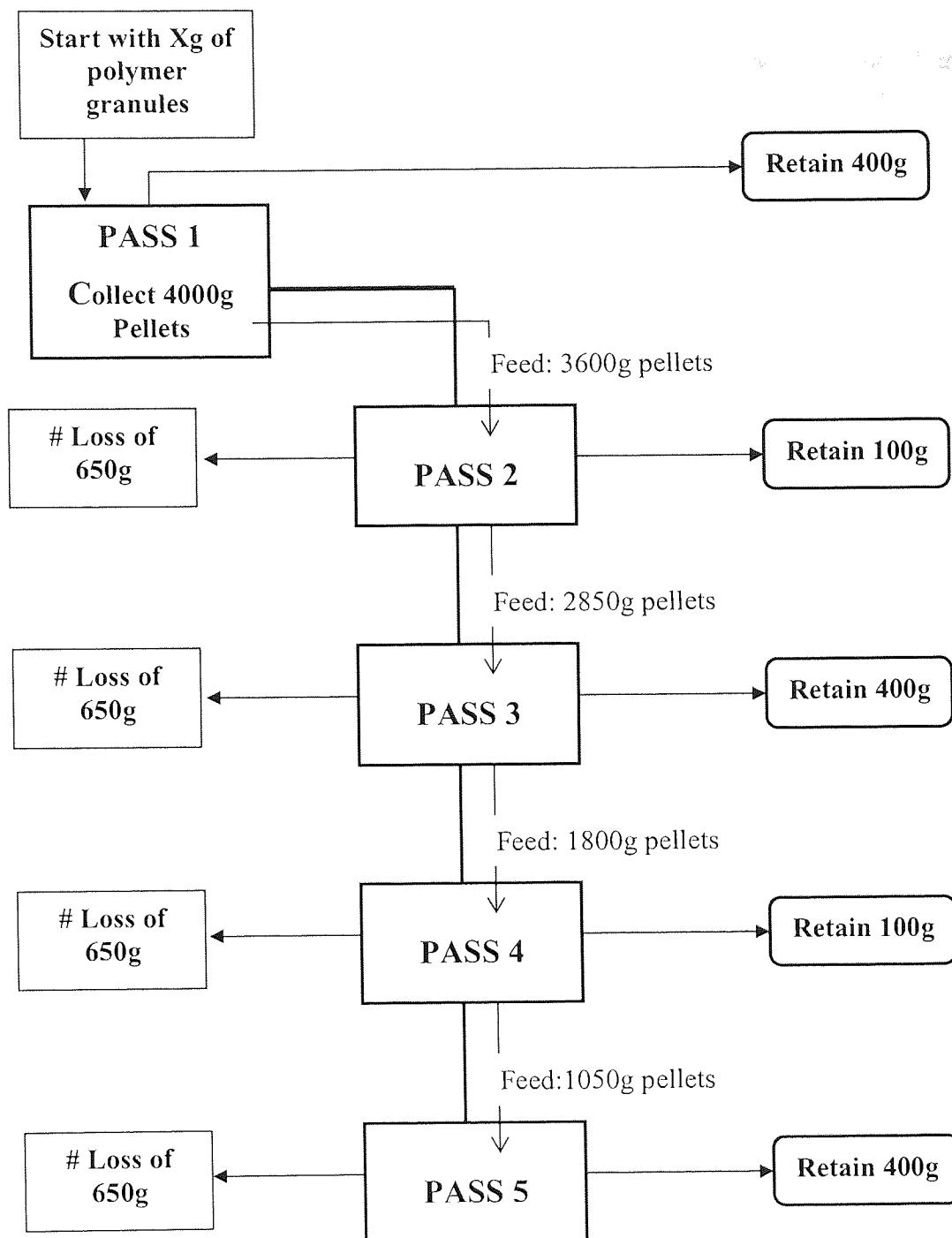


Figure 2.2 Twin-Screw extrusion line and arrangements shown for Po stabilisation (under nitrogen) and Multi-pass extrusion (under atmospheric conditions).





Scheme 2.1 Method used for the multi-pass extrusion of m-LLDPE at 100rpm, extrusion temperature 210°C, output rate 4.0kg.h<sup>-1</sup>. # Loss due to collection of mid-cut only, i.e. discarding first and last fractions of extrudate for sampling consistency.

Table 2.4: Flow feeding rates (ml/min) used for the addition of the Weston 399 (phosphite) and Irganox E201 (at 100rpm only) during Po stabilisation of **m-LLDPE and z-LLDPE** at various screw speeds (rpm); 50,100, 150 and 200 and concentrations (ppm).

Polymer	Screw Speed/rpm	Target Concentration of Phosphite(ppm)	Flow Rate (feeding) /ml/min
z-LLDPE	50	1000	0.5
	100		0.8
	150		1.1
m-LLDPE	50	1000	0.4
	100		0.7
	150		1.0
z-LLDPE	50	1500	0.8
	100		1.2
	150		1.7
m-LLDPE	50	1500	0.6
	100		1.0
	150		1.6
z-LLDPE	50	2000	1.1
	100		1.6
	150		2.2
m-LLDPE	50	2000	0.8
	100		1.3
	150		2.1
Polymer	Screw Speed/rpm	Target Concentration of E201/TMP (ppm)	Flow Rate (feeding) /ml/min
z-LLDPE	100	1350	1.2
m-LLDPE	100	1350	1.0

Table 2.5: Flow feeding rates (ml/min) used for the addition of liquid antioxidants during Po stabilisation of **m-LLDPE only** at a screw speed of 100rpm and an extrusion temperature of 210°C; see tables 4.1 and 5.1-5.2 for identification of codes.

Code	Screw Speed/rpm	Flow rate (ml/min)under nitrogen	Comment
S4	100	1.2	Traditional 1076/399 blend
S11	100	1.0	A number of various single liquid antioxidants Tested in m-LLDPE only
S17	100	0.7	
S19	100	0.2	
S20	100	1.4	
S21	100	0.7	
S22	100	1.2	Lactone (Irganox HP136) containing formulations with liquid Weston 399 (phosphite).
S23	100	1.0	
S24	100	1.0	
S25	100	1.0	
S26	100	1.0	Irg. FSO42 containing Liquid; Irg.E201/TMP.
S27	100	1.0	
S28	100	1.2	Irg. FSO42 containing formulations with W399.
S29	100	1.2	
S30	100	1.0	Hindered phenol/ liquid R-HALS combinations with W399 in m-LLDPE only
S31	100	1.0	
S32	100	1.2	

Table 2.6: Flow feeding rates (ml/min) used for the addition of liquid antioxidants during Po stabilisation of **m-LLDPE only** at a screw speed of 100rpm and an extrusion temperature of 210°C; see table 5.2 for identification of codes.

Code	Screw Speed/rpm	Flow rate (ml/min) under nitrogen	Comment
S37	100	0.84	<b>XP-60 based system with W399</b>
S42	100	0.93	<b>XP-490 based system with W399</b>
S43	100	0.2	<b>Vitamin E based systems with the addition of W399.</b>
S44	100	0.2	
S45	100	0.2	
S46	100	0.2	
S47	100	1.0	
S48	100	1.0	
S49	100	0.2	

Table 2.7 **Preliminary stabilisation work for formulations s1, s2, s3, s4, s11 and s12.** Sample codes and conditions used for twin-screw multi-pass extrusion experiment (extrusion temperatures 210 and 285°C, screw speed of 50-200rpm under atmospheric conditions) of **Pass-zero stabilised m-LLDPE.** Initially compounded (Po) the polymer under nitrogen at 210°C at 100rpm.

Code Number	Target Total Concentration /ppm wt/wt ratio	Polymer	Code <sup>1</sup>	Extrusion Passes	Screw speed /rpm	Die Temp/°C (multi-pass extrusion)
S1 1076:399	2000 1:3	Metallocene	m-S1-210-P1	1	50	210
			m-S1-210-P3	3		
			m-S1-210-P5	5		
			m-S1-285-P1	1	50	285
			m-S1-285-P3	3		
			m-S1-285-P5	5		
			m-S1-285-P1	1	200	285
			m-S1-285-P3	3		
			m-S1-285-P5	5		
S2 1076:399	1750 1:1.3		m-S2-210-P1	1	50	210
			m-S2-210-P3	3		
			m-S2-210-P5	5		
			m-S2-285-P1	1	50	285
			m-S2-285-P3	3		
			m-S2-285-P5	5		
S3 1076:399	2750 1:2.7		m-S3-210-P1	1	50	210
			m-S3-210-P3	3		
			m-S3-210-P5	5		
S4 1076:399	2500 1:4	m-S4-285-P1	1	50	285	
		m-S4-285-P3	3			
		m-S4-285-P5	5			
		m-S4-285-P1	1	200	285	
		m-S4-285-P3	3			
		m-S4-285-P5	5			
S11 E201:U626:TMP.	1350 1:2:1.5	m-S11-285-P1	1	50	285	
		m-S11-285-P3	3			
		m-S11-285-P5	5			
		m-S11-285-P1	1	200	285	
		m-S11-285-P3	3			
		m-S11-285-P5	5			
S12 1076:399	1500 1:2	m-S12-285-P1	1	50	285	
		m-S12-285-P3	3			
		m-S12-285-P5	5			
		m-S12-285-P1	1	200	285	
		m-S12-285-P3	3			
		m-S12-285-P5	5			

<sup>1</sup> Code denoted as m-S1-210-P1 signifies type of polymer (m-LLDPE), Pass-zero stabilised formulation number (S1), multi-pass extrusion temperature (210) and the pass (pass 1).

Table 2.8 **Preliminary stabilisation work using formulations s1, s2, s3, s4, s11 and s12.** Sample codes and conditions used for twin-screw multi-pass extrusion experiment (extrusion temperatures 210 and 285°C, screw speed of 50-200rpm under atmospheric conditions) of **Pass-zero stabilised z-LLDPE**. Initially compounded (Po) the polymer under nitrogen at 210°C at 100rpm.

Code Number	Total Concentration /ppm wt/wt ratio	Polymer	Code <sup>2</sup>	Extrusion Passes	Screw speed /rpm	Die Temp/°C (multi-pass extrusion)
<b>S1</b> 1076:399	2000 1:3	Ziegler	z-S1-210-P1	1	50	210
			z-S1-210-P3	3		
			z-S1-210-P5	5		
			z-S1-285-P1	1	50	285
			z-S1-285-P3	3		
			z-S1-285-P5	5		
			z-S1-285-P1	1	200	285
			z-S1-285-P3	3		
			z-S1-285-P5	5		
<b>S2</b> 1076:399	1750 1:1.3		z-S2-210-P1	1	50	210
			z-S2-210-P3	3		
			z-S2-210-P5	5		
			z-S2-285-P1	1	50	285
			z-S2-285-P3	3		
			z-S2-285-P5	5		
<b>S3</b> 1076:399	2750 1:2.7		z-S3-210-P1	1	50	210
			z-S3-210-P3	3		
			z-S3-210-P5	5		
<b>S4</b> 1076:399	2500 1:4	z-S4-285-P1	1	50	285	
		z-S4-285-P3	3			
		z-S4-285-P5	5			
		z-S4-285-P1	1	200	285	
		z-S4-285-P3	3			
		z-S4-285-P5	5			
<b>S11</b> E201:U626: TMP.	1350 1:2:1.5	z-S11-285-P1	1	50	285	
		z-S11-285-P3	3			
		z-S11-285-P5	5			
		z-S11-285-P1	1	200	285	
		z-S11-285-P3	3			
		z-S11-285-P5	5			
<b>S12</b> 1076:399	1500 1:2	z-S12-285-P1	1	50	285	
		z-S12-285-P3	3			
		z-S12-285-P5	5			
		z-S12-285-P1	1	200	285	
		z-S12-285-P3	3			

<sup>2</sup> Code denoted as z-S1-210-P1 signifies type of polymer (z-LLDPE), Pass-zero stabilised formulation number (S1), multi-pass extrusion temperature (210) and the pass (pass 1).

Table 2.9 **Preliminary stabilisation work using formulations s4, s11 and s13**. Sample codes and conditions used for twin-screw multi-pass extrusion experiment (extrusion temperatures 285°C, screw speed of 50-200rpm under atmospheric conditions) of **Pass-zero stabilised m-LLDPE and z-LLDPE**. Initially compounded (Po) the polymer under nitrogen at 210°C at 100rpm.

Code Number	Total Conc. /ppm wt/wt ratio	Polymer	Code <sup>3</sup>	Extrusion Passes	Screw speed /rpm	Die Temp/°C (multi-pass extrusion)
<b>S4</b> 1076:399	2500 1:4	Metallocene	m-S4-285-P1	1	100	285
			m-S4-285-P3	3		
			m-S4-285-P5	5		
<b>S11</b> E201:U626:TMP	1350 1:2:1.5		m-S11-285-P3	1	100	285
			m-S11-285-P3	3		
			m-S11-285-P5	5		
<b>S13</b> E201:U626:TMP	1350 1:2:1.5		m-S13-285-P3	1	50	285
			m-S13-285-P3	3		
			m-S13-285-P5	5		
			m-S13-285-P3	1	100	285
			m-S13-285-P3	3		
			m-S13-285-P5	5		
			m-S13-285-P3	1	200	285
			m-S13-285-P3	3		
			m-S13-285-P5	5		
<b>S4</b> 1076:399	2500 1:4	Ziegler	z-S4-285-P1	1	100	285
			z-S4-285-P3	3		
			z-S4-285-P5	5		
<b>S11</b> E201:U626:TMP	1350 1:2:1.5		z-S11-285-P3	1	100	285
			z-S11-285-P3	3		
			z-S11-285-P5	5		
<b>S13</b> E201:399:TMP	1350 1:2:1.5		z-S13-285-P3	1	50	285
			z-S13-285-P3	3		
			z-S13-285-P5	5		
			z-S13-285-P3	1	100	285
			z-S13-285-P3	3		
			z-S13-285-P5	5		
			z-S13-285-P3	1	200	285
			z-S13-285-P3	3		
			z-S13-285-P5	5		

<sup>3</sup> Code denoted as m-S1-210-P1 signifies type of polymer (m-LLDPE), Pass-zero stabilised formulation number (S1), multi-pass extrusion temperature (210) and the pass (pass 1).

Table 2.10. Sample codes and conditions used for twin-screw multi-pass extrusion experiment (extrusion temperatures 260°C, screw speed of 100rpm under atmospheric conditions) of **Pass-zero stabilised m-LLDPE containing single antioxidant formulations – s14 to s21**. Initially compounded (Po) the polymer under nitrogen at 210°C at 100rpm.

Code Number	Total Concentration/ ppm	Polymer	Code <sup>4</sup>	Extrusion Passes	Screw speed /rpm	Die Temp/°C
<b>S14</b> Irg.1076	500	Metallocene	m-S14-260-P1	1	100	100
			m-S14-260-P3	3		
			m-S14-260-P5	5		
<b>S15</b> HP 136	300		m-S15-260-P1	1	100	100
			m-S15-260-P3	3		
			m-S15-260-P5	5		
<b>S16</b> Irgs. FS042	1000		m-S16-260-P1	1	100	100
			m-S16-260-P3	3		
			m-S16-260-P5	5		
<b>S17</b> Tin. 765	1000		m-S17-260-P1	1	100	100
			m-S17-260-P3	3		
			m-S17-260-P5	5		
<b>S18</b> Tin. 622LD	1000		m-S18-260-P1	1	100	100
			m-S18-260-P3	3		
			m-S18-260-P5	5		
<b>S19</b> Irg. E201	300		m-S19-260-P1	1	100	100
			m-S19-260-P3	3		
			m-S19-260-P5	5		
<b>S20</b> Weston 399	2000		m-S20-260-P1	1	100	100
			m-S20-260-P3	3		
			m-S20-260-P5	5		
<b>S21</b> Chims 119	1000	m-S21-260-P1	1	100	100	
		m-S21-260-P3	3			
		m-S21-260-P5	5			

<sup>4</sup> Code denoted as m-S14-260-P1 signifies type of polymer (m-LLDPE), Pass-zero stabilised formulation number (S14), multi-pass extrusion temperature (260) and the pass number (pass 1).



Table 2.11. Sample codes and conditions used for twin-screw multi-pass extrusion experiment (extrusion temperatures 260°C, screw speed of 100rpm under atmospheric conditions) of **Pass-zero stabilised m-LLDPE containing combination antioxidant formulations – s22 to s32**. These were initially compounded (Po) in the polymer under nitrogen at 210°C at 100rpm.

Code Number	Total Concentration /ppm wt/wt ratio	Polymer	Code	Extrusion Passes	Screw speed /rpm	Die Temp/°C
<b>S22</b> 1076+HP136+W399	2800 1.7:1:6.7	Metallocene	m-S22-260-P1	1	100	260
			m-S22-260-P1	3		
			m-S22-260-P5	5		
<b>S23</b> 1076+HP136+W399+TMP	3250 1.7:1:6.7		m-S23-260-P1	1	100	260
			m-S23-260-P1	3		
			m-S23-260-P5	5		
<b>S24</b> 1076+HP136+W399	4300 5:1:8.3		m-S24-260-P1	1	100	260
			m-S24-260-P1	3		
			m-S24-260-P5	5		
<b>S25</b> 1076+HP136+W399	2300 1.7:1:3		m-S25-260-P1	1	100	260
			m-S25-260-P1	3		
			m-S25-260-P5	5		
<b>S26</b> FS042+E+U626+TMP	1850 1:1.7:2		m-S26-260-P1	1	100	260
			m-S26-260-P1	3		
			m-S26-260-P5	5		
<b>S27</b> FS042+E+U626+TMP	2350 1:3.3:2		m-S27-260-P1	1	100	260
			m-S27-260-P1	3		
			m-S27-260-P5	5		
<b>S11</b> E+U626+TMP	1350 1:2:1.5		m-S11-260-P1	1	100	260
			m-S11-260-P1	3		
			m-S11-260-P5	5		
<b>S28</b> 1076+FS042+W399	3000 1:1:4		m-S28-260-P1	1	100	260
			m-S28-260-P1	3		
			m-S28-260-P5	5		
<b>S29</b> 1076+FS042+W399	3500 1:2:2		m-S29-260-P1	1	100	260
			m-S29-260-P1	3		
			m-S29-260-P5	5		
<b>S30</b> 1076+FS042+T765+W399	4000 1:1:4:2		m-S30-260-P1	1	100	260
			m-S30-260-P1	3		
			m-S30-260-P5	5		
<b>S31</b> 1076+FS042+T622LD+W399	4000 1:1:4:2		m-S31-260-P1	1	100	260
			m-S31-260-P1	3		
		m-S31-260-P5	5			
<b>S32</b> 1076+FS042+C119+W399	4000 1:1:4:2	m-S32-260-P1	1	100	260	
		m-S32-260-P1	3			
		m-S32-260-P5	5			
<b>S4</b> 1076+W399	2500 1:4	m-S4-260-P1	1	100	260	
		m-S4-260-P1	3			
		m-S4-260-P5	5			

Table 2.12. Sample codes and conditions used for twin-screw multi-pass extrusion experiment (extrusion temperatures 260°C, screw speed of 100rpm under atmospheric conditions) of **Pass-zero stabilised m-LLDPE containing combinations of antioxidant formulations based on XP-60 and XP-490 systems (s33 to s42)**. These were initially compounded (Po) in the polymer under nitrogen at 210°C at 100rpm. Formulation s4 used for comparison.

Code Number	Total Concentration /ppm wt/wt ratio	Polymer	Code	Extrusion Passes	Screw speed /rpm	Die Temp/°C
<b>XP-60 based Systems</b>						
<b>S33</b> XP-60	861 1:2.3	Metallocene	m-S33-260-P1	1	100	260
			m-S33-260-P1	3		
			m-S33-260-P5	5		
<b>S34</b> HP136+U626	861 1:2.3		m-S34-260-P1	1	100	260
			m-S34-260-P1	3		
			m-S34-260-P5	5		
<b>S35</b> HP136+PEPQ	1435 1:2.3		m-S35-260-P1	1	100	260
			m-S35-260-P1	3		
			m-S35-260-P5	5		
<b>S36</b> HP136+Dover.S9228	1230 1:2.3		m-S36-260-P1	1	100	260
			m-S36-260-P1	3		
			m-S36-260-P5	5		
<b>S37</b> HP136+W399	1722 1:2.3	m-S37-260-P1	1	100	260	
		m-S37-260-P1	3			
		m-S37-260-P5	5			
<b>XP-490 based Systems</b>						
<b>S38</b> XP-490	2870 1:2.3:3.3	Metallocene	m-S38-260-P1	1	100	260
			m-S38-260-P1	3		
			m-S38-260-P5	5		
<b>S39</b> 1076+HP136+PEPQ	2870 1:2.3:3.3		m-S39-260-P1	1	100	260
			m-S39-260-P1	3		
			m-S39-260-P5	5		
<b>S40</b> 1076+HP136+U626	1720 1:2.3:3.3		m-S40-260-P1	1	100	260
			m-S40-260-P1	3		
			m-S40-260-P5	5		
<b>S41</b> 1076+HP136+Dover.S9228	2470 1:2.3:3.3		m-S41-260-P1	1	100	260
			m-S41-260-P1	3		
			m-S41-260-P5	5		
<b>S42</b> 1076+HP136+W399	3820 1:2.3:3.3	m-S42-260-P1	1	100	260	
		m-S42-260-P1	3			
		m-S42-260-P5	5			
<b>S4</b> 1076+W399	2500 1:4	m-S4-260-P1	1	100	260	
		m-S4-260-P1	3			
		m-s4-260-P5	5			

Table 2.13. Sample codes and conditions used for twin-screw multi-pass extrusion experiment (extrusion temperatures 260°C, screw speed of 100rpm under atmospheric conditions) of Pass-zero stabilised m-LLDPE containing combinations of antioxidant formulation based on Vitamin E systems (s43 to s49). These were initially compounded (Po) in the polymer under nitrogen at 210°C at 100rpm.

Code Number	Total Concentration /ppm wt/wt ratio	Polymer	Code	Extrusion Passes	Screw speed /rpm	Die Temp/°C	
<b>Vitamin E based Systems</b>							
<b>S43</b> E201+HP136+PEPQ	1735 <b>1:0.7:2.3</b>	Metallocene	m-S43-260-P1	1	100	260	
			m-S43-260-P1	3			
			m-S43-260-P5	5			
	<b>S44</b> E201+HP136+U626		1160 <b>1:1.1:2.3</b>	m-S44-260-P1	1	100	260
				m-S44-260-P1	3		
				m-S44-260-P5	5		
	<b>S45</b> E201+HP136+U626+TMP		1660 <b>1:1.1:2.3</b>	m-S45-260-P1	1	100	260
				m-S45-260-P1	3		
				m-S45-260-P5	5		
	<b>S46</b> E201+HP136+D.S9228		1535 <b>1:0.8:2.3</b>	m-S46-260-P1	1	100	260
				m-S46-260-P1	3		
				m-S46-260-P5	5		
	<b>S47</b> E201+HP136+W399		2710 <b>1:0.5:2.3</b>	m-S47-260-P1	1	100	260
				m-S47-260-P1	3		
				m-S47-260-P5	5		
	<b>S48</b> E201+HP136+W399+ZnSt		2210 <b>1:0.5:2.3</b>	m-S48-260-P1	1	100	260
				m-S48-260-P1	3		
				m-S48-260-P5	5		
<b>S49</b> E201+U626+ZnSt	1400 <b>1:2</b>	m-S49-260-P1	1	100	260		
		m-S49-260-P1	3				
		m-S49-260-P5	5				

## 2.3 Sample Preparation and Analysis

### a. Polymer plaques for Colour analysis.

Extruded LLDPE polymer samples, using the Betol TSE, were pressed into plaques for colour analysis. The plaques were prepared by compression moulding using an electric Daniels press machine. Approximately 7g of the processed LLDPE polymer sample was placed in each of the 9 compartments of a mould which was  $5 \times 5 \text{cm}^2$  and 3mm in depth. The whole mould was wrapped in a special high temperature grade cellophane film and placed between two stainless steel metal plates (thoroughly cleaned before to ensure a smooth surface). The whole preparation was then placed in a Daniels press set at  $160^\circ\text{C}$  and the polymer was preheated for 3.5min without applying any pressure. The samples were then subjected to full pressure for 1.5min, followed, by cooling to  $100^\circ\text{C}$  and finally by quenching of the polymer in cold water. Three plaques were prepared for each processed polymer sample and stored in a cool dark place.

The plaques were then analysed using ASTM 1925 method for colour, using a Minolta CM5081 spectrophotometer, taken with the settings as illuminate C and an observer angle of  $2^\circ$ . Colour measurements, were targeted against a white background, and the YI (Yellow index) measurement was taken. For example,  $\text{YI}_1 = 7.00$ ,  $\text{YI}_2 = 7.66$  and  $\text{YI}_3 = 7.38$ , hence the average YI was taken as 7.35 with a standard deviation of 0.8. The % experimental error of these colour plaques, YI data, obtained from the three average readings for each plaque of the triplicate samples was found to be between 4-5%.

### b. Polymer films for FTIR analysis

Virgin LLDPE samples were pressed to thin films for infrared analysis. The films were prepared by compression moulding, using an electric Daniels press machine. About 2.5g of polymer sample was used for films of up to 0.25mm thickness. The polymer sample was placed between a paper spacer of  $10 \times 15 \text{cm}^2$  surface and 0.2mm thickness. The resulting preparation was placed between two polished stainless steel plates, which were thoroughly cleaned before use to ensure a smooth surface and laminated with smooth PTFE coated glass fabric sheets to prevent the polymer from sticking to the plates. First the polymer sample was preheated for 3min without pressure at  $150^\circ\text{C}$  and then a pressure of  $120 \text{kg.cm}^{-2}$  was applied for 1.5min. Finally, the sample was cooled down to  $100^\circ\text{C}$  under full pressure using cold running water, before taking it out.

Films of 0.1 to 0.25mm thickness were then cut out for infrared analysis. All infra red analysis was carried out on a Perkin Elmer 1710 Fourier Transform spectrophotometer.

## 2.4 Rheology

### a. Melt Flow Index (MFI)

The melt flow index (MFI) is defined as the mass (g) of the molten polymer extruded through a standard die in a given time (normally 10 minutes) based on ASTM D-1238. The measurement of the melt viscosity of the polymer is inversely proportional to the molecular weight of the polymer, hence its MFI gives an indication of the extent of degradation after processing, i.e. melt stability. The MFI of virgin, processed stabilised and unstabilised LLDPE samples were examined. About 2g of each of the LLDPE polymer samples were measured on a Davenport melt flow indexer, (see figure 2.3) at a constant temperature of  $190^{\circ}\text{C} \pm 0.1^{\circ}\text{C}$ . The barrel of the indexer was charged with the material using a charging tool to exclude air and, at that moment, the stopwatch was started ( $t = 0\text{min}$ ). The charging time did not exceed one minute. A piston was placed on top of the sample and the sample was left to reach an equilibrium temperature ( $t = 5\text{min}$ ). A load of 2.16kg (low load melt index, MI) or 21.6kg (high load melt index, HLMI) was then placed on top of the piston to extrude the molten polymer through a die (internal diameter of  $2.0955\text{mm} \pm 0.0051\text{mm}$ ). For MI measurements, each extrudate was cut off after 60 seconds. For HLMI measurements, each extrudate was cut off after 10 seconds. For both MI and HLMI measurements, five successive cut-offs (after 60 or 10 seconds for MI and HLMI respectively) were taken. All extrudates were weighed and an average MI or HLMI was calculated from the amount of polymer melt (in grams), which passed through the die within a set period, i.e. 10 seconds or 1 minute, using equation 2.4. Samples were done in triplicate to establish the experimental error. For example,  $\text{MI}_1 = 1.02$ ,  $\text{MI}_2 = 1.00$  and  $\text{MI}_3 = 0.98$ , hence the average MI was taken as  $1.00 \pm 0.05$  (g/10min). And, for example,  $\text{HLMI}_1 = 31.4$ ,  $\text{HLMI}_2 = 32.8$  and  $\text{HLMI}_3 = 31.3$ , hence the average HLMI was taken as  $31.8 \pm 0.8$  (g/10min). Thus, the %, MI and HLMI experimental error was found to be between 2% and 2-3% respectively. The melt flow ratio (MFR, according to equation 2.5) and % MI change or %HLMI change were calculated using equation 2.6. It is important to note here that the more negative % MI or HLMI value would reflect a higher extent of crosslinking of the polymer (during extrusion), whereas, a more positive value would indicate overall chain scission.

$$\text{MI or HLMI} = 10 \cdot \frac{m}{t} \text{ (g/10min)} \quad (2.4)$$

$$\text{MFR} = \text{HLMI} / \text{MI} \quad (2.5)$$

$$\% \text{ HLMI change or MI change} = (\text{MI}_{\text{sample}} - \text{MI}_{\text{virgin}}) / \text{MI}_{\text{virgin}} * 100 \quad (2.6)$$

Where:-

m is the average weight of the extrudates (g).

t is time of extrusion (min).

MFR is the melt flow ratio.

HLMI is the high load melt flow index (g/10min)

MI is the low load melt flow index (g/10min)

MI<sub>sample</sub> is the low load melt flow index of a stabilised sample (g/10min)

MI<sub>virgin</sub> is the low melt flow index of the virgin sample (g/10min)

% HLMI is the change in HLMI between a stabilised and virgin sample.

% MI is the change in MI between a stabilised and virgin sample.

#### b. Twin Bore Capillary Rheometry

The rheological characteristics of virgin/stabilised metallocene and Ziegler LLDPE granules were measured in a Rosand twin bore capillary rheometer RH2000 (see figure 2.4) controlled by computer software (REO 7.0). All test parameters barrel temperature, die diameter and shear rate range were entered *via* the computer interface. Amplifiers were calibrated and autozeroed, dies for the two barrels; (1) long die, 16mm length with a 1mm diameter (2) zero length die, 0mm length, 1mm diameter; were used for the Bagley correction. The Bagley correction takes account of the pressure drops at the entry and exit from a capillary die.

From the values of the pressures at the long die ( $P_l$ ) and at the zero length die ( $P_0$ ), the shear stress ( $\sigma_s$ ), shear viscosity ( $\eta$ ), extensional stress ( $\sigma_E$ ), elongational viscosity ( $\eta_E$ ) and power law

index,  $n$ , (indicates the level of pseudoplasticity exhibited by the polymer, if  $n < 1$  the higher the pseudoplasticity) for each shear rate were calculated automatically by the Rosand REO 7.0 software, according to equations 2.7 to 2.11.

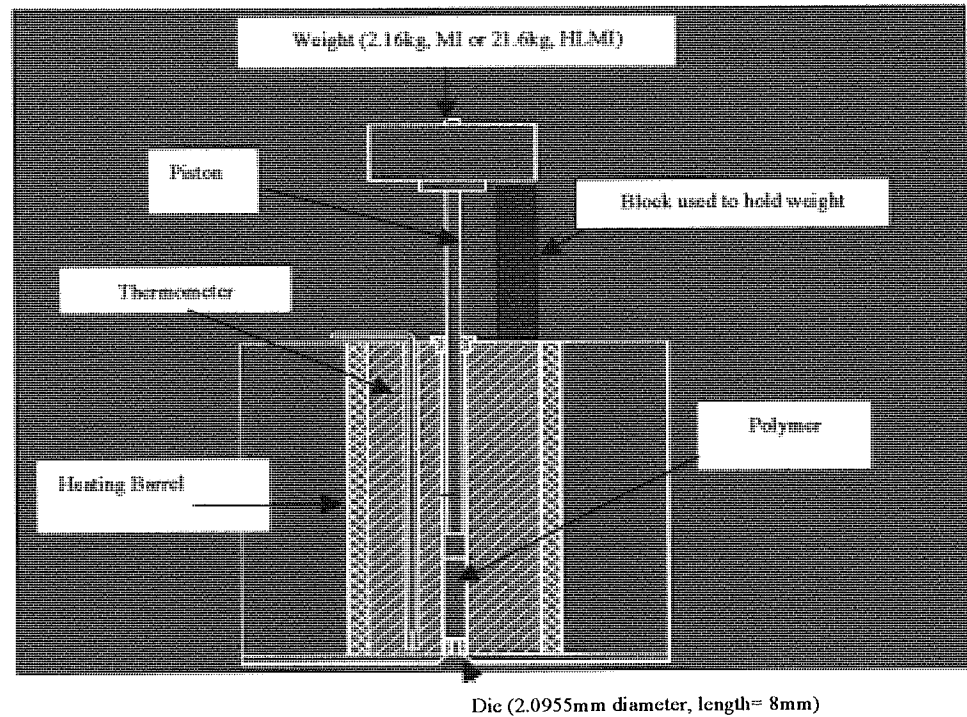


Figure 2.3. Schematic diagram of the Davenport melt flow indexer.

$$\text{Apparent shear rate } \dot{\gamma} = \frac{4Q}{\pi^3} \quad (2.7)$$

$$\text{Shear stress } \sigma_s = \frac{(P_1 - P_0)r}{2L} \quad (2.8)$$

$$\text{Shear viscosity } \eta = \frac{\sigma_s}{\dot{\gamma}} \quad (2.9)$$

$$\text{Extensional stress } \sigma_E = \frac{3}{8}(n+1)P_0 \quad \text{with } \sigma_s \propto \dot{\gamma}^n \quad (2.10)$$

$$\text{Elongational viscosity } \eta_E = \frac{9}{32} \frac{(n+1)^2}{\eta} \left( \frac{P_0}{\dot{\gamma}} \right)^2 \quad (2.11)$$

where:

Q is the volumetric flow rate of the polymer ( $\text{m}^3 \cdot \text{s}^{-1}$ )

r is the radius of the long and short die (0.5mm)

$P_1$  is the pressure measured at the long die (16mm length, 1mm diameter)

$P_0$  is the pressure measured at the zero length die (0mm length, 1mm diameter).

L is the length of each rheometric barrel (22mm)

$\eta$  is the shear viscosity at a specific shear rate.

n is the power law index.

**(i) Shear and Elongational viscosity measurements of Virgin m-LLDPE and z-LLDPE polymers.**

The capillary rheometer was used to determine the changes in shear and elongational viscosity of virgin m-LLDPE and z-LLDPE granules. All rheological experiments were carried out in the shear rate range of,  $100\text{-}2500\text{s}^{-1}$ , and at temperatures of 210, 260 or  $285^\circ\text{C}$ , simulated conditions experienced by polymers during processing. Ascending and descending of shear rates during a test run provided information as to the melt stability of the polymer during analysis. Hence, the more stable the material during the test, the narrower the hysteresis loop. Typically, two tests were carried out for each sample to cover the entire shear rate range; 100 to  $2500\text{s}^{-1}$ , in the following order:

**Test 1:** 100-150-200-250-300-350-400-450-500-600-700-600-500-400-300 $\text{s}^{-1}$

**Test 2:** 500-600-750-1000-1500-1750-2000-2500-2000-1750-1500-1250-1000-750-500 $\text{s}^{-1}$ .

**(ii) Material Degradation Test - Shear and Elongational viscosity measurements of Processed Stabilised and Unstabilised m-LLDPE polymers.**

The rheological characteristics (corrected shear stress, shear and extensional viscosity) of processed; stabilised and unstabilised m-LLDPE polymers, using a material degradation test were evaluated with the aid of the RH2000 capillary rheometer. The material degradation test involved five degradation cycles. Each cycle entailed ascending shear rate steps from 200-400-600-800-1000-1200-1400-1600 $\text{s}^{-1}$  followed by a five minute waiting time interval then similarly repeating the procedure a further four times (see figure 2.5).





Aston University

Content has been removed due to copyright restrictions

Figure 2.4 Schematic diagram of the Rosand RH2000 Twin bore capillary Rheometer .  
[Courtesy of D. Fleming “Polymer rheology – a number science”, *in Progress in rubber and plastics technology*, **12 (2)**, 674, (1996)].

All processed stabilised m-LLDPE polymer samples were initially compounded with low concentrations of antioxidants (formulations s24 and s26, table 2.11, see section 2.2) using a

Betol TSE at a screw speed of 100rpm and an extrusion temperature of 210°C under nitrogen (see table 2.5, using temperature profile number one). The stabilised m-LLDPE polymer samples were subjected to multi-pass extrusion (Passes 1 to 5) at an extrusion screw speed of 100rpm at an extrusion temperature of 210°C under atmospheric conditions.

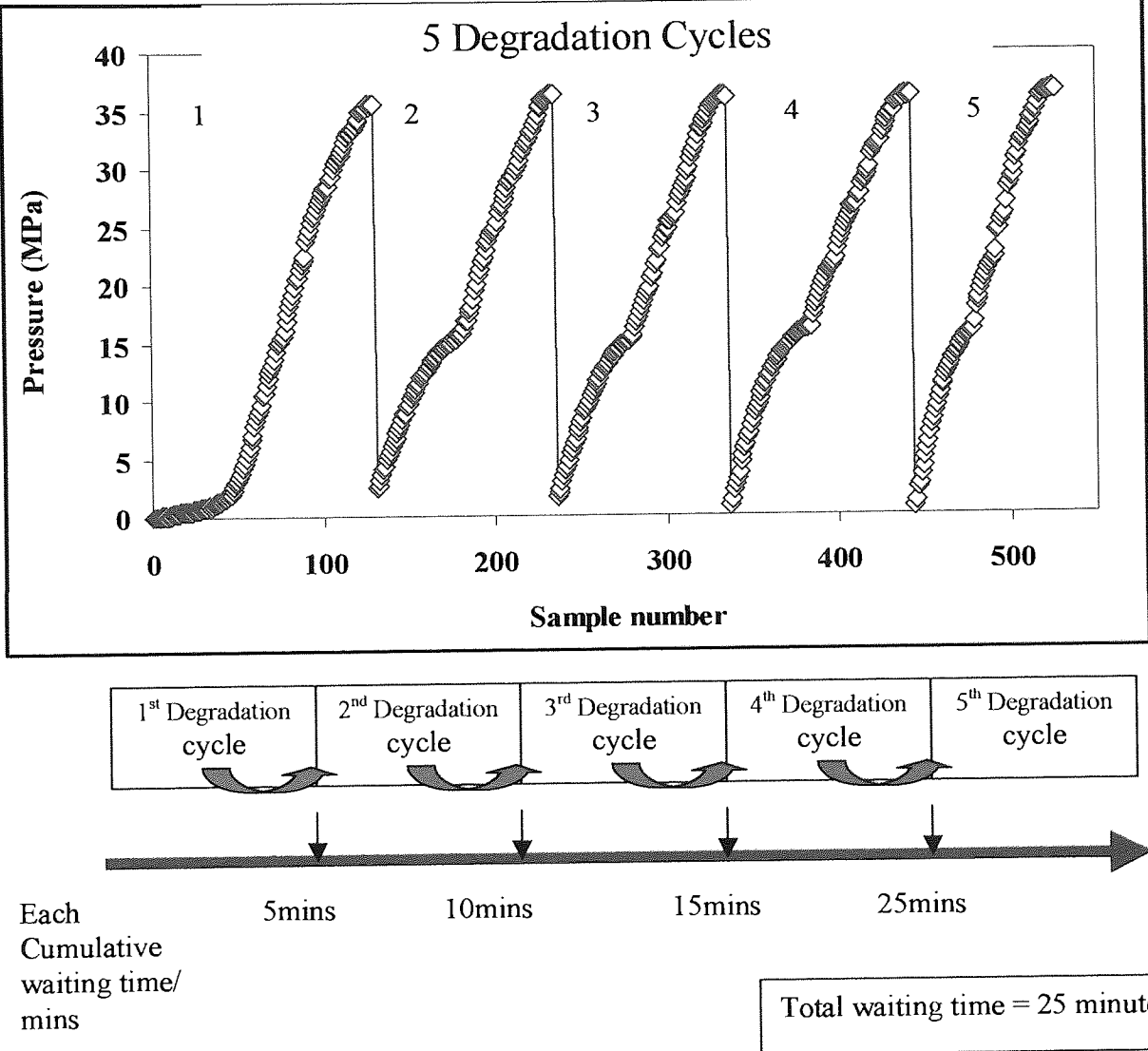


Figure 2.5 Outline of the Material degradation test of stabilised m-LLDPE polymer samples. Five degradation cycles. Each cycle entailed ascending shear rates from 200-1600s<sup>-1</sup>, followed by a 5 minute waiting time. Change in shear viscosity of the stabilised polymer was recorded.

## 2.5 Gel Permeation Chromatography (GPC)

GPC analyses of selected of m-LLDPE and z-LLDPE polymer samples virgin and processed (under varying extrusion conditions, see table 2.14-2.15) were performed by Exxon, Baytown (USA) [91]. For comparative purposes a stabilised processed sample (see s4, in table 2.7) was also examined.

LLDPE molecular weight values were calculated based upon a four part 'broad calibration'.

1. NBS 1475 (a linear PE standard from NIST, National institute of Standards and Testing) was used to calibrate over the 5,000-350,000 molecular weight range. Three runs of NBS 1475 were made and summed.
2. A series of n-alkanes (e.g. C<sub>18</sub>-C<sub>60</sub>) were used to calibrate over the 250-850 MW range.
3. Polystyrene standards were used to calibrate for MW>350,000 using the 'universal calibration' method and the following Mark-Houwink coefficients

Polymer	k(dl/g)	a
PS	$1.75 \times 10^{-4}$	0.67
PE	$5.17 \times 10^{-4}$	0.70

4. A single PE calibration curve was constructed using these 3 data sets. A series of PS standards was run and the peak retention was recorded. Hence, by entering PS results into a PE calibration curve a relationship between PS retention volume and PE equivalent MW was correlated.

Once the calibration graph had been established polymer samples were ready to be analysed. To tri-chlorobenzene (the mobile phase), 300pm of antioxidant were added. Accurately weighed polymer samples (4-6mg) were put in 4ml glass vials. This was followed by placing the vials in a hot sample carousel. The carousel was inserted into an injector compartment of the GPC instrument.

The following conditions were used to run the GPC instrument: -

- Injection and compartment, temperature 145°C.
- 1.0 ml/min flow rate.
- 50 minute run time
- 300µl injection
- 270 bar maximum pressure
- 2 hour initial delay time.
- Inject sample.

The results were automatically recorded by a PC.

Table 2.14. Sample and codes of unstabilised m-LLDPE polymer samples sent for GPC analysis; processed under varying extrusion conditions using a twin-screw extruder, under atmospheric conditions.

Code	Polymer	Number of Passes	Die Temp./°C	Screw Speed/rpm
M LL MA1-P1	Metallocene	1	210	50
M LL MA1-P3		3		
M LL MA1-P5		5		
M LL MA9-P1		1	210	200
M LL MA9-P3		3		
M LL MA9-P5		5		
m LL MA2-P1		1	235	50
m LL MA2-P3		3		
m LL MA2-P5		5		
m LL MA10-P1		1	235	200
m LL MA10-P3		3		
m LL MA10-P5		5		
m LL MA3-P1		1	260	50
m LL MA3-P3		3		
m LL MA3-P5		5		
m LL MA11-P1		1	260	200
m LL MA11-P3		3		
m LL MA11-P5		5		
m LL MA4-P1		1	285	50
m LL MA4-P3		3		
m LL MA4-P5		5		
m LL MA12-P1	1	285	200	
m LL MA12-P3	3			
m LL MA12-P5	5			

Table 2.15. Sample and codes of unstabilised z-LLDPE polymer samples sent for GPC analysis; processed under varying extrusion conditions using a twin-screw extruder, under atmospheric conditions.

Code	Polymer	Number of Passes	Die Temp./°C	Screw Speed/rpm
z LL MA1-P1	Ziegler	1	210	50
z LL MA1-P3		3		
z LL MA1-P5		5		
z LL MA9-P1		1	210	200
z LL MA9-P3		3		
z LL MA9-P5		5		
z LL MA2-P1		1	235	50
z LL MA2-P3		3		
z LL MA2-P5		5		
z LL MA10-P1		1	235	200
z LL MA10-P3		3		
z LL MA10-P5		5		
z LL MA3-P1		1	260	50
z LL MA3-P3		3		
z LL MA3-P5		5		
z LL MA11-P1		1	260	200
z LL MA11-P3		3		
z LL MA11-P5		5		
z LL MA4-P1		1	285	50
z LL MA4-P3		3		
z LL MA4-P5		5		
z LL MA12-P1		1	285	200
z LL MA12-P3		3		
z LL MA12-P5		5		

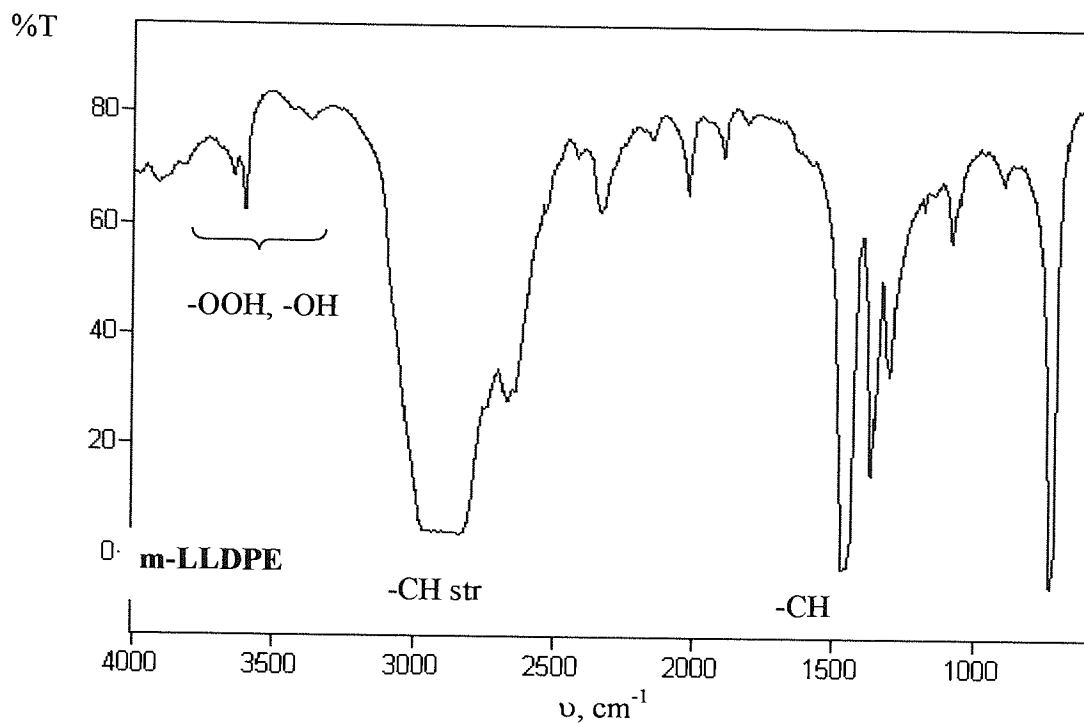


Figure 2.6: Infrared spectrum of a virgin m-LLDPE film (0.18mm thickness).

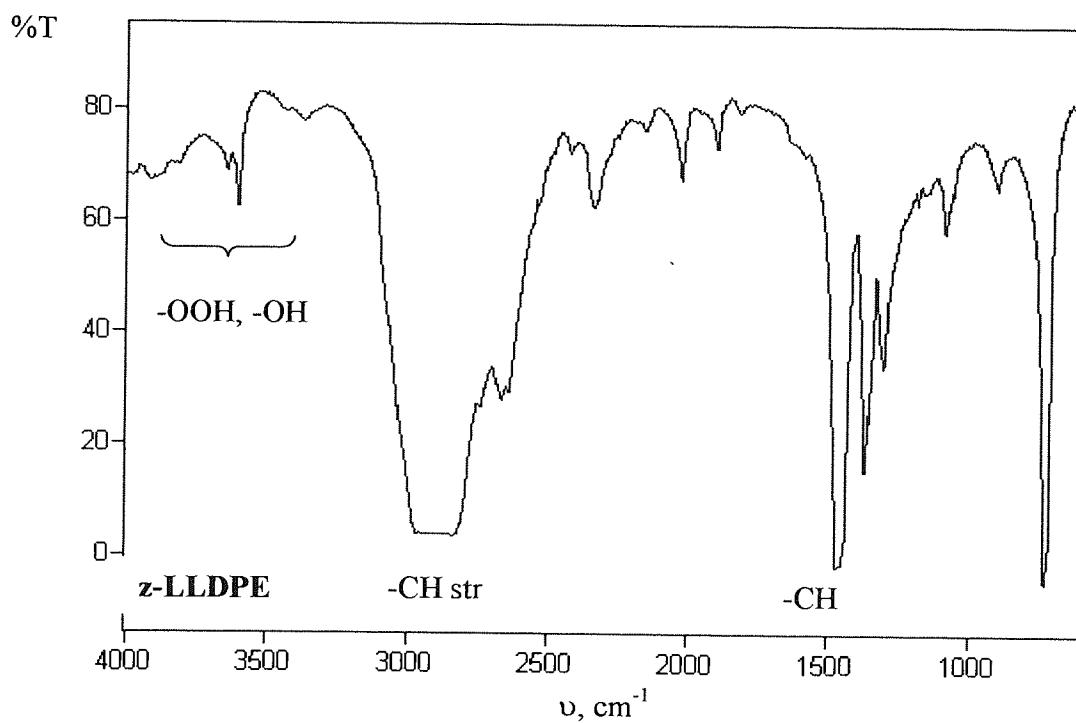


Figure 2.7: Infrared spectrum of a virgin z-LLDPE thin film (0.17mm thickness).

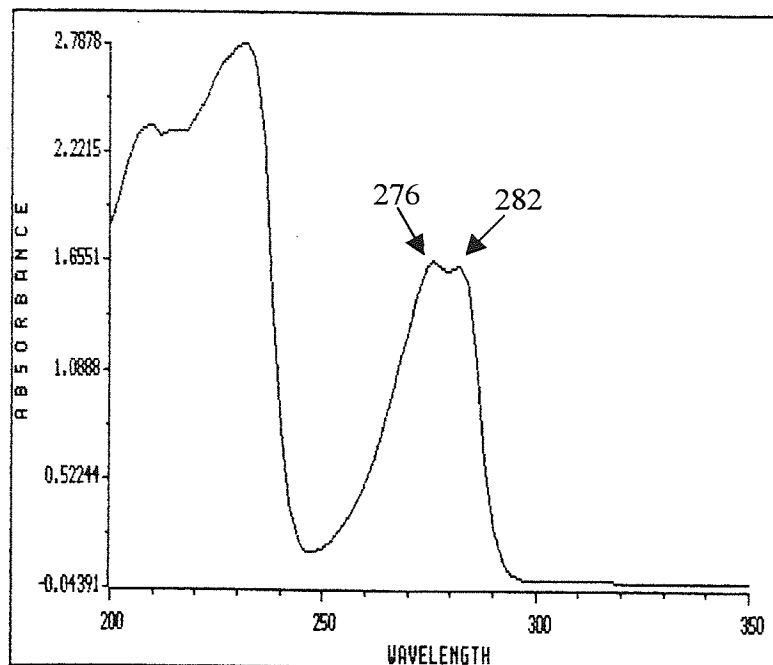


Figure 2.8a: UV spectrum of Irg.1076 in hexane.

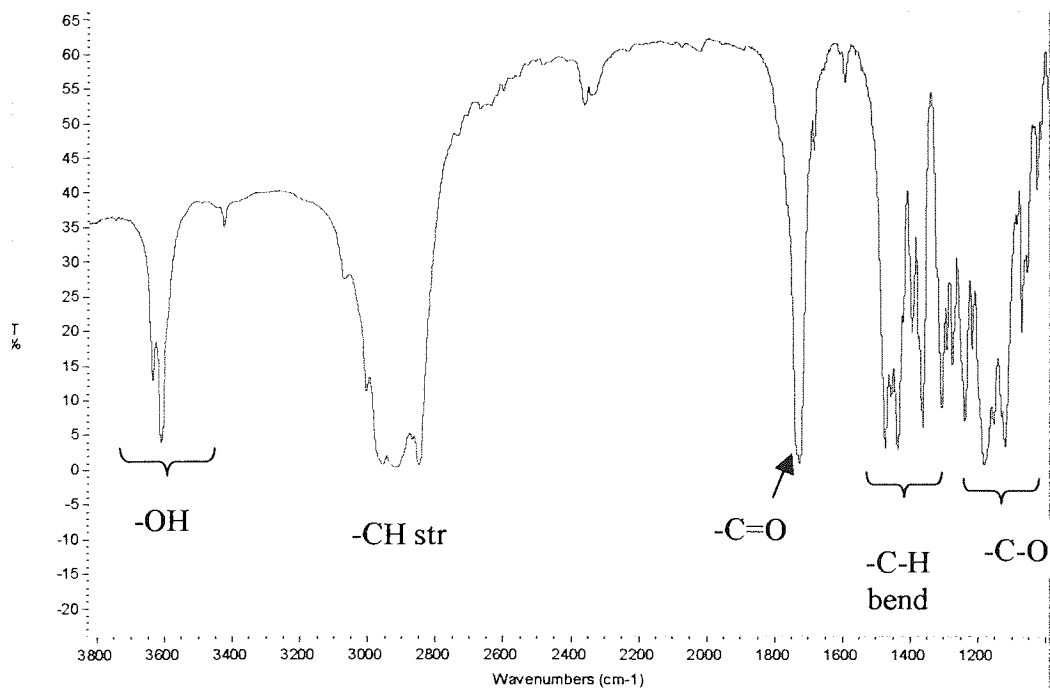


Figure 2.8b: IR spectrum of Irganox 1076, KBR windows.

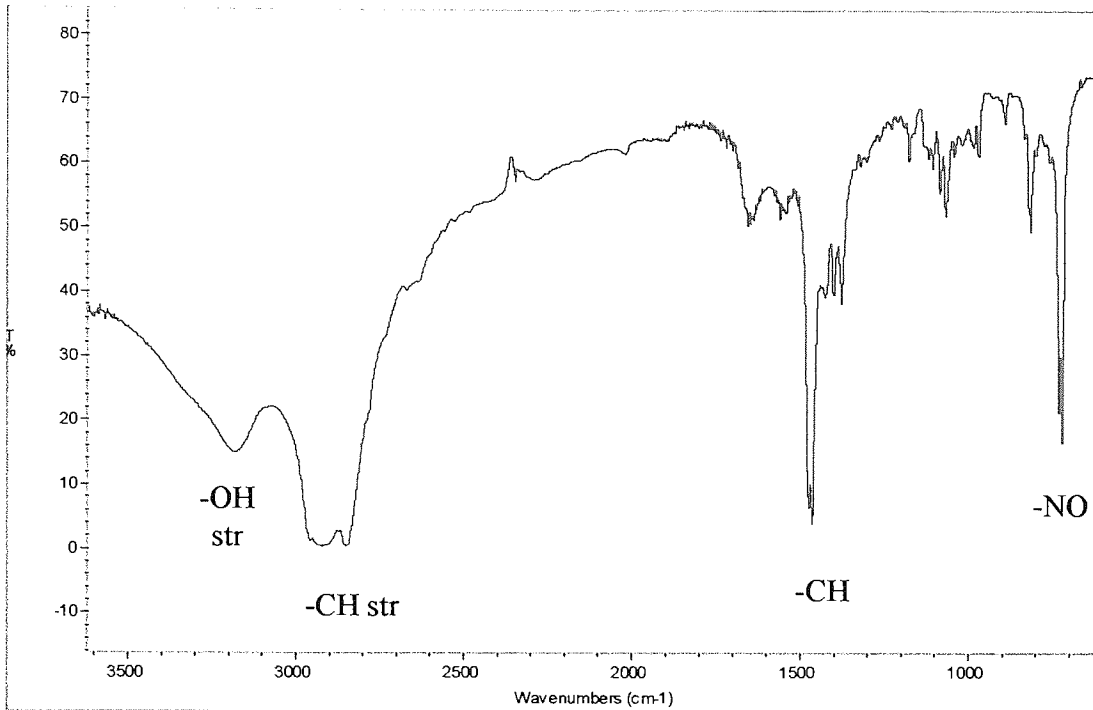


Figure 2.9: IR spectrum of Irg.FS042, KBR windows.



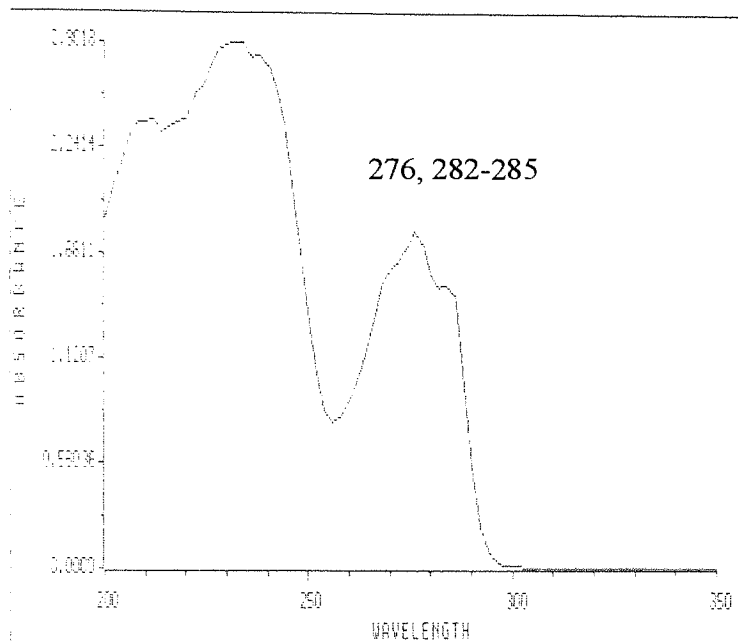


Figure 2.10a: UV spectrum of HP136 in a hexane.

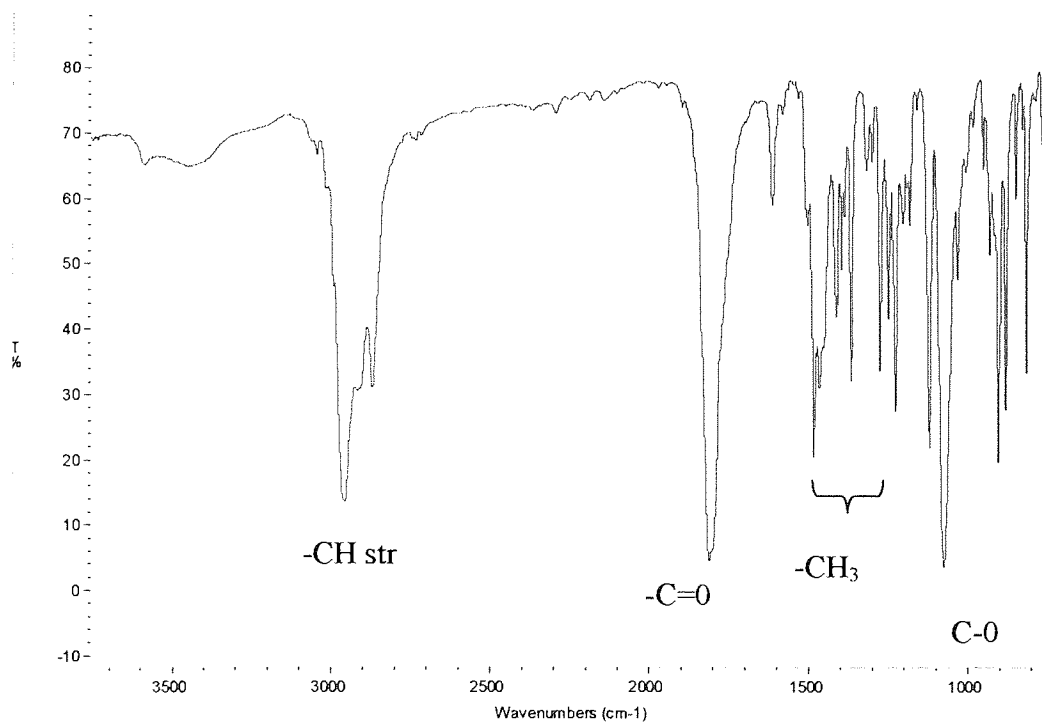


Figure 2.10b: IR spectrum of HP136, KBR windows.

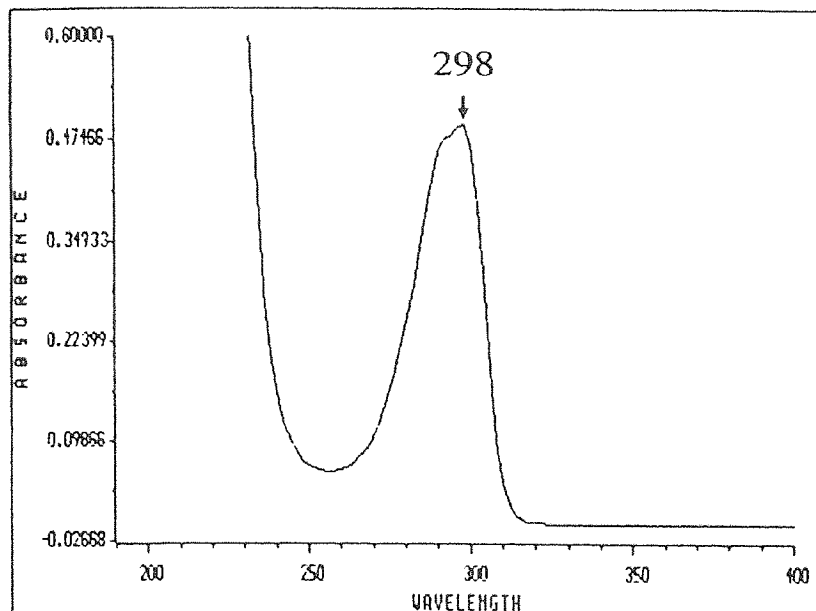


Figure 2.11a: UV spectrum of Irganox E201 in hexane.

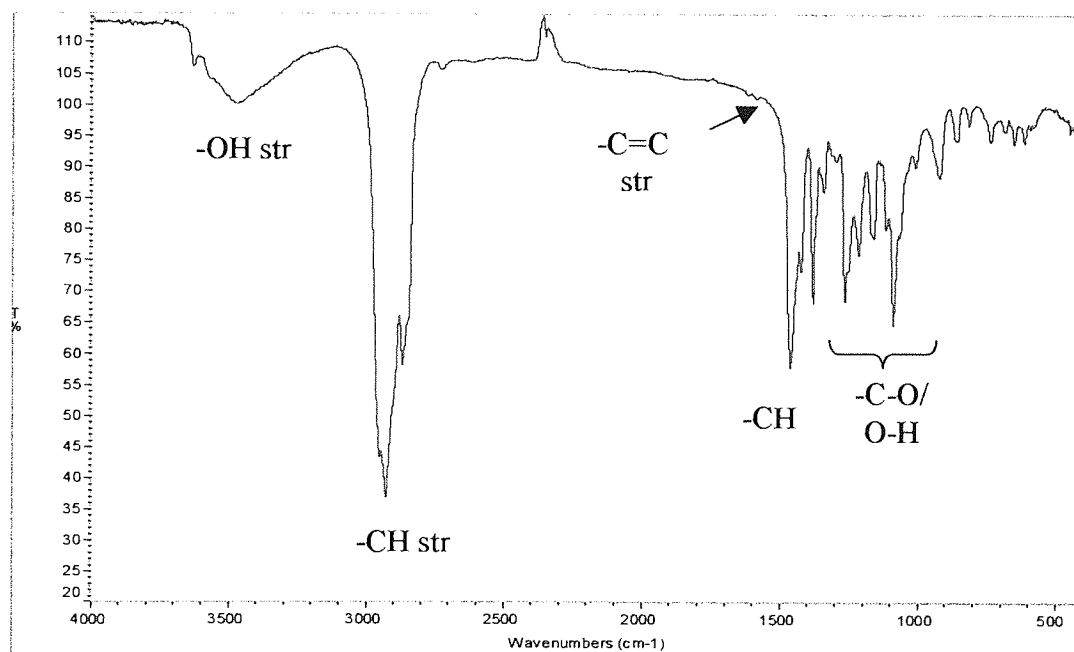


Figure 2.11b: IR spectrum of Irganox E201, KBR windows.

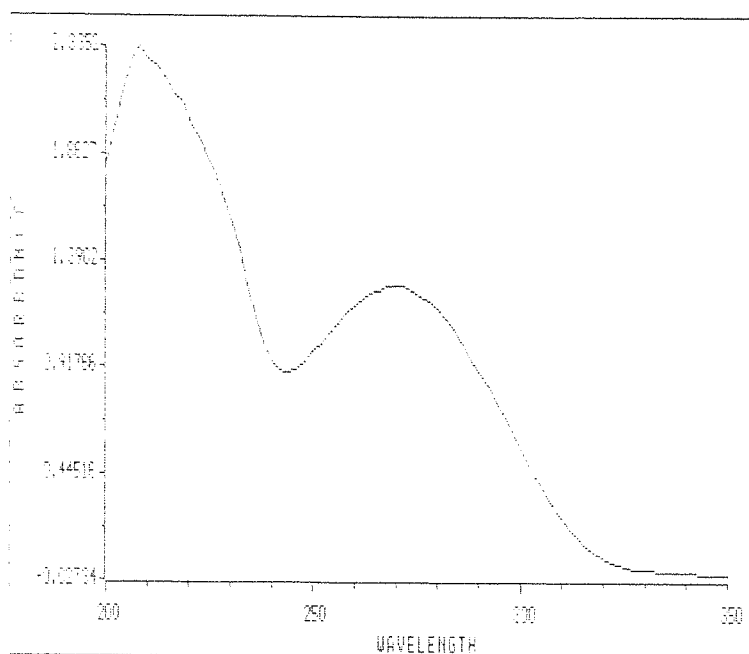


Figure 2.12a: UV spectrum of Irgafos P-EPQ in hexane. Peak at 275nm.

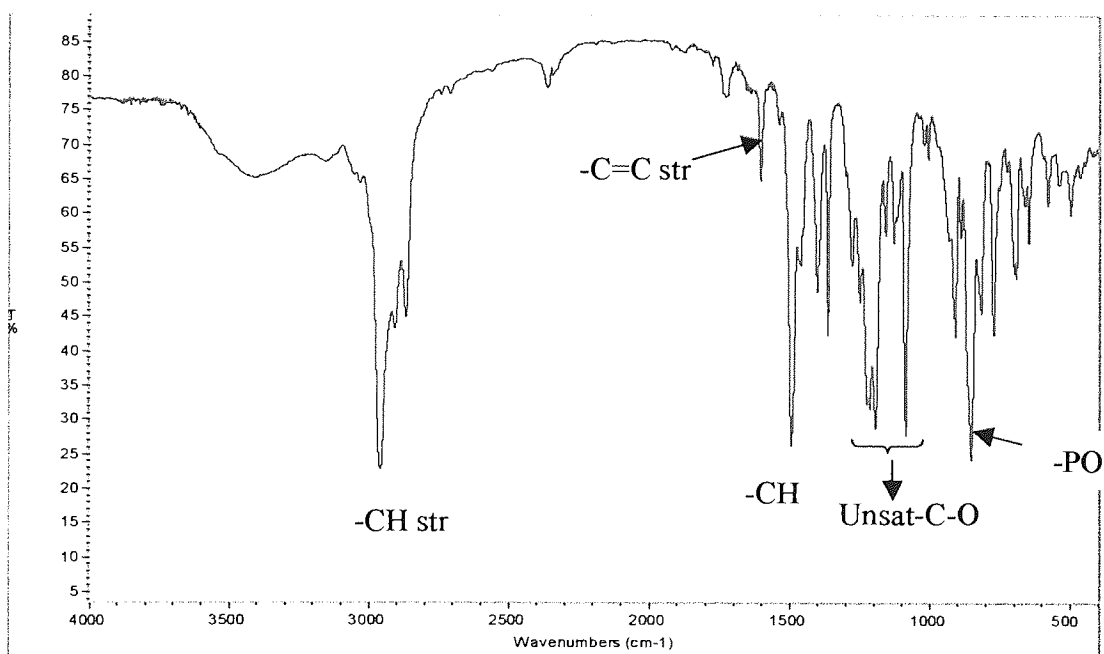


Figure 2.12b: IR spectrum of Irgafos P-EPQ, KBR windows.

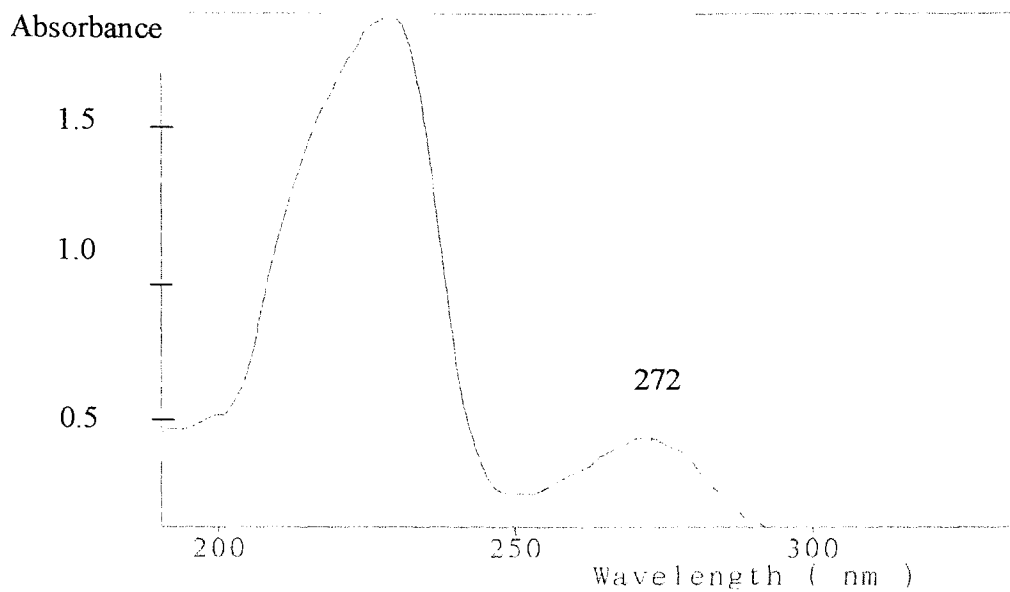


Figure 2.13a: UV spectrum of Weston 399 in hexane.

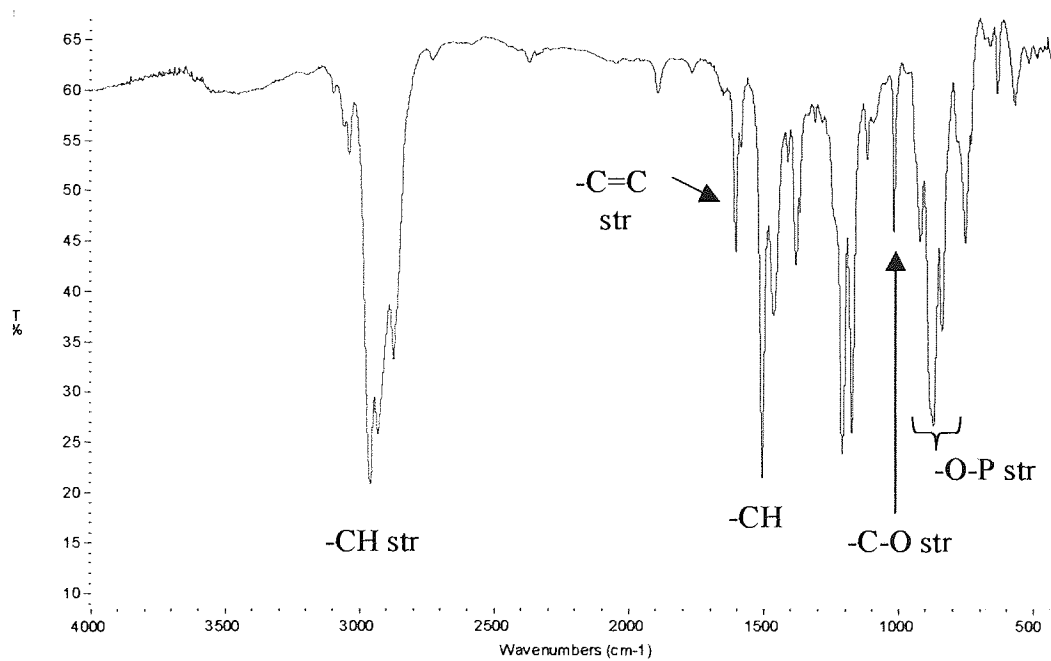


Figure 2.13b: IR spectrum of Weston 399, KBr windows.

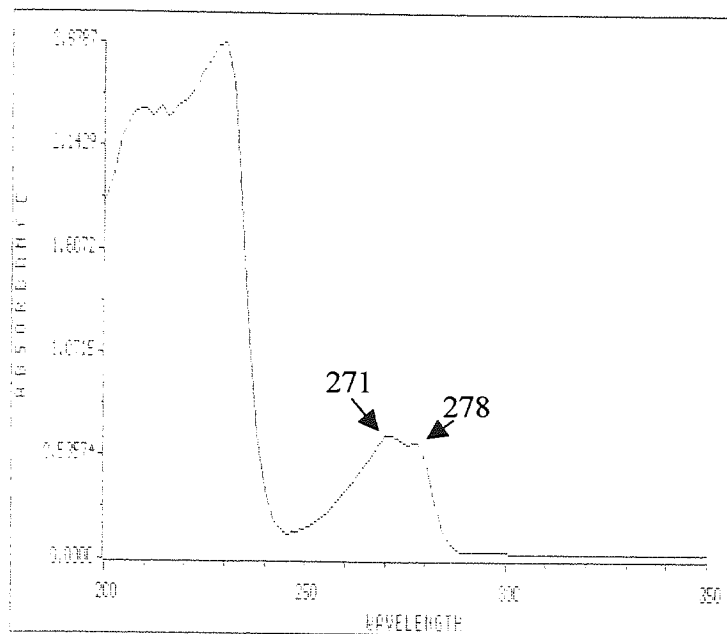


Figure 2.14a: UV spectrum of Ultrinox 626 in hexane.

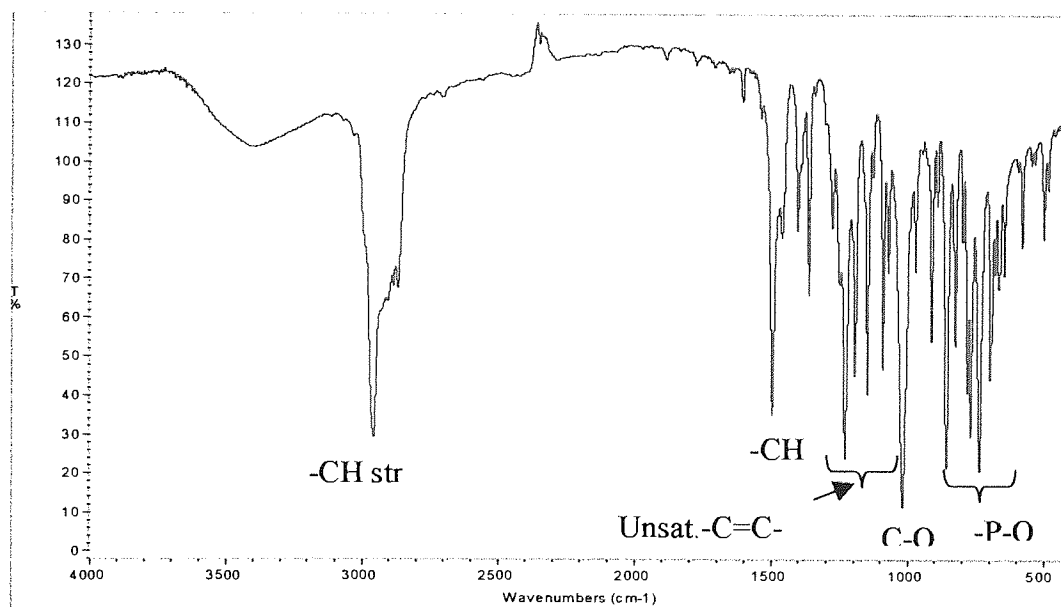


Figure 2.14b: IR spectrum of Ultrinox 626, KBr windows.

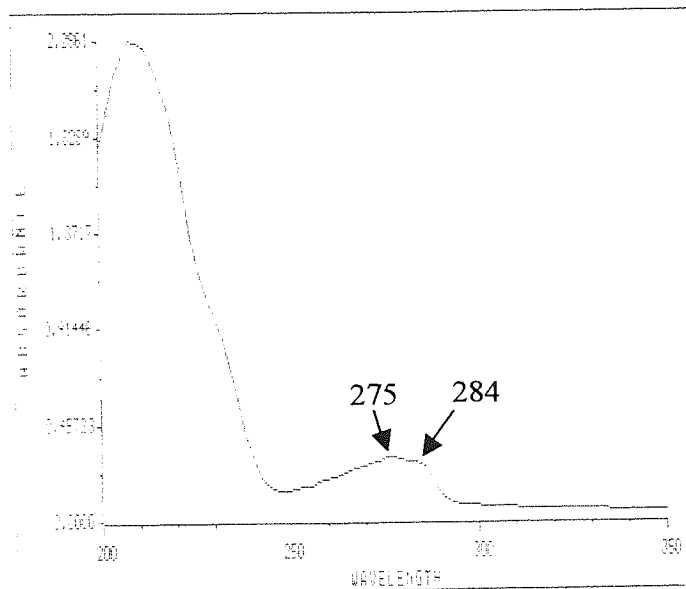


Figure 2.15a: UV spectrum of Doverphos S-9228 in hexane.

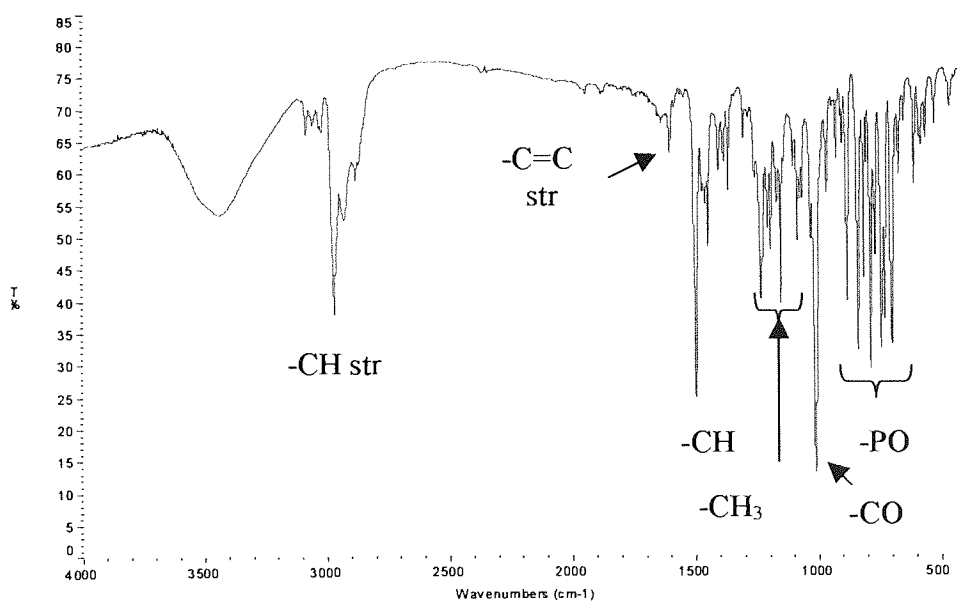


Figure 2.15b: IR spectrum of Doverphos S-9228, KBr windows.

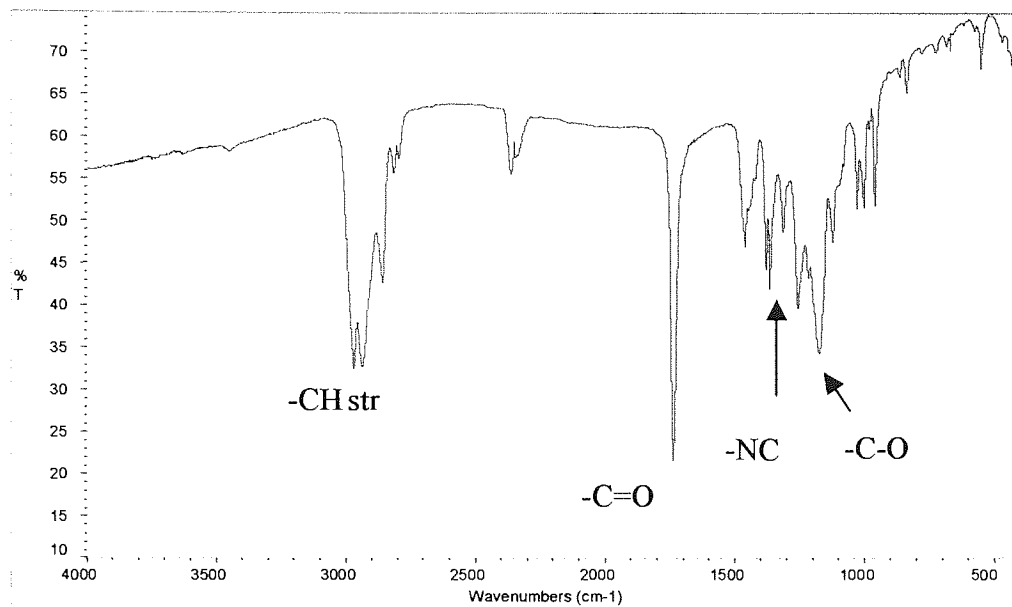


Figure 2.16: IR spectrum of Tinuvin 765, KBr windows.

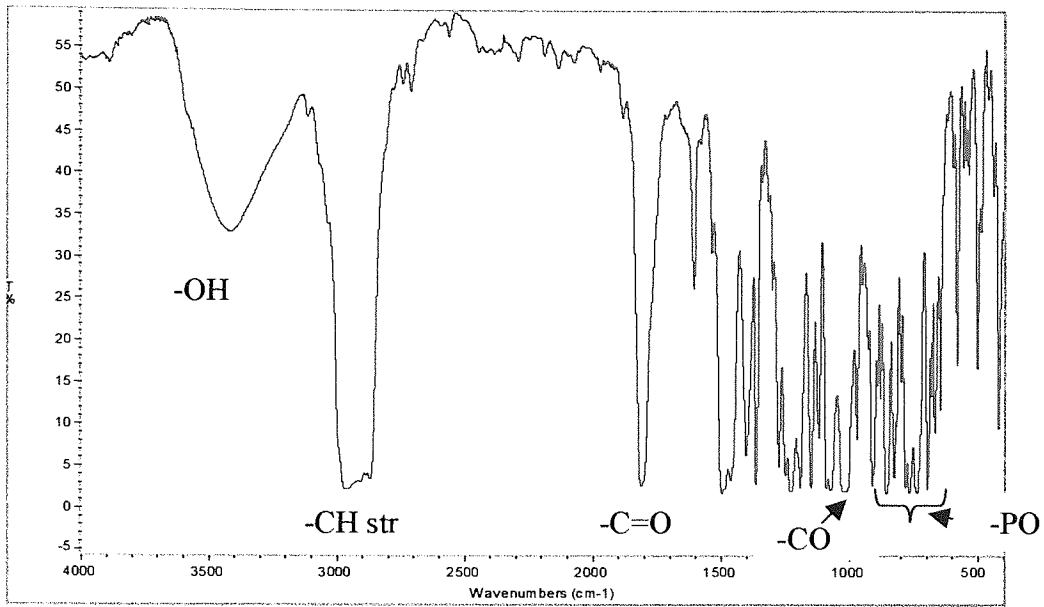


Figure 2.17: IR spectrum of XP-60, KBr windows.

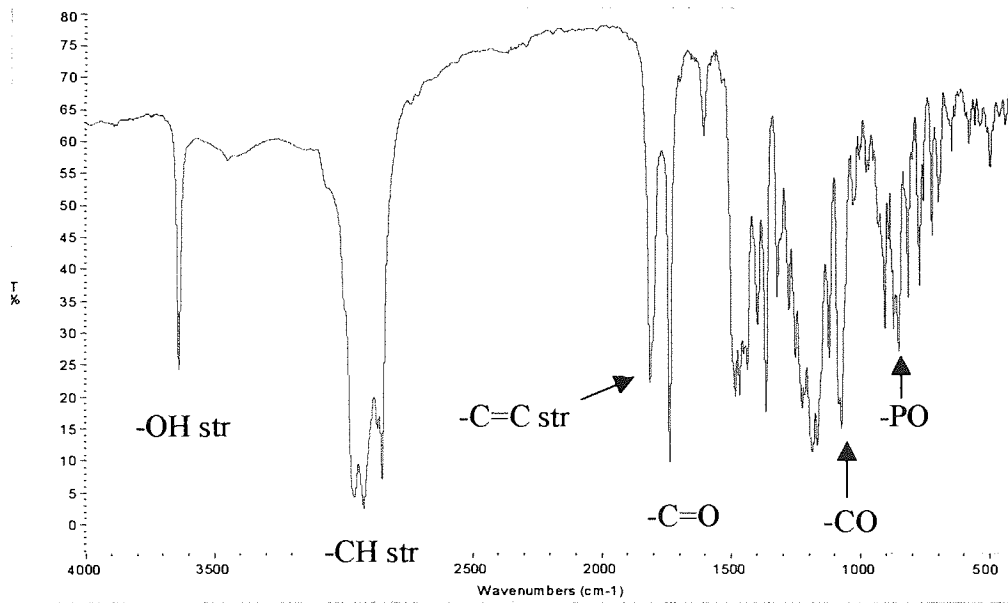


Figure 2.28: IR spectrum of XP-490, KBr windows.



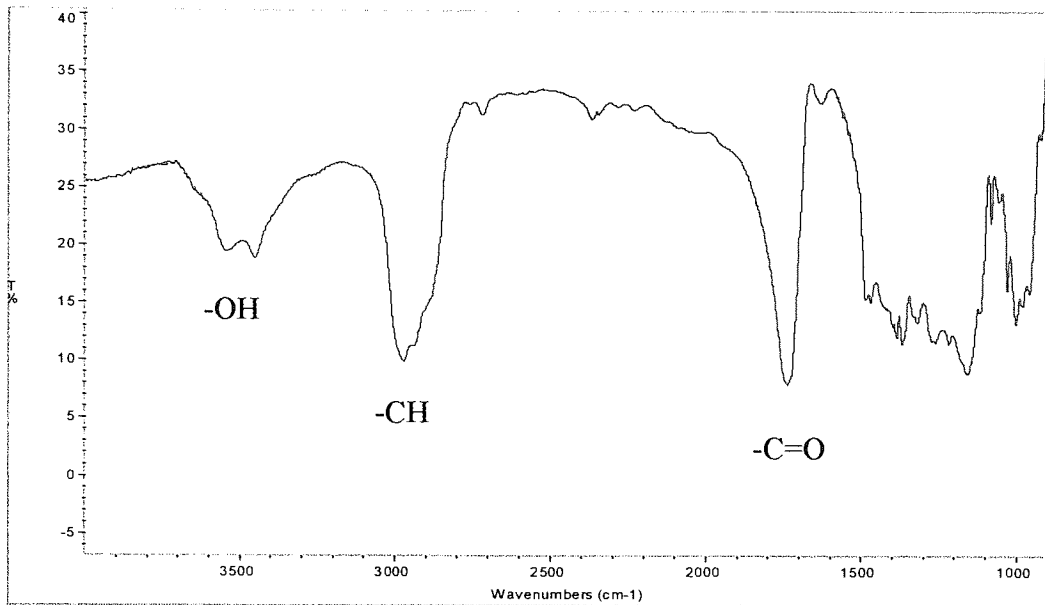


Figure 2.19: IR spectrum of Tinuvin 622LD, KBr windows.

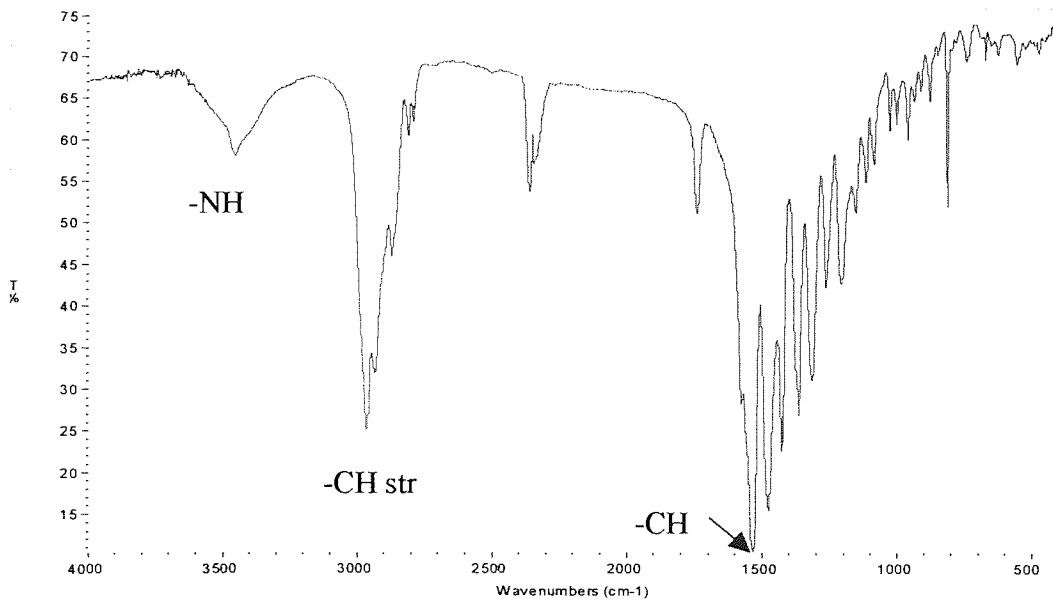


Figure 2.20: IR spectrum of Chimassorb 119D, KBr windows.

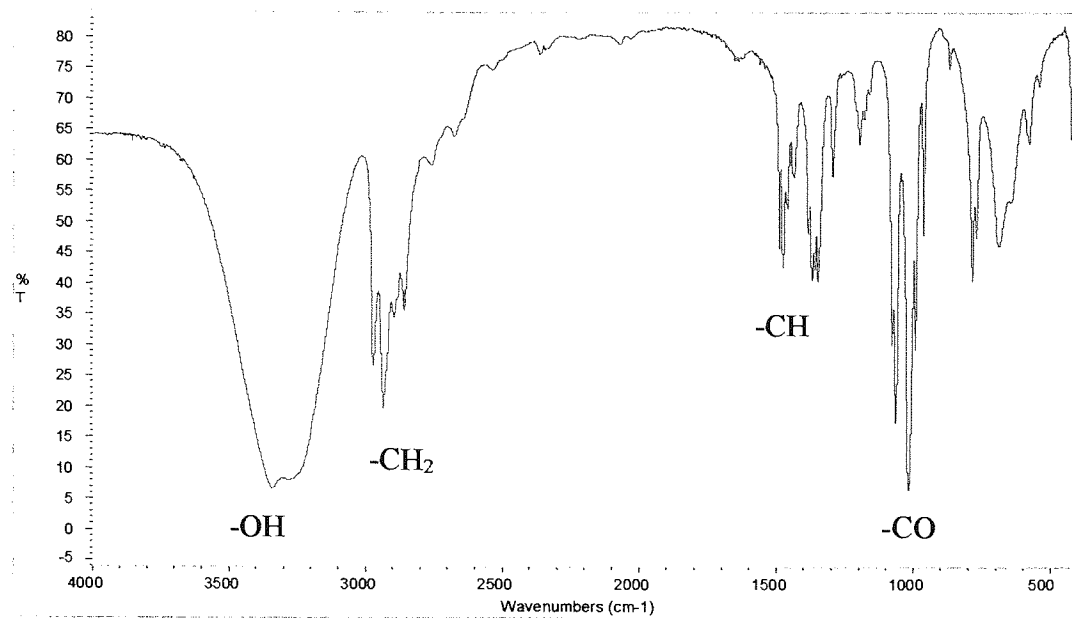


Figure 2.21: IR spectrum of TMP, KBr windows.

## **Chapter 3. Rheological and Structural Characteristics of Unstabilised, Virgin and Extruded Metallocene and Ziegler Polymers.**

### **3.1 Objectives and Methodology**

Manufacturing LLDPE into useful products such as films, for the packaging industry requires the use of high shear mixing machinery (i.e. a twin screw extruder, TSE) at elevated temperatures. A combination of high shearing, processing temperatures and small residual concentrations of oxygen can result in prominent changes in polymer structure (due to thermal oxidative degradation) thereby drastically affecting its physical and mechanical performance 'in-service'. The work described in this chapter was carried out by two researchers. The author's work (which is the subject of this thesis) on the stabilisation of m-LLDPE and z-LLDPE polymers has followed an investigation conducted by another researcher on the effect of melt extrusion on the rheological and structural characteristics of both unstabilised m-LLDPE and z-LLDPE polyethylenes [92]; the author has carried out some of the melt flow measurements of the extruded unstabilised polymers. Additional work on capillary rheometry of some of the polymer samples was also conducted as part of undergraduate projects helped by the author [93,94]. The salient findings of this work on the unstabilised polymers [92-94] are reported here in order to attain a better understanding of the stabilisation work on the same polymers described in chapters 4 and 5.

Unstabilised m-LLDPE and z-LLDPE polymers were extruded [92] in a Betol TSE using the same experimental set up used in the stabilisation work described in this work (see chapter 2). The extrusion was conducted using different temperatures (210-285°C) and varying screw speeds (50-200rpm). The rheological (melt flow and capillary rheometry) and the structural characteristics (Mw data, changes in functional groups; carbonyl, double bonds and extent of short chain branching), as well as colour changes of both of the virgin and the extruded unstabilised polymers were investigated using a range of analytical techniques [92]. The capillary rheometric measurements were conducted on m-LLDPE and z-LLDPE polymers using a Rosand twin-bore capillary rheometer using virgin, unstabilised extruded and two stabilised samples (formulation s24 and s26, see chapter 2).

## 3.2 RESULTS AND DISCUSSION

### 3.2.1 Molecular and Rheological Characteristics of Virgin m-LLDPE and z-LLDPE polymers

The structural characteristics govern the rheological behaviour of polymer melts during extrusion. Polymers are characterised by their molecular weight ( $M_w$ ) and the associated molecular weight distribution, MWD [95]. The high degree of control exerted by metallocene catalysts during the co-polymerisation of ethylene with an  $\alpha$ -olefin (e.g. 1-hexene) is known to result in a narrow MWD and uniform short chain branch distribution (SCBD), which is in direct contrast to a much wider MWD and SCBD of traditional z-LLDPE polymers [1,96]. Both MWD and branching, therefore, exert an important effect on the processing properties of polymers and their rheological characteristics (see section 1.3.1) [28,29,97]. The major differences in the molecular weight characteristics of the virgin m-LLDPE and z-LLDPE polymers used in this study are shown in table 3.1 and figure 3.1; thereby confirming the much narrower MWD of the m-LLDPE polymer. It is also clear from figure 3.1 that the m-LLDPE polymer has a much lower fraction of very high molecular weight chains (see  $\overline{M}_z$  in table 3.1) and a higher fraction of low molecular weight chains (see  $\overline{M}_n$  in table 3.1).

The viscosity or resistance to deformation, of a polymer melt under processing conditions is of great importance as it determines the ease with which a polymer is fabricated into a final product [27]. The shear viscosity (a shearing deformation), measured by capillary flow, is defined as the ratio of the wall shear stress to the wall shear rate [27,34]. Upon examining the shear viscosity, the melt flow appears as laminates of fluid sliding past each other having a zero velocity at the capillary wall and some maximum value at the centre of the fluid flow. In a polymer melt, the viscosity changes with the rate of deformation and, hence, it cannot be described adequately by one value, thus the shear viscosity is described as a function of shear rate [97].

Figure 3.2 [92] shows clearly that although both m-LLDPE and z-LLDPE polymers are shear thinning (non-Newtonian behaviour), the m-LLDPE has a higher viscosity at the range of shear rates typically experienced by the polymers during extrusions (e.g.  $100-1000\text{s}^{-1}$ ) [27,98]. Figure 3.3 [92] shows that the shear viscosity of both polymers decreases with increasing extrusion temperature and this can be related to the observed decrease in melt pressure of the polymers during twin-screw extrusions at higher extrusion temperatures (see chapter 4). Figure 3.4 [92] shows that the extent of reduction in shear viscosity at the different temperatures (i.e. difference between  $210^\circ\text{C}$  and  $285^\circ\text{C}$ ) is higher at higher shear rates in the case of m-LLDPE (compared to

z-LLDPE) reflecting the fact that higher shear rate the m-LLDPE polymer has a lower fraction of molecular chains having higher molecular weight (i.e.  $\overline{M}_w$ ), see also figure 3.31 as well as a more uniform SCBD. This suggests that the disentanglement of the m-LLDPE polymer chains is easier at all temperatures under a higher shearing motion [28]. However, for the z-LLDPE polymer, disentanglement of the fractions of molecular chains with high molecular weight ( $\overline{M}_w$ ) and the much higher molecular weight ( $\overline{M}_z$ ) fraction, together with the more irregular SCBD, results in greater inhibition of the disentanglement of the chains at lower extrusion temperatures, and consequently at higher temperatures the change in viscosity is also smaller (see figure 3.4).

Melt fracture, which arises from a periodic loss of melt adhesion at the capillary (or die wall) at a critical wall shear stress, is a real processing problem [97]. It is observed as a dramatic change from a laminar to a non-laminar (plug) flow, giving rise to extrudate surface irregularities such as sharkskin [97]. These transitions result in pressure fluctuations during extrusion in the capillary rheometer. Melt fracture can be observed from both the raw pressure data of capillary rheometric results, where pressure fluctuations occur, and as a discontinuity becomes clearer in the log shear stress versus log shear rate plot (see figures 3.5-3.7) [92]. It is clear that the z-LLDPE undergoes melt fracture only at low extrusion temperatures (e.g. 210°C) and this occurs at a high critical shear rate of 1000 s<sup>-1</sup>. On the other hand, m-LLDPE melt fractures at much lower shear rates when extruded (in the capillary rheometer) under the same conditions, and suffers melt fracture over the whole temperature range examined (210-285°C, see figure 3.7).

Examination of the elongational viscosity function (calculated from the shear viscosity function, see chapter 2),  $\eta_E$ , provides useful information on polymer melt elasticity [28]. Polymers with a high elongational viscosity exhibit high melt elasticity [34]. Elongational viscosity involves the stretching of a polymer and is essentially a tensile deformation. Elongational flow measurements provide an advantage over shear measurements in that the former does not involve an interface with the wall of the instrument, so that slip is not a problem [97]. Furthermore,  $\eta_E$  is extremely sensitive to molecular weight distribution (MWD) [28,97,98] and the degree of chain branching of the polymer [28,98,99].

Figures 3.8 and 3.9 [92] compare the  $\eta_E$  for virgin m-LLDPE and z-LLDPE tested (in the rheometer) at 210 and 260°C. In both polymers,  $\eta_E$  shows a decreasing trend with increasing extensional stress, hence the polymer melts exhibit tension thinning behaviour (confirmed also from shear viscosity measurements, see figure 3.2). However, the elongational viscosity of the

m-LLDPE polymer is much greater than z-LLDPE polymer, suggesting a higher melt elasticity of the former. Further, the rate of tension thinning appears also to be substantially higher in the case of the m-LLDPE polymer at both 210 and 260°C.

PE can be extruded *via* a tubular film blowing process into films with high mechanical properties such as high tensile strength [99]. Tension thinning behaviour improves the tubular film blowing characteristics and facilitates extensive drawdown (downgauging) of the film [28,99]. The elongational viscosity measurements of the m-LLDPE polymer has demonstrated its high melt elasticity, considerable tension thinning behaviour and high viscosity (compared to the z-LLDPE) which would be expected to result in advantageous tubular film blowing processability.

### **3.2.2 Effect of Multiple Extrusion on Changes in Molecular and Rheological Characteristics of Unstabilised m-LLDPE and z-LLDPE polymers**

Capillary rheometric measurements were conducted after the unstabilised polymers were processed (in a Betol TSE) with the rheological test being conducted at a low temperature of 210°C. The rheological behaviour of the processed polymer samples using different extrusion temperatures and speeds followed by multi extrusion (passes 1 to 5) [92] was examined. Figure 3.10 [93] shows that there is no difference in the trend of viscosity change with shear rate after processing of the polymers (e.g. pass 1 at 210°C and 200rpm) when compared to the behaviour of the corresponding virgin polymers (tested in the rheometer at the same temperature), see figures 3.2 and 3.10.

Raw pressure data from the capillary rheometric measurements for the multiple extruded m-LLDPE and z-LLDPE polymers showed similar behaviour to that of the virgin polymers, under all extrusion conditions, whereby the m-LLDPE polymer undergoes much more severe melt fracture than the z-LLDPE polymer. Figure 3.11 [93] shows that no melt fracture occurs in the z-LLDPE polymer that was extruded at high temperature of 285°C/200rpm, whereas the m-LLDPE polymer undergoes severe melt fracture under the same conditions as reflected clearly from the sharp pressure fluctuations.

Figures 3.12-3.15 and 3.16-3.17 [93] show the rheometric pressure data for multi-extruded (P1, P3 and P5) m-LLDPE and z-LLDPE polymers processed under different temperatures and screw speeds. Melt fracture in the z-LLDPE polymer is only observed at an extrusion temperature of

210°C and only at higher shear rates (see figure 3.16 versus figure 3.17) whereas the m-LLDPE polymer shows pressure fluctuations, reflecting melt fracture, under all conditions examined; generally melt fracture is reduced with increasing extrusion temperatures, see figures 3.16 and 3.17 and reducing speed, see figure 3.12 and 3.13. In analogy with the virgin polymers, the extruded m-LLDPE shows also higher melt elasticity when compared to the extruded z-LLDPE. Figure 3.18a [93] confirms this and shows that while the elongational viscosity of both polymers decreases with increasing extensional stress, in the case of the extruded m-LLDPE polymer, the elongational viscosity decreases more steeply (compared to z-LLDPE) suggesting that it undergoes higher extent of broadening of MWD (possibly due to crosslinking) under the shear rates and temperatures typically experienced during extrusion, see also figure 3.30 that compare MWD curves for both polymers at different shear rates with respect to that of their virgin counterparts. Multiple extrusion increases this effect (see figure 3.18b), this again suggests that further MWD broadening occurs on multiple extrusions. The 'back tracking' observed in figure 3.18a & b is believed to be attributed to a glitch in the software. The higher extent of shear thinning observed in the extruded metallocene polymers (see figure 3.18 and see also figure 3.9 for virgin polymer) may be attributed to the more regular SCB distribution and presence of smaller fraction of molecular weight chains with a low molecular weight, which would lead to more shear thinning. Whereas, the higher fraction of chains with low molecular weight in the z-LLDPE polymer (that has a more irregular SCBD and has also a higher fraction of chains with very high molecular weight,  $\overline{M}_z$ ) is responsible for the observed reduced extent of shear thinning, see figure 3.1. Melt flow index (MFI) measurements can be related to changes in the molecular weight of a polymer [48,97]. A drop in MFI of a polymer is indicative of an increase in molecular weight (increase in viscosity) due to crosslinking reactions [48]. The higher the molecular weight of a polymer, the greater the number of points of attachments and entanglements between polymer chains, thereby retarding melt flow [29,100]. On the other hand, an increase in MFI (decrease in viscosity) is due to a decrease in molecular weight as a result of degradation *via* prevalent chain scission reactions [48]. Under normal extrusion conditions, crosslinking and chain scission reactions are in direct competition [48]. It has been shown that [30,45,100] the extent of contribution of each of these reactions to the overall degradation mechanism is very much dependent upon the structural and morphological characteristics of a polymer and the processing conditions (i.e. the amount of oxygen present) [101]. The effect of processing severity (increasing extrusion passes under different conditions) on the melt stability of extruded unstabilised polymers is shown in tables 3.2-3.3. Figure 3.19 shows the effect of processing severity (temperatures and screw speed) on changes in melt flow at two

different shear rates. The difference in the behaviour of the m-LLDPE and z-LLDPE polymers is quite clear particularly at the high shear (high load, HLMI) measurements. The overall continuous drop in the melt flow (HLMI) curves with extrusion passes in the case of m-LLDPE suggests that oxidative degradation occurs predominantly by crosslinking reactions under all conditions examined. The z-LLDPE, on the other hand, appears to change mechanism, from an initial crosslinking route to predominantly a chain scission path, with processing severity; this is reflected in the observed initial drop in the melt flow (HLMI) curves followed by a rise under all processing conditions (see figures 3.19). To take account of initial differences in the HLMI values of the metallocene (17 g/10min) and Ziegler polymers (32 g/10min), the % change in HLMI and in MI are also plotted at extrusion temperatures of 210°C and 285°C for two screw speeds. Figures 3.20 and 3.21 clearly support the above argument, that chain scission seems to become the predominant mechanism for z-LLDPE, particularly at high temperatures and high screw speeds. It is also clear that the extent of degradation of both sets of polymers increases with processing severity and the mechanism of degradation appears to be dependent upon the screw speed (i.e. residence time and shear rate) and temperature employed during extrusion.

The molecular weight characteristics of the unstabilised m-LLDPE and z-LLDPE polymers (extruded at Aston [92]) were measured at Exxon, Baytown by GPC. Tables 3.4-3.6 give the molecular weight and % changes in  $\bar{M}_w$  and polydispersity of these polymers. Under normal extrusion conditions, both crosslinking and chain scission reactions are in direct competition [23,45]. The rate and extent of these reactions, however, is dependent upon the nature of the polymer and its molecular mobility as well as the extrusion conditions, particularly temperature and shear [93]. Figure 3.22 show the %  $\bar{M}_w$  change (with respect to values of the corresponding virgin polymers) with multi-pass extrusion. A positive change in  $\bar{M}_w$  indicates crosslinking and a negative change in  $\bar{M}_w$  values point out to chain scission, with a zero change meaning the values are the same as that of the virgin unprocessed polymer. The  $\bar{M}_w$  results confirm those results obtained from melt flow measurements (see figures 3.20 & 3.21) and show that overall the m-LLDPE polymer undergoes more crosslinking, than the z-LLDPE polymer under all conditions tested; z-LLDPE undergoes more chain scission particularly at higher extrusion temperatures and higher shear rates (e.g. screw speed of 200rpm). Under the highest extrusion temperature of 285°C used in this work, a higher shear rate (200rpm) gives rise to an increase in the melt temperatures (shear temperature) of the polymers, see table 3.7. The higher melt temperatures incurred at 200rpm (compared to that measured at a lower extrusion shear rate of 50rpm) coupled with a shorter residence time in conditions relatively high in oxygen concentrations (as more material, containing more residual oxygen, is fed into the extruder as compared to 50rpm)



may lead to an increase in the concentration of alky peroxy ( $\text{ROO}\bullet$ ) radicals in the polymers and this could lead to predominance of chain scission reactions.

On the other hand, extrusion of both polymers at the same temperature of  $285^\circ\text{C}$  but at the lower shear rate of 50rpm gives rise to lower extent of increase in melt temperatures (lower shear heat generated), see table 3.7. Under these conditions, the polymer is subjected to longer residence time (compared to 200rpm), which would result in more oxygen-deficient environment with relative predominance of alky ( $\text{R}\bullet$ ) radicals that could result in higher extent of crosslinking reactions in the polymers, as confirmed from molecular weight results of the polymers (see figures 3.23a&b). Under these conditions of high extrusion temperatures ( $285^\circ\text{C}$ ) both the Ziegler and metallocene polymers were found to give higher  $\overline{M}_w$  at lower shear rates (50rpm) than in the case of higher shear rates (200rpm), see figures 3.23a &b. However, at both shear rates, in spite of the fact that the molecular weight of the virgin (unextruded) z-LLDPE polymer is higher than that of the m-LLDPE polymer (see tables 3.4 & 3.5), after extrusion the m-LLDPE gives rise to higher molecular weights at all extrusion passes (at  $285^\circ\text{C}$ ) compared to that of the z-LLDPE (see figures 3.23c & d) again suggesting that m-LLDPE undergoes mainly crosslinking reactions. At lower shear rates (50rpm) there appears to be a higher extent of crosslinking (see figures 3.23a), which is paralleled by a broader MWD curve as reflected in the higher extent of polydispersity values, see figure 3.24a. The z-LLDPE polymer, on the other hand, tends to undergo mainly chain scission reactions especially at higher shear rates (200rpm) as illustrated in figure 3.23d and this is paralleled by a narrowing of MWD distribution reflected in lower polydispersity values (compared to that at 50rpm), see figure 3.24b.

Figure 3.25 compares the changes in molecular weights and polydispersity of the two polymers extruded at  $285^\circ\text{C}$  with respect to their virgin (unprocessed) analogues. It is clear that the m-LLDPE polymer shows an increase in the extent of crosslinking with extrusion passes with a higher overall degree of crosslinking occurring at 50rpm; more oxygen deficient conditions. This is supported by the broader MWD curves as reflected in a larger increase in % PD change, as shown in figure 3.25b. The extruded z-LLDPE polymer, on the other hand, shows a predominance of chain scission reactions with respect to its virgin analogue, with higher extent of chain scission at 200rpm; conditions of relative high oxygen concentration, see figure 3.25a. A comparison of the MWD curves of the extruded polymers at  $285^\circ\text{C}$  and 200rpm (pass 5) with that of the corresponding virgin polymers, (see figures 3.26b & c), show that under these conditions the m-LLDPE gives rise to a broader MWD with a larger shift towards the high

molecular weight end of the distribution curve, see figure 3.26b, supporting predominance of crosslinking reactions, whereas the z-LLDPE polymer results also in a broader overall MWD (compared to its virgin analogue, though the difference is relatively small), the shift is seen to be more predominantly towards the lower molecular weight end of the distribution curve, see figure 3.26c, indicating the larger role that chain scission reactions play in the case of the z-LLDPE polymer.

The effect of extrusion temperature at speeds of 50 and 200rpm in passes 1 and 5 on changes in  $\overline{M}_w$  and P.D. of the m-LLDPE and z-LLDPE polymers with respect to their virgin analogues is shown in figures 3.27 & 3.28. Again, at all extrusion temperatures, the  $\overline{M}_w$  of both polymers is higher at the lower shear rate of 50rpm than in the case of 200rpm (figures 3.27a & 3.28a), with the m-LLDPE polymer showing an overall higher extent of increase in its  $\overline{M}_w$  (with respect to its virgin analogue) at all temperatures compared to the z-LLDPE, thus reflecting the overall higher extent of crosslinking. After the first extrusion pass, the z-LLDPE polymer shows a predominance of chain scission at both shear rates (50 and 200rpm) and all temperatures (when compared to its virgin analogue), with higher extent of chain scission reactions occurring at the higher shear rate, see figure 3.27a. This confirms the more oxidative conditions are dominant at 200rpm (compared to 50rpm). The change in PD of the z-LLDPE at 200rpm (pass 1) at all temperatures also supports this observation and reflects narrower MWD curves, i.e. lower PD values compared to the virgin sample (see figure 3.27b).

Figure 3.29 compares the MWD curves of the extruded polymers at 285°C and both speeds of 50 and 200rpm (passes 1 and 5). Figure 3.30 shows a comparison of the distribution curves (with respect to virgin) after the fifth extrusion pass, it is clear that both polymers give rise to broadening of the MWD curves, though a much lower extent of broadening occurs at 200rpm than at 50rpm (see figure 3.30b). With the metallocene polymer showing a clear shift to the high molecular weight end of the distribution curves (see figure 3.30b & d) confirming the importance of crosslinking reactions whereas the z-LLDPE polymer gives rise to a shift to the lower Mw end of the curves (figures 3.30 a& c) reflecting the predominance of chain scission reaction pathway. In both polymers (at 285°C) the narrower MWD is clearly evident at the higher shear rates, see figure 3.30, with the z-LLDPE polymer showing consistently a shift to the lower molecular weight end of the distribution curves, at both 50 and 200rpm, compared to that of the m-LLDPE polymer, which results in a higher fraction of higher molecular weight, see figure 3.30b & d. Figure 3.31 shows also a comparison of MWD curves of m-LLDPE with that of the z-LLDPE polymer at different screw speeds.

### 3.2.3 Twin Bore Capillary rheometry of stabilised m-LLDPE polymer samples.

A material degradation test was conducted in the capillary rheometer on two stabilised m-LLDPE samples (s24 and s26) tested under simulated extrusion conditions; high shear rates of  $1600\text{s}^{-1}$ , and run temperatures of  $260^\circ\text{C}$ . The material degradation test entailed 5 cycles (see chapter 2) with ascending shear rates ranging from 200-400-600-800-1000-1200-1400-1600 $\text{s}^{-1}$  in each cycle and five minute waiting time intervals (in between each cycle). The maximum pressure on the long die PL max (related to the rheological properties of the polymer) was taken at the end of each degradation cycle at the shear rate of  $1600\text{s}^{-1}$  (see figure 3.32). The polymer samples were initially subjected to multiple extrusion (passes 1, 3 and 5) at an extrusion temperature of  $210^\circ\text{C}$  and screw speed of 100rpm under atmospheric conditions. A virgin m-LLDPE polymer sample was also tested for comparison. The stabilised samples s24 contained the AO blend Irganox 1076:Irganox HP136: Weston 399 (1500:300:2500ppm w/w ratio respectively) and s26 had the AO blend Irganox E201:Irgastab FS042:Ultranox 626 and TMP (300:500:600:450ppm w/w ratio respectively).

Figure 3.32 shows plots of the maximum pressure at the long die (PL) with waiting time between the degradation cycles (5 minute intervals). A high PL value is indicative of a polymer with a high viscosity, thereby requiring a large amount of shear stress for extrusion. Sharp increases in PL during the material degradation are indicative of structural changes, i.e. due to cross-linking reactions. Figure 3.32-3.34 show changes during the first, third and fifth extrusion passes and shows that the unstabilised extruded polymer undergoes severe degradation as reflected in the sharp increase in PL max values, indicating crosslinking, (passes 1 and 3) followed by sharp drops in  $P_{\text{max}}$  at the end of the 5<sup>th</sup> degradation cycle, indicating chain scission to become the predominant reaction (see figure 3.34). The aim of the antioxidant combinations incorporated into the m-LLDPE polymer during the compounding step,  $P_0$ , is to inhibit the deleterious oxidative reactions, which lead to changes in the Mw and MWD of the polymer. The extruded stabilised (s24 and s-26) polymers show lower extent of degradation with time in this test. This is supported by the high melt stabilising effectiveness of both antioxidant packages in the polymer (see chapter 5) even after five multiple extrusion passes. Figure 3.38 [94] shows changes in shear viscosity during the material degradation test. This lower extent of change exhibited during the test by samples s24 and s26 may be attributed to the high extent of synergism between the various antioxidant functions in the blend (see chapter 5).

The extensional viscosity function plotted against waiting time provides useful information about changes in molecular weight and MWD of a polymer [28,34]. Figure 3.39 shows the effect of extrusion severity (passes 1, 3 and 5) at a shear rate of,  $600\text{s}^{-1}$ ; on the extensional viscosity functions of multi-processed m-LLDPE polymers samples. The extruded unstabilised m-LLDPE (pass 1) polymer shows generally a higher extensional viscosity than the stabilised samples and hence higher, melt elasticity. The extensional viscosity of the stabilised m-LLDPE polymer samples (s24 and s26) does not appear to change drastically with extrusion severity (passes 1, 3 and 5) and increasing waiting time, whereas that of the unstabilised polymer shows an upward shift at pass 5. This suggests that the stabilised polymers undergo broadening of their molecular weight distribution curves to a much lower extent when compared with the unstabilised polymer. This is supported by findings (in chapter 5), which showed there are only small changes in the MFR (related to the MWD of a polymer) of polymer samples containing these stabiliser packages.

### 3.2.4 Thermal Oxidative Degradation mechanism of LLDPE

Based on the results shown in this chapter and changes in functional groups observed previously [92], some of the oxidative reactions which can take place under multiple extrusion conditions used here are proposed in scheme 3.1. Initially, the temperature and shear employed during processing cause some of the polymer chains to undergo homolytic chain scission, primarily at an allylic carbon atom (scheme 3.1, reaction 1) [30,45]. In the presence of oxygen, alkyl radicals from peroxy radicals (reaction 2), followed by hydrogen abstraction from the polymer substrate to give hydroperoxides (reaction 3). These peroxides are responsible for the formation of secondary macroalkyl radicals along the polymer chain (reactions 4 and 5 scheme 3.1) and lead to the formation of carbonyl (through reactions 6-8 and 14, scheme 3.1) and unsaturated groups (reactions 9, see scheme 3.1), as well as cross-linked polymer chains (reaction 10, scheme 3.1), the concentrations of each of these groups depends on the relative amount of oxygen present in the extruder. In the presence of higher oxygen concentrations (e.g. high temperature and high shear rate of 200rpm), the secondary alkyl radicals yield secondary hydroperoxides (scheme 3.1, reaction 6) which lead to the formation of aldehyde groups via the  $\beta$  scission of the alkoxy radical (scheme 3.1, reaction 8), resulting in a decrease of the molecular weight of the polymer [45]. It was shown that aldehyde and acid groups are formed in the polymer most likely from the breakdown of peroxy radicals [30]. Aldehyde groups generally react further leading to the formation of acid groups, which are the main final carbonyl groups formed in oxidised polymers [17]. Under more oxygen deficient conditions, e.g. 50rpm, which coexist in the extruder, alkyl

radicals formed initially may recombine, react by disproportionation reactions to yield carbon-carbon double bonds, abstract hydrogen from the polymer chain to yield secondary alkyl radicals which react further. Disproportionation reactions of primary alkyl radicals lead to the formation of vinyl groups, whereas trans-vinylene groups are formed from the disproportionation of secondary alkyl radicals and chain scission reactions. Cross-linking reactions, leading to an increase in the molecular weight of the polymer, occur *via* the combinations of two secondary alkyl radical or a secondary alkyl radical with a secondary alkoxy radical, as well as from the addition reaction of two primary alkyl radicals to a vinyl group. However, it was shown [92] that the concentration of vinyl groups does not significantly change after extrusions for both polymers, suggesting that these reactions have minor contributions. On the other hand, the amount of trans-vinylidene groups increases after extrusions, especially after the first extrusion pass, suggesting that these reactions are favoured.

Table 3.1. Molecular weight characteristics of Virgin m-LLDPE and z-LLDPE polymers.

Characteristics	m-LLDPE	z-LLDPE
Weight Average, $\bar{M}_w$	101 146	112 720
Number Average, $\bar{M}_n$	49 171	32 008
Z Average, $\bar{M}_z$	173 087	333 159
$M_w/M_n$	2.06	3.52
$M_z/M_w$	1.71	2.96
Density, g/cm <sup>3</sup>	0.918	0.918

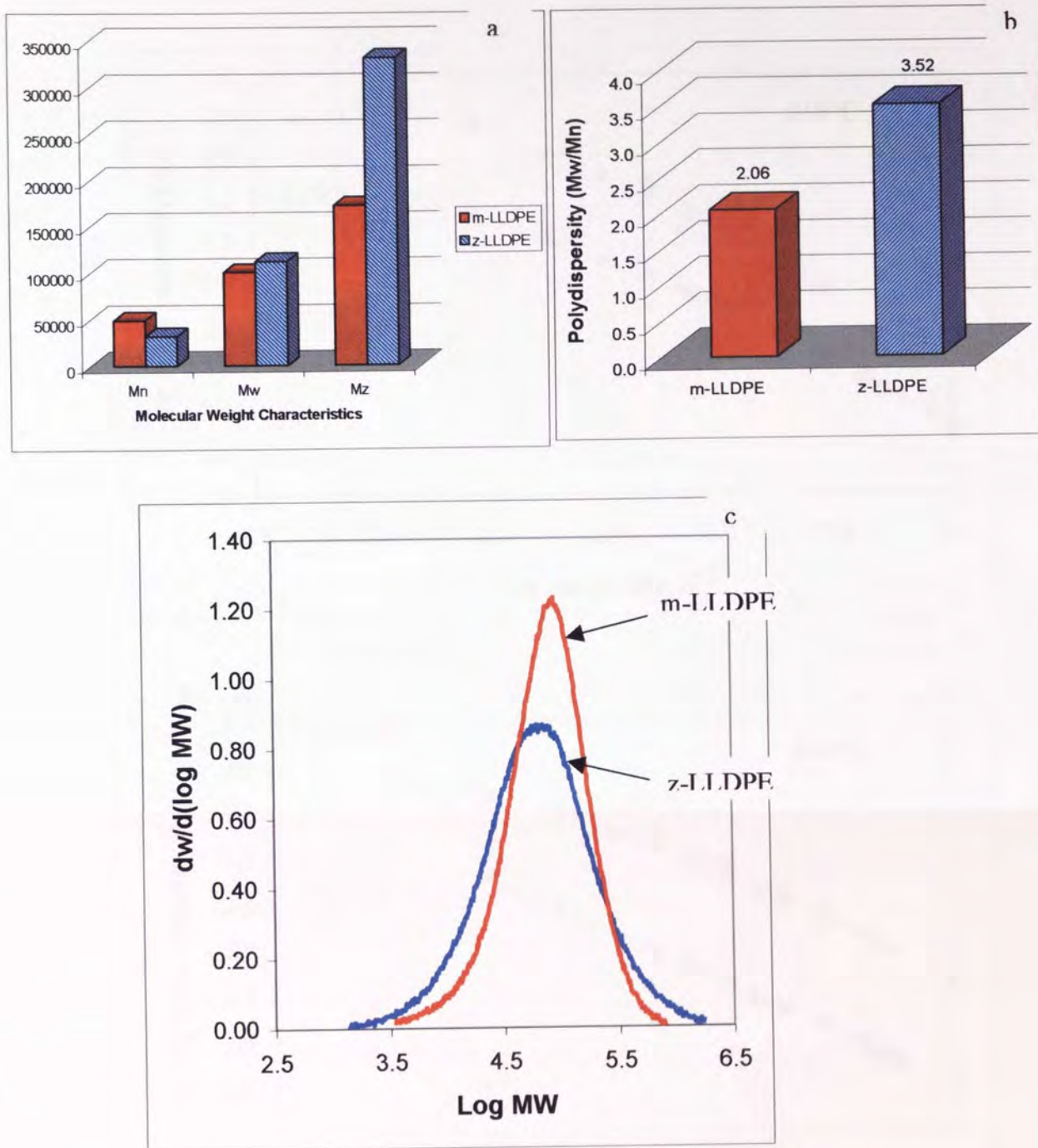


Figure 3.1 Differences in molecular weight characteristics of Virgin m-LLDPE and z-LLDPE polymers; a. Molecular weight features, b. Polydispersity, c. MWD.



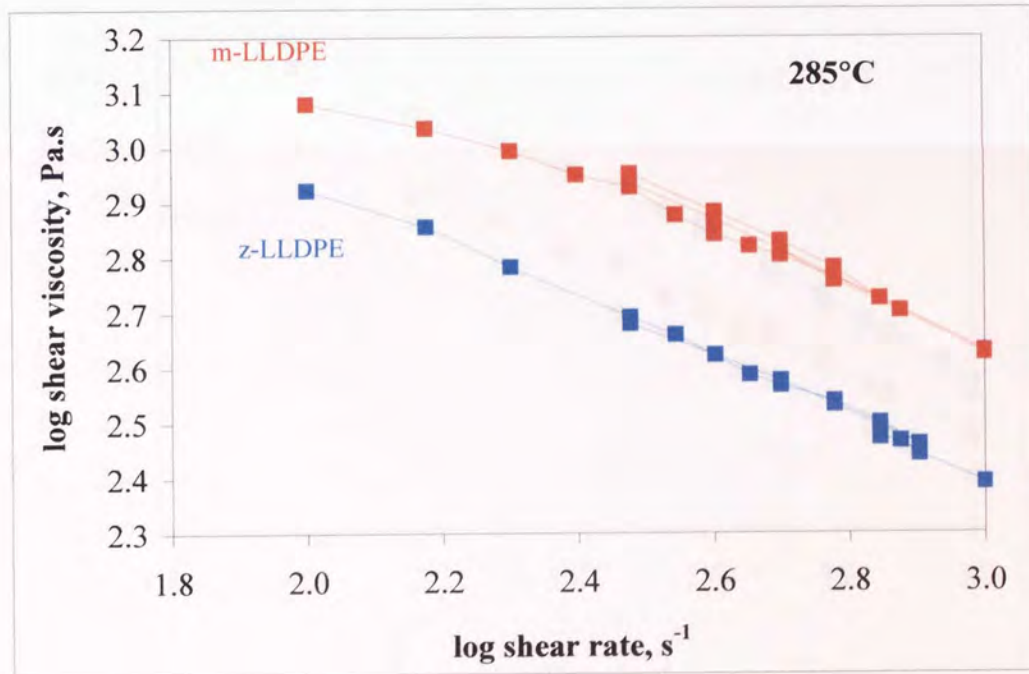
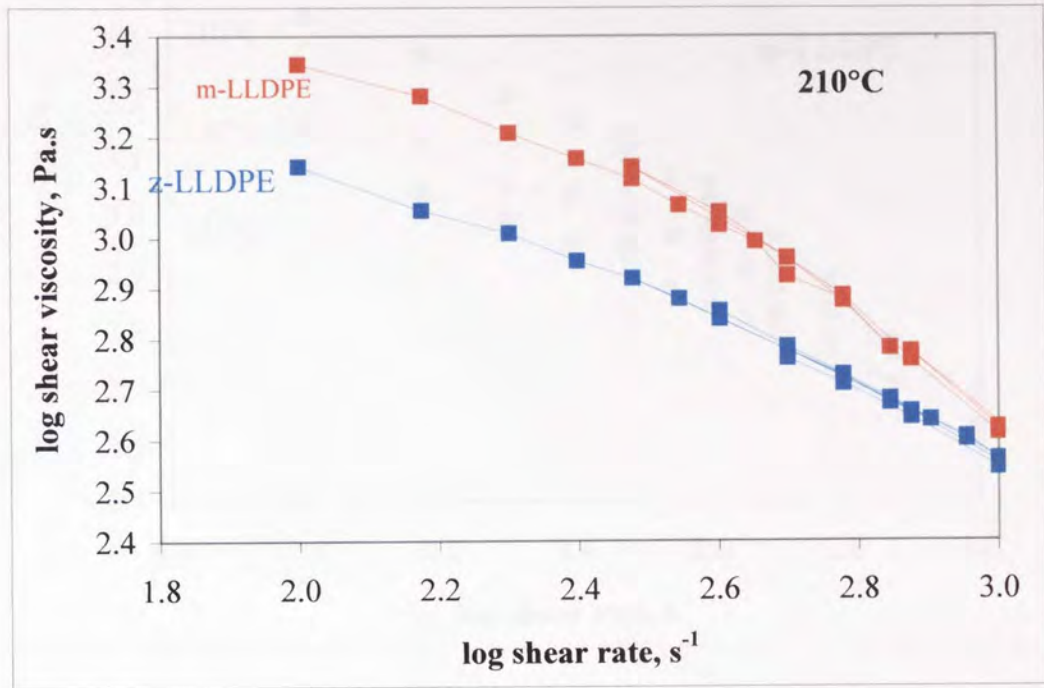


Figure 3.2: Shear viscosity functions of virgin unstabilised m-LLDPE and z-LLDPE extruded in a capillary rheometer at 210°C and 285°C, 1mm diameter dies (long die of 16mm length and short die of zero length) were used [92].



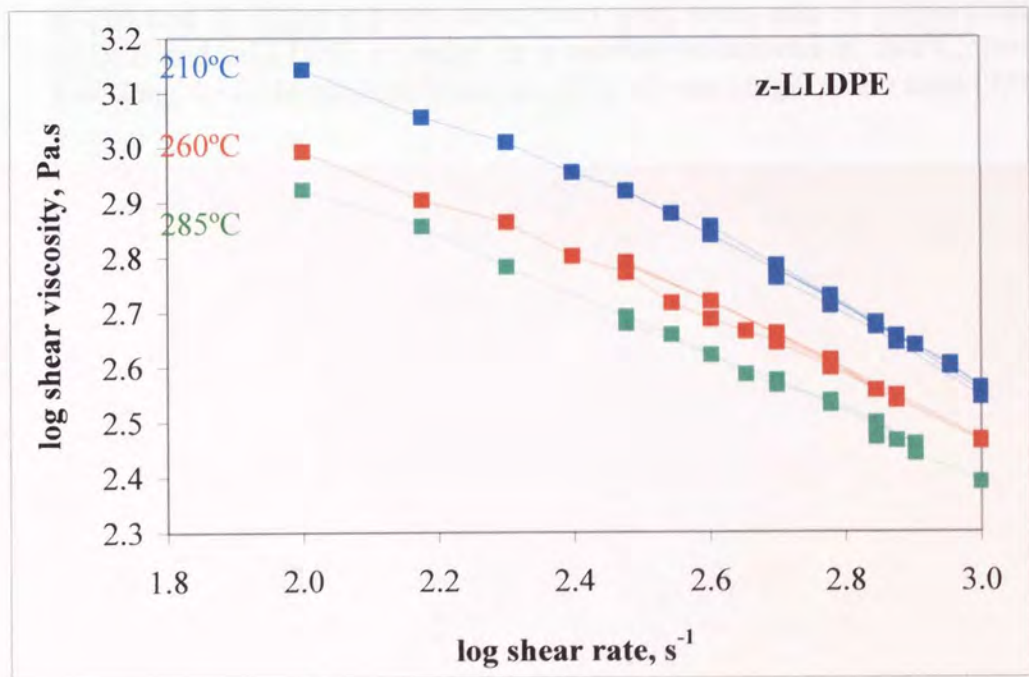
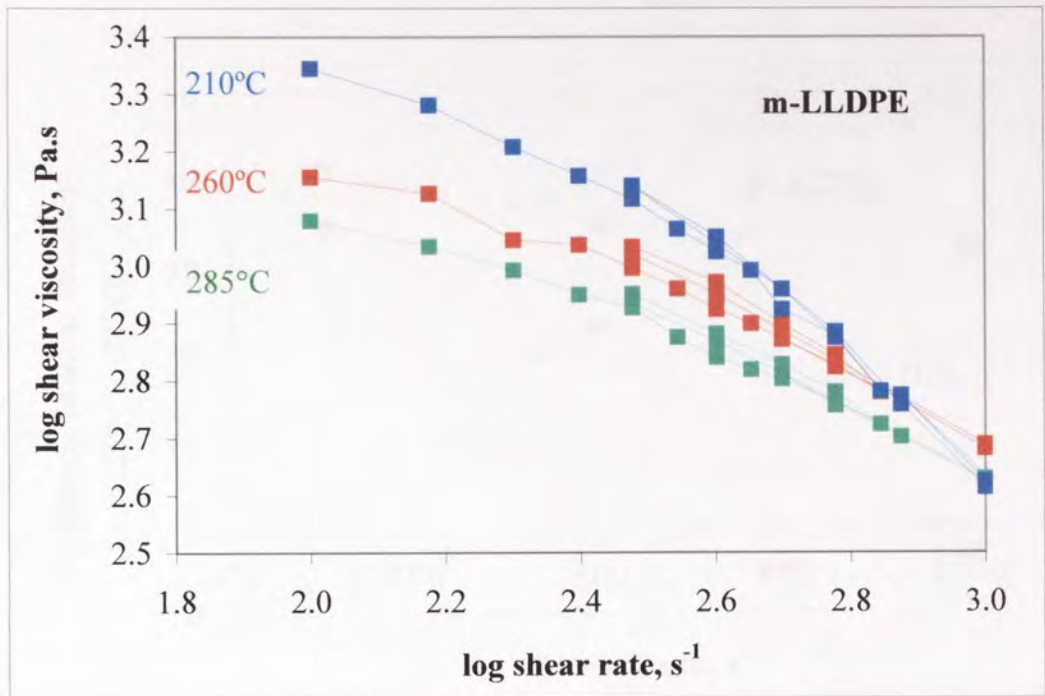


Figure 3.3: Effect of temperature on the shear viscosity functions of virgin unstabilised m-LLDPE and z-LLDPE, extruded in a capillary rheometry, 1mm diameter dies (long die of 16mm length and short die of zero length) were used [92].

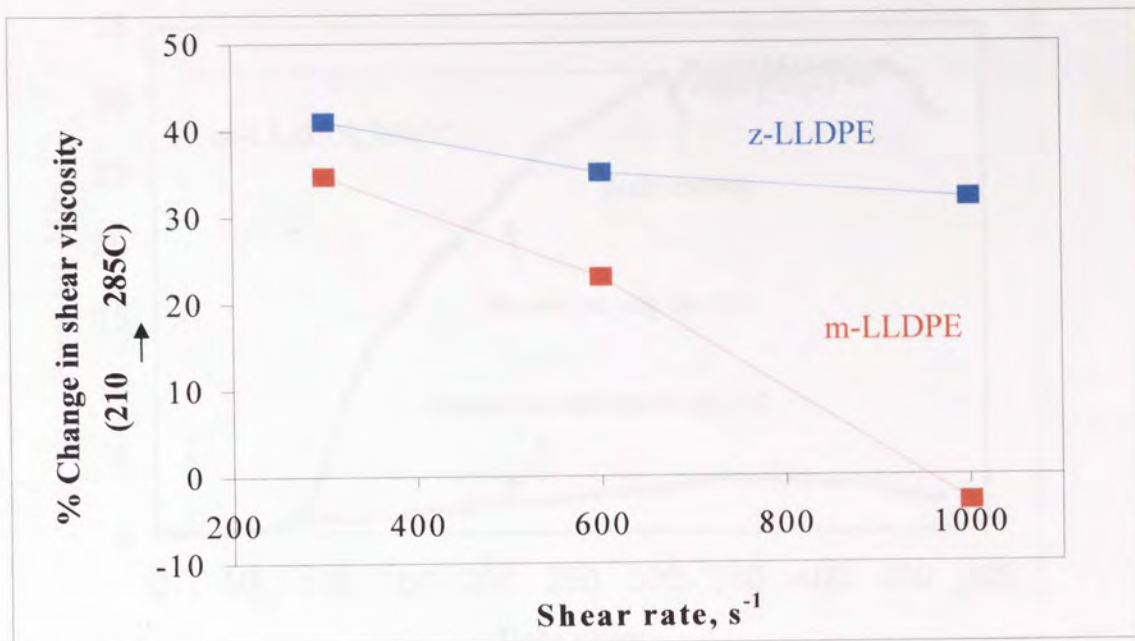


Figure 3.4: % Change in shear viscosity (calculated from the difference in viscosities at 210 and 285°C at a given shear rate) with shear rate of virgin unstabilised m-LLDPE and z-LLDPE, extruded in a capillary rheometer at 210°C; 1mm diameter dies (long die of 16mm length and short die of zero length) were used [92].

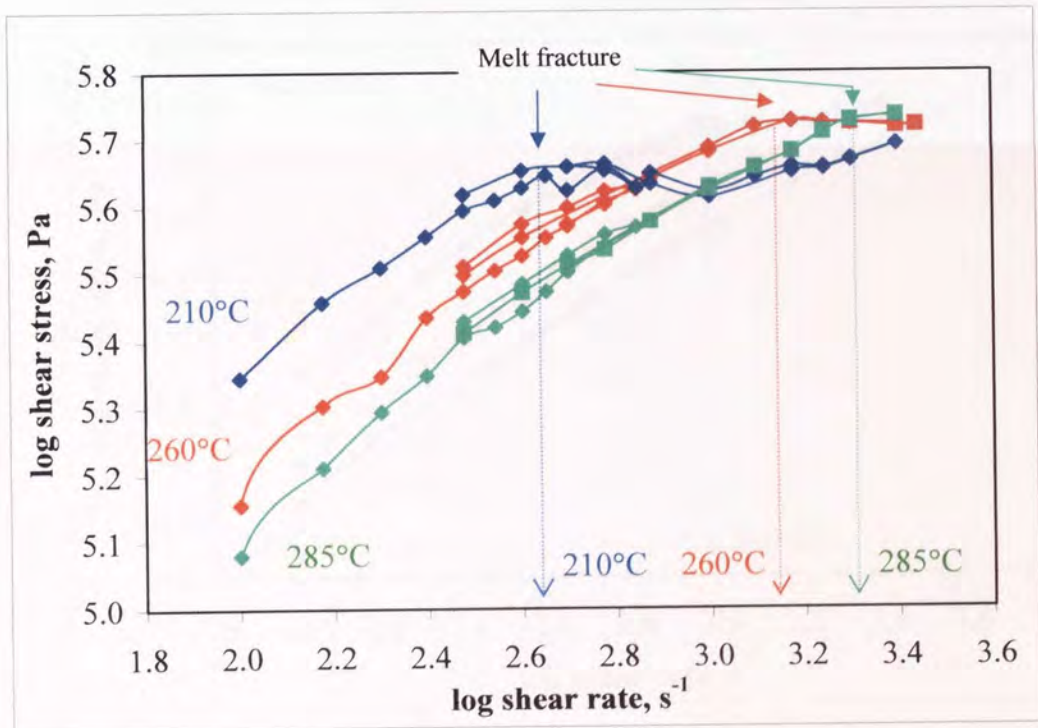
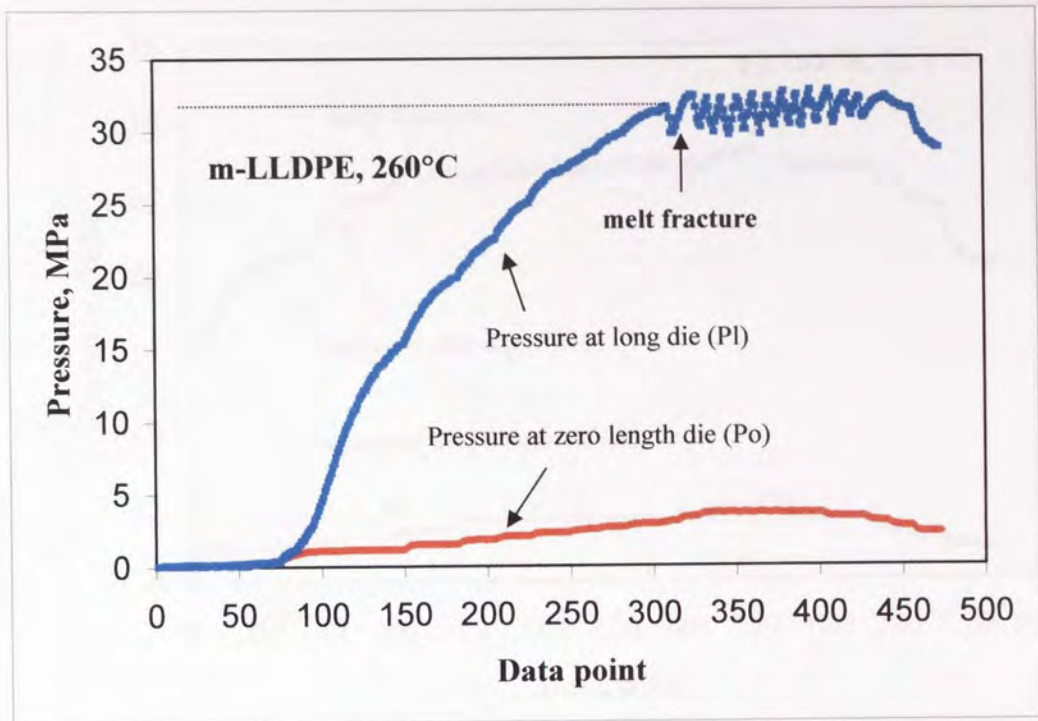


Figure 3.5: Melt fracture of virgin unstabilised m-LLDPE, extruded in a capillary rheometry at 210, 260 and 285°C, 1mm diameter dies (long die of 16mm length and short die of zero length) were used [92].



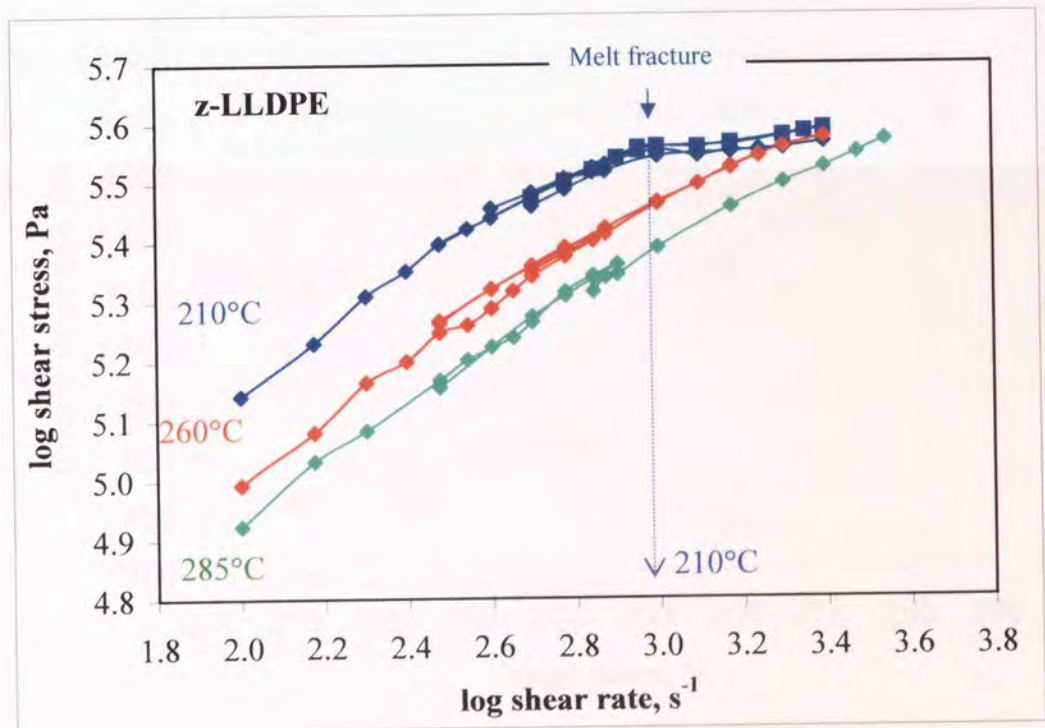
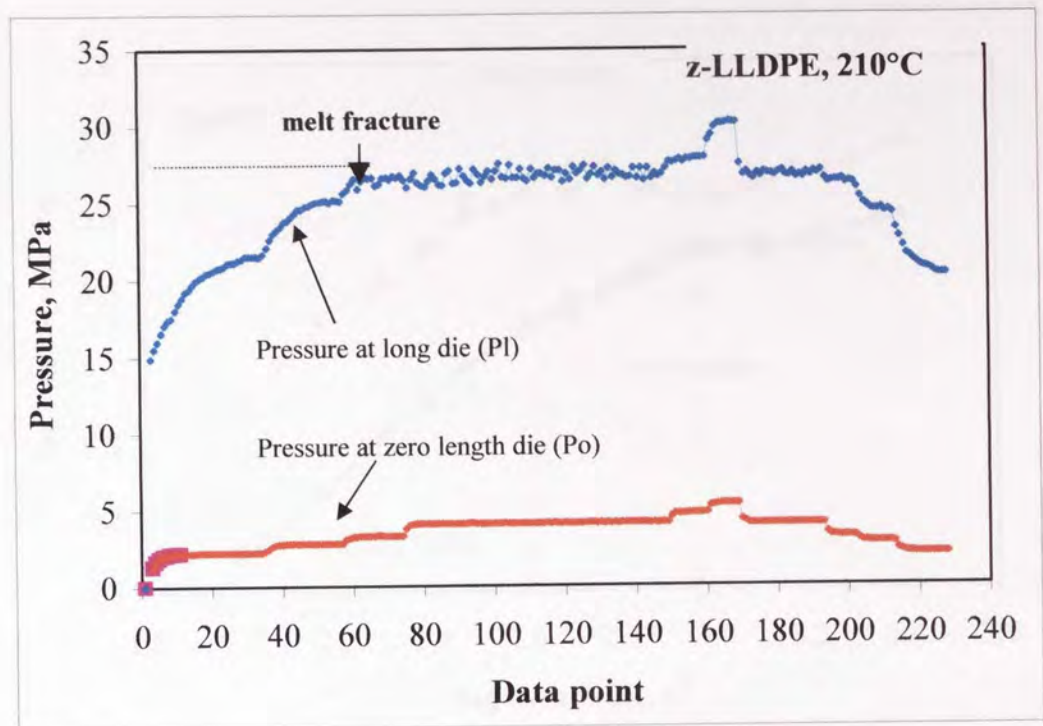


Figure 3.6: Melt fracture of unstabilised virgin z-LLDPE, extruded in a Capillary rheometry at 210, 260 and 285°C, 1mm diameter dies (long die of 16mm length and short die of zero length) were used [92].

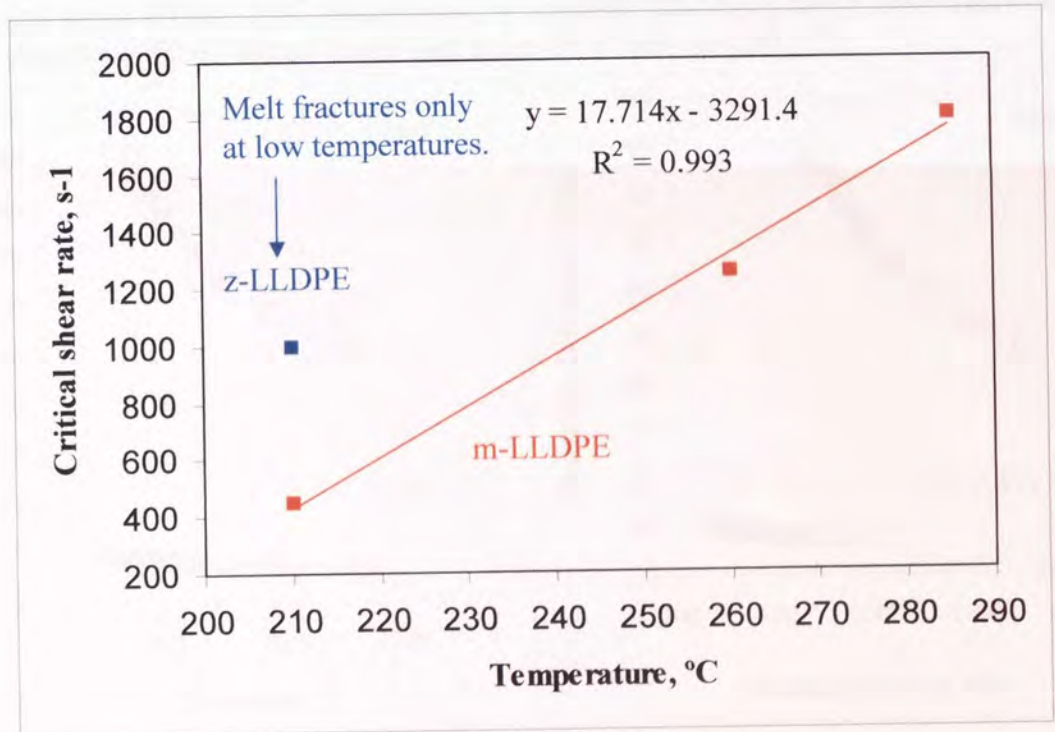
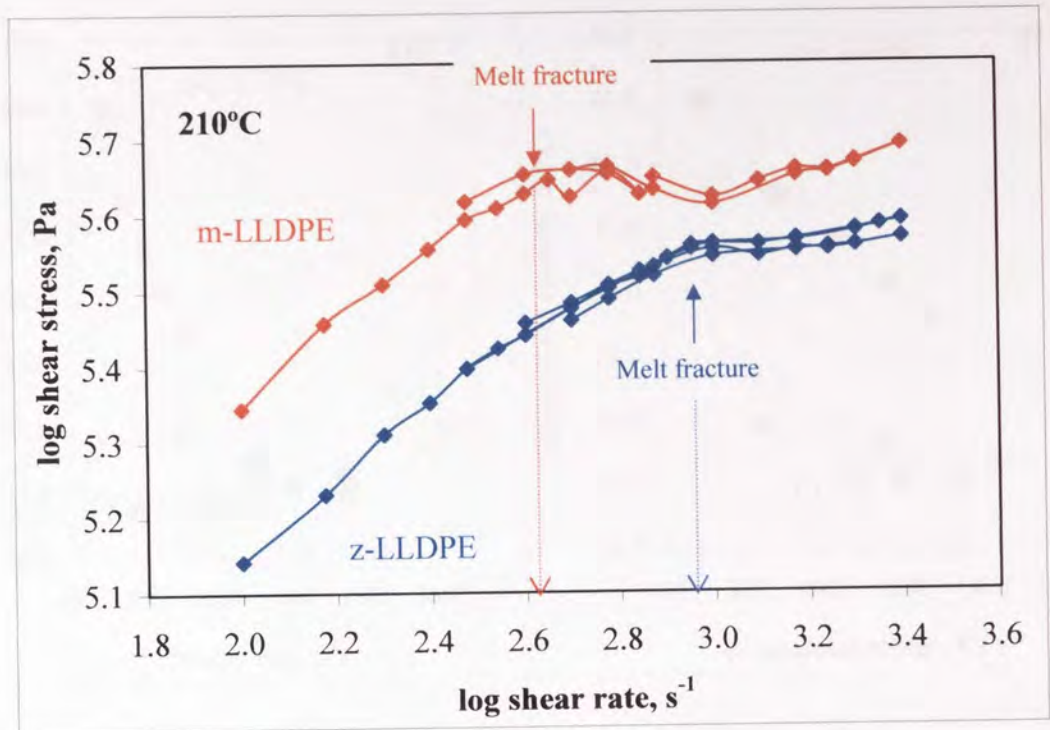


Figure 3.7: Critical shear rates at which melt fracture of unstabilised virgin m-LLDPE and z-LLDPE occurs, in function of the extrusion temperature, determined by capillary rheometry using 1mm diameter dies (long die of 16mm length and a short die of zero length) (z-LLDPE only shows melt fracture at 210°C) [92].



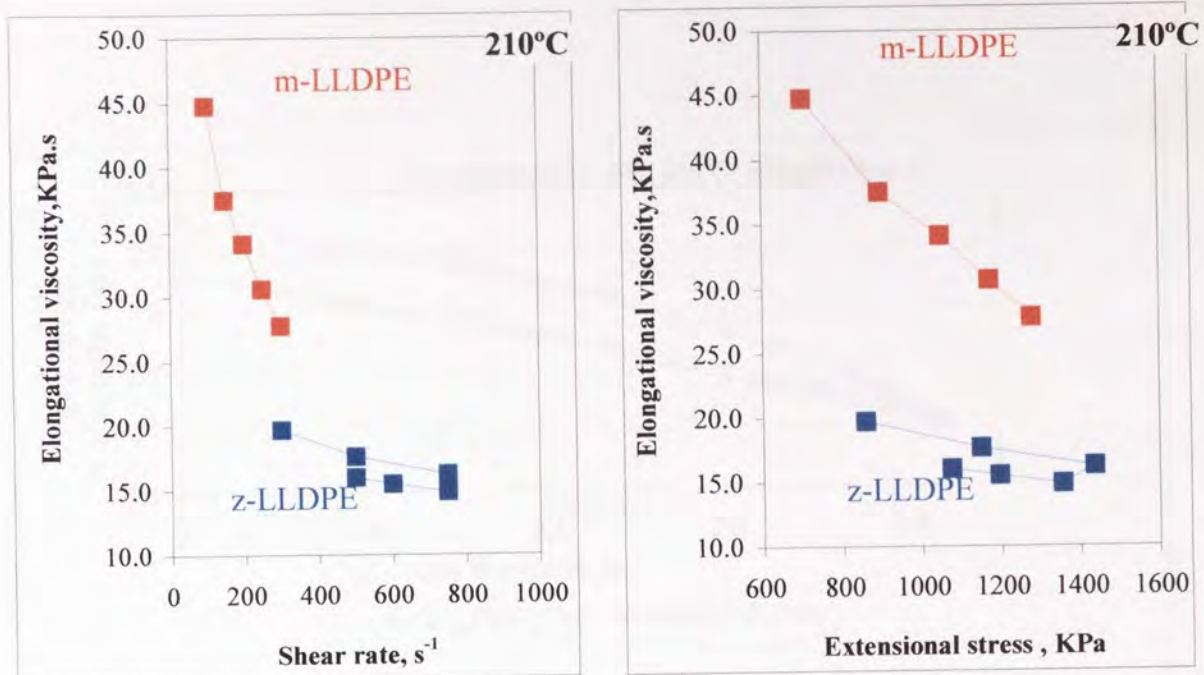


Figure 3.8: Elongational viscosity functions of unstabilised virgin m-LLDPE and z-LLDPE at 210°C, determined by capillary rheometry using 1mm diameter dies (long die of 16mm length and short die of zero length) [92].

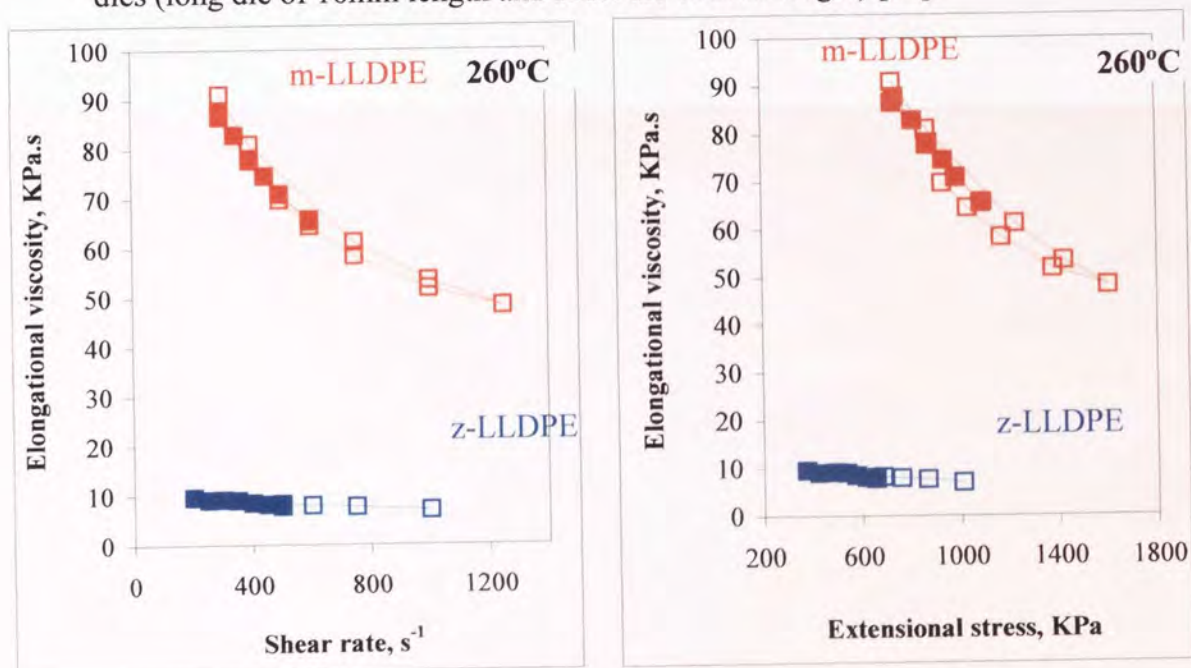


Figure 3.9: Elongational viscosity functions of unstabilised virgin m-LLDPE and z-LLDPE at 260°C, extruded in a capillary rheometry, 1mm diameter dies (long die of 16mm length and short die of zero length) were used [92].

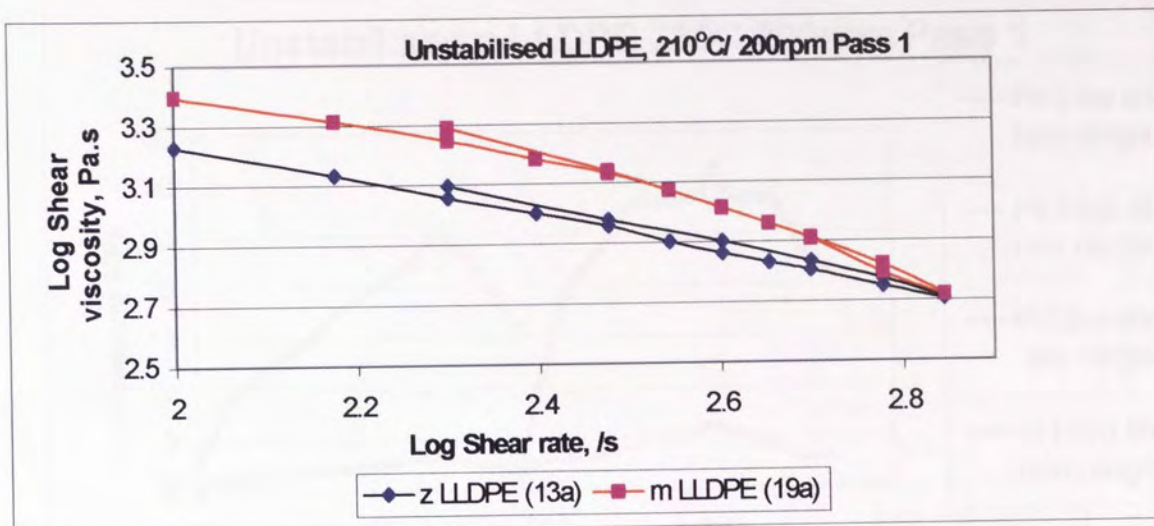


Figure 3.10 Comparison of log shear viscosity against log shear rate for unstabilised m-LLDPE and z-LLDPE after processing in an extruder at 210°C/200rpm Pass 1 [93].



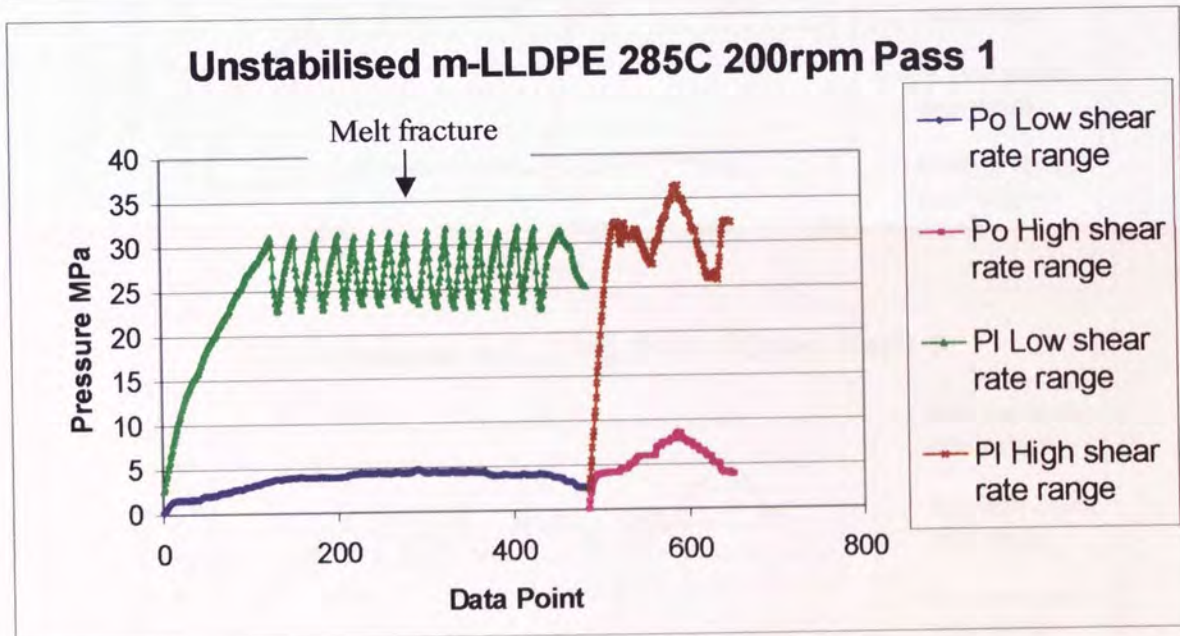
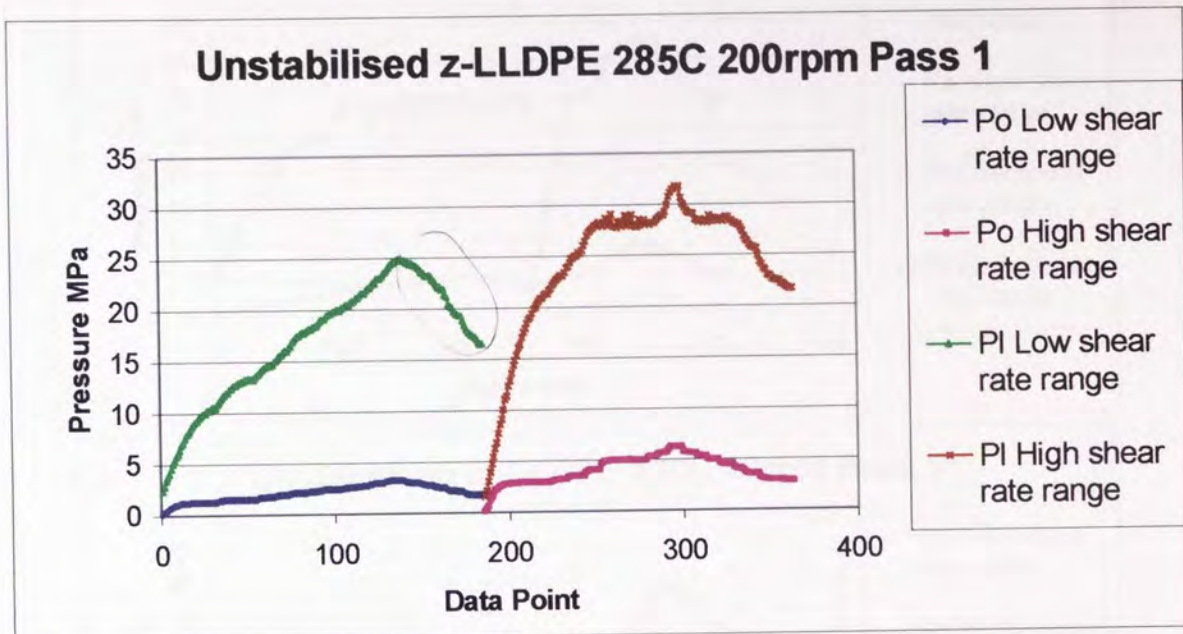


Figure. 3.11. Comparison of severity of melt fracture between unstabilised m-LLDPE and z-LLDPE after processing in an extruder at 285°C and 200rpm for Pass 1 [93].



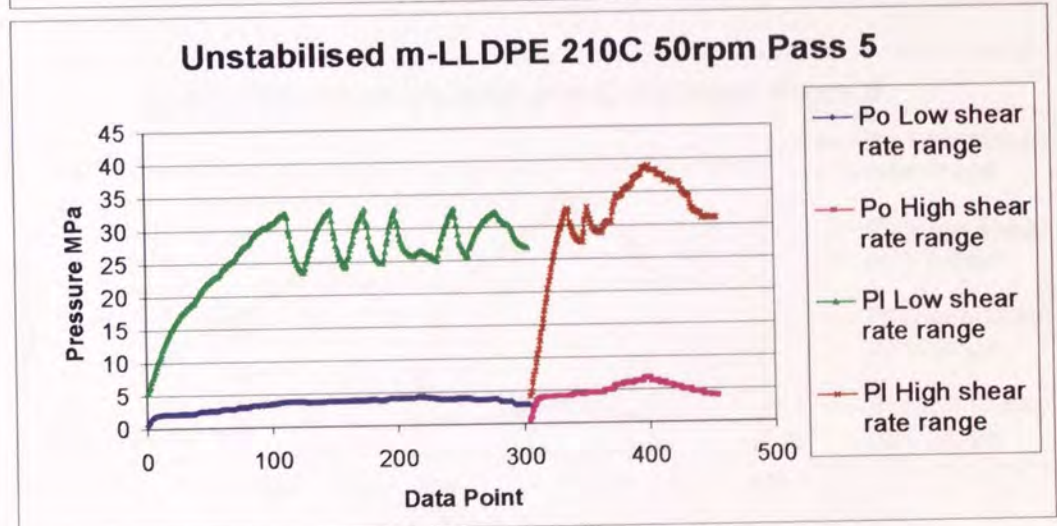
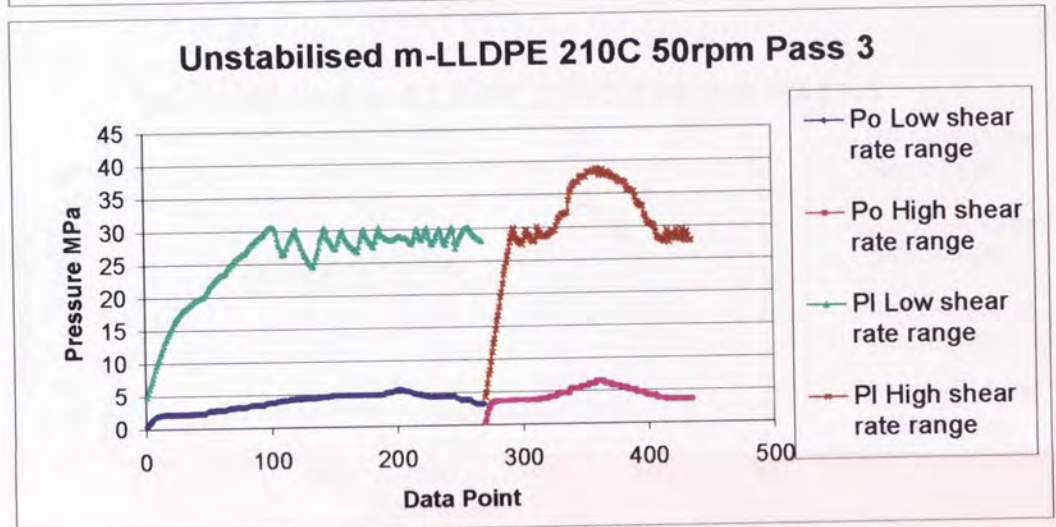
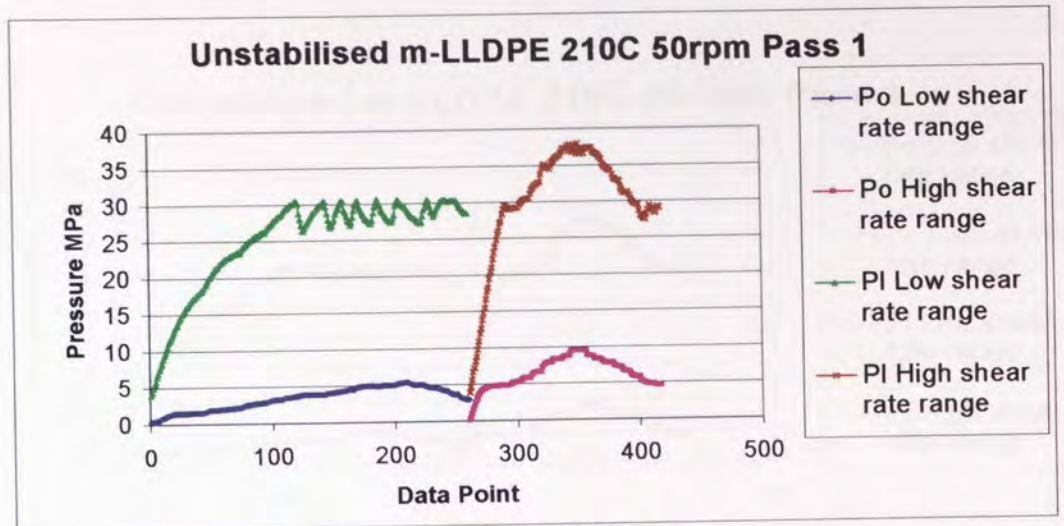


Figure 3.12. Comparison of severity of melt fracture between unstabilised m-LLDPE after processing in an extruder at 210oC and 50rpm for Pass 1,3 and 5 [93].

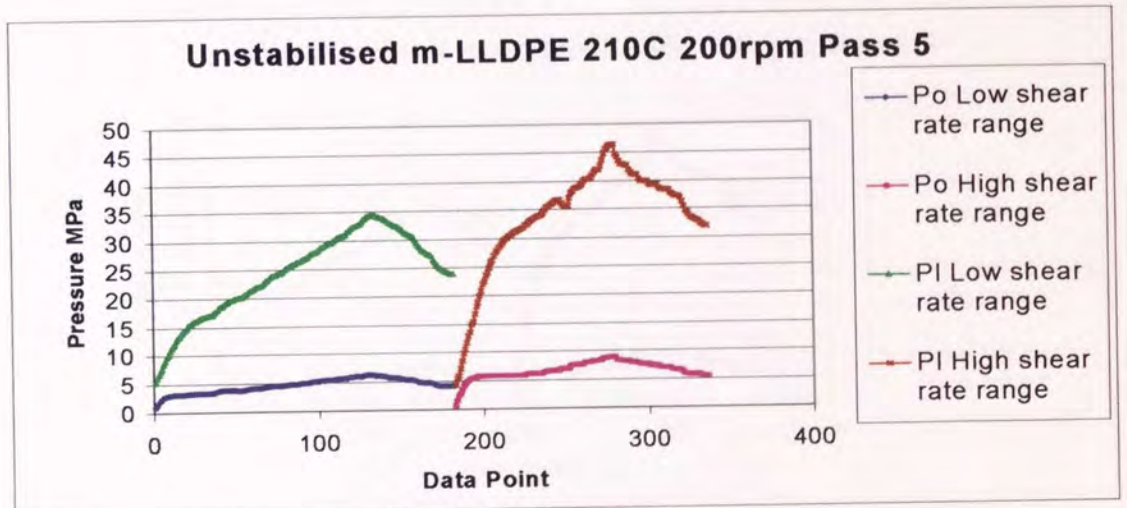
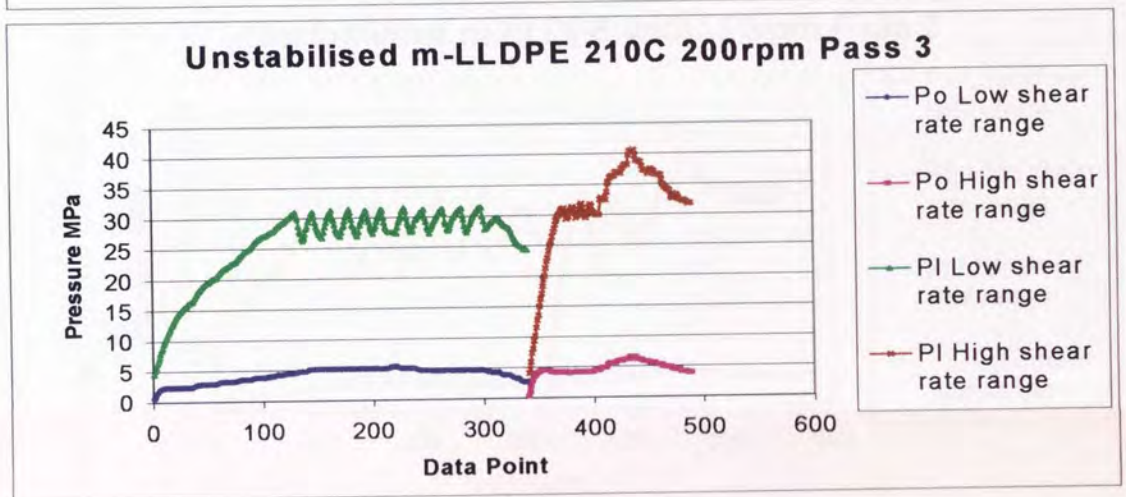
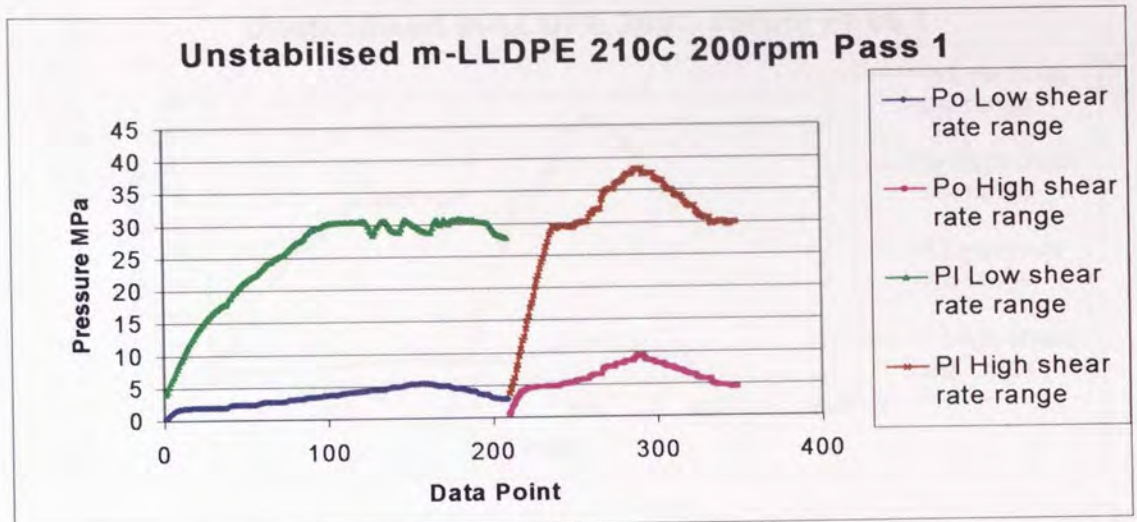


Figure 3.13. Comparison of severity of melt fracture between unstabilised m-LLDPE after processing in an extruder at 210°C and 50rpm for Pass 1,3 and 5 [93].



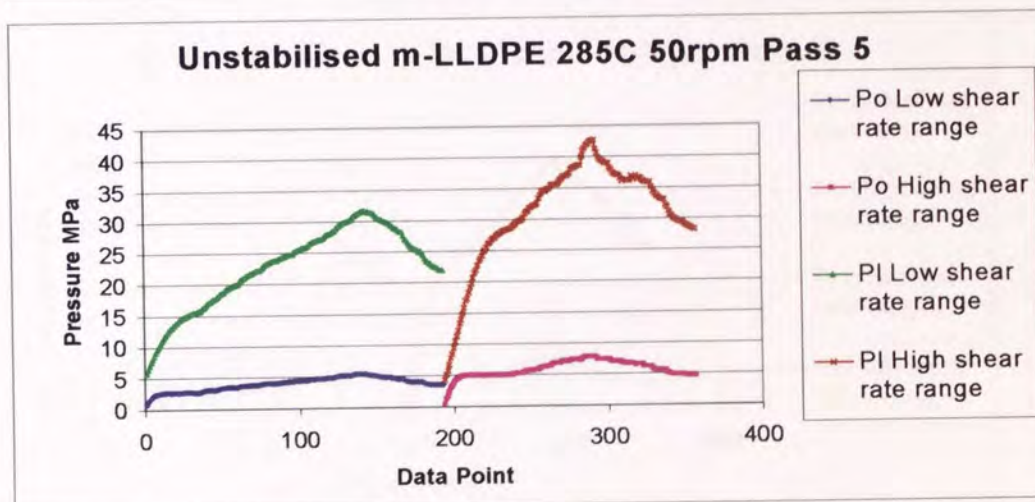
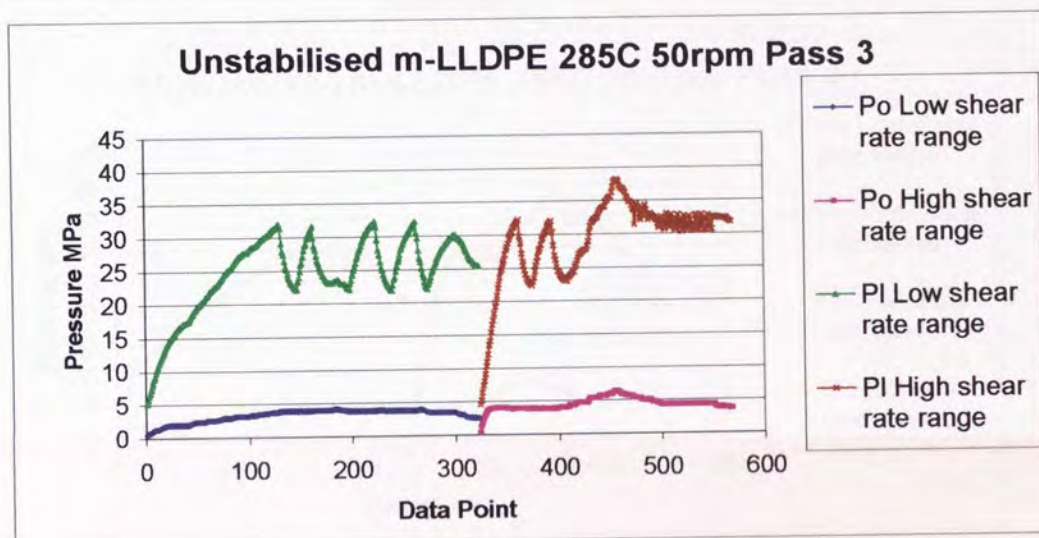
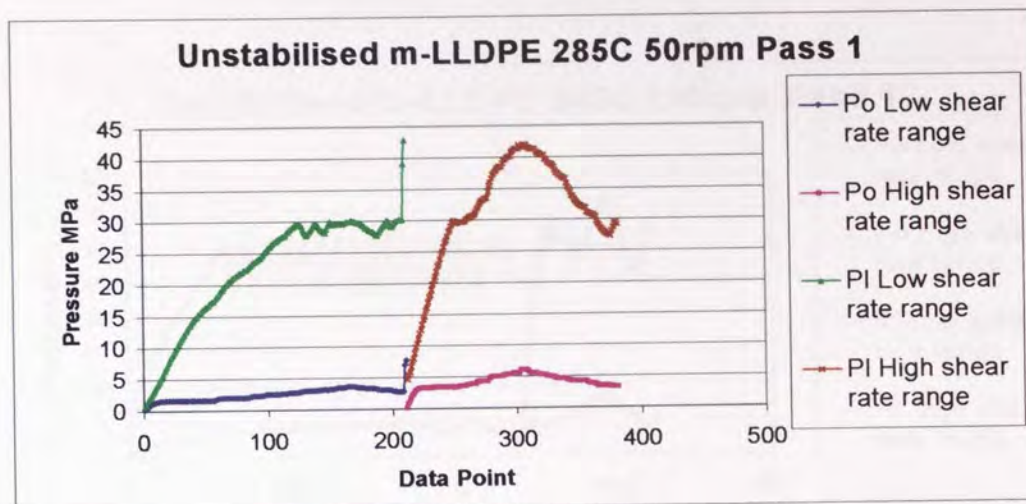


Figure 3.14. Comparison of severity of melt fracture between unstabilised m-LLDPE after processing in an extruder at 285°C and 50rpm for Pass 1, 3 and 5 [93].

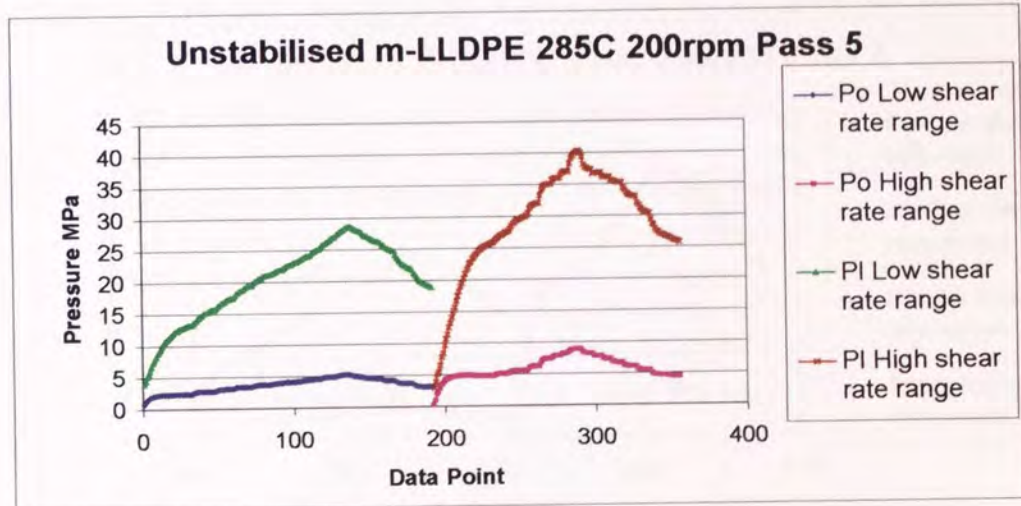
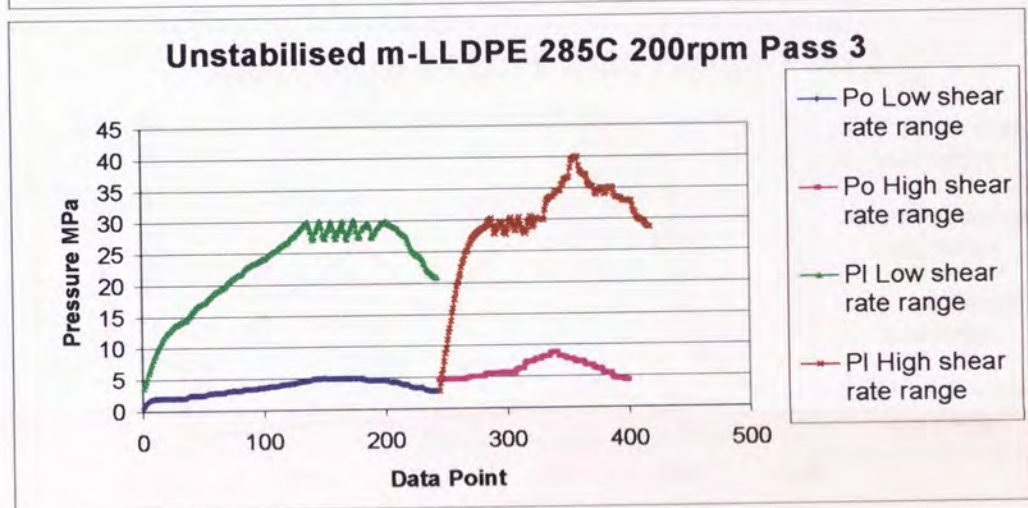
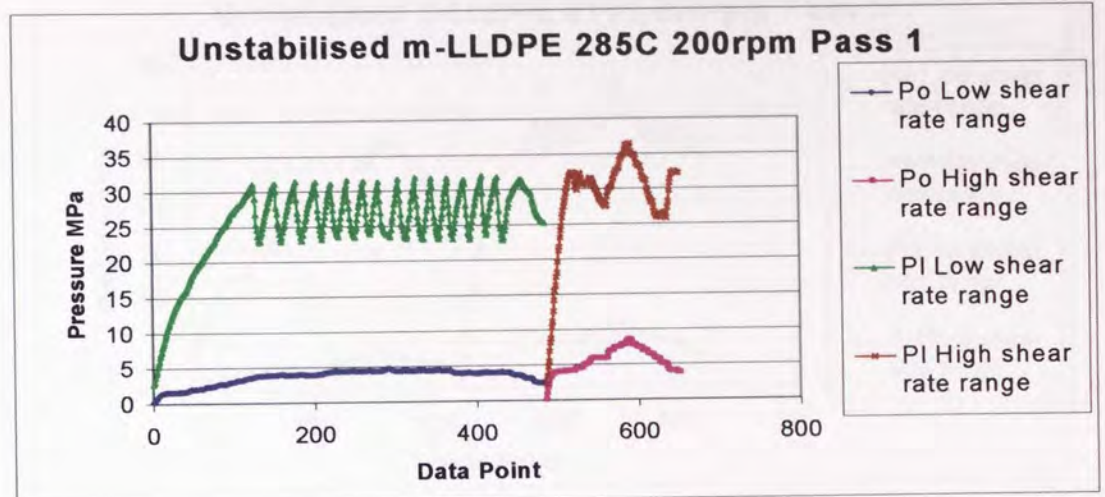


Figure 3.15. Comparison of severity of melt fracture between unstabilised m-LLDPE after processing in an extruder at 285°C and 50rpm for Pass 1, 3 and 5 [93].



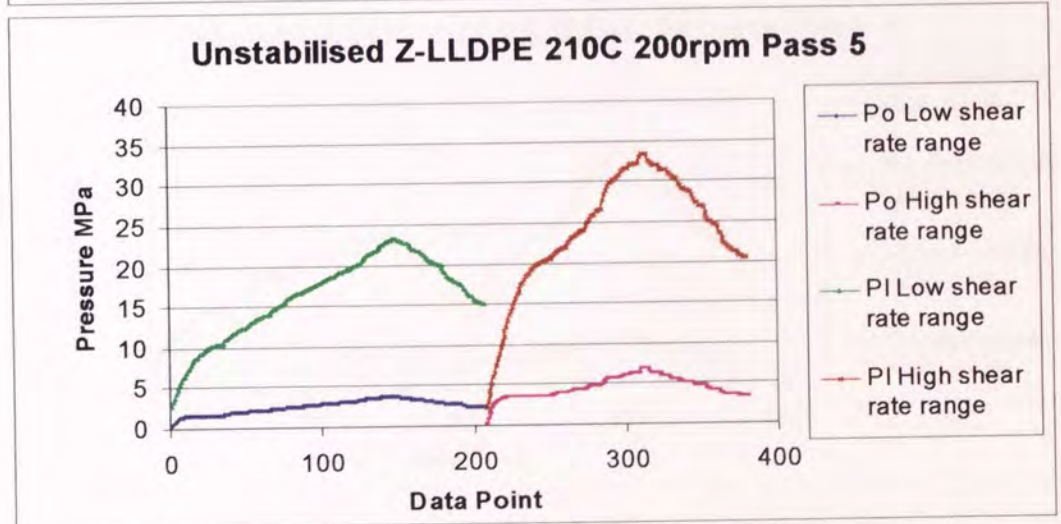
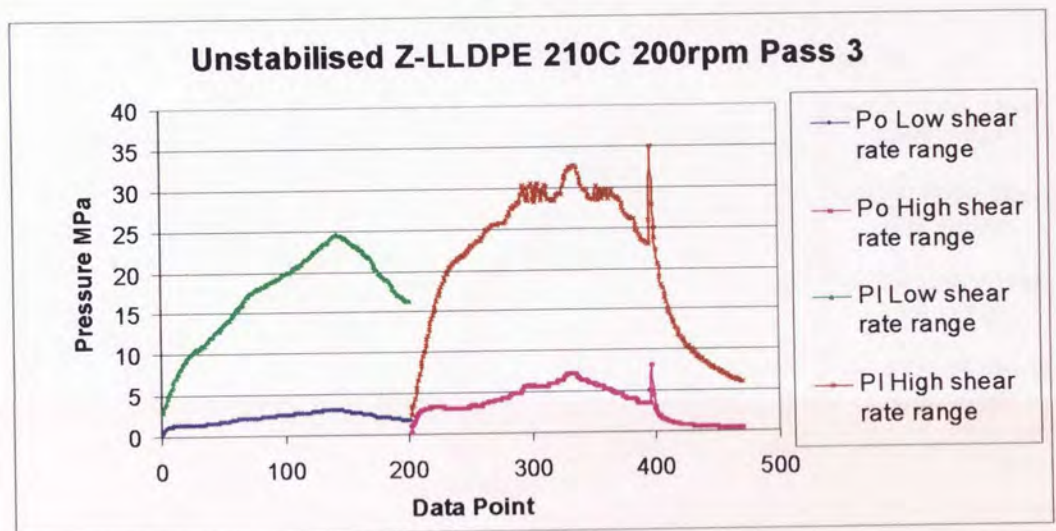
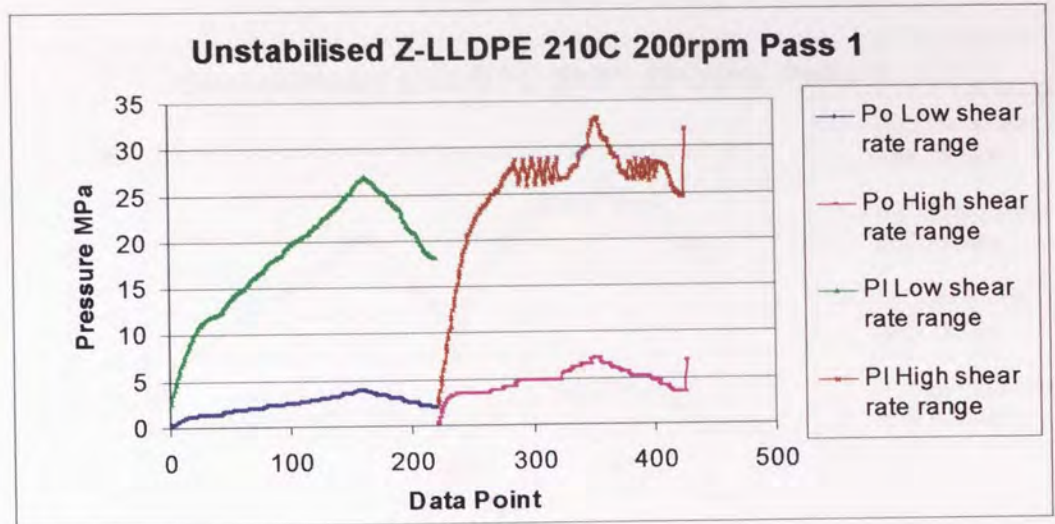


Figure 3.16. Comparison of severity of melt fracture between unstabilised z-LLDPE after processing in an extruder at 210 C and 200rpm for Pass 1, 3 and 5 [93].

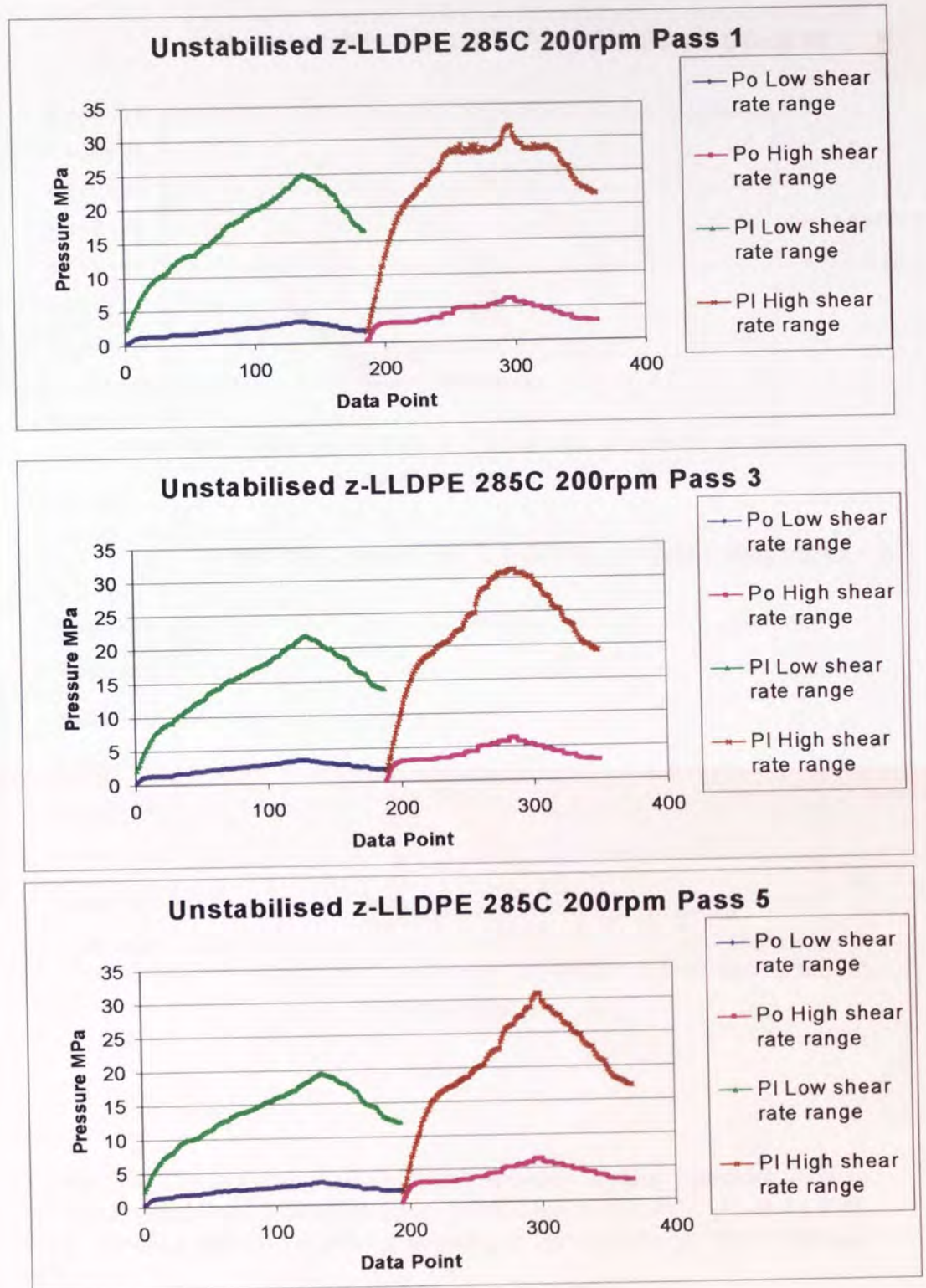


Figure 3.17. Comparison of severity of melt fracture between unstabilised m-LLDPE after processing in an extruder at 285 C and 200rpm for Pass 1, 3 and 5 [93].



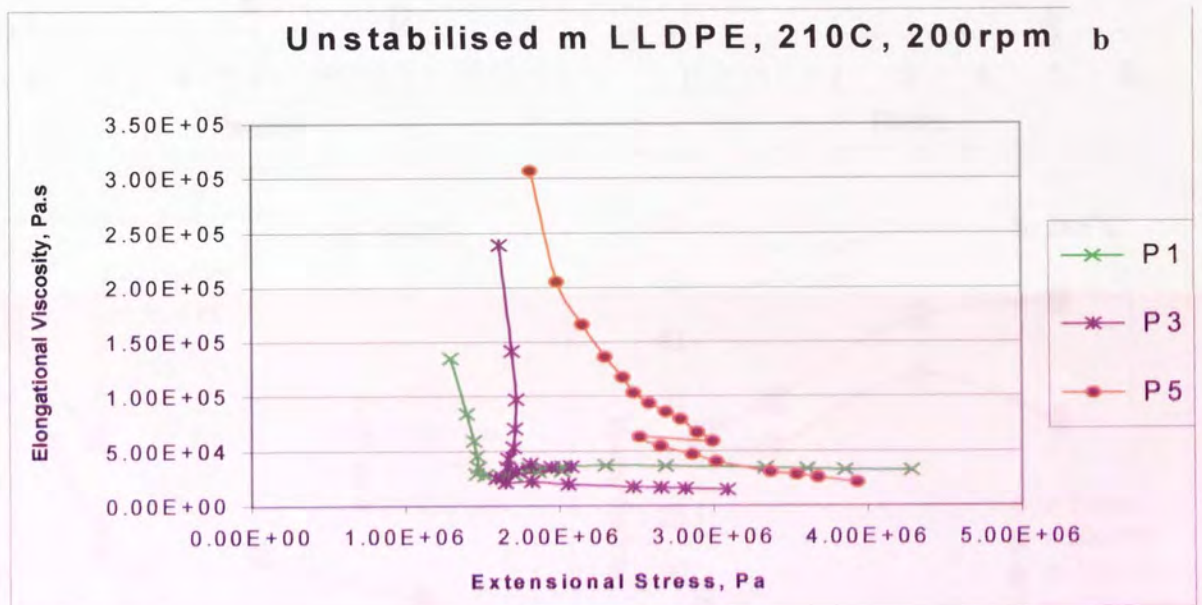
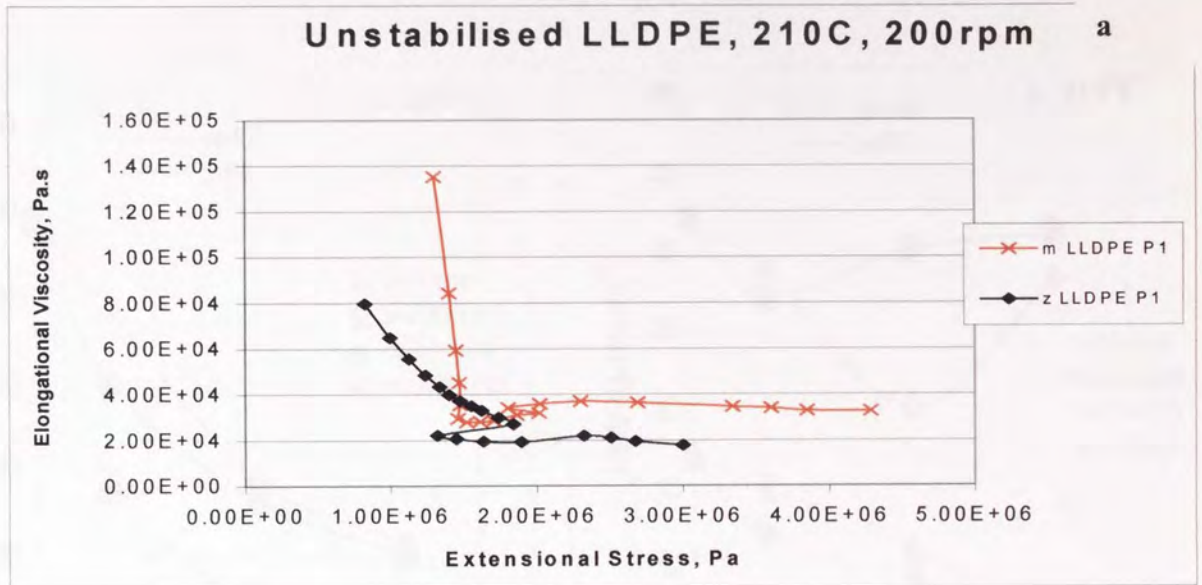


Figure 3.18 Comparison of elongational viscosity against extensional stress (a) unstabilised Pass 1 samples of z-LLDPE and m-LLDPE, (b) m-LLDPE multi-extruded m-LLDPE after processing in an extruder at 210°C/200rpm [93].

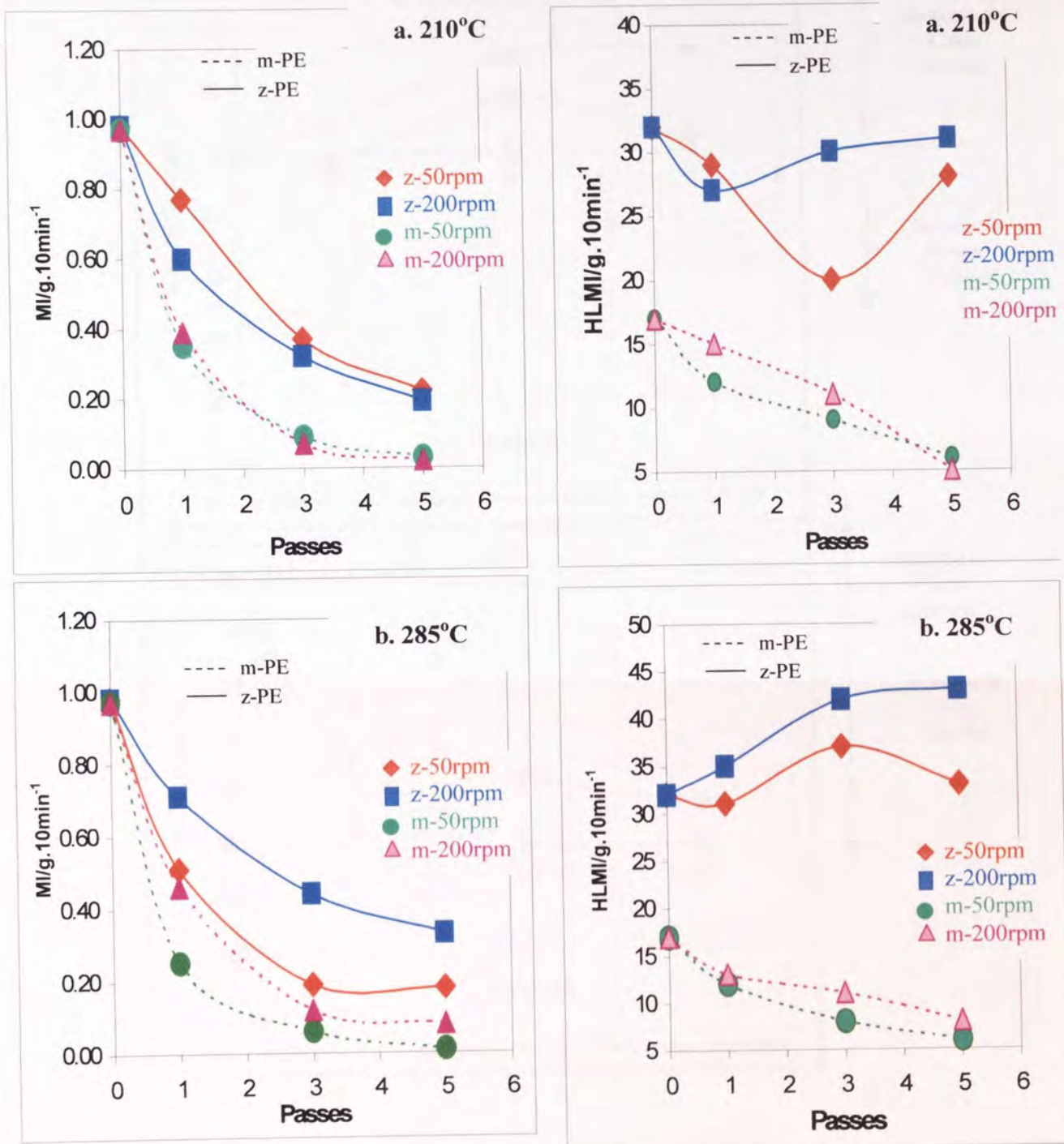


Figure 3.19. Effect of processing severity at fixed temperatures; a. 210°C, b. 285°C, and varying screw speeds (50-200rpm) on the MI and HLMI for unstabilised m-LLDPE and z-LLDPE polymer samples.



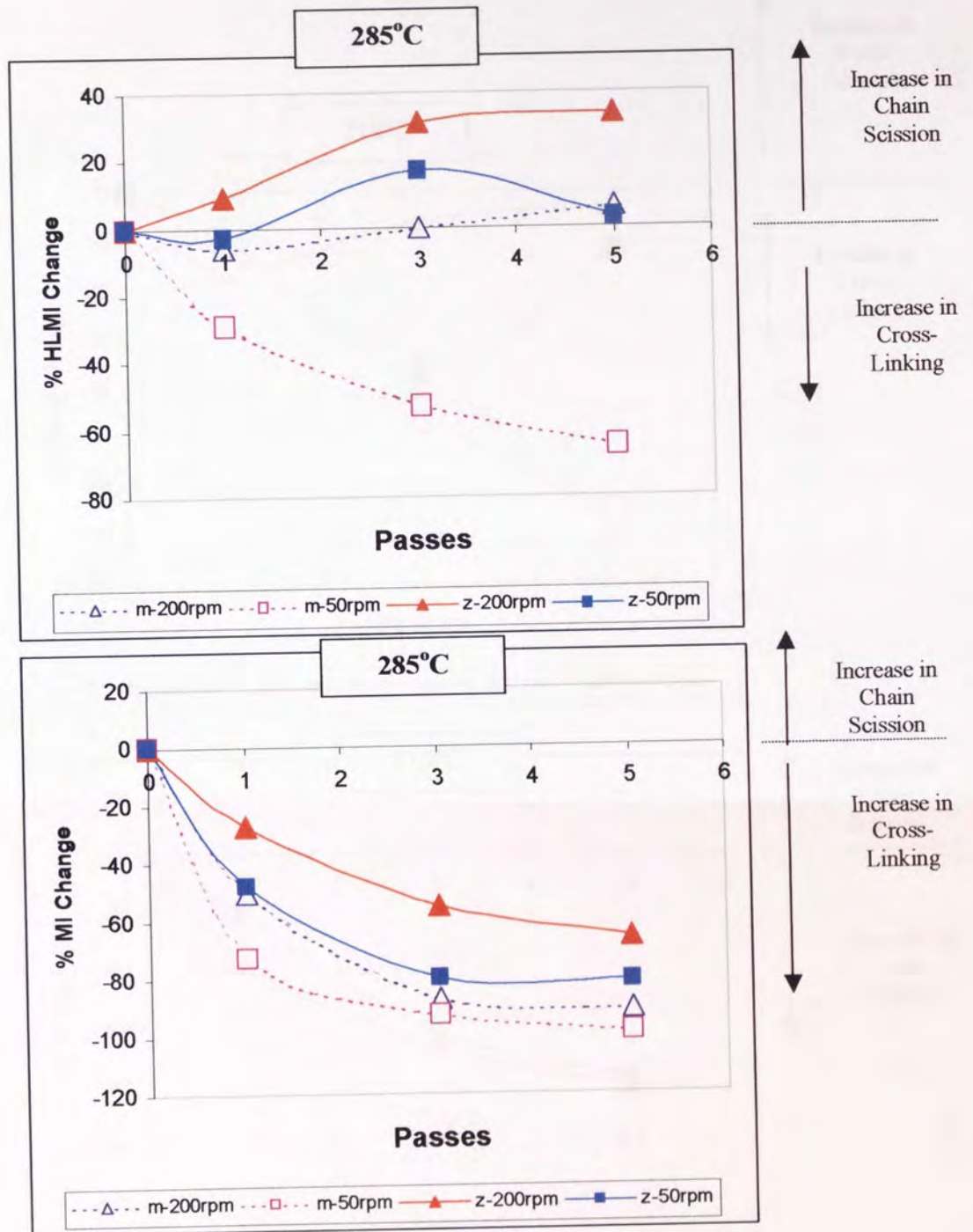


Figure 3.20 Changes in MI and HLMI for multiple extruded m-LLDPE and z-LLDPE polymers at **285°C** at various screw speeds (50-200rpm).

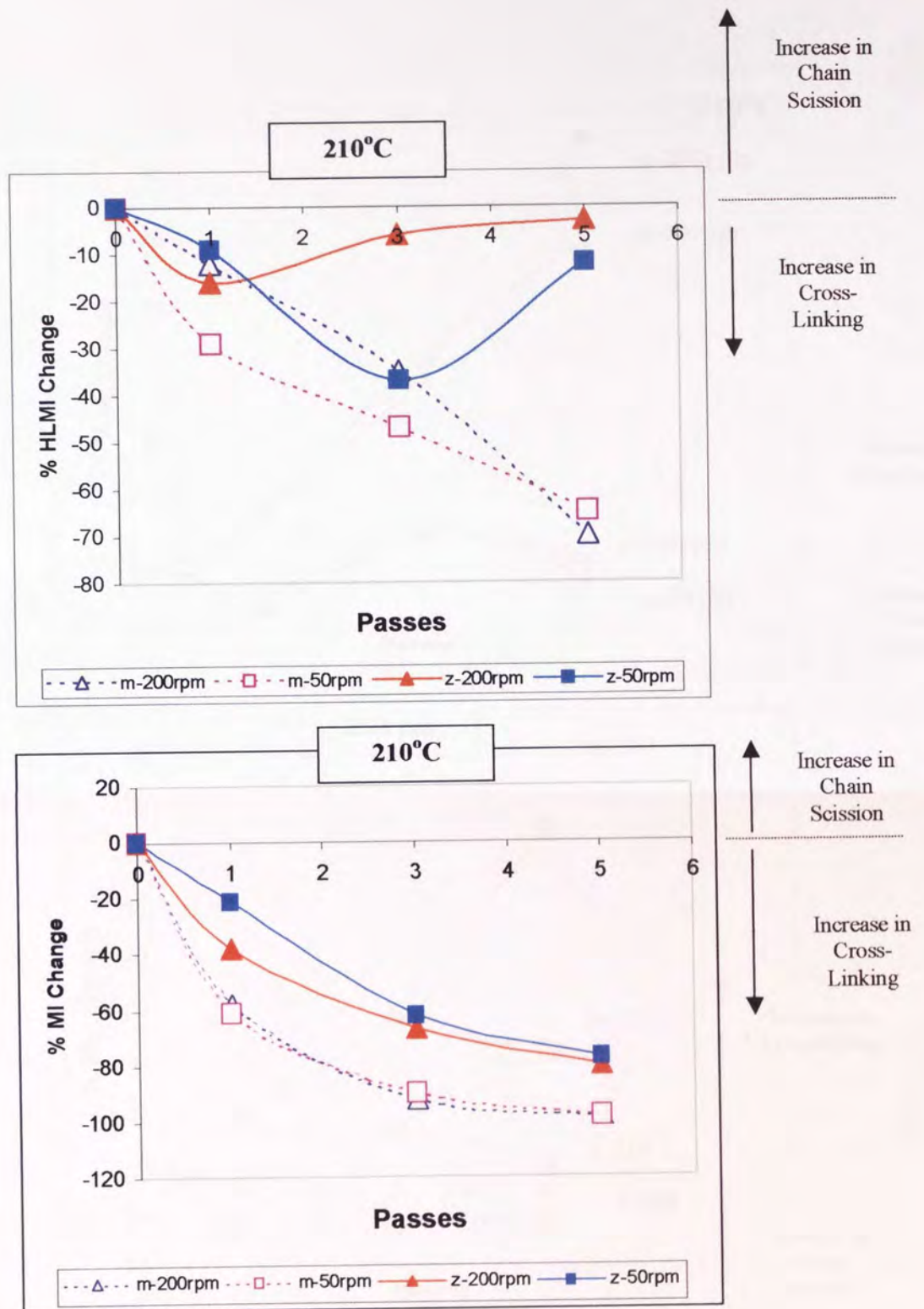


Figure 3.21 Changes in MI and HMI for multiple extruded m-LLDPE and z-LLDPE polymers at **210°C** at various screw speeds (50-200rpm).

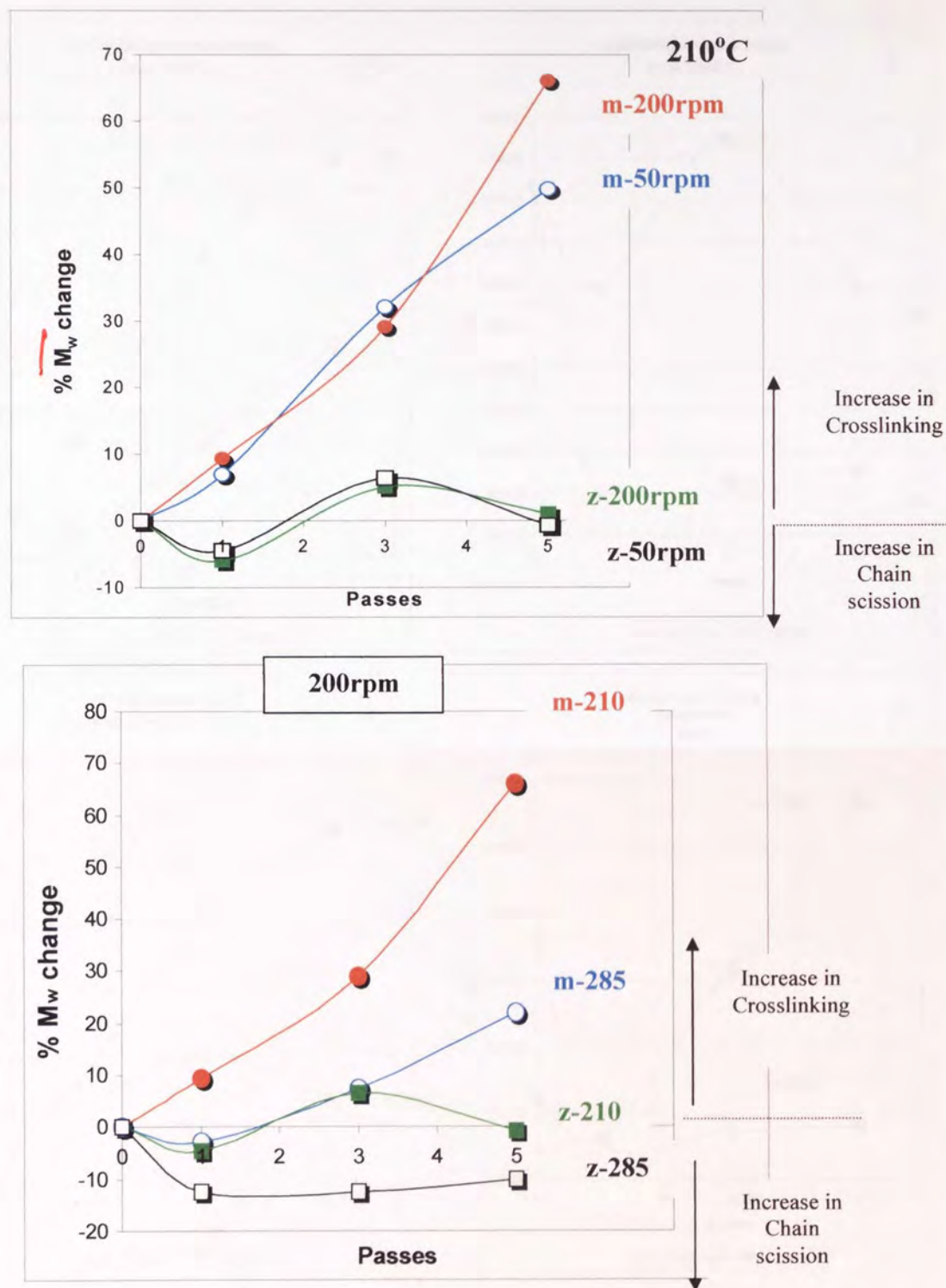


Figure 3.22. Effect of shear rate (screw speed); 50-200rpm at extrusion temperatures of 210-285°C upon the  $M_w$  (as measured by GPC) of extruded m-LLDPE and z-LLDPE polymer samples.



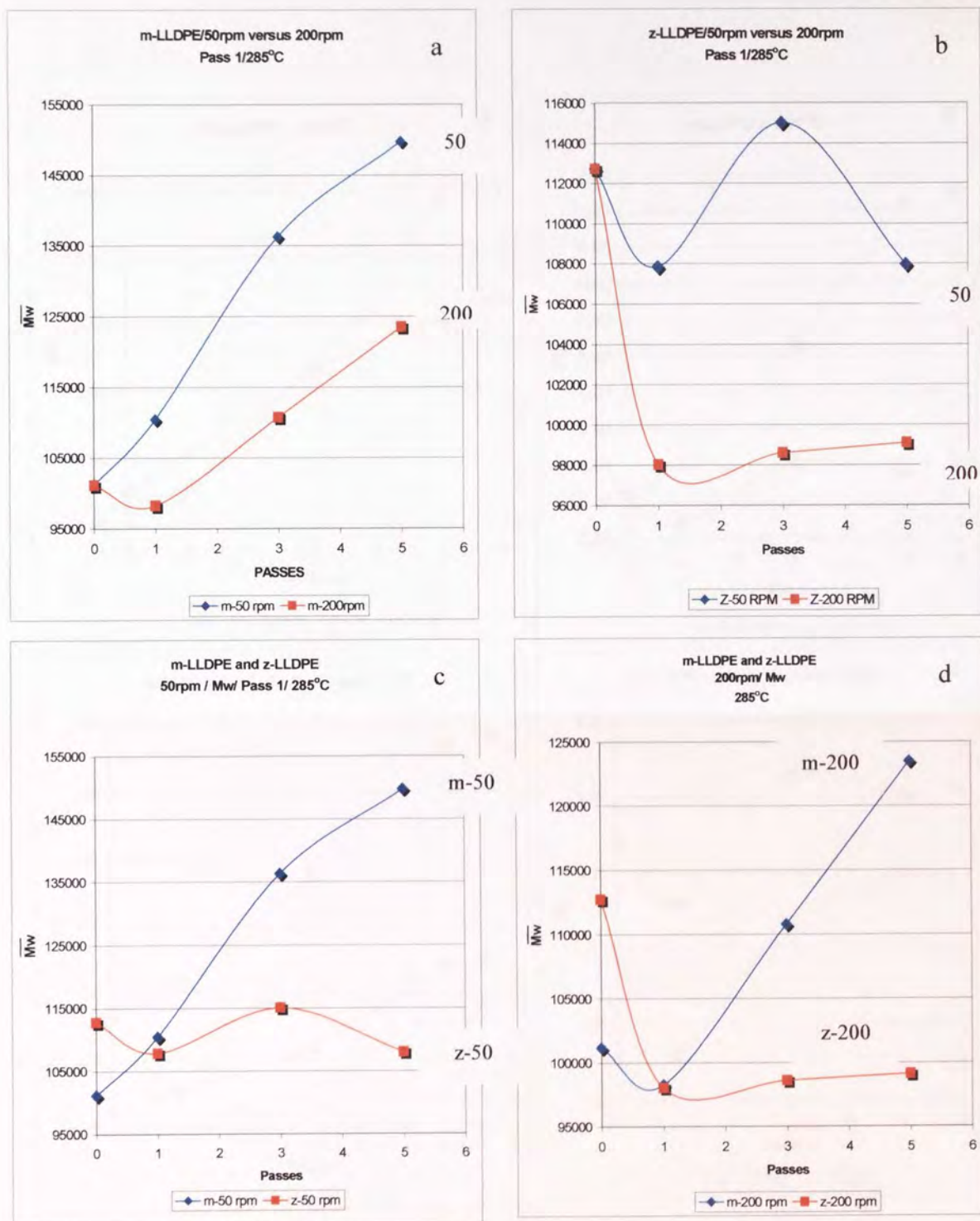


Figure 3.23 Effect of extrusion speed (50rpm and 200rpm) at an extrusion temperature of 285°C upon the  $\bar{M}_w$  (as measured by GPC) of multiply extruded m-LLDPE and z-LLDPE polymer samples.

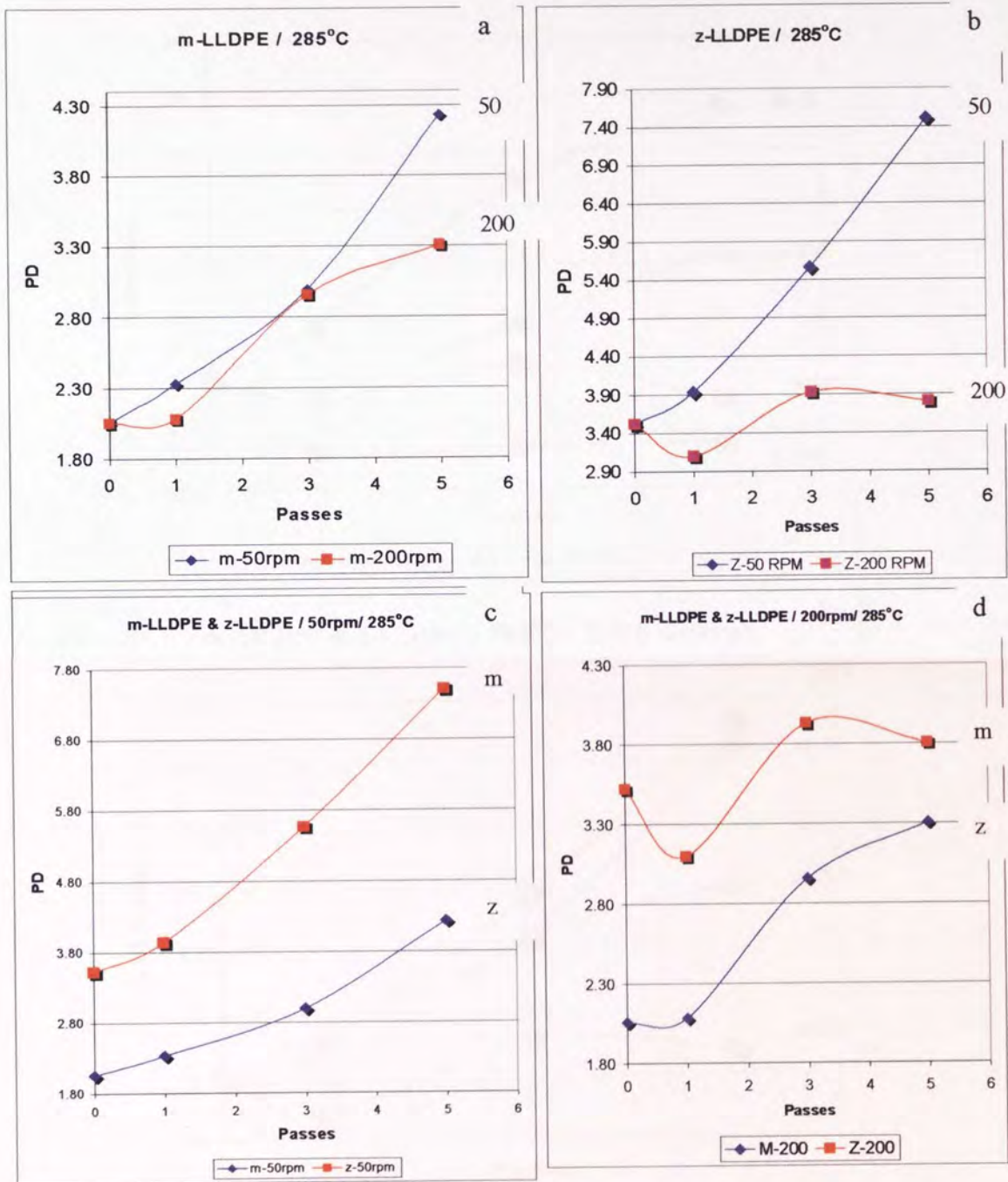


Figure 3.24. Effect of extrusion speed (50rpm-200rpm) at an extrusion temperature of 285°C upon the MWD (as measured by GPC) of multiply extruded m-LLDPE and z-LLDPE polymer samples.



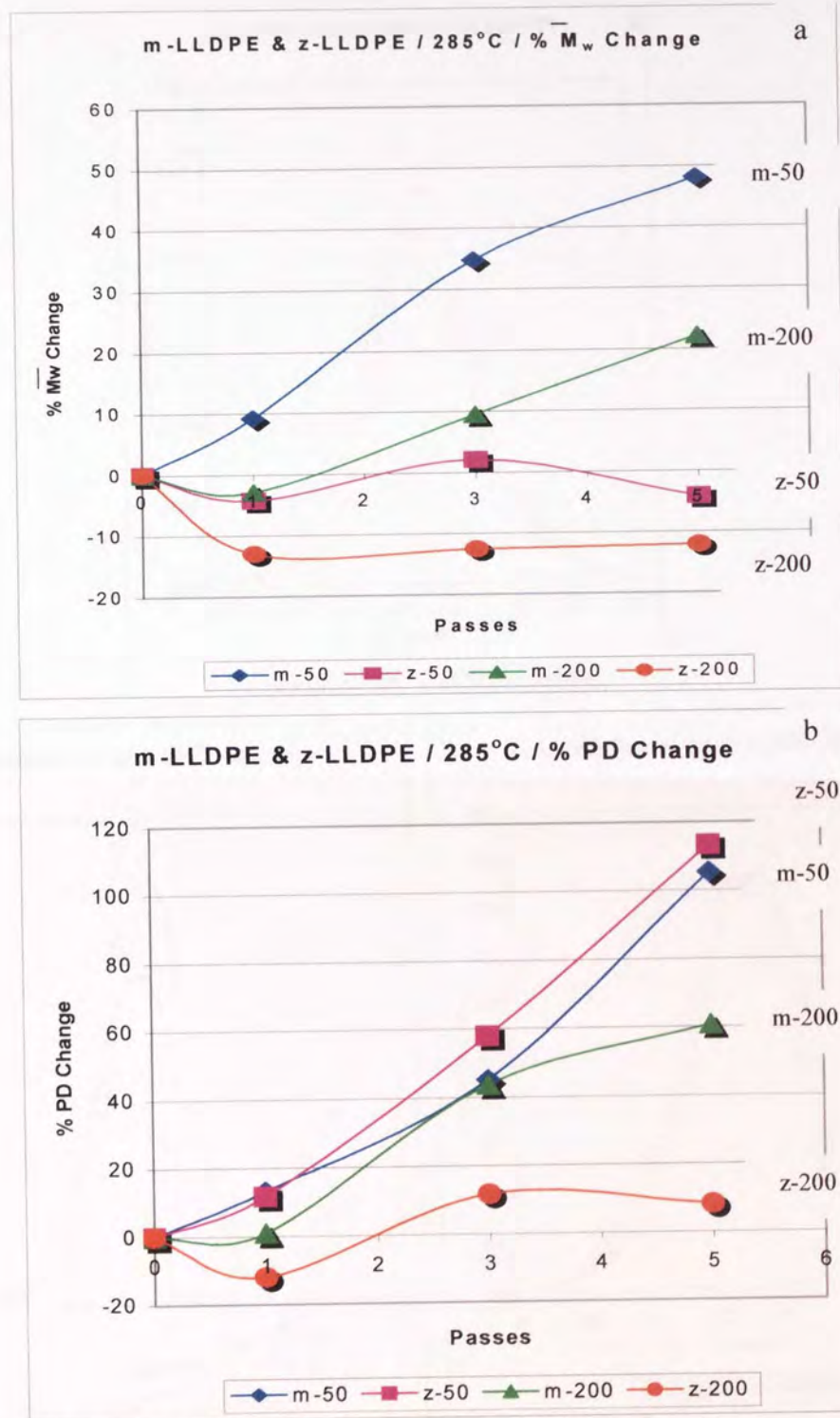


Figure 3.25 Effect of extrusion speed (50rpm and 200rpm) at an extrusion temperature of 285°C upon the % change (with respect to values of respective virgin polymers) in  $\bar{M}_w$  and polydispersity (as measured by GPC) of multiply extruded m-LLDPE and z-LLDPE polymer samples.

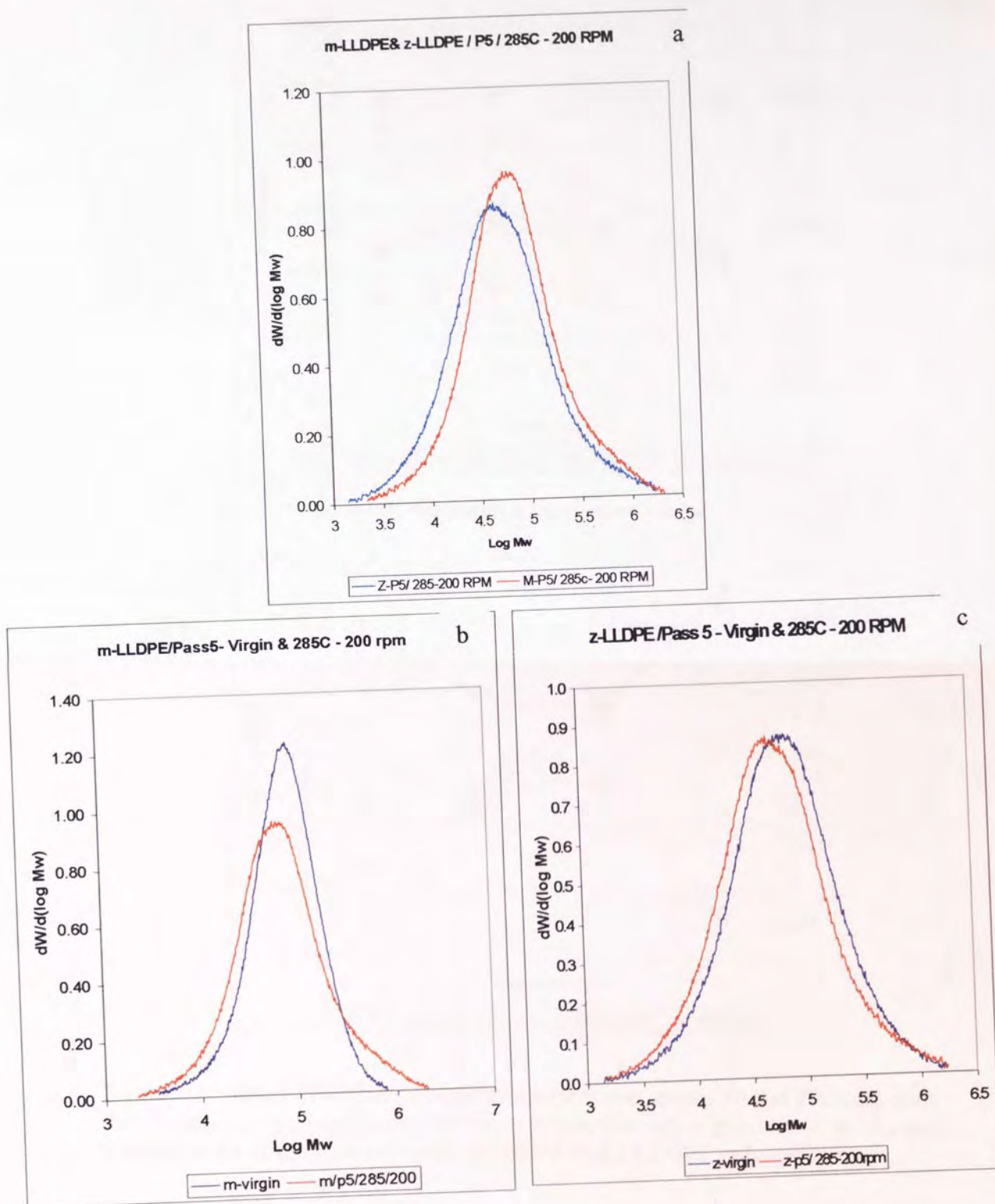


Figure 3.26. Shifts in MWD of Virgin m-LLDPE and z-LLDPE polymers relative to their multi-extruded Pass 5 analogues (285°C/200rpm).

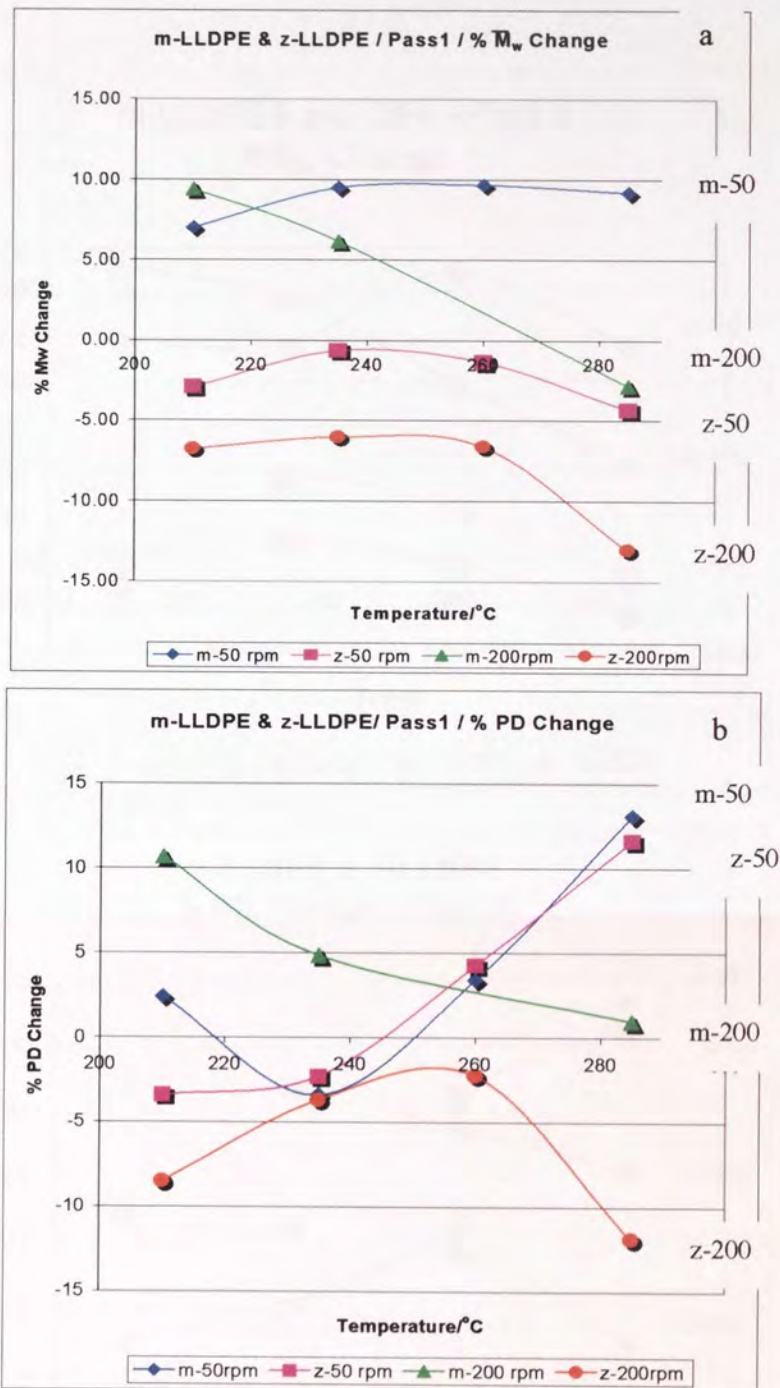


Figure 3.27. Effect of extrusion temperature (at screw speeds 50 and 200rpm) upon the % changes (with respect to values of respective virgin polymers) in  $M_w$  and polydispersity of multiple extruded m-LLDPE and z-LLDPE polymer samples.



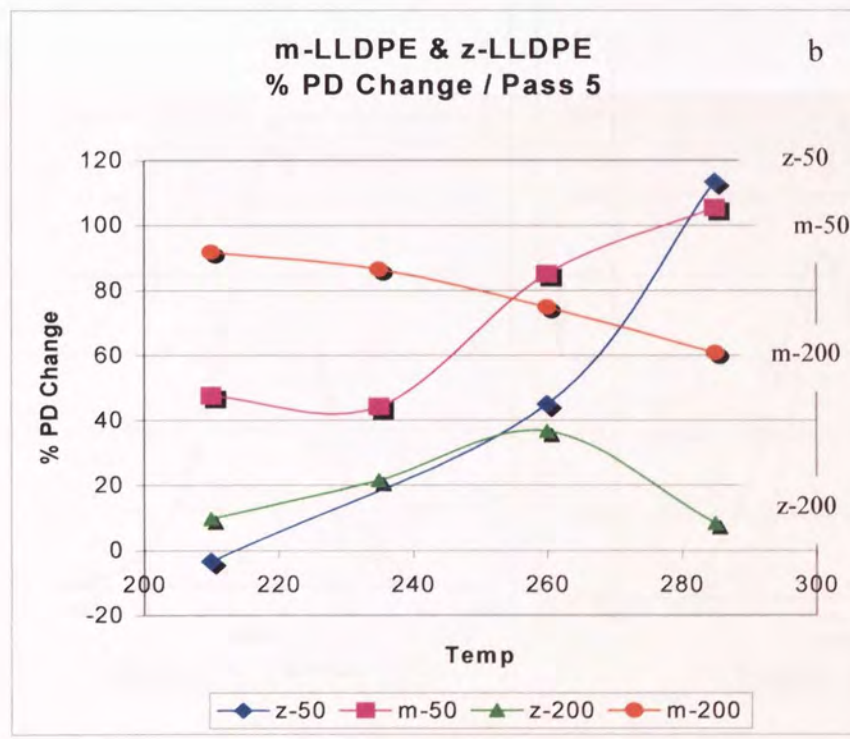
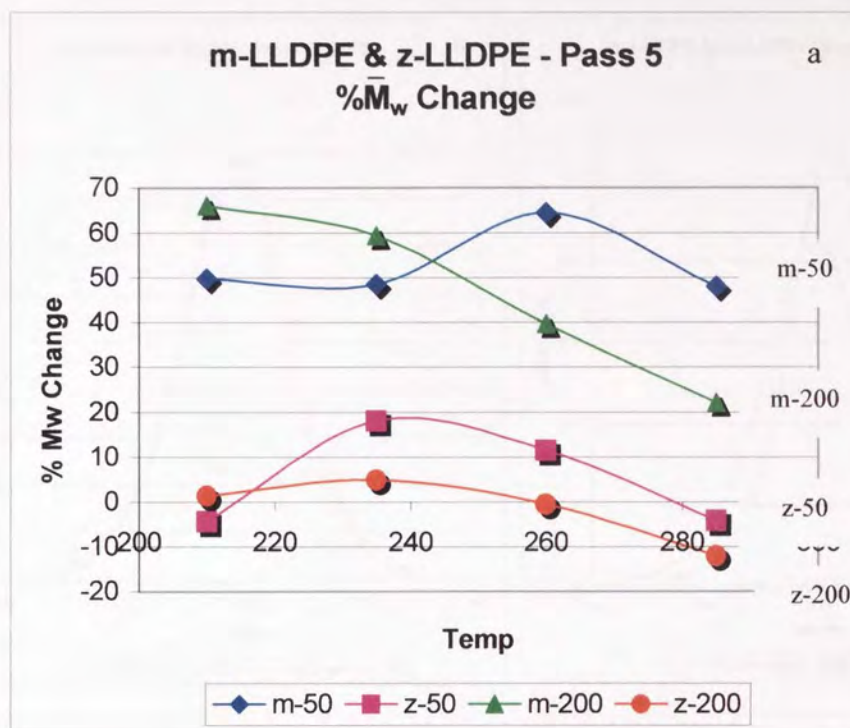


Figure 3.28. Effect of extrusion temperatures (at screw speeds 50 and 200rpm) upon the % changes (with respect to virgin polymers) in  $\bar{M}_w$  and MWD of Pass 5 extruded m-LLDPE and z-LLDPE polymer samples.

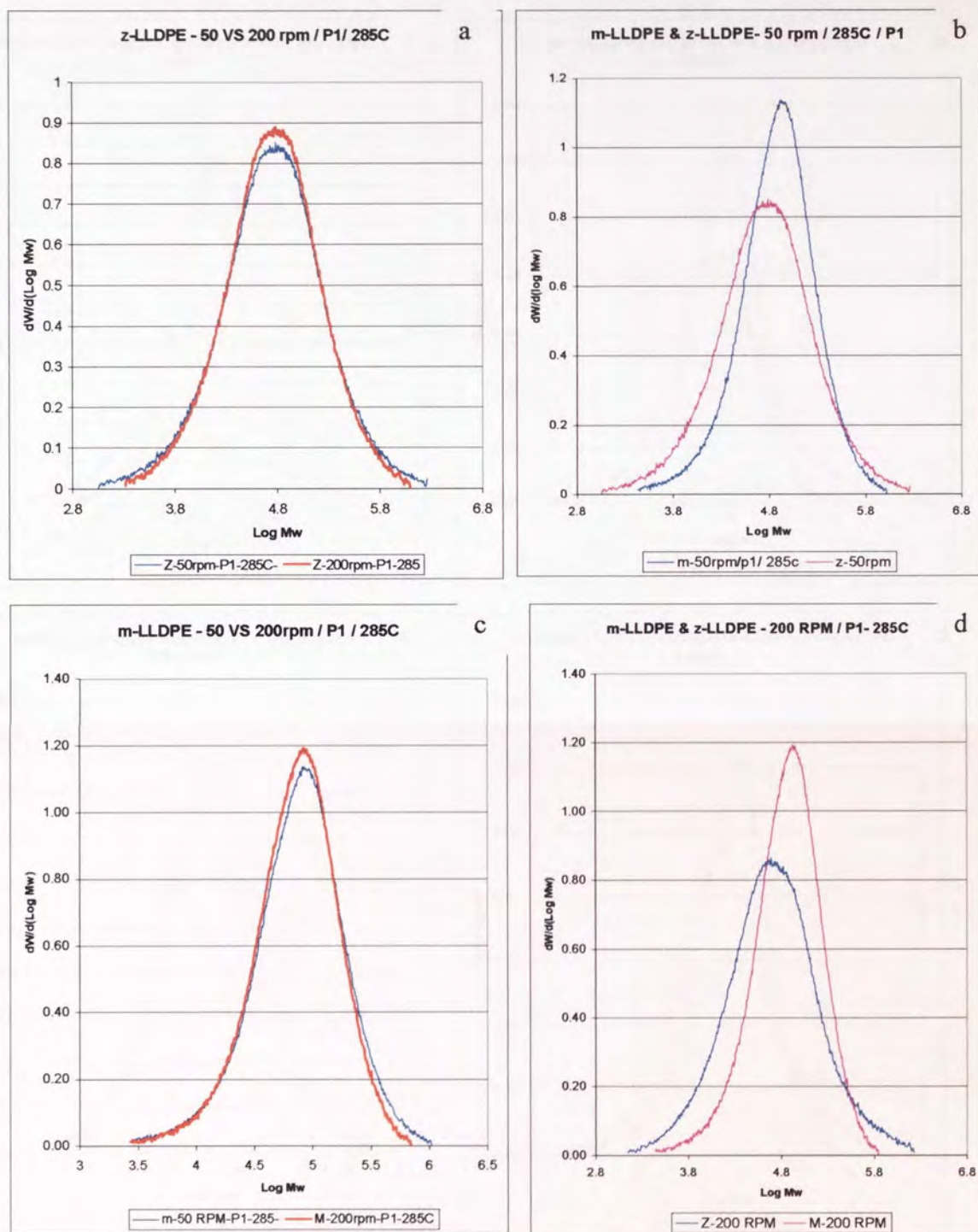


Figure 3.29. Shifts in MWD of Virgin m-LLDPE and z-LLDPE polymers relative to their multi-extruded Pass 1 analogues (285°C/50-200rpm).



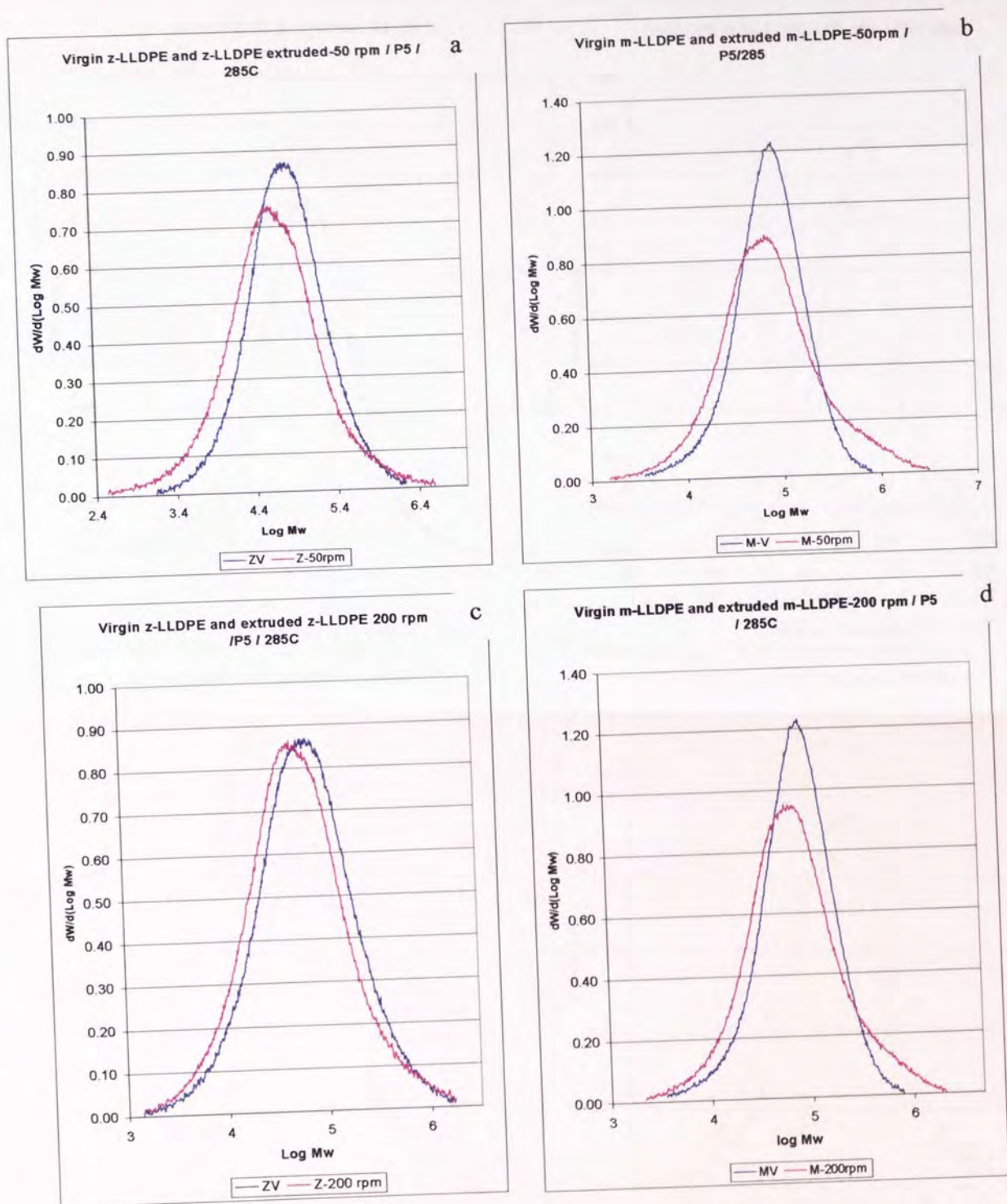


Figure 3.30. Shifts in MWD of Virgin m-LLDPE and z-LLDPE polymers relative to their multi-extruded Pass 5 analogues (285°C/50-200rpm).

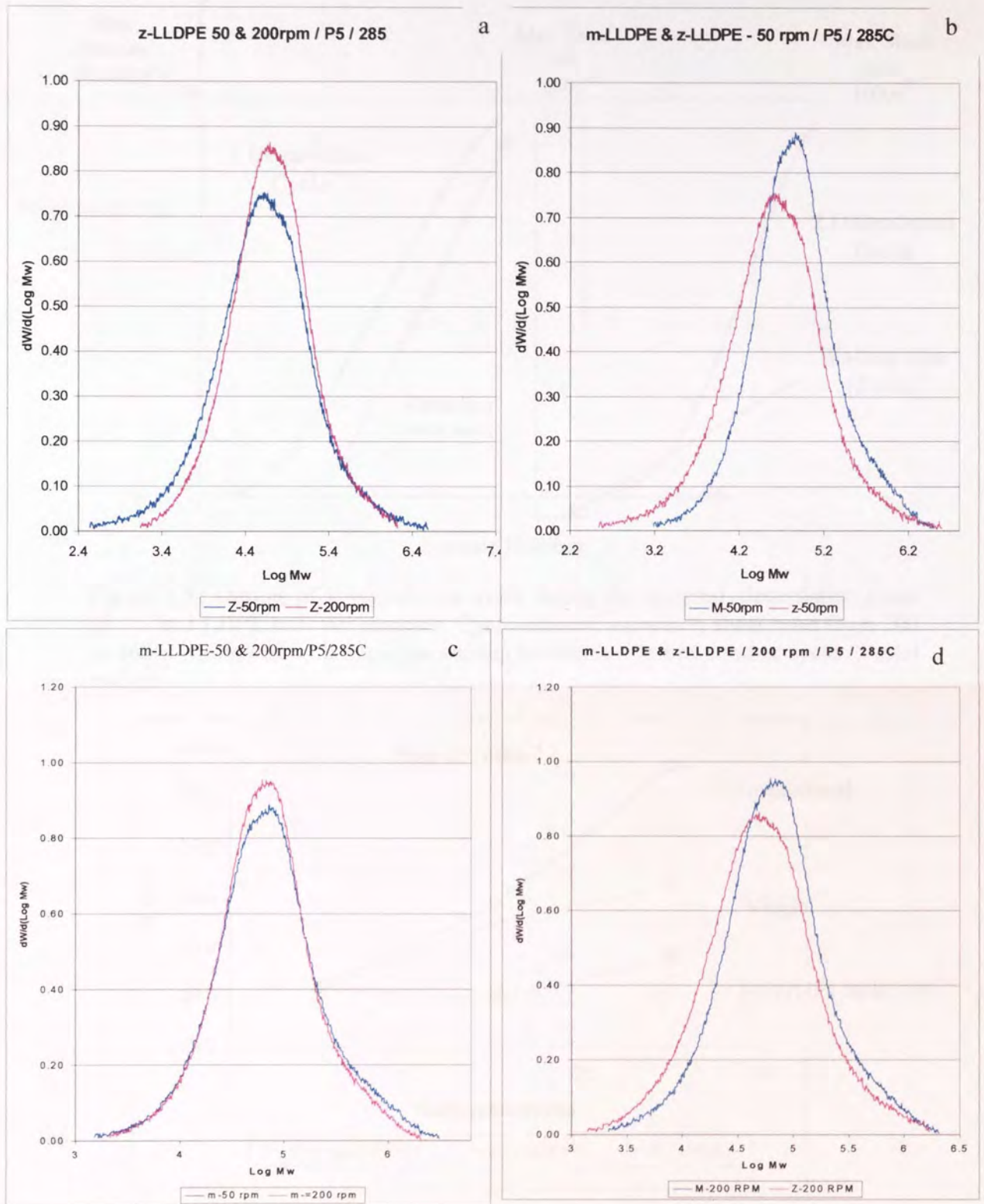


Figure 3.31. Shifts in MWD of Virgin m-LLDPE and z-LLDPE polymers relative to their multi-extruded Passes 1 and 5 analogues (285°C/50-200rpm).



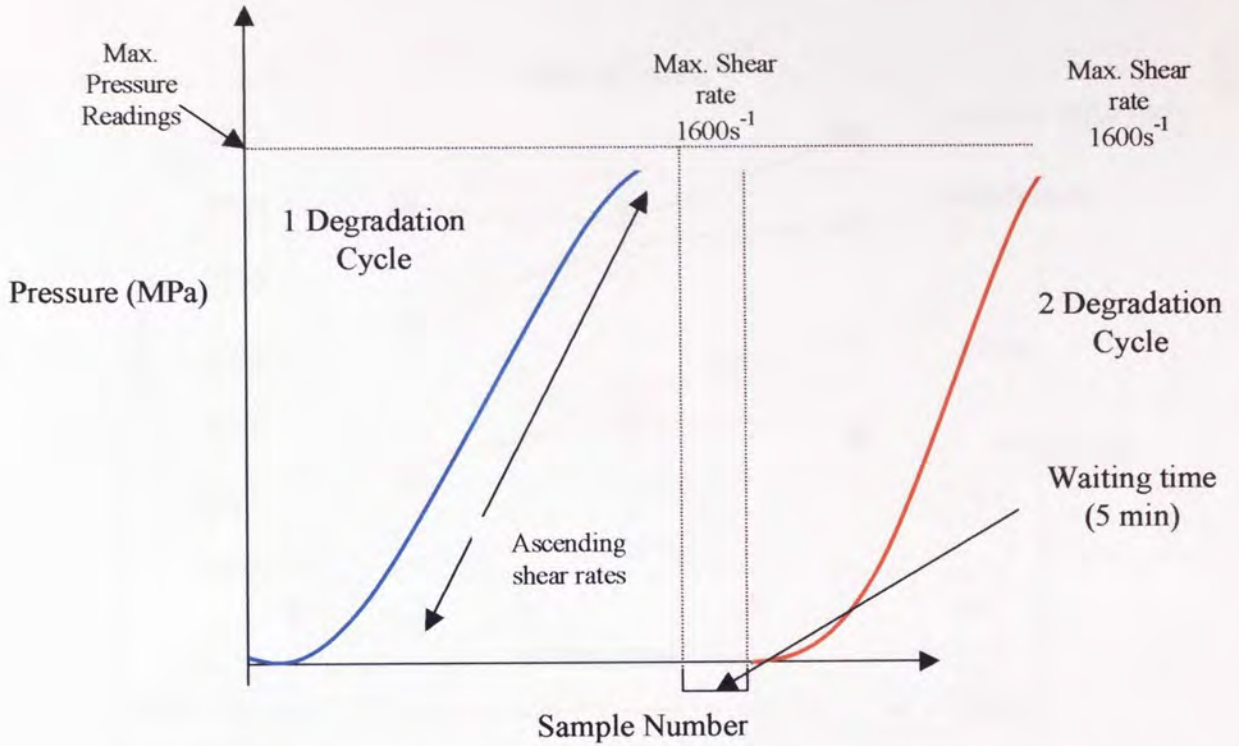


Figure 3.32 Outline of 1 degradation cycle during the material degradation cycle of m-LLDPE polymer samples. Cycle entailed ascending shear rates from 200 to 1600s<sup>-1</sup> followed by a 5 minute waiting before the start of another cycle (5 total cycles).

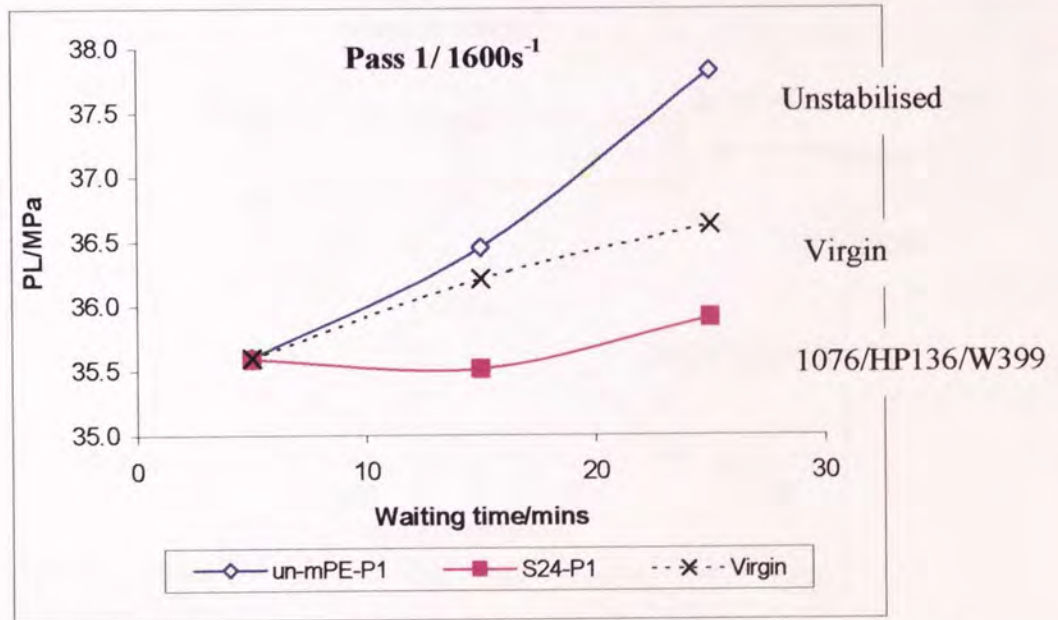


Figure 3.33 Change in Max. pressure on long die (PL) of **Pass 1**; Unstabilised extruded, Stabilised and that of Virgin m-LLDPE polymer samples during **Material Degradation test** (a shear rate; 1600s<sup>-1</sup> and temperature; 260°C, 5 degradation cycles, 5 minute waiting intervals). Stabilised and unstabilised extruded at 260°C/100rpm.

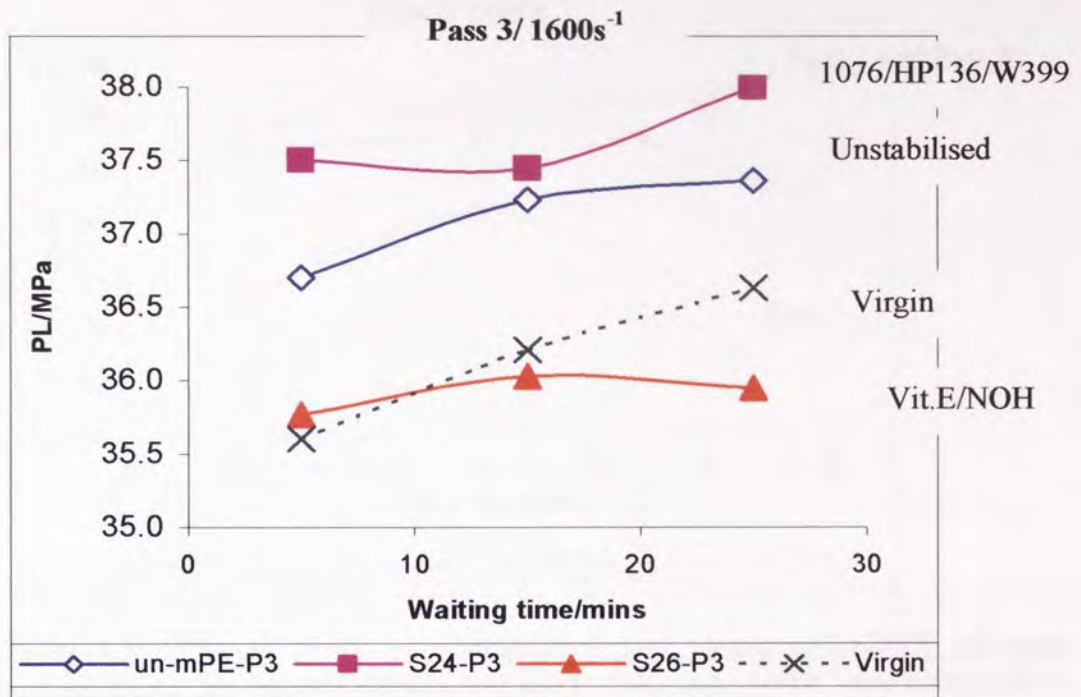


Figure 3.34. Change in PL of **Pass 3**; unstabilised, stabilised and virgin m-LLDPE polymer samples during the **Material Degradation Test** (a shear rate;  $1600\text{s}^{-1}$  and temperature;  $260^\circ\text{C}$ , 5 degradation cycles, 5 minute waiting intervals).

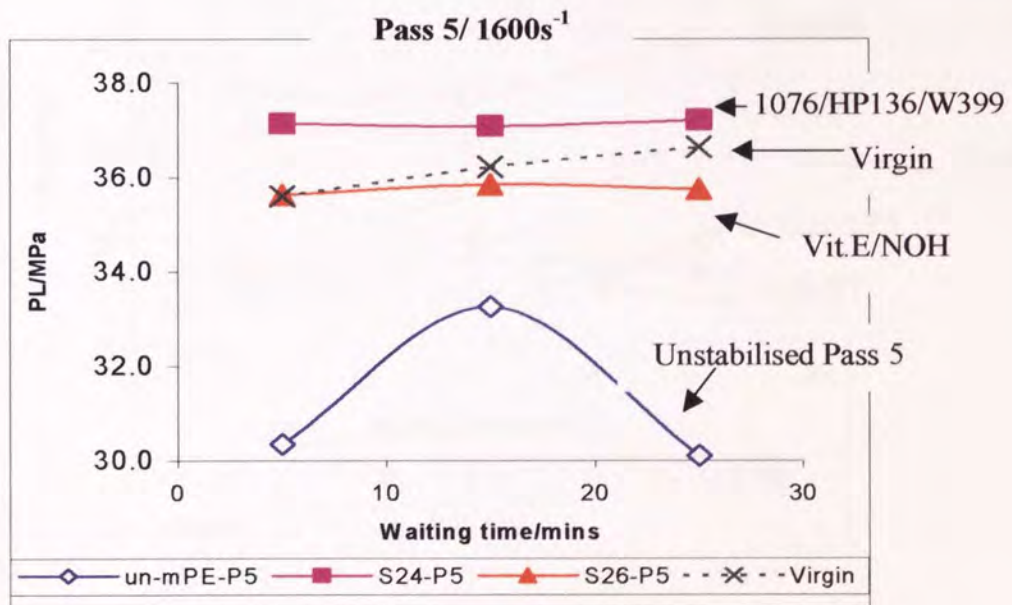


Figure 3.35. Change in PL of **Pass 5**; unstabilised, stabilised and virgin m-LLDPE polymer samples during the **Material Degradation Test** (a shear rate;  $1600\text{s}^{-1}$  and temperature;  $260^\circ\text{C}$ , 5 degradation cycles, 5 minute waiting intervals).



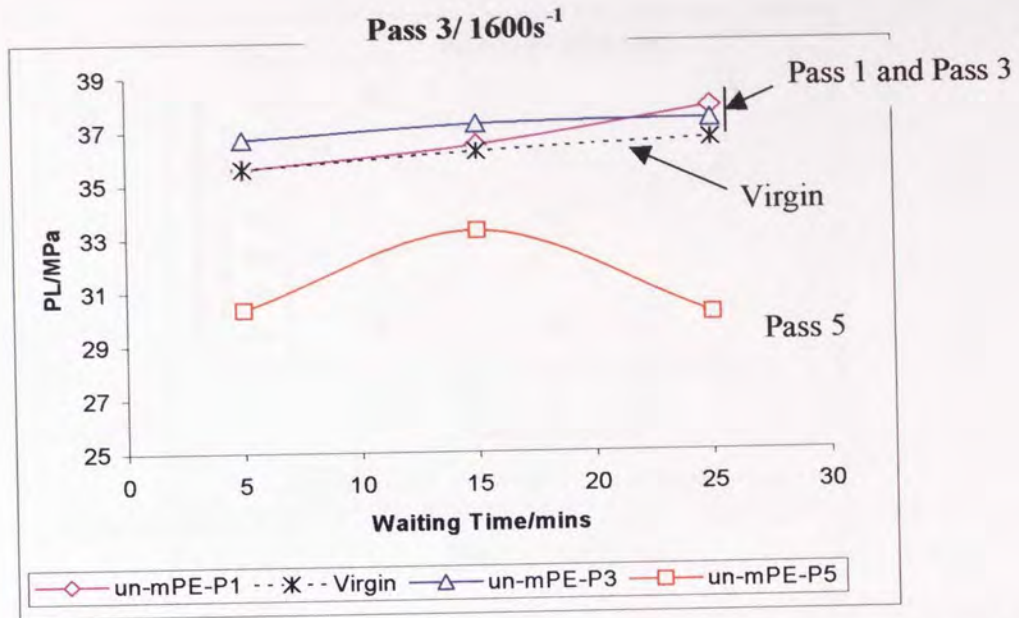


Figure 3.36. Change in PL of unstabilised and virgin m-LLDPE polymer samples during the material degradation test (a shear rate;  $1600s^{-1}$  and temperature;  $260^{\circ}C$ , 5 degradation cycles, 5 minute waiting intervals).

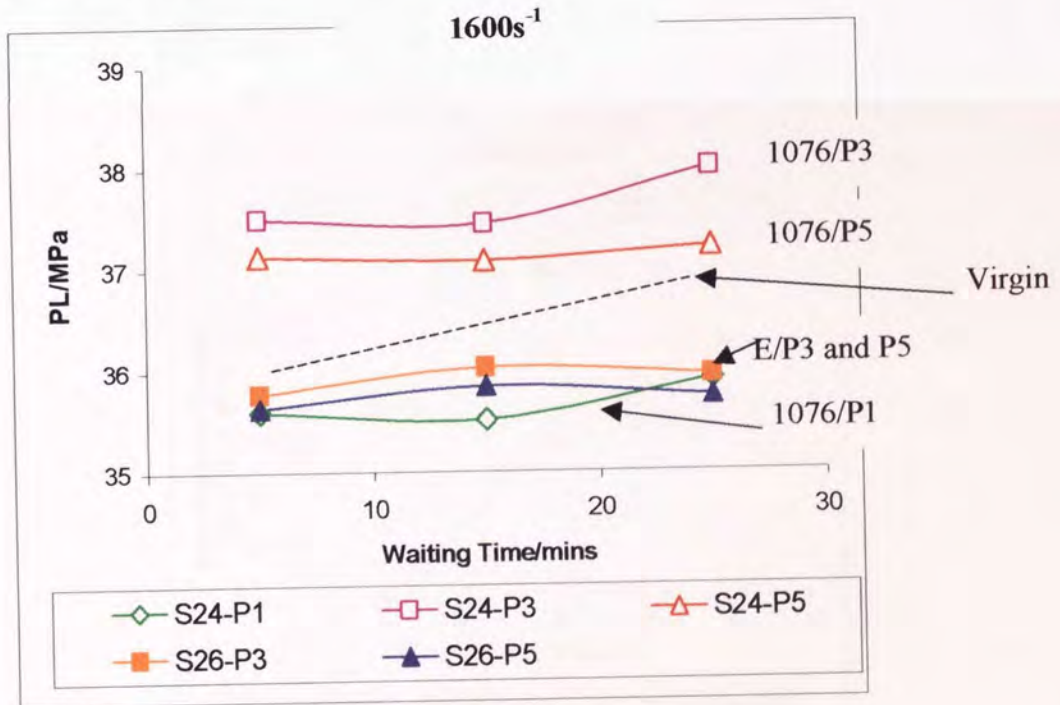


Figure 3.37. Change in PL of multi-processed (P1, P3 and P5), Po stabilised m-LLDPE polymer samples (using formulations s24 and s26, see table 5.1) during the material degradation test (a shear rate;  $1600s^{-1}$  and temperature;  $260^{\circ}C$ , 5 degradation cycles, 5 minute waiting intervals).

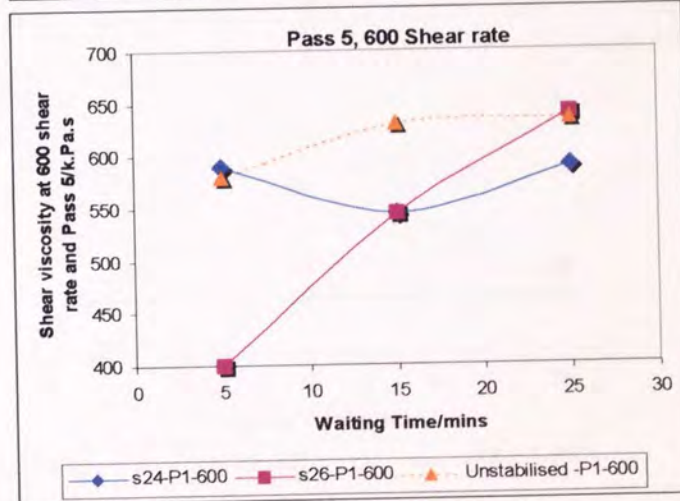
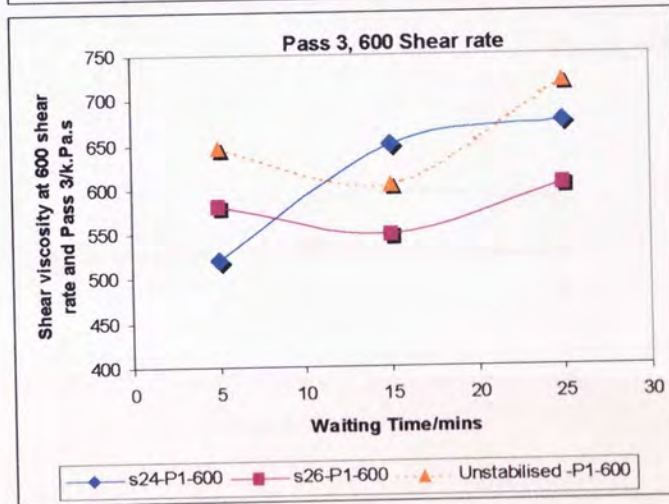
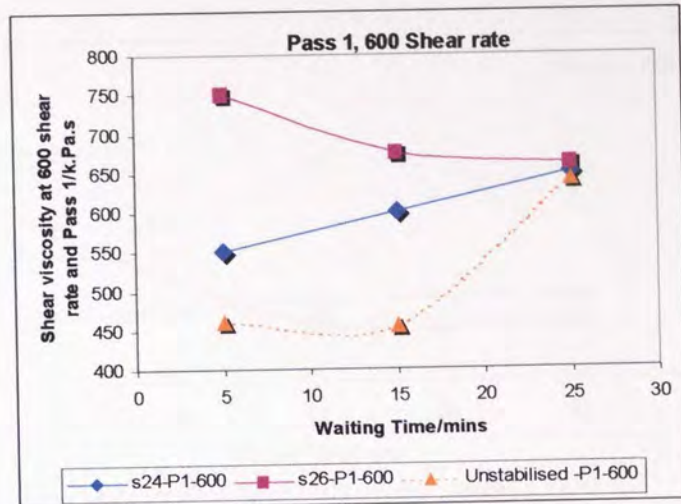


Figure 3.38. Change in Shear viscosity of multi-processed (P1, P3 and P5), Po stabilised m-LLDPE polymer samples (using formulations s24 and s26) during the material degradation test (at a shear rate of  $600\text{s}^{-1}$  and temperature;  $260^\circ\text{C}$ , 5 degradation cycles, 5 minute waiting intervals).



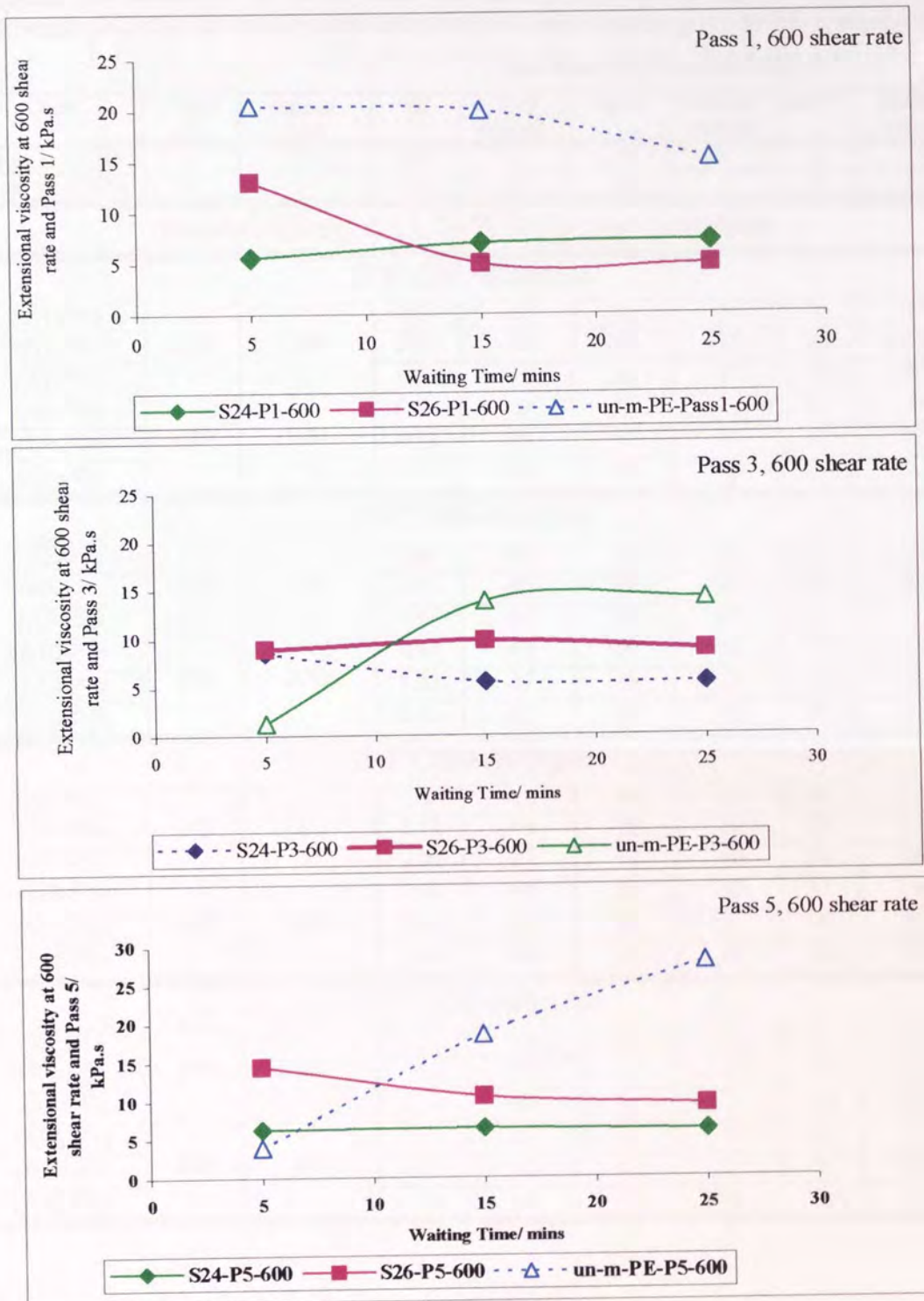


Figure 3.39. **Extensional viscosity functions** of unstabilised, stabilised and virgin multi-processed m-LLDPE polymer samples during the material degradation test (a shear rate;  $600\text{s}^{-1}$  and temperature;  $260^\circ\text{C}$ , 5 degradation cycles, 5 minute waiting intervals).

Table 3.2 Effect of Processing parameters on unstabilised extruded **z-LLDPE polymer samples**. The subscript 's' in the code denotes the addition of Irganox 1076 (0.2%w/w) by swelling in DCM to the unstabilised extruded polymer samples prior to MI measurements.

Code	Temp /°C	Speed /rpm	Melt flow measurements /10g.min <sup>-1</sup>					
			MI	%MI change <sup>1</sup>	HLMI	%HLMI change <sup>2</sup>	MFR <sup>3</sup>	%MFR <sup>4</sup> change
Virgin z-LLDPE	-	-	0.98	0	32	0	0	32
Virgin z-LLDPEs	-	-	0.97	0	32	0	0	33
<b>Unstabilised z-LLDPE Polymer samples</b>								
<b>210°C/50-200rpm</b>								
zA1-P1s	210	50	0.77	-21	29	-9	38	19
zA1-P3s			0.37	-62	20	-37	54	69
zA1-P5s			0.22	-77	28	-12	127	303
zA9-P1s	210	200	0.60	-38	27	-16	45	41
zA9-P3s			0.32	-67	30	-6	93	191
zA9-P5s			0.19	-80	31	-3	163	419
<b>235°C/50-200rpm</b>								
zA2-P1s	235	50	0.40	-60	23	-28	57	78
zA2-P3s			0.15	-85	22	-31	150	369
zA2-P5s			0.07	-93	18	-44	257	703
zA10-P1s	235	200	0.47	-53	26	-19	55	72
zA10-P3s			0.23	-67	28	-12	122	281
zA10-P5s			0.13	-87	26	-19	196	512
<b>260°C/50-200rpm</b>								
zA3-P1s	260	50	0.37	-63	26	-19	69	116
zA3-P3s			0.12	-88	25	-22	206	544
zA3-P5s			0.08	-92	19	-40	243	660
zA11-P1s	260	200	0.52	-48	28	-12	54	69
zA11-P3s			0.25	-75	33	3	133	316
zA11-P5s			0.15	-85	29	-9	195	509
<b>285°C/50-200rpm</b>								
zA4-P1s	285	50	0.51	-48	31	-3	62	94
zA4-P3s			0.19	-80	37	17	195	509
zA4-P5s			0.18	-81	33	3	183	472
zA12-P1s	285	200	0.71	-27	35	9	53	66
zA12-P3s			0.44	-55	42	31	96	200
zA12-P5s			0.33	-66	43	34	129	363

<sup>1</sup> %MI change = (MI<sub>sample</sub> - MI<sub>virgin</sub>)/MI<sub>virgin</sub> × 100

<sup>2</sup> % HLMI change = (HLMI<sub>sample</sub> - HLMI<sub>virgin</sub>)/HLMI<sub>virgin</sub> × 100

<sup>3</sup> MFR = HLMI/MI

<sup>4</sup> %MFR change = (MFR<sub>sample</sub> - MFR<sub>virgin</sub>)/MFR<sub>virgin</sub> × 100



Table 3.3 Effect of Processing parameters on unstabilised extruded **m-LLDPE polymer samples**. The subscript 's' in the code denotes the addition of Irganox 1076 (0.2%w/w) by swelling in DCM to the unstabilised extruded polymer samples prior to MI measurements.

Code	Temp /°C	Speed /rpm	Melt flow measurements /10g.min <sup>-1</sup>					
			MI	%MI change <sup>5</sup>	HLMI	%HLMI change <sup>6</sup>	MFR <sup>7</sup>	%MFR change <sup>8</sup>
Virgin m-LLDPE	-	-	0.97	0	17	0	17	0
Virgin m-LLDPEs	-	-	0.93	0	17	0	18	0
<b>Unstabilised m-LLDPE Polymer samples</b>								
<b>210°C/50-200rpm</b>								
mA1-P1	210	50	0.35	-61	12	-29	34	100
mA1-P3			0.09	-90	9	-47	100	488
mA1-P5			0.03	-98	6	-65	200	1076
mA1-P1s	210	50	0.36	-61	12	-29	33	94
mA1-P3s			0.09	-90	9	-47	100	488
mA1-P5s			0.02	-98	6	-65	300	1664
mA9-P1s	210	200	0.39	-58	15	-12	38	124
mA9-P3s			0.07	-92	11	-35	157	824
mA9-P5s			0.02	-98	5	-70	250	1370
<b>235°C/50-200rpm</b>								
mA2-P1s	235	50	0.41	-59	13	-24	30	76
mA2-P3s			0.11	-89	8	-53	76	347
mA2-P5s			0.04	-96	6	-65	153	800
mA10-P1s	235	200	0.29	-71	13	-24	43	153
mA10-P3s			0.04	-96	10	-41	245	1341
mA10-P5s			0.01	-99	5	-71	460	2606
<b>260°C/50-200rpm</b>								
mA3-P1s	260	50	0.37	-63	12	-29	33	94
mA3-P3s			0.05	-95	8	-53	152	794
mA3-P5s			0.01	-99	4	-76	430	2429
mA11-P1s	260	200	0.27	-73	13	-24	48	182
mA11-P3s			0.07	-93	11	-35	163	859
mA11-P5s			0.02	-98	8	-53	380	2135
<b>285°C/50-200rpm</b>								
mA4-P1s	285	50	0.25	-73	12	-29	48	182
mA4-P3s			0.06	-93	8	-53	133	682
mA4-P5s			0.01	-99	6	-65	600	3429
mA12-P1s	285	200	0.46	-50	18	-6	39	129
mA12-P3s			0.12	-87	17	0	142	735
mA12-P5s			0.08	-91	16	6	200	1076

$$^5 \text{ \%MI change} = (\text{MI}_{\text{sample}} - \text{MI}_{\text{virgin}}) / \text{MI}_{\text{virgin}} \times 100$$

$$^6 \text{ \% HLMI change} = (\text{HLMI}_{\text{sample}} - \text{HLMI}_{\text{virgin}}) / \text{HLMI}_{\text{virgin}} \times 100$$

$$^7 \text{ MFR} = \text{HLMI} / \text{MI}$$

$$^8 \text{ \%MFR change} = (\text{MFR}_{\text{sample}} - \text{MFR}_{\text{virgin}}) / \text{MFR}_{\text{virgin}} \times 100$$

Table 3.4: GPC results (provided by Exxon) of virgin and extruded m-LLDPE samples (50-200rpm, 210-285°C, atmospheric conditions, 4mm diameter, die).

				Molecular Weight Characteristics						
Code		Temp /°C	Speed /rpm	M <sub>n</sub>	M <sub>p</sub>	M <sub>w</sub>	M <sub>z</sub>	M <sub>z+1</sub>	M <sub>w</sub> /M <sub>n</sub>	M <sub>z</sub> /M <sub>w</sub>
Virgin m-LLDPE		-	-	49171	90414	101146	173087	267480	2.06	1.71
<b>Unstabilised m-LLDPE Polymer samples</b>										
<b>210°C/50-200rpm</b>										
mA1-P1s		210	50	51346	87800	108214	196166	316085	2.11	1.81
mA1-P3s				47151	96624	122115	270474	504280	2.59	2.21
mA1-P5s				49934	101156	151552	432701	876637	3.04	2.86
mA9-P1s		210	200	48532	86100	110642	224846	431185	2.28	2.03
mA9-P3s				44012	78094	133231	380852	803543	3.03	2.86
mA9-P5s				42503	83614	167985	655938	1308259	3.95	3.90
<b>235°C/50-200rpm</b>										
MA2-P1s		235	50	55597	89534	110722	200060	329051	1.99	1.81
MA2-P3s				-	-	-	-	-	-	-
MA2-P5s				50557	86946	150236	417523	838904	2.97	2.78
MA10-P1s		235	200	49650	85263	107354	197262	317325	2.16	1.84
MA10-P3s				-	-	-	-	-	-	-
MA10-P5s				42048	68138	161250	607943	1178834	3.83	3.77
<b>260°C/50-200rpm</b>										
MA3-P1s		260	50	51974	91303	110905	201031	323983	2.13	1.81
MA3-P3s				-	-	-	-	-	-	-
MA3-P5s				43606	86342	166278	604459	1280626	3.81	3.64
MA11-P1s		260	200	45675	80801	113701	250714	466229	2.49	2.21
MA11-P3s				-	-	-	-	-	-	-
MA11-P5s				39224	81201	141226	492267	997336	3.60	3.49
<b>285°C/50-200rpm</b>										
MA4-P1s		285	50	47352	83614	110406	215823	368552	2.33	1.95
MA4-P3s				45514	94025	136286	394610	859891	2.99	2.90
MA4-P5s				35437	72238	149742	609086	1303563	4.23	4.07
MA12-P1s		285	200	47131	83614	98245	168444	254966	2.08	1.71
MA12-P3s				37439	75844	110741	290972	618255	2.96	2.63
MA12-P5s				37341	62420	123484	401286	832981	3.31	3.25

Table 3.5: GPC results (provided by Exxon) of virgin and extruded z-LLDPE samples (50-200rpm, 210-285°C, atmospheric conditions, 4mm diameter, die).

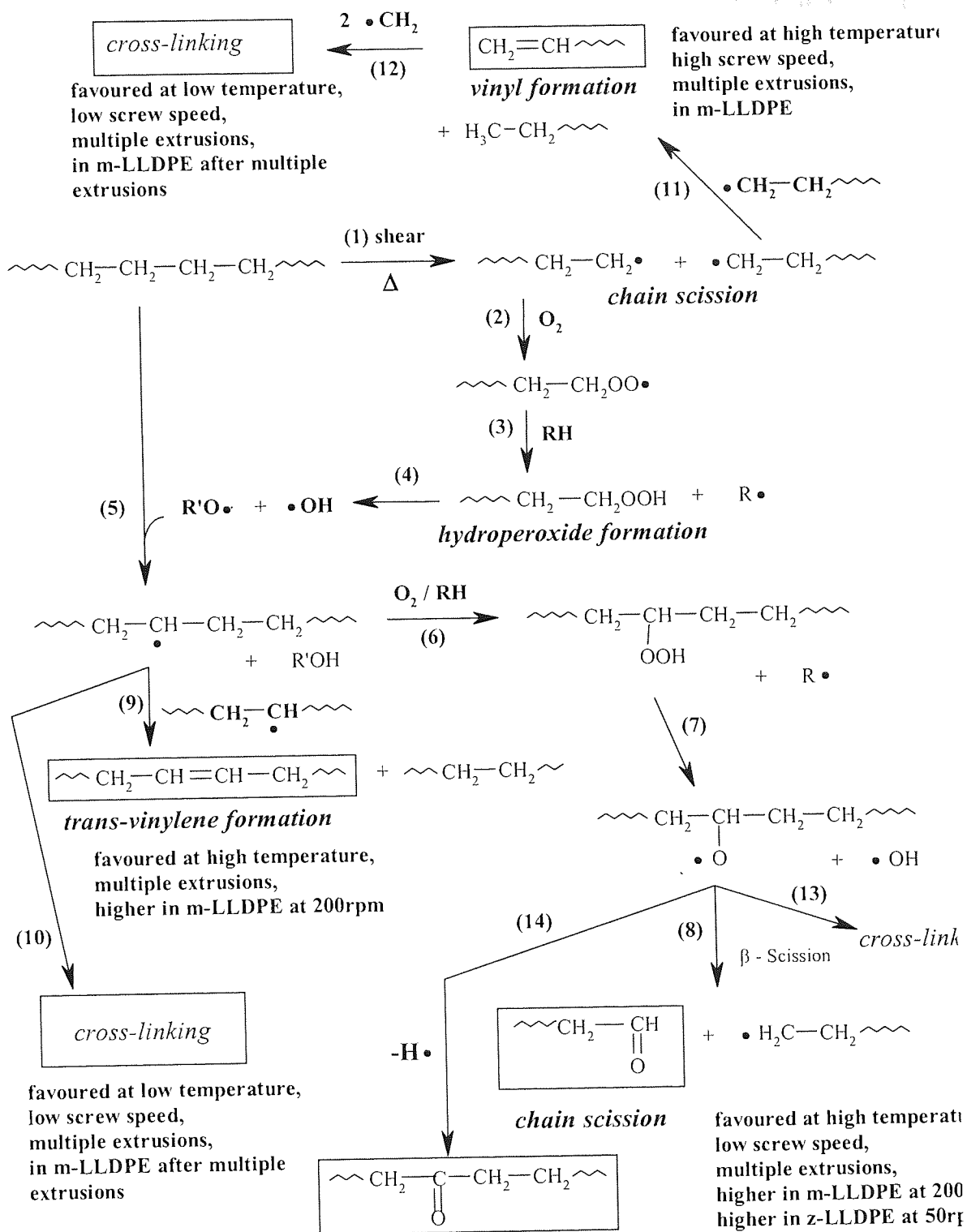
				Molecular Weight Characteristics						
Code		Temp /°C	Speed /rpm	M <sub>n</sub>	M <sub>p</sub>	M <sub>w</sub>	M <sub>z</sub>	M <sub>z+1</sub>	M <sub>w</sub> /M <sub>n</sub>	M <sub>z</sub> /M <sub>w</sub>
Virgin z-LLDPE		-	-	32008	70844	112720	333159	684148	3.52	2.96
<b>Unstabilised z-LLDPE Polymer samples</b>										
<b>210°C/50-200rpm</b>										
zA1-P1s		210	50	32159	76587	109420	309536	635763	3.40	2.83
zA1-P3s				28572	72370	114601	342431	673102	4.01	2.99
zA1-P5s				31695	65535	107839	305543	589924	3.40	2.83
zA9-P1s		210	200	32639	72945	105085	278409	531809	3.22	2.65
zA9-P3s				28894	70844	119718	444401	1056477	4.14	3.71
zA9-P5s				29609	46568	114220	396094	820901	3.86	3.47
<b>235°C/50-200rpm</b>										
zA2-P1s		235	50	32559	66824	111983	325609	671971	3.44	2.91
zA2-P3s				-	-	-	-	-	-	-
zA2-P5s				25408	47957	133117	579654	1267559	5.24	4.35
zA10-P1s		235	200	31232	66176	105923	296714	593395	3.39	2.80
zA10-P3s				-	-	-	-	-	-	-
zA10-P5s				27621	45976	118220	480004	1065087	4.28	4.06
<b>260°C/50-200rpm</b>										
zA3-P1s		260	50	30289	68138	111184	350354	756194	3.67	3.15
zA3-P3s				-	-	-	-	-	-	-
zA3-P5s				24615	43474	125644	628306	1505476	5.10	5.00
zA11-P1s		260	200	30620	70844	105252	306595	648414	3.44	2.91
zA11-P3s				-	-	-	-	-	-	-
zA11-P5s				23298	47958	112101	461963	980912	4.81	4.12
<b>285°C/50-200rpm</b>										
zA4-P1s		285	50	27415	61216	107839	346612	739721	3.93	3.21
zA4-P3s				20683	49387	115025	461691	1003006	5.56	4.01
zA4-P5s				14384	36030	107967	689803	1797530	7.51	6.39
zA12-P1s		285	200	31630	60623	98021	255402	486003	3.10	2.61
zA12-P3s				25072	49873	98590	304219	644262	3.93	3.09
zA12-P5s				26026	48906	99092	356526	763190	3.81	3.60

Table 3.6: Changes in the %  $\overline{M}_w$  and % PD characteristics (calculated from GPC measurements, provided by Exxon) of extruded m-LLDPE and z-LLDPE samples relative to their respective virgin polymers; 285°C/50-200rpm.

Polymer	Sample code	Pass	Speed/ rpm	Die temp./ °C	% Mw Change	% MWDChange
m-LLDPE	MA4-P1	1	50	285	9.16	13.1
	MA4-P3	3			34.74	45.14
	MA4-P5	5			48.04	105.33
	MA12-P1	1	200	285	-2.87	0.97
	MA12-P3	3			9.48	43.68
	MA12-P5	5			22.08	60.67
z-LLDPE	zA4-P1	1	50	285	-4.3	11.64
	zA4-P3	3			2.04	57.9
	zA4-P5	5			-4.2	113.35
	zA12-P1	1	200	285	-13.04	-11.9
	zA12-P3	3			-12.53	11.6
	zA12-P5	5			-12.09	8.2

Table 3.7. Effect of screw speed on the observed melt temperature of unstabilised multi-extruded (passes 1, 3 and 5) **m-LLDPE and z-LLDPE polymer samples**.

Polymer	Die (T1) Temp./°C	Screw Speed/rpm	Pass	Observed Melt (T2) Temp/°C	Temp. Difference (T2-T1)
Metallocene m-LLDPE	285	50	1	281	-4
			3	281	-4
			5	281	-4
		200	1	311	+26
			3	311	+26
			5	311	+26
Ziegler z-LLDPE	285	50	1	277	-8
			3	277	-8
			5	277	-8
		200	1	295	+15
			3	295	+15
			5	295	+15



Scheme 3.1 Proposed thermal oxidative mechanism of LLDPE.



## Chapter 4. Melt and Colour Stabilisation of m-LLDPE during processing using different classes of antioxidants Used singly.

### 4.1 Objectives and Methodology

It was shown previously (see chapter 3) that the thermal oxidative degradation route of m-LLDPE in the melt occurs mainly *via* crosslinking reactions. Based on this finding the effect of a number of antioxidants (AO) of different classes, used singly on the melt stability of m-LLDPE was investigated. These antioxidants operate primarily *via* different mechanisms; alkyl (R•), alkylperoxyl (ROO•) radical scavengers and hydroperoxide (ROOH) decomposers. These systems were examined in order to establish their individual performance in the polymer melt and to have a better understanding of their role when used in combination with other antioxidants (see chapter 5). In this chapter the extrusion characteristics and stabilising performance of different AOs used in m-LLDPE during compounding and multiple extrusion is discussed.

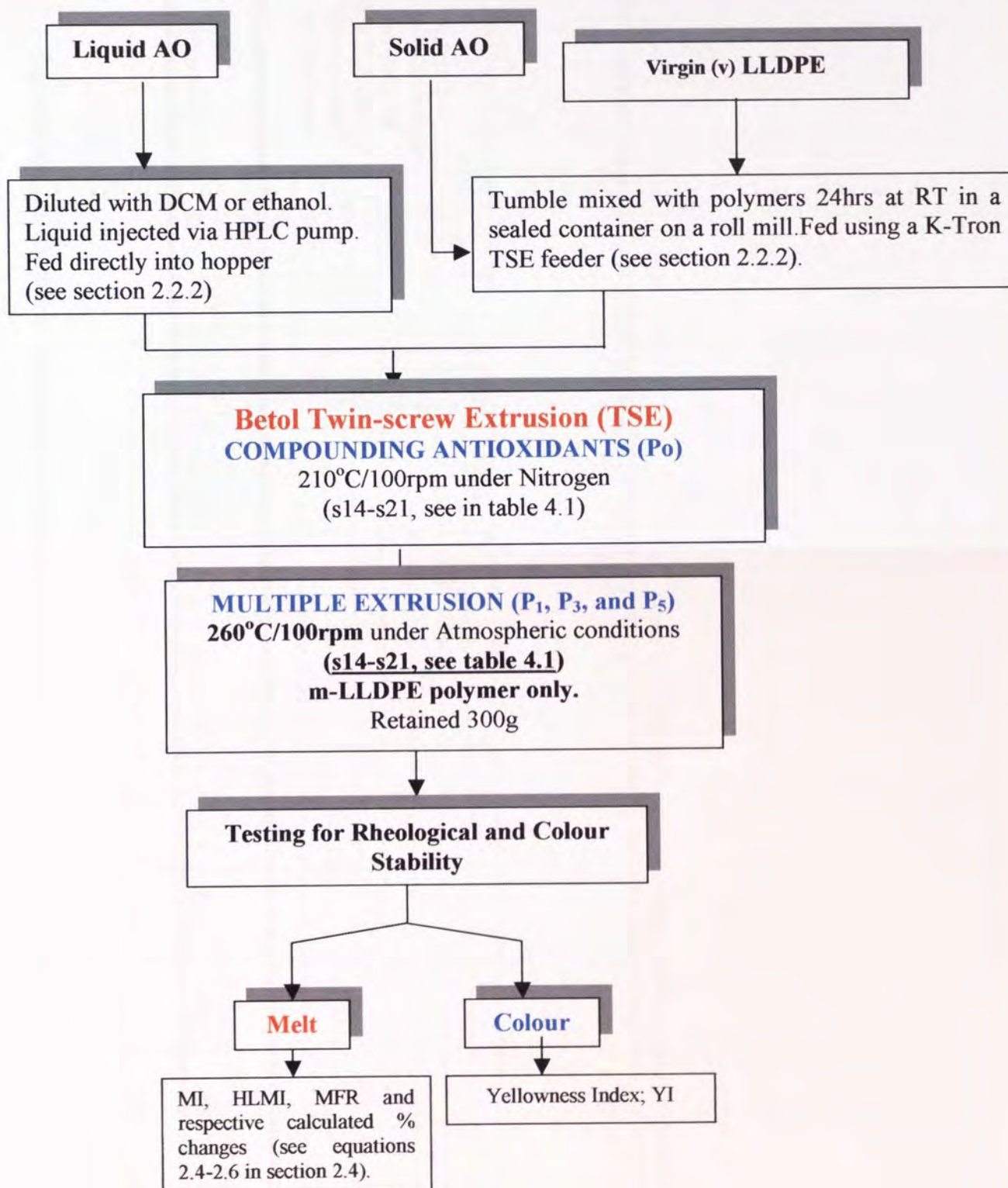
Table 4.1 displays the different AO systems used; including a synthetic (Irganox 1076) and biological (Irganox E201) hindered phenols; a lactone (Irganox HP136); an alkylated hydroxylamine (Irgastab FS042); a phosphite (Weston 399) and alkyl hydroxyl amine light stabilisers, R-HALS (Tinuvin 765, Tinuvin 622LD and Chimassorb 119D, see table 2.2 in chapter 2, for chemical structures). Table 4.2 shows selected stabilised polymer samples, which have been repeatedly processed in order to establish experimental error.

Different low concentrations of AO were initially compounded with the polymer (Po), during extrusion at an extrusion temperature of 210°C and screw speed of 100rpm under nitrogen (see section 2.2 for a detailed description). Polymer characterisation of all resultant extruded Po stabilised samples was carried out by examining their melt flow (MF) characteristics (MI, HLMI and MFR). A criterion for an acceptable level of Po stabilisation was based on the difference between the MI of the stabilised m-LLDPE polymer (Po) and the MI of the virgin m-LLDPE polymer being within the range of  $\pm 10\%$ .

All Po compounded m-LLDPE polymer samples were subsequently subjected to multiple extrusions using the TSE at an extrusion temperature of 260°C and screw speed of 100rpm,



under atmospheric conditions. To differentiate between the effectiveness of different AO, the melt flow and colour characteristics of the polymer samples were monitored after the first, third and fifth passes (multi-pass extrusion). Scheme 4.1 summarises the methodology used in this work.



Scheme 4.1. Overview of the methodology used in the stabilisation of m-LLDPE using single antioxidants.

Table 4.1 Metallocene catalysed LLDPE polymer samples containing different antioxidant formulations compounded (Po) in a TSE at 210°C/100rpm under nitrogen.

Cost/ \$/kg	0.04	0.44	-	0.31	0.13	0.33	0.02	-				
CODE	Irg. 1076	Irg. HP 136	Irgs. FS042	T.765	T.622LD	Irg. E201	W399	C119D	Total [AO] /ppm	Ratio /w/w	Cost <sup>1</sup> \$/kg of PE	Comments
S14	500								500	-	0.04	Analysing the effect of single AO systems upon the melt and colour stability of m-LLDPE
S15		300							300	-	0.44	
S16			1000						300	-	0.33	
S17				1000					1000	-	-	
S18					1000				2000	-	0.02	
S19						300			1000	-	0.31	
S20							2000		1000	-	0.13	
S21								1000	1000	-	-	

<sup>1</sup> To determine the total cost of a stabiliser package, calculate the cost of each individual AO then total i.e. [A:B:C] packages cost: ADDITIVE A COST = (Price of additive \$/kg) x (additive concentration/ppm) / 10<sup>4</sup> = \$/kg/PE. Repeat calculation for additive B and C.

Table 4.2 Metallocene catalysed Polyethylene (m-LLDPE) samples containing antioxidants received from Exxon Chemicals Baytown (USA) in May 2000; Irganox 1076, Irganox HP 136 and Irgastab FS042.

Code	Irg. 1076	Irg. HP136	Irg. FS042	Comments
S14	500			All stabilisation work conducted was carried out using 'new' and 'old' batches of AO obtained from Exxon.
S15		300		
S16			1000	

## 4.2 RESULTS

### 4.2.1 Extrusion characteristics of Pass-zero (Po) and Multiple extrusion (P1, P3 and P5) of stabilised (using single antioxidants) metallocene polymers.

The extrusion characteristics; power consumption, melt pressure, the appearance of the polymer lace, differences in melt and die temperature ( $\Delta T$ ) of stabilised m-LLDPE polymer samples containing different commercially available antioxidants (used singly); Irganox 1076, Irganox E201, Irganox HP136, Irgastab FS042, Weston 399, Tinuvin 622LD, Tinuvin 765, Chimassorb 119D; (see s14-s42 in table 4.1) were monitored (see section 2.2). All unstabilised m-LLDPE polymer samples were initially compounded, whereby the antioxidants were homogenised with the polymer using nitrogen and a low extrusion temperature of 210°C and screw speed of 100rpm, in order to minimise the effect of thermal oxidative degradation (see section 2.2a). The effectiveness of the single antioxidants (upon the melt and colour stability) in the m-LLDPE polymer was then examined by subjecting the compounded (Po) metallocene polymers to multiple extrusion (passes 1 to 5), under atmospheric conditions, extrusion temperature of 260°C and screw speed of 100rpm (see section 2.2b). The criterion chosen for the optimum feed rate values, were taken as those, which lead to minimum variation in pressure of  $\pm 5\%$ . The optimum output rate values used to process pass-zero Po stabilised and multiple extruded metallocene polymers were 4.0 kg.h<sup>-1</sup> and 4.8 kg.h<sup>-1</sup>, respectively. A virgin m-LLDPE polymer sample was also processed under the same multiple extrusion conditions. This allowed the extrusion characteristics of the unstabilised metallocene polymer to be compared to their stabilised counterpart.

#### a. Pass zero (Po) extrusion characteristics

Table 4.3 and figures 4.1-4.4 present the various extrusion characteristics recorded from m-LLDPE polymer samples processed in the presence of different antioxidants (see s14-s42 in table 4.1) during the compounding (Po) step and clearly show that the addition of either liquid or solid antioxidants to m-LLDPE during the compounding step lead to only minor differences in extrusion characteristics. It is also clear from these figures that there is little difference between the extrusion characteristics of the unstabilised m-LLDPE polymer and the stabilised samples, e.g. an unstabilised m-LLDPE polymer shows melt pressure values similar to that of an Irganox 1076 (s14) stabilised polymer under similar extrusion conditions (see table 4.3). Melt fracture, a real processing problem, is observed

as a dramatic change from a smooth extrusion to a non-laminar flow, sometimes giving rise to extrudate irregularities such as shark skin, zig-zag and basket weave [29]. Figure 4.2 and table 4.3 show that all polymers (in the presence and absence of antioxidants) exhibited severe melt fracture during the compounding step.

b. Multi-pass extrusion characteristics (Passes 1, 3 and 5)

Table 4.4 highlights the multi-pass extrusion characteristics of stabilised m-LLDPE polymers (s14-s21, in table 4.1). Figure 4.5 compares the effect of multi-pass steps on the extrusion characteristics of unstabilised and a selected m-LLDPE polymer sample containing Irganox 1076 (s14). It is clearly evident that the power consumption, melt pressures and  $\Delta T$  values of stabilised and unstabilised m-LLDPE polymer samples do not significantly change with increasing processing severity. Although there is no significant difference between the overall extrusion characteristics of the stabilised and unstabilised metallocene polymers (with increasing processing severity), the appearance of the polymer lace does however show a significant difference. Table 4.4 shows clearly that the unstabilised m-LLDPE polymer (with increasing processing severity) exhibits a distinct change in opacity (relative to its stabilised counterparts). It is interesting to note that m-LLDPE polymer samples containing R-HALS (relative to the other stabilised samples) show a noticeable change in opacity (with each successive extrusion pass). Repeating the extrusion process for selected stabilised samples in order to establish experimental error showed very little change in the extrusion characteristics of repeatedly processed samples, see table A1 in appendix 1.

#### **4.2.2 Effect of $P_0$ and Multiple Extrusions ( $P_1$ , $P_3$ and $P_5$ ) on the Melt stability of m-LLDPE.**

a. Pass-zero ( $P_0$ ) Compounding step

Table 4.5 and figures 4.6 & 4.7 compare the effect of the compounding ( $P_0$ ) step (210°C/100rpm under nitrogenous conditions) on the melt stability of compounded m-LLDPE using different antioxidants, with that of an extruded ( $P_1$ ) unstabilised m-LLDPE polymer sample. The high thermal melt stabilising performance of all antioxidants examined is clearly illustrated, showing no significant increase or decrease in melt flow characteristics with the exception of the two R-HALS AOs, Tinuvin 765 (s17) and Chimassorb 119D (s21). Both

R-HALS show overall lower MI values (see figure 4.6 & 4.7) and a negative value for the % MI change suggesting some crosslinking reactions taking place. Similarly, the unstabilised m-LLDPE polymer shows a drastic drop in MI and % MI change indicating a much higher crosslinking level even after only one extrusion process (260°C/100rpm). All samples appeared to be colourless after the compounding step.

b. Multiple Extrusion of Po stabilised m-LLDPE polymer samples.

(i) Effect of Synthetic and Biological Hindered Phenols, Lactones, Hydroxylamines and Phosphites

Tables 4.6 and figure 4.8 show the effect of processing severity (multi-pass extrusion) on the rheological characteristics of stabilised m-LLDPE polymers and clearly illustrate the far superior polymer melt stability imparted by the Irganox 1076, Irganox HP136 and Irganox E201 antioxidants in comparison to the phosphite (Weston 399) containing m-LLDPE polymer sample, (see s14, s15, s19 versus s20 in figure 4.8). It is also important to note that these former antioxidants were used at a fraction of the concentration used for Weston 399 (300-500ppm compared to 2000ppm, see in table 4.1).

Figure 4.8 also shows that the hydroxylamine, Irgastab FS042 (s16), imparted a slightly lower level of melt stability to the m-LLDPE (with increasing processing severity) compared to the hindered phenols and lactones, although it still outperformed the phosphite, Weston 399. Table 4.6 also calls attention to the different melt flow behaviour of the stabilised metallocene polymers relative to the unstabilised m-LLDPE polymer sample. It can be seen that the unstabilised m-LLDPE undergoes severe crosslinking and broadening of MWD, as reflected by the drastic drop in MI and rapid rise in the MFR.

Table 4.7 and figure 4.9 show the colour stability of m-LLDPE stabilised with different AOs' during multiple extrusion. It can be clearly seen that colour development increases with each successive extrusion pass for all stabilised polymer samples. Figure 4.9 also demonstrates that the lactone (Irganox HP136) and Vitamin E (Irganox E201) impart similar levels of colour stability to m-LLDPE with increasing processing severity (see s15 versus s19). The hydroxylamine (Irgastab FS042) imparts the most intense discolouration with increasing processing severity.

(ii) Alkyl Hydroxylamines (R-HALS).

Table 4.6 and figure 4.10 show the very low stabilising melt stability characteristics of m-LLDPE polymer samples containing three R-HALS antioxidants; Tinuvin 765 (s17), Tinuvin 622LD (s18) and Chimassorb 119D (s21). This is clearly illustrated by the drastic drop in MI and significant changes in MI and MFR (indicating extensive crosslinking and shifts in MWD) with increasing processing severity. Although it is important to note that the level of crosslinking incurred by R-HALS stabilised polymers (during multiple extrusion) is not as severe as that exhibited by the unstabilised metallocene polymer (see table 4.6).

Table 4.7 and figure 4.11 show that these samples also result in discolouration (with increasing processing severity) of the polymer with Chimassorb 119D giving the lowest intense yellowing, whereas Tinuvin 622 imparts the highest extent of discolouration. Although the R-HALS systems have demonstrated lower ineffectiveness as melt stabilisers to the m-LLDPE polymer (see figure 4.10), the extent of discolouration caused by these antioxidants appear to be lower than that offered by the hindered phenols, lactone and hydroxylamine.

### 4.3 DISCUSSION

Metallocene catalysed polyethylene (m-LLDPE) is widely used in a broad range of end-user applications covering all major consumer products such as films. The fabrication of these films is carried out almost exclusively using a twin-screw extrusion process (TSE) [25]. Agasant and co-workers [102] have shown that the advantages of the TSE method is derived from a short polymer melt residence time, good shear rate and temperature control, a positive pumping action, reduced melt slipping and a self-wiping screw action. The commercial interest in m-LLDPE is centred upon its unique molecular structural characteristics, i.e. narrow molecular weight (MWD) and short chain branch (SCB) distribution, features which govern advantageous physical properties (e.g. high optical clarity and impact strength) [21,24,103-104]. However, it is well documented in the literature that m-LLDPE primary molecular parameters lead to processing difficulties (due to high viscosities) often requiring the use of high processing temperatures and shearing conditions (in the presence of residual oxygen) [25,26,28]. It has been shown that the melt rheological properties of a polymer (under severe processing conditions) change drastically as a consequence of thermal oxidative degradation (as shown in section 1.4) thereby resulting in a loss in highly desirable



mechanical properties (see section 1.3.3) [32,45,105]. To inhibit such deleterious free radical oxidative reactions entails the use of 'powerful' antioxidants such as hindered phenols and phosphites, e.g. Irganox 1076 and Weston 399 (see section 1.5.1) [61]. To investigate the effects of different antioxidants (acting *via* different mechanisms) which have the potential of stabilising the m-LLDPE polymer, entails effective compounding of the AOs' in the polymer followed by multiple extrusion and measurement of melt and colour stability characteristics of the resultant stabilised m-LLDPE polymer samples. The difference in the effectiveness of different antioxidants representing different mechanistic classes is described here.

#### **4.3.1 Twin screw extrusion characteristics of Pass zero (Po) and Multi-pass (P1, P3 and P5) stabilised Metallocene polymers.**

It has been shown [22] that better film properties, i.e. optical clarity, maybe attained when a m-LLDPE polymer sample is compounded at a low temperature profile (under nitrogen) and then blown at a high temperature profile. In this work the compounding (Po) step was conducted at an extrusion temperature of 210°C and screw speed of 100rpm under nitrogen (using low concentrations of different antioxidants), whereas, the multiple extrusion process was carried out at 260°C/100rpm under atmospheric conditions. It has been clearly shown (see figures 4.1- 4.5), that the extrusion characteristics of all stabilised PE samples are not different from those of the unstabilised polymers. The level of power consumed (during extrusion) may be attributed to the amount of power required to shear the polymer melt during processing and is a reflection of the overall rheological characteristics of the m-LLDPE polymer [25]. The m-LLDPE polymer, by virtue of its narrow MWD, contains a low fraction of low molecular weight chains and a low fraction of high molecular weight chains (see table 2.1 in chapter 2, p.73, molecular weight characteristics,), thereby resulting in a high degree of entanglement (i.e. high viscosity) and irregular flow. This has been shown to result in the use of large amounts of energy from the extruder motor (the main source of energy to the polymer melt) and higher overall higher power consumption than the Ziegler polymer. The high melt temperatures compared to the die temperature (note that  $\Delta T$  is correlated to the melt flow of the polymers) shown by the metallocene polymer (higher than the Ziegler polymer) must be due to the high shear rates, (as indicated by the high power consumption, see figure 4.1) experienced during processing which generates more heat in the melt during extrusion. The melt pressures measured by the pressure transducers at the die, is governed by the viscosity of the polymer, higher viscosities result in higher melt pressures.



Melt fracture, a real processing problem [29], was clearly shown in the case of both stabilised and unstabilised metallocene polymers under all extrusion conditions examined (see figure 4.2). It has been suggested [29,106] that melt fracture arises from a periodic loss of melt adhesion at the die wall at a critical shear stress. It is observed as a dramatic change from laminar to a non-laminar flow thereby giving rise to extrudate surface irregularities such as shark-skin [29]. It has been demonstrated [106] that the magnitude of melt fracture incurred by a m-LLDPE polymer during film blowing extrusion has a strong influence on its ultimate mechanical properties, i.e. dart impact strength. In this study the melt fracture observed at 210°C/100rpm was found to be the most severe (as compared to 260°C/100rpm), see table 4.3 & 4.4 and figure 4.2. This suggests that polymer samples processed at 210°C/100rpm may exhibit undesirable mechanical properties, i.e. lower dart impact strength, as compared to analogue polymer samples extruded at 260°C/100rpm. In addition, these results demonstrate the important role that temperature exerts upon the severity of melt fracture encountered during processing, i.e. the higher the extrusion temperature, the less melt fracture but the greater probability of thermal oxidative degradation. This may be rationalised if considering that an increase in temperature results in increasing polymer chain movement; translation, rotation and vibration of the main backbone and the SCB [22], thereby reducing the overall melt viscosity (less entanglements between polymeric chains) and increasing the 'availability' of more mobile polymer chains susceptible to the deleterious free radical reactions leading to thermal oxidative degradation. The occurrence of melt fracture in m-LLDPE under simulated extrusion conditions at low shear rates was also clearly evident from capillary rheometric measurements (see chapter 3). It was shown recently [107] that the addition of a branched polymer, as a processing aid for m-LLDPE used in tubular film blowing, not only increases the processing rate but successfully eliminates melt fracture without changing the overall physical properties of m-LLDPE films. This was attributed to the migration of the branched polymer to the surface during extrusion, thereby forming a lubricating layer between the metal surfaces and the bulk material [107].

It is interesting to note that although the overall extrusion characteristics of the stabilised m-LLDPE polymer appear to be not too different from those of their unstabilised counterparts (under all extrusion conditions examined, see in figures 4.1-4.5), there however appears to be a distinct difference in the appearance of the extrudates (i.e. opacity) after multiple extrusion.

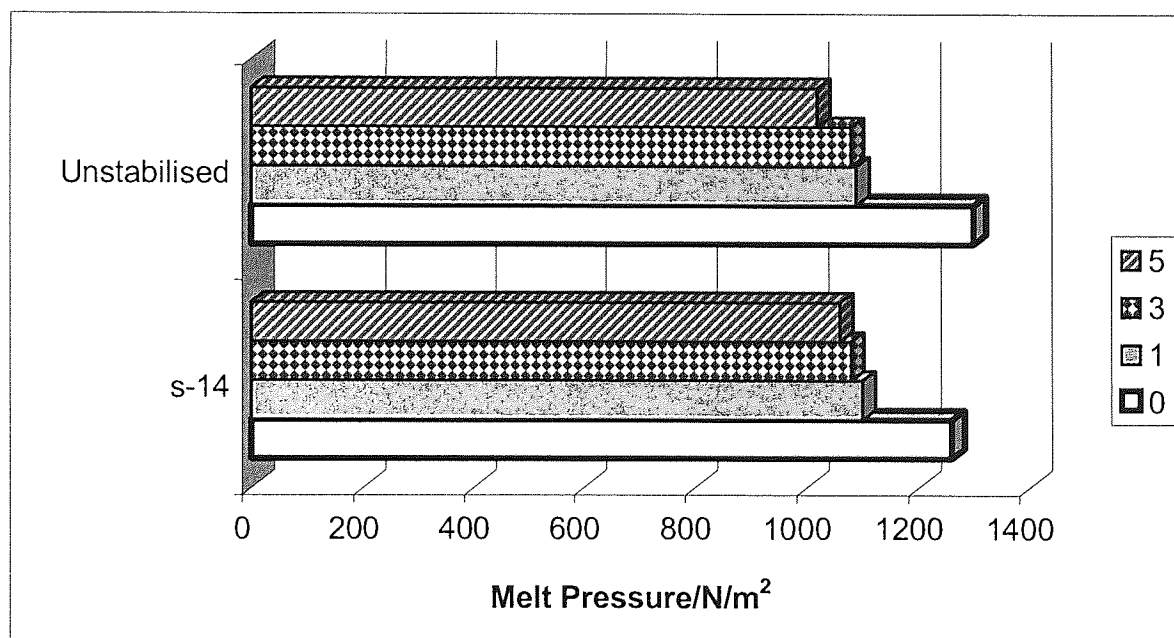
Table 4.4 highlights the fact that the unstabilised m-LLDPE polymer samples display the greatest change in opacity (appeared less clear) with increasing processing severity compared to the stabilised m-LLDPE polymer samples. This may be explained by earlier findings (see chapter 3) that the unstabilised m-LLDPE polymer undergoes a significant increase in its viscosity (i.e. polymer Mw) due to prevalent crosslinking reactions (see figure 4.10). This significant change in the unstabilised polymer structure may be responsible for the noticeable change in opacity. On the other hand, the high levels of melt stability offered by the different antioxidants (i.e. effective inhibition of free radical crosslinking reactions), to the metallocene polymer during multiple extrusion appears to be associated with minimal changes in polymer opacity. Qu and Ranby [108] have demonstrated that when LDPE undergoes drastic structural changes (e.g. increase in crosslinking) and a change in its physical properties during extrusion there is an overall decrease in polymer opacity. A noticeable change in opacity (with increasing processing severity) was observed in the case of m-LLDPE polymer samples containing R-HALS antioxidants, which have imparted much lower extents of melt stability and higher levels of crosslinking reactions (see figure 4.9) during multiple extrusion this lends further support to this argument.

#### **4.3.2 Effect of a Lactone, Hydroxylamine and Synthetic/Biological hindered phenols and a phosphite on the melt and colour stability of m-LLDPE during processing.**

MFI can provide useful information with regard to structural changes in polymers processed under different conditions [48]. A decrease in MI is caused by an increase in the molecular weight (Mw) of the polymer due to the dominance of crosslinking reactions, whilst an increase in MI is associated with a decrease in the Mw of the polymer due to chain scission [48]. The calculation of the melt flow ratio, MFR (see equation 2.5, in section 2.4), from MFI measurements can be directly related to the changes in a primary molecular parameter (see section 1.3.1, p. 5), the molecular weight distribution (MWD) [34].

The mild conditions (210°C/100rpm under nitrogen) used for the compounding step is important as this results in almost no change in melt characteristics of the polymers compared to the virgin polymer samples (see figure 4.8). It has been shown in the literature [22] that the effect of thermal oxidative degradation may be minimised by blanketing material feeders and the hopper above the extruder with nitrogen. The lack of colour imparted by the Po stabilised

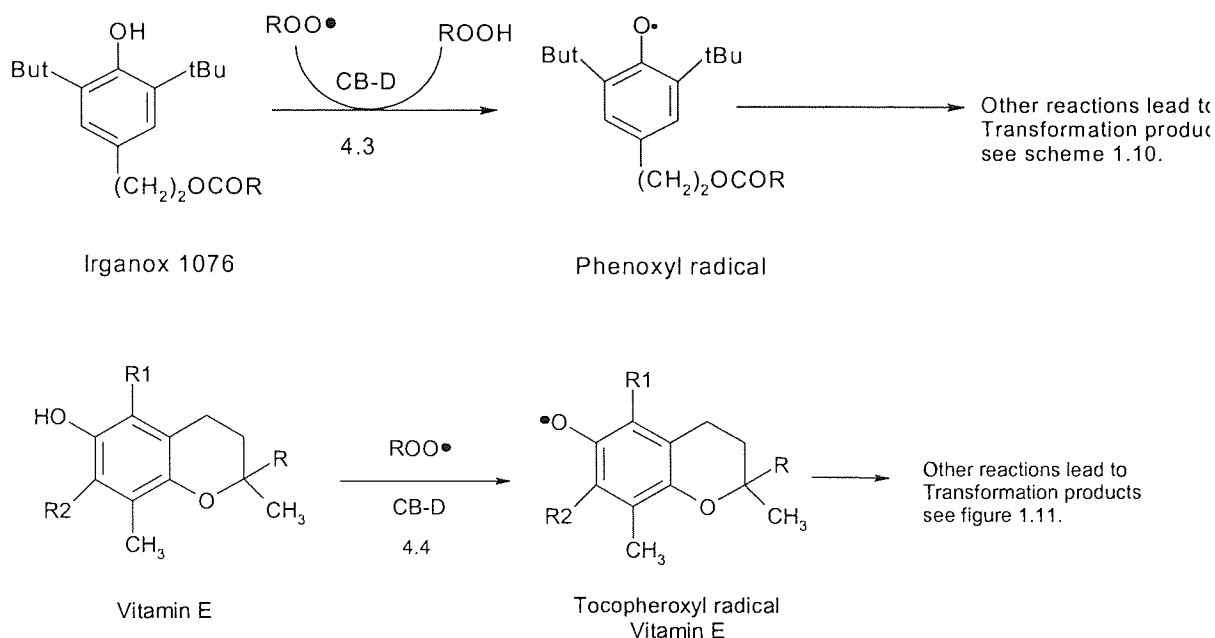
m-LLDPE polymer samples imply low concentrations of transformation products produced as a consequence of the antioxidant action of individual stabilisers. The marked improvement in melt flow retention of multiple extruded m-LLDPE stabilised with different AOs' may be attributed to the effective scavenging ability of these antioxidants of the detrimental polymer propagating radicals [49]. In contrast the unstabilised polymer shows a rapid rise in calculated MFR (indicating broadening of MWD) and drastic change in MI (reflecting a high level of crosslinking), see figure 4.8. The two hindered phenols, Vitamin E and Irganox 1076, and the lactone (Irganox HP136) have shown a superior melt stabilising effect in m-LLDPE under the multiple extrusion conditions used here (figure 4.8). The high antioxidant efficiency of the lactone (Irganox HP136) shown during multiple processing (see table 4.1 and figure 4.10) may be attributed to its efficient complementary CB-D and CB-A antioxidant functions. Many studies have demonstrated that 3 arylbenzofuran-2-one operates efficiently under conditions where both alkyl,  $R\bullet$ , and alkyl peroxy,  $ROO\bullet$ , radicals are present in the system, i.e. under normal extrusion conditions, thereby inhibiting effectively both crosslinking and chain scission reactions (see reaction 4.1 & 4.2) [78-81,109].



A further important contribution to the antioxidant activity of Irganox HP136 stems from the activity of the highly stable radical produced 3 arylbenzofuran-2-one (A), which is formed *via* the facile donation of a weakly bonded benzylic hydrogen atom as a consequence of the CB-D/CB-A activity of the parent hindered phenol (Irganox HP136) [78-80,109]. Model experiments have also shown that the 3 arylbenzofuran-2-one radical may either readily

dimerise or react further with other alkylperoxyl or alkyl free radicals (see figures 1.12&1.13, p. 35&36), thereby increasing the potent antioxidant activity of Irganox HP136 [78]. It is important to note that the Irganox HP136 was utilised at low concentration levels, 300ppm, a fraction of that used for Irganox 1076, Irgastab FS042 and Weston 399 concentration (500-2000ppm). It is also worth mentioning here that the lactone, Irganox HP136 is considered a 'safe' antioxidant for food contact applications in PE and PP [79]. The effect of synergistic combinations of Irganox HP136, synthetic/biological hindered phenols and phosphites on the melt and colour stability of m-LLDPE during multiple extrusion (260°C/100rpm under atmospheric conditions) has therefore been examined and will be discussed in chapter 5.

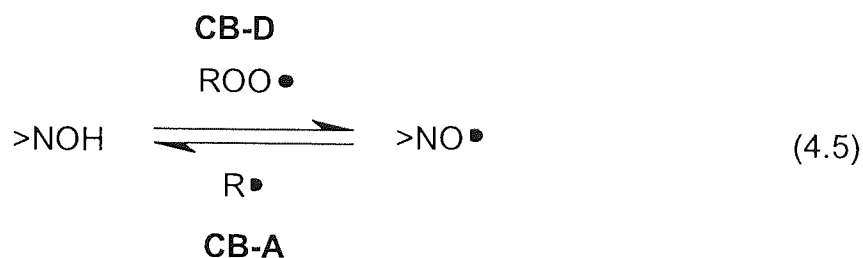
It is known that synthetic and biological hindered phenols (e.g. Irganox 1076 and Irganox E201) act primarily by CB-D mechanism *via* removing alkylperoxyl radicals, ROO•, (see reactions 4.3 and 4.4) and producing a stabilised phenoxyl radical [88]. The latter undergoes further transformations giving rise to antioxidants and/or pro-oxidant products some of which may be highly coloured (see reaction 1.23 in scheme 1.10 & figure 1.11) [53,56,58,60, 74,88,110].



Most of the transformation products of Vitamin E and Irganox 1076 formed during melt extrusion of polymers were shown to exhibit extremely effective antioxidant properties

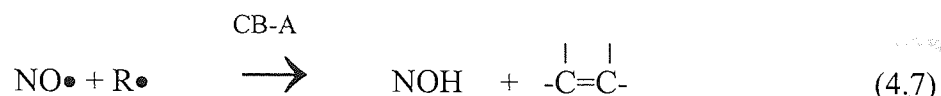
[56,58,74,110,111]. Indeed figure 4.8 shows clearly that both hindered phenols are very effective processing antioxidants for m-LLDPE.

Compared to the hindered phenols and lactones, the hydroxylamine, Irganox FS042, (s16) was shown to impart a slightly lower extent of melt stabilisation (see figure 4.8). Many studies [53,78,82,112] have shown that hydroxylamines such as Irgastab FS042, operate effectively in conditions where both alkyperoxyl (ROO•) and alkyl (R•) radicals are present in the system (see section 1.5.5) and are thought to operate *via* a complementary CB-A/CB-D mechanism (see reactions 4.5 and 4.6) [82]. It has been shown that [112,113] that hydroxylamines formed during processing via the formation of the corresponding nitroxyl radical formed from hindered amine light stabilisers based on 2, 2, 6, 6-tetramethyl piperidines are very effective melt stabilisers for polyolefins [113]. The effectiveness of the hydroxylamine and of the corresponding nitroxyl radical were shown to be due to their CB-A/CB-D redox characteristics allowing the couple to scavenge both alkyperoxyl (ROO•) and alkyl (R•) radicals (see reaction 4.5).

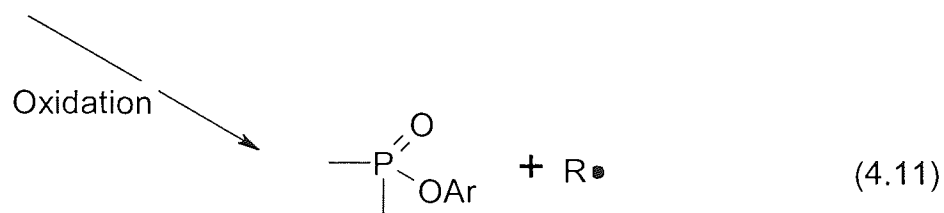
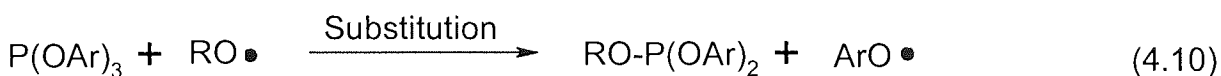
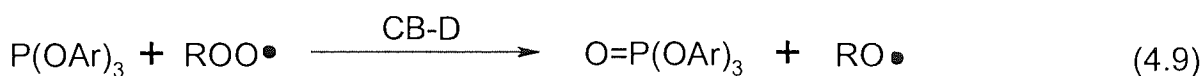
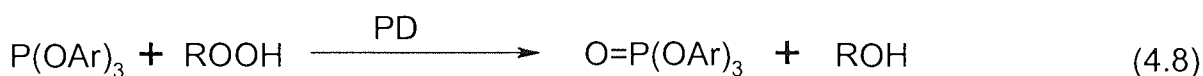


The lower extent of melt stabilising ability observed here for the aliphatic hydroxylamine, Irgastab FS042, may be explained at least in part by the production of hydroperoxides in the first CB-D antioxidant step (see reaction 4.6) which are the main source of initiating radicals that propagate the autoxidative chain. This suggests that the addition of a good hydroperoxide decomposer may lead to high melt stability (see chapter 5). It is also possible that the unhindered hydroxylamine function has a lower effectiveness than the fully hindered hydroxylamine such as those formed from 2, 2, 6, 6-tetramethylpiperidine derivatives.





A multi-extruded m-LLDPE polymer sample containing the peroxidolytic phosphite antioxidant, Weston 399 (used at a 2000ppm) gave a much lower stabilising effect compared to the other antioxidants examined in this work, see figure 4.8. The sharp drop in MI and increase in MFR with increasing processing severity suggest significant crosslinking and MWD broadening of the polymer sample. Schwetlick and co-workers [83-85,114] have shown that organic aryl phosphites, such as Weston 399, function primarily by a preventive mechanism reducing hydroperoxides to alcohols (see reaction 4.8). However, their overall catalytic peroxidolytic activity is known to be much lower than for example sulphur-containing catalytic peroxidolytic antioxidants. Although Weston 399 can also contribute to some CB activity through deactivating both ROO• (see reaction 4.9) and RO• (see reaction 4.10) radicals [83]. This aryl phosphite is not a highly effective chain breaking antioxidant due to the formation of non-sterically hindered phenoxyl radical (see reaction 4.10) which would be expected to have only a minor CB-activity. If an oxidation reaction occurs instead of substitution (as shown in reaction 4.11) then alky (R•) radicals are formed which can propagate the autoxidative chain. Generally, therefore, phosphites are not used on their own, but instead they are used in combination with 'powerful' alkylperoxyl and/or alkyl radical scavengers, in order to improve the melt stability of polymers (see chapter 5).



All antioxidants resulted in increasing intensities of yellowing in the polymer when subjected to multiple extrusion passes (see figure 4.11). This may be attributed to many factors

including the formation of increasing quantities of coloured oxidation transformation products, e.g. quinonoidal type structures [58,60]. The extent of discolouration depends upon the chemical structure of the parent antioxidant, the oxidation products and the type and amount of catalyst residues in the polymer [58,60].

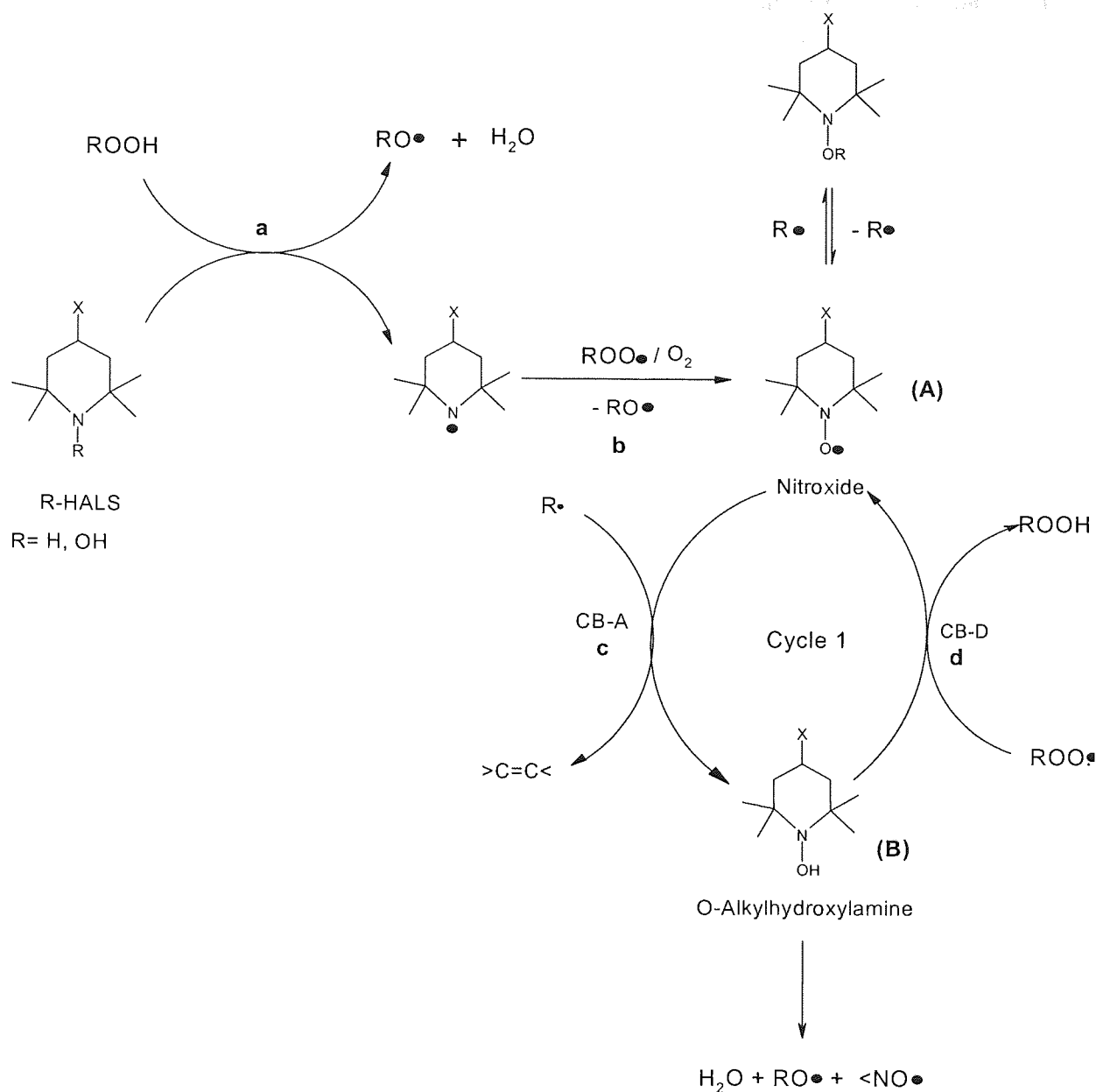
Irganox HP136 and Irganox E201 resulted in comparable levels of discolouration (with increasing processing severity) with the only exception to this finding occurring for pass 5, with the Vitamin E stabilised polymer sample yielding a slightly lower intensity of discolouration (as compared to its Irganox 1076 stabilised counterpart). Previous work at Aston [56,74] has shown that discolouration caused by Irganox E201 is due to, at least in part, the formation of greater quantities of coloured transformation products, e.g. spirodimer (SPD), trimer (see section 1.5.3b) and aldehydes (ALD). The Aston work [56,74] demonstrated further that the addition of a phosphite antioxidant such as Ultrinox 626 to tocopherol reduces drastically the level of discolouration of the polymer samples (see section 5.3.1.2). The yellowing resulted from Irganox HP136 and Irganox 1076 (see figure 4.9) is most certainly due to the formation of coloured oxidation products produced as a consequence of the antioxidant action of the parent antioxidants. The slightly lower discolouration produced in multi-extruded m-LLDPE containing Irganox E201 (for pass 5) suggests that a lower concentration of the coloured transformation products may be formed due to the AO action of the parent AO (Vitamin E versus Irganox 1076). The hydroxylamine, Irgastab FS042, resulted in the most severe discolouration which is probably also due to the formation of greater coloured oxidation products (compared to the other antioxidants).

#### **4.3.3 Effect of Alkyl Hydroxylamine Antioxidants (R-HALS) on the melt and colour stability of m-LLDPE during processing.**

It is clear that all the R-HALS antioxidants examined here (s17, s18 and s21, see table 4.1) have been found not to be highly effective processing stabilisers when compared to for example, the hindered phenols as reflected by the large change in their MI characteristics during multiple extrusion, see figure 4.10. The high negative change in MI suggests a high extent of crosslinking reactions of the polymer upon extrusion (see figure 4.10). This ineffectiveness of Tinuvin 765, Tinuvin 622LD and Chimisorb 119D as melt stabilisers for m-LLDPE may be attributed to the fact that these tertiary amines can undergo reactions with hydroperoxides formed during processing resulting in the formation of alkoxyl radicals (see



reaction a in scheme 4.3) thereby propagating further chain oxidation. However the fact that these R-HALS offer some melt stability to m-LLDPE (during multiple processing) when compared to the behaviour of the unstabilised polymer processed under the same conditions (which exhibited severe crosslinking during multiple extrusion, see figure 4.10) must be due to the formation of the nitroxyl radical. This may form via a reaction with hydroperoxides similar to that proposed for hindered amines hydrolyse amines [112] (see reaction b in scheme 4.3). It has been shown that under normal processing conditions (i.e. oxygen deficient) the relatively high  $[R\bullet]/[ROO\bullet]$  ratio may allow the stable nitroxyl radical ( $NO\bullet$ ), to compete as CB-A antioxidant with oxygen for the polymer radical ( $R\bullet$ ) giving rise to O-alkylhydroxylamine,  $>NOH$  (**B**), see reaction c in scheme 4.3.



Scheme 4.3 Chain breaking activity (CB-A) and redox reactions of R-HALS during the melt extrusion of m-LLDPE.

It has been reported [85,115-116] that the rate of reaction of oxygen with nitroxyl radicals is comparable to that of an alkyl radical with oxygen. An important contribution to the antioxidant activity of R-HALS must be centered upon the redox reaction which regenerates the Nitroxyl radical, ( $>\text{NO}\bullet$ ), and O-alkylhydroxylamine ( $>\text{NOH}$ , see cycle 1, reactions c&d in scheme 4.3) [112,115-117]. The redox couple may function as a melt stabiliser by a complementary CB-A/CB-D mechanism hence the concentration of the nitroxyl and hydroxylamine would change reciprocally throughout the processing. It is expected that the

formation of the free O-alkylhydroxylamine, >NOH is also accompanied by the formation of unsaturation in the polymer (see reaction c, in scheme 4.3) [112, 115-117].

The slightly higher melt stabilising efficiency of a m-LLDPE polymer containing Tinuvin 622LD when compared to the other two R-HALS examined here (Tinuvin 765 and Chimassorb 119D) even when the melt stabilising effect is compared during the compounding step (Po), i.e. before multiple extrusion (see figure 4.10, s18 versus s17 and s21) may be attributed to its superior physiochemical properties i.e. lower volatility and higher molecular weight. It has been shown [118] that the performance of AOs including HALS is governed not only by this chemical activity but also by important physiochemical parameters such as volatility, solubility and Mw. Analysis of both rheological properties and colour data suggest that the performance of these particular antioxidants (R-HALS) may be improved by utilising them in combination with alkyl and alkylperoxyl radical scavengers and hydroperoxide decomposers. The effect of synergistic combinations comprising of different R-HALS/lactones/synthetic hindered phenols/phosphites on the melt and colour stability of m-LLDPE during multiple extrusion (260°C/100rpm under atmospheric conditions) is examined in chapter 5.

#### 4.4 Overall Perspective of Stabilisation Work Using a Single AO

The excellent chain breaking (CB) activity (*via* different mechanisms) of commercially available antioxidants such as Irganox HP136 (a lactone), Irganox E201 (vitamin E), Irganox 1076 and Irgastab FS042 (a hydroxylamine), used here singly, in polyolefins was clearly illustrated by their high efficiency as melt processing stabilisers, with no significant increase or decrease in melt flow (MF), in m-LLDPE during multiple extrusion. In the absence of these potent stabilisers, the degradation of m-LLDPE was found to proceed at a rapid rate. From MF and gel permeation chromatographic measurements (GPC, see chapter 3) it is clearly evident that unstabilised m-LLDPE polymer samples undergo predominantly crosslinking reactions (coupled with significant changes in MWD), which is indicative of the importance of reactions involving the macroalkyl radicals ( $R\bullet$ )

The high melt stabilising activity of Irganox HP136 in m-LLDPE was attributed, at least in part, to its efficient complementary CB-D and CB-A functions, thereby efficiently trapping both detrimental propagating alkyl ( $R\bullet$ ) and alkylperoxyl ( $ROO\bullet$ ), free radicals, whereas the high antioxidant functions of the hindered phenols Irganox 1076 and Irganox E201, is primarily centered upon their 'powerful' CB-D antioxidant action which results in the removal of alkylperoxyl ( $ROO\bullet$ ) free radicals from the autoxidative chain. The findings in this study have, however, also shown that the Irgastab FS042 (a hydroxylamine) imparts a slightly lower overall melt stabilising efficiency to the m-LLDPE polymer under multiple extrusion conditions (as compared to that offered by Irganox HP136, Irganox E201 and Irganox 1076). This was attributed to the production of hydroperoxides ( $ROOH$ ) in the first CB-D antioxidant step, which are considered to be the main source of initiating radicals that propagate the autoxidative chain. The poor performance of Irgastab FS042 may be improved by the addition of an alkyl, alkylperoxyl traps and a good hydroperoxide decomposer (see chapter 5). The high levels of melt stability of m-LLDPE polymer containing Irganox HP136, Irganox E201, Irganox 1076 and even Irgastab FS042 were obtained by using low concentration levels of 0.03, 0.03, 0.05 and 0.1% w/w, respectively. This implies that the AOs' are present in sufficient concentrations at the various oxidisable sites to prevent severe thermal oxidative degradation during multiple extrusion. This also suggests that the AOs suffered minimal loss of antioxidant (due to blooming and volatilisation) and have excellent

compatibility with the m-LLDPE polymer matrix. It is important to note that both Vitamin E and the lactone are generally considered as safe AOs by the FDA (food and drug administration) and are approved for use in food packaging and medical applications.

Other antioxidants such as a phosphite, Weston 399, and R-HALS; Tinuvin 765, Tinuvin 622LD and Chimassorb 119D offered much lower levels of melt stability to the m-LLDPE polymer during multiple extrusion. The lower extent in melt stability offered by these antioxidants may be attributed to their lower overall CB activity; reactions with alkylperoxyl,  $\text{ROO}\bullet$  and alkoxy,  $\text{RO}\bullet$ , radicals (as compared to the lactone, vitamin E, Irganox 1076 and hydroxylamine antioxidants). Weston 399 (used at a concentration level of 0.2%w/w) operates primarily *via* a PD-S mechanism; non-radical deactivation of hydroperoxides (ROOH) into alcohols and phosphates. The results in this work imply that the melt flow performance of Weston 399 and R-HALS may be improved by the addition of powerful alkylperoxyl,  $\text{ROO}\bullet$  and alkyl,  $\text{R}\bullet$ , radical traps.

The colour, an important characteristic of a processed polymer, can also be related to the chemical reactions, i.e. consumption of antioxidants (as a consequence of their antioxidant action), taking place during the processing of a polymer. The development of colour in m-LLDPE containing all single antioxidants generally increased with increasing processing severity (produced as a consequence of their antioxidant action during processing). In this work, the Irganox HP136 and Irganox E201 antioxidants produced comparable low levels of discolouration to the m-LLDPE polymer (with increasing processing severity). The introduction of a commercially available hindered aromatic phosphite such as Ultrinox 626 (as part of a synergistic blend) in m-LLDPE containing either Irganox E201 or Irganox HP136 may prevent colour development (see chapter 5).

Table 4.3 Processing characteristics for Pass-zero stabilisation of m-LLDPE at an extrusion temperature of 210°C and a screw speed of 100rpm (in a Betol TSE under nitrogenous conditions, 4mm die) using single antioxidants (see s14-s22 in table 4.1).

Processing characteristics of stabilised m-LLDPE, P <sub>0</sub>											
Code and AO All processed Under nitrogen	Screw speed, rpm	T <sub>die</sub> , °C	Output Rate, kg.h <sup>-1</sup>	P/N/m <sup>2</sup> ±5%	I, A (±0.5)	actual T <sub>melt</sub> , °C (± 2)	ΔT <sup>1</sup>	Power Consumption		Observ.	
								kW	kW.h/kg		
<b>Single Antioxidants</b>											
S-14	Irg. 1076	100	210	4.0	1260	13.0	233	+23	1.58	0.40	Severe Melt fracture
S-15	HP136	100	210	4.0	1250	13.5	232	+22	1.64	0.41	Severe Melt fracture
S-16	FS042	100	210	4.0	1280	13.0	231	+21	1.58	0.39	Severe Melt fracture
S-17	T.765	100	210	4.0	1260	13.0	233	+23	1.58	0.40	Severe Melt fracture
S-18	T.622	100	210	4.0	1250	13.5	232	+22	1.64	0.41	Severe Melt fracture
S-19	E201	100	210	4.0	1280	13.0	231	+21	1.58	0.39	Severe Melt fracture
S-20	W399	100	210	4.0	1250	13.5	232	+22	1.64	0.41	Severe Melt fracture
S-21	Chim.119D	100	210	4.0	1280	13.0	231	+21	1.58	0.39	Severe Melt fracture
<b>Unstabilised m-LLDPE polymer</b>											
Unstabilised		100	210	4.0	1300	13.0	232	+22	1.58	0.39	Severe Melt fracture

<sup>1</sup> ΔT= T<sub>melt</sub> - T<sub>die</sub>



Table 4.4 The **multiple extrusion characteristics** of stabilised **m-LLDPE** samples containing **single antioxidants** (see table 4.1) carried out at 260°C/100rpm under atmospheric conditions, P1, P3 and P5. Values for an unstabilised m-LLDPE polymer is shown for comparative purposes.

Formulation No.	Sample code	Screw Speed /rpm	Die Temp. /°C	Output rate/ kg.h <sup>-1</sup>	P/ N/m <sup>2</sup> ±5%	I (A) ±0.5	Actual Melt Temp/ °C	ΔT <sup>1</sup>	P.C. <sup>2</sup>		Observ.
									kW	kW.h /kg	
<b>Unstabilised</b>	m-260-P1	100	260	4.8	1090	14.0	273	+13	1.70	0.36	SlightMF/opacity change
	m-260-P3			4.8	1080	14.0	273	+13	1.70	0.36	SlightMF/opacity change
	m-260-P5			4.8	1020	14.0	273	+13	1.70	0.36	SlightMF/opacity change
s-14 <b>Irg. 1076</b>	m-260-P1	100	260	4.8	1100	14.5	272	+12	1.77	0.37	Slight MF
	m-260-P3			4.8	1080	14.5	272	+12	1.77	0.37	Slight MF
	m-260-P5			4.8	1060	14.0	272	+12	1.70	0.36	Slight MF
s-15 <b>Irg. HP136</b>	m-260-P1	100	260	4.8	1030	14.5	274	+14	1.70	0.36	Slight MF
	m-260-P3			4.8	1010	14.0	274	+14	1.70	0.36	Slight MF
	m-260-P5			4.8	1050	14.0	274	+14	1.70	0.36	Slight MF
s-16 <b>Irg. FS042</b>	m-260-P1	100	260	4.8	1100	14.0	272	+12	1.70	0.36	Slight MF
	m-260-P3			4.8	1040	14.0	272	+12	1.70	0.36	Slight MF
	m-260-P5			4.8	980	14.0	272	+12	1.70	0.36	Slight MF
s-17 <b>T. 765</b>	m-260-P1	100	260	4.8	1080	14.0	273	+13	1.70	0.36	SlightMF
	m-260-P3			4.8	1060	14.0	273	+13	1.70	0.36	SlightMF/opacity change
	m-260-P5			4.8	1030	14.0	273	+13	1.70	0.36	SlightMF/opacity change
s-18 <b>T. 622LD</b>	m-260-P1	100	260	4.8	1040	14.0	273	+13	1.70	0.36	SlightMF
	m-260-P3			4.8	1080	14.0	273	+13	1.70	0.36	SlightMF/opacity change
	m-260-P5			4.8	950	14.0	272	+12	1.70	0.36	SlightMF/opacity change
s-19 <b>Irg. E201</b>	m-260-P1	100	260	4.8	1100	14.0	273	+13	1.70	0.36	Slight MF
	m-260-P3			4.8	1070	14.0	273	+13	1.70	0.36	Slight MF
	m-260-P5			4.8	1060	14.0	272	+12	1.70	0.36	Slight MF
s-20 <b>W. 399</b>	m-260-P1	100	260	4.8	1090	14.0	273	+13	1.70	0.36	Slight MF
	m-260-P3			4.8	1080	14.0	273	+13	1.70	0.36	Slight MF
	m-260-P5			4.8	1000	14.0	273	+13	1.70	0.36	Slight MF
s-21 <b>Chims. 119D</b>	m-260-P1	100	260	4.8	1090	14.0	272	+12	1.70	0.36	Slight MF
	m-260-P3			4.8	1040	14.0	273	+13	1.70	0.36	Slight MF
	m-260-P5			4.8	1000	14.0	273	+12	1.70	0.36	SlightMF/opacity change

<sup>1</sup> ΔT is defined as the difference in melt and die temperature.

<sup>2</sup> P.C. is defined as the power consumption.



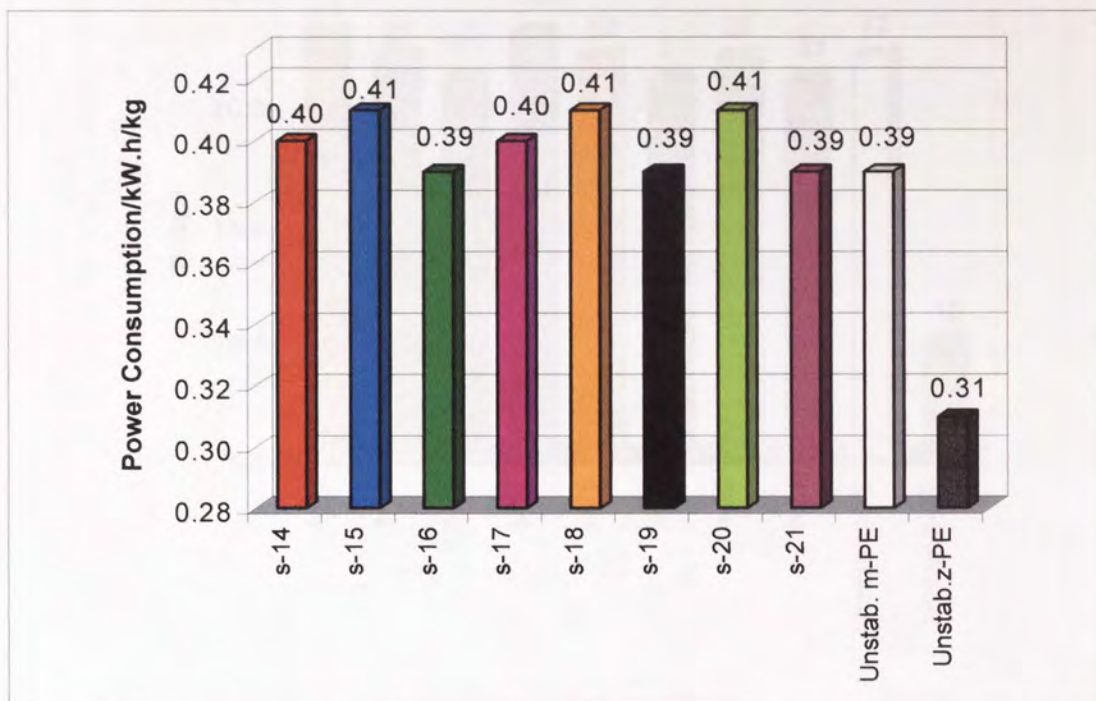


Figure 4.1. Change in Power consumption during twin screw extrusion of stabilised m-LLDPE (Po, formulation numbers s14-s21 see tables 4.3); N<sub>2</sub>, 210°C, 100rpm. Changes in unstabilised polymers extruded under similar conditions is shown for comparison. Values for unstabilised z-LLDPE polymers shown for comparison.

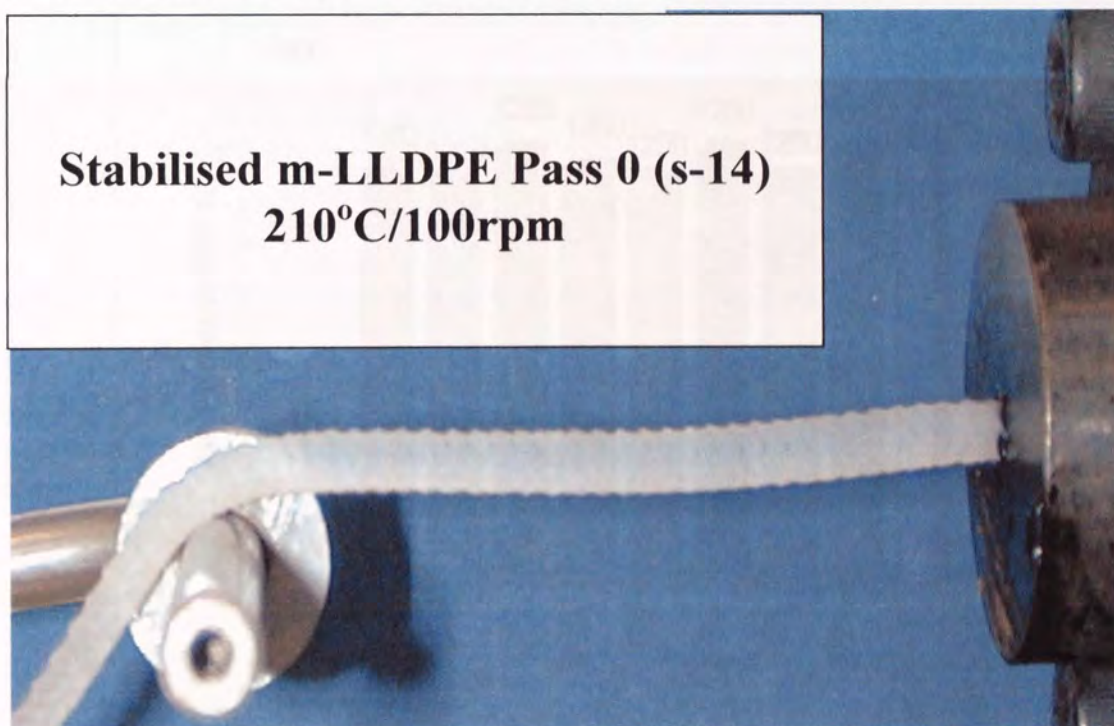


Figure 4.2 Effect of processing of stabilised polymers on the appearance of the extruded laces (4mm die) of m-LLDPE melt fracture is shown in the case of the metallocene polymer.



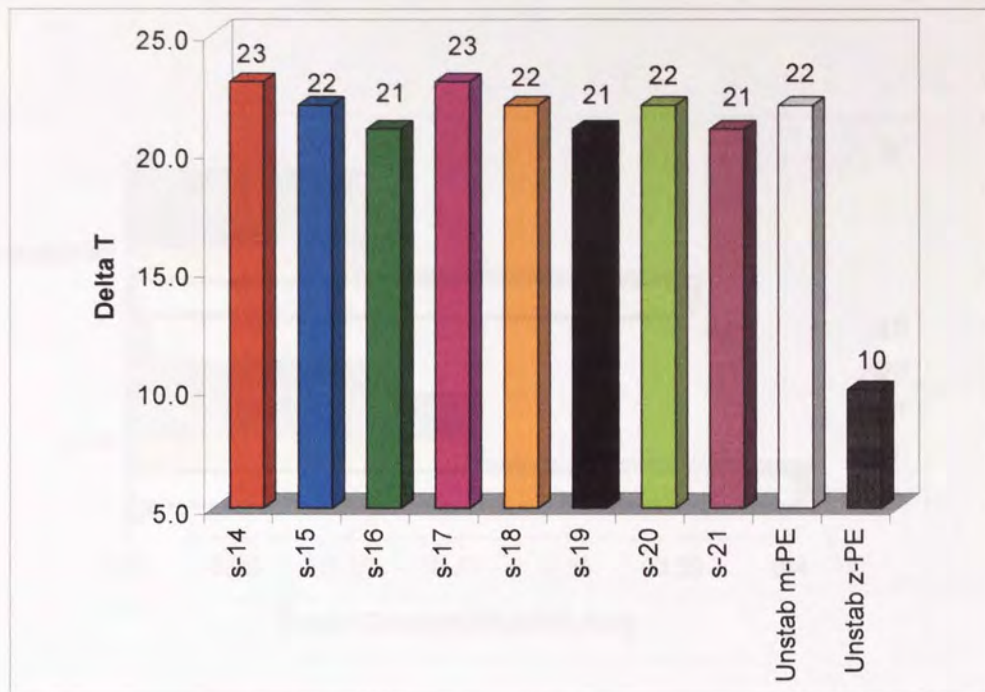


Figure 4.3: A comparison of  $\Delta T$  (defined as the temperature difference between the die and melt) stabilised ( $P_0$ , formulation number s14-s21, see table 4.1) and unstabilised ( $P_1$ ) m-LLDPE. Values for unstabilised z-LLDPE polymers shown for comparison

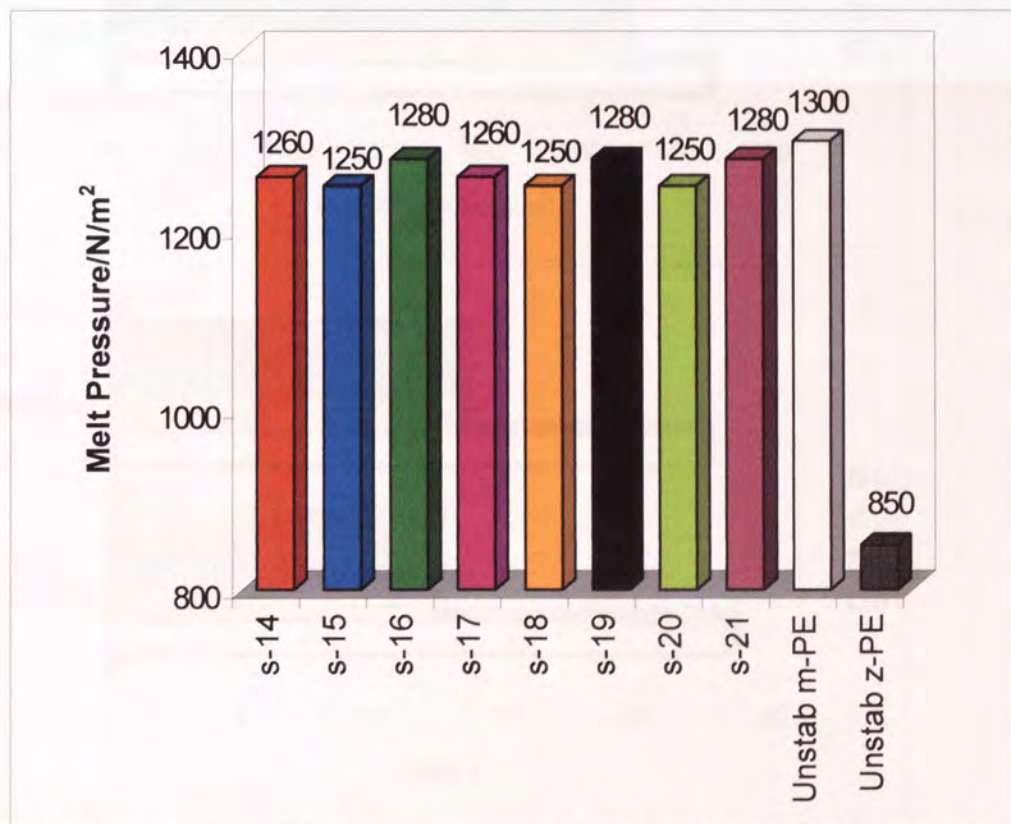


Figure 4.4: Changes in melt pressure during processing of stabilised ( $P_0$ , formulation number s14-s21, see table 4.1) and unstabilised ( $P_1$ ) m-LLDPE. Values for unstabilised z-LLDPE polymers shown for comparison

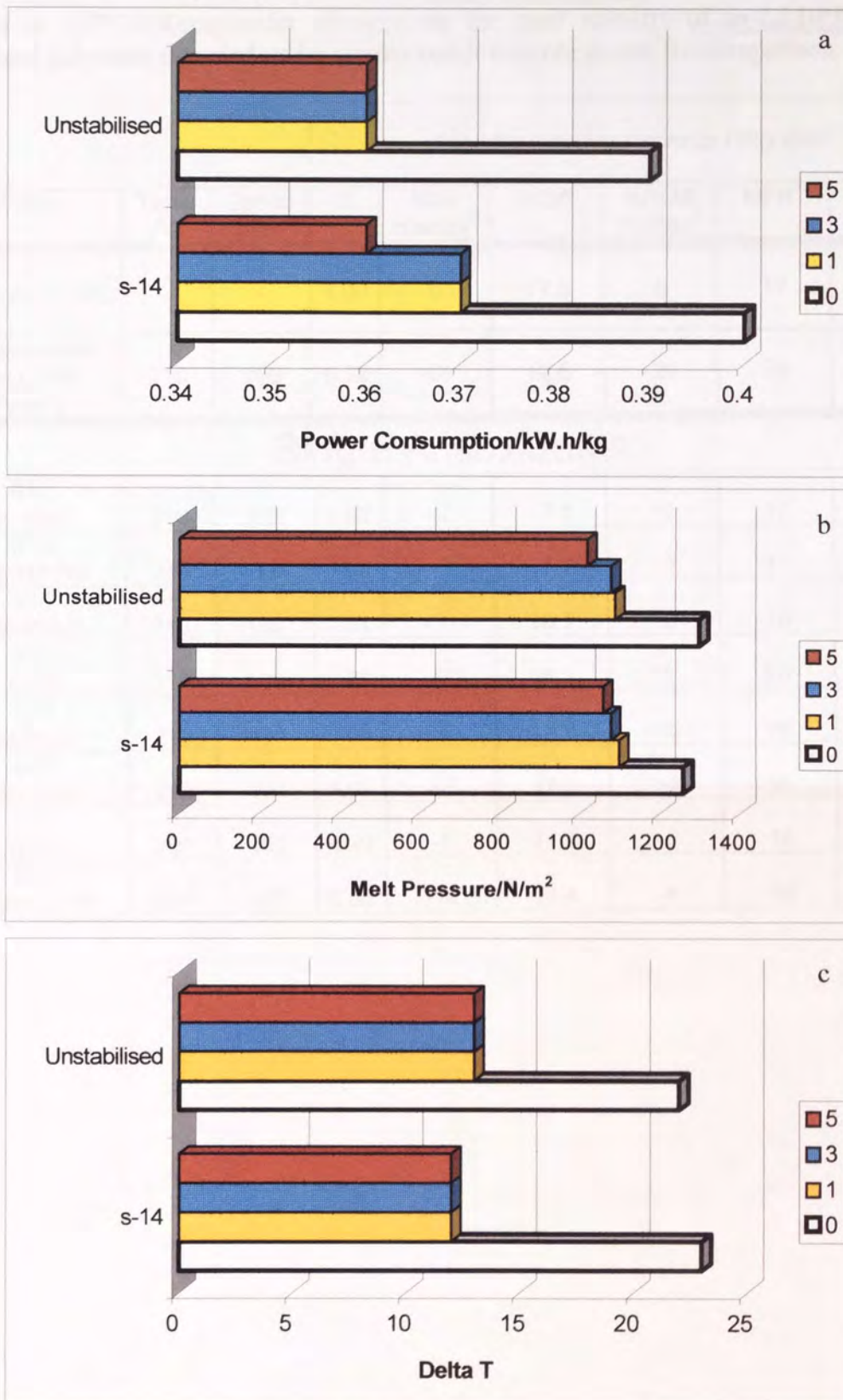


Figure 4.5 Changes in (a). Power Consumption, (b). Melt Pressure, (c).  $\Delta T$  (difference between the die and actual melt temperature) of unstabilised and stabilised (Irganox 1076, s14) m-LLPDE polymer samples during multi-pass extrusion; Passes 1,3 and 5 (260°C, 100rpm under atmospheric conditions)..



Table 4.5 Effect of Pass zero (Po) stabilised **single antioxidants** (see s14-s21 in table 4.1); processed at 210°C/100rpm/under nitrogen on the melt stability of **m-LLDPE** samples. Unstabilised polymers extruded under similar conditions are shown for comparison.

			Melt flow measurements /10g.min <sup>-1</sup>					
Code	Temp /°C	Speed /rpm	MI	%MI change <sup>3</sup>	HLMI	%HLMI change <sup>4</sup>	MFR <sup>5</sup>	%MFR change <sup>6</sup>
Virgin m-LLDPE	-	-	1.00	0	17.0	0	17	0
Unstabilised m-LLDPE Pass 1	210	100	0.32	-68	12.6	-26	39	129
<b>Single Antioxidants</b>								
S14 <b>Ir. 1076</b>	210	100	1.02	+2	17.1	+1	17	-1
S15 <b>Irg. HP136</b>	210	100	1.05	+5	17.7	+4	17	-1
S16 <b>Irgs.FS042</b>	210	100	1.11	+11	18.1	+6	16	-6
S17 <b>T.765</b>	210	100	0.83	-17	16.7	-2	20	18
S18 <b>T.622LD</b>	210	100	1.06	+6	17.2	+1	16	-6
S19 <b>Irg. E201</b>	210	100	1.07	+7	17.7	+4	16	-6
S20 <b>W399</b>	210	100	0.99	-1	17.5	+3	18	+6
S21 <b>Chims.119D</b>	210	100	0.86	-14	16.4	-4	19	+12

<sup>3</sup> %MI change = (MI<sub>sample</sub> - MI<sub>virgin</sub>)/MI<sub>virgin</sub> x 100

<sup>4</sup> % HLMI change = (HLMI<sub>sample</sub> - HLMI<sub>virgin</sub>)/HLMI<sub>virgin</sub> x 100

<sup>5</sup> MFR = HLMI/MI

<sup>6</sup> %MFR change = (MFR<sub>sample</sub> - MFR<sub>virgin</sub>)/MFR<sub>virgin</sub> x 100

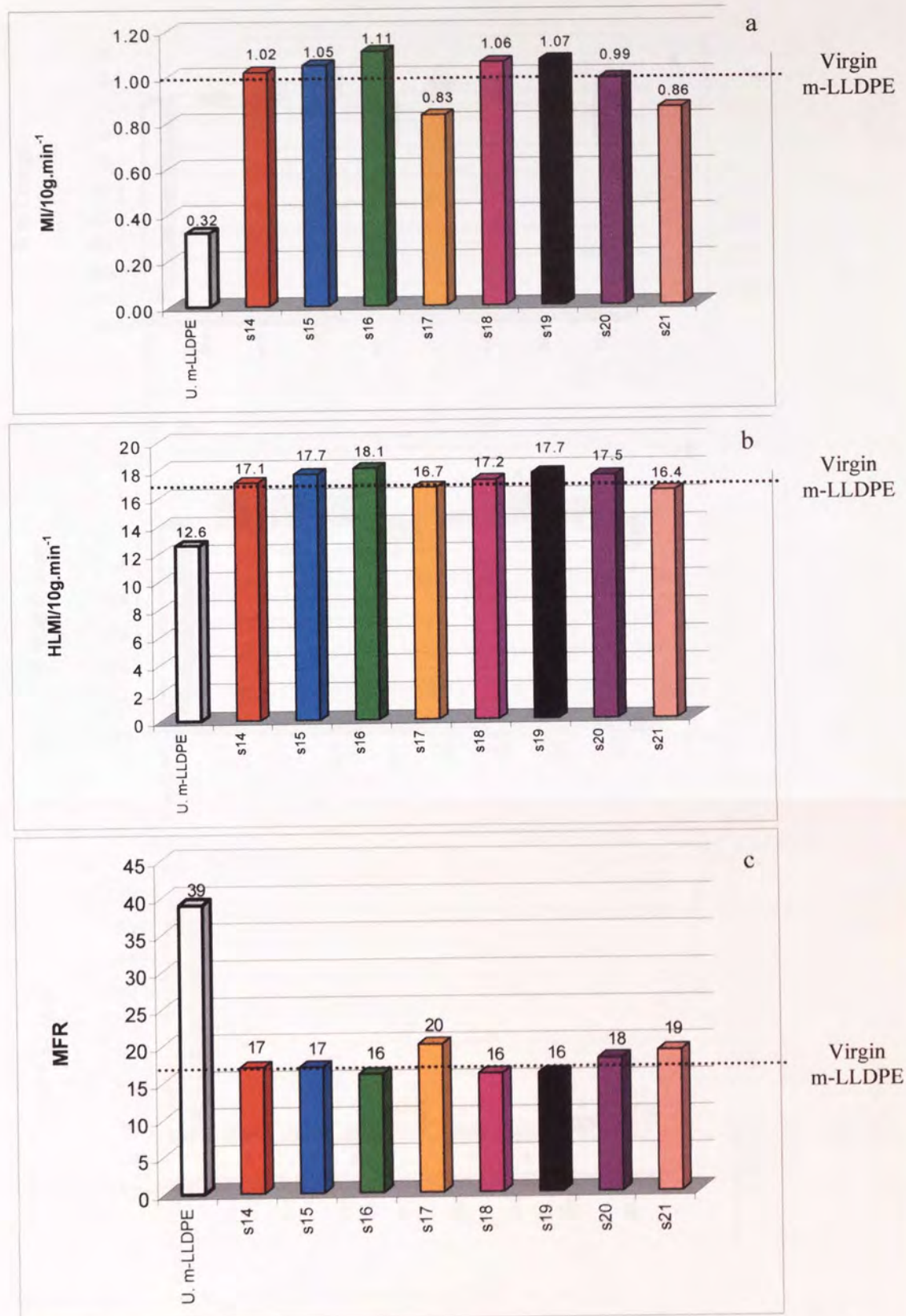


Figure 4.6 Melt stability characteristics; a. MI, b. HLMI and c. MFR; of stabilised (see s14-s21, in table 4.1) during the Po compounding step (210°C, 100rpm, N<sub>2</sub>). Unstabilised extruded (P1) m-LLDPE polymer samples are shown for comparison



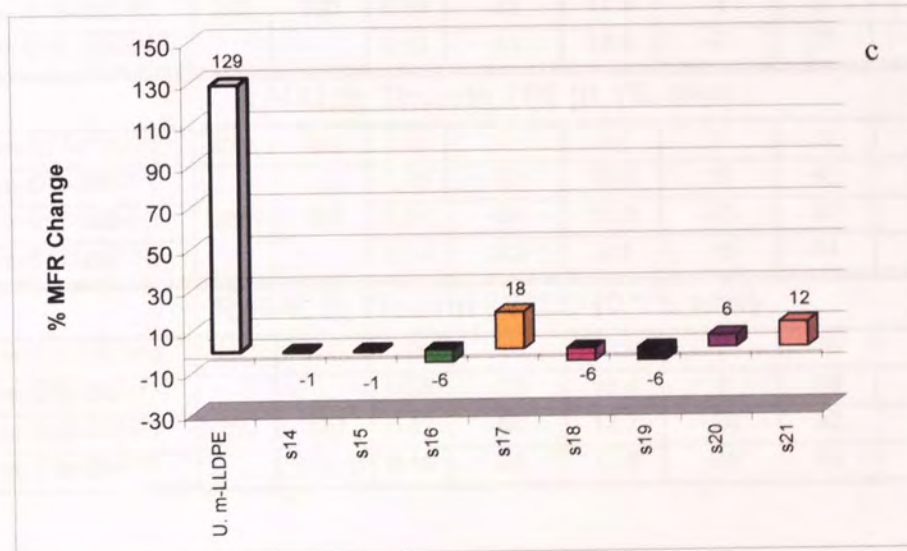
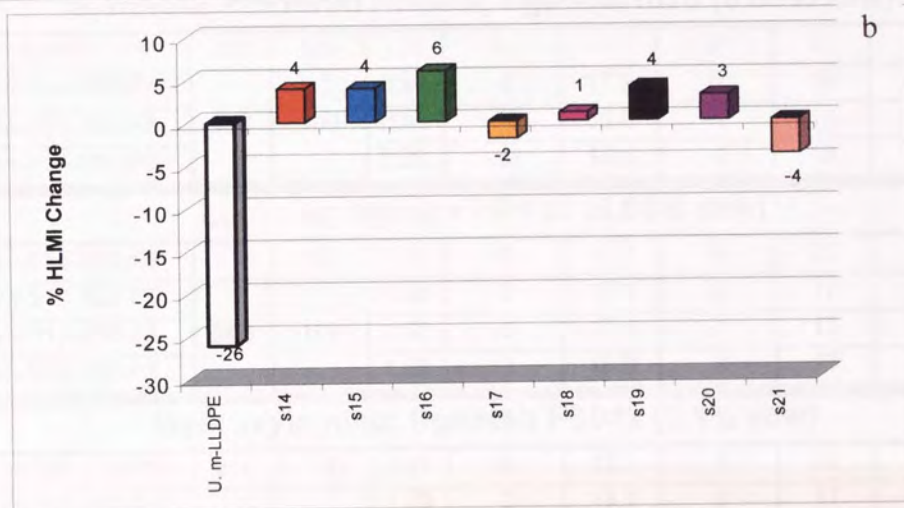
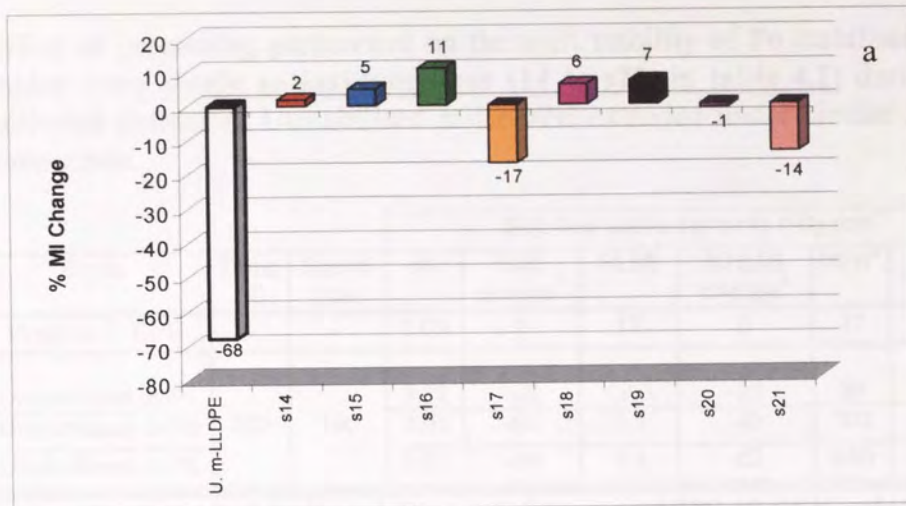


Figure 4.7 Changes in the melt stability characteristics; a. %MI, b. %HLMI and c. %MFR; of stabilised (see s14-s21, in table 4.1) during the Po compounding step (210°C, 100rpm, N<sub>2</sub>). Unstabilised extruded (P1) m-LLDPE polymer samples are shown for comparison

Table 4.6. Effect of processing parameters on the melt stability of Po stabilised **m-LLDPE** polymer samples using **single antioxidants (see s14 to s21, in table 4.1)** during Pass-zero (Po) and multi-pass extrusion. Unstabilised m-LLDPE extruded under similar conditions is shown for comparison.

Code	Temp /°C	Speed /rpm	Melt flow measurements /10g.min <sup>-1</sup>					
			MI	%MI change <sup>7</sup>	HLMI	%HLMI change <sup>8</sup>	MFR <sup>9</sup>	%MFR <sup>10</sup> change
Virgin m-LLDPE	-	-	1.00	0	17	0	17	0
Unstabilised m-P1	260	100	0.32	-68	12.6	-26	39	129
Unstabilised m-P3			0.03	-97	9.1	-46	303	1682
Unstabilised m-P5			0.01	-99	6.4	-62	640	3664
<b>Synthetic hindered Phenol; Irganox 1076 (0.05% w/w)</b>								
m-S14-210-P0	210	100	1.02	0	17.0	0	17	0
m-S14-260-P1	260	100	0.97	-5	17.0	0	18	6
m-S14-260-P3			0.92	-10	16.8	-1	18	6
m-S14-260-P5			0.87	-15	16.5	-3	19	12
<b>Lactone; Irganox HP136 (0.03% w/w)</b>								
m-S15-210-P0	210	100	1.05	0	17.7	0	17	0
m-S15-260-P1	260	100	1.05	0	17.4	2	17	0
m-S15-260-P3			1.02	-3	17.6	-1	17	0
m-S15-260-P5			1.02	-3	16.9	-4	17	0
<b>Hydroxylamine; Irgastab FS042 (0.1% w/w)</b>								
m-S16-210-P0	210	100	1.11	0	18.1	0	16	0
m-S16-260-P1	260	100	1.09	-2	18.1	0	17	6
m-S16-260-P3			0.83	-25	17.3	-4	21	31
m-S16-260-P5			0.68	-39	16.8	-7	25	56
<b>R-HALS; Tinuvin 765 (0.1% w/w)</b>								
m-S17-210-P0	210	100	0.83	0	16.7	0	20	0
m-S17-260-P1	260	100	0.39	-53	15.9	-5	41	105
m-S17-260-P3			0.34	-59	12.6	-25	37	85
m-S17-260-P5			0.15	-82	9.6	-43	64	220
<b>R-HALS; Tinuvin 622LD (0.1% w/w)</b>								
m-S18-210-P0	210	100	1.06	0	17.2	0	16	0
m-S18-260-P1	260	100	0.85	-20	16.4	-5	19	19
m-S18-260-P3			0.42	-60	13.7	-20	33	106
m-S18-260-P5			0.16	-85	11.8	-31	74	363

<sup>7</sup> %MI change =  $(MI_{\text{Sample}} - MI_{\text{Po}}) / MI_{\text{Po}} \times 100$  in the case of the virgin replace MI<sub>Po</sub> with MI<sub>virgin</sub>.

<sup>8</sup> % HLMI change =  $(HLMI_{\text{sample}} - HLMI_{\text{Po}}) / HLMI_{\text{Po}} \times 100$  in the case of the virgin replace HLMI<sub>Po</sub> with HLMI<sub>virgin</sub>.

<sup>9</sup> MFR = HLMI/MI

<sup>10</sup> %MFR change =  $(MFR_{\text{sample}} - MFR_{\text{Po}}) / MFR_{\text{Po}} \times 100$  in the case of the virgin replace MFR<sub>Po</sub> with MFR<sub>virgin</sub>.



Table 4.6 continued.....

Code	Temp /°C	Speed /rpm	Melt flow measurements /10g.min <sup>-1</sup>					
			MI	%MI change <sup>11</sup>	HLMI	%HLMI change <sup>12</sup>	MFR <sup>13</sup>	%MFR change <sup>14</sup>
Virgin m-LLDPE	-	-	1.00	0	17	0	17	0
Unstabilised m-P1	260	100	0.32	-68	12.6	-26	39	129
Unstabilised m-P3			0.03	-97	9.1	-46	303	1682
Unstabilised m-P5			0.01	-99	6.4	-62	640	3664
<b>Biological hindered Phenol; Irganox E201 (0.03% w/w)</b>								
m-S19-210-P0	210	100	1.07	0	17.7	0	16	0
m-S19-260-P1	260	100	1.06	-1	17.5	-1	16	0
m-S19-260-P3			1.00	-7	17.1	-3	17	6
m-S19-260-P5			0.96	-10	16.8	-5	18	12
<b>Phosphite; Weston 399 (0.2% w/w)</b>								
m-S20-210-P0	210	100	0.99	0	17.5	0	18	0
m-S20-260-P1	260	100	0.89	-10	17.2	-2	19	5
m-S20-260-P3			0.30	-70	13.0	-26	43	139
m-S20-260-P5			0.14	-86	10.8	-38	77	328
<b>R-HALS; Chimassorb 119D (0.1% w/w)</b>								
m-S21-210-P0	210	100	0.86	0	16.4	0	19	0
m-S21-260-P1	260	100	0.69	-20	15.9	-3	23	21
m-S21-260-P3			0.22	-74	11.3	-31	51	168
m-S21-260-P5			0.13	-85	9.7	-41	75	295

<sup>11</sup> %MI change = (MI<sub>sample</sub> - MI<sub>P0</sub>)/MI<sub>P0</sub> x 100 in the case of the virgin replace MI<sub>P0</sub> with MI<sub>virgin</sub>.

<sup>12</sup> % HLMI change = (HLMI<sub>sample</sub> - HLMI<sub>P0</sub>)/HLMI<sub>P0</sub> x 100 in the case of the virgin replace HLMI<sub>P0</sub> with HLMI<sub>virgin</sub>.

<sup>13</sup> MFR = HLMI/MI

<sup>14</sup> %MFR change = (MFR<sub>sample</sub> - MFR<sub>P0</sub>)/MFR<sub>P0</sub> x 100 in the case of the virgin replace MFR<sub>P0</sub> with MFR<sub>virgin</sub>.



Table 4.7. Effect of processing parameters (260°C/100rpm, atmospheric conditions) on the **Colour Stability** of Po stabilised **m-LLDPE** polymer samples using **single antioxidants** (see s14 to s21, in table 4.1) during Pass-zero (Po) and multi-pass extrusion (260°C/100rpm, under atmospheric conditions, P1, P3 and P5). Unstabilised m-LLDPE extruded under similar conditions is shown for comparison.

Code	Temp/°C	Speed/rpm	YI
Virgin m-LLDPE	-	-	-7.80
Unstabilised m-P1	260	100	8.92
Unstabilised m-P3			12.14
Unstabilised m-P5			15.02
<b>Synthetic hindered Phenol; Irganox 1076 (0.05% w/w)</b>			
m-S14-260-P1	260	100	12.41
m-S14-260-P3			17.50
m-S14-260-P5			20.66
<b>Lactone; Irganox HP136 (0.03% w/w)</b>			
m-S15-260-P1	260	100	11.39
m-S15-260-P3			17.89
m-S15-260-P5			17.97
<b>Hydroxylamine; Irgastab FS042 (0.1% w/w)</b>			
m-S16-260-P1	260	100	12.25
m-S16-260-P3			20.48
m-S16-260-P5			24.73
<b>R-HALS; Tinuvin 765 (0.1% w/w)</b>			
m-S17-260-P1	260	100	9.23
m-S17-260-P3			11.97
m-S17-260-P5			14.38
<b>R-HALS; Tinuvin 622LD (0.1% w/w)</b>			
m-S18-260-P1	260	100	8.34
m-S18-260-P3			10.47
m-S18-260-P5			17.76
<b>Biological hindered Phenol; Irganox E201 (0.03% w/w)</b>			
m-S19-260-P1	260	100	12.25
m-S19-260-P3			15.80
m-S19-260-P5			18.17
<b>Phosphite; Weston 399 (0.2% w/w)</b>			
m-S20-260-P1	260	100	11.64
m-S20-260-P3			15.66
m-S20-260-P5			21.22
<b>R-HALS; Chimassorb 119D (0.1% w/w)</b>			
m-S21-260-P1	260	100	9.99
m-S21-260-P3			12.24
m-S21-260-P5			10.98

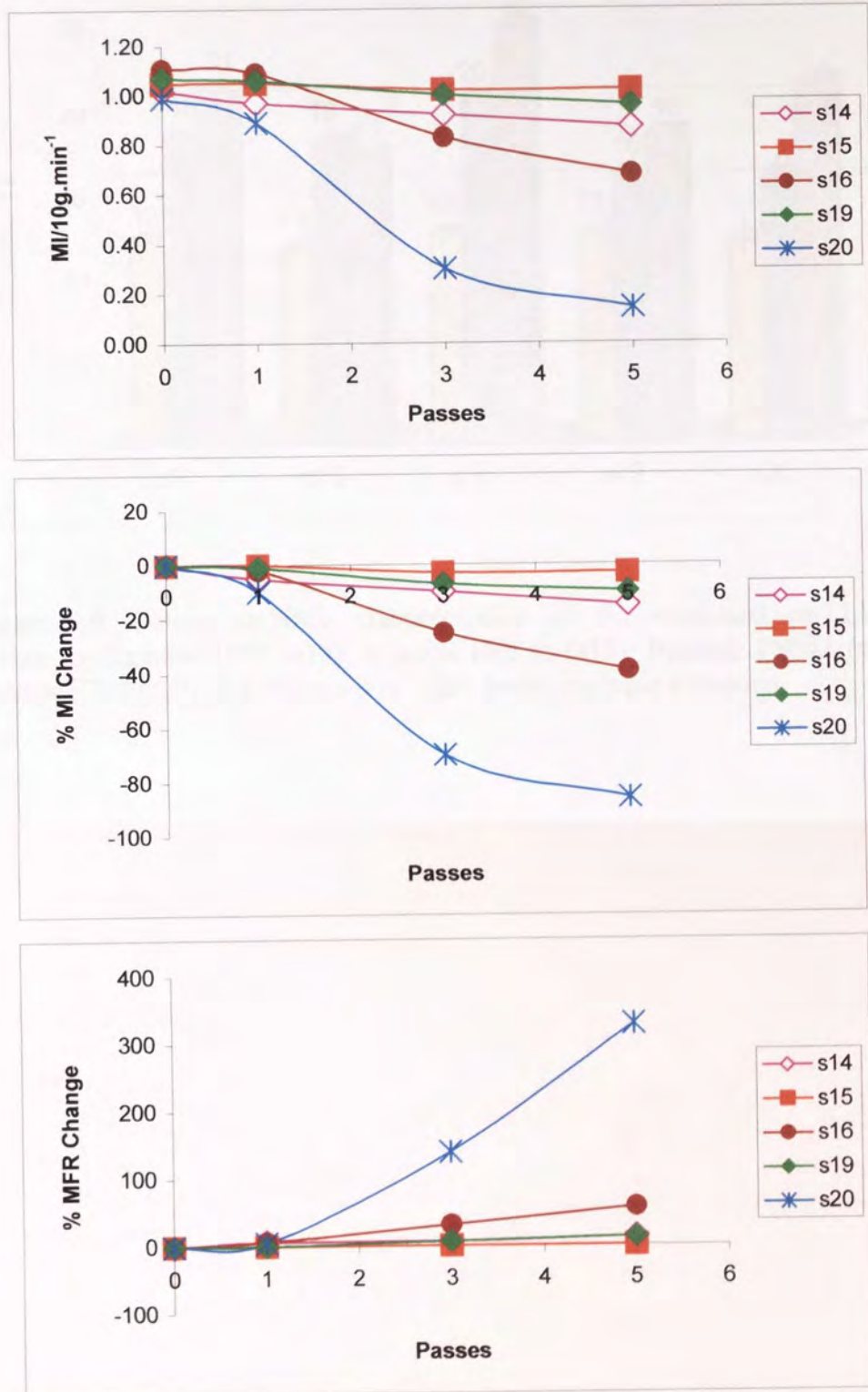


Figure 4.8 Melt stability characteristics a. MI, b. % MI and c. % MFR; of stabilised m-LLDPE containing Irganox 1076 (s14), Irganox HP136 (s15), Irgastab FS042 (s16), Irganox E201 (s19) and Weston 399 (s20) during multiple extrusion.



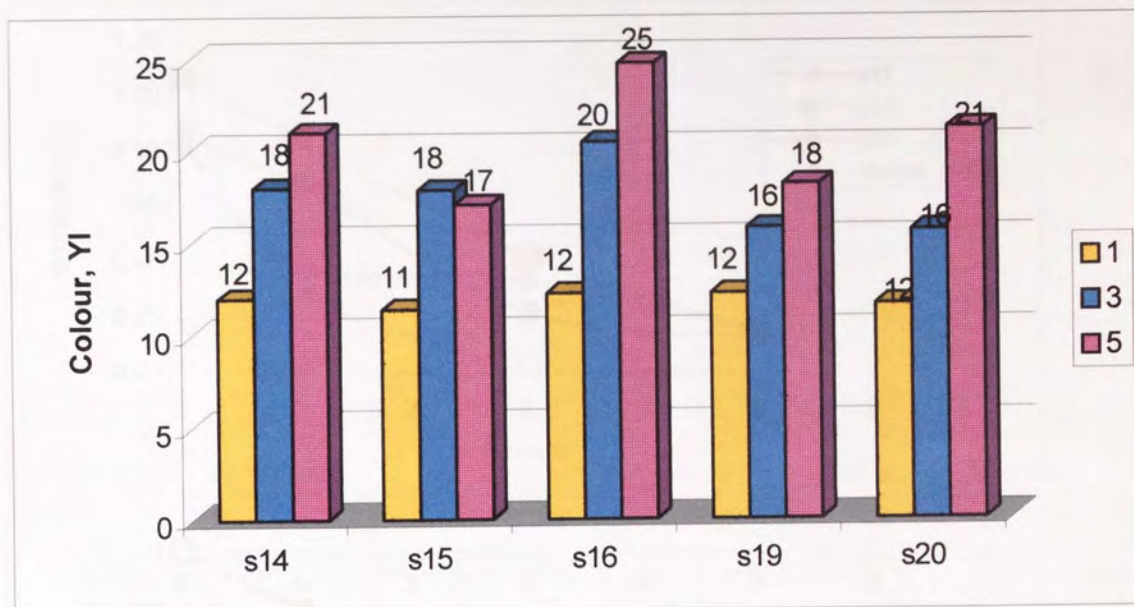


Figure 4.9 Colour stability characteristics of Po stabilised m-LLDPE containing Irganox 1076 (s14), Irganox HP136 (s15), Irgastab FS042 (s16), Irganox E201 (s19) and Weston 399 (s20) during multiple extrusion.

The second surface of the lens was an atoric surface of a rotational symmetry and had an astigmatic effect. The overall astigmatism along the main line was constant with regard to amount and axial position also being provided in the region respectively the regions having at least practically a constant optic power. The main line and the region surrounding was characterized by the following performance function

$$F = \int_{Y_{\min}}^{Y_{\max}} [(A - A_v)^2 + (H - H_v)^2 + (\varepsilon - \varepsilon_v)^2] dy$$

with  $A_v(y)$ ,  $H_v(y)$  and  $\varepsilon_v(y)$  being the prescribed surface astigmatism, surface power, and axial position of the surface in relation to the horizontal X plane, respectively, and with  $A(y)$ ,  $H(y)$ , and  $\varepsilon(y)$  being the surface astigmatism, surface power, and axial position of the surface in relation to the horizontal x plane, respectively.

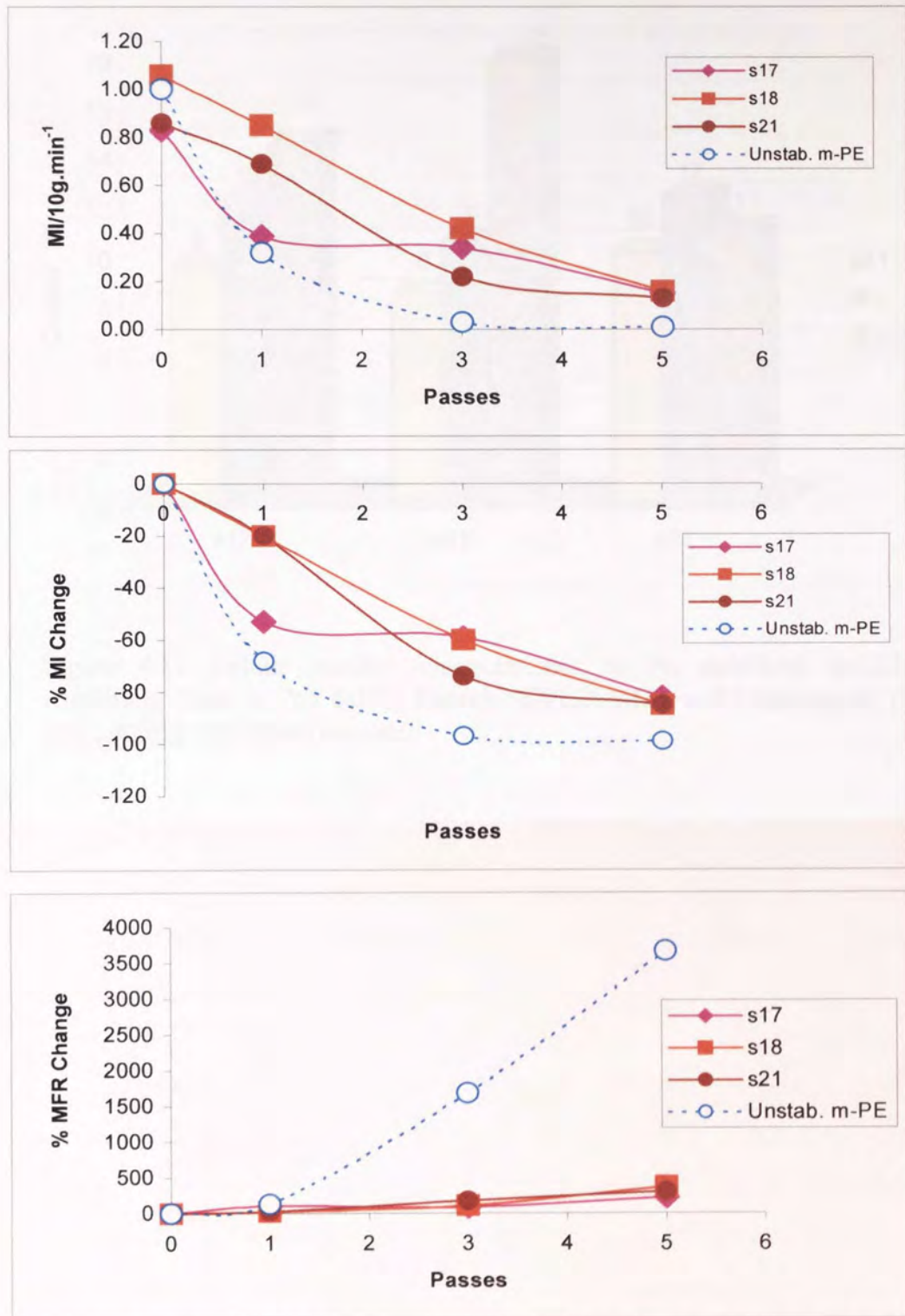


Figure 4.10 Melt stability characteristics a. MI, b. % MI and c. % MFR; of stabilised m-LLDPE containing Tinuvin 765 (s17), Tinuvin 622LD (s18), and Chimassorb 119D (s21) during multiple extrusion.



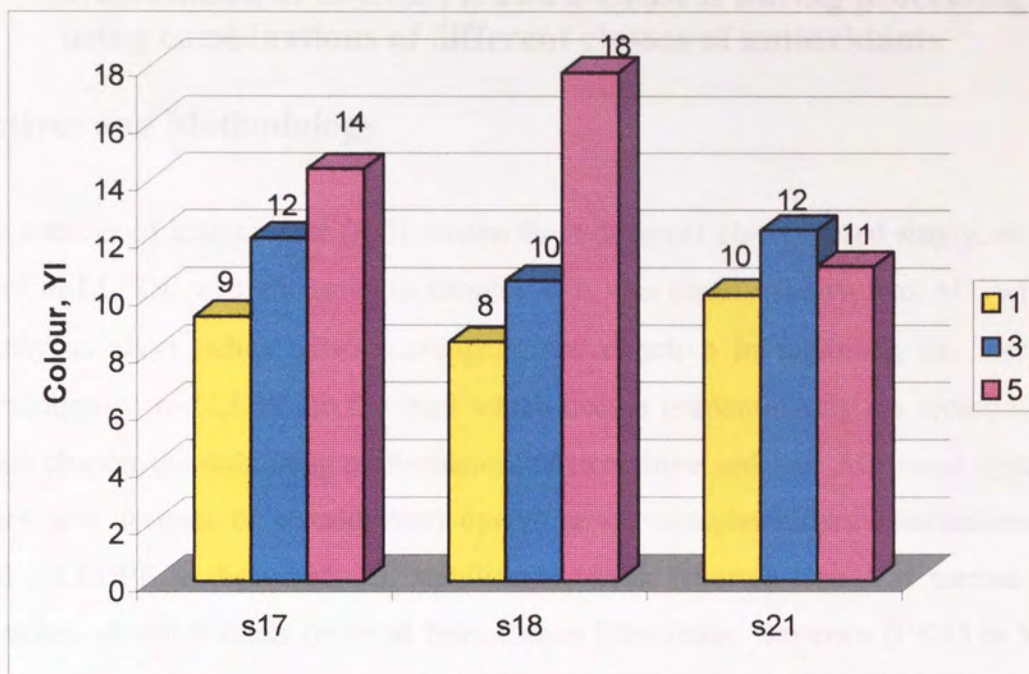


Figure 4.11 Colour stability characteristics of Po stabilised m-LLDPE containing Tinuvin 765 (s17), Tinuvin 622LD (s18) and Chimassorb 119D (s21) during multiple extrusion.

## Chapter 5. Stabilisation of m-LLDPE and z-LLDPE during processing using combinations of different classes of antioxidants

### 5.1 Objectives and Methodology

The effect of a number of antioxidants (AO) chosen from different classes, used singly, on the melt stability of m-LLDPE was presented in chapter 4. It was clearly shown that AO, which operate primarily as alkyl radical ( $R\bullet$ ) scavengers, are effective in inhibiting the thermal oxidative degradation of m-LLDPE, in the melt which occurs predominantly *via* crosslinking reactions. In this chapter the stabilising performances of two, three and four AO based systems (in the presence and absence of co-additives) operating *via* complementary mechanisms in m-LLDPE and z-LLDPE is discussed. All stabilisation work reported here was carried out using 'new' batches of antioxidants received from Exxon Chemicals, Baytown (USA) in May 2000 (see table 2.2, for chemical structures, chapter 2).

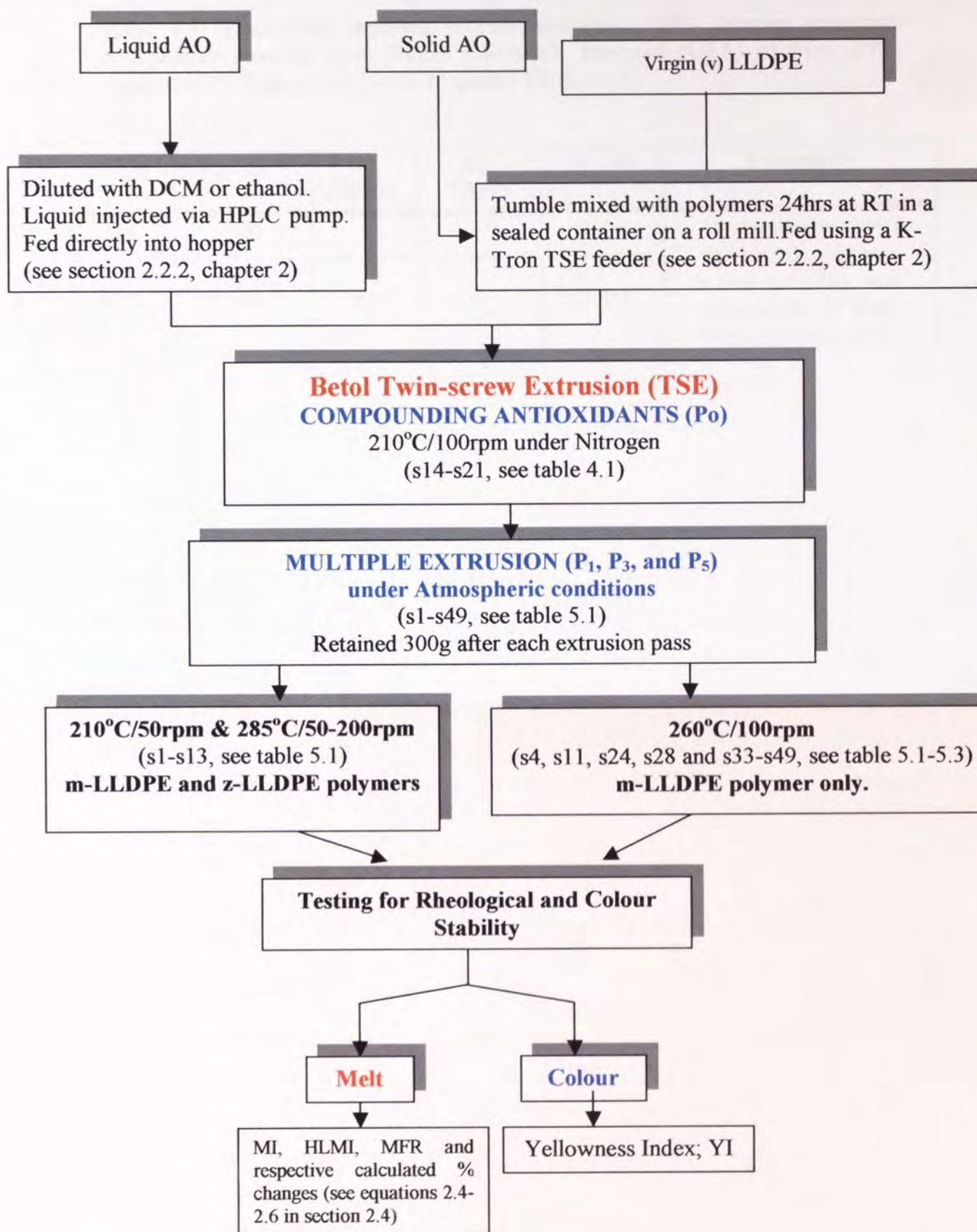
Tables 5.1 & 5.2 display the two, three and four AO combinations utilised throughout this study. This work involved using combinations comprising of synthetic and biological hindered phenols Irganox 1076 and Irganox E201 (Vitamin E); a lactone (Irganox HP136); alkylated hydroxylamine (Irgastab FS042); various phosphites: Weston 399, Irgafos P-EPQ, Doverphos S9228 and Ultrinox 626, and alkyl hydroxyl amine light (R-HALS) stabilisers: Tinuvin 765, Tinuvin 622LD and Chimassorb 119D; in the presence/absence of co-additives Zinc Stearate (ZnSt) and trimetholoypropane (TMP). The performance of these systems was compared with that of commercially available AO blends; XP-60 (1:2.3 w/w ratio of Irganox HP136:Ultrinox 626) and XP-490 (1:2.3:3.3 w/w ratio of HP136:PEPQ:Irganox 1076). It is important to point out here that samples s33-s48 (see table 5.2) are based on combinations of Lactone:Phosphite AO, having constant (0.6 %) phosphite content with AO ratio of 1:2.3 w/w ratio, respectively. This provided the advantage of comparing the performance of the different phosphites at the same phosphorus level in each combination. It is also worth mentioning here that the synergistic combinations s1 to 13 were used in both m-LLDPE and z-LLDPE polymers whilst AO blends s22 to s49 were only used in the m-LLDPE polymer (see table 5.1 & 5.2). Table 5.3 shows two samples, which have been processed more than once in order to establish experimental error.

Different low concentrations of AO were initially compounded (homogenised) with the polymer (Po), during extrusion (in a Betol twin screw extruder, TSE, l/d=33:1, 4mm die) at an



extrusion temperature of 210°C and a screw speed of 100rpm (see section 2.2), with the K-Tron feeder (with solid AOs mixed with polymer powder) and hopper above the extruder blanketed with nitrogen in order to minimise thermal oxidative degradation. Polymer characterisation of all the extruded Po stabilised samples was carried out by examining their melt flow (MF) characteristics (MI, HLMI and MFR). A criterion for an acceptable level of Po stabilisation was based on the difference between the MI of stabilised polymers (Po) and the MI of virgin polymers being within the range of  $\pm 10\%$ .

All Po stabilised LLDPE polymers were then subjected to multiple extrusion using the TSE under varying temperatures 210-285°C and screw speeds of 50-200rpm (under atmospheric conditions). To differentiate between the effectiveness of different AO systems, the melt flow and colour characteristics of the polymer samples were monitored after multi-pass extrusion (first, third and fifth passes). Scheme 5.1 summarises the methodology used in this work.



Scheme 5.1. Overview of the methodology used in the stabilisation of m-LLDPE using two, three and four based AO based systems.



Table 5.1 Metallocene and Ziegler/Natta catalysed LLDPE polymer samples containing different antioxidant formulations compounded (Po) in a TSE at 210°C/100rpm under nitrogen.

AO State Cost/ \$/kg	Target Concentrations/ppm										Total [AO] /ppm	Ratio <sup>1</sup> w/w	Cost <sup>1</sup> \$/kg of PE	Comments	
	Solid	Liquid	Solid	Liquid	Solid	Liquid	Solid	Liquid	Solid	Liquid					
	0.04	0.44	0.33	0.02	0.14	0.31	0.13								
<b>CODE</b>	<b>Irg.</b> 1076	<b>Irg.</b> HP 136	<b>Irg.</b> E201	<b>W</b> 399	<b>U. 626</b>	<b>T. 622LD</b>	<b>TMP</b>	<b>Chims</b> 119D							
S1	500			1500											
S2	750			1000											
S3	750			2000											
S4	500			2000			450								
S11		300			600										
S12	500			1000											
S13			300	600			450								
Constant lactone 0.03% w/w content; Irganox 1076; lactone: Phosphite respectively															
S22	500	300		2000											
S23	500	300		2000			450								
S24	1500	300		2500											
S25	500	300		1500											
Constant Vt. E 0.02% w/w content; Irganox E201; Irgastab FS042; Phosphite respectively															
S26		300	500		600		450								
S27		300	1000		600		450								
Constant W399 2.0% w/w content; Irgastab FS042; Phosphite respectively															
S28	500		500	2000											
S29	500		1000	2000											
Constant Irgastab FS042; Phosphite and R-HALS content: 0.05, 2.0 and 1.0 % w/w respectively															
S30	500		500	2000		1000									
S31	500		500	2000		1000									
S32	500		500	2000		1000		1000							

<sup>1</sup> To determine the total cost of a stabiliser package, calculate the cost of each individual AO then total i.e. [A:B:C] packages cost: ADDITIVE A COST = (Price of additive \$/kg x additive concentration/ppm) / 10<sup>4</sup> = \$/kg/PE. Repeat calculation for additive B and C. \* excluding price of TMP, # excluding price of Chims. 119D



Table 5.2 Metalocene catalysed polyethylene (m-LLDPE) samples containing XP-60, XP-490 and Irganox E201 based systems; each combination comprised of a constant 0.6% Phosphite content and 1:2:3 ratio w/w (phosphite:lactone); compounded (Po) in a twin screw extruder at 210°C/100rpm under nitrogen.

Target Concentrations/ppm										
AO State	Solid	Solid	Liquid	Liquid	Solid	Solid	Solid	Solid	Solid	Solid
Cost/\$/kg	0.04	0.44	0.33	0.02	0.18	0.26	0.14	-	-	-
CODE	Irg. 1076	Irg. HP 136	Irg. E201	W	Dover. S9228	PEPQ	U. 626	Irg. XP-60	Irg. XP-490	Zinc Stearate (ZnSt)
Constant: 0.6% Phosphite content and ratio 1:2:3 (Irganox HP136 : Phosphite)										
S33								861		861
S34		261				600				861
S35		435			1000					1435
S36		373			857					1230
S37		522		1200						1722
Constant: 0.6% Phosphite content and ratio 1:2:3:3 (Irganox HP136 : Phosphite : Irganox 1076)										
S38									2870	2870
S39	1435	435			1000					2870
S40	860	260				600				1720
S41	1235	375			860					2470
S42	1910	580		1330						3820
Constant: 0.03% w/w Vitamin E, 0.6% Phosphite and lactone content; ratio of 1:2:3 of Irganox HP136: Phosphite										
S43		435	300			1000				1735
S44		260	300				600			1160
S45		260	300				600		500	1160+ZnSt
S46		375	300			860				1535
S47		580	300	1330					500	2210+ZnSt
S48		580	300	1530						2210
S49			300				600		500	900+ZnSt
Constant: 0.03% w/w Vitamin E, 0.6% Phosphite and lactone content; ratio of 1:2:3 of Irganox HP136: Phosphite										
S43		435	300			1000				1735
S44		260	300				600			1160
S45		260	300				600		500	1160+ZnSt
S46		375	300			860				1535
S47		580	300	1330					500	2210+ZnSt
S48		580	300	1530						2210
S49			300				600		500	900+ZnSt

Prior to Po stabilisation  
Liquid AO; Weston 399 dissolved in DCM  
Liquid AO; Vitamin E dissolved in Ethanol.

Irganox XP-60  
AO systems  
(XP-60 is a 1:2:3 ratio  
of HP136:U626).

Irganox  
XP-490 AO systems  
(XP-490 is a 1:2:3 ratio  
of HP136:U626).

Vitamin E  
(Irganox E201)  
Based  
Systems

2 To determine the total cost of a stabiliser package, calculate the cost of each individual AO then total i.e. [A:B:C] packages cost: ADDITIVE A COST = (Price of additive \$/kg) x (additive concentration/ppm) / 10<sup>4</sup> = \$/kg/PE. Repeat calculation for additive B and C. # excluding price of ZnSt.

CONFIDENTIAL

Table 5.3 Metallocene catalysed polyethylene (m-LLDPE) samples containing antioxidants received from Exxon Chemicals Baytown (USA) in May 2000; Irganox 1076, Irganox HP 136 and Irgastab FS042.

Code	Irg. 1076	Irg. HP136	Irg. FS042	W. 399	Comments
S4	500			2000	All stabilisation work conducted using was carried out using 'new' batches of AO from Exxon in May 2000
S22	500	300		2000	



## 5.2 RESULTS

Polymer processing i.e. extrusion, a manufacturing process, converts polymer granules into products with desired shapes and sizes via phase transformation and melt deformation. A typical extrusion process involves applying high shear rates ( $100-1000s^{-1}$ ) to polymer melts under atmospheric conditions [25,119]. A combination of high shear, elevated processing temperatures and small residual concentrations of oxygen during processing result in a number of considerable changes in the chemical and morphological structure of a polymer, i.e. due to the effects of thermal oxidative degradation (see section 1.4, chapter 1). Antioxidants may inhibit these undesirable changes during melt extrusion (see section 1.5, chapter 1). To investigate the effects of possible interactions between different antioxidants, which have the potential for being used together as physical mixtures in stabilisation packages, requires the examinations of varying combinations of antioxidants under extrusion conditions. This, allows the performance optimisation of the stabiliser package and leads to an understanding the underlying of the chemistry responsible for the observed effects in the AO combinations. Melt flow index (MFI) measurements, can be related to changes in the molecular weight of a polymer. A drop in melt flow (increase in viscosity) is indicative of an increase in polymer molecular weight due to crosslinking reactions, whereas an increase in MFI (decrease in viscosity) is due to a decrease in molecular weight due to chain scission reactions. Under normal extrusion conditions both crosslinking and chain scission reactions are in direct competition. In this section the extrusion characteristics of the Po and multiply extruded m-LLDPE and z-LLDPE polymers (in the presence/absence of antioxidants) is described.

### 5.2.1 Extrusion characteristics of homogenised (Pass zero, Po) and Multiply extruded (Pass 1-5) m-LLDPE and z-LLDPE polymer samples.

The Betol twin screw extrusion characteristics power consumption, melt pressure, the appearance of the polymer lace and  $\Delta T$ ; of stabilised m-LLDPE and z-LLDPE polymer samples containing different synergistic combinations of commercially available antioxidants (see s1-s13 & s22-s49 in table 5.1&5.2) were monitored after the homogenisation (Po) and the multiple extrusion processes. As mentioned before (section 4.2.1) the compounding (homogenisation) step (referred to as pass zero, Po) was conducted under mild extrusion conditions ( $210^{\circ}C$ , 100rpm, under nitrogen) in order to minimise the effect of thermal oxidative degradation (see section 2.2a, chapter 2). Other screw speeds of 50, 100, 150 and 200rpm were also examined and found to have no significant effect on

the melt stability, see tables A1-2 and figures A1-A5, in appendix 2. The criterion chosen for the optimum feed rate values, were taken as those which lead to minimum variation in pressure ( $\pm 5\%$ ). Note that the optimum output rate values used to compound the various AOs' in metallocene and Ziegler polymers were  $4.0\text{kg}\cdot\text{h}^{-1}$  and  $4.6\text{kg}\cdot\text{h}^{-1}$ , respectively. The effectiveness of the AO blends (melt and colour) in the m-LLDPE and z-LLDPE polymers was then examined by subjecting the compounded (Po) polymers to multiple extrusions (passes 1 to 5). An unstabilised m-LLDPE polymer sample was also processed under the same multiple extrusion conditions for comparison. The extrusion characteristics of the compounded (Po) and multiply extruded (P1, P3 and P5) polymers are described.

#### a. Extrusion characteristics of Compounded (Po) Polymer samples

Table 5.4 and figures 5.1-5.4 present the extrusion characteristics ( $210^\circ\text{C}/100\text{rpm}$  under nitrogen) of the compounding step exhibited by selected by m-LLDPE and z-LLDPE polymer samples processed in the presence of different synergistic combinations; s4, s1-s12, s24, s28, s33, s43 in table 5.1 & 5.2) during the Po compounding step. The extrusion characteristics of all Po stabilised extruded polymer samples are displayed in table A3, see appendix 2. As was shown earlier (section 4.2.1) the compounding of different AO blends does not appear to alter significantly the processing characteristics of the m-LLDPE and z-LLDPE polymers when compared to their unstabilised counterparts. This is clearly reflected in figures 5.1 and 5.3-5.4 and table 5.4, which show a series of plots of power consumption, melt pressure and  $\Delta T$  values against various polymer samples. It is also clear that the m-LLDPE polymer behaves differently during extrusion compared to the Ziegler polymer. In all cases, the metallocene polymer consumes more power, yields higher melt pressures and presents higher  $\Delta T$ . Melt fracture, a real processing problem, is observed as a dramatic change from a smooth extrusion to a non-laminar flow, sometimes giving rise to extrudate irregularities such a shark skin, zig-zag and basket weave. Table 5.4 and figure 5.2 show clearly that the m-LLDPE polymer samples (in the presence/absence of antioxidants) exhibit far more severe melt fracture than is the case with the Ziegler polymer.

#### b. Multi-pass extrusion characteristics

The extrusion characteristics of all multi-extruded stabilised polymer samples are shown in tables A4-A11 in appendix 2. Table 5.5 highlights the extrusion characteristics of stabilised m-LLDPE



and z-LLDPE of unstabilised and one representative stabilised system, s4, (a 1:4 w/w ratio of Irganox 1076:Weston 399 respectively). It is clear that the overall extrusion characteristics of the stabilised polymers; power consumption, melt pressure, extent of melt fracture and actual melt temperature (see figures 5.5-5.7) are again not too different from those of the unstabilised multi-extruded polymer samples with overall higher values for the m-LLDPE polymers. Furthermore, compared to the compounding step (Po), the extrusion parameters of all multiple passes for both polymers are generally lower (see figures 5.5 & 5.6) with the exception of  $\Delta T$ , whereby the melt temperature of multiply extruded polymers is lower than the set die temperature in contrast to a considerably higher melt temperatures exhibited during compounding. This higher melt temperature at Po reflects high shear rates in the first extrusion pass (Po) due to the higher viscosities of the polymers and the much lower melt temperature of P1-P5 (compared to the die temperature) is supported by a decrease in viscosity and hence lower power consumption and melt pressure.

### 5.2.2 Effect of the compounding step (Po) on the stability of m-LLDPE and z-LLDPE.

Tables 5.6 & 5.7 and figures 5.8 & 5.9 present the effect of the Po compounding step (210°C/100rpm under nitrogen conditions) on the melt stability of stabilised m-LLDPE and z-LLDPE polymer samples using different synergistic combinations (see table 5.1 & 5.2) in a Betol TSE. It is clear in table 5.6 & 5.7 and figures 5.8 & 5.9 that at Po all stabilised m-LLDPE and z-LLDPE polymers exhibit very minor changes in their melt flow characteristics compared to the virgin (as received) polymers (see tables 5.6 & 5.7). The effectiveness of all AO combinations after compounding is clearly shown by comparing the high levels of polymer melt stability with that of the unstabilised but similarly extruded (P1) polymers; the latter (unstabilised) which undergo much more extensive oxidative degradation predominantly *via* crosslinking (decrease in MI), as an example see figure 5.9. To compare the effectiveness of the different synergistic AO combinations (see table 5.1&5.2) in m-LLDPE and z-LLDPE, changes in melt characteristics of multiply extruded polymer samples (Pass 1, Pass 3 and Pass 5) were examined.

### 5.2.3 Effects of Combinations of Two Antioxidant on the Melt and Colour Stability of m-LLDPE and z-LLDPE during Multiple extrusion (P1, P3 and P5)

#### A. Multiple Extrusions of Stabilised m-LLDPE and z-LLDPE polymers at 285°C under Variable speeds

##### (a). Blends of Irganox 1076 and Weston 399.

Combinations of the synthetic hindered phenol, Irganox 1076, and the phosphite, Weston 399, (at optimum molar ratios of the individual components) have been shown to act synergistically offering high levels of melt stabilisation to polyolefins [88]. The effect of processing severity (increasing extrusion passes under different extrusion conditions) on the melt stability of unstabilised and stabilised m-LLDPE and z-LLDPE polymer samples containing different weight ratios of Irganox 1076 and Weston 399 (see s1-s12 in table 5.1) is given in tables 5.8 & 5.9 and figures 5.10-5.16.

It is clear that unstabilised m-LLDPE polymer suffers more extensive thermal oxidative degradation, (predominantly *via* crosslinking reactions, under all conditions examined), with increasing extrusion passes, when compared to that of unstabilised z-LLDPE samples processed under the same extrusion conditions. This is clearly reflected in the difference in the level of reduction of MI with extrusion passes (see figures 5.12 & 5.14). Calculation of the MFR (from MI measurements) can be related to changes in molecular weight distribution (MWD) of polymers. Figures 5.10 & 5.16 show that both m-LLDPE and z-LLDPE polymers give rise to higher MFR values with increasing extrusion passes but the extent of MFR increase in the case of the m-LLDPE is again higher than is the case for the z-LLDPE. This would indicate that multiple extrusions result in a much more rapid shift of the MWD to higher values in the case of the m-LLDPE compared to the z-LLDPE polymer. This is particularly noticeable at the higher extrusion temperatures (285°C) with screw speeds of 50 to 200rpm (see figures 5.16).

Tables 5.8&5.9 and figures 5.12-5.14 show the effect of processing severity (screw speeds 50 to 200rpm at a processing temperature of 285°C) on the melt stability of stabilised m-LLDPE and z-LLDPE polymer samples containing different combinations of Irganox 1076 and Weston 399. It is clear that the higher concentration of Weston 399 in the Irganox 1076:Weston 399 combination (i.e. s4) results in a much better overall stabilisation effect in both the Metallocene and Ziegler polymers, see figures 5.17 to 5.21. However, overall at the high extrusion temperatures of 285°C at

both screw speeds of 50 and 200rpm the Irganox 1076:Weston 399 AO system offers higher overall melt stability to the z-LLDPE polymer compared to that for the m-LLDPE polymer, see figures 5.20 & 5.21.

Figures 5.12 & 5.22 show that the stabilised formulations reduce drastically the extent of broadening of MWD reflected by a smaller extent of change in MFR in both m-LLDPE and z-LLDPE polymers at the higher phosphite containing AO combination (i.e. 1:4 ; s4). Moreover, at the higher screw speed of 200rpm at an extrusion temperature of 285°C, the above AO system (wt ratio of 1:4) gives rise to a better stabilising effect (less crosslinking reflected in less decrease in MI) in both polymers when compared to lower screw speeds, e.g. 50 and 100rpm, see figures 5.23 & 5.24. The extent of discolouration of the polymers caused by the Irganox 1076:Weston 399 AO system is shown in figures 5.25 and 5.26. It is clear that at 285°C, lower screw speeds and increasing number of passes results in higher extents of discolouration (figure 5.25), with the AO system imparting more overall discolouration to the metallocene polymer than the Ziegler analogue (see figure 5.26).

**(b). Blends of Irganox E201 and different phosphites with TMP.**

The effect of processing severity (285°C at different screw speeds) on the melt stability of polymers containing a biological hindered phenol (Irganox E201), a phosphite (Weston 399 or Ultrinox 626) and a polyhydric alcohol (TMP), (see s11 and s13, in table 5.1) was compared with that of polymers containing Irganox 1076:Weston 399 used at a 1:4 wt ratio. Screw speeds of 50, 100 and 200rpm were used in the case of the m-LLDPE whereas the Ziegler polymer samples were extruded at 100rpm only (see tables 5.10 & 5.11).

Figures 5.27 & 5.28 show that in the m-LLDPE, the Vitamin E:phosphite AO systems generally show higher melt stability than those containing Irganox 1076:Weston 399, with the Vitamin E:Ultrinox 626 system showing the best overall stabilising performance (reflected in lower extent of change in MI and MFR). Furthermore, this AO system (s11) was shown to be more effective in m-LLDPE than in z-LLDPE (see figures 5.28-5.30) which is in direct contrast to the trend shown by the Irganox 1076:Weston 399 system as was highlighted earlier (see figure 5.22).

Furthermore, in the case of m-LLDPE polymer, the vitamin E combinations give rise to better colour stability than for the Irganox 1076/Weston 399 system, with a slight difference as to which phosphite is used (Ultranox 626 or Weston 399), especially at 285°C/200rpm, passes 3 and 5 (see figures 5.32-5.35 and tables 5.12-5.13). Figures 5.32 & 5.33 show that generally both the Vitamin E:phosphite and Irganox 1076:phosphite AO systems (processed at 285°C/100rpm) cause further extents of discolouration in the m-LLDPE polymer than in the z-LLDPE polymer.

## **B. Multiple Extrusions of Stabilised m-LLDPE polymers at 260°C at 100rpm.**

### **(a). Blends of Lactone and different Phosphites**

The effect of processing severity (multi-pass extrusion at 260°C/100rpm) on the melt and colour stability of m-LLDPE in the presence of different antioxidant combinations based on the lactone, Irganox HP136, used with different phosphites (see s34-s37, a ratio of 1:2.3 w/w ratio of lactone:phosphite, in table 5.2) is shown in figures 5.36-5.37 and tables 5.14-5.15. The phosphorus content in all combinations was kept constant at 0.6%P and the AO ratio was 1:2.3 w/w of lactone:phosphite.

Table 5.14 and figure 5.36 show the very high thermal melt stabilising effect of all lactone antioxidant based systems with no significant change in melt flow characteristics even after five multiple extrusions. A comparison of the effect of the different phosphites in the combinations has revealed that the system containing tris (nonyl) phenyl phosphite (Weston 399, s37), gives rise to slightly lower melt stability to the polymer (at the concentration examined) compared to the other phosphites. Furthermore, Weston 399 containing system was also found to give rise to higher extent of discolouration in the m-LLDPE polymer when compared to the other phosphites used, see figure 5.37. The initial colour stability after the first and third extrusion pass was best in the case of the lactone containing phosphite PEP-Q. Figure 5.38 highlights the cost effectiveness of each of the Irganox HP136:Phosphite stabiliser packages (HP136:Phos.). It is clear that HP136:Ultranox 626 containing m-LLDPE, which produced excellent levels of melt and colour stability with increasing extrusion severity is also the cheapest (0.91\$/lb) formulation .

#### 5.2.4 Effects of Three Antioxidant Combinations on the Melt and Colour Stability of m-LLDPE during Multiple extrusion (P1, P3 and P5) at 260°C/100rpm.

##### (a). Blends of Lactone, Irganox 1076 and different Phosphites.

The effect of extrusion severity on the melt and colour stability of stabilised m-LLDPE polymers of a number of three AO systems were examined. Synergistic combinations of Irganox 1076, Irganox HP136 and Weston 399 in the presence/absence of a co-additive, TMP (see s22-s25 in table 5.1) were used containing a fixed lactone content 0.03% w/w in the presence of varying concentrations of Weston 399 and Irganox 1076. When different phosphites (Weston 399, Doverphos S9228, Ultrinox 626 and Irgafos P-EPQ) were used in the Irganox 1076:Irganox HP136 systems, the P content was kept fixed at 0.6% and the ratio of lactone:phosphite:Irganox 1076 was also kept fixed at 1:2.3:3.3 (see s39-s42, in table 5.2). The melt and colour stabilising efficiencies of these synergistic combinations were compared under identical extrusion conditions with those of a commercial stabiliser package, XP-490 (a synergistic combination of Irganox 1076, Irganox HP136 and P-EPQ, used in a w/w ratio of 3.3:1:2.3, as stated by the manufacturer). A blend with similar composition was also prepared and tested in m-LLDPE during multi-pass extrusion (s39, see table 5.2).

Figure 5.39 and table 5.16 compare the effect of varying concentrations and ratios of the AO-combination Irganox 1076:Weston 399 in the presence and absence of the polyhydric alcohol, TMP in blends containing a fixed low concentration (300ppm) of the lactone, Irganox HP136. In blends containing constant ratios of Irganox 1076:Weston 399 of 1:4 and Irganox 1076 concentration of 500ppm, the addition of TMP (s23 versus s22) results in slightly improved melt stability, as reflected by a lower change in MI and less MWD broadening (see % MI and %MFR change in figure 5.39). However, a much more drastic improvement is achieved when a higher concentration of Irganox 1076 (a three fold increase) is used even at lower phenol to phosphite ratio of 1:1.75 only, see sample s24 in figure 5.39. However, such a high hindered phenol concentration in the blend also gives rise to higher extent of discolouration as shown in figure 5.40. It is clear from figure 5.40 that the addition of the lactone to blends of Irganox 1076:Weston 399 increases the discolouration of the polymer.



The effect of varying the type of phosphite AOs in blends of Irganox 1076:Irganox HP136:phosphite is shown in figures 5.41 & 5.42 (see also table 5.18). It is clear that there is not much difference in the stabilising effect exerted by the different phosphites and there appears to be no additional benefit in using higher concentrations of the Irganox 1076 in the blends, e.g. compare s40 and s42 in figure 5.41. Furthermore, laboratory blended AO system showed very similar behaviour to an equivalent commercial AO blend, (e.g. compare XP-490 designated here as sample s38 and sample s39, figure 5.42). Although, the different phosphites do not seem to have any significant effect on the extent of melt stability of the polymer, they do affect the discolouration to different extents. Figure 5.43 shows that blends containing Weston 399 (s24 and s42) give the worst discolouration.

Cost analysis of these AO systems compared at the concentrations used, shows that the s40 sample (Ultranox 626 containing blend) which produced high melt and colour stability in m-LLDPE have the lowest cost (1.1\$/lb). Although the P-EPQ has slightly outperformed the Ultranox 626, in colour, it is the most expensive formulation (2.3\$/lb). A cost comparison with other AO systems discussed earlier is also shown in this figure.

**(b). Blends of Hydroxylamine, Irganox E201 and Ultranox 626 with TMP.**

The effect of varying concentrations of hydroxylamine (Irgastab FS042) in AO blends containing Vitamine E:Ultranox 626 (and containing a small concentration of TMP, sample s11) on the melt stability of m-LLDPE is shown in table 5.20 and figure 5.45 & 5.46. The hydroxylamine does not seem to have any significant additional effect on the melt stability of the polymer as shown from the minimal changes in the melt rheological measurements given by samples s26 and s27 when compared to sample s11 (containing no hydroxylamine). The presence of the hydroxylamine in the AO system does however give rise to a slight increase in discolouration of the polymer as shown in figure 5.47 (see also table 5.21).

**(c). Blends of Hydroxylamine, Irganox 1076 and Weston 399.**

The effect of the hydroxylamine, Irgastab FS042, on the melt and colour stability of the m-LLDPE containing Irganox 1076 with Weston 399 was also examined. Table 5.22 and figure 5.48 & 5.49 show again that the addition of the hydroxylamine does not have any significant effect on the melt



stability of the polymer. However, the presence of the hydroxylamine in the hindered phenol:phosphite-containing polymer does give a definite increase in the extent of discolouration of the polymer, see figure 5.50 and table 5.23.

**(d). Blends of Lactone, Irganox E201 and different phosphites with/without Zinc Stearate.**

The effect of different phosphites on the melt and colour stability of m-LLDPE containing AO combinations based on Vitamin E:Irganox HP136 and extruded in the presence or absence of the co-additives TMP and Zinc stearate (ZnSt) has been examined. Neither the different phosphites nor the co-additives (TMP or ZnSt) show any significant effect on the melt stability of the lactone:Vitamin E stabilised polymers, as shown in figures 5.51-5.53 and table 5.24. The presence of the ZnSt in the formulations, however, tends to have a slight improvement on the colour stability, see figure 5.55 and an even slightly better improvement is observed in the presence of the polyhydric alcohol, TMP, see figure 5.56 and table 5.25. Overall, the presence of the phosphite Weston 399 (s48) in these samples gives rise to the least colour stability, see figure 5.54 and table 5.25.

The cost effectiveness of each combination is shown in figure 5.57. The vitamin E/HP136 in combination with ultranox 626 (s44) that presented high extents of melt and colour stability (with increasing extrusion severity) is among the lower priced (1.4\$/lb) formulations.

**5.2.5 Effects of Combinations of Four Antioxidants on the Melt and Colour Stability of m-LLDPE during Multiple extrusion (P1, P3 and P5) at 260°C/100rpm.**

**(a). Blends of Hydroxylamine, Irganox 1076, Weston 399 and different R-HALS**

The effect of different alkylated hindered amine light stabilisers (R-HALS); Tinuvin 765, Tinuvin 622LD and Chimassorb 119D on the melt and colour stability of m-LLDPE containing Irganox 1076:Irgastab FS042:Weston 399 (1:1:4 w/w ratio respectively) was examined (see s30-s32 in table 5.2). Table 5.26 and figure 5.58 shows that the effect of the HALS is overall not a significant one although blends containing Tinuvin 765 (s30) give rise to lower melt stability upon multiple extrusion, see figure 5.58. However, all R-HALS, similar to the case where the hydroxylamine is present, contribute to increasing discolouration of the polymer as clearly shown in figure 5.59. The

formulation containing Chimassorb 119D (s32) which produced high levels of melt and poor colour stability has the lowest price (0.15\$/lb, see table 5.2).

### 5.3 DISCUSSION

#### 5.3.1 Extrusion characteristics of stabilised Metallocene and Ziegler polymers and the effect of the Compounding step (Po) Process on their Melt Stability.

The amount of power required to shear a polymer melt during extrusion is a reflection of the rheological characteristics of that polymer (i.e. its shear viscosity), which is in turn a direct consequence of the structural architecture of the polymer. The melt pressures (measured by pressure transducers at the die) is also governed by the viscosity of the polymer, large viscosities result in higher melt pressures. The difference between the melt and die temperatures,  $\Delta T$ , may be correlated to the melt flow characteristics of polymers. The extrusion characteristics of all stabilised and multiply extruded metallocene and Ziegler polymers suggest that the low concentrations of varying blends of additives do not alter significantly the overall extrusion characteristics of both sets of polymers compared to their unstabilised counterparts (see figures 5.1-5.2 & 5.5-5.7). These results (polymers containing AO blends) are in line with the extrusion characteristics of those polymers containing single AOs' (as discussed in chapter 4) and confirm that the stabilised m-LLDPE polymer samples require higher power consumption and melt pressures than is the case for the z-LLDPE.

The higher power consumption needed for the stabilised m-LLDPE polymer is almost certainly due to its narrower molecular weight distribution (MWD) [25,28,119] and higher shear viscosity [28] relative to the Ziegler polymer. The virgin z-LLDPE polymer, which has a broad MWD, contains a high fraction of high molecular weight chains and a high fraction of low molecular weight chains (determined from the molecular weight measurements shown in table 2.1 in section 2.1 and figure 3.1). Disentanglement caused by the interaction of fractions of chains with low and higher molecular weight, i.e. lubrication, results in irregular flow [28]. The melt flow is improved by the presence of high fraction of low molecular weight chains in z-LLDPE (less entanglement, compared to the m-LLDPE polymer), which improves melt processability [28]. However, this processing advantage occurs at the expense of solid-state properties (see section 1.1 for structure/property relations), which become inferior [28]. Cogswell [120] has suggested that a narrow MWD polymer (such as the case with m-LLDPE) would experience a more difficult flow,

greater entanglement and is generally characterised by defects such as melt fracture. This was clearly shown in the case of m-LLDPE stabilised polymer samples, which suffered from a higher extent of melt fracture compared to the z-LLDPE stabilised polymer samples processed under the same conditions (see figure 5.2). The occurrence of melt fracture in m-LLDPE under all processing temperatures at lower critical shear rates was also evident from capillary rheometric measurements. The results in this investigation are in good agreement with work reported by others [28] who showed that metallocene catalysed LLDPE polymers consume more energy (as compared to that presented by its Ziegler counterpart) during film blow extrusion.

The temperature difference between the die and the polymer melt,  $\Delta T$ , showed the largest increase (with increasing screw speed) in the case of the metallocene stabilised samples (see figures 5.3 & 5.7 and also tables 5.4 & 5.5), which is a direct consequence of the higher shear rates (as indicated by the higher power consumption, see figure 5.3) required by this polymer.

### **5.3.2 Effect of Two Antioxidant Combinations on the melt and colour stabilisation of m-LLDPE and z-LLDPE during multiple extrusion.**

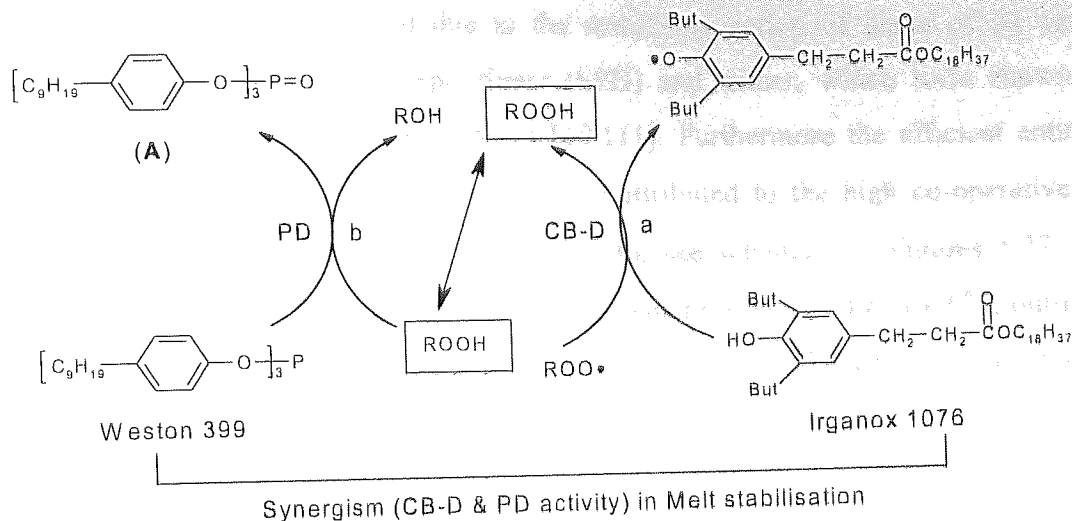
#### **(a). Blends of Irganox 1076 and Weston 399 (285°C/variable speeds).**

It was shown in chapter 3 that unstabilised m-LLDPE undergoes predominantly crosslinking reactions during multiple extrusion at all temperatures examined, whereas the Ziegler polymer undergoes mainly chain scission reactions, though its behaviour was shown to be more temperature dependent. In practice, these degradative reactions result in deleterious changes in the mechanical properties of polymers leading to unpredictable performance and catastrophic failure [34]. Consequently, PE is rarely used without stabilisation and generally chain-breaking antioxidants are used in combination with peroxidolytic antioxidants to provide the necessary protection during melt extrusion (see section 1.5).

The higher effectiveness of this AO system (Irganox 1076:Weston 399) in the Zeigler polymer (compared to m-LLDPE) under all conditions examined is clearly illustrated by the lower extent of change in both MI and HLMI, see figures 5.12-5.15 & 5.60-5.63. However, as in the case of the unstabilised polymers, a similar trend was observed in the above stabilised samples, i.e. a higher extent of crosslinking is observed (reflected in an increased negative change in MI and HLMI values) in the stabilised m-LLDPE (compared to z-LLDPE), though in both polymers the overall

extent of crosslinking reactions is lower than that observed in their unstabilised analogues, see as an example figures. 5.12 & 5.14 and 5.60. Figure 5.60 also shows clearly that the effectiveness of this Irganox 1076:Weston 399 (1:4 w/w) AO system becomes much higher when the polymer is extruded at a lower temperatures (260°C).

In both cases (m-LLDPE and z-LLDPE polymers), the higher effectiveness of the AO system at the higher screw speed (200 rpm and 285°C) as shown in figure 5.61 must be due partly to the shorter residence time experienced by the polymers at higher speeds, thus resulting in a lower extent of oxidative degradation. This argument is further supported by the lower extent of discoloration imparted in the polymer at such higher screw speed (200 rpm), see figure. 5.25. Weston 399 is known to act *via* a PD mechanism [83,84] leading to deactivation of ROOH *via* reduction to alcohol while the phosphite is oxidised to the corresponding phosphate (A) (scheme 5.2, reaction b). In addition, the presence of Irganox 1076 [60,88] in the blend will contribute to deactivation of alkylperoxyl (ROO●) radicals (scheme 5.2, reaction a) and hence resulting in a 'powerful' synergistic effect. It was shown earlier (see chapter 3) that Ziegler polymers undergo higher extents of chain scission reactions compared to the metallocene polymers with the latter resulting in mainly crosslinking reactions upon extrusion [32]. Figure 5.61 shows this clearly for the Irganox 1076:Weston 399 stabilised polymers, where the Ziegler polymers give increasing extents of chain scission (compared to the m-LLDPE polymer which shows increasing extents of crosslinking) during multi-extrusion at both screw speeds of 50-200rpm. Since Irganox 1076 operates *via* mainly trapping alkylperoxyl (ROO●) radicals (not R●), it may be expected that blends containing Weston 399:Irganox 1076 would offer higher stabilisation to the Ziegler polymer (compared to the m-LLDPE polymer). This indeed is the case as seen from the higher extent of stabilisation offered by such an AO blend to the Ziegler polymer (lower extent of melt flow changes, see figures 5.61 & 5.62).



Scheme 5.2 Co-operative interactions between Irganox 1076 and Weston 399 under melt processing conditions.

(b). **Blends of Irganox E201 and different Phosphites with TMP (285°C/variable speeds).**

Previous work at Aston has shown the  $\alpha$ -tocopherol is a highly effective melt stabiliser in LDPE giving a better performance than Irganox 1076 [56,74,110,111]. It was further demonstrated that a 1:2 w/w ratio of  $\alpha$ -tocopherol:Ultranox 626 (with a small concentration of TMP) imparted a high extent of melt and colour stability to LDPE during multi-pass extrusion conditions [56,74,110,111]. It was interesting therefore to examine the effectiveness of such AO systems (Vitamin E and Ultranox 626) as a processing stabiliser in m-LLDPE and z-LLDPE polymers and to compare its performance to that of the Irganox 1076:Weston 399 system.

It is clear from figures 5.27-5.30 that the Vitamin E system (Irganox E201:Ultranox 626:TMP, denoted as formulation s11) is a much more highly effective melt stabiliser compared to Irganox 1076:Weston 399 AO system (s4) even at the much lower concentration of Vitamin E (compared to Irganox 1076) that is used here. Further, figure 5.27-5.30 shows that the Vitamin E system is more effective in the m-LLDPE compared to its performance in the z-LLDPE polymer. The higher antioxidant activity of the  $\alpha$ -tocopherol-based system may be attributed, at least in part, to its highly efficient alkylperoxyl ( $\text{ROO}\bullet$ ) radical trapping capability and the higher stability of the formed tocopheroxyl radical, compared to the phenoxyl radical formed from Irganox 1076. The stereoelectronic effects of  $\alpha$ -tocopherol result in enhanced stability of the tocopheroxyl radical *via*

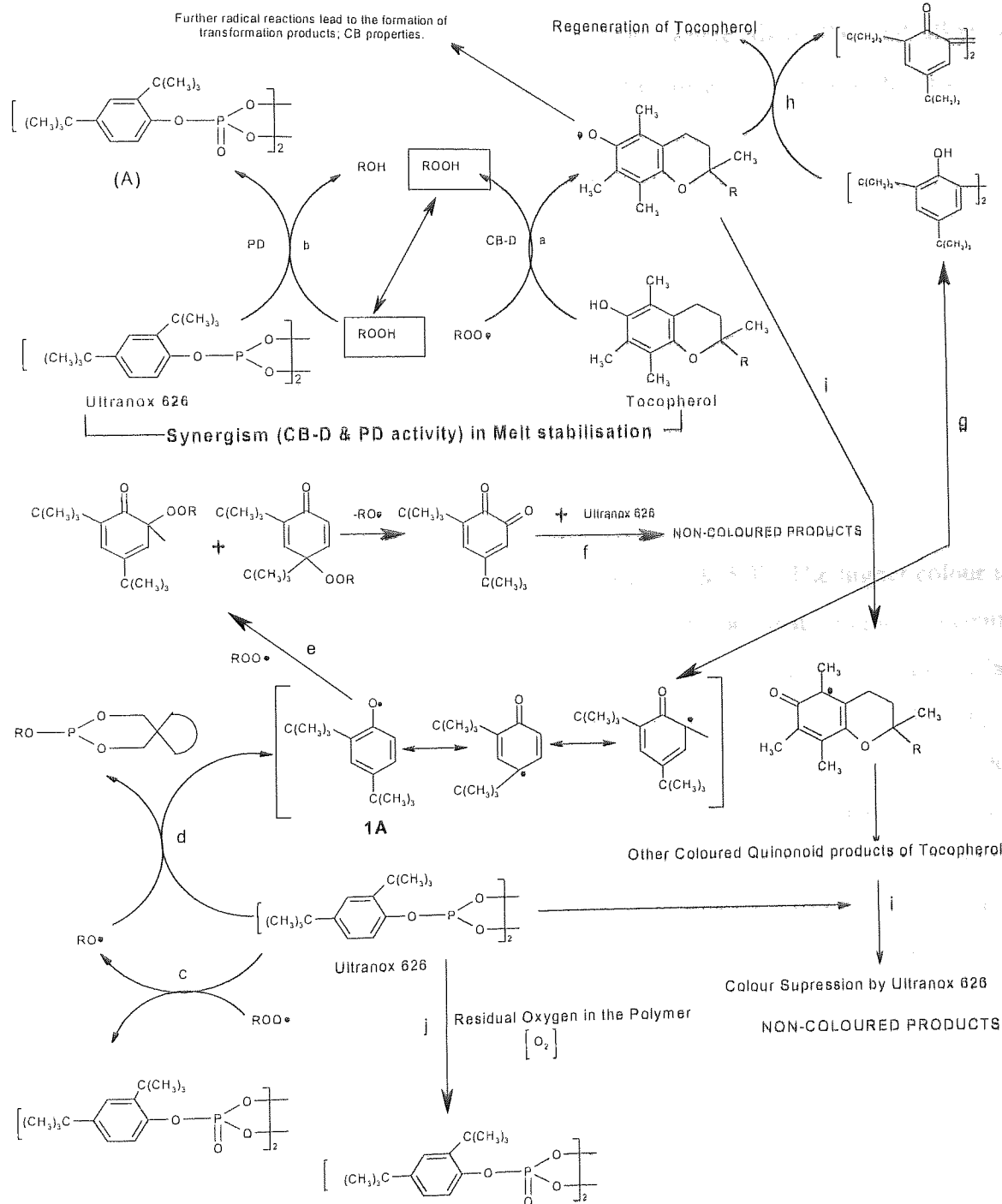
interaction between the *p*-orbitals, and due to the stabilising action of some of its oxidation products, i.e. dihydroxydimer (DHD), spirodimer (SPD) and trimer, which were shown to be themselves effective polymer antioxidants [56,74,110,111]. Furthermore the efficient antioxidant activity of the  $\alpha$ -tocopherol-based system can also be attributed to the high co-operative action between  $\alpha$ -tocopherol and the phosphite (Ultranox 626), see scheme 5.3. Figures 5.27 & 5.29 clearly show that blends of Vitamin E with the peroxidolytic phosphite, Ultranox 626, out-perform blends of Vitamin E with Weston 399 in stabilising the melt of m-LLDPE and z-LLDPE polymers, under all extrusion conditions examined (285°C with variable speeds).

In contrast to the aryl phosphite Weston 399, which has only a weak chain breaking activity, the hindered phosphite Ultranox 626 exhibits both peroxide decomposing activity and a strong chain breaking activity where both alkylperoxyl (ROO•) and alkoxy (RO•) radicals can be deactivated. Further, it has been suggested previously [111] that the co-operative AO mechanism between  $\alpha$ -tocopherol and Ultranox 626 also results in the regeneration of the  $\alpha$ -tocopherol, as shown in scheme 5.5 [111], whereas such a regeneration mechanism is unlikely to occur in the presence of the unhindered phosphite Weston 399. Figure 5.27 shows that the  $\alpha$ -tocopherol:Ultranox 626 combination (s11) is more effective than  $\alpha$ -tocopherol:Weston 399 as a melt stabiliser in m-LLDPE extruded under all extrusion conditions examined. These results support the above arguments and confirm the higher extent of synergism that occur in the  $\alpha$ -tocopherol:Ultranox 626 system (s11). In addition to the higher melt stabilising effectiveness of the Vitamin E:Ultranox 626:TMP blend this system also imparts a lower extent of discolouration to the m-LLDPE polymer when compared to the performance of the Irganox 1076:Weston 399 system, see figures 5.32 & 5.34. Although  $\alpha$ -tocopherol has been shown previously [111] to cause higher discolouration in PE when compared to Irganox 1076, the blend of Vitamin E with Ultranox 626 which also contains a small concentration of the polyhydric alcohol, TMP, gives a lower extent of discolouration than Irganox 1076:Weston 399 as shown above.

The additional colour stability observed in the Vitamin E system must be, at least in part, due to the presence of the polyhydric alcohol, TMP, in the system. It has been shown [111] that the use of TMP with Vitamin E and phosphite gives rise to a significant reduction in the concentration of one



of the most discolouring oxidation products of  $\alpha$ -tocopherol, namely, the corresponding aldehyde, hence increasing drastically the colour stability of the polymer.



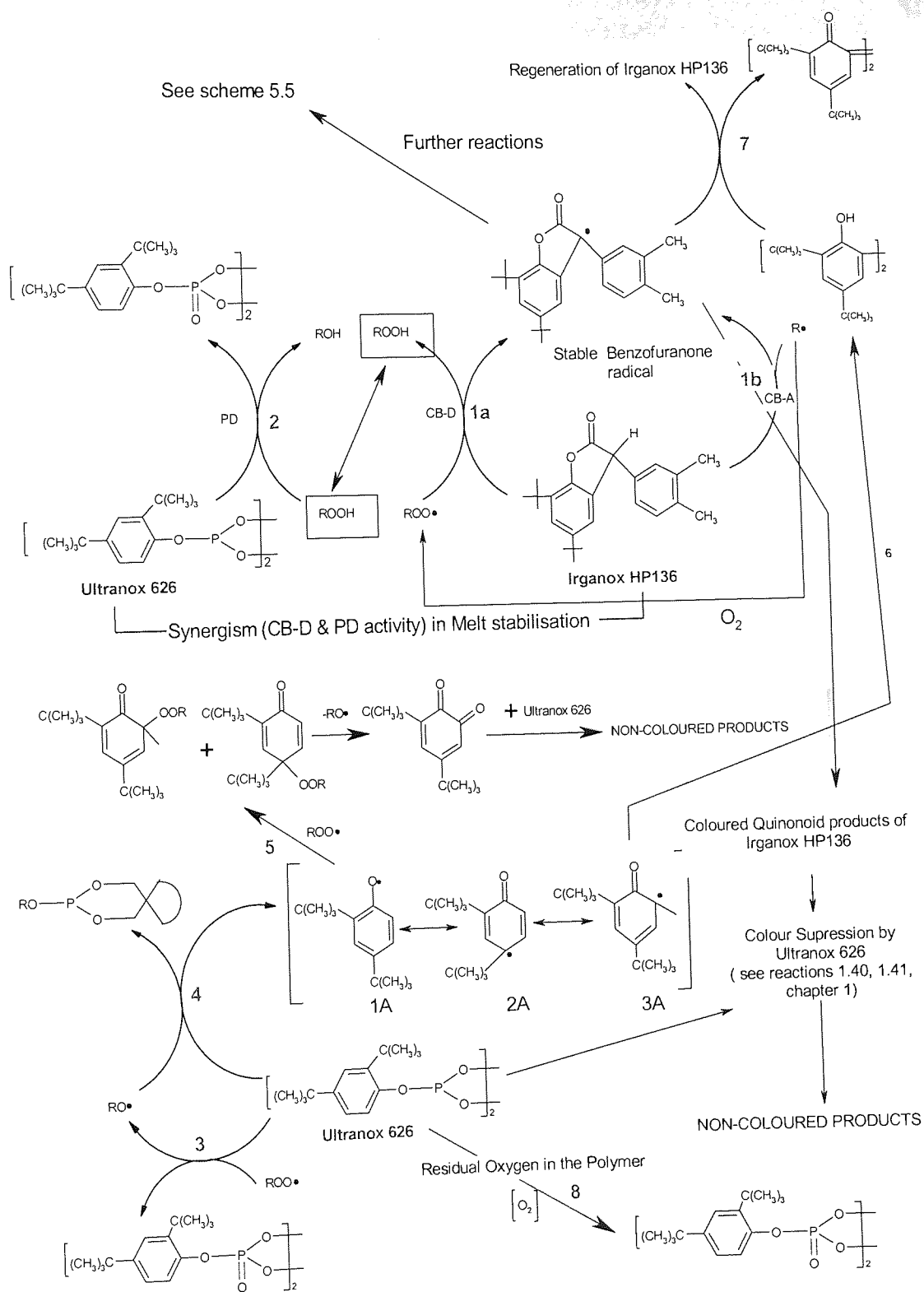
Scheme 5.3. Co-operative interactions between Tocopherol and Ultrinox 626 under melt extrusion conditions [111].

(c). **Blends of Lactone and different phosphites (260°C/100rpm).**

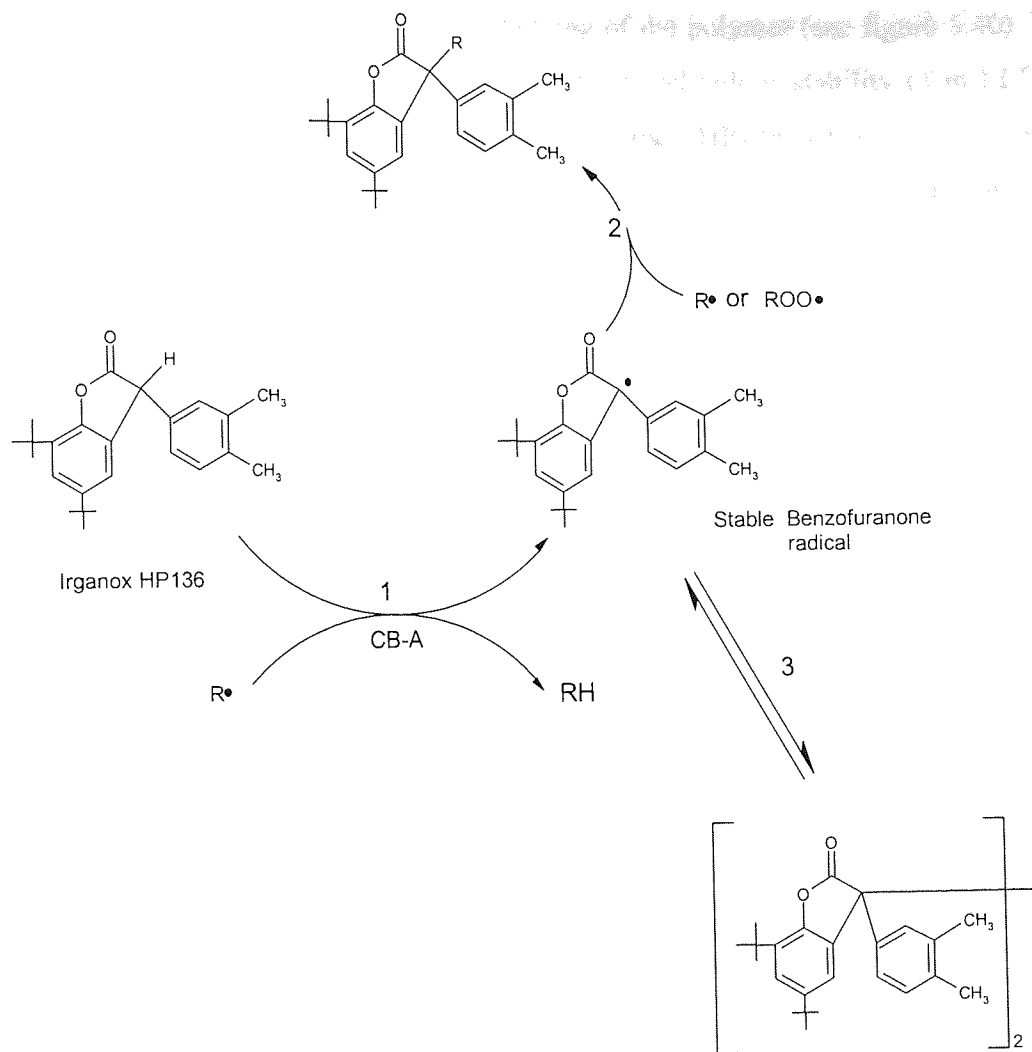
Pauquet [79,109] and Nesvadba *et. al.* [78] have demonstrated that 3 arylbenzofuran-2-one (a lactone) can function effectively as a complementary chain breaking; donor (CB-D) and acceptor (CB-A) antioxidant, operating efficiently under conditions where alkyl,  $R\bullet$ , and alkyl peroxy,  $ROO\bullet$ , radicals are present in a system, i.e. under normal extrusion conditions, thereby having the ability to retard or inhibit crosslinking and chain scission reactions [32] (see reactions a & b in figure 1.13, chapter 1). The use of such good CB-A/CB-D AO blends with a phosphite, which act as peroxide decomposers, have been shown to be effective in the stabilisation of polymer melts [80,81,115].

A range of different hindered phosphites used at the same phosphorus content (0.6%P) in blends with the lactone Irganox HP136 (applied at a fixed ratio of 1:2.3), gave quite similar levels of melt stability to m-LLDPE (see figure 5.36 for the phosphites Ultrinox 626, PEP-Q, Doverphos S9228). In comparison, the sterically unhindered phosphite, Weston 399, [83] used under the same conditions, gave a slightly lower stabilising efficiency and a higher extent of discolouration especially after five multiple extrusion passes, see figures 5.36 & 5.37. The higher colour in pass 5 imparted by the blend containing Weston 399 may be due to the fact that a higher concentration of Irganox HP136 was used for this sample (s37), done in order to keep the weight ratio of lactone to phosphite constant, see table 5.2. Another possible reason for the slightly lower stabilising effect of Weston 399, compared to the other hindered aryl phosphites (Ultrinox 626, PEP-Q and Doverphos S9228), in blends containing Irganox HP136, may be due to the lower thermal hydrolytic stability of the former unhindered phosphite. Stevenson *et. al.* [120] has shown that the higher lattice energy and hydrophobic substituents characteristic of Ultrinox 626, Irgafos P-EPQ and Doverphos S9228 (compared to Weston 399) makes it slightly more difficult for water to penetrate the tightly packed crystal structure and subsequently less potential to hydrolysing of these phosphites (see chemical structures, section 2.1). Moreover, any partial destruction of Weston 399 through either volatilisation or hydrolysis would lead to a reduction in effective stabilisation of m-LLDPE during multi-pass extrusion. Furthermore, non-termination of the propagating radicals ( $ROO\bullet$  and  $RO\bullet$ ), which can occur *via* oxidation reactions of the Weston 399 with those radicals (see reaction 4.11, in chapter 4) may result in rapid consumption of 3 arylbenzofuran-2-one. This may also be responsible for the more pronounced yellowing of the polymer stabilised with Irganox HP136:Weston 399 AO system (s37) with increasing processing severity (see figure 5.37).

Reaction scheme 5.4 shows a proposed mechanism for the possible transformations and interactions between 3 arylbenzofuran-2-one, Irganox HP136 and the phosphite, Ultrinox 626 (representative of blends and other sterically hindered aryl phosphites). As an effective CB-D antioxidant, the lactone is able to react with alkyl and alkyperoxyl radicals to give the highly stable arylbenzofuran-2-one radical and hydroperoxides (see reaction 1a-b in scheme 5.4) [79]. The stabilised arylbenzofuran-2-one radical, formed as consequence of the CB-D/CB-A activity of Irganox HP136, may either readily dimerise or react further with other alkyperoxyl or alkyl free radicals (see reactions 2 and 3 in scheme 5.5) [78]. The synergistic action of the aryl hindered aromatic phosphite, Ultrinox 626 with hindered phenols was discussed in the literature [111]. By virtue of its PD activity the phosphites will deactivate effectively hydroperoxides thereby leading to the formation of a phosphate and alcohol (see reaction 2 in scheme 5.4). The additional CB activity of Ultrinox 626 may also lead to trapping of alkyl peroxy and alkoxy radicals, resulting in the formation of a hindered phenoxy radical, IA (see reactions 3-5 in scheme 5.4). Further, reactions of IA can lead to the formation of 3A, which via C-C coupling forms a hindered dimer (see reaction 6 in scheme 5.4). There is evidence in the literature for the formation of this dimer in the  $\alpha$ -tocopherol:Ultrinox 626 AO system [121]. The dimer may be able to regenerate the parent hindered phenol, 3 arylbenzofuran-2-one *via* a redox reaction (see reaction 7 in scheme 5.4). This co-operative antioxidant action of the lactone and phosphite may be responsible, at least in part, for the observed high extents of melt stability of m-LLDPE under multiple extrusion conditions. Colour suppression reactions between Ultrinox 626 and the coloured transformation products formed from Irganox 1076 lead to the formation of colourless products (see reaction 1.40-1.42, chapter 1). By analogy, reactions between the phosphite Ultrinox 626 and coloured 3 arylbenzofuran-2-one products formed during high temperature processing could possibly result in colourless products (see reaction 7 in scheme 5.4).



Scheme 5.4 Co-operative interactions between 3-Aryl benzofuranone (Irganox HP136) and Ultranox 626 under melt processing conditions



Scheme 5.5 CB-A activity of 3 Arylbenzofuranone (Irganox HP136) under melt processing conditions [78].

### 5.3.3 Effect of Three Antioxidant Combinations on the melt and colour stabilisation of m-LLDPE during multiple extrusion at 260°C at 100rpm.

#### a. Effect of Phosphites on blends containing Irganox 1076 and Irganox HP136.

Examining the effect of concentration of Irganox 1076 in blends containing Irganox 1076:Weston 399:Irganox HP136 has clearly shown the advantage of using higher concentrations of the hindered phenol in the blends, e.g. 1500ppm against 500ppm and higher ratios of Irganox 1076:Weston 399 (e.g. 1:4), see figure 5.39. However, in general, the addition of the lactone to the Irganox

1076:Weston 399 blend results in increasing yellowing of the polymer (see figure 5.40). Based on this finding, the effect of various phosphites on the melt and colour stability of m-LLDPE were examined in blends based on Irganox 1076:phosphite:Irganox HP136, where the concentration of Irganox 1076 used was high (generally over 1000ppm) and the ratio of phenol:lactone:phosphite was kept at 1:2.3:3.3 %w/w with all the phosphites compared at the same phosphorus content concentration of 0.06%.

Figure 5.39 shows clearly that neither the presence nor the nature of phosphite used seem to have any significant effect on the excellent performance of these blends (when compared with sample s24 which has no phosphite). This may be attributed to the effective synergistic effect between Irganox 1076 and lactone Irganox HP136 when used at these concentration ratios, even without the phosphite, due to their complementary AO mechanism of action, i.e. CB-D/CB-A/PD. Indeed the commercial AO blend XP-60 (Irganox 1076:Ultranox 626, weight ratio of 1:2.3 %w/w respectively) examined in this work has been shown in the literature to offer excellent stability performance in polyolefins [70, 79,78,80,109,115].

The high effectiveness of blends based on similar AO combinations has also been referred to by others. [70,81]. Horton *et. al.* have recently reported [81] that the addition of a XP system (containing Irganox 1010:Irganox HP136:Irgafos 168 in a w/w ratio of 3:1:3) to polypropylene film, leads to high levels of melt flow control, optical clarity, increased processing times, good control of film profile, improved orientation and a wider processing window during multiple extrusion. Kenny [80] has also reported that high levels of melt flow and colour stabilisation in film grade LLDPE may be achieved by the addition of XP-490 (Irganox 1076:Irganox HP136:Irgafos P-EPQ in a w/w ratio of 3:1:2.3) when compared with a traditional formulation containing Irganox 1076/Irgafos P-EPQ system. It was shown that although both the total concentration of the XP system is 33% and the phosphite concentration of the XP system is 66% is less than the traditional formulation, the melt flow and colour performance was reported to be equivalent to that of the traditional formulation [80].

The cost effectiveness of each of the stabiliser packages examined above revealed that the Irganox 1076:HP136:Ultranox 626 (s40) which produced excellent levels of melt and colour stability with increasing extrusion severity had the lowest price.



**b. Effect of Hydroxylamine and Lactone blends containing Hindered Phenols; Irganox E201 or Irganox 1076, and phosphites in the presence or absence of hindered amine stabilisers.**

Horsey [82], Nesvadaba *et. al.* [78] and Zweifel [115] have claimed that hydroxylamines operate effectively in conditions where alkyl radicals,  $R\bullet$ , are present in a system in high concentrations (see section 1.5.5, chapter 1). It is thought that the chemistry of the hydroxylamine is not too different from that of the more traditional hindered amine light stabilisers (R-HALS) [115]. They are thought to operate *via* a CB-A mechanism thereby producing a nitron radical which is able to trap further alkyl radicals (see figures 1.14&1.15, chapter 1). It has also been reported that hydroxylamines readily decompose peroxides, ROOH (considered to be the main source of initiating radicals), see figure 1.16, chapter 1 [78, 82,115].

However, figure 5.45 shows that the addition of varying concentrations of the hydroxylamine Irgastab FS042 to a m-LLDPE polymer containing a blend of Vitamin E:Ultranox 626 at 1:2 %w/w ratio respectively (with TMP) does not have any effect on the melt stability of the polymer, but the presence of the hydroxylamine does contribute to reducing the colour stability of this polymer (increasing yellowing, see figure 5.47). Similarly, the addition of varying concentrations of hydroxylamine to a polymer containing an Irganox 1076:Weston 399 blend has no major effect on the melt stability (slight improvement) but again the presence of the hydroxylamine in the blend does increase the extent of polymer discolouration, see figures 5.48 & 5.50. It was shown earlier that the melt stabilising effectiveness of the hydroxylamine (used alone) at 1000ppm in m-LLDPE (see chapter 4, see figure 4.8) is considerably lower than that of either of the hindered phenols (concentrations of 300-500ppm) or the lactone (300ppm) (when each is used separately). This would suggest that even at more than double the concentration, the chain breaking (CB) AO activity of the hydroxylamine (under the experimental conditions used here) is lower than the CB activity of the hindered phenols and that of the lactone.

However, and in contrast to the minimal effect on melt stability, the presence of the phosphite in these blends gives rise to a significant improvement in the colour stability of the polymer. Amongst the various phosphites examined here, the hindered aryl phosphite PEP-Q gives the lowest extent of yellowing (s39) whereas the unhindered phosphite Weston 399 (s42) gave the highest discolouration to the polymer, see figure 5.43. The high extent of yellowing imparted by the blend

containing Weston 399 (s42) may partly be due to the fact that in order to keep the ratio and phosphorous content constant, the actual amount (ppm concentration) of the AOs used in this blend is much higher than in the other blends and this can be expected to give higher concentrations of the coloured transformation products contributing to yellowing of the polymer. Some suggestions have been forwarded earlier (see section 4.3.2 in chapter 4) for the reasons of the lower effectiveness of the hydroxylamine; this may be due to their aliphatic non-sterically hindered hydroxylamine functions (as hindered hydroxylamines have been shown in the literature to be very highly effective melt stabilisers in polyolefins) [113] and also possibly due to the production of the initiating radicals (mainly alkyl, R•, radicals) during their reaction with hydroperoxides (ROOH) which are formed during their AO function, see reactions 4.5 and 4.6 (see chapter 4). The very high effectiveness of the powerful synergistic AO blends based on Irganox E201:Ultranox 626 (s11) and Irganox 1076:Weston 399 (s4) means that the addition of the hydroxylamine as a third AO does neither improve nor deteriorate the stabilising effect of the blends as shown in figures 5.45 & 5.48. Why the hydroxylamine imparts more colour to the polymer both when used singly or in combination with other AOs is more difficult to explain without further evidence.

The effect of the lactone Irganox HP136 on the melt stabilising performance of AO blends containing Irganox E201 and different phosphites (compared at the same phosphorus content of 0.6%) is minimal, see figure 5.51. Again, this is most likely due to the already highly powerful stabilising performance of the Irganox E201:Phosphite blends where there is almost no change in the melt flow characteristics of the polymer even after 5 extrusion passes at 260°C.

However, the presence of the lactone in a blend of Irganox E201:Ultranox 626 (s44) does seem to improve the colour stability of the polymer compared to the performance of the same blend but which does not contain the lactone (s11), see figure 5.54b. In the absence of any evidence, a possible suggestion for the reduction in extent of discolouration is *via* additional reactions of the lactone with some of the discolouring transformation products of Vitamin E, thus reducing their concentration and their adverse effect on yellowing or/and possible reactions with traces of transition metal ions to prevent the formation of coloured phenoxyl complexes.

Although the different phosphites in blends of Irganox HP136:Irganox E201:Phosphite (1:(0.5-1):2.3 %w/w ratio respectively) have no effect on their melt stability performance, they do affect

the colour stability of the polymer to varying extents, with Weston 399 giving the highest extent of discolouration (see figure 5.54c, s48). It is important to point out here that in order to keep the phosphorus content in all phosphites constant, higher weight concentrations of Weston 399 had to be used (1330ppm) compared to other phosphites examined (600-1000ppm) and this may also have an effect on colour as this non-hindered aryl phosphite is hydrolytically unstable.

The addition of a very small concentration of ZnSt to blends of Irganox HP136: Irganox E201:Weston 399 (s48) leads to an improvement in the colour stability of the m-LLDPE (figure 5.53d) without any significant effect on its melt stability (figures 5.53) during multiple extrusion. Kresta *et. al.* [122] and Pospisil [88] showed that a small concentration of metallic ion residue from a Ziegler-Natta catalysed polymerisation stage of a polymer has a drastic effect on the colour, antioxidant efficiency and basicity of a system. Under high processing temperatures ( $>250^{\circ}\text{C}$ ) thermal de-alkylation of hindered phenols readily occurs in positions 2 and 6, residues of polymerisation catalysts remaining in the polymer react at these sites thereby lowering effective stabilisation of phenols and increasing the discolouration of the polymer by the formation of metal phenolates [88]. Kresta and Majer [122] reported that a reaction of metallic ions with a PP polymer melt leads to the generation of hydrogen chloride which owing to its diffusion mobility is able to interact with more phenolic antioxidant molecules thereby catalysing dealkylation reactions. It is important to mention here that the manufacturer of the metallocene LLDPE polymer stated that the polymer used throughout this investigation was polymerised in the absence of chlorine. However, one can suggest that the hydrolysis of a hydrolysable phosphite such as Weston 399 (see reactions 1.37-1.39, chapter 1) may lead to the formation of a phosphorus acid, which may catalyse de-alkylation of the parent hindered phenols. This would explain why ZnSt does not appear to have a positive effect on colour suppression (with increasing processing severity) when used in combination with a the more hydrolytically stable phosphite Ultrinox 626 (see figure 5.53a, s44). Hence the effective colour suppression by the ZnSt when used in combination with Irganox HP136: Irganox E201 and Weston 399 (s48) may be explained by the preferential reaction of metallic ion residues with ZnSt giving stable colourless products at the expense of coloured metal ion phenolates and efficient neutralisation of phosphorus acids.

Compared to the polyhydric alcohol, TMP, which is also known to react with metal ions and prevent the formation of the highly coloured phenolate-metal complexes [111,121], the use of ZnSt.

with AO blends containing Irganox E201:Ultranox 626 (s49) gives rise to higher extent of yellowing to m-LLDPE compared to the same blend but containing TMP (s11), see figure 5.56. The ZnSt is most likely unable to reduce the concentration of the highly discolouring transformation products, e.g. aldehyde, formed from Vitamin E during extrusion in the same way as does the polyhydric alcohol TMP as was shown previously [121].

#### **5.3.4 Effect of Four Antioxidant Combinations on the melt and colour stability of m-LLDPE during multiple extrusion at 260°C/100rpm.**

##### **5.3.4.1 Effect of Hindered Amine stabilisers (HAS) on blends of hydroxylamine, Irganox 1076 and Weston 399.**

The addition of various HAS examined here does not seem to have any significant effect on the melt stabilising performance in m-LLDPE containing Irganox 1076:Irgastab FS042:Weston 399 (the HAS Tinuvin 765 gives a slightly lowering performance), see figure 5.58. However, all the HAS give rise to improvement in the colour stability of the polymer with Tinuvin 765 giving the highest improvement as shown in figure 5.59.

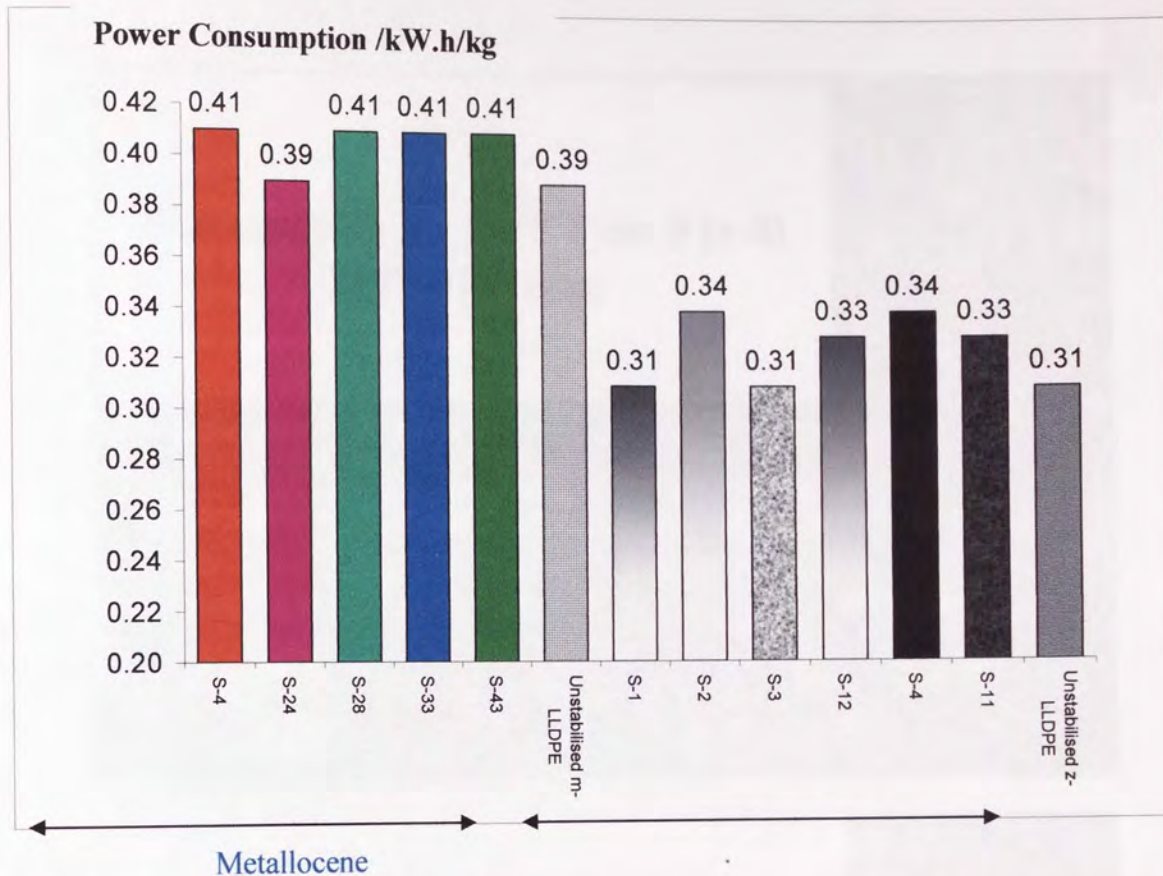
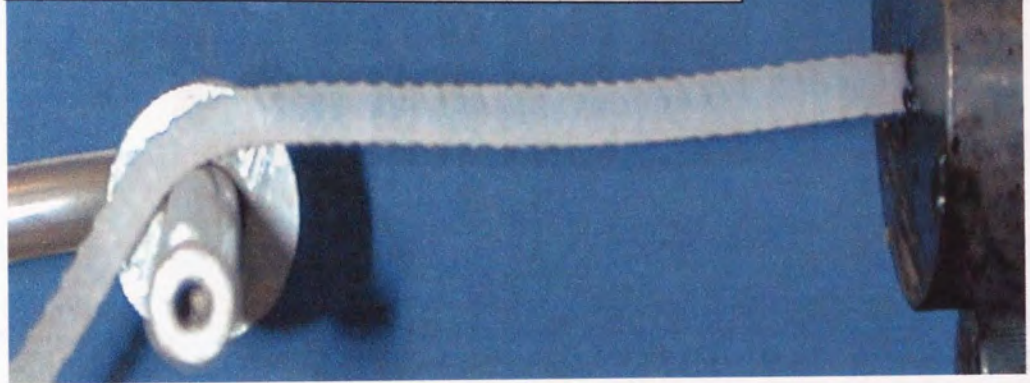


Figure 5.1. Change in Power consumption during twin screw extrusion of stabilised m-LLDPE ( $P_o$ , formulation numbers s4 to s43, see tables 5.1-5.2) and z-LLDPE ( $P_o$ , formulation numbers s1 to s12, see tables 5.1-5.2). Changes in unstabilised polymers extruded (atmospheric conditions, 210°C, 100rpm,  $P_1$ ) under similar conditions are shown for comparison.



**Stabilised m-LLDPE Pass 0 (s-4)**  
**210°C/100rpm**



**Stabilised z-LLDPE Pass 0 (s-4)**  
**210°C/100rpm**



Figure 5.2 Effect of processing of stabilised polymers on the appearance of the extruded laces (4mm die) of m-LLDPE and z-LLDPE polymers extruded under the same conditions (using formulation s-4, see table 5.1). Clear melt fracture is shown in the case of the metallocene polymer.



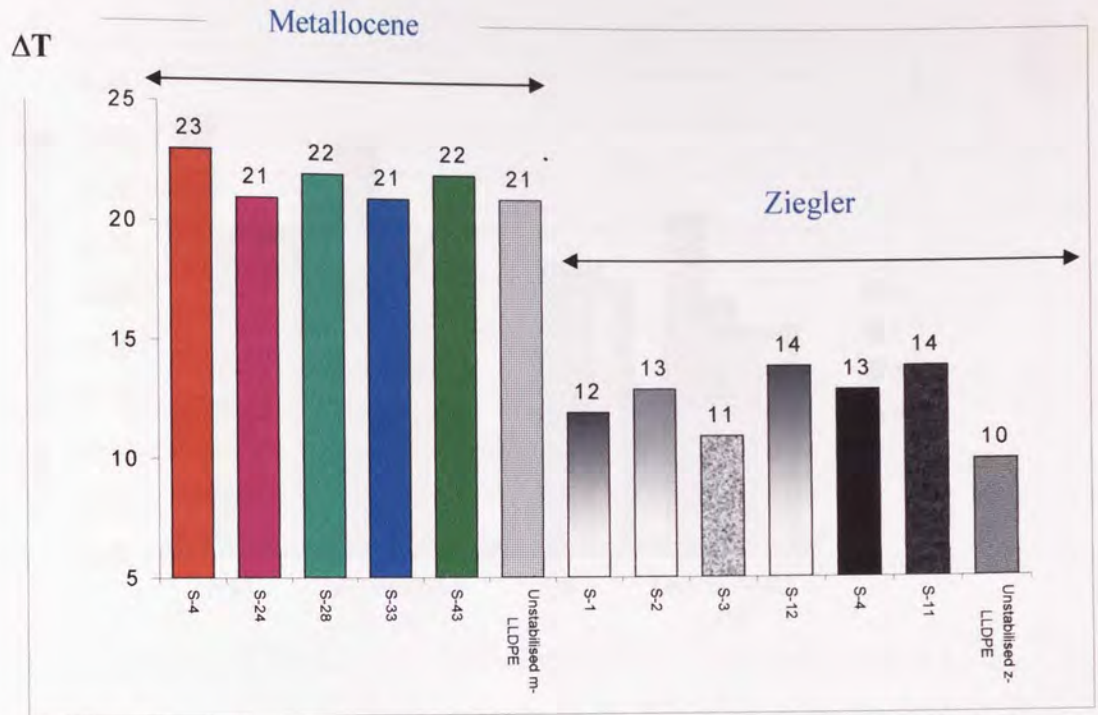


Figure 5.3: A comparison of  $\Delta T$  during twin screw extrusion of stabilised m-LLDPE (s4 to s43, see tables 5.1-5.2) and z-LLDPE (s1 to s12, see tables 5.1-5.2). Changes in unstabilised polymers extruded (atmospheric conditions, 210°C, 100rpm,  $P_1$ ) under similar conditions are shown for comparison.

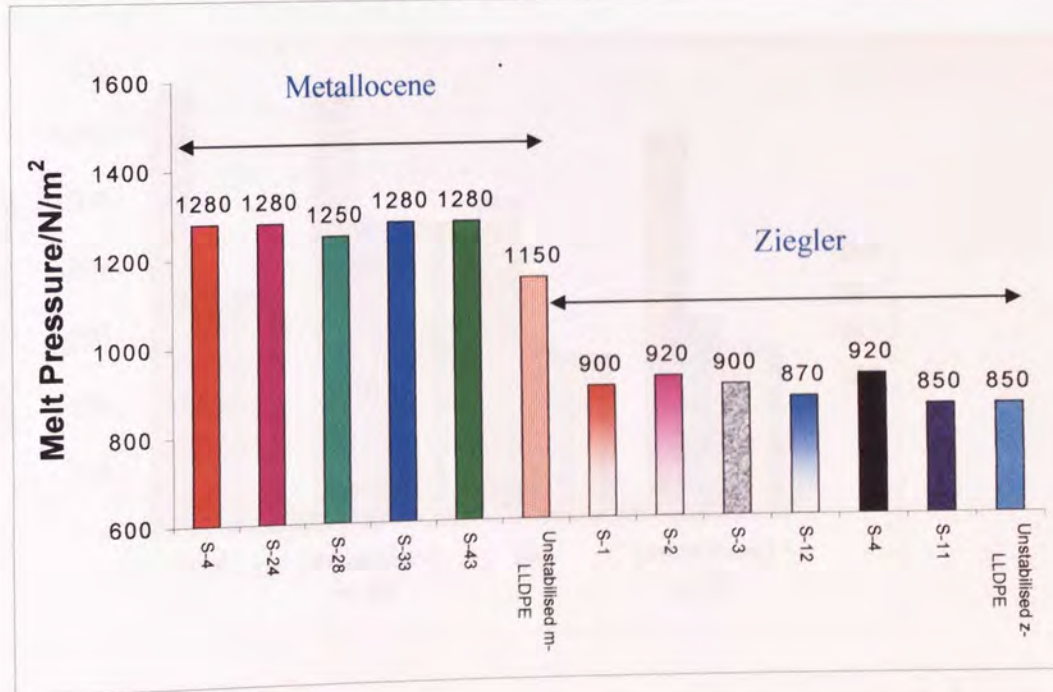


Figure 5.4: Changes in melt pressure during of stabilised m-LLDPE (s4 to s43, see tables 5.1-5.2) and z-LLDPE (s1 to s12, see tables 5.1-5.2). Changes in unstabilised polymers extruded (atmospheric conditions, 210°C, 100rpm,  $P_1$ ) under similar conditions are shown for comparison.

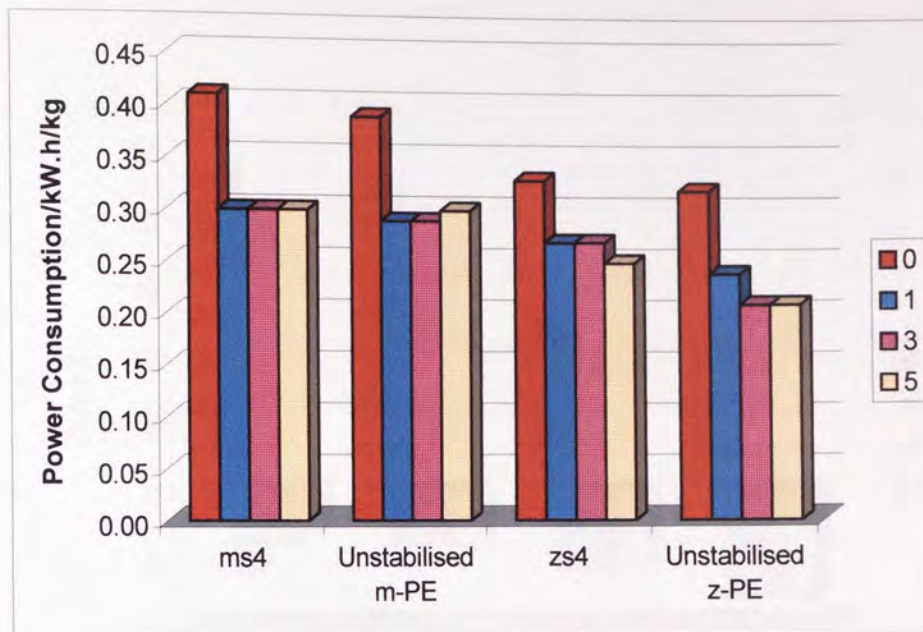


Figure 5.5. Changes in power consumption of stabilised (Po, formulation S-4, see table m-LLDPE and z-LLDPE during multi-pass extrusion; Passes 1,3 and 5 (285°C, 50rpm under atmospheric conditions). Unstabilised multi-pass extruded m-LLDPE and z-LLDPE samples are shown for comparison.

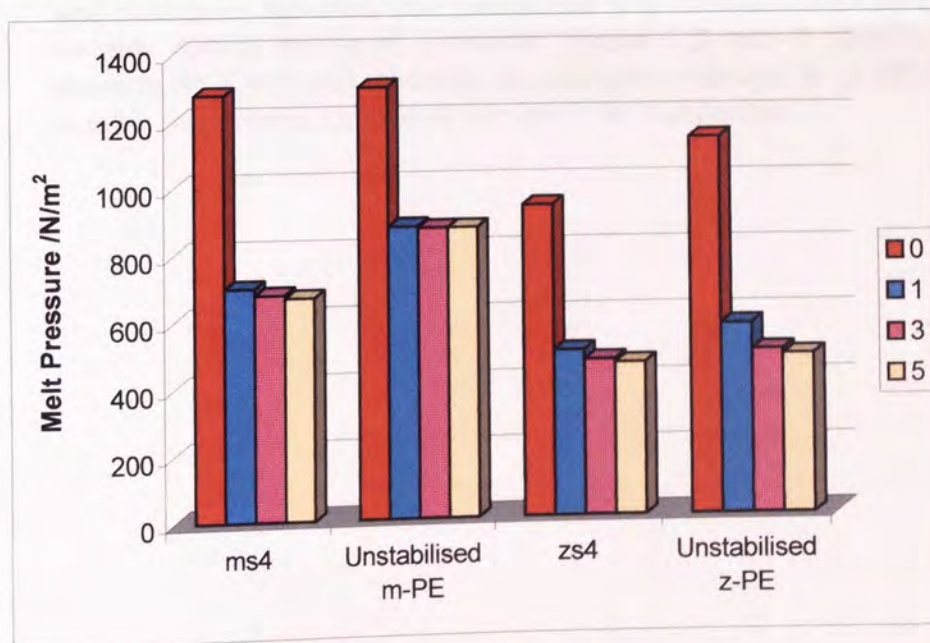


Figure 5.6 Changes in melt pressure of stabilised (Po, formulation S-4, see table 5.1, nitrogen) m-LLDPE and z-LLDPE during multi-pass extrusion; Passes 1,3 and 5 (285°C, 50rpm under atmospheric conditions). Unstabilised multipass extruded m-LLDPE and z-LLDPE samples (using same conditions) are shown for comparison.



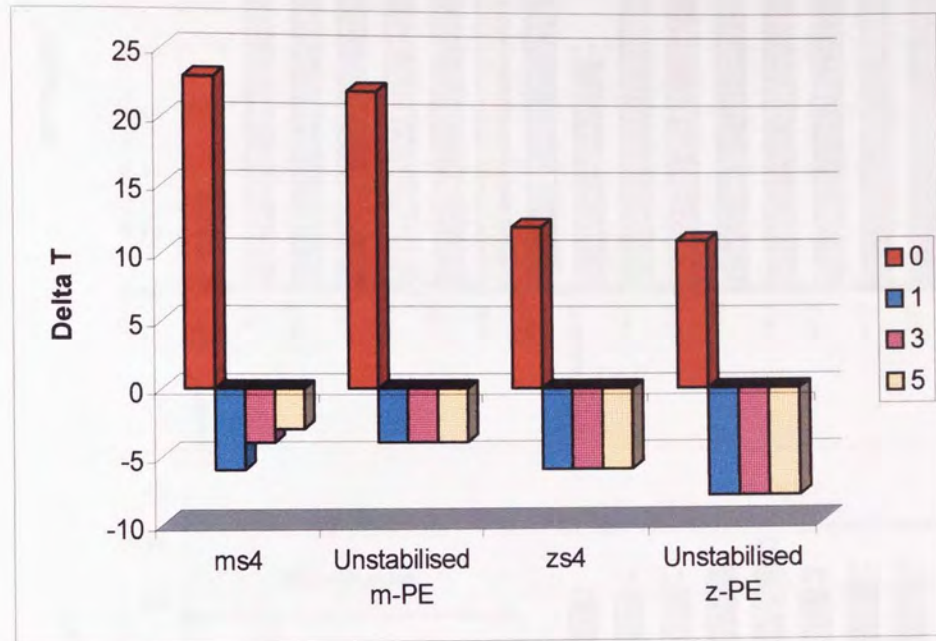


Figure 5.7 Changes in  $\Delta T$  (difference between the die and actual melt temperature) of stabilised (Po, formulation S-4, nitrogen) m-LLDPE and z-LLDPE samples during multi-pass extrusion; Passes 1,3 and 5 (285°C, 50rpm under atmospheric conditions). Unstabilised multipass extruded m-LLDPE and z-LLDPE samples (using same conditions) are shown for comparison.

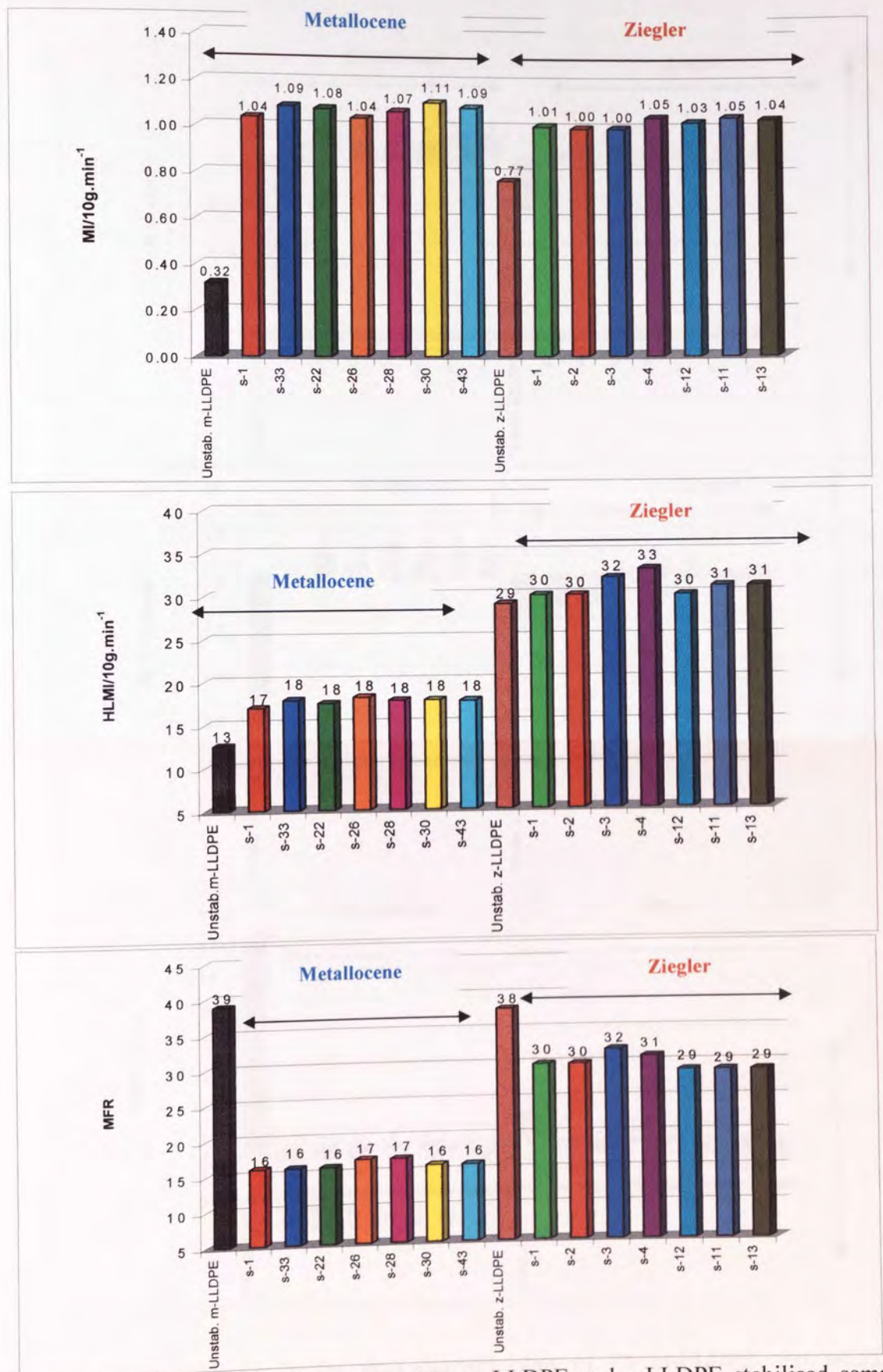


Figure 5.8 The melt characteristics of Po m-LLDPE and z-LLDPE stabilised samples (see tables 5.1 & 5.2). Unstabilised m-LLDPE and z-LLDPE polymers extruded once (P1) are shown for comparison.



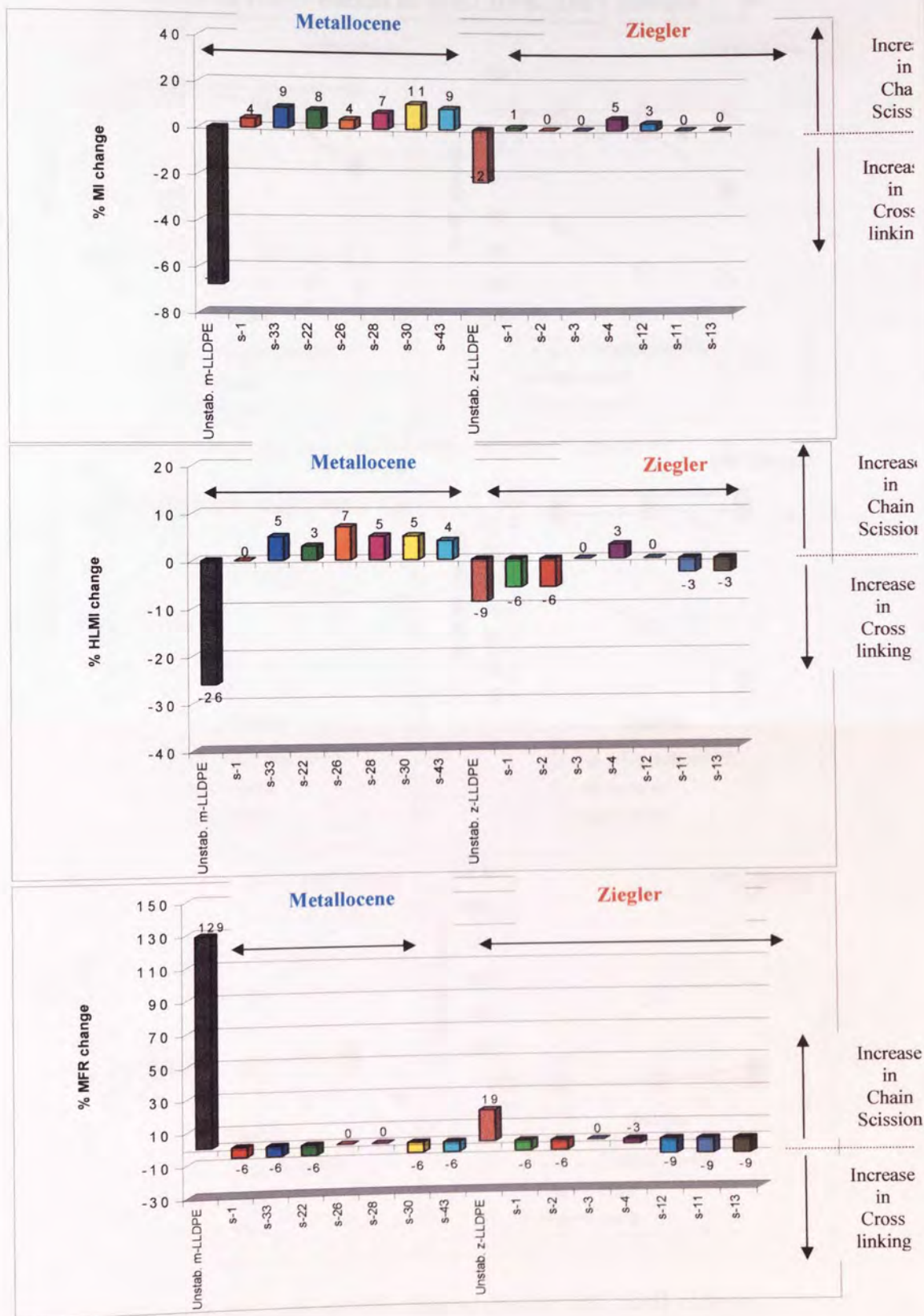


Figure 5.9 % Changes in the melt characteristics of Po m-LLDPE and z-LLDPE stabilised samples (see tables 5.1 & 5.2). Unstabilised m-LLDPE and z-LLDPE polymers extruded once (P1) are shown for comparison.

Irg.1076:W.399 Blends in m-LLDPE; 210°C/50rpm

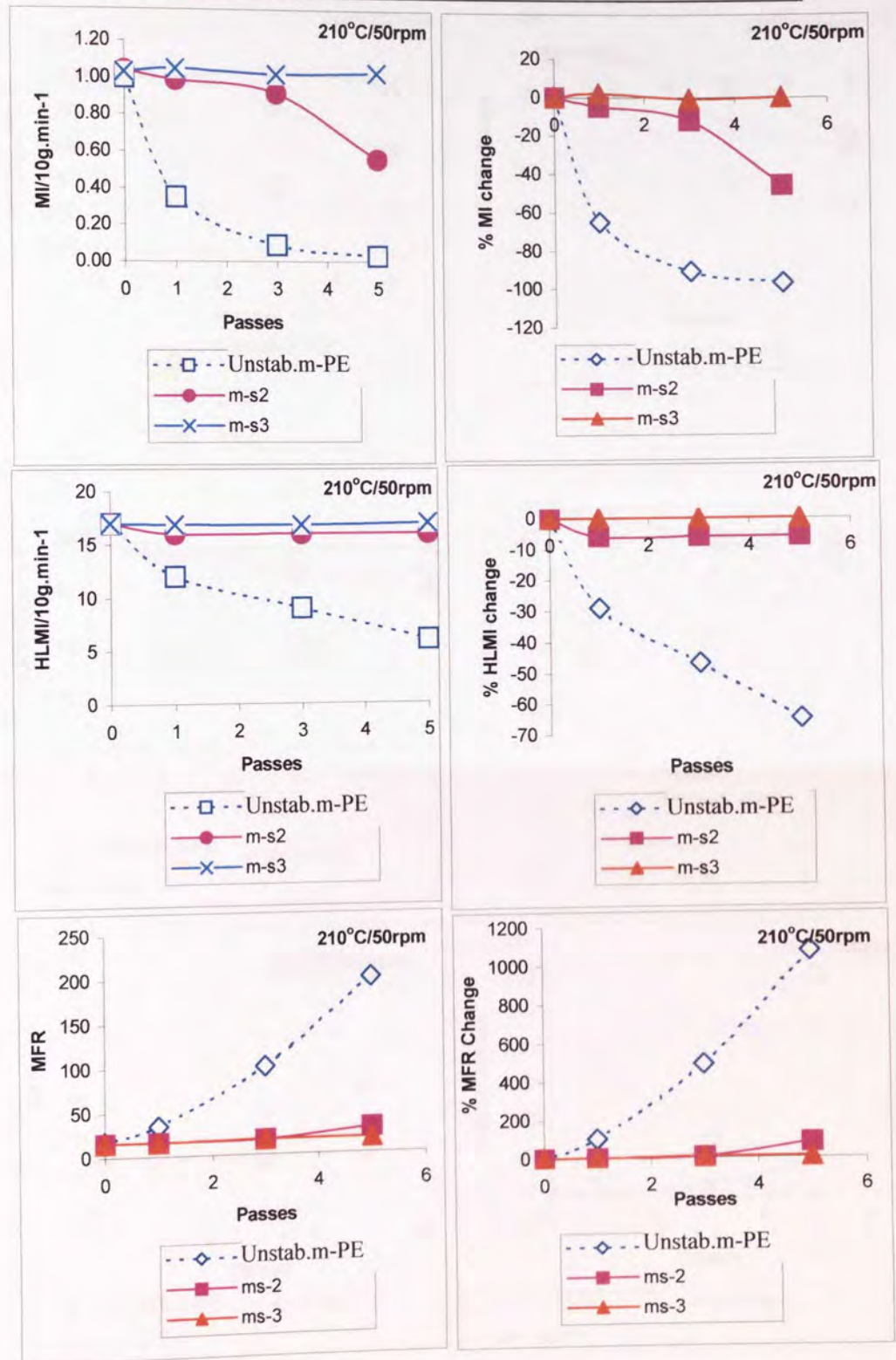


Figure 5.10. Effect of on the melt stability characteristics; MI, %MI change, HLMI, % HLMI change, MFR and %MFR change of stabilised m-LLDPE polymer samples; using Synthetic hindered Phenol/Phosphite combinations (see s2 and s3 in table 5.1); during multi-pass extrusion at 210°C/50rpm (P1, P3 and P5 under atmospheric conditions). Unstabilised m-LLDPE polymers processed under the same conditions are shown here for comparison.



**Irg.1076:W.399 Blends in z-LLDPE; 210°C/50rpm**

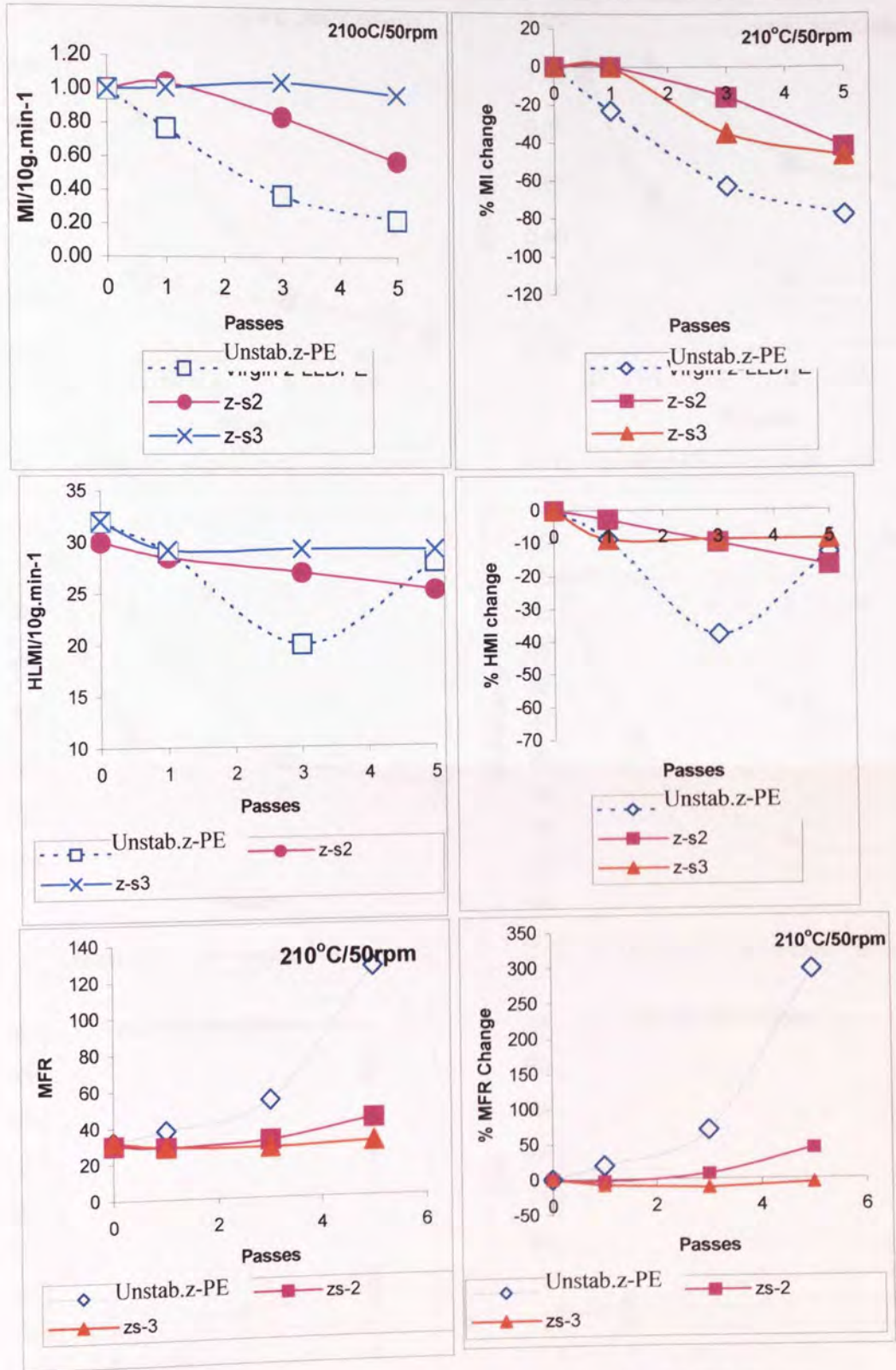


Figure 5.11. Effect of on the melt stability characteristics; MI, %MI change, HLM, % HLM change, MFR and %MFR change of stabilised **z-LLDPE polymer samples**; using Synthetic hindered Phenol/Phosphite combinations (see s2 and s3 in table 5.1); during multi-pass extrusion at **210°C/50rpm** (P1, P3 and P5 under atmospheric conditions). Unstabilised z-LLDPE polymers processed under the same conditions are shown here for comparison.

s2 and s4 in m-LLDPE and z-LLDPE 285°C/50rpm

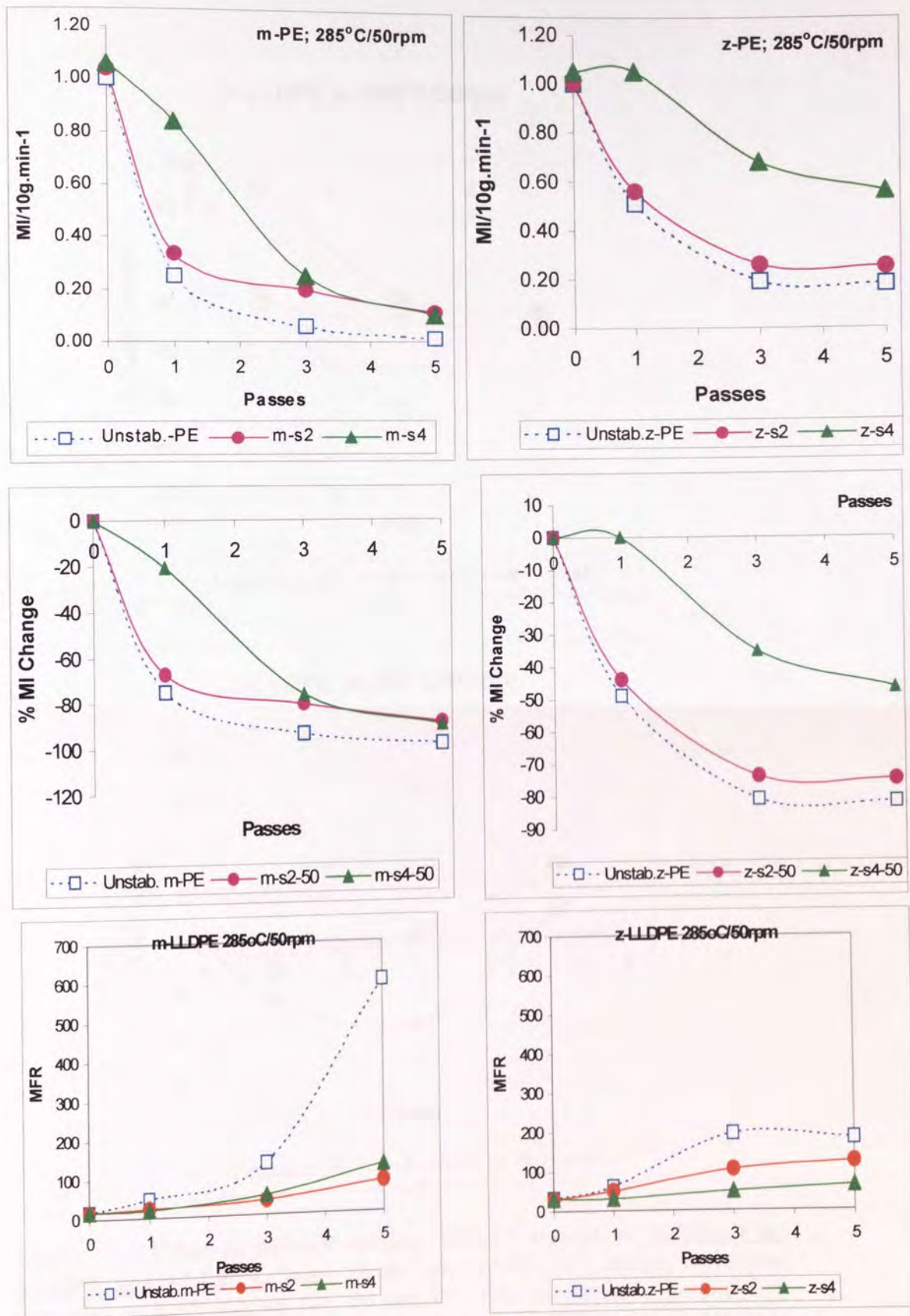


Figure 5.12. Effect of processing severity (P1, P3 and P5); multi-pass extrusion at **285°C/50rpm** on the melt stability characteristics; MI, %MI change and % MFR change; of unstabilised and stabilised **m-LLDPE** and **z-LLDPE** polymer samples containing different combinations of Irganox 1076:Weston 399 blend (see s2 and s4, in table 5.1).



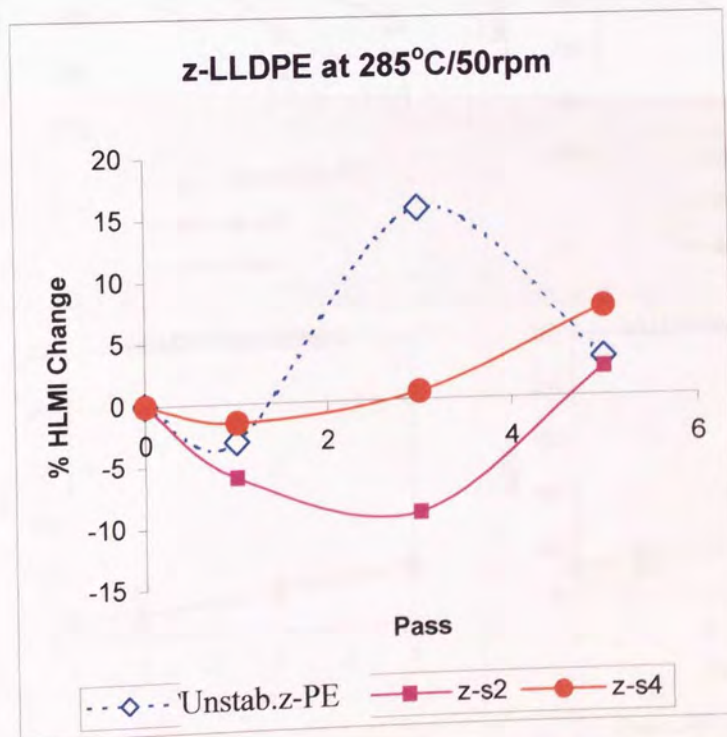
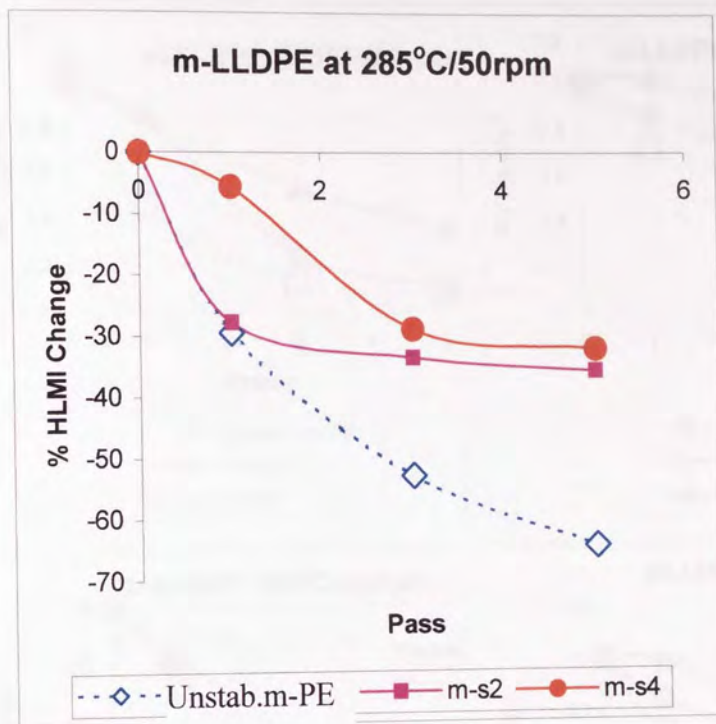


Figure 5.13. Effect on the melt stability, %HLMI change, of **stabilised m-LLDPE and z-LLDPE** (using s2 and s4, in table 5.1) during multi-pass extrusion at **285°C/50rpm** (P1, P3 and P5 under atmospheric conditions). Unstabilised samples processed under the same conditions are shown here for comparison

s2 and s4 in m-LLDPE and z-LLDPE 285°C/200rpm

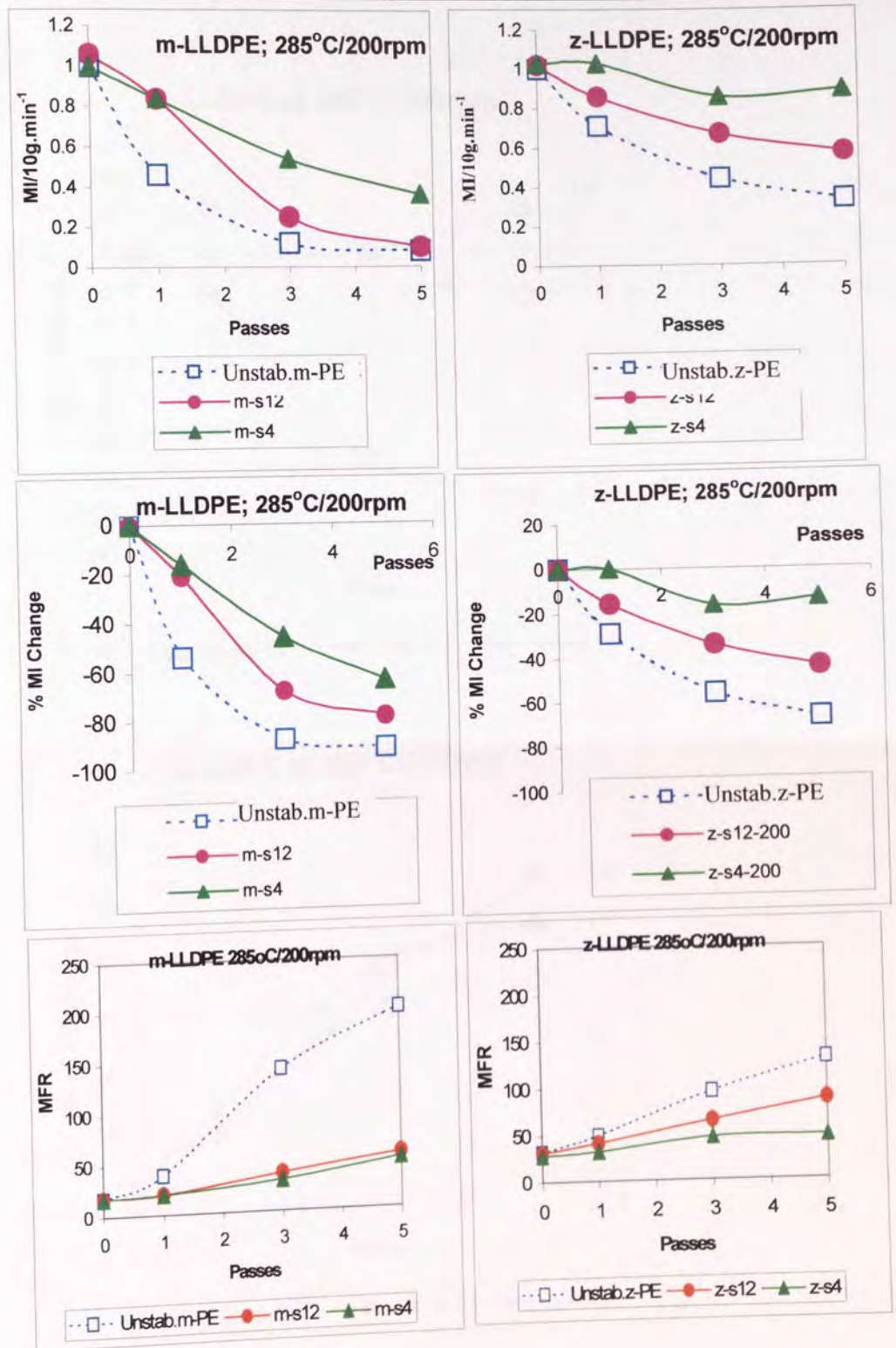


Figure 5.14. Effect of processing severity (P1, P3 and P5); multi-pass extrusion at **285°C/200rpm** on the melt stability characteristics; MI, % MI change and %MFR change of stabilised **m-LLDPE** and **z-LLDPE** polymer samples containing different combinations of a Irganox 1076:Weston 399 AO blend (see s2 and s4 in table 5.1). Unstabilised m-LLDPE and z-LLDPE values are shown here for comparison.



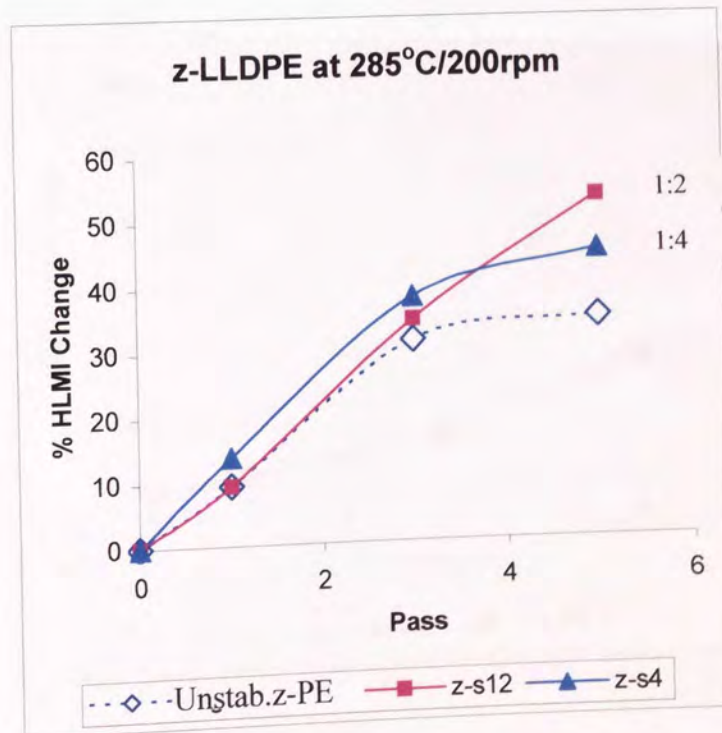
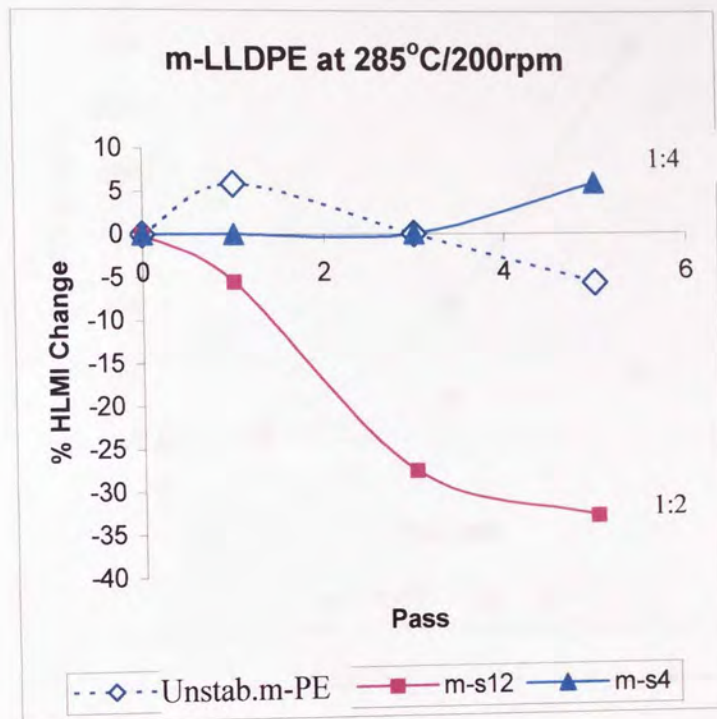


Figure 5.15. Effect on the melt stability, %HLMI change, of **stabilised m-LLDPE and z-LLDPE** (using s2 and s4, in table 5.1) during multi-pass extrusion at **285°C/200rpm** (P1, P3 and P5 under atmospheric conditions). Unstabilised samples processed under the same conditions are shown here for comparison.

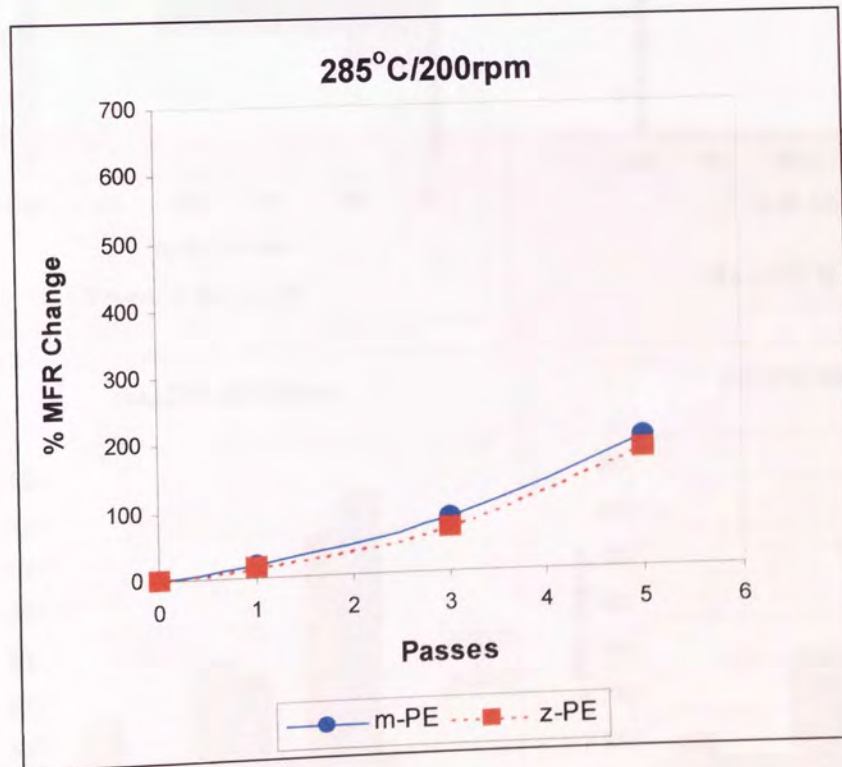
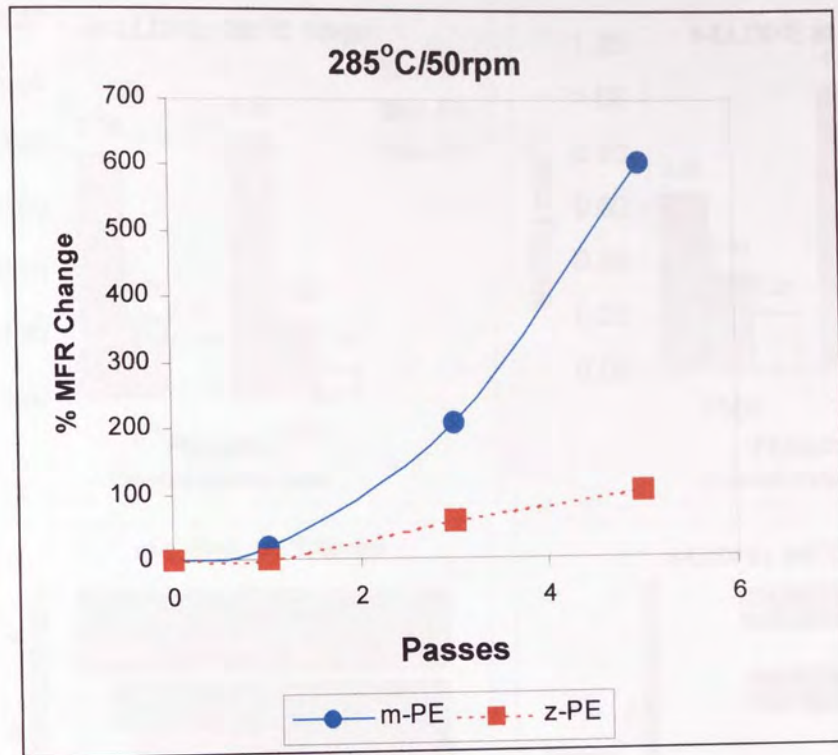


Figure 5.16. Effect on the melt stability, %MFR change, of stabilised m-LLDPE and z-LLDPE (using s4, in table 5.1) during multi-pass extrusion at an extrusion temperature of 285°C and different screw speeds (50-200rpm) (P1, P3 and P5 under atmospheric conditions).



**Effect of W399 Concentration in m-LLDPE and z-LLDPE; 285°C/50rpm**

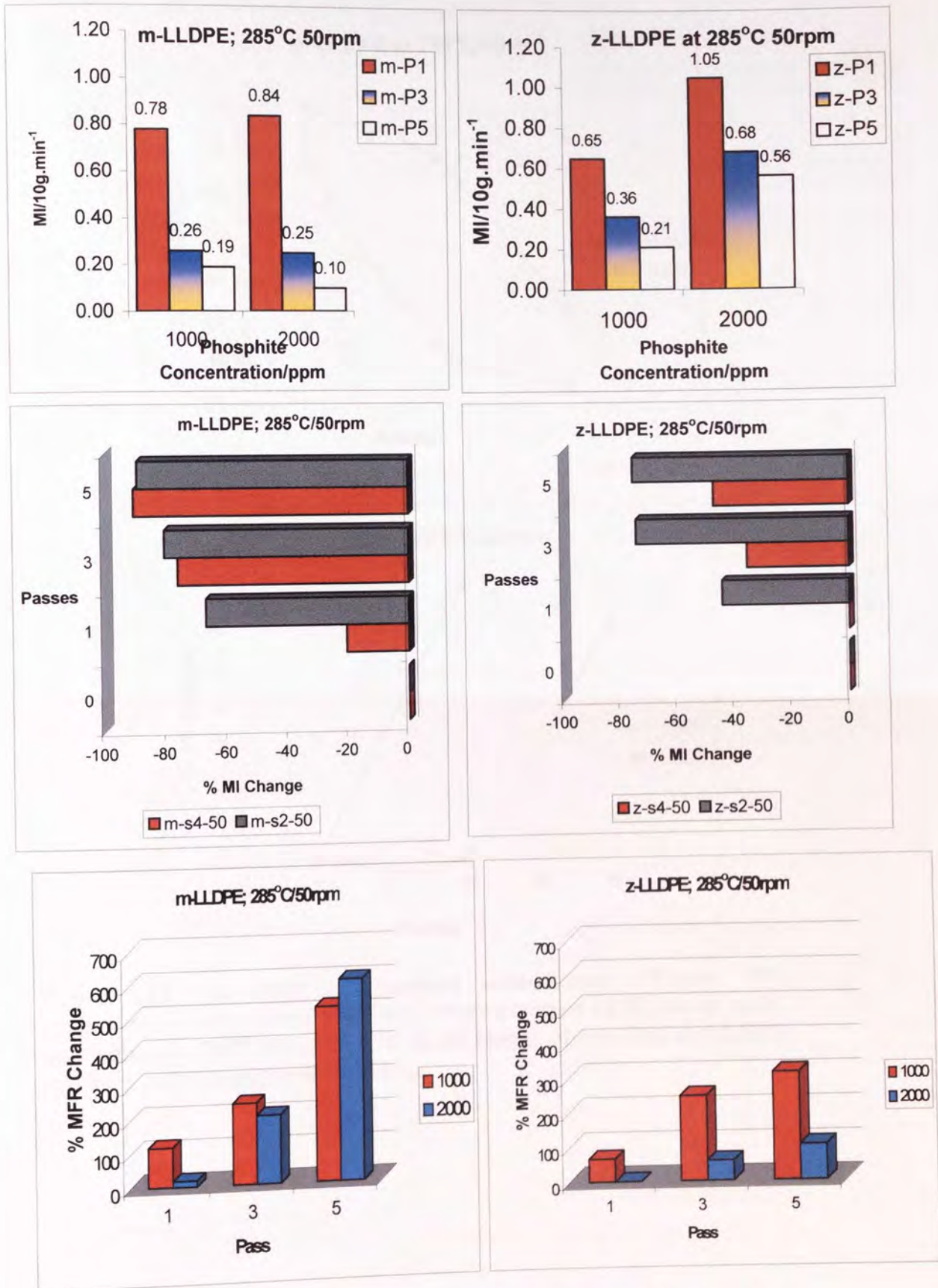


Figure 5.17 The effect of phosphite concentration (Weston 399) during multi-pass concentration (formulations containing 500ppm Irganox 1076) during multi-pass extrusion (285°C/50rpm) on MI, %MI change and % MFR change of stabilised m-LLDPE and z-LLDPE polymers under atmospheric conditions.

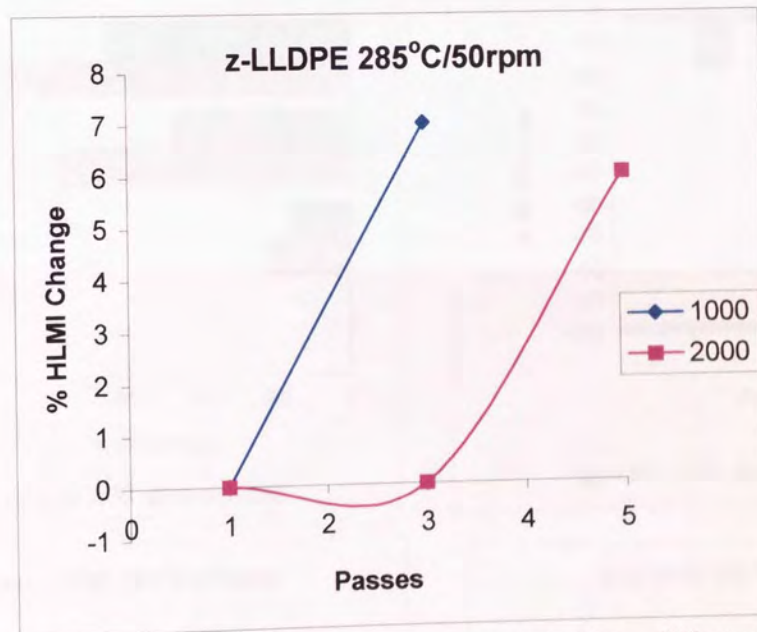
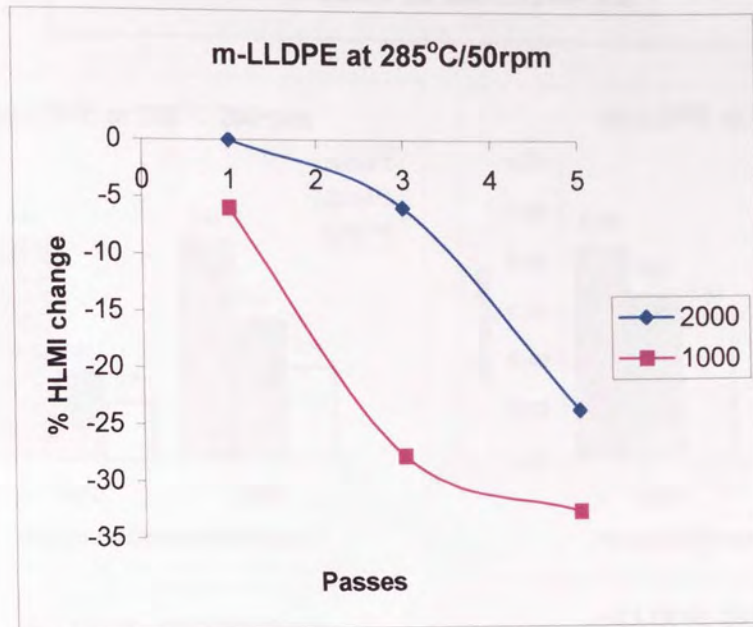


Figure 5.18 The effect of Phosphite concentration (Weston 399) concentration (formulations containing 500ppm Irganox 1076) during multi-pass extrusion (285°C/50rpm) on % HLMI change of stabilised **m-LLDPE** polymers under atmospheric conditions.



## Effect of Weston 399 Concentration in m-LLDPE and z-LLDPE; 285°C/200rpm

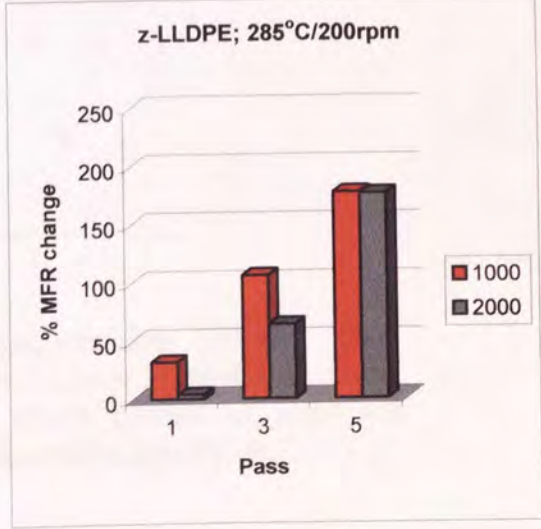
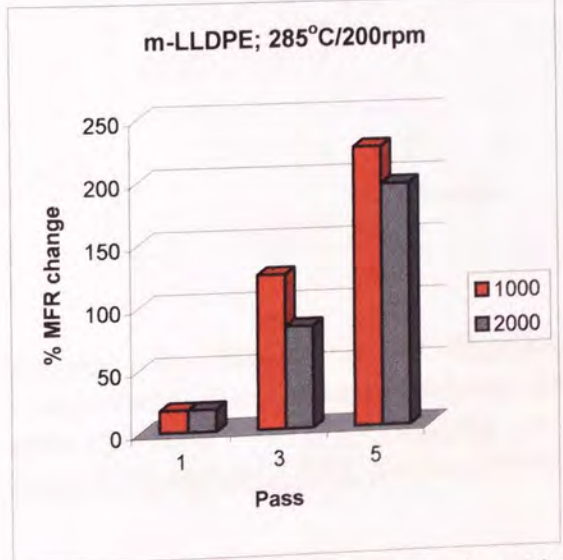
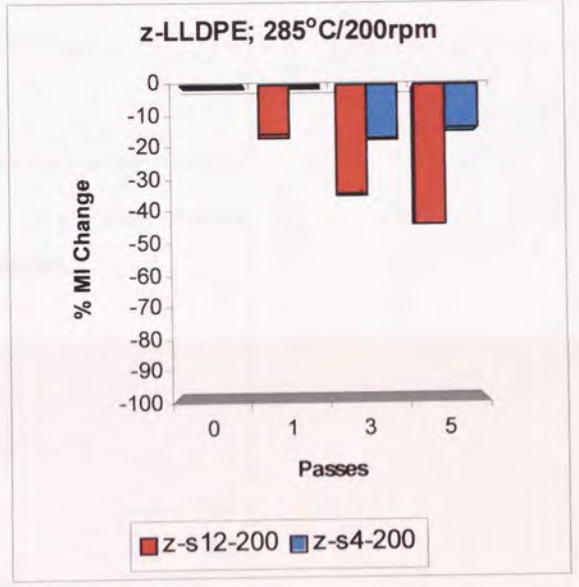
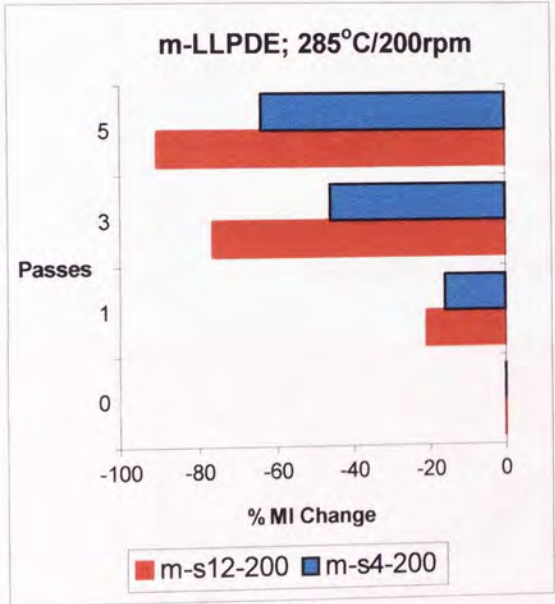
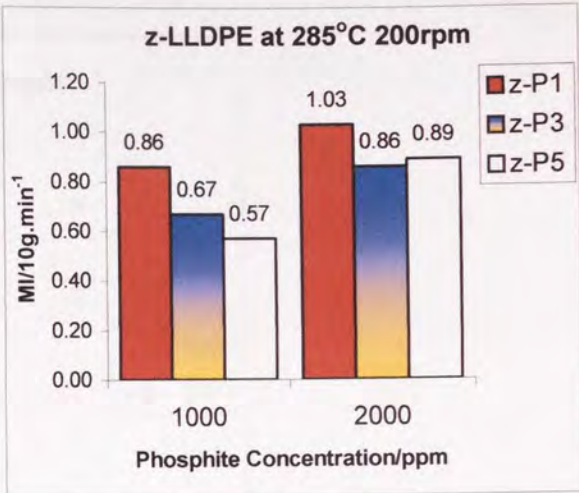
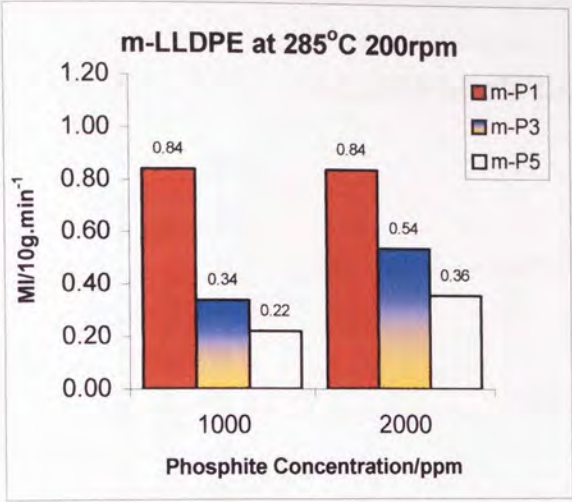


Figure 5.19 The effect of phosphite concentration (Weston 399) concentration (formulations containing 500ppm Irganox 1076) during multi-pass extrusion at **285°C/200rpm** on MI, %MI change and % MFR change of **stabilised m-LLDPE and z-LLDPE** polymers under atmospheric conditions.

Irganox 1076: Weston 399

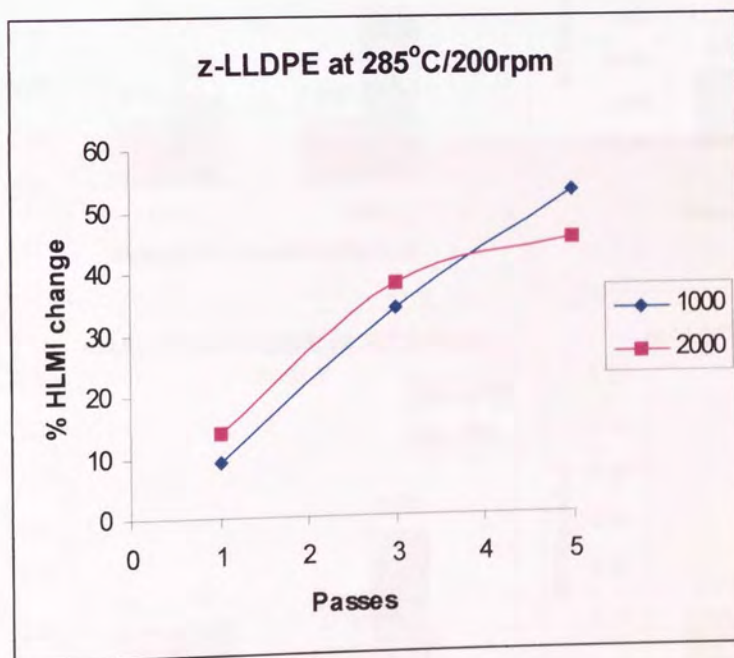
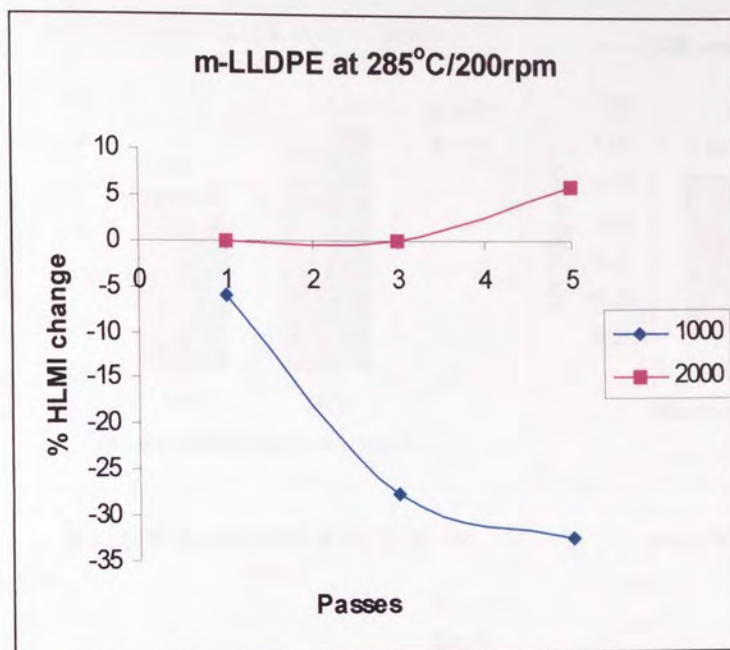


Figure 5.20 The effect of Phosphite concentration (Weston 399) concentration (formulations containing 500ppm Irganox 1076) during multi-pass extrusion at 285°C/200rpm on % HLMI change of stabilised m-LLDPE and z-LLDPE polymers under atmospheric conditions.



**Effect of Weston 399 Concentration in m-LLDPE and z-LLDPE; 285°C/50-200rpm for PASSES 1, 3 and 5**

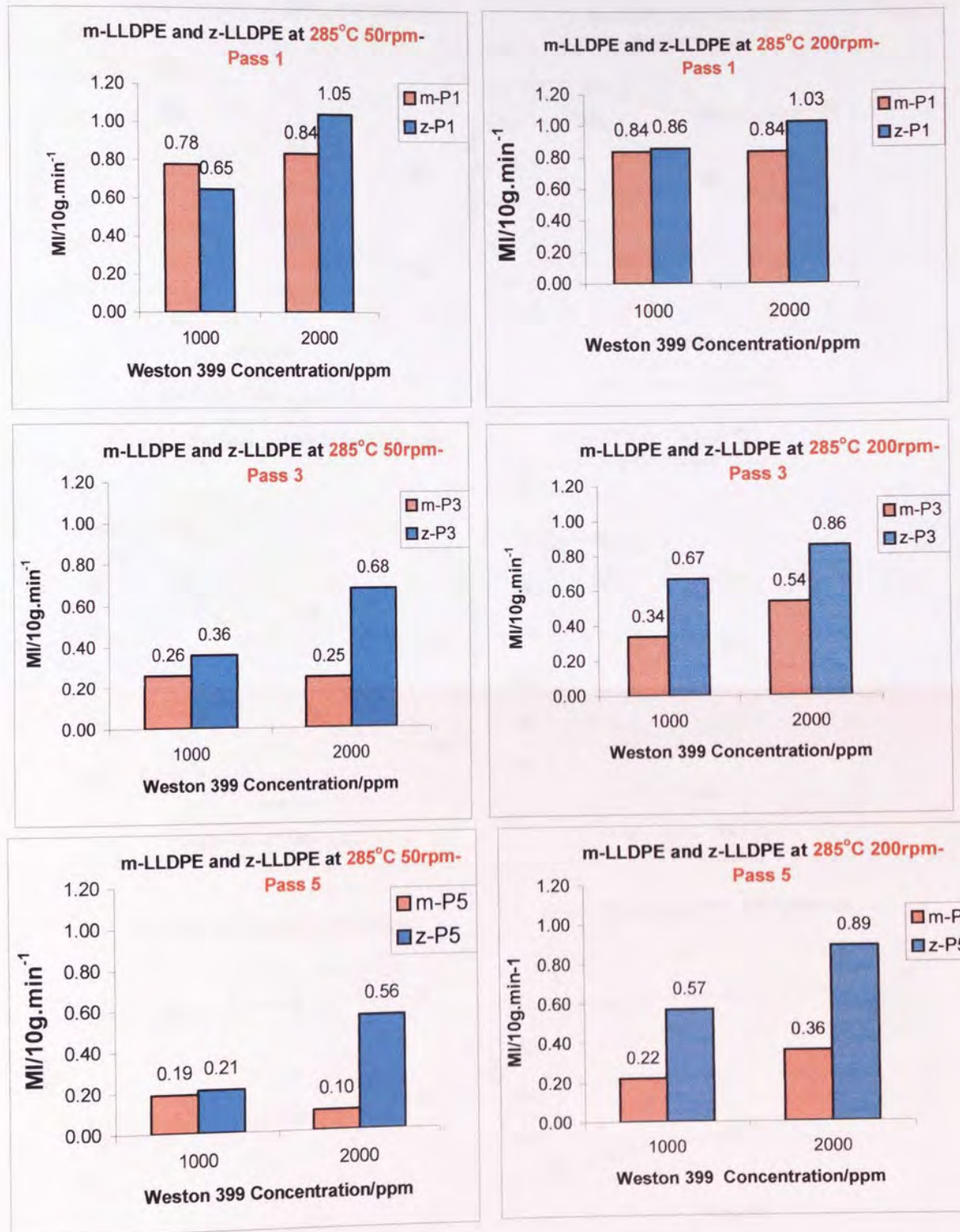


Figure 5.21 Compares the effect on melt stability, MI, of increasing Weston 399 concentrations (fixed Irganox [1076] of 500ppm on each successive pass (1, 3 and 5) during multi-pass extrusion at 285°C at 50 and 200rpm under atmospheric conditions of stabilised m-LLDPE and z-LLDPE polymer samples.

**s4 in m-LLDPE and z-LLDPE;  
285°C/50-200rpm**

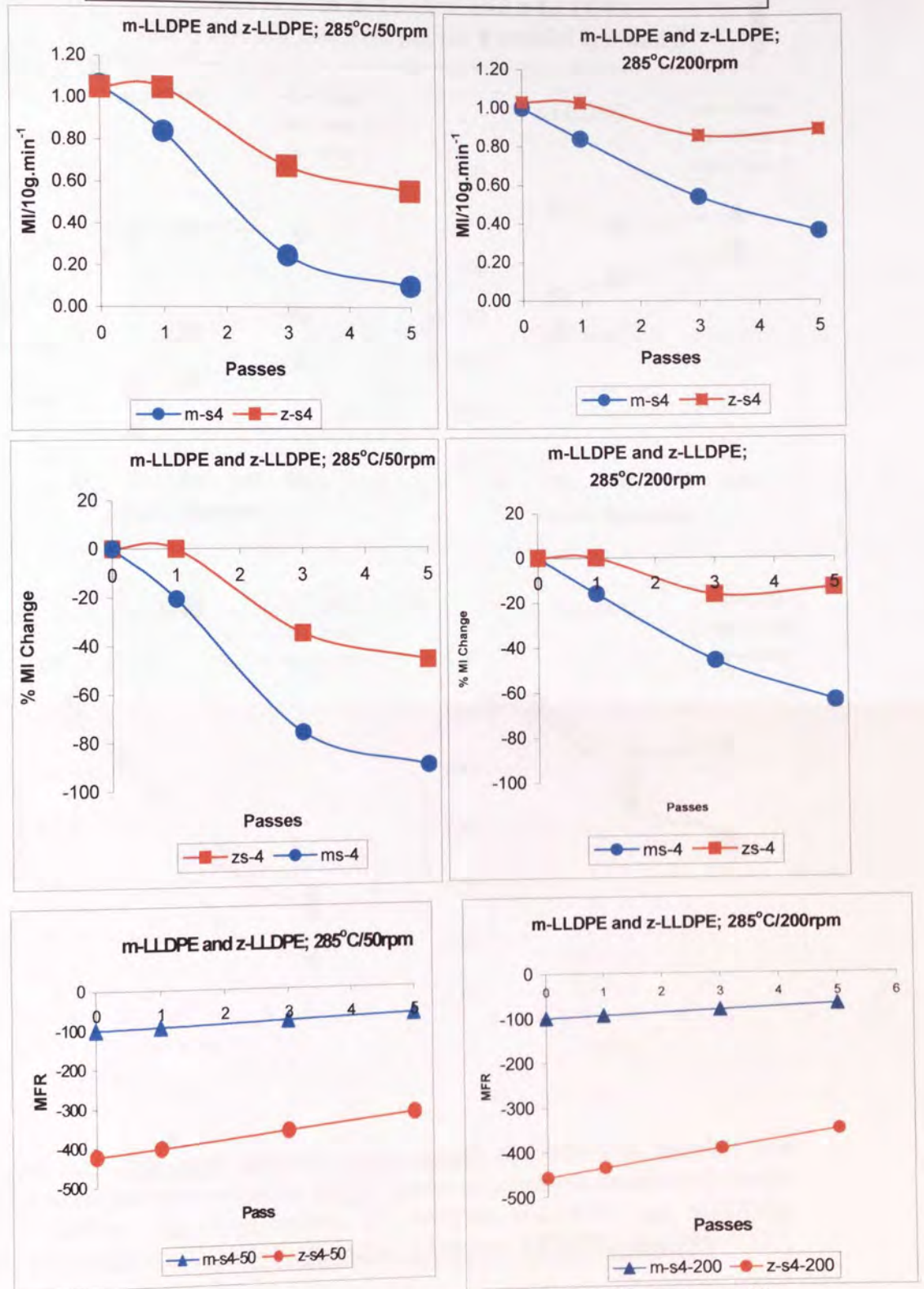


Figure 5.22. Compares the effect of processing severity on the melt stability characteristics of m-LLDPE and z-LLDPE polymers containing a **1:4 w/w ratio of Irganox 1076:Weston 399** (see s-4 in table 5.1) during multi-pass extrusion conditions with an **extrusion temperature of 285°C at screw speeds of 50 and 200rpm** under atmospheric conditions.



**Effect of s4 in m-LLDPE and z-LLDPE;  
285°C and 50, 100, 200rpm for PASSES 1, 3 and 5**

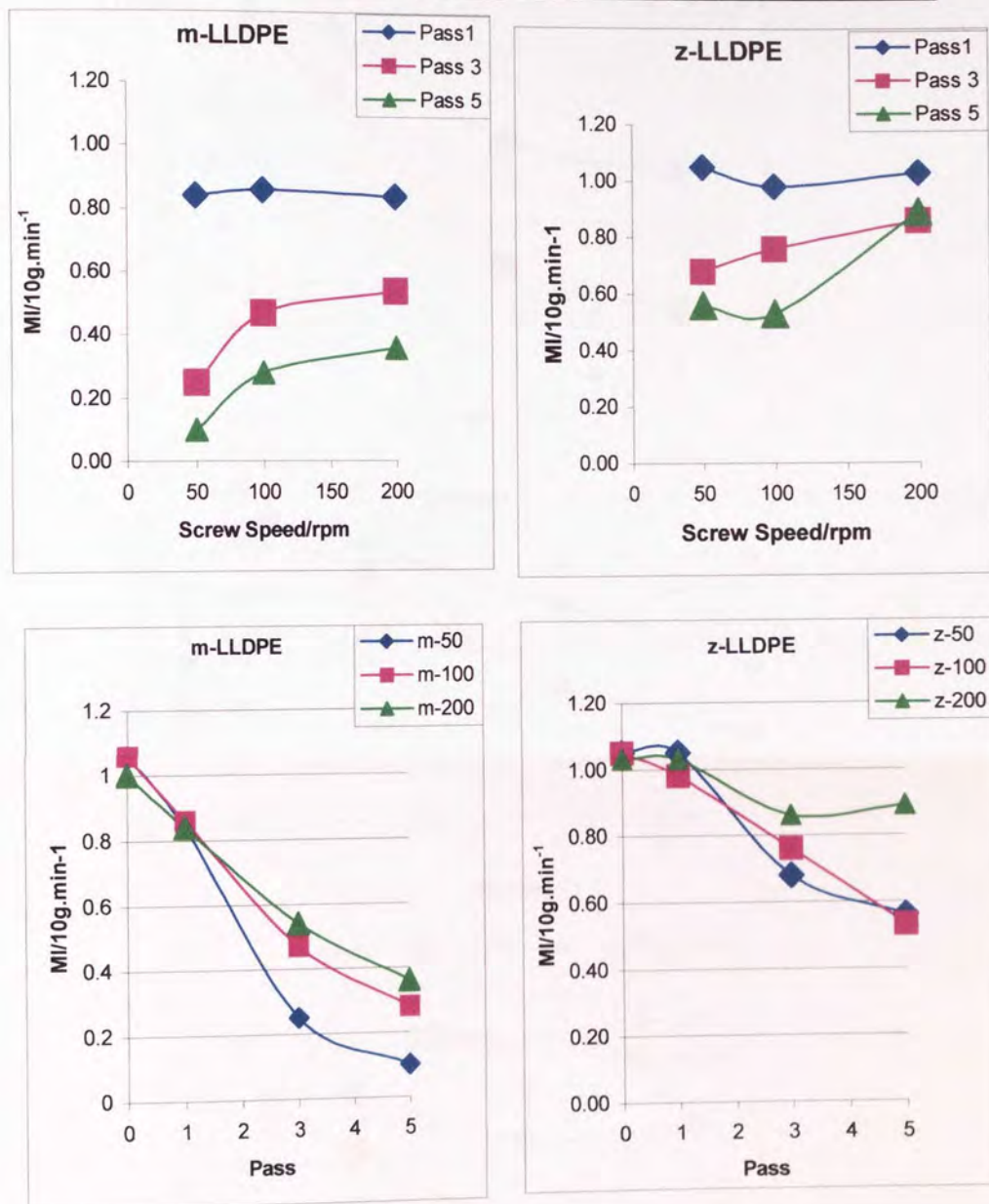


Figure 5.23. **Effect of different screw speeds** (50, 100 and 200rpm) at a fixed extrusion temperature of **285°C** (under atmospheric conditions) on the melt stability, MI, characteristics of stabilised m-LLDPE and z-LLDPE polymer sample, using a **1:4 w/w ratio of Irganox 1076:Weston 399**.

Compares s4 in m-LLDPE and z-LLDPE;  
285°C at Screw speeds 50, 100 and 200rpm.

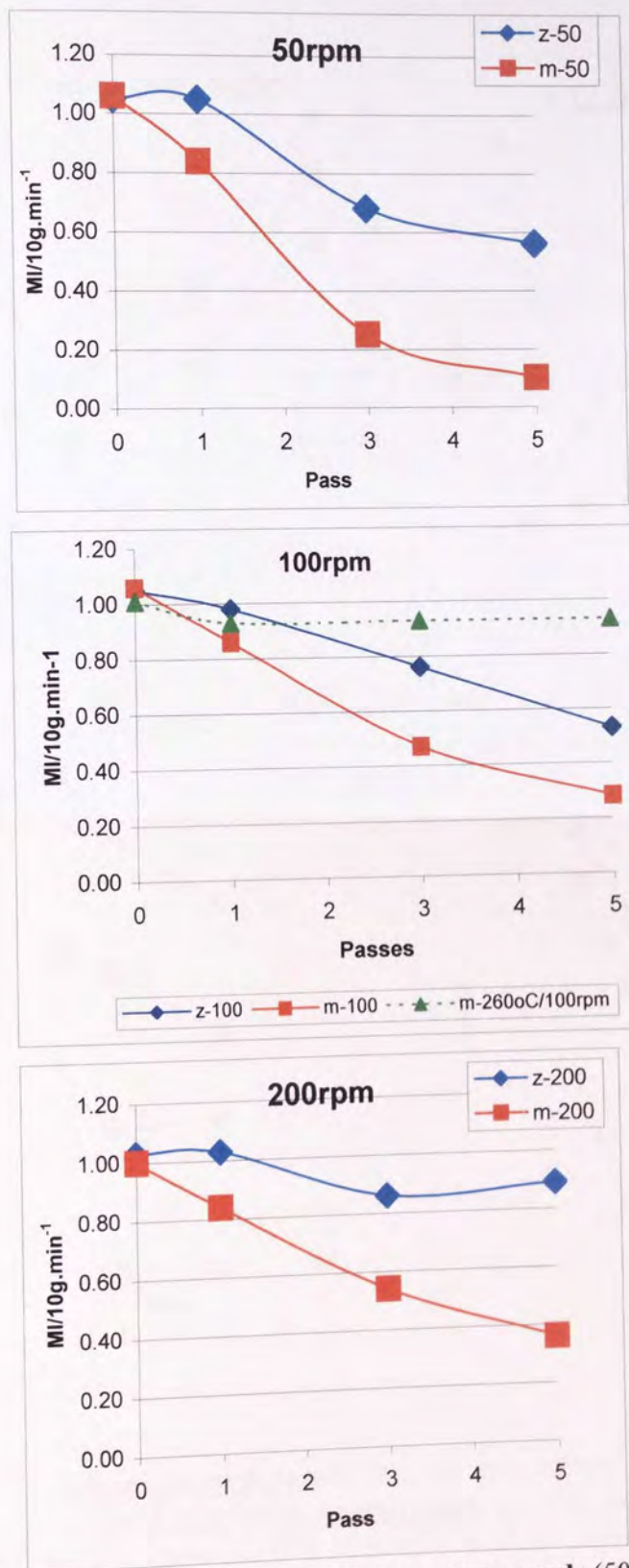


Figure 5.24. **Compares the effect of different screw speeds** (50, 100 and 200rpm) at a **fixed temperature** (285°C, under atmospheric conditions) with increasing processing severity on the melt stability; using a **1:4 ww/w ratio of a Irganox 1076:Weston 399 (500:2000ppm)**; of stabilised m-LLDPE and z-LLDPE polymer samples. The stability of the stabilised m-LLDPE polymer (with the same AO blend ratio) extruded at 260°C/100rpm is shown for comparison.



**Effect of s4 on Colour in m-LLDPE and z-LLDPE;  
285°C/50-200rpm for PASSES 1, 3 and 5**

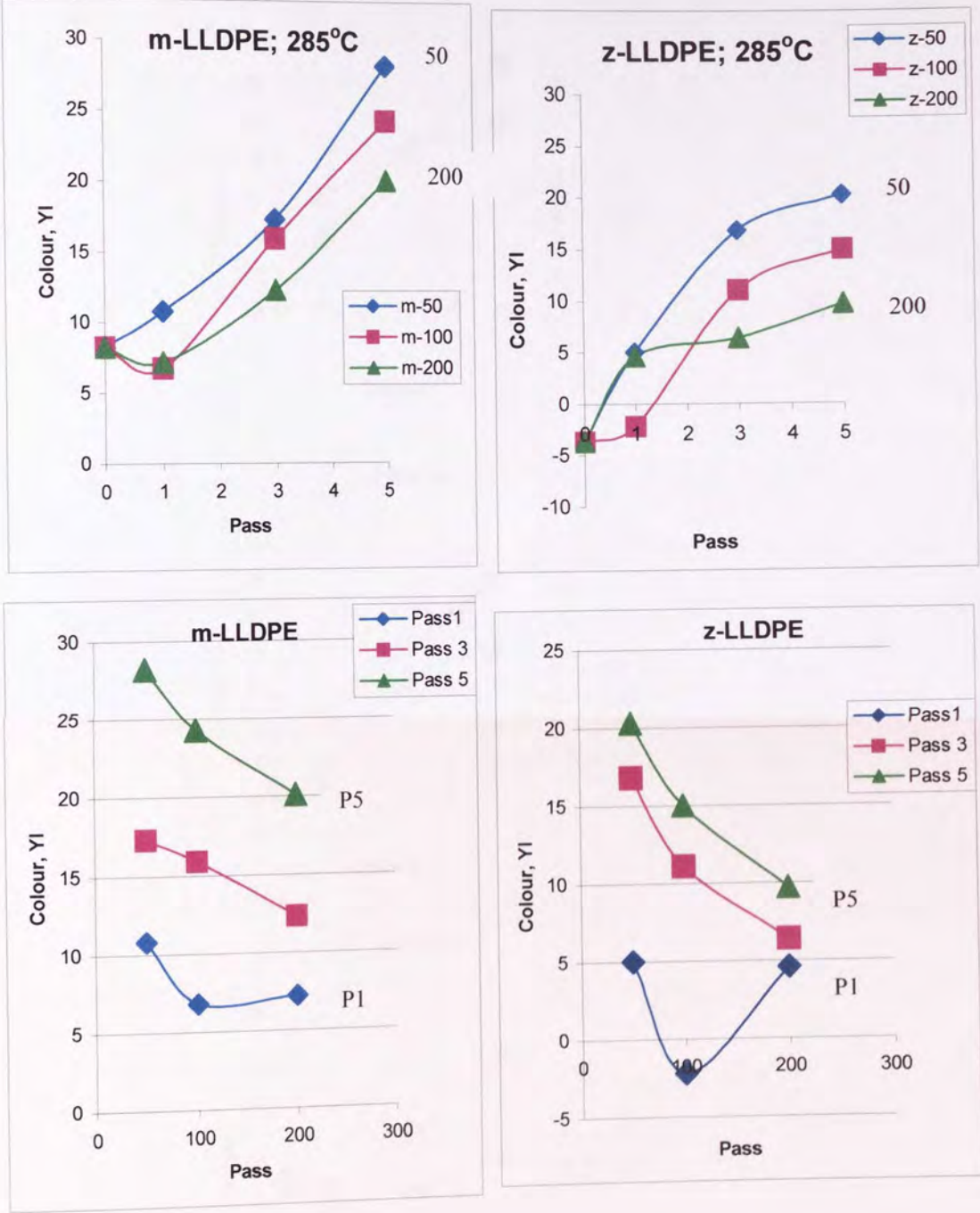


Figure 5.25. **Effect of screw speed** (50, 100 and 200rpm) with multi-pass extrusion at a **fixed extrusion temperature** (285°C under atmospheric conditions) on the colour stability of stabilised m-LLDPE and z-LLDPE polymer samples using a **1:4 w/w ratio of Irganox 1076:Weston 399** stabiliser package.

**Effect of s4 on Colour in m-LLDPE and z-LLDPE;  
285°C/50-200rpm for PASSES 1, 3 and 5**

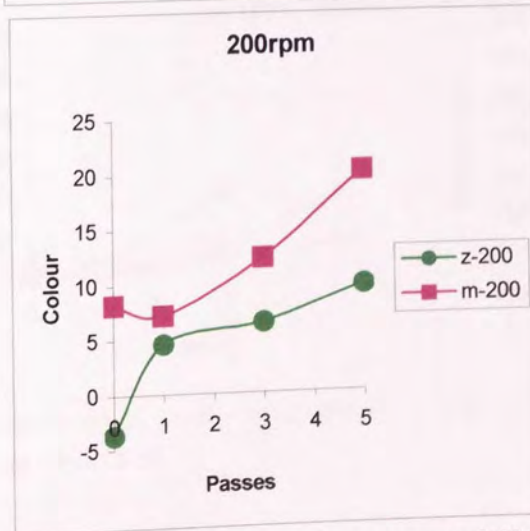
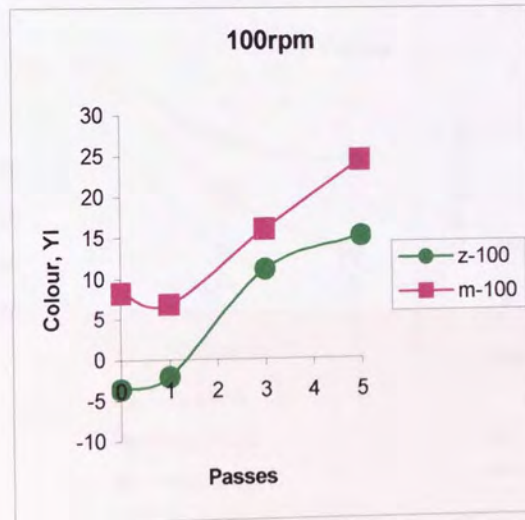
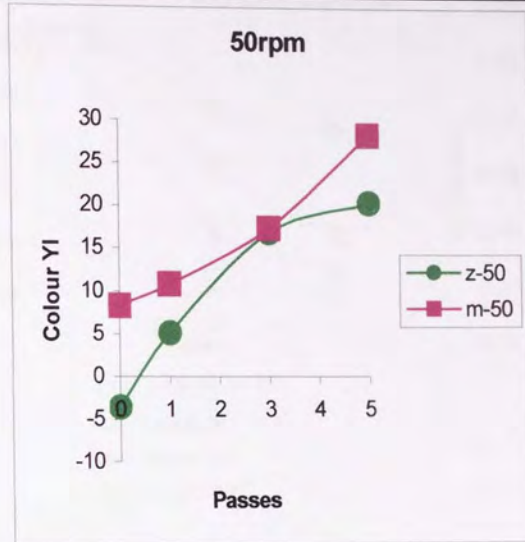


Figure 5.26. Comparison of the effect of screw speed (50, 100 and 200rpm) with increasing processing severity at a fixed extrusion temperature (285°C under atmospheric conditions) on the colour stability of stabilised of m-LLDPE and z-LLDPE polymer samples using a 1:4 w/w ratio of Irganox 1076:Weston 399 stabiliser package.



**Effect of s4, s11 and s13 in m-LLDPE;  
285°C at 50-200rpm**

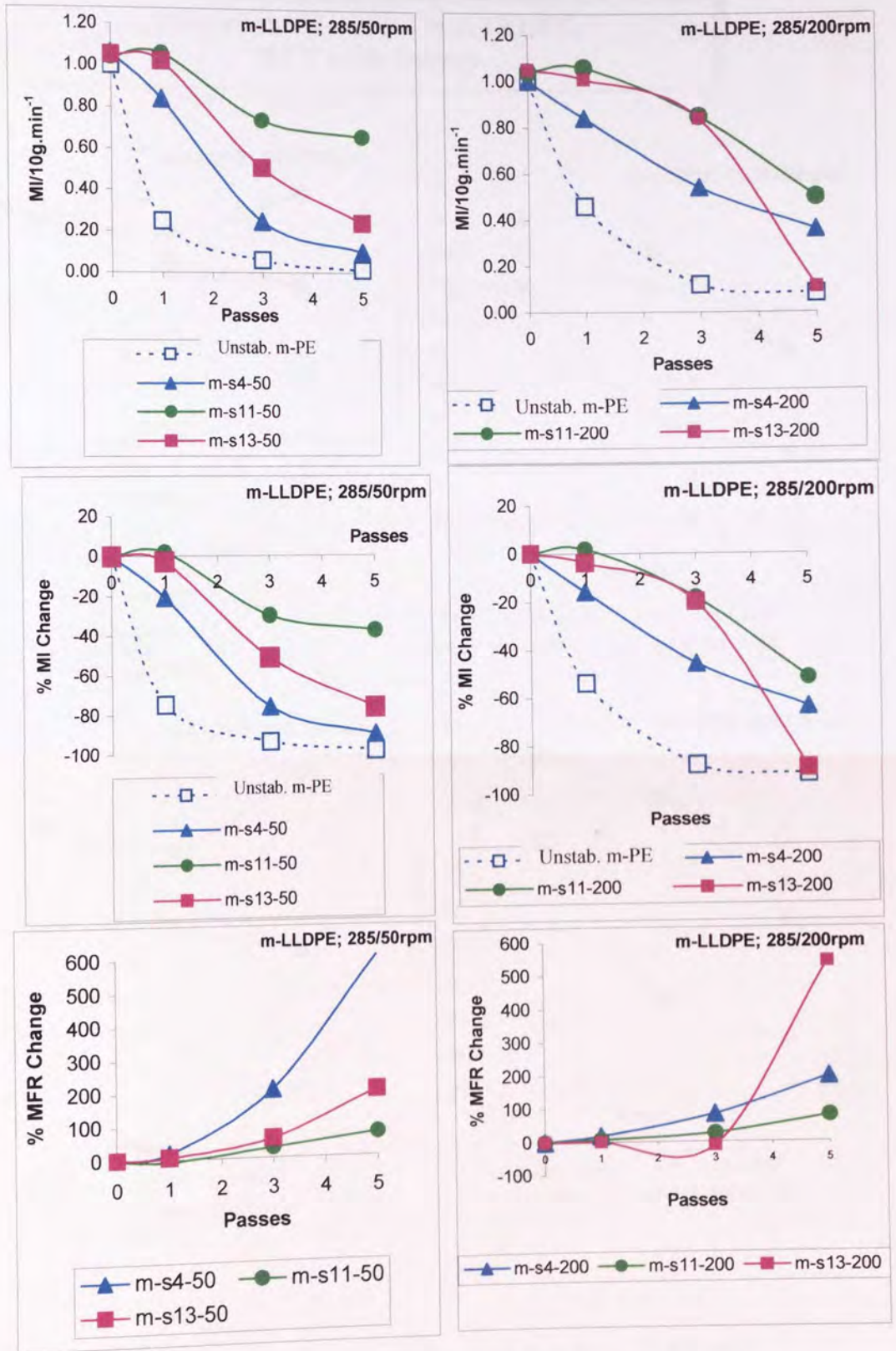


Figure 5.27. **Comparison** of at the effect of AOs' on the melt stability, MI, %MI change and % MFR change, in **stabilised m-LLDPE**; using a Irganox 1076:Weston 399 (s4) and Vit.E in **combination with phosphites** (s11 and s13) see table 5.1 during multi-pass extrusion (**285°C with two different screw speeds, 50 and 200rpm**).



**Effect of s4, s11 and s13 in m-LLDPE;  
285°C at 50-200rpm**

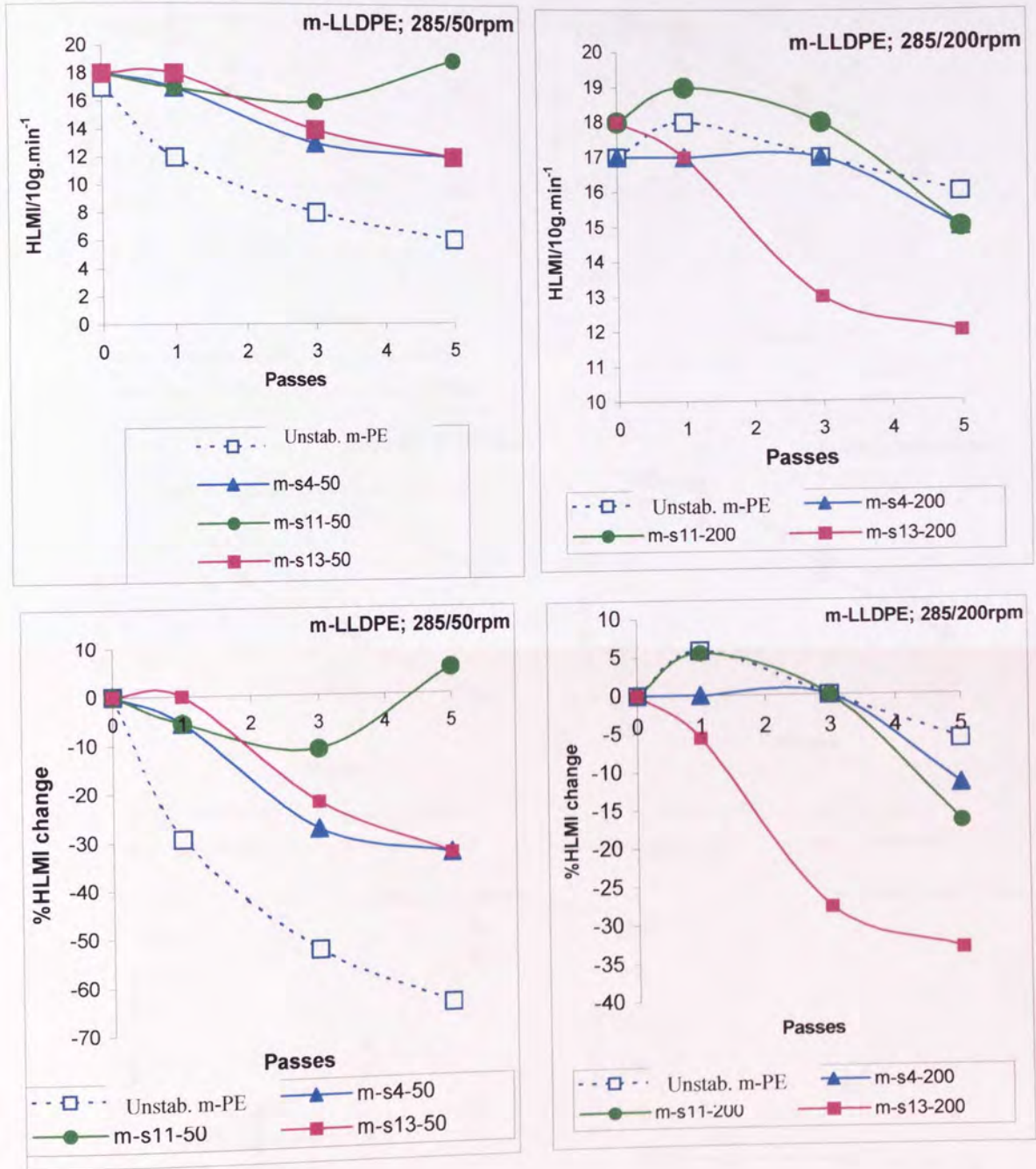


Figure 5.28. **Comparison** of the effect of AOs' on the melt stability, HLMi and %HLMi change, of **m-LLDPE**; using Irganox 1076:Weston 399(s4) and Vitamin E **in combination with phosphites** (s11 and s13) see table 5.1 during multi-pass extrusion (**285°C with two different screw speeds, 50 and 200rpm**).

**Effect of s4 in m-LLDPE and z-LLDPE;  
285°C/100rpm**

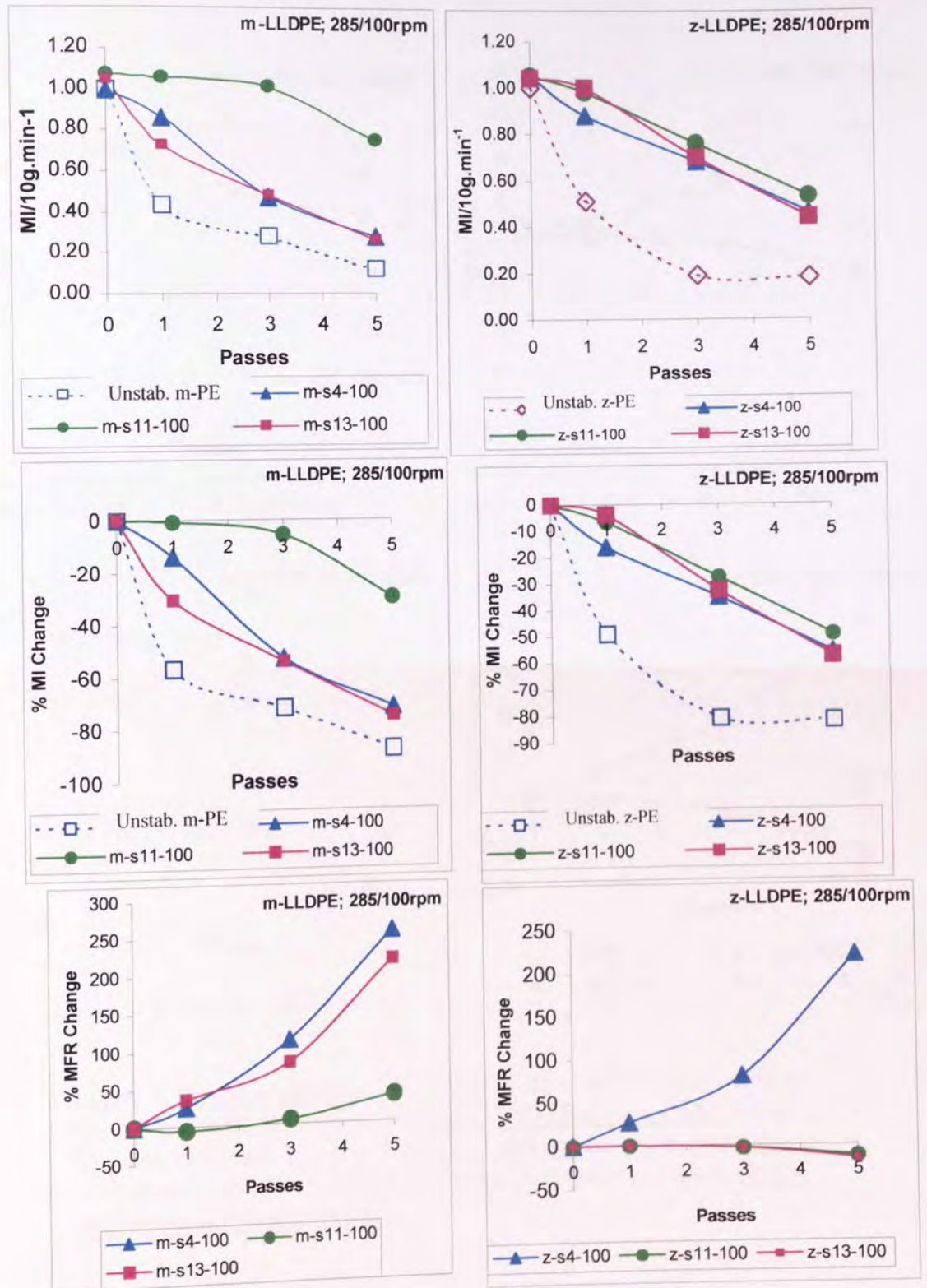


Figure 5.29. Comparison of the effect of AOs on the melt stability, MI, %MI change and % MFR change, of stabilised **m-LLDPE** and **z-LLDPE**; using Irganox 1076 and Irganox E201 in combination with phosphites (see s4, s11 and s13 in table 5.1) during multi-pass extrusion (**285°C at a screw speed of 100rpm**).



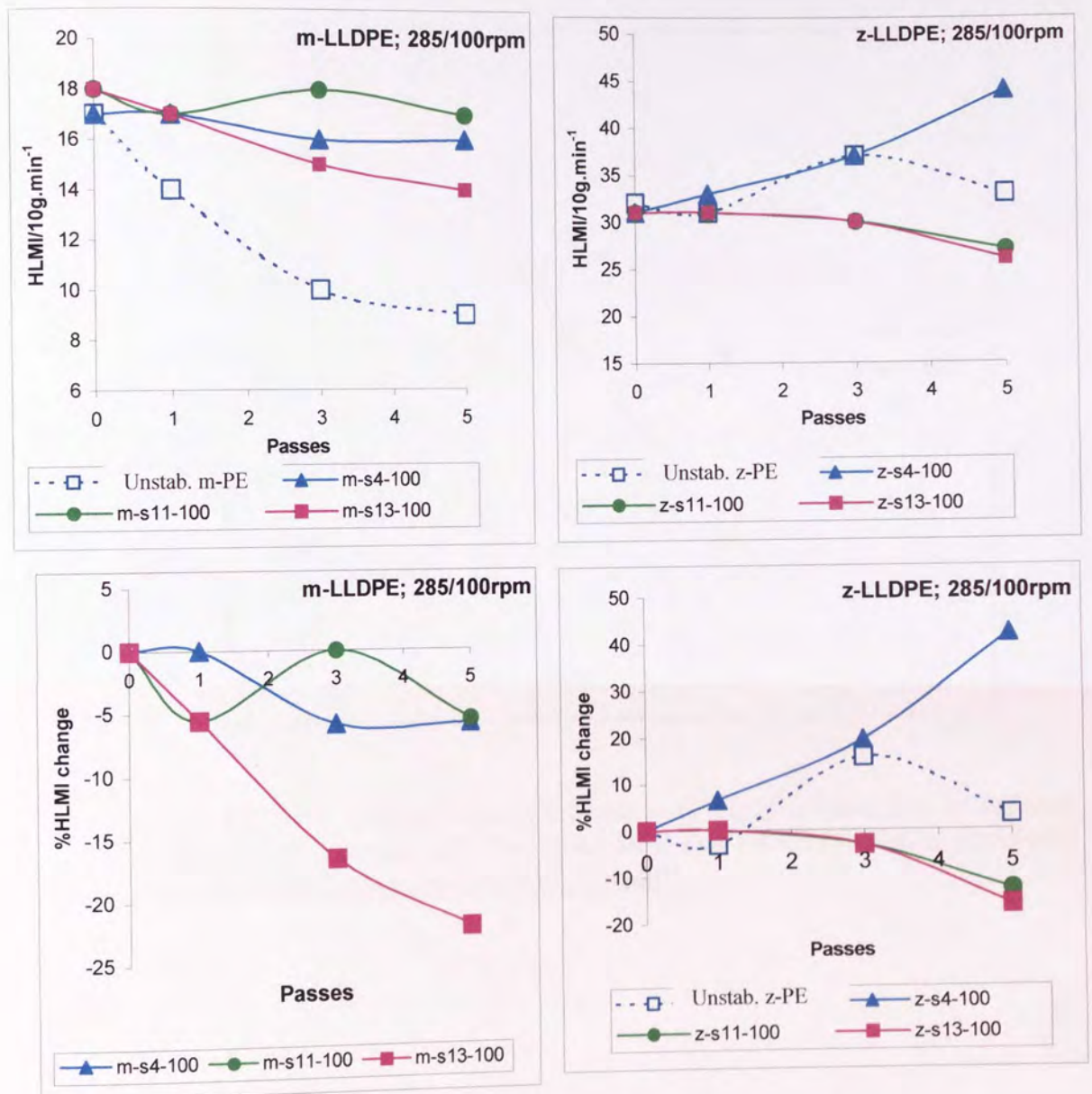


Figure 5.30. **Comparison** of the effect of AOs' on the melt stability, HLM and %HLM change, of **m-LLDPE and z-LLDPE**; using a Irganox 1076 and Irganox E201 **in combination with phosphites** (see s4, s11 and s13 in table 5.1) during multi-pass extrusion (**285°C at a screw speed of 100rpm**).

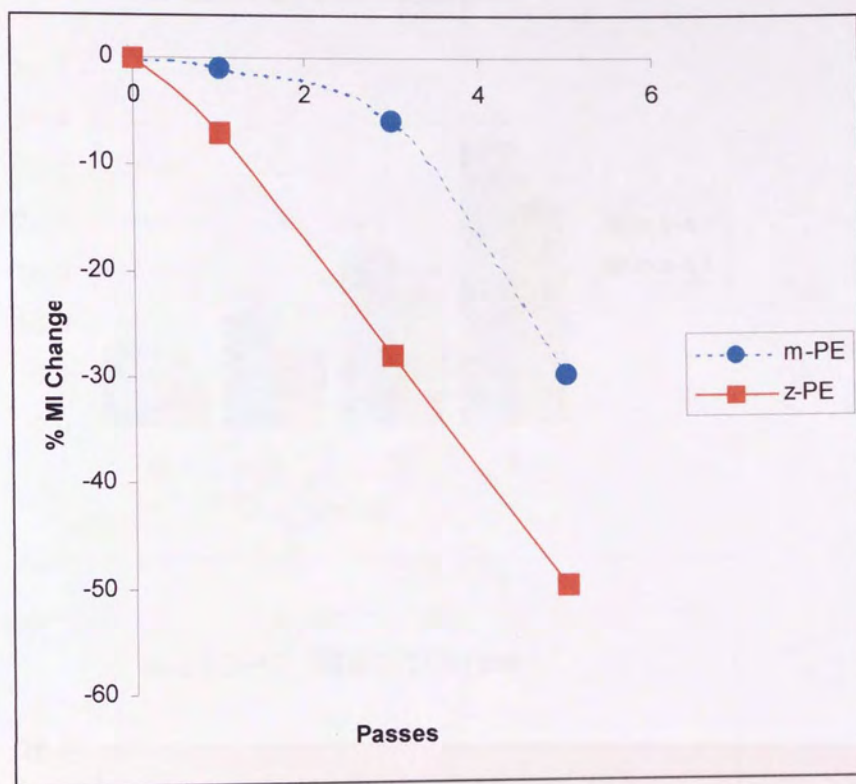


Figure 5.31. The effect of Vitamin E:Ultranox 626 (s11 in table 5.1) on the melt stability, %MI change of stabilised **m-LLDPE** and **z-LLDPE**; during multi-pass extrusion (285°C at a screw speed of 100rpm).



**Effect of s4 and s11 on Colour in m-LLDPE; 285°C/50-200rpm for PASSES 1, 3 and 5.**

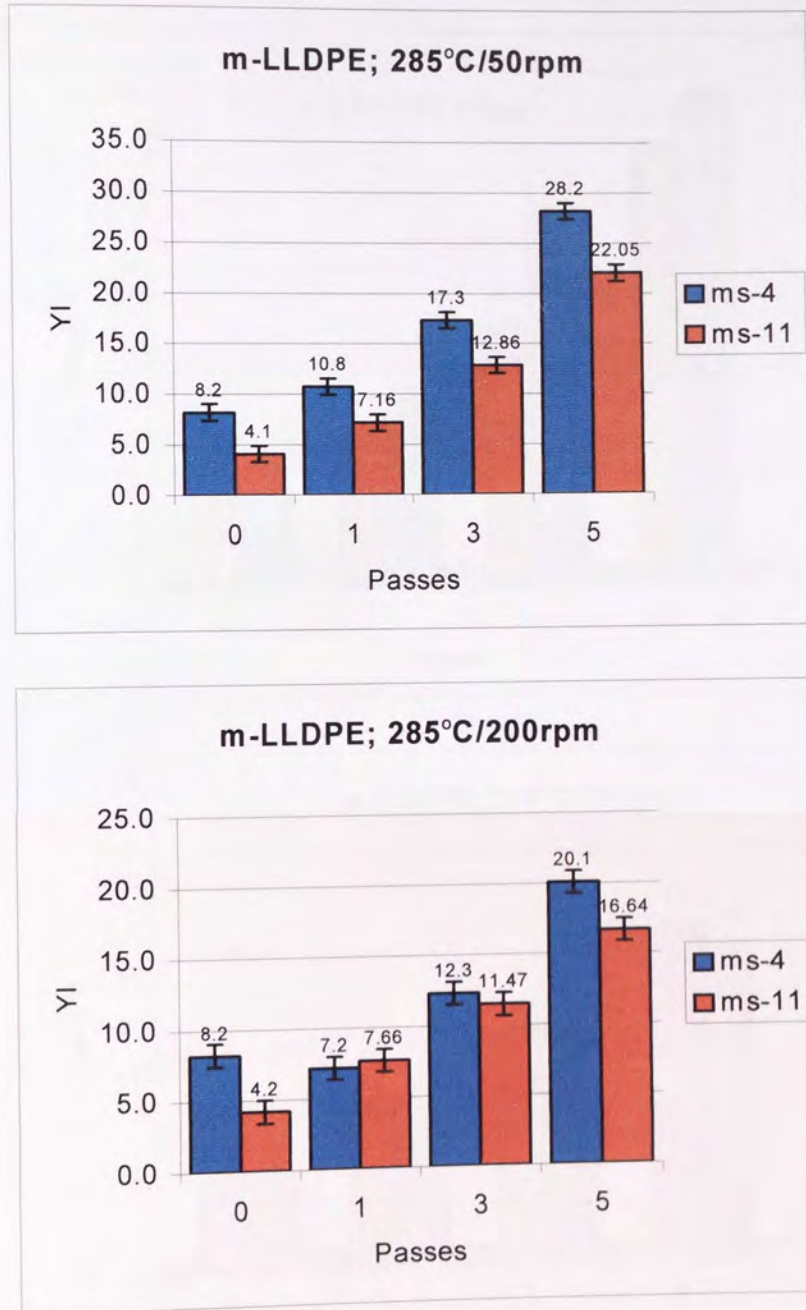


Figure 5.32 Comparison of the colour stability of stabilised m-LLDPE polymers; using Irganox 1076 and Irganox E201 in combination with different phosphites (see s4 and s11 (see table 5.1) during multi-pass extrusion at an extrusion temperature of 285°C with screw speeds of 50 and 200rpm (under atmospheric conditions).



**Effect of Weston 399 and Ultrinox 626 in combination with Irganox E201 on Colour in m-LLDPE; 285°C/50-200rpm for PASSES 1, 3 and 5.**

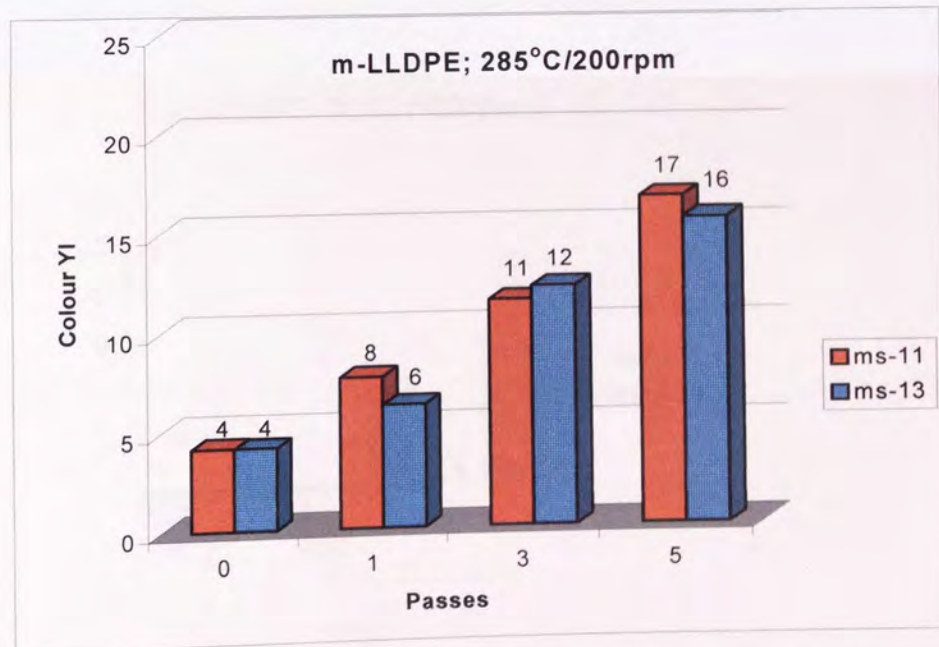
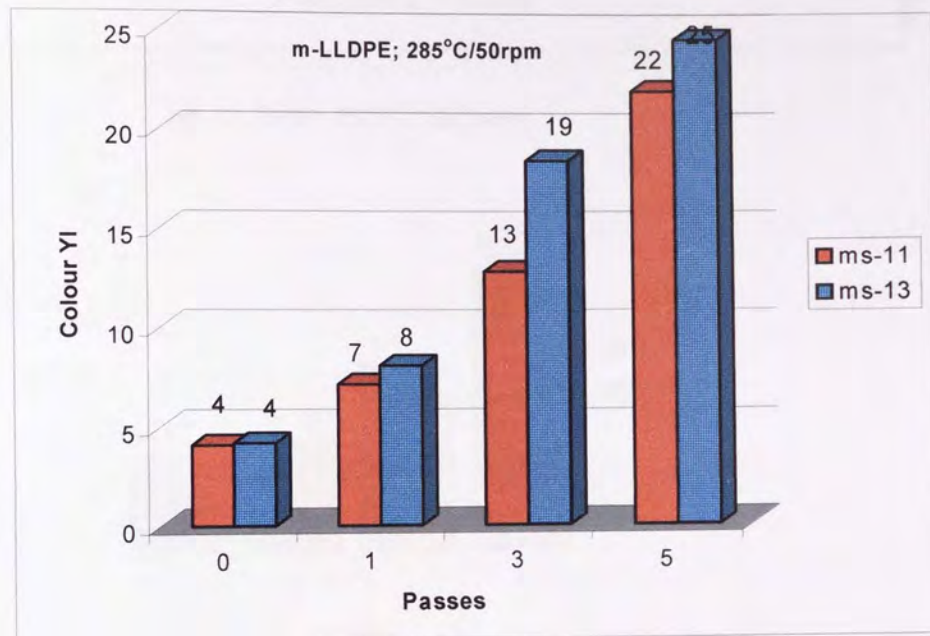


Figure 5.33 Comparison of the colour stability of stabilised m-LLDPE polymers; using Irganox 1076 and Irganox E201 in combination with different phosphites; s11 and s13 (see table 5.1) during multi-pass extrusion at an extrusion temperature of 285°C with screw speeds of 50 and 200rpm (under atmospheric conditions).

**Effect of s4 and s11 on Colour in m-LLDPE; 285°C/100rpm for PASSES 1, 3 and 5.**

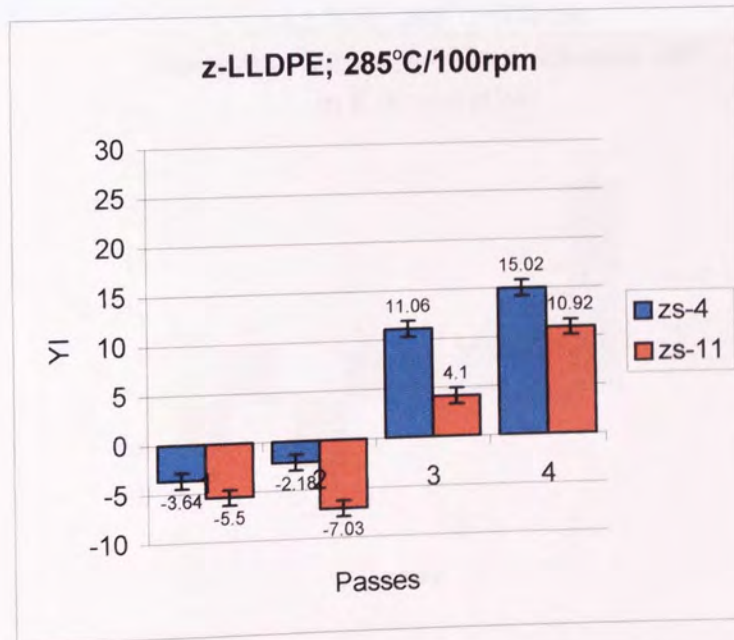
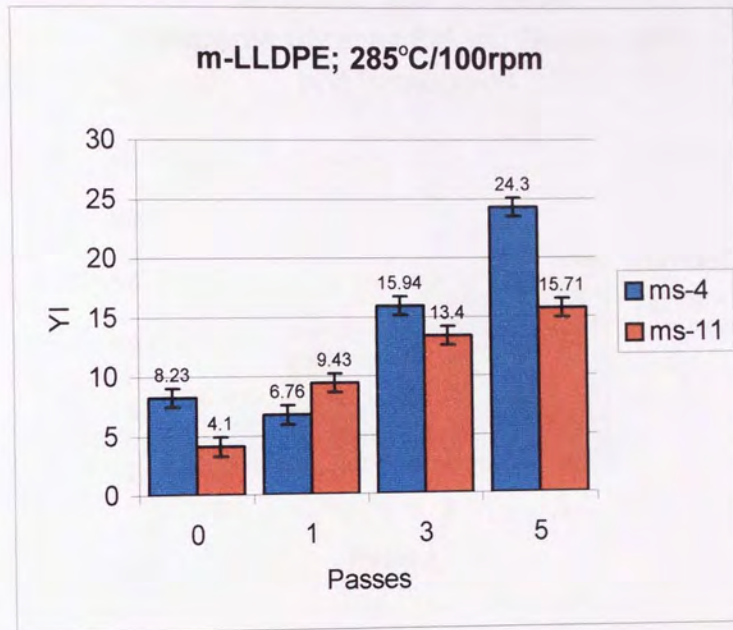


Figure 5.34 Comparison of the colour stability of stabilised m-LLDPE and z-LLDPE polymers; using Irganox 1076 and Irganox E201 in combination phosphites (see s4 and s11 in table 5.1); during multi-pass extrusion at an extrusion temperature of 285°C with a screw speed of 100rpm (under atmospheric conditions).



**Effect of Weston 399 and Ultrinox 626 in combination with Irganox E201 on Colour in m-LLDPE; 285°C/100rpm for PASSES 1, 3 and 5.**

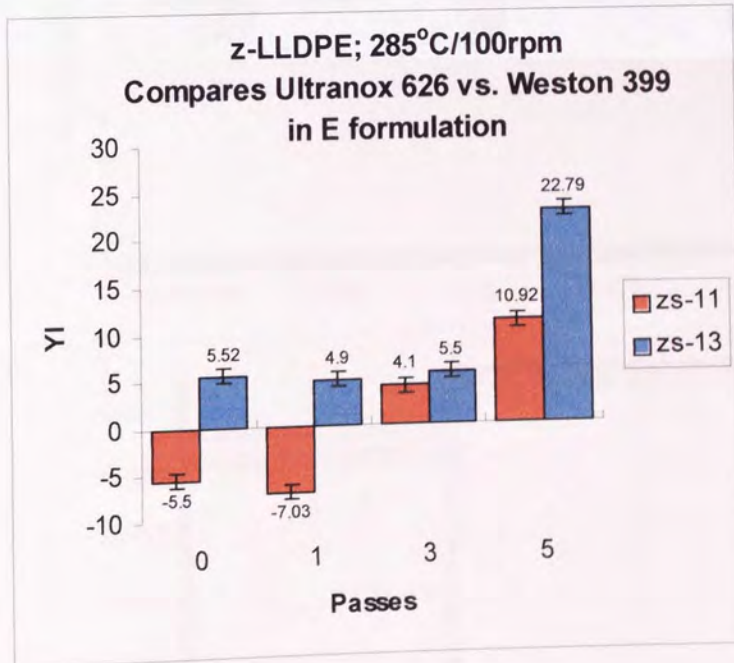
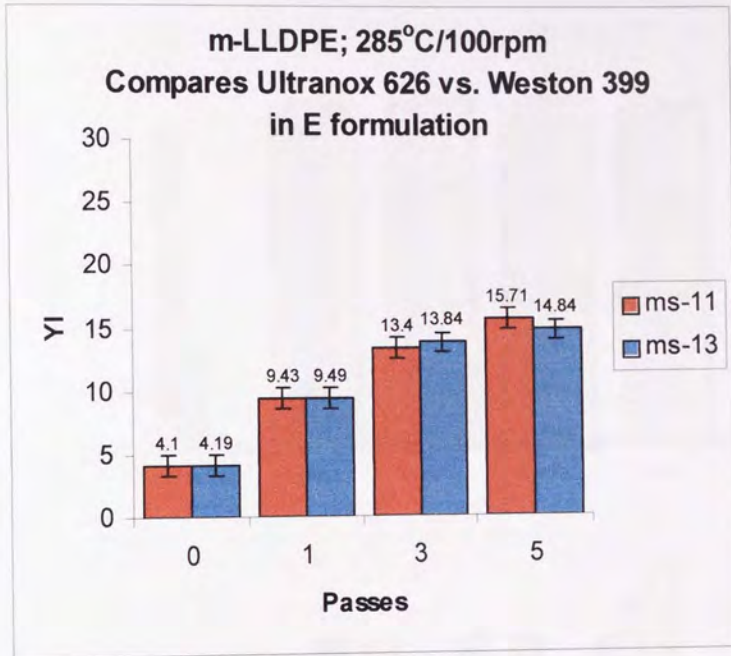


Figure 5.35 Comparison the colour stability of stabilised m-LLDPE and z-LLDPE polymers; using Irganox E201 in combination with different phosphites (see s4 and s11 in table 5.1); during multi-pass extrusion at an extrusion temperature of 285°C with a screw speed of 100rpm (under atmospheric conditions).

**Irganox HP136 and Phosphites**  
**Effect of 2 AO based systems on melt stability of m-LLDPE;**  
**260°C/100rpm for PASSES 1, 3 and 5.**

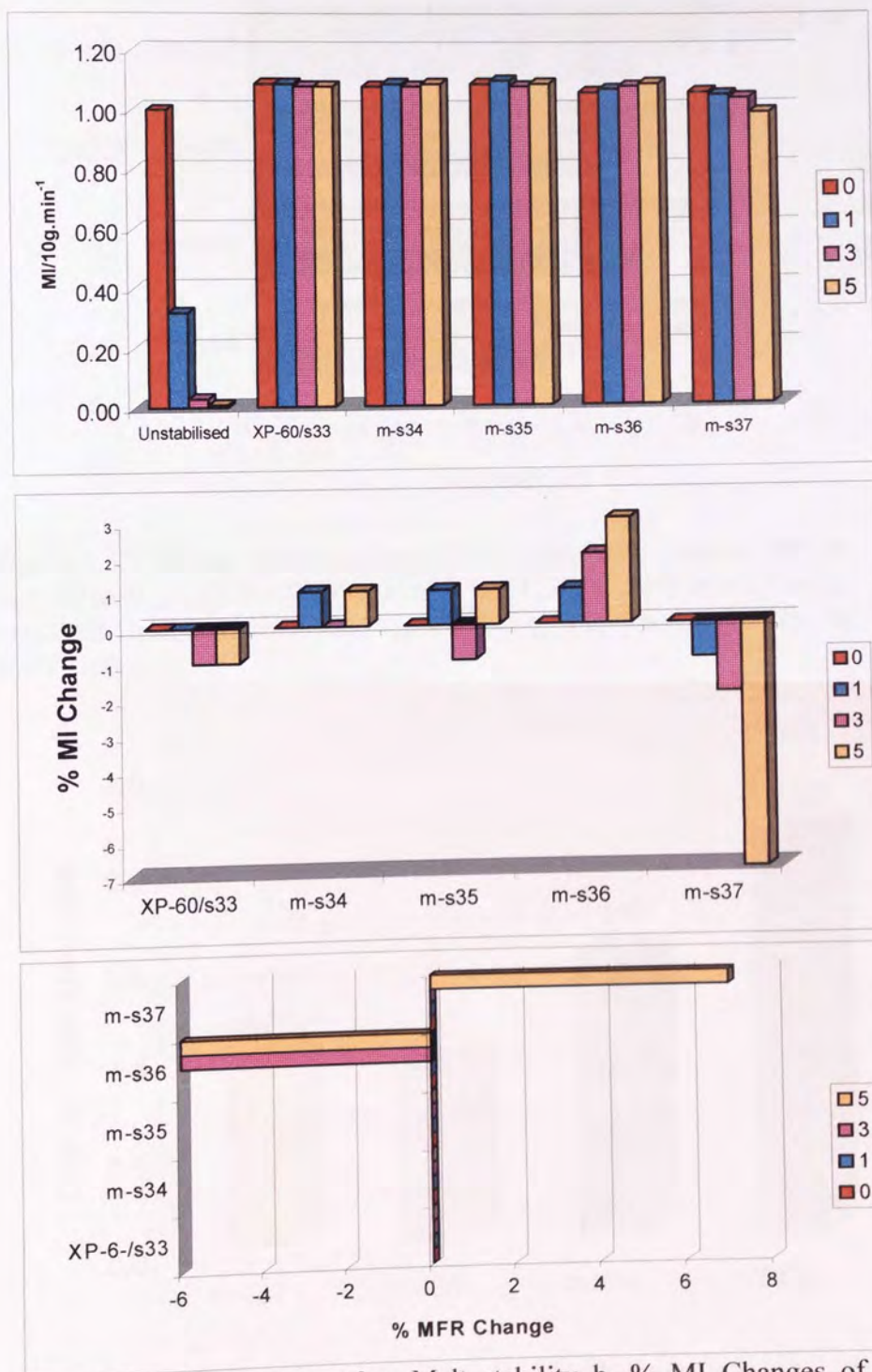


Figure 5.36. Comparison of a. Melt stability b. % MI Changes of m-LLDPE containing Irganox HP136 in combination with different Phosphites; U626 (s33 & s34), PEPQ (s35), Doverphos S9228 (s36) and W.399 (s37); see table 5.1; multi-extruded at 260°C/100rpm.



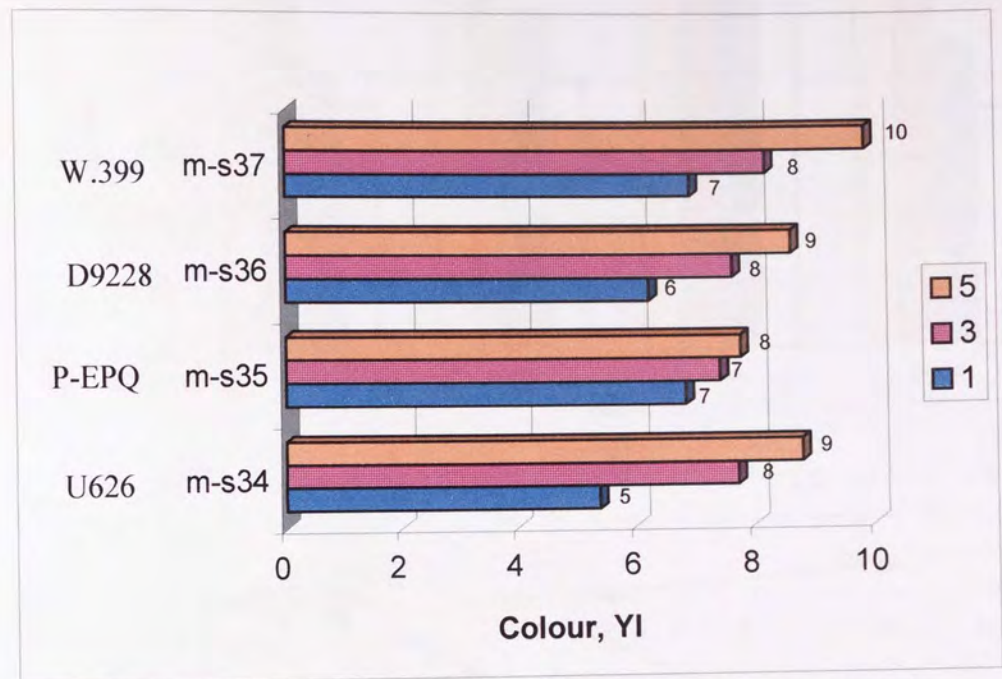


Figure 5.37. Colour Stability of m-LLDPE containing Irganox HP136 and different phosphites (PEPQ, U.626, D.S9228, W.399) in a 2.3 ratio; stabilised formulations s34-s37, see table 5.1; multi-extruded at 260°C/100rpm.

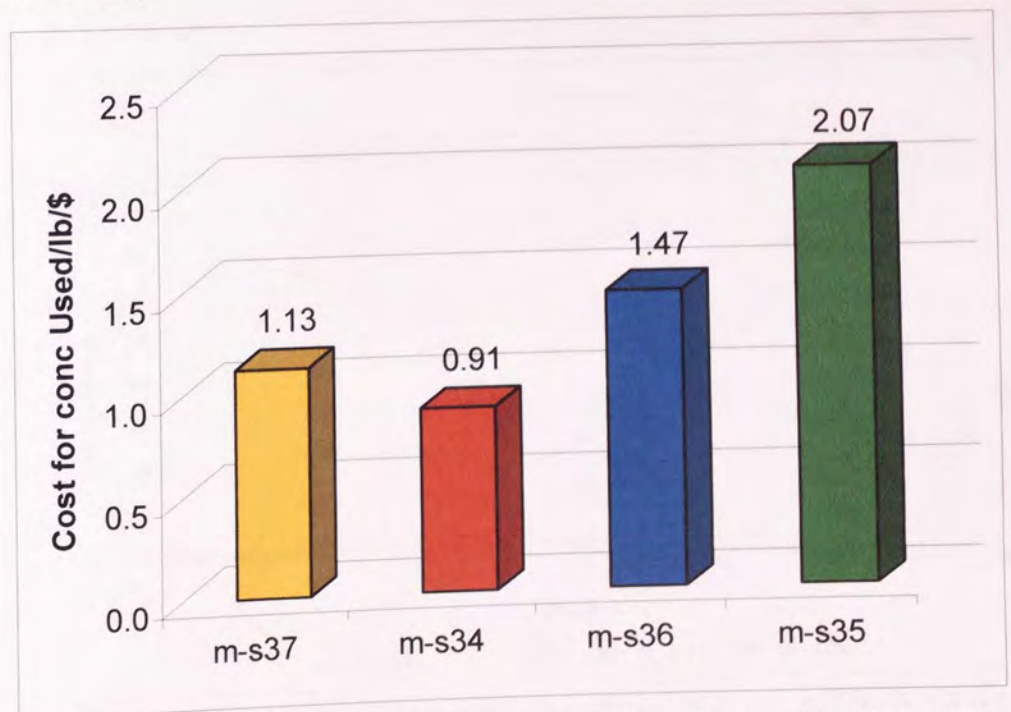


Figure 5.38. Cost effectiveness of Irganox HP136:Phosphite combinations. Cost for the concentration used.



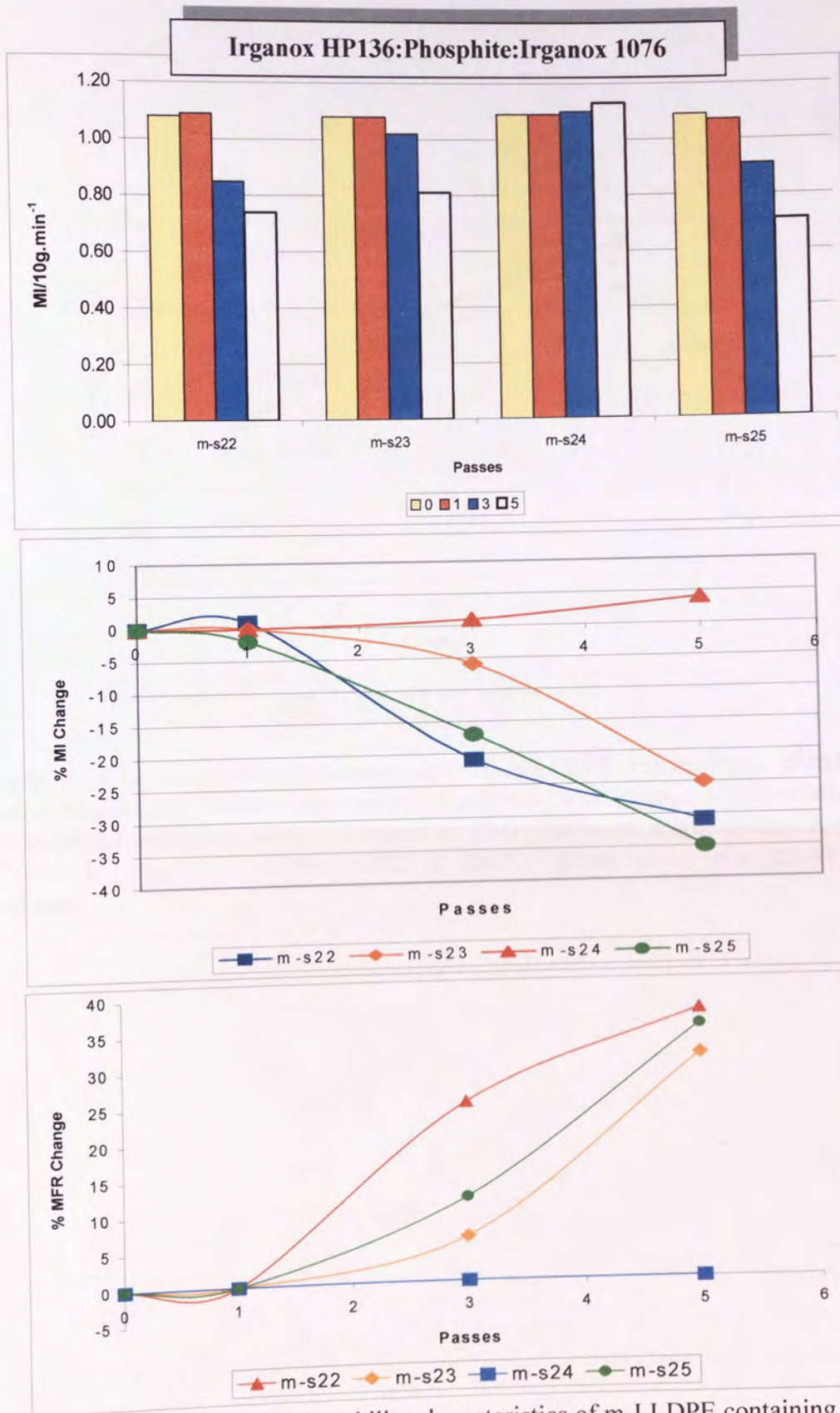


Figure 5.39 Comparison of melt stability characteristics of m-LLDPE containing a fixed lactone content (0.03%w/w) and varying concentrations of Irganox 1076/weston 399 combinations in the presence/absence of TMP; stabilised formulations (see s22-s-25 in table 5.1); multi-extruded at 260°C/100rpm under atmospheric conditions.

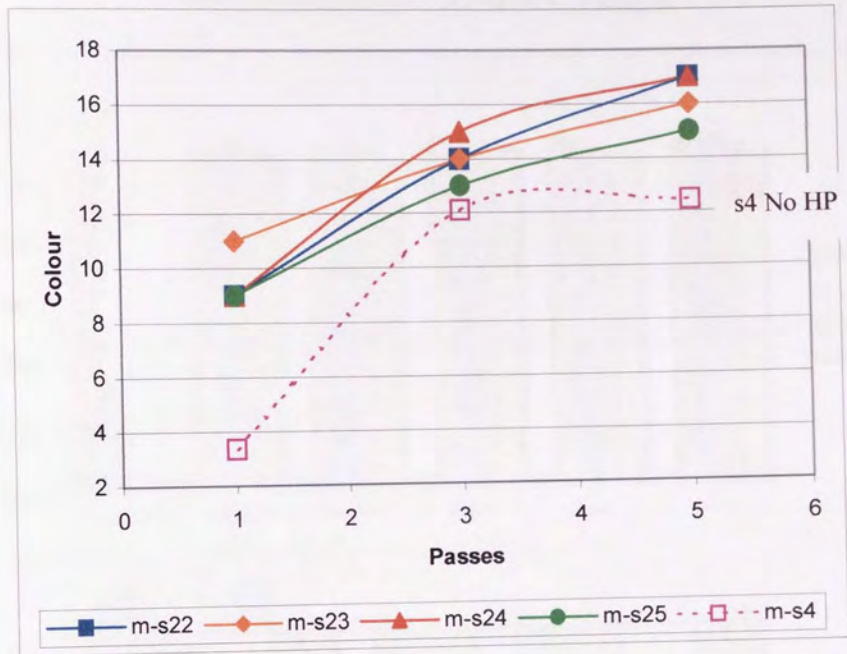


Figure 5.40 Colour stability characteristics of m-LLDPE containing a fixed lactone content (0.03%w/w) and varying concentrations of Irganox 1076/weston 399 combinations in the presence/absence of TMP; stabilised formulations (see s22-s-25 in table 5.1); multi-extruded at 260°C/100rpm under atmospheric conditions.



**Irganox 1076:Irganox HP136:Phosphites**  
**Effect of 3 AO based systems on melt stability of m-LLDPE;**  
**260°C/100rpm for PASSES 1, 3 and 5.**

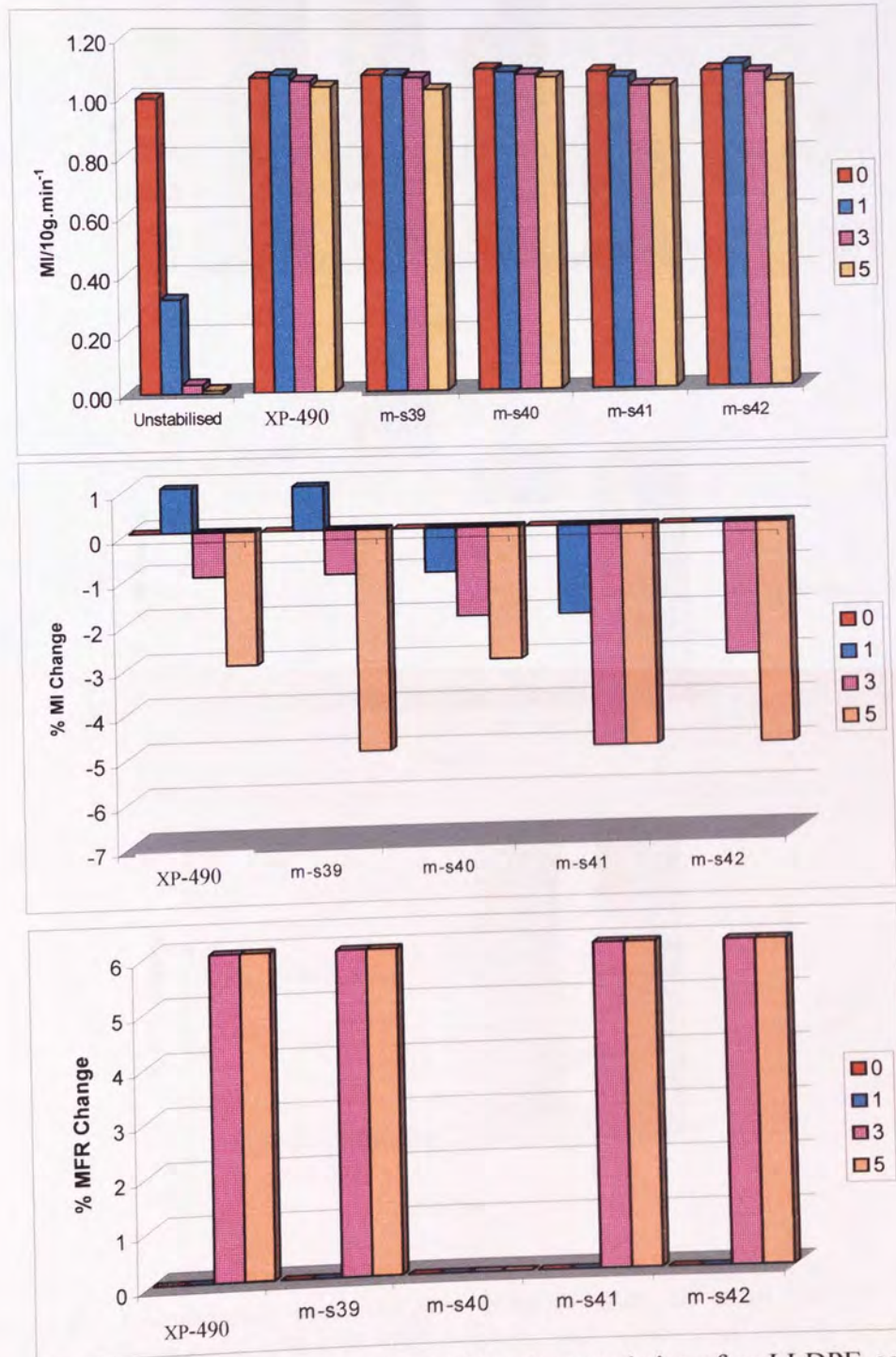


Figure 5.41 Comparison of melt stability characteristics of m-LLDPE containing Irganox 1076:Irganox HP136 in combination with different phosphites (P-EPQ, U626, Doverphos S9228 and W.399); stabilised formulations (see s39-s42 in table 5.1); multi-extruded at 260°C/100rpm.

Irganox HP136:Irganox 1076:Irgafos P-EPQ

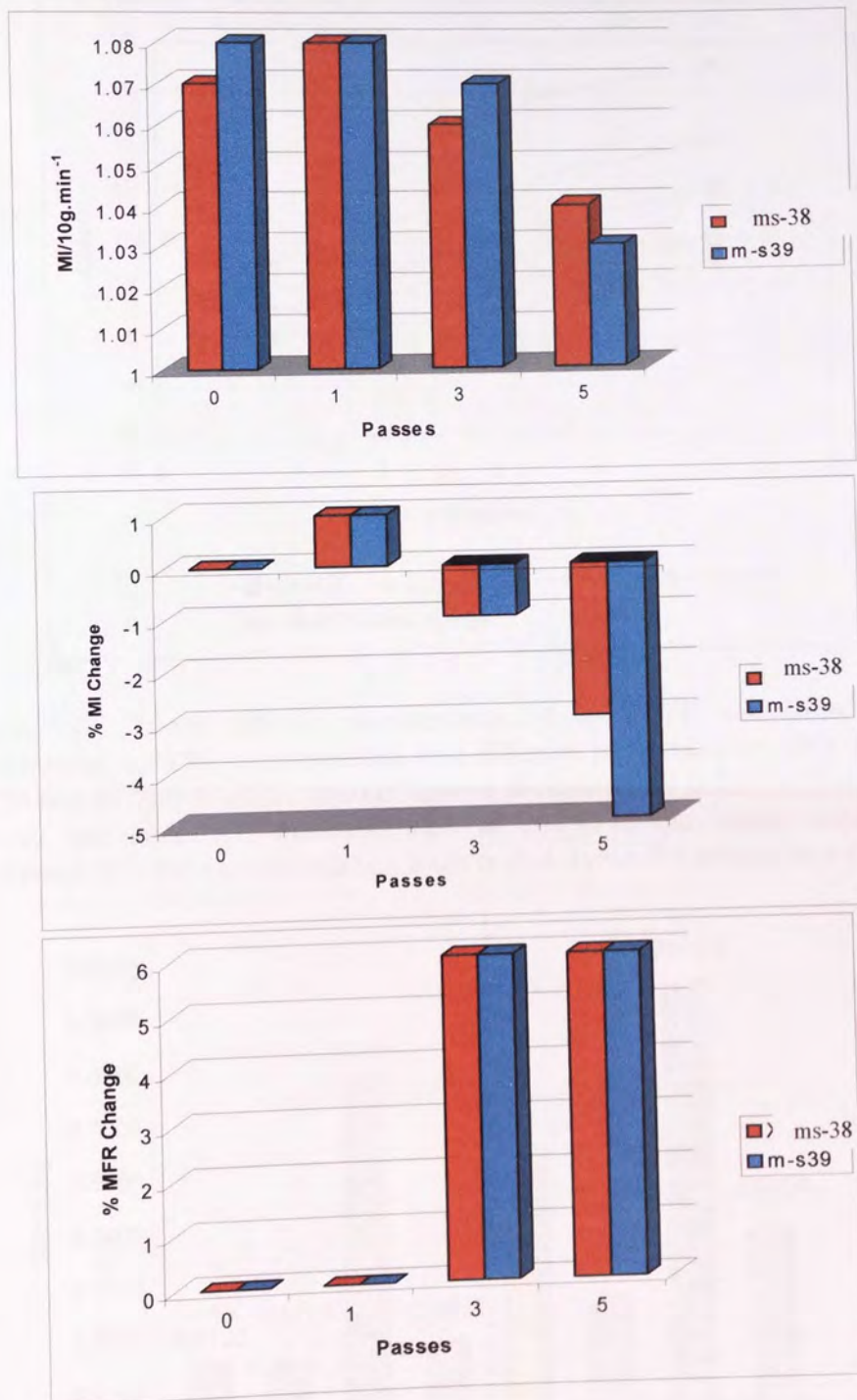


Figure 5.42. Comparative melt stability characteristics of a m-LLDPE polymer containing a commercial, s38 (XP-490) package and a blend of similar composition prepared at Aston, s39, based on a Irganox 1076:Irganox HP136 and PEP-Q system; multi-extruded at 260°C/100rpm under atmospheric conditions.



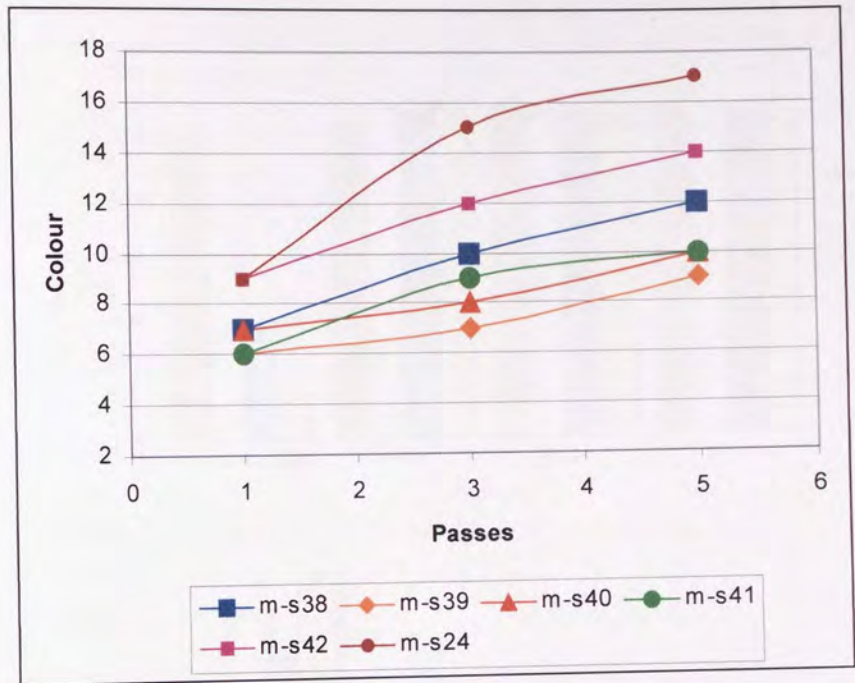


Figure 5.43 Colour stability characteristics of m-LLDPE containing Irganox 1076:Irganox HP136 in combination with different phosphites (P-EPQ, U626, D. S9228 and W.399) in a 1:2.3 ratio of lactone:phosphite; P0 stabilised formulations s39-s42 see table 5.1; multi-extruded at 260°C/100rpm under atmospheric conditions; XP-490 a commercial package is also shown for comparison (s38).

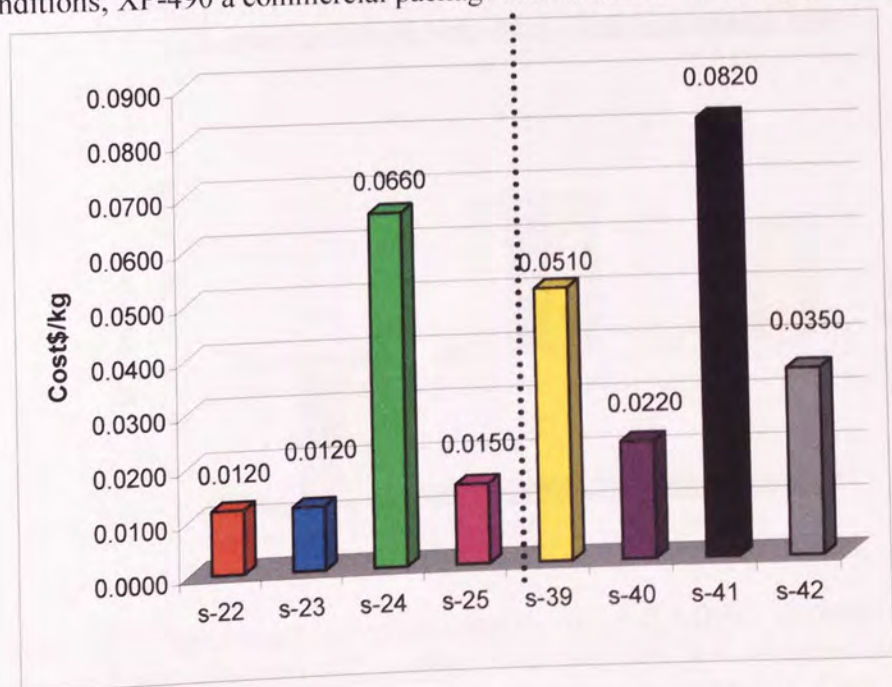


Figure 5.44. Cost effectiveness of a Irganox 1076:Irganox HP136 in combination with different phosphites. Cost for the concentration used. Note that s-23 expresses cost excluding price of TMP.



**Irganox E201:Ultranox 626 in the presence/absence  
of Hydroxylamine (Irgastab FS042)**

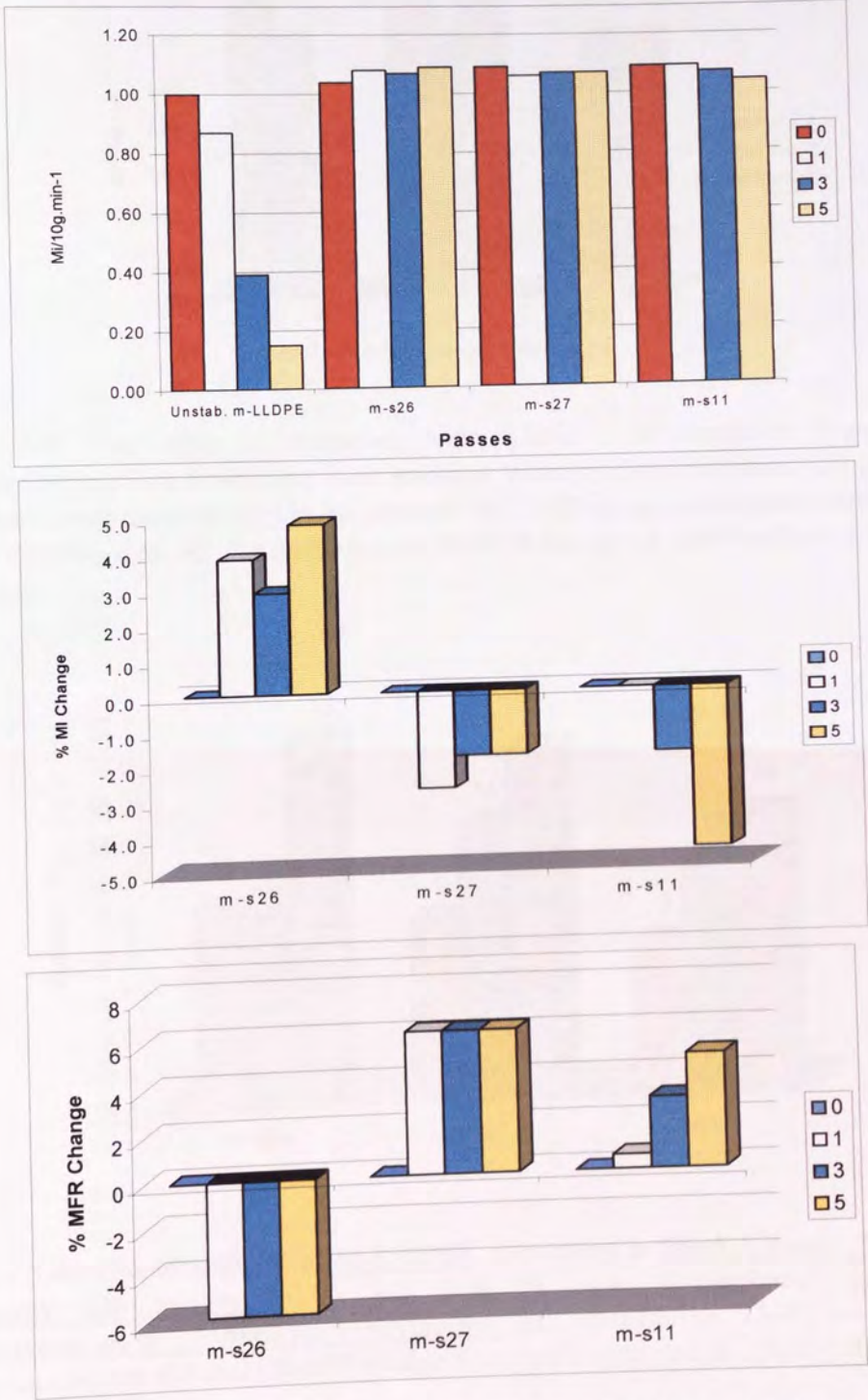


Figure 5.45 Comparison of melt stability of m-LLDPE containing a fixed Vitamin E and Ultranox 626 content (0.03 and 0.06 % w/w respectively) in the presence/absence of dialkyhydroxylamine and co-additive TMP; stabilised formulations (see s11 and s26-s27 in table 5.1); multi-extruded at 260°C/100rpm.

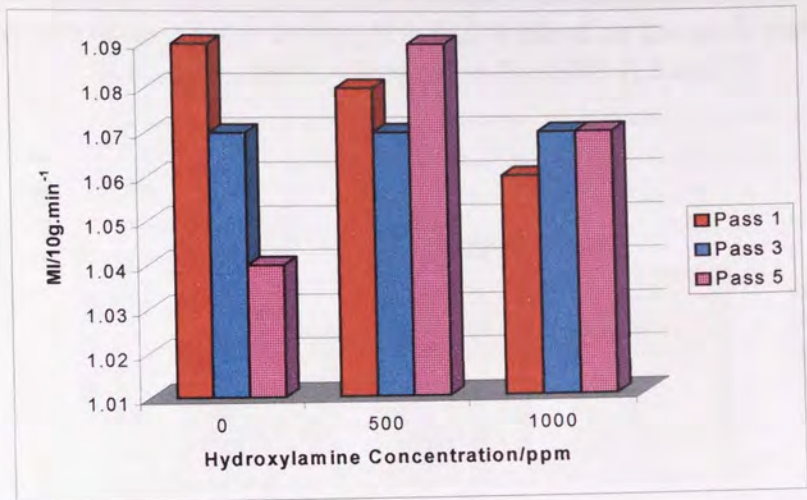


Figure 5.46 The effect of increasing hydroxylamine concentration (Irgastab FS042); formulations containing fixed levels of Vitamin E and Ultrinox 626 (0.03 and 0.06 % w/w respectively) in the presence of TMP during multi-pass extrusion at 260°C/100rpm on MI, %MI change and % MFR change of stabilised m-LLDPE polymers.

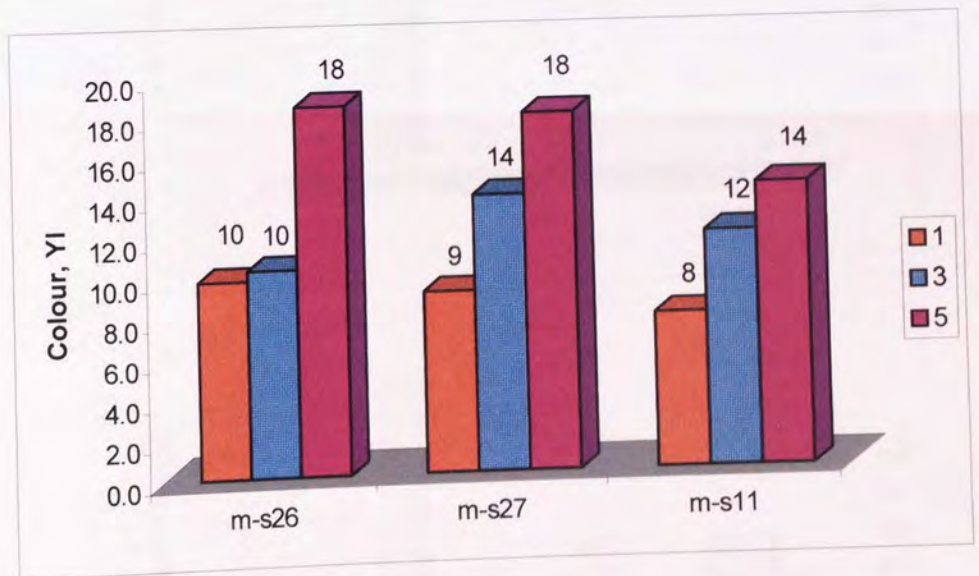


Figure 5.47 Colour stability of m-LLDPE containing a fixed Vitamin E and Ultrinox 626 content (0.03 and 0.06 % w/w respectively) in the presence/absence of dialkyhydroxylamine and co-additive TMP; stabilised formulations (see s11 and s26-s27 in table 5.1); multi-extruded at 260°C/100rpm.



Effect of hydroxylamine in Irg.1076/W.399 blend on the melt stability of m-LLDPE; 260°C/100rpm for PASSES 1, 3 and 5.

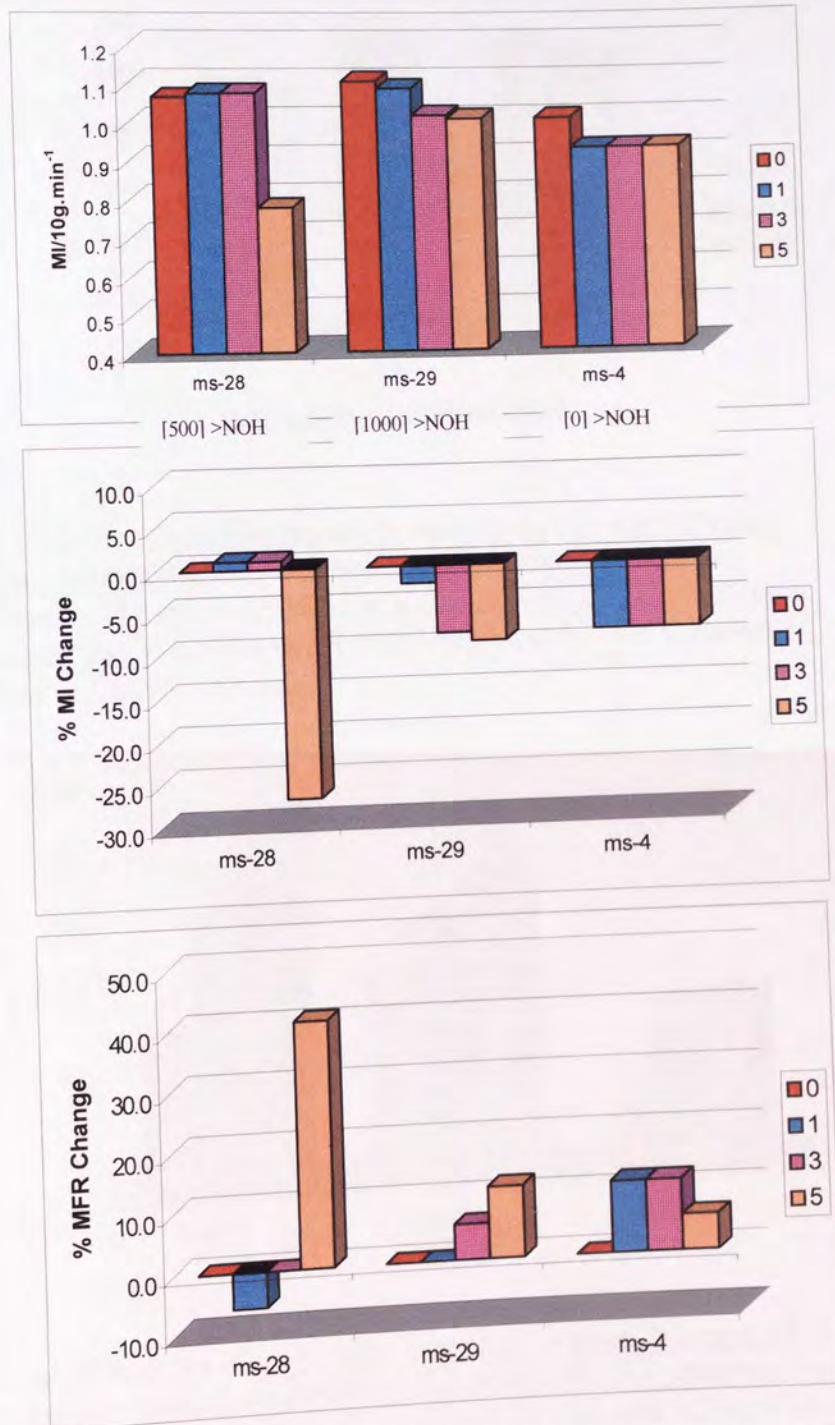


Figure 5.48 Comparison of melt stability of m-LLDPE containing a fixed Irganox 1076 and Weston 399 content (0.05 and 0.2 % w/w respectively) in the presence/absence of dialkyhydroxylamine; stabilised formulations (see s4 and s28-s29 in table 5.1); multi-extruded at 260°C/100rpm.

**Effect of increasing hydroxylamine in Irg.1076/W399 blend on melt stability of m-LLDPE; 260°C/100rpm for PASSES 1, 3 and 5.**

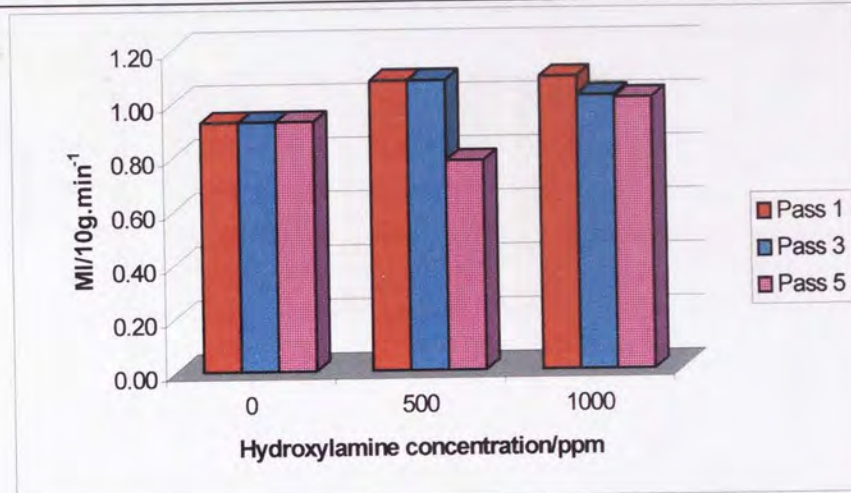


Figure 5.49 The effect of **increasing hydroxylamine concentration (Irgastab FS042)**; formulations containing a constant of Irganox 1076/Weston 399 (0.05 and 0.2 % w/w respectively) during multi-pass extrusion at 260°C/100rpm on MI, %MI change and % MFR change of stabilised m-LLDPE polymers.

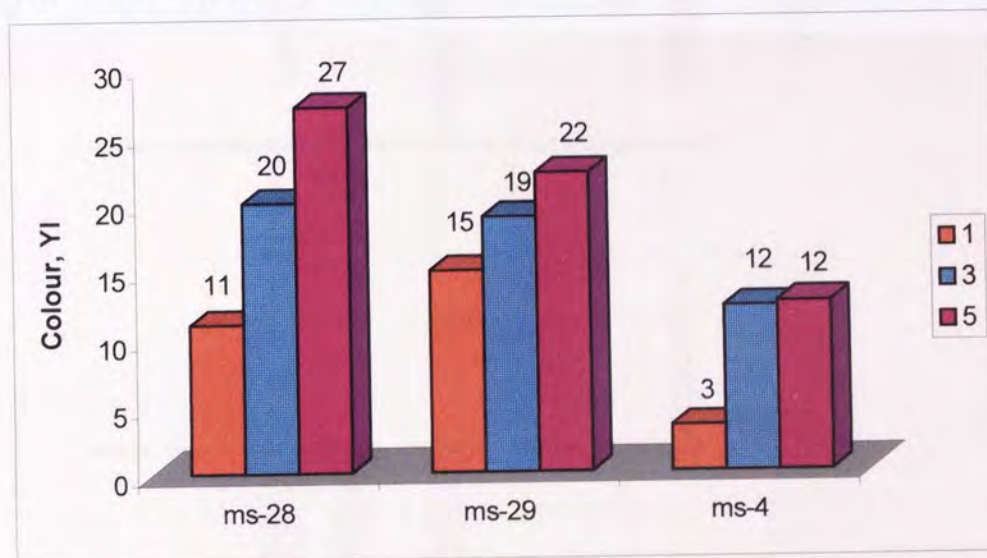


Figure 5.50 Colour stability of **m-LLDPE** containing a **fixed Irganox 1076 and Weston 399 content** (0.05 and 0.2 % w/w respectively) **in the presence/absence of dialkyhydroxylamine**; stabilised formulations (see s4 and s28-s29 in table 5.1); multi-extruded at 260°C/100rpm.



**Irg.HP136:Irg.E201:Phosphite  
1:(0.5-1):2.3**

**Effect of a 1:2.3 w/w ratio of lactone:with different phosphites in a combination with a fixed level of E on the melt stability of m-LLDPE; 260°C/100rpm for PASSES 1, 3 and 5.**

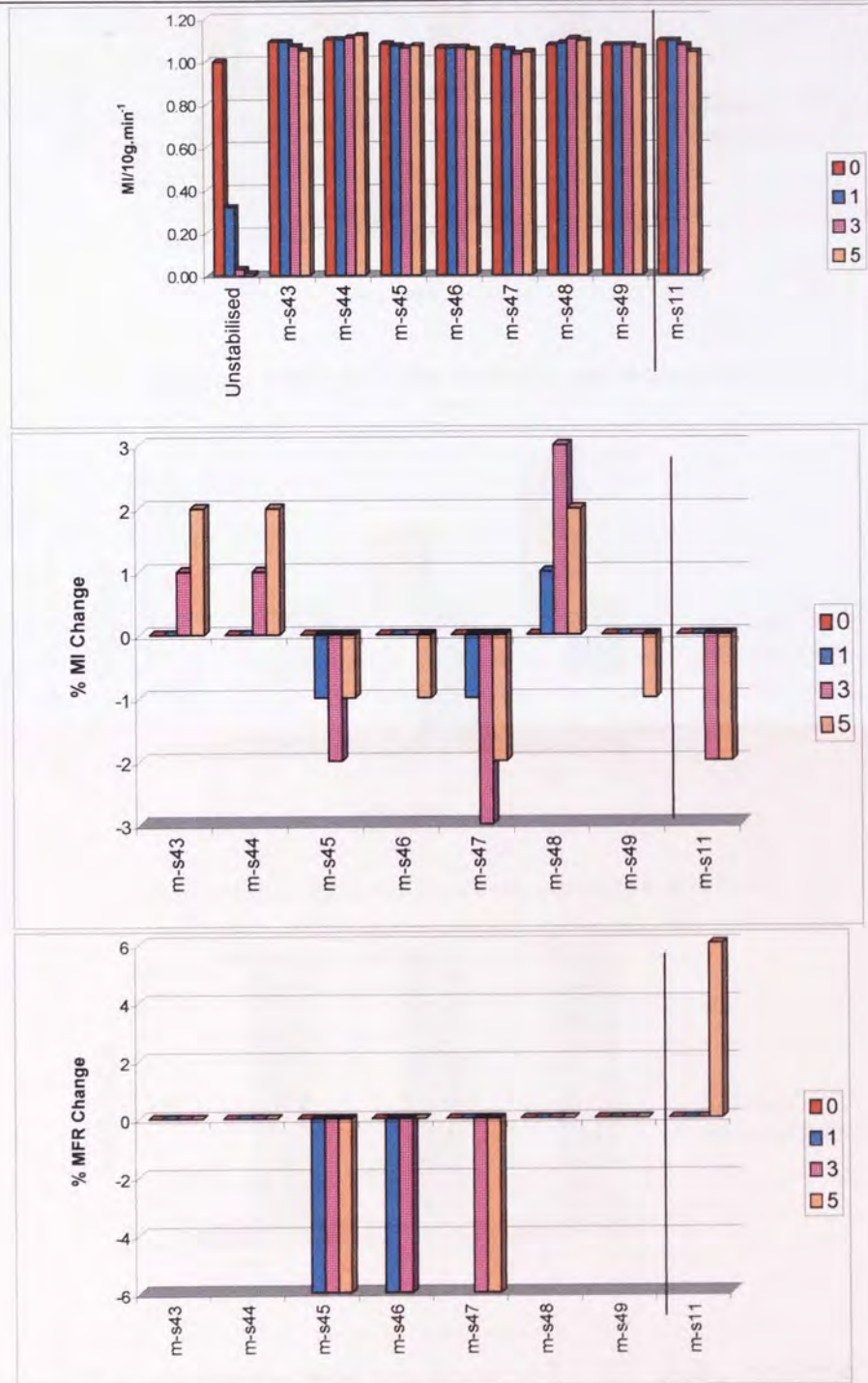


Figure 5.51 Comparison of melt stability of m-LLDPE in the presence and absence of co-additives containing Irganox HP136 in combination with different phosphites (P-EPQ, U626, Doverphos S9228 and W.399); in a 1:2.3 w/w ratio with a fixed concentration of Irganox E201 (see s43-s-49 in table 5.1); multi-extruded at 260°C/100rpm. Formulation ms-11 contains no Irg. HP136 shown for comparison



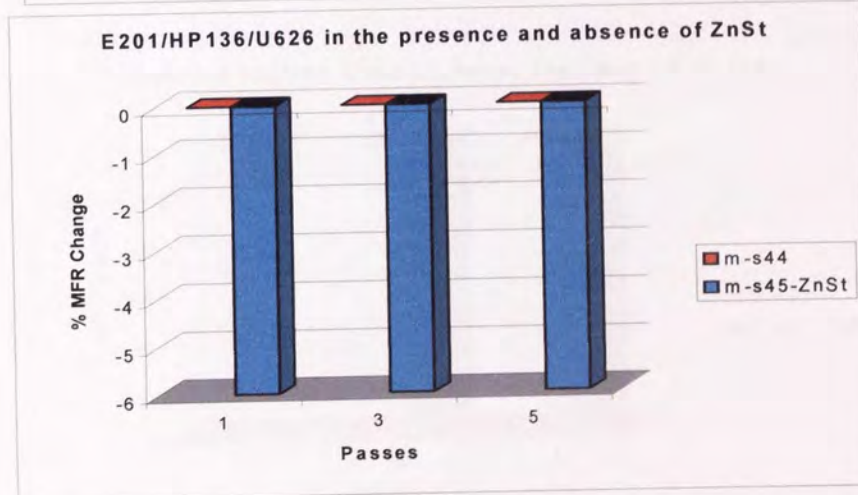
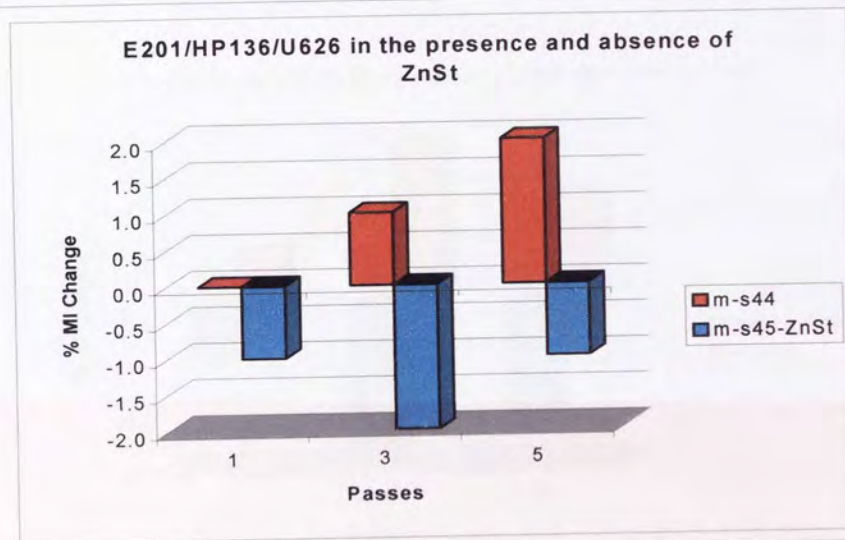
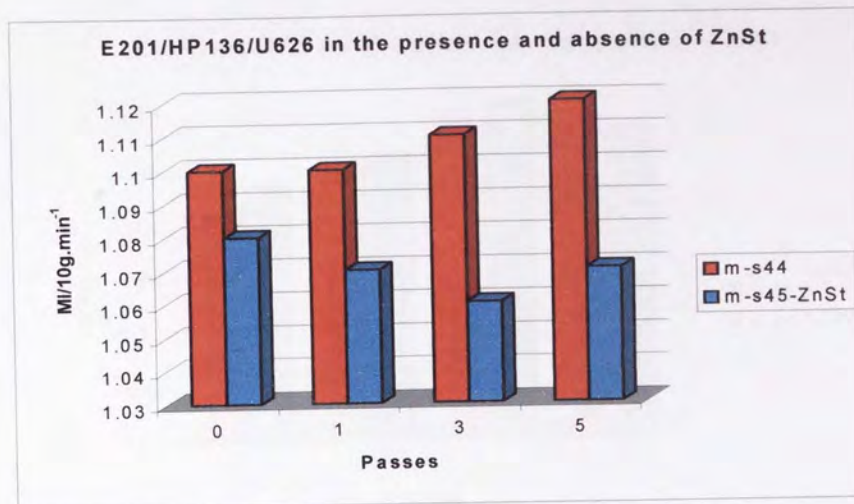


Figure 5.52 Comparison of melt stability of m-LLDPE in the presence and absence of co-additive, ZnSt, containing Irganox HP136 in combination with phosphite Ultrinox 626; stabilised formulations in a 1:2.3 w/w ratio with a fixed concentration of Irganox E201 (see s43-s-49 in table 5.1); multi-extruded at 260°C/100rpm.

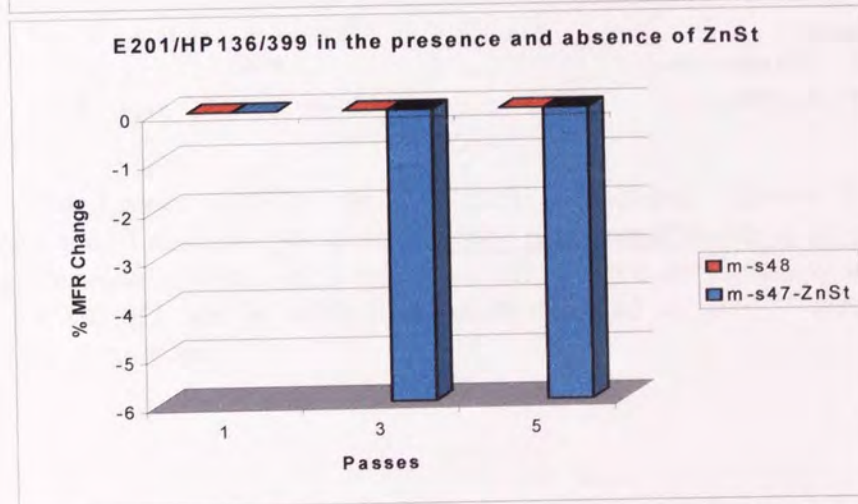
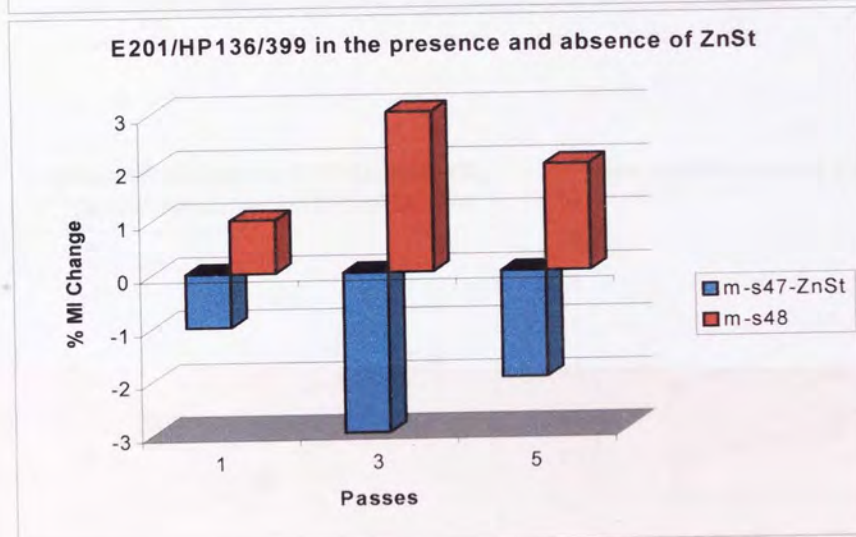
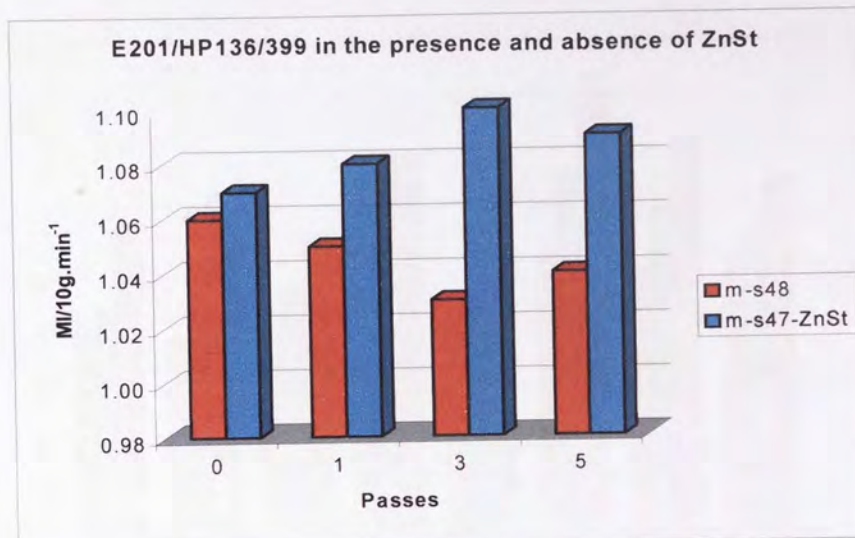


Figure 5.53 Comparison of melt stability characteristics of m-LLDPE **in the presence and absence of co-additive, ZnSt**, containing Irganox HP136 in combination **with phosphite Weston 399**; stabilised formulations in a 1:2.3 w/w ratio with a fixed concentration of Irganox E201 (see s43-s-49 in table 5.1); multi-extruded at 260°C/100rpm.



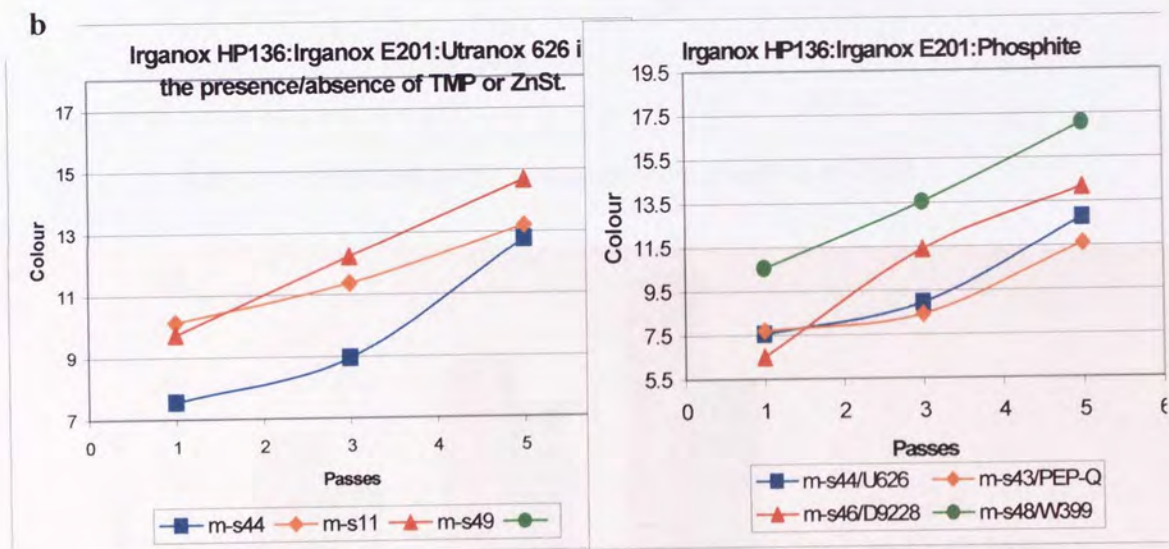
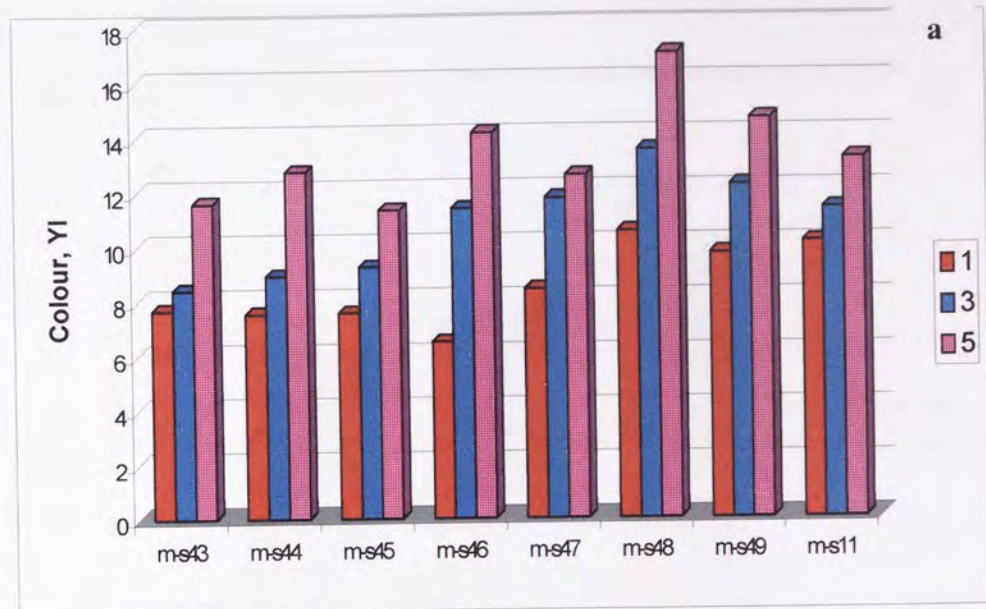


Figure 5.54 Colour stability of m-LLDPE containing Irganox HP136 in combination with different phosphites; **in the presence/absence of co-additives**; stabilised formulations in a 1:2.3 w/w ratio with a fixed concentration of Irganox E201 (see s43-s11 see in table 5.1); multi-extruded at 260°C/100rpm under atmospheric conditions.

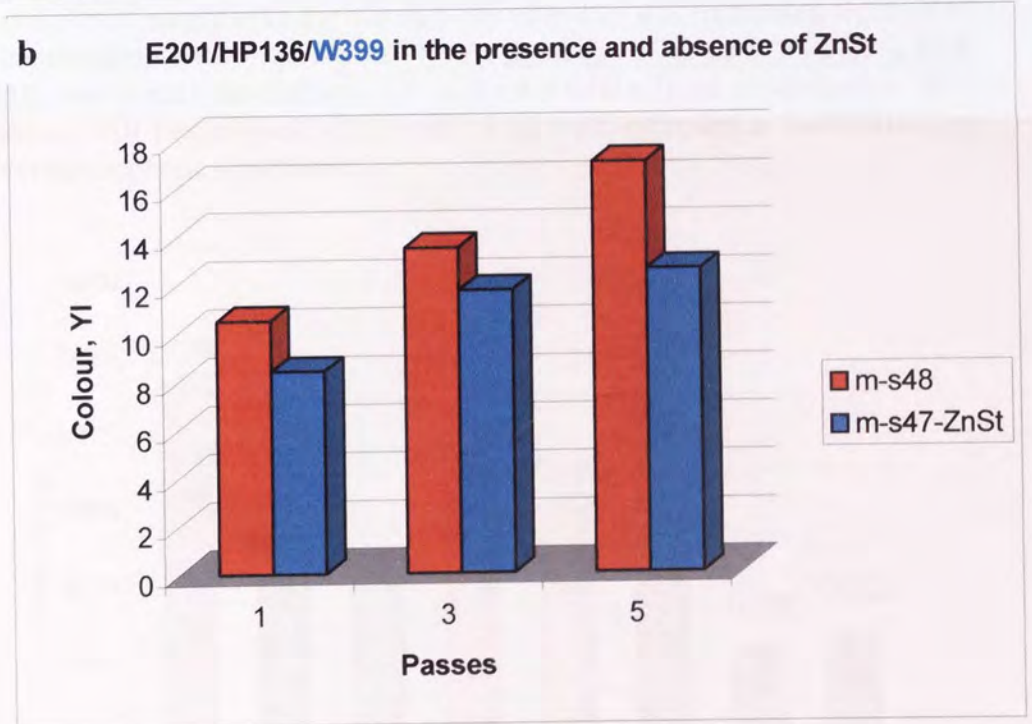
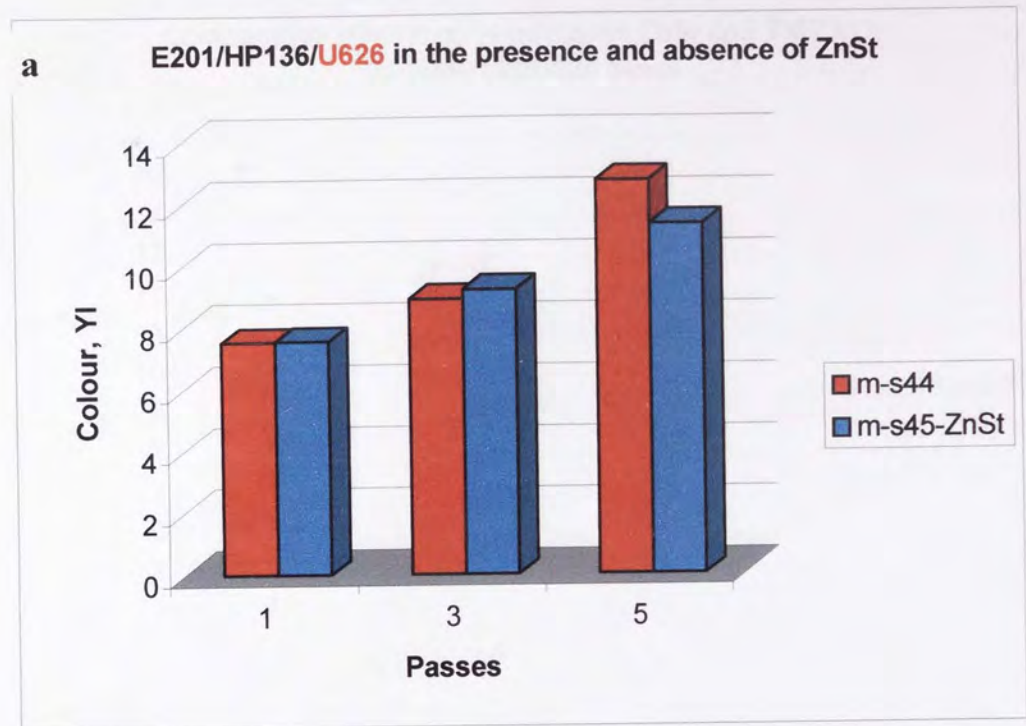


Figure 5.55 Colour stability of m-LLDPE containing Irganox HP136 in combination with different phosphites; a. U626 b. W.399; **in the presence/absence of co-additive ZnSt**; stabilised formulations in a 1:2.3 ratio with a fixed concentration of Irganox E201 (see s44, s45, s47 and s48 in table 5.1); multi-extruded at 260°C/100rpm under atmospheric conditions.



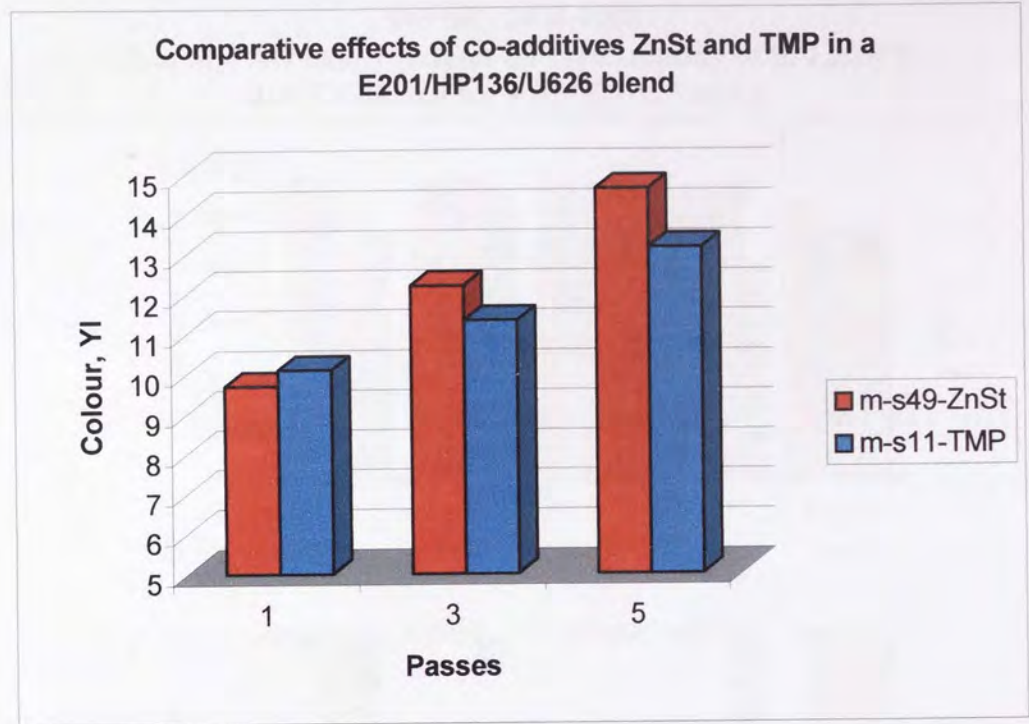


Figure 5.56 Comparative Colour stability of m-LLDPE containing Irganox E201 in combination with Ultrinox 626 **in the presence of co-additives ZnSt and TMP**; stabilised formulations in a 1:2.3 ratio with a fixed concentration of Irganox E201 (see s49 and s11 in table 5.1); multi-extruded at 260°C/100rpm under atmospheric conditions.

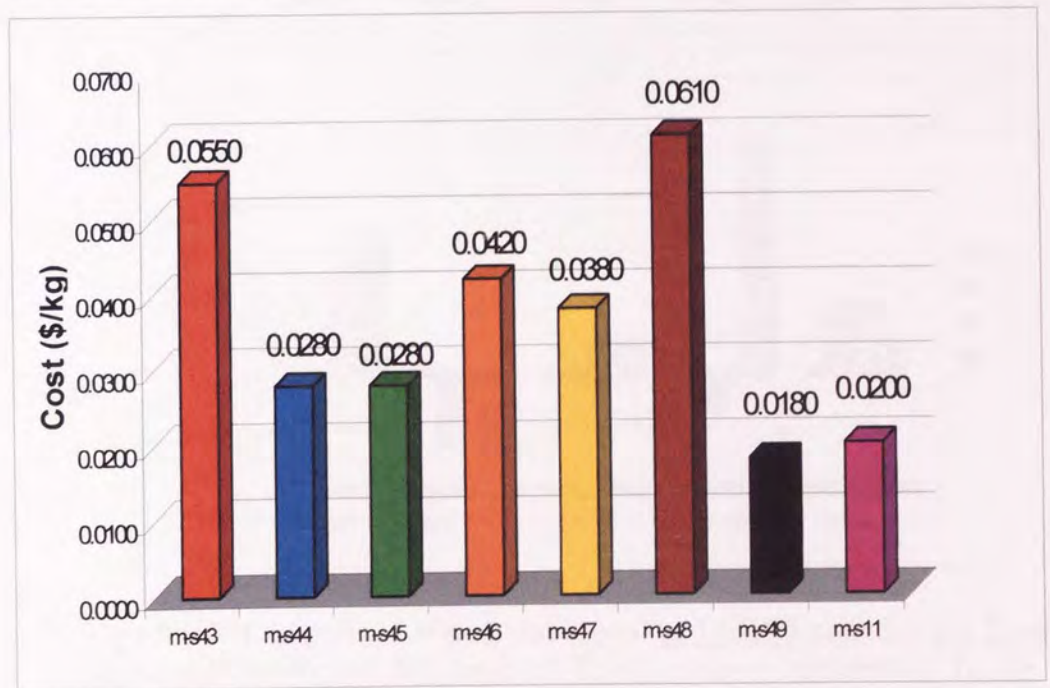


Figure 5.57. Cost effectiveness of Irganox HP136:Irganox E201:Phosphite combinations. Cost for the concentration used.



**Irg.1076:FS042:Wes.399:HALS  
500:500:2000:1000**  
**Effect of 4 AO based systems on melt stability of m-LLDPE;  
260°C/100rpm for PASSES 1, 3 and 5.**

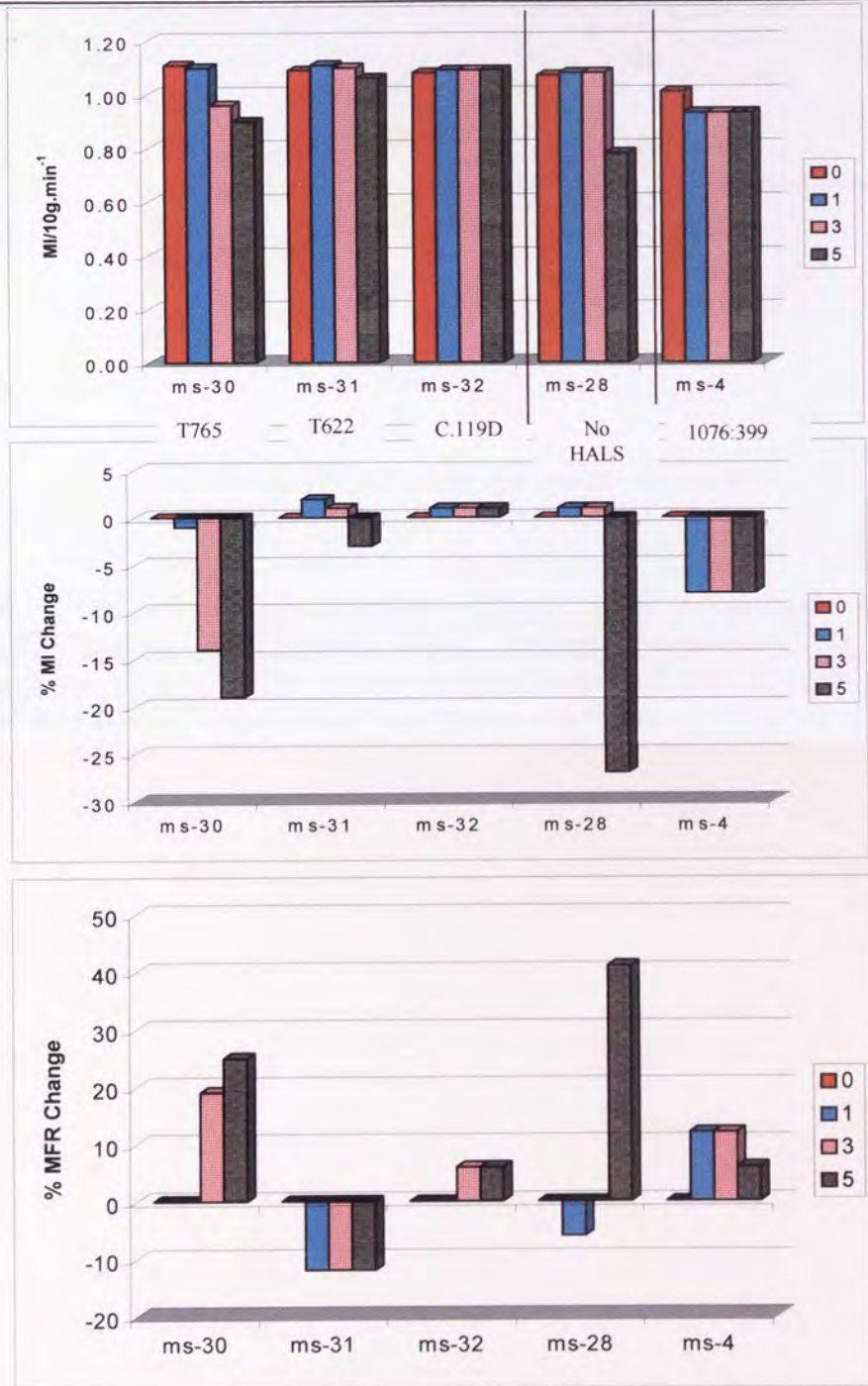


Figure 5.58 Comparison of melt stability of m-LLDPE containing a **fixed Irganox 1076/Weston 399/Irgastab FS042 content** respectively) **in the presence/absence of HALS**; stabilised formulations (s30-s32 in table 5.2); multi-extruded at 260°C/100rpm under atmospheric conditions. For comparison a Irganox 1076/Weston 399 blend is shown (s4).

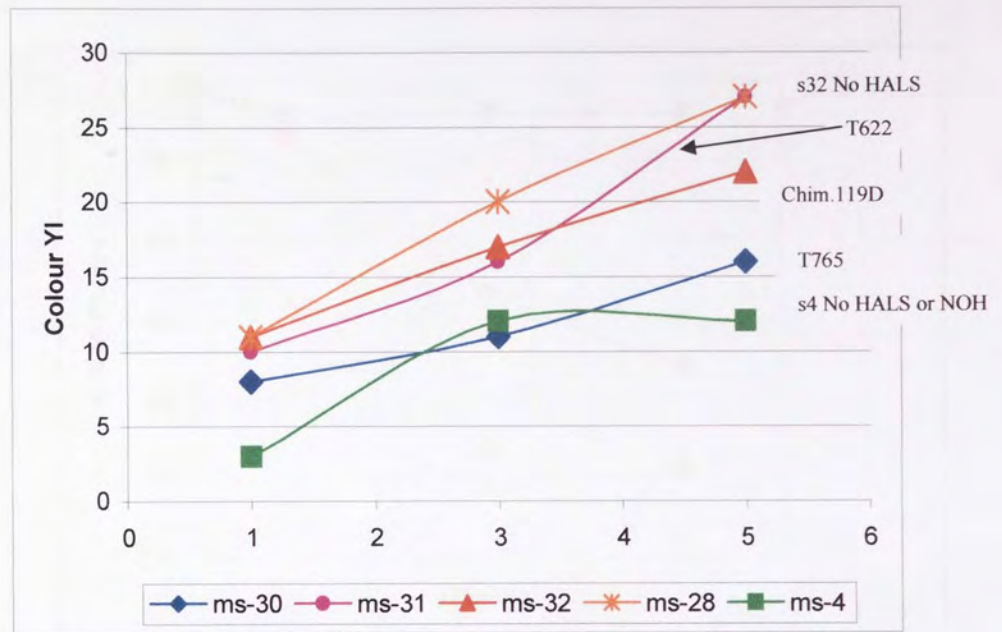


Figure 5.59 Colour stability characteristics of m-LLDPE containing a fixed Irganox 1076/Weston 399/Irgastab FS042 content respectively) in the presence/absence of HALS; PO stabilised formulations (s30-s32 in table 5.2); multi-extruded at 260°C/100rpm under atmospheric conditions.

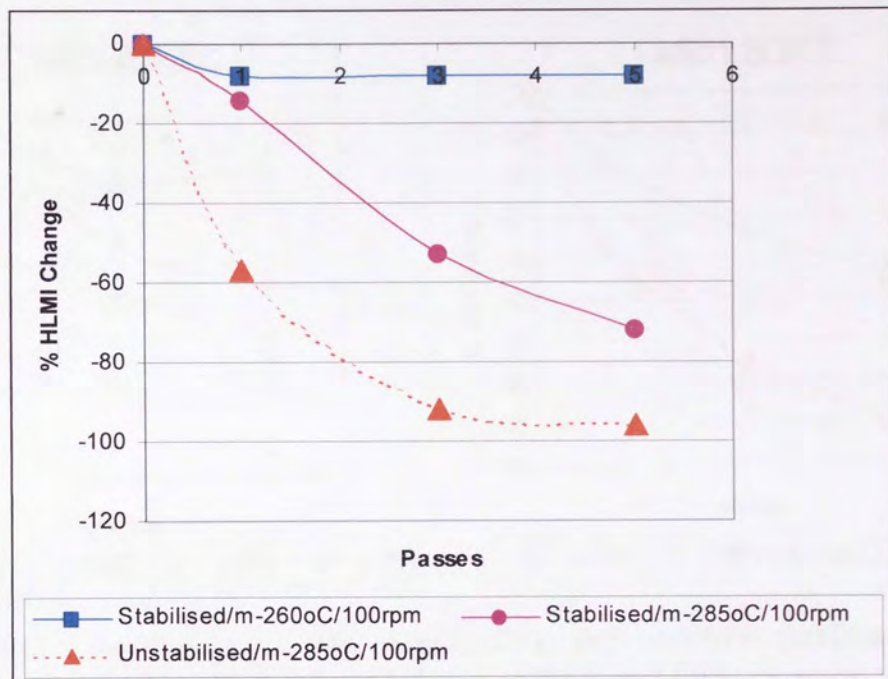


Figure 5.60 % Changes in MI of m-LLDPE stabilised with a 1:4 w/w ratio of Irganox 1076 :Weston 399; extruded at 260-285°C/100rpm. Unstabilised m-LLDPE extruded at 285°C but the same screw speed shown for comparison.



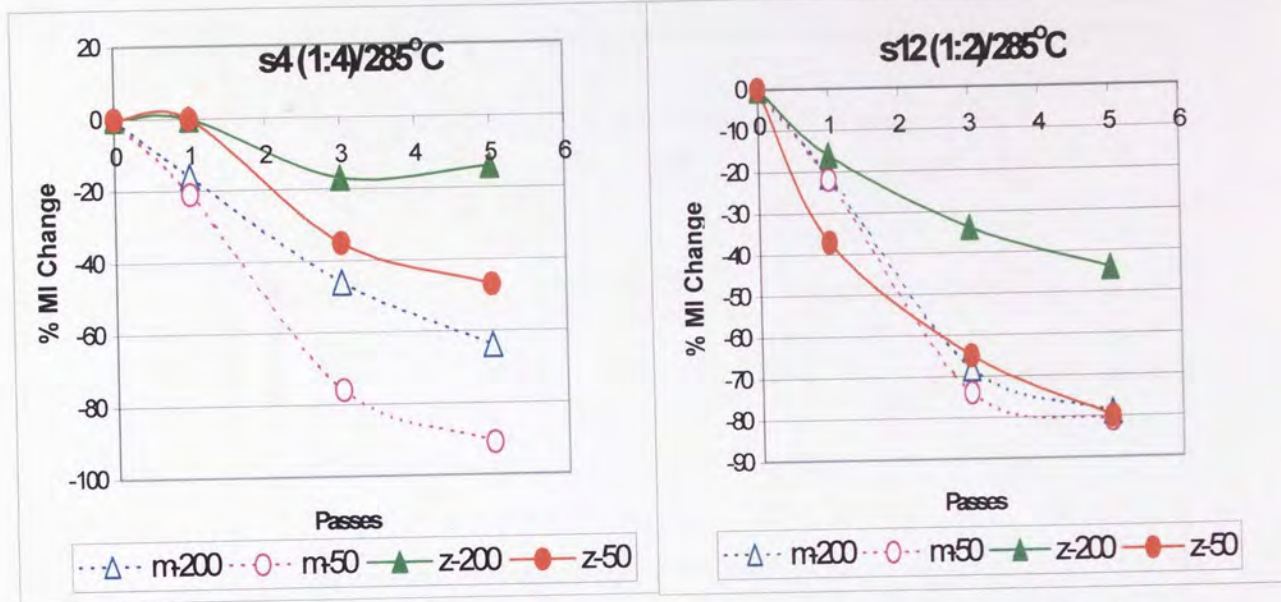


Figure 5.61 % Changes in MI of m-LLDPE and z-LLDPE stabilised with Irganox 1076:Weston 399 at 1:2 and 1:4 w/w at 285°C and different screw speeds.

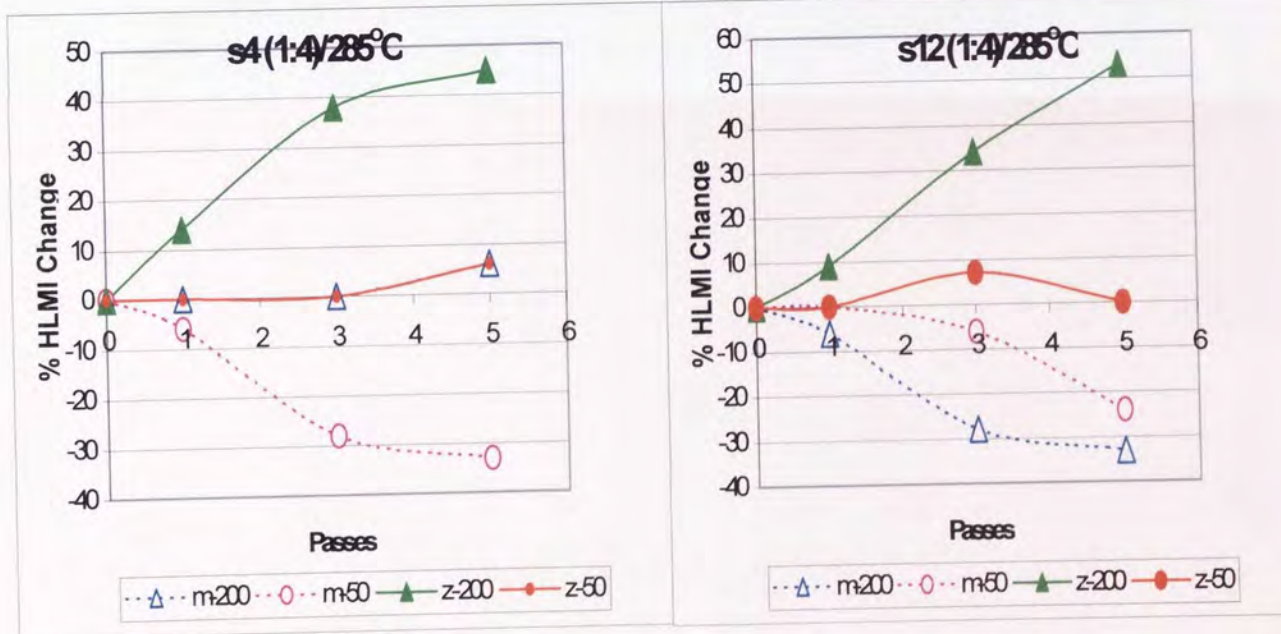


Figure 5.62 % Changes in HLMI of m-LLDPE and z-LLDPE stabilised with Irganox 1076:Weston 399 at 1:2 and 1:4 w/w at 285°C and different screw speeds.

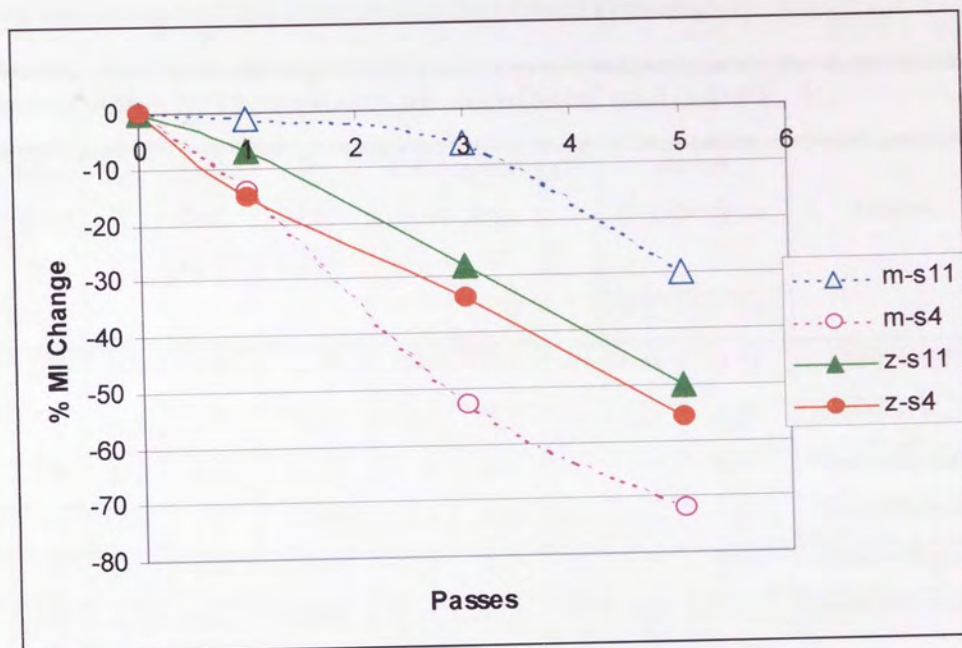


Figure 5.63 % Changes in MI of m-LLDPE and z-LLDPE stabilised with Irganox 1076 :Weston 399 at 1:2 and 1:4 w/w at 285°C/100rpm.



Table 5.4 Processing characteristics for Pass-zero stabilisation of m-LLDPE and z-LLDPE at an extrusion temperature of 210°C and a screw speed of 100rpm (under nitrogenous conditions, 4mm die) using two and three antioxidant based systems.

Processing characteristics of stabilised m-LLDPE, P <sub>0</sub>										
Formulation No. [ppm]	Screw speed, rpm	T <sub>die</sub> , °C	Output Rate, kg.h <sup>-1</sup>	P, N/m <sup>2</sup> (±5%).	I, A (±0.5)	actual T <sub>melt</sub> , °C (± 2)	ΔT <sup>1</sup>	Power Consumption		Observ.
								kW	kW.h/kg	
Virgin m-LLDPE	100	210	4.0	1150	13.0	231	+21	1.58	0.39	Melt fracture
S-4	100	210	4.0	1280	13.5	233	+23	1.64	0.41	Severe Melt fracture
S-24	100	210	4.0	1280	13.0	231	+21	1.58	0.39	Severe Melt fracture
S-28	100	210	4.0	1250	13.5	232	+22	1.64	0.41	Severe Melt fracture
S-33	100	210	4.0	1280	13.5	231	+21	1.64	0.41	Severe Melt fracture
S-43	100	210	4.0	1280	13.5	232	+22	1.64	0.41	Severe Melt fracture
Processing characteristics of stabilised z-LLDPE, P <sub>0</sub>										
Virgin z-LLDPE	100	210	4.7	850	12.0	220	+10	1.46	0.31	Slight Melt fracture
S-1	100	210	4.7	900	12.0	222	+12	1.46	0.31	Slight Melt fracture
S-2	100	210	4.6	920	12.5	223	+13	1.52	0.34	Slight Melt fracture
S-3	100	210	4.7	900	12.0	221	+11	1.46	0.31	Slight Melt fracture
S-12	100	210	4.6	870	12.5	224	+14	1.52	0.33	Slight Melt fracture
S-4	100	210	4.7	920	13.0	223	+13	1.58	0.34	Slight Melt fracture
S-11	100	210	4.6	850	12.5	224	+14	1.52	0.33	Slight Melt fracture

$$^1 \Delta T = T_{\text{melt}} - T_{\text{die}}$$

Table 5.5 Multiple extrusion characteristics of stabilised m-LLDPE and z-LLDPE polymer samples under an extrusion temperature of 285°C and a screw speed of 50rpm (under nitrogenous conditions, 4mm die) using a two antioxidant based systems. Unstabilised values are shown for comparative purposes.

Formulation No.	Sample code	Screw Speed /rpm	Die Temp. /°C	Output rate/kg.h <sup>-1</sup>	P/N/m <sup>2</sup> (±5%).	I (A) ±0.5	Actual Melt Temp/ °C	ΔT	P.C.	
									kW	kV h/k
<b>Unstabilised m-LLDPE Polymer</b>										
Unstabilised	m-285-P1	50	285	2.8	880	13.5	281	-4	0.82	0.2
	m-285-P3			2.9	875	14.0	281	-4	0.85	0.2
	m-285-P5			2.8	875	14.0	281	-4	0.85	0.3
<b>Unstabilised z-LLDPE Polymer</b>										
Unstabilised	z-285-P1	50	285	3.2	575	12.5	277	-8	0.76	0.2
	z-285-P3			3.3	495	11.5	277	-8	0.70	0.2
	z-285-P5			3.4	480	11.5	277	-8	0.70	0.2
<b>Two AO Based systems m-LLDPE Polymer Synthetic Hindered Phenol : Phosphite</b>										
m-s4	m-285-P1	50	285	2.7	700	13.5	279	-6	0.82	0.3
	m-285-P3			2.7	680	13.5	281	-4	0.82	0.3
	m-285-P5			2.7	670	13.5	282	-3	0.82	0.3
m-s4	m-285-P1	100	285	4.5	1000	14.5	290	+5	1.76	0.3
	m-285-P3			4.5	1020	14.5	293	+8	1.76	0.3
	m-285-P5			4.5	950	14.5	294	+9	1.76	0.3
m-s4	m-285-P1	200	285	8.0	965	12.5	313	+28	3.04	0.3
	m-285-P3			8.0	920	12.5	311	+26	3.04	0.3
	m-285-P5			7.9	900	12.0	311	+26	2.92	0.3
<b>Two AO Based systems z-LLDPE Polymer Synthetic Hindered Phenol : Phosphite</b>										
z-s4	z-285-P1	50	285	3.1	500	13.5	279	-6	0.82	0.2
	z-285-P3			3.1	470	13.5	279	-6	0.82	0.2
	z-285-P5			3.1	460	12.5	279	-6	0.76	0.2
z-s4	z-285-P1	100	285	6.2	690	14.0	285	0	1.70	0.2
	z-285-P3			6.2	690	14.0	285	0	1.70	0.2
	z-285-P5			6.2	660	14.0	283	-2	1.70	0.2
z-s4	z-285-P1	200	285	8.0	650	12.0	294	+9	2.92	0.3
	z-285-P3			7.4	580	11.5	301	+16	2.80	0.3
	z-285-P5			7.4	560	11.5	300	+15	2.80	0.3

Table 5.6: Melt stability characteristics of Pass-zero (Po) stabilised **m-LLDPE** samples processed at 210°C/100rpm/under nitrogen; containing 'combinations' s1-s49 (see table 5.1&5.2).

Code	Screw Speed /rpm	Melt Flow Measurements/g10.min <sup>-1</sup>					
		MI	% MI Change <sup>5</sup>	HLMI	% HLMI Change <sup>6</sup>	MFR <sup>7</sup>	% MFR Change <sup>8</sup>
Virgin	-	1.00	0	17.0	0	17	0
Unstabilised Pass 1	100	0.32	-68	12.6	-26	39	+129
<b>Two AO Based systems</b>							
<b>Synthetic hindered phenol (Irganox 1076): Phosphite (Weston 399)</b>							
S-1	100	1.04	+4	17.0	0	16	-6
S-2	100	1.04	+4	17.0	0	16	-6
S-3	100	1.03	+3	17.0	0	16	-6
S-4	100	1.01	+1	17.0	0	17	0
S-12	100	1.00	0	17.0	0	17	0
<b>XP-60 Two AO Based systems</b>							
<b>Lactone (HP136): Phosphite</b>							
S-33	100	1.09	+9	17.9	+5	16	-6
S-34	100	1.08	+8	17.7	+4	16	-6
S-35	100	1.09	+9	17.6	+3	16	-6
S-36	100	1.06	+6	18.1	+6	17	0
S-37	100	1.06	+6	17.6	+3	17	0
<b>XP-490 Three AO Based systems</b>							
<b>Synthetic Hindered Phenol (Irg.1076): Lactone (HP136) : Phosphite</b>							
S-22	100	1.08	+8	17.5	+3	16	-6
S-23	100	1.08	+8	17.3	+2	16	-6
S-24	100	1.09	+9	17.4	+2	16	-6

<sup>5</sup> MI is defined as the MI of the virgin polymer; % MI change = (MI sample-MI virgin)/MI virgin \* 100

<sup>6</sup> % HLMI change same as above except using HLMI.

<sup>7</sup> MFR = HLMI/MI

<sup>8</sup> % MFR change = (MFR sample-MFR virgin)/ MFR virgin \* 100

Table 5.6: continued.....

Code	Screw Speed /rpm	Melt Flow Measurements/g10.min <sup>-1</sup>					
		MI	% MI Change <sup>5</sup>	HLMI	% HLMI Change <sup>6</sup>	MFR <sup>7</sup>	% MFR Change <sup>8</sup>
Virgin	-	1.00	0	17.0	0	17	0
Unstabilised Pass 1	100	0.32	-68	12.6	-26	39	+129
S-25	100	1.09	+9	18.0	+6	17	0
S-38	100	1.07	+7	17.5	+3	16	-6
S-39	100	1.08	+8	17.5	+3	16	-6
S-40	100	1.10	+10	17.6	+3	16	-6
S-41	100	1.09	+9	17.4	+2	16	-6
S-42	100	1.09	+9	17.7	+4	16	-6
<b>Three AO Based systems</b>							
<b>Biological hindered phenol (Irg.E201): Hydroxylamine (FS042): Phosphite (U.626): TMP</b>							
S-26	100	1.04	+4	18.2	+7	17	0
S-27	100	1.04	+9	17.8	+5	16	-6
<b>Three AO Based systems</b>							
<b>Synthetic hindered phenol (Irg.1076): Hydroxylamine (FS042): Phosphite (W399)</b>							
S-28	100	1.07	+7	17.8	+5	17	0
S-29	100	1.11	+11	17.4	+2	16	-6
<b>Four AO Based systems</b>							
<b>Synthetic hindered phenol (Irg.1076): Hydroxylamine (FS042): Phosphite (W399): R-HALS</b>							
S-30	100	1.11	+11	17.8	+5	16	-6
S-31	100	1.09	+9	18.1	+6	17	0
S-32	100	1.08	+8	17.7	+4	16	-6

<sup>5</sup> MI is defined as the MI of the virgin polymer; % MI change = (MI sample-MI virgin)/MI virgin \* 100

<sup>6</sup> % HLMI change same as above except using HLMI.

<sup>7</sup> MFR = HLMI/MI

<sup>8</sup> % MFR change = (MFR sample-MFR virgin)/ MFR virgin \* 100

Table 5.6: continued.....

Code	Screw Speed /rpm	Melt Flow Measurements/g10.min <sup>-1</sup>					
		MI	% MI Change <sup>5</sup>	HLMI	% HLMI Change <sup>6</sup>	MFR <sup>7</sup>	% MFR Change <sup>8</sup>
Virgin	-	1.00	0	17.0	0	17	0
Unstabilised Pass 1	100	0.32	-68	12.6	-26	39	+129
Three AO Based systems							
Biological Hindered Phenol (Irg.201): Lactone (HP136): Phosphite							
S-43	100	1.09	+9	17.7	+4	16	-6
S-44	100	1.10	+10	18.0	+6	16	-6
S-45	100	1.08	+8	17.9	+5	17	0
S-46	100	1.06	+6	17.7	+4	17	0
S-47	100	1.06	+6	17.6	+3	17	0
S-48	100	1.07	+7	17.6	+3	16	-6
S-49	100	1.07	+7	17.3	+2	16	-6
S-11	100	1.09	+9	17.4	+2	16	-6
S-13	100	1.05	+5	18.0	+6	17	0

<sup>5</sup> MI is defined as the MI of the virgin polymer; % MI change = (MI sample-MI virgin)/MI virgin \* 100

<sup>6</sup> % HLMI change same as above except using HLMI.

<sup>7</sup> MFR = HLMI/MI

<sup>8</sup> % MFR change = (MFR sample-MFR virgin)/ MFR virgin \* 100



Table 5.7: Melt stability characteristics of Pass-zero (Po) stabilised **z-LLDPE** samples processed at 210°C/100rpm/under nitrogen; containing 'combinations' s1-s13 (see table 5.1). Unstabilised values are shown for comparison.

Code	Screw Speed /rpm	Melt Flow Measurements/g10.min <sup>-1</sup>					
		MI	% MI Change <sup>5</sup>	HLMI	% HLMI Change <sup>6</sup>	MFR <sup>7</sup>	% MFR Change <sup>8</sup>
Virgin	-	1.00	0	32.0	0	32	0
Unstabilised Pass 1	50	0.77	-23	29	-9	38	+19
<b>Two AO Based systems</b>							
<b>Synthetic hindered phenol (Irganox 1076): Phosphite (Weston 399)</b>							
S-1	100	1.01	+1	30	-6	30	-6
S-2	100	1.00	0	30	-6	30	-6
S-3	100	1.00	0	32	0	32	0
S-4	100	1.05	+5	33	+3	31	-3
S-12	100	1.03	+3	30	0	29	-9
<b>Three AO Based systems</b>							
<b>Biological Hindered Phenol (Irg.201): Lactone (HP136): Phosphite</b>							
S-11	100	1.05	0	31	-3	29	-9
S-13	100	1.04	0	31	-3	29	-9

<sup>5</sup> MI is defined as the MI of the virgin polymer; % MI change = (MI sample-MI virgin)/MI virgin \* 100

<sup>6</sup> % HLMI change same as above except using HLMI.

<sup>7</sup> MFR = HLMI/MI

<sup>8</sup> % MFR change = (MFR sample-MFR virgin)/ MFR virgin \* 100

Table 5.8 Effect of **Irganox 1076:Weston 399 AO systems** (at varying concentrations, see s1 to s12, in table 5.1) on the melt stability of **m-LLDPE** during Pass zero (Po) and Multi-pass extrusion conditions. Unstabilised polymers extruded under similar conditions are shown for comparison.

Code	Temp /°C	Speed /rpm	Melt flow measurements /10g.min <sup>-1</sup>					
			MI	%MI change <sup>1</sup>	HLMI	%HLMI change <sup>2</sup>	MFR <sup>3</sup>	%MFR <sup>4</sup> change
Virgin m-LLDPE	-	-	1.00	0	17	0	17	0
Unstab m-P1	210	50	0.35	-65	12	-29	34	100
Unstab m-P3			0.09	-91	9	-47	100	488
Unstab m-P5			0.03	-97	6	-65	200	1076
Unstab m-P1	285	50	0.25	-75	12	-29	48	182
Unstab m-P3			0.06	-94	8	-53	133	382
Unstab m-P5			0.01	-99	6	-65	600	3429
Unstab m-P1	285	200	0.46	-54	18	6	39	129
Unstab m-P3			0.12	-88	17	0	142	735
Unstab m-P5			0.08	-92	16	-6	200	1076
<b>Synthetic Hindered Phenol (Irganox 1076) : Phosphite (Wes.399)</b>								
<b>S2 1:1.3 w/w ratio (750:1000ppm)</b>								
m-S2-210-PO	210	100/N2	1.04	0	17	0	16	0
m-S2-210-P1	210	50	0.99	-5	16	-6	16	0
m-S2-210-P3			0.92	-12	16	-6	17	6
m-S2-210-P5			0.56	-46	16	-6	29	81
m-S2-210-PO	210	100/N2	1.04	0	17	0	16	6
m-S2-285-P1	285	50	0.34	-67	12	-29	35	119
m-S2-285-P3			0.20	-81	11	-35	55	244
m-S2-285-P5			0.11	-89	11	-35	100	525
<b>S12 1:2.0 w/w ratio (500:1000ppm)</b>								
m-S12-210-P0	210	100/N2	1.00	0	17	0	17	0
m-S12-285-P1	285	50	0.78	-22	17	0	17	0
m-S12-285-P3			0.26	-74	16	-6	30	76
m-S12-285-P5			0.19	-81	13	-24	45	165
m-S12-210-P0	210	100/N2	1.06	0	18	0	17	0
m-S12-285-P1	285	200	0.84	-21	17	-6	20	18
m-S12-285-P3			0.34	-68	13	-28	38	124
m-S12-285-P5			0.22	-79	12	-33	55	224
<b>S1 1:2.7 w/w ratio (500:1500ppm)</b>								
m-S1-210-P0	210	100/N2	1.04	0	17	0	16	0
m-S1-210-P1	210	50	1.02	-2	17	0	17	6
m-S1-210-P3			1.01	-3	17	0	17	6
m-S1-210-P5			1.00	-4	17	0	17	6

<sup>1</sup> %MI change = (MI<sub>sample</sub> - MI<sub>virgin</sub>)/MI<sub>virgin</sub> x 100

<sup>2</sup> % HLMI change = (HLMI<sub>sample</sub> - HLMI<sub>virgin</sub>)/HLMI<sub>virgin</sub> x 100

<sup>3</sup> MFR = HLMI/MI

<sup>4</sup> %MFR change = (MFR<sub>sample</sub> - MFR<sub>virgin</sub>)/MFR<sub>virgin</sub> x 100

Table 5.8 .....Continued

Code	Temp /°C	Speed /rpm	Melt flow measurements /10g.min <sup>-1</sup>					
			MI	%MI change <sup>5</sup>	HLMI	%HLMI change <sup>6</sup>	MFR <sup>7</sup>	%MFR change <sup>8</sup>
m-S1-210-P0	210	100/N2	1.04	0	17	0	16	0
m-S1-285-P1	285	50	0.65	-37	15	-12	23	44
m-S1-285-P3			0.36	-65	14	-18	39	144
m-S1-285-P5			0.15	-85	12	-29	80	400
<b>S3 1:3.0 w/w ratio (750:2000ppm)</b>								
m-S3-210-P0	210	100/N2	1.03	0	17	0	16	0
m-S3-210-P1	210	50	1.05	2	17	0	16	0
m-S3-210-P3			1.02	-1	17	0	17	6
m-S3-210-P5			1.03	0	17	0	17	6
<b>S4 1:4.0 w/w ratio (500:2000ppm)</b>								
m-S4-210-P0	210	100/N2	1.06	0	18	0	17	0
m-S4-285-P1	285	50	0.84	-21	17	-6	20	18
m-S4-285-P3			0.25	-76	13	-28	52	206
m-S4-285-P5			0.10	-91	12	-33	120	606
m-S4-210-P0	210	100/N2	1.00	0	17	0	17	0
m-S4-285-P1	285	200	0.84	-16	17	0	20	18
m-S4-285-P3			0.54	-46	17	0	31	82
m-S4-285-P5			0.36	-64	18	6	50	194

<sup>5</sup> %MI change = (MI<sub>sample</sub> - MI<sub>virgin</sub>)/MI<sub>virgin</sub> x 100

<sup>6</sup> % HLMI change = (HLMI<sub>sample</sub> - HLMI<sub>virgin</sub>)/HLMI<sub>virgin</sub> x 100

<sup>7</sup> MFR = HLMI/MI

<sup>8</sup> %MFR change = (MFR<sub>sample</sub> - MFR<sub>virgin</sub>)/MFR<sub>virgin</sub> x 100

Table 5.9 Effect of **Irganox 1076:Weston 399 AO systems** (at varying concentrations, see s1 to s12, in table 5.1) on the melt stability of **z-LLDPE** during Pass zero (Po) and Multi-pass extrusion conditions. Unstabilised polymers extruded under similar conditions are shown for comparison.

Code	Temp /°C	Speed /rpm	Melt flow measurements /10g.min <sup>-1</sup>					
			MI	%MI change <sup>9</sup>	HLMI	%HLMI change <sup>10</sup>	MFR <sup>11</sup>	%MFR <sup>12</sup> change
Virgin z-LLDPE	-	-	1.00	0	32	0	32	0
Unstab z-P1	210	50	0.77	-23	29	-9	38	19
Unstab z-P3			0.37	-63	20	-38	54	69
Unstab z-P5			0.22	-78	28	-13	127	297
Unstab z-P1	285	50	0.51	-49	31	-3	61	91
Unstab z-P3			0.19	-81	37	16	195	509
Unstab z-P5			0.18	-82	33	3	183	472
Unstab z-P1	285	200	0.71	-29	35	9	49	53
Unstab z-P3			0.44	-56	42	31	95	197
Unstab z-P5			0.33	-67	43	34	130	306
<b>Synthetic Hindered Phenol (Irganox 1076) : Phosphite (Wes. 399)</b>								
<b>S2 1:1.3 w/w ratio (750:1000ppm)</b>								
z-S2-210-PO	210	100/N2	1.00	0	30	0	30	0
z-S2-210-P1	210	50	1.00	0	29	-3	29	-3
z-S2-210-P3			0.84	-16	27	-10	32	7
z-S2-210-P5			0.58	-42	25	-17	43	43
z-S2-210-PO	210	100/N2	1.00	0	30	0	30	0
z-S2-285-P1	285	50	0.56	-44	28	-7	50	67
z-S2-285-P3			0.26	-74	27	-10	104	247
z-S2-285-P5			0.25	-75	31	3	124	313
<b>S12 1:2.0 w/w ratio (500:1000ppm)</b>								
z-S12-210-P0	210	100/N2	1.03	0	30	0	29	0
z-S12-285-P1	285	50	0.65	-37	30	0	46	59
z-S12-285-P3			0.36	-65	32	7	89	207
z-S12-285-P5			0.21	-80	30	0	143	393
z-S12-210-P0	210	100/N2	1.02	0	32	0	31	0
z-S12-285-P1	285	200	0.86	-16	35	9	41	32
z-S12-285-P3			0.67	-34	43	34	64	106
z-S12-285-P5			0.57	-44	49	53	86	177
<b>S1 1:2.7 w/w ratio (500:1500ppm)</b>								
z-S1-210-P0	210	100/N2	1.01	0	30	0	30	0
z-S1-210-P1	210	50	1.01	0	31	3	31	3
z-S1-210-P3			0.94	-7	30	0	32	7
z-S1-210-P5			0.62	-39	27	-10	44	47

$$^9 \%MI \text{ change} = (MI_{\text{sample}} - MI_{\text{virgin}}) / MI_{\text{virgin}} \times 100$$

$$^{10} \%HLMI \text{ change} = (HLMI_{\text{sample}} - HLMI_{\text{virgin}}) / HLMI_{\text{virgin}} \times 100$$

$$^{11} MFR = HLMI / MI$$

$$^{12} \%MFR \text{ change} = (MFR_{\text{sample}} - MFR_{\text{virgin}}) / MFR_{\text{virgin}} \times 100$$

Table 5.9 .....Continued

Code	Temp /°C	Speed /rpm	Melt flow measurements /10g.min <sup>-1</sup>					
			MI	%MI change <sup>13</sup>	HLMI	%HLMI change <sup>14</sup>	MFR <sup>15</sup>	%MFR change <sup>16</sup>
z-S1-210-P0	210	100/N2	1.01	0	30	0	30	0
z-S1-285-P1	285	50	1.01	0	32	7	32	7
z-S1-285-P3			0.56	-44	34	13	61	103
z-S1-285-P5			0.33	-67	35	17	106	253
<b>S3 1:3.0 w/w ratio (750:2000ppm)</b>								
z-S3-210-P0	210	100/N2	1.00	0	32	0	32	0
z-S3-210-P1	210	50	1.01	0	29	-9	29	-9
z-S3-210-P3			1.05	5	29	-9	28	-13
z-S3-210-P5			0.98	-2	29	-9	30	-6
<b>S4 1:4.0 w/w ratio (500:2000ppm)</b>								
z-S4-210-P0	210	100/N2	1.05	0	33	0	31	0
z-S4-285-P1	285	50	1.05	0	33	0	31	0
z-S4-285-P3			0.68	-35	33	0	49	58
z-S4-285-P5			0.56	-47	35	6	63	103
z-S4-210-P0	210	100	1.03	0	29	0	28	0
z-S4-285-P1	285	200	1.03	0	33	14	32	14
z-S4-285-P3			0.86	-17	40	38	46	64
z-S4-285-P5			0.89	-14	42	45	47	176

$$^{13} \%MI \text{ change} = (MI_{\text{sample}} - MI_{\text{virgin}}) / MI_{\text{virgin}} \times 100$$

$$^{14} \% \text{ HLMI change} = (HLMI_{\text{sample}} - HLMI_{\text{virgin}}) / HLMI_{\text{virgin}} \times 100$$

$$^{15} \text{ MFR} = HLMI / MI$$

$$^{16} \% \text{ MFR change} = (MFR_{\text{sample}} - MFR_{\text{virgin}}) / MFR_{\text{virgin}} \times 100$$



Table 5.10 Effect of Synthetic and Biological hindered phenol in combination with different phosphites on the melt stability of stabilised **z-LLDPE** polymer samples; (see s4 to s13, in table 5.1), during Pass zero (Po) and Multi-pass extrusion conditions. Unstabilised z-LLDPE extruded under similar conditions is shown for comparison.

Code	Temp /°C	Speed /rpm	Melt flow measurements /10g.min <sup>-1</sup>					
			MI	%MI change <sup>17</sup>	HLMI	%HLMI change <sup>18</sup>	MFR <sup>19</sup>	%MFR <sup>20</sup> change
Virgin z-LLDPE	-	-	1.00	0	32	0	32	0
Unstab z-P1	285	50	0.51	-49	31	-3	61	91
Unstab z-P3			0.19	-81	37	16	195	509
Unstab z-P5			0.18	-82	33	3	183	472
Unstab z-P1	285	100	0.68	-32	29	-9	43	34
Unstab z-P3			0.32	-68	30	-6	97	203
Unstab z-P5			0.22	-78	30	-6	136	325
Unstab z-P1	285	200	0.71	-29	35	9	49	53
Unstab z-P3			0.44	-56	42	31	95	197
Unstab z-P5			0.33	-67	43	34	130	306
<b>Synthetic Hindered Phenol (Irganox 1076) : Phosphite (Wes. 399)</b>								
<b>S4 1:4.0 w/w ratio</b>								
z-S4-210-PO	210	100/N2	1.05	0	31	0	30	0
z-S4-285-P1	285	100	0.88	-15	33	6	38	27
z-S4-285-P3			0.68	-34	37	20	54	80
z-S4-285-P5			0.46	-56	44	41	96	220
<b>Biological Hindered Phenol (Irg. E201) : Phosphite (Wes. 399): TMP</b>								
<b>S13 1:2.0:1.5 w/w ratio</b>								
z-S13-210-PO	210	100/N2	1.04	0	31	0	30	0
z-S13-285-P1	285	100	1.00	-4	31	-1	31	3
z-S13-285-P3			0.70	-33	30	-5	43	4
z-S13-285-P5			0.44	-58	26	-15	59	97
<b>Biological Hindered Phenol (Irg. E201) : Phosphite (U.626): TMP</b>								
<b>S11 1:2.0:1.5 w/w ratio</b>								
z-S11-210-PO	210	100/N2	1.05	0	31	0	30	0
z-S11-285-P1	285	100	0.98	-7	31	-2	32	7
z-S11-285-P3			0.76	-28	30	-5	39	30
z-S11-285-P5			0.53	-50	27	-14	51	70

<sup>17</sup> %MI change = (MI<sub>sample</sub> - MI<sub>virgin</sub>)/MI<sub>virgin</sub> x 100

<sup>18</sup> % HLMI change = (HLMI<sub>sample</sub> - HLMI<sub>virgin</sub>)/HLMI<sub>virgin</sub> x 100

<sup>19</sup> MFR = HLMI/MI

<sup>20</sup> %MFR change = (MFR<sub>sample</sub> - MFR<sub>virgin</sub>)/MFR<sub>virgin</sub> x 100

Table 5.11 Effect of Synthetic and Biological hindered phenol in combination with different phosphites on the melt stability of stabilised m-LLDPE polymer samples; (see s4 to s13, in table 5.1), during Pass zero (Po) and Multi-pass extrusion conditions. Unstabilised z-LLDPE extruded under similar conditions is shown for comparison.

Code	Temp /°C	Speed /rpm	Melt flow measurements /10g.min <sup>-1</sup>					
			MI	%MI change <sup>21</sup>	HLMI	%HLMI change <sup>22</sup>	MFR <sup>23</sup>	%MFR <sup>24</sup> change
Virgin m-LLDPE	-	-	1.00	0	17	0	17	0
Unstab m-P1	285	50	0.25	-75	12	-29	48	182
Unstab m-P3			0.06	-94	8	-53	133	382
Unstab m-P5			0.01	-99	6	-65	600	3429
Unstab m-P1	285	100	0.43	-57	14	-20	33	94
Unstab m-P3			0.08	-92	10	-41	125	635
Unstab m-P5			0.04	-96	9	-46	225	1224
Unstab m-P1	285	200	0.46	-54	18	6	39	129
Unstab m-P3			0.12	-88	17	0	142	735
Unstab m-P5			0.08	-92	16	-6	200	1076
<b>Synthetic Hindered Phenol (Irganox 1076) : Phosphite (Wes. 399)</b>								
<b>S4 1:4.0 w/w ratio</b>								
m-S4-210-PO	210	100/N2	1.06	0	18	0	17.0	0
m-S4-285-P1	285	50	0.84	-21	17	-6	20	18
m-S4-285-P3			0.25	-76	13	-28	52	206
m-S4-285-P5			0.10	-91	12	-33	120	606
m-S4-210-PO	210	100/N2	1.06	0	17	0	16	0
m-S4-285-P1	285	100	0.86	-14	17	2	20	25
m-S4-285-P3			0.47	-53	16	-5	34	113
m-S4-285-P5			0.28	-72	16	-6	57	256
m-S4-210-PO	210	100/N2	1.00	0	17	0	17	0
m-S4-285-P1	285	200	0.84	-16	17	0	20	18
m-S4-285-P3			0.54	-46	17	0	31	82
m-S4-285-P5			0.36	-64	15	-11	50	194
<b>Biological Hindered Phenol (Irg. E201) : Phosphite (Wes. 399): TMP</b>								
<b>S13 1:2.0:1.5 w/w ratio</b>								
m-S13-210-PO	210	100/N2	1.05	0	18	0	17	0
m-S13-285-P1	285	50	1.02	-3	18	-1	18	6
m-S13-285-P3			0.51	-51	14	-21	27	59
m-S13-285-P5			0.24	-77	12.2	-33	51	200
m-S13-210-PO	210	100/N2	1.05	0	18	0	17	0
m-S13-285-P1	285	100	0.73	-30	17	-8	23	35
m-S13-285-P3			0.48	-54	15	-17	31	82
m-S13-285-P5			0.26	-75	14	-25	54	218

<sup>21</sup> %MI change = (MI<sub>sample</sub> - MI<sub>virgin</sub>)/MI<sub>virgin</sub> x 100

<sup>22</sup> % HLMI change = (HLMI<sub>sample</sub> - HLMI<sub>virgin</sub>)/HLMI<sub>virgin</sub> x 100

<sup>23</sup> MFR = HLMI/MI

<sup>24</sup> %MFR change = (MFR<sub>sample</sub> - MFR<sub>virgin</sub>)/MFR<sub>virgin</sub> x 100

Table 5.11 ....Continued

Code	Temp /°C	Speed /rpm	Melt flow measurements /10g.min <sup>-1</sup>					
			MI	%MI change <sup>25</sup>	HLMI	%HLMI change <sup>26</sup>	MFR <sup>27</sup>	%MFR change <sup>28</sup>
m-S13-210-PO	210	100/N2	1.05	0	18	0	17	0
m-S13-285-P1	285	200	1.01	-4	17	-8	17	0
m-S13-285-P3			0.84	-20	13	-29	15	-12
m-S13-285-P5			0.11	-90	12	-35	109	541
<b>Biological Hindered Phenol (Irg. E201) : Phosphite (U.626): TMP</b>								
<b>S11 1:2.0:1.5 w/w ratio</b>								
m-S11-210-PO	210	100/N2	1.04	0	18	0	17	0
m-S11-285-P1	285	50	1.06	2	17	-8	16.0	-6
m-S11-285-P3			0.74	-29	16	-14	22	29
m-S11-285-P5			0.66	-37	19	2	29	71
m-S11-210-PO	210	100/N2	1.07	0	18	0	17	0
m-S11-285-P1	285	100	1.06	-1	17	-7	16	-6
m-S11-285-P3			1.01	-6	18	-4	18	6
m-S11-285-P5			0.75	-30	17	-9	23	35
m-S11-210-PO	210	100/N2	1.04	0	18	0	17	0
m-S11-285-P1	285	200	1.06	2	19	3	18	6
m-S11-285-P3			0.85	-19	18	-3	21	24
m-S11-285-P5			0.50	-52	15	-17	30	76

$$^{25} \% \text{MI change} = (\text{MI}_{\text{sample}} - \text{MI}_{\text{virgin}}) / \text{MI}_{\text{virgin}} \times 100$$

$$^{26} \% \text{HLMI change} = (\text{HLMI}_{\text{sample}} - \text{HLMI}_{\text{virgin}}) / \text{HLMI}_{\text{virgin}} \times 100$$

$$^{27} \text{MFR} = \text{HLMI} / \text{MI}$$

$$^{28} \% \text{MFR change} = (\text{MFR}_{\text{sample}} - \text{MFR}_{\text{virgin}}) / \text{MFR}_{\text{virgin}} \times 100$$

Table 5.12 Effect of **Synthetic and Biological hindered phenols in combination with different phosphites** on the Colour stability of stabilised **m-LLDPE** polymer samples; (see s4 to s13, in table 5.1), during Pass zero (Po) and Multi-pass extrusion conditions. Unstabilised z-LLDPE extruded under similar conditions is shown for comparison.

Code	Temp /°C	Speed /rpm	YI
<b>Synthetic Hindered Phenol: Phosphite Irganox 1076: Weston 399 S4; 1:4 w/w ratio (Total concentration 2500ppm)</b>			
m-S4-285-P0	285	50	8.2
m-S4-285-P1			10.8
m-S4-285-P3			17.3
m-S4-285-P5			28.2
m-S4-285-P0	285	100	8.2
m-S4-285-P1			6.8
m-S4-285-P3			15.9
m-S4-285-P5			24.3
m-S4-285-P0	285	200	8.2
m-S4-285-P1			7.2
m-S4-285-P3			12.3
m-S4-285-P5			20.1
<b>Biological Hindered Phenol: Phosphite:TMP Irganox E201: Weston 399:TMP S13; 1:2:0.5 w/w ratio (Total concentration 1350ppm)</b>			
m-S13-285-P0	285	50	4.2
m-S13-285-P1			8.1
m-S13-285-P3			18.1
m-S13-285-P5			24.7
m-S13-285-P0	285	100	4.2
m-S13-285-P1			9.5
m-S13-285-P3			13.8
m-S13-285-P5			14.8
m-S13-285-P0	285	200	4.2
m-S13-285-P1			6.2
m-S13-285-P3			12.1
m-S13-285-P5			15.6
<b>Biological Hindered Phenol: Phosphite:TMP Irganox E201: Ultrinox 626:TMP S11; 1:2:0.5 w/w ratio (Total concentration 1350ppm)</b>			
m-S11-285-P0	285	50	4.1
m-S11-285-P1			7.2
m-S11-285-P3			12.9
m-S11-285-P5			22.0
m-S11-285-P0	285	100	4.1
m-S11-285-P1			9.4
m-S11-285-P3			13.4
m-S11-285-P5			15.7
m-S11-285-P0	285	200	4.1
m-S11-285-P1			7.7
m-S11-285-P3			11.5
m-S11-285-P5			16.6

Table 5.13 Effect of **Synthetic and Biological hindered phenols in combination with different phosphites** on the Colour stability of stabilised **z-LLDPE** polymer samples; (see s4 to s13, in table 5.1), during Pass zero (Po) and Multi-pass extrusion conditions. Unstabilised z-LLDPE extruded under similar conditions is shown for comparison.

Code	Temp /°C	Speed /rpm	YI
<b>Synthetic Hindered Phenol: Phosphite Irganox 1076: Weston 399 S4; 1:4 w/w ratio (Total concentration 2500ppm)</b>			
z-S4-285-P0	285	50	-3.6
z-S4-285-P1			5.0
z-S4-285-P3			16.8
z-S4-285-P5			20.3
z-S4-285-P0	285	100	-3.6
z-S4-285-P1			-2.2
z-S4-285-P3			11.1
z-S4-285-P5			15.0
z-S4-285-P0	285	200	-3.6
z-S4-285-P1			4.6
z-S4-285-P3			6.4
z-S4-285-P5			9.7
<b>Biological Hindered Phenol: Phosphite:TMP Irganox E201: Weston 399:TMP S13; 1:2:0.5 w/w ratio (Total concentration 1350ppm)</b>			
z-S13-285-P0	285	100	-5.5
z-S13-285-P1			4.9
z-S13-285-P3			5.5
z-S13-285-P5			22.8
<b>Biological Hindered Phenol: Phosphite:TMP Irganox E201: Ultrinox 626:TMP S11; 1:2:0.5 w/w ratio (Total concentration 1350ppm)</b>			
z-S11-285-P0	285	100	-5.5
z-S11-285-P1			-7.0
z-S11-285-P3			4.1
z-S11-285-P5			10.9



Table 5.14. Effect of processing parameters on the melt stability of stabilised **XP-60 Two antioxidant based systems (s33 to s37, see table 5.2) m-LLDPE** samples during Pass-zero (Po) and multi-pass extrusion (260°C/100rpm, under atmospheric conditions, P1, P3 and P5). Unstabilised m-LLDPE extruded under similar conditions is shown for comparison. All formulations with a constant; 0.6% P content and 1:2.3 ratio (lactone :Phosphite)

Code	Temp /°C	Speed /rpm	Melt flow measurements /10g.min <sup>-1</sup>					
			MI	%MI change <sup>29</sup>	HLMI	%HLMI change <sup>30</sup>	MFR <sup>31</sup>	%MFR <sup>32</sup> change
Virgin m-LLDPE	-	-	1.00	0	17	0	17	0
Unstabilised m-P1	260	100	0.32	-68	12.6	-26	39	129
Unstabilised m-P3			0.03	-97	9.1	-46	303	1682
Unstabilised m-P5			0.01	-99	6.4	-62	640	3664
<b>XP-60 Two AO Based systems</b>								
<b>Lactone (Irganox HP136): Phosphite</b>								
<b>XP-60 Irganox HP136: Ultrinox 626 (1:2.3)</b>								
m-S33-210-P0	210	100	1.09	0	17.9	0	16	0
m-S33-260-P1	260	100	1.09	0	18.1	1	16	0
m-S33-260-P3			1.08	-1	18.1	1	16	0
m-S33-260-P5			1.08	-1	18.0	0	16	0
<b>Irganox HP136: Ultrinox 626 (1:2.3)</b>								
m-S34-210-P0	210	100	1.08	0	17.7	0	16	0
m-S34-260-P1	260	100	1.09	1	17.3	-2	16	0
m-S34-260-P3			1.08	0	17.3	-2	16	0
m-S34-260-P5			1.09	1	16.9	-4	16	0
<b>Irganox HP136: Irgafos P-EPQ (1:2.3)</b>								
m-S35-210-P0	210	100	1.09	0	17.6	0	16	0
m-S35-260-P1	260	100	1.10	1	17.2	-2	16	0
m-S35-260-P3			1.08	-1	17.3	-2	16	0
m-S35-260-P5			1.09	1	17.1	-3	16	0
<b>Irganox HP136: Doverphos S9228 (1:2.3)</b>								
m-S36-210-P0	210	100	1.06	0	18.1	0	17	0
m-S36-260-P1	260	100	1.07	1	17.8	-2	17	0
m-S36-260-P3			1.08	2	17.8	-2	16	-6
m-S36-260-P5			1.09	3	18.0	-1	16	-6

<sup>29</sup> %MI change = (MI<sub>sample</sub> - MI<sub>Po</sub>)/MI<sub>Po</sub> x 100 in the case of the virgin replace MI<sub>Po</sub> with MI<sub>virgin</sub>.

<sup>30</sup> % HLMI change = (HLMI<sub>sample</sub> - HLMI<sub>Po</sub>)/HLMI<sub>Po</sub> x 100 in the case of the virgin replace HLMI<sub>Po</sub> with HLMI<sub>virgin</sub>.

<sup>31</sup> MFR = HLMI/MI

<sup>32</sup> %MFR change = (MFR<sub>sample</sub> - MFR<sub>Po</sub>)/MFR<sub>Po</sub> x 100 in the case of the virgin replace MFR<sub>Po</sub> with MFR<sub>virgin</sub>.

Table 5.14. continued....

Code	Temp /°C	Speed /rpm	Melt flow measurements /10g.min <sup>-1</sup>					
			MI	%MI change <sup>33</sup>	HLMI	%HLMI change <sup>34</sup>	MFR <sub>35</sub>	%MFR <sub>36</sub> change
Virgin m-LLDPE	-	-	1.00	0	17	0	17	0
Unstabilised m-P1	260	100	0.32	-68	12.6	-26	39	129
Unstabilised m-P3			0.03	-97	9.1	-46	303	1682
Unstabilised m-P5			0.01	-99	6.4	-62	640	3664
<b>Irganox HP136: Weston 399 (1:2.3)</b>								
m-S37-210-P0	210	100	1.06	0	17.6	0	17	0
m-S37-260-P1	260	100	1.05	-1	17.4	-1	17	0
m-S37-260-P3			1.04	-2	17.9	2	17	0
m-S37-260-P5			0.99	-7	17.6	0	18	7
<b>Two AO Based systems Synthetic hindered Phenol: Phosphite</b>								
<b>Irganox 1076: Weston 399 (1:4)</b>								
m-S4-210-P0	210	100	1.01	0	17.7	0	17	0
m-S4-260-P1	260	100	0.93	-8	17.3	-2	19	12
m-S4-260-P3			0.93	-8	17.3	-2	19	12
m-S4-260-P5			0.93	-8	17.2	-3	19	6

<sup>33</sup> %MI change =  $(MI_{\text{Sample}} - MI_{P0})/MI_{P0} \times 100$  in the case of the virgin replace  $MI_{P0}$  with  $MI_{\text{virgin}}$ .

<sup>34</sup> % HLMI change =  $(HLMI_{\text{sample}} - HLMI_{P0})/HLMI_{P0} \times 100$  in the case of the virgin replace  $HLMI_{P0}$  with  $HLMI_{\text{virgin}}$ .

<sup>35</sup> MFR = HLMI/MI

<sup>36</sup> %MFR change =  $(MFR_{\text{sample}} - MFR_{P0})/MFR_{P0} \times 100$  in the case of the virgin replace  $MFR_{P0}$  with  $MFR_{\text{virgin}}$ .

Table 5.15. Effect of processing parameters (260<sup>0</sup>C/100rpm, atmospheric conditions) on the **Colour Stability of XP antioxidant based systems (s33 to s37**, see table 5.2) m-LLDPE samples containing antioxidant combinations during Po and multi-pass extrusion (P1, P3 and P5). Unstabilised m-LLDPE extruded under similar conditions is shown for comparison.

Code	Temp/°C	Speed/rpm	YI
Virgin m-LLDPE	-	-	-7.80
Unstabilised m-P1	260	100	8.92
Unstabilised m-P3			12.14
Unstabilised m-P5			15.02
<b>XP-60 Two AO Based systems</b>			
Lactone (HP136): Phosphite			
m-S33-260-P1	260	100	6.36
m-S33-260-P3			8.32
m-S33-260-P5			9.44
m-S34-260-P1	260	100	5.38
m-S34-260-P3			7.72
m-S34-260-P5			8.80
m-S35-260-P1	260	100	7.49
m-S35-260-P3			9.93
m-S35-260-P5			12.24
m-S36-260-P1	260	100	6.24
m-S36-260-P3			7.65
m-S36-260-P5			8.63
m-S37-260-P1	260	100	6.94
m-S37-260-P3			8.22
m-S37-260-P5			9.87
m-S4-260-P1	260	100	3.37
m-S4-260-P3			12.11
m-S4-260-P5			12.43

Table 5.16 Effect of processing parameters on the melt stability of stabilised **Three antioxidant based systems (s22 to s25, see table 5.1) m-LLDPE** samples during Pass-zero (Po) and multi-pass extrusion (260°C/100rpm, under atmospheric conditions, P1, P3 and P5). Unstabilised m-LLDPE extruded under similar conditions is shown for comparison. All formulations with a constant lactone content and varying concentrations of Irganox 1076/Weston 399.

Code	Temp /°C	Speed /rpm	Melt flow measurements /10g.min <sup>-1</sup>					
			MI	%MI change <sup>37</sup>	HLMI	%HLMI change <sup>38</sup>	MFR <sup>39</sup>	%MFR change <sup>40</sup>
Virgin m-LLDPE	-	-	1.00	0	17	0	17	0
Unstabilised m-P1	260	100	0.32	-68	12.6	-26	39	129
Unstabilised m-P3			0.03	-97	9.1	-46	303	1682
Unstabilised m-P5			0.01	-99	6.4	-62	640	3664
<b>Three AO Based systems</b>								
Synthetic Hindered Phenol (Irg.1076): Lactone (HP136) : Weston 399								
Irganox 1076:Lactone:Weston 399 (1.7:1:6.7)								
m-S22-210-P0	210	100	1.08	0	17.5	0	16	0
m-S22-260-P1	260	100	1.09	1	17.7	1	16	0
m-S22-260-P3			0.85	-21	17.1	-3	20	25
m-S22-260-P5			0.74	-31	16.5	-6	22	37
Irganox 1076:Lactone:Weston 399:TMP (1.7:01:6.7)								
m-S23-210-P0	210	100	1.08	0	17.3	0	16	0
m-S23-260-P1	260	100	1.08	0	17.7	2	16	0
m-S23-260-P3			1.02	-6	17.2	-1	17	6
m-S23-260-P5			0.81	-25	17.0	-2	21	31
Irganox 1076:Lactone:Weston 399 (5:1:8.3)								
m-S24-210-P0	210	100	1.09	0	17.4	0	16	0
m-S24-260-P1	260	100	1.09	0	17.2	-1	16	6
m-S24-260-P3			1.10	1	17.7	2	16	6
m-S24-260-P5			1.13	4	17.5	3	16	6
Irganox 1076:Lactone:Weston 399 (1.7:1:3.0)								
m-S25-210-P0	210	100	1.09	0	18.0	0	17	0
m-S25-260-P1	260	100	1.07	-2	17.8	-1	17	0
m-S25-260-P3			0.91	-17	17.6	-2	19	12
m-S25-260-P5			0.71	-35	16.2	-10	23	35

<sup>37</sup> %MI change =  $(MI_{\text{Sample}} - MI_{\text{Po}}) / MI_{\text{Po}} \times 100$  in the case of the virgin replace  $MI_{\text{Po}}$  with  $MI_{\text{virgin}}$ .

<sup>38</sup> % HLMI change =  $(HLMI_{\text{Sample}} - HLMI_{\text{Po}}) / HLMI_{\text{Po}} \times 100$  in the case of the virgin replace  $HLMI_{\text{Po}}$  with  $HLMI_{\text{virgin}}$ .

<sup>39</sup> MFR =  $HLMI / MI$

<sup>40</sup> %MFR change =  $(MFR_{\text{Sample}} - MFR_{\text{Po}}) / MFR_{\text{Po}} \times 100$  in the case of the virgin replace  $MFR_{\text{Po}}$  with  $MFR_{\text{virgin}}$ .

Table 5.17. Effect of processing parameters (260<sup>0</sup>C/100rpm, atmospheric conditions) on the **Colour Stability of Three antioxidant based systems (s22 to s25, see table 5.1)** m-LLDPE samples containing antioxidant combinations during Po and multi-pass extrusion (P1, P3 and P5). Unstabilised m-LLDPE extruded under similar conditions is shown for comparison.

Code	Temp/ <sup>o</sup> C	Speed/rpm	YI
Virgin m-LLDPE	-	-	-7.80
Unstabilised m-P1	260	100	8.92
Unstabilised m-P3			12.14
Unstabilised m-P5			15.02
<b>Three AO Based systems</b>			
Biological hindered phenol (Irg.E201): Lactone (HP136): Phosphite			
m-S22-260-P1	260	100	8.56
m-S22-260-P3			14.06
m-S22-260-P5			16.89
m-S23-260-P1	260	100	10.55
m-S23-260-P3			13.97
m-S23-260-P5			15.52
m-S24-260-P1	260	100	9.22
m-S24-260-P3			15.27
m-S24-260-P5			17.12
m-S25-260-P1	260	100	9.09
m-S25-260-P3			13.49
m-S25-260-P5			14.98



Table 5.18. Effect of processing parameters on the melt stability of stabilised **XP-490 Three antioxidant based systems** (s38 to s42, see table 5.2) **m-LLDPE** samples during Pass-zero (Po) and multi-pass extrusion (260°C/100rpm, under atmospheric conditions, P1, P3 and P5). Unstabilised m-LLDPE extruded under similar conditions is shown for comparison. All formulations with a constant; 0.6% P content and 1:2.3:3.3 w/w ratio (lactone :Phosphite:1076)

Code	Temp /°C	Speed /rpm	Melt flow measurements /10g.min <sup>-1</sup>					
			MI	%MI change <sup>41</sup>	HLMI	%HLMI change <sup>42</sup>	MFR <sup>43</sup>	%MFR change <sup>44</sup>
Virgin m-LLDPE	-	-	1.00	0	17	0	17	0
Unstabilised m-P1	260	100	0.32	-68	12.6	-26	39	129
Unstabilised m-P3			0.03	-97	9.1	-46	303	1682
Unstabilised m-P5			0.01	-99	6.4	-62	640	3664
<b>XP-490 Three AO Based systems</b>								
Synthetic Hindered Phenol (Irg.1076): Lactone (HP136) : Phosphite								
XP-490 Irganox HP136:Irgafos P-EPQ:Irganox 1076 (1:2.3:3.3)								
m-S38-210-P0	210	100	1.07	0	17.5	0	16	0
m-S38-260-P1	260	100	1.08	1	17.7	1	16	0
m-S38-260-P3			1.06	-1	17.7	1	17	6
m-S38-260-P5			1.04	-3	17.6	1	17	6
Irganox HP136:Irgafos P-EPQ:Irganox 1076 (1:2.3:3.3)								
m-S39-210-P0	210	100	1.08	0	17.5	0	16	0
m-S39-260-P1	260	100	1.08	1	17.6	1	16	0
m-S39-260-P3			1.07	-1	18.0	3	17	6
m-S39-260-P5			1.03	-5	18.0	3	17	6
Irganox HP136:Irgafos Ultrinox 626:Irganox 1076 (1:2.3:3.3)								
m-S40-210-P0	210	100	1.10	0	17.6	0	16	0
m-S40-260-P1	260	100	1.09	-1	17.7	1	16	0
m-S40-260-P3			1.08	-2	17.8	1	16	0
m-S40-260-P5			1.07	-3	17.5	1	16	0
Irganox HP136:Doverphos S9228:Irganox 1076 (1:2.3:3.3)								
m-S41-210-P0	210	100	1.09	0	17.4	0	16	0
m-S41-260-P1	260	100	1.07	-2	17.3	-1	16	0
m-S41-260-P3			1.04	-5	17.7	2	17	6
m-S41-260-P5			1.04	-5	17.5	1	17	6
Irganox HP136:Weston 399:Irganox 1076 (1:2.3:3.3)								
m-S42-210-P0	210	100	1.09	0	17.7	0	16	0
m-S42-260-P1	260	100	1.11	0	17.8	1	16	0
m-S42-260-P3			1.08	-3	18.3	3	17	6
m-S42-260-P5			1.05	-5	18.1	2	17	6

<sup>41</sup> %MI change =  $(MI_{\text{Sample}} - MI_{\text{Po}}) / MI_{\text{Po}} \times 100$  in the case of the virgin replace  $MI_{\text{Po}}$  with  $MI_{\text{virgin}}$ .

<sup>42</sup> % HLMI change =  $(HLMI_{\text{Sample}} - HLMI_{\text{Po}}) / HLMI_{\text{Po}} \times 100$  in the case of the virgin replace  $HLMI_{\text{Po}}$  with  $HLMI_{\text{virgin}}$ .

<sup>43</sup> MFR = HLMI/MI

<sup>44</sup> %MFR change =  $(MFR_{\text{Sample}} - MFR_{\text{Po}}) / MFR_{\text{Po}} \times 100$  in the case of the virgin replace  $MFR_{\text{Po}}$  with  $MFR_{\text{virgin}}$ .

Table 5.19. Effect of processing parameters (260°C/100rpm, atmospheric conditions) on the **Colour Stability of XP 490 antioxidant based systems (s38 to s42**, see table 5.2) m-LLDPE samples containing antioxidant combinations during Po and multi-pass extrusion (P1, P3 and P5). Unstabilised m-LLDPE extruded under similar conditions is shown for comparison.

Code	Temp/°C	Speed/rpm	YI
Virgin m-LLDPE	-	-	-7.80
Unstabilised m-P1	260	100	8.92
Unstabilised m-P3			12.14
Unstabilised m-P5			15.02
<b>XP-490 Three AO Based systems</b>			
Synthetic hindered phenol (Irg.1076): Lactone (HP136): Phosphite			
m-S38-260-P1	260	100	7.19
m-S38-260-P3			10.00
m-S38-260-P5			11.70
m-S39-260-P1	260	100	5.88
m-S39-260-P3			6.90
m-S39-260-P5			8.57
m-S40-260-P1	260	100	6.57
m-S40-260-P3			8.06
m-S40-260-P5			9.79
m-S41-260-P1	260	100	5.81
m-S41-260-P3			8.79
m-S41-260-P5			9.76
m-S42-260-P1	260	100	8.76
m-S42-260-P3			11.60
m-S42-260-P5			13.53

Table 5.20 Effect of processing parameters on the melt stability of stabilised **Three antioxidant based systems (s26 to s27, see table 5.1) m-LLDPE** samples during Pass-zero (Po) and multi-pass extrusion (260°C/100rpm, under atmospheric conditions, P1, P3 and P5). Unstabilised m-LLDPE extruded under similar conditions is shown for comparison. All formulations with a constant Vitamin E, Ultrinox 626 and TMP content in the presence and absence of Irgastab FS042.

Code	Temp /°C	Speed /rpm	Melt flow measurements /10g.min <sup>-1</sup>					
			MI	%MI change <sup>45</sup>	HLMI	%HLMI change <sup>46</sup>	MFR <sup>47</sup>	%MFR change <sup>48</sup>
Virgin m-LLDPE	-	-	1.00	0	17	0	17	0
Unstabilised m-P1	260	100	0.32	-68	12.6	-26	39	129
Unstabilised m-P3			0.03	-97	9.1	-46	303	1682
Unstabilised m-P5			0.01	-99	6.4	-62	640	3664
<b>Three AO Based systems</b>								
<b>Biological Hindered Phenol (Irg.E201): Irgastab FS04: Ultrinox 626</b>								
<b>Irganox E201:Irgastab FS042:Ultrinox 626:TMP (1 : 1.7 : 2.0)</b>								
m-S26-210-P0	210	100	1.04	0	18.2	0	17	0
m-S26-260-P1	260	100	1.08	4	17.7	-3	16	-6
m-S26-260-P3			1.07	3	17.5	-4	16	-6
m-S26-260-P5			1.09	5	17.8	-2	16	-6
<b>Irganox E201:Irgastab FS042:Ultrinox 626:TMP (1 : 3.3 : 2.0)</b>								
m-S27-210-P0	210	100	1.09	0	17.8	0	16	0
m-S27-260-P1	260	100	1.06	-3	17.9	1	17	6
m-S27-260-P3			1.07	-2	17.9	1	17	6
m-S27-260-P5			1.07	-2	18.3	3	17	6
<b>Two AO Based systems</b>								
<b>Biological Hindered Phenol (Irg.E201): Ultrinox 626</b>								
<b>Irganox E201: Ultrinox 626:TMP (1 : 2.0)</b>								
m-S11-210-P0	210	100	1.09	0	17.4	0	16	0
m-S11-260-P1	260	100	1.09	0	17.6	1	16	0
m-S11-260-P3			1.07	-2	17.7	2	16	0
m-S11-260-P5			1.04	-2	17.5	1	17	6

<sup>45</sup> %MI change = (MI<sub>sample</sub> - MI<sub>Po</sub>)/MI<sub>Po</sub> x 100 in the case of the virgin replace MI<sub>Po</sub> with MI<sub>virgin</sub>.

<sup>46</sup> % HLMI change = (HLMI<sub>sample</sub> - HLMI<sub>Po</sub>)/HLMI<sub>Po</sub> x 100 in the case of the virgin replace HLMI<sub>Po</sub> with HLMI<sub>virgin</sub>

<sup>47</sup> MFR = HLMI/MI

<sup>48</sup> %MFR change = (MFR<sub>sample</sub> - MFR<sub>Po</sub>)/MFR<sub>Po</sub> x 100 in the case of the virgin replace MFR<sub>Po</sub> with MFR<sub>virgin</sub>

Table 5.21 Effect of processing parameters (260<sup>0</sup>C/100rpm, atmospheric conditions) on the **Colour Stability of Three antioxidant based systems (s26-27**, see table 5.1) m-LLDPE samples containing antioxidant combinations during Po and multi-pass extrusion (P1, P3 and P5). Unstabilised m-LLDPE extruded under similar conditions is shown for comparison. All formulations with a constant Vitamin E, Ultrinox 626 and TMP content in the presence and absence of Irgastab FS042.

Code	Temp/ <sup>o</sup> C	Speed/rpm	YI
Virgin m-LLDPE	-	-	-7.80
Unstabilised m-P1	260	100	8.92
Unstabilised m-P3			12.14
Unstabilised m-P5			15.02
<b>Three AO Based systems</b>			
<b>Biological hindered phenol (Irg.E201): Irgastab FS042:Ultrinox 626: TMP</b>			
m-S26-260-P1	260	100	9.86
m-S26-260-P3			10.34
m-S26-260-P5			18.46
m-S27-260-P1	260	100	9.07
m-S27-260-P3			13.84
m-S27-260-P5			17.92
<b>Two AO Based systems</b>			
<b>Biological hindered phenol (Irg.E201): Ultrinox 626: TMP</b>			
m-S11-260-P1	260	100	7.74
m-S11-260-P3			11.81
m-S11-260-P5			14.17

Table 5.22 Effect of processing parameters on the melt stability of stabilised **Three antioxidant based systems** (s28 to s29, see table 5.1) **m-LLDPE** samples during Pass-zero (Po) and multi-pass extrusion (260°C/100rpm, under atmospheric conditions, P1, P3 and P5). Unstabilised m-LLDPE extruded under similar conditions is shown for comparison. All formulations with a constant 1:4 w/w ratio of Irg. 1076 and Weston 399 respectively.

Code	Temp /°C	Speed /rpm	Melt flow measurements /10g.min <sup>-1</sup>					
			MI	%MI change <sup>49</sup>	HLMI	%HLMI change <sup>50</sup>	MFR <sub>51</sub>	%MFR <sub>52</sub> change
Virgin m-LLDPE	-	-	1.00	0	17	0	17	0
Unstabilised m-P1	260	100	0.32	-68	12.6	-26	39	129
Unstabilised m-P3			0.03	-97	9.1	-46	303	1682
Unstabilised m-P5			0.01	-99	6.4	-62	640	3664
<b>Three AO Based systems</b>								
<b>Synthetic Hindered Phenol (Irg.1076): Irgastab FS04: Weston 399</b>								
<b>Irganox 1076:Irgastab FS042:Weston 399 (1 : 1 : 4) TMP</b>								
m-S28-210-P0	210	100	1.07	0	17.8	0	17	0
m-S28-260-P1	260	100	1.08	1	17.7	-1	16	-6
m-S28-260-P3			1.08	1	18.2	2	17	0
m-S28-260-P5			0.78	-27	19.1	7	24	41
<b>Irganox 1076:Irgastab FS042:Weston 399 (1 : 2 : 4) TMP</b>								
m-S29-210-P0	210	100	1.11	0	17.8	0	16	0
m-S29-260-P1	260	100	1.09	-2	17.6	-1	16	0
m-S29-260-P3			1.02	-8	17.1	-4	17	6
m-S29-260-P5			1.01	-9	16.9	-5	17	12
<b>Two AO Based systems</b>								
<b>Synthetic Hindered Phenol (Irg.1076): Weston 399</b>								
<b>Irganox 1076: Weston 399 (1 : 4)</b>								
m-S4-210-P0	210	100	1.01	0	17.7	0	17	0
m-S4-260-P1	260	100	0.93	-8	17.3	-2	19	12
m-S4-260-P3			0.93	-8	17.3	-2	19	12
m-S4-260-P5			0.93	-8	17.2	-3	19	6

<sup>49</sup> %MI change =  $(MI_{\text{Sample}} - MI_{\text{Po}}) / MI_{\text{Po}} \times 100$  in the case of the virgin replace  $MI_{\text{Po}}$  with  $MI_{\text{virgin}}$ .

<sup>50</sup> % HLMI change =  $(HLMI_{\text{Sample}} - HLMI_{\text{Po}}) / HLMI_{\text{Po}} \times 100$  in the case of the virgin replace  $HLMI_{\text{Po}}$  with  $HLMI_{\text{virgin}}$ .

<sup>51</sup> MFR =  $HLMI / MI$

<sup>52</sup> %MFR change =  $(MFR_{\text{Sample}} - MFR_{\text{Po}}) / MFR_{\text{Po}} \times 100$  in the case of the virgin replace  $MFR_{\text{Po}}$  with  $MFR_{\text{virgin}}$ .



Table 5.23 Effect of processing parameters (260<sup>0</sup>C/100rpm, atmospheric conditions) on the **Colour Stability** of **Three antioxidant based systems (s28-29)**, see table 5.1) m-LLDPE samples containing antioxidant combinations during Po and multi-pass extrusion (P1, P3 and P5). Unstabilised m-LLDPE extruded under similar conditions is shown for comparison. All formulations with a constant 1:4 w/w ratio of Irg. 1076 and Weston 399 respectively.

Code	Temp/ <sup>0</sup> C	Speed/rpm	YI
Virgin m-LLDPE	-	-	-7.80
Unstabilised m-P1	260	100	8.92
Unstabilised m-P3			12.14
Unstabilised m-P5			15.02
<b>Three AO Based systems</b>			
<b>Synthetic hindered phenol (Irg.1076): Irgastab FS042:Weston 399</b>			
m-S28-260-P1	260	100	11.12
m-S28-260-P3			19.89
m-S28-260-P5			26.94
m-S29-260-P1	260	100	14.89
m-S29-260-P3			18.81
m-S29-260-P5			22.01
<b>Two AO Based systems</b>			
<b>Synthetic hindered phenol (Irg.1076): Weston 399</b>			
m-S4-260-P1	260	100	3.37
m-S4-260-P3			12.11
m-S4-260-P5			12.43

Table 5.24. Effect of processing parameters on the melt stability of stabilised **Vitamin E (Irganox E201) Three antioxidant based systems (s43 to s49**, see table 5.2) **m-LLDPE** samples during Pass-zero (Po) and multi-pass extrusion (260°C/100rpm, under atmospheric conditions, P1, P3 and P5). Unstabilised m-LLDPE extruded under similar conditions is shown for comparison.

Code	Temp /°C	Speed /rpm	Melt flow measurements /10g.min <sup>-1</sup>					
			MI	%MI change <sup>53</sup>	HLMI	%HLMI change <sup>54</sup>	MFR <sup>55</sup>	%MFR <sup>56</sup> change
Virgin m-LLDPE	-	-	1.00	0	17	0	17	0
Unstabilised m-P1	260	100	0.32	-68	12.6	-26	39	129
Unstabilised m-P3			0.03	-97	9.1	-46	303	1682
Unstabilised m-P5			0.01	-99	6.4	-62	640	3664
<b>Three AO Based systems</b>								
Biological Hindered Phenol (Irg.201): Lactone (HP136): Phosphite								
HP136:E201:P-EPQ (1:0.7:2.3)								
m-S43-210-P0	210	100	1.09	0	17.7	0	16	0
m-S43-260-P1	260	100	1.09	0	17.7	-1	16	0
m-S43-260-P3			1.07	1	17.6	-2	16	0
m-S43-260-P5			1.05	2	17.3	-3	16	0
HP136:E201:U626 (1:1.1:2.3)								
m-S44-210-P0	210	100	1.10	0	18.0	0	16	0
m-S44-260-P1	260	100	1.10	0	17.9	0	16	0
m-S44-260-P3			1.11	1	17.9	0	16	0
m-S44-260-P5			1.12	2	18.0	0	16	0
HP136:E201:U626:ZnSt (1:1.1:2.3)								
m-S45-210-P0	210	100	1.08	0	17.9	0	17	0
m-S45-260-P1	260	100	1.07	-1	17.4	-3	16	-6
m-S45-260-P3			1.06	-2	17.4	-3	16	-6
m-S45-260-P5			1.07	-1	17.4	-3	16	-6
HP136:E201:D.S9228 (1:0.8:2.3)								
m-S46-210-P0	210	100	1.06	0	17.7	0	17	0
m-S46-260-P1	260	100	1.06	0	17.5	-1	16	-6
m-S46-260-P3			1.06	0	17.5	-1	16	-6
m-S46-260-P5			1.05	-1	17.7	0	17	0
HP136:E201:W399: ZnSt (1:0.5:2.3)								
m-S47-210-P0	210	100	1.06	0	17.6	0	17	0
m-S47-260-P1	260	100	1.05	-1	17.2	-2	17	0
m-S47-260-P3			1.03	-3	17.0	-3	16	-6
m-S47-260-P5			1.04	-2	16.6	-6	16	-6

<sup>53</sup> %MI change = (MI<sub>Sample</sub> - MI<sub>Po</sub>)/MI<sub>Po</sub> x 100 in the case of the virgin replace MI<sub>Po</sub> with MI<sub>virgin</sub>.

<sup>54</sup> % HLMI change = (HLMI<sub>Sample</sub> - HLMI<sub>Po</sub>)/HLMI<sub>Po</sub> x 100 in the case of the virgin replace HLMI<sub>Po</sub> with HLMI<sub>virgin</sub>.

<sup>55</sup> MFR = HLMI/MI

<sup>56</sup> %MFR change = (MFR<sub>Sample</sub> - MFR<sub>Po</sub>)/MFR<sub>Po</sub> x 100 in the case of the virgin replace MFR<sub>Po</sub> with MFR<sub>virgin</sub>.

Table 5.24 continued.....

Code	Temp /°C	Speed /rpm	Melt flow measurements /10g.min <sup>-1</sup>					
			MI	%MI change <sup>57</sup>	HLMI	%HLMI change <sup>58</sup>	MFR <sup>59</sup>	%MFR <sup>60</sup> change
Virgin m-LLDPE	-	-	1.00	0	17	0	17	0
Unstabilised m-P1	260	100	0.32	-68	12.6	-26	39	129
Unstabilised m-P3			0.03	-97	9.1	-46	303	1682
Unstabilised m-P5			0.01	-99	6.4	-62	640	3664
<b>Three AO Based systems</b>								
Biological Hindered Phenol (Irg.201): Lactone (HP136): Phosphite								
HP136:E201:W399 (1:0.5:2.3)								
m-S48-210-P0	210	100	1.07	0	17.6	0	16	0
m-S48-260-P1	260	100	1.08	1	17.6	0	16	0
m-S48-260-P3			1.10	3	18.1	3	16	0
m-S48-260-P5			1.09	2	17.9	2	16	0
E201:U 626:ZnSt (1:2) NO lactone								
m-S49-210-P0	210	100	1.07	0	17.3	0	16	0
m-S49-260-P1	260	100	1.07	0	17.4	1	16	0
m-S49-260-P3			1.07	0	17.4	1	16	0
m-S49-260-P5			1.06	-1	17.2	-1	16	0
E201:U 626:TMP (1:2) NO lactone								
m-S11-210-P0	210	100	1.09	0	17.4	0	16	0
m-S11-260-P1	260	100	1.09	0	17.6	1	16	0
m-S11-260-P3			1.07	-2	17.7	2	16	0
m-S11-260-P5			1.04	-2	17.5	1	17	6
Irganox 1076:Weston 399								
m-S4-210-P0	210	100	1.01	0	17.7	0	17	0
m-S4-260-P1	260	100	0.93	-8	17.3	-2	19	12
m-S4-260-P3			0.93	-8	17.3	-2	19	12
m-S4-260-P5			0.93	-8	17.2	-3	19	6
Irganox 1076: Irgastab FS042: Weston 399								
m-S29-210-P0	210	100	1.11	0	17.8	0	16	0
m-S29-260-P1	260	100	1.09	-2	17.6	-1	16	0
m-S29-260-P3			1.02	-8	17.1	-4	17	6
m-S29-260-P5			1.01	-9	16.9	-5	17	12

<sup>57</sup> %MI change =  $(MI_{\text{Sample}} - MI_{\text{Po}}) / MI_{\text{Po}} \times 100$  in the case of the virgin replace MI<sub>Po</sub> with MI<sub>virgin</sub>.

<sup>58</sup> % HLMI change =  $(HLMI_{\text{Sample}} - HLMI_{\text{Po}}) / HLMI_{\text{Po}} \times 100$  in the case of the virgin replace HLMI<sub>Po</sub> with HLMI<sub>virgin</sub>.

<sup>59</sup> MFR = HLMI/MI

<sup>60</sup> %MFR change =  $(MFR_{\text{Sample}} - MFR_{\text{Po}}) / MFR_{\text{Po}} \times 100$  in the case of the virgin replace MFR<sub>Po</sub> with MFR<sub>virgin</sub>.

Table 5.25. Effect of processing parameters (260<sup>0</sup>C/100rpm, atmospheric conditions) on the **Colour Stability** of **Vitamin E, antioxidant based systems (s43 to s49**, see table 5.2) m-LLDPE samples containing antioxidant combinations during Po and multi-pass extrusion (P1, P3 and P5). Unstabilised m-LLDPE extruded under similar conditions is shown for comparison.

Code	Temp/ <sup>0</sup> C	Speed/rpm	YI
Virgin m-LLDPE	-	-	-7.80
Unstabilised m-P1	260	100	8.92
Unstabilised m-P3			12.14
Unstabilised m-P5			15.02
<b>Three AO Based systems</b>			
Biological Hindered Phenol (Irg.201): Lactone (HP136): Phosphite			
m-S43-260-P1	260	100	7.69
m-S43-260-P3			8.43
m-S43-260-P5			11.60
m-S44-260-P1	260	100	7.55
m-S44-260-P3			8.94
m-S44-260-P5			12.76
m-S45-260-P1	260	100	7.58
m-S45-260-P3			9.25
m-S45-260-P5			11.34
m-S46-260-P1	260	100	6.49
m-S46-260-P3			11.38
m-S46-260-P5			14.15
m-S47-260-P1	260	100	8.43
m-S47-260-P3			11.75
m-S47-260-P5			12.59
m-S48-260-P1	260	100	10.54
m-S48-260-P3			13.52
m-S48-260-P5			17.05
m-S49-260-P1	260	100	9.72
m-S49-260-P3			12.23
m-S49-260-P5			14.66
m-S11-260-P1	260	100	10.13
m-S11-260-P3			11.36
m-S11-260-P5			13.19
m-S4-260-P1	260	100	3.37
m-S4-260-P3			12.11
m-S4-260-P5			12.43
m-S29-260-P1	260	100	14.89
m-S29-260-P3			18.81
m-S29-260-P5			22.01

Table 5.26 Effect of processing parameters on the melt stability of stabilised **four antioxidant based systems (s30 to s32, see table 5.2) m-LLDPE** samples during Pass-zero (Po) and multi-pass extrusion (260°C/100rpm, under atmospheric conditions, P1, P3 and P5). Unstabilised m-LLDPE extruded under similar conditions is shown for comparison. All formulations with a constant 1:1:4:2 w/w ratio of Irg. 1076/Irgastab FS042/Weston 399/HALS respectively.

Code	Temp /°C	Speed /rpm	Melt flow measurements /10g.min <sup>-1</sup>					
			MI	%MI change <sup>61</sup>	HLMI	%HLMI change <sup>62</sup>	MFR <sup>63</sup>	%MFR change <sup>64</sup>
Virgin m-LLDPE	-	-	1.00	0	17	0	17	0
Unstabilised m-P1	260	100	0.32	-68	12.6	-26	39	129
Unstabilised m-P3			0.03	-97	9.1	-46	303	1682
Unstabilised m-P5			0.01	-99	6.4	-62	640	3664
<b>Four AO Based systems</b>								
<b>Synthetic Hindered Phenol (Irg.1076): Irgastab FS04: Weston 399:HALS</b>								
Irganox 1076:Irgastab FS042:Weston 399: Tinuvin 765 (1 : 1 : 4: 2)								
m-S30-210-P0	210	100	1.11	0	17.8	0	16	0
m-S30-260-P1	260	100	1.10	-1	17.6	-1	16	0
m-S30-260-P3			0.96	-14	18.2	2	19	19
m-S30-260-P5			0.90	-19	18.4	3	20	25
Irganox 1076:Irgastab FS042:Weston 399: Tinuvin 622LD (1 : 1 : 4: 2)								
m-S31-210-P0	210	100	1.09	0	18.1	0	17	0
m-S31-260-P1	260	100	1.11	2	16.9	-7	15	-12
m-S31-260-P3			1.10	1	16.9	-7	15	-12
m-S31-260-P5			1.06	-3	15.8	-13	15	-12
Irganox 1076:Irgastab FS042:Weston 399: Chimassorb 119D (1 : 1 : 4: 2)								
m-S32-210-P0	210	100	1.08	0	17.7	0	16	0
m-S32-260-P1	260	100	1.09	1	17.8	1	16	0
m-S32-260-P3			1.09	1	18.2	3	17	6
m-S32-260-P5			1.09	1	18.7	6	17	6
<b>Two and Three AO Based systems</b>								
Irganox 1076:Irgastab FS042:Weston 399 (1 : 1 : 4)								
m-S28-210-P0	210	100	1.07	0	17.8	0	17	0
m-S28-260-P1	260	100	1.08	1	17.7	-1	16	-6
m-S28-260-P3			1.08	1	18.2	2	17	0
m-S28-260-P5			0.78	-27	19.1	7	24	41
Irganox 1076: Weston 399 (1 : 4)								
m-S4-210-P0	210	100	1.01	0	17.7	0	17	0
m-S4-260-P1	260	100	0.93	-8	17.3	-2	19	12
m-S4-260-P3			0.93	-8	17.3	-2	19	12
m-S4-260-P5			0.93	-8	17.2	-3	19	6

<sup>61</sup> %MI change = (MI<sub>Sample</sub> - MI<sub>Po</sub>)/MI<sub>Po</sub> x 100 in the case of the virgin replace MI<sub>Po</sub> with MI<sub>virgin</sub>.

<sup>62</sup> % HLMI change = (HLMI<sub>sample</sub> - HLMI<sub>Po</sub>)/HLMI<sub>Po</sub> x 100 in the case of the virgin replace HLMI<sub>Po</sub> with HLMI<sub>virgin</sub>

<sup>63</sup> MFR = HLMI/MI

<sup>64</sup> %MFR change = (MFR<sub>sample</sub> - MFR<sub>Po</sub>)/MFR<sub>Po</sub> x 100 in the case of the virgin replace MFR<sub>Po</sub> with MFR<sub>virgin</sub>



Table 5.27 Effect of processing parameters (260<sup>0</sup>C/100rpm, atmospheric conditions) on the **Colour Stability** of **Four antioxidant based systems (s30-32**, see table 5.2) m-LLDPE samples containing antioxidant combinations during Po and multi-pass extrusion (P1, P3 and P5). Unstabilised m-LLDPE extruded under similar conditions is shown for comparison. All formulations with a constant 1:1:4:2 w/w ratio of Irg. 1076/Irgastab FS042/Weston 399/HALS respectively.

Code	Temp/ <sup>o</sup> C	Speed/rpm	YI
Virgin m-LLDPE	-	-	-7.80
Unstabilised m-P1	260	100	8.92
Unstabilised m-P3			12.14
Unstabilised m-P5			15.02
<b>Three AO Based systems</b>			
<b>Synthetic hindered phenol (Irg.1076): Irgastab FS042:Weston 399</b>			
m-S30-260-P1	260	100	8.20
m-S30-260-P3			11.36
m-S30-260-P5			15.98
m-S31-260-P1	260	100	9.86
m-S31-260-P3			15.73
m-S31-260-P5			27.07
m-S32-260-P1	260	100	10.99
m-S32-260-P3			17.45
m-S32-260-P5			21.85
<b>Two and Three AO Based systems</b>			
m-S28-260-P1	260	100	11.12
m-S28-260-P3			19.89
m-S28-260-P5			26.94
m-S4-260-P1	260	100	3.37
m-S4-260-P3			12.11
m-S4-260-P5			12.43

## Chapter 6. Overall Conclusions and Recommendations For Future Work

### 6.1 Conclusions.

The following conclusions can be drawn from the results discussed in chapters 3 to 5:-

1. Rheological characterisation of the unstabilised m-LLDPE and z-LLDPE using a twin-bore capillary rheometer (under simulated processing conditions) has shown some main differences in the shear viscosity of the polymers due to differences in their molecular structure; m-LLDPE has a narrower MWD (PD=2.06) whereas z-LLDPE has a broad distribution (PD=3.52). Both unstabilised polymers are shear thinning (non-newtonian behaviour; a highly desirable feature, which improves the tubular film blowing characteristics and facilitates extensive draw-down of film during processing); the viscosity reduces with increasing shear rates under all conditions, with the m-LLDPE polymer shear thinning the most (see figures 3.2-3.4). Elongational viscosity measurements of both polymers have clearly indicated differences in the change in MWD; with the m-LLDPE polymer exhibiting higher melt elasticity (see figures 3.8 & 3.9). Elongational viscosity data coupled with MFR data (related to changes in MWD) reflect the difference in the extent of thermal oxidative degradation that occurs during processing for the two virgin polymers. Melt fracture, a real processing problem, which gives rise to surface irregularities, is also clearly evident from the rheological data and appears to be most severe in the case of the m-LLDPE almost certainly due to its narrower MWD (see figure 3.11).
2. The twin-screw extrusion (TSE) processing characteristics of the metallocene and Ziegler polymers were shown to be quite different. The main parameter affecting the different behaviour of the polymers is the differences in their initial viscosities and MWD (confirmed also by capillary rheometry measurements). The higher shear viscosity of the m-LLDPE polymer (see figure 3.2), is responsible for the higher melt pressures observed at higher screw speeds (see figure 4.4), which in turn leads to higher power consumption (see figure 4.1). The higher shear rates encountered during processing by the m-LLDPE polymer have led to more heat being generated in the melt and this explains the higher

differences between die and melt temperatures (see figure 4.3). The TSE characteristics of the unstabilised m-LLDPE and z-LLDPE polymer are not too different from their stabilised analogues, although there appeared, however, to be a distinct difference in the extrudate appearance (i.e. opacity) after multiple extrusion; the stabilised polymers display minor changes in opacity, thereby suggesting slight changes in polymer structure (see figure 4.5).

3. From melt flow measurements and molecular weight characteristics of the unstabilised extruded m-LLDPE and z-LLDPE polymers it was clear that both polymers undergo degradation during processing. Both cross-linking and chain scission reactions take place (with corresponding increase and decrease in Mw) with the extent of contribution of each to the overall oxidation mechanism being very dependent on the extrusion conditions, i.e. residence time, extrusion temperature and shear rate. The evidence suggests that the m-LLDPE undergoes predominantly cross-linking reactions under all processing conditions whereas z-LLDPE undergoes both cross-linking and chain scission reactions with the latter occurring predominantly under more severe processing conditions (higher temperatures and screw speeds, 285°C/200rpm, with  $[ROO\bullet] > [R\bullet]$ ), see figures 3.20-3.23. MFR and GPC measurements also confirmed that the initial narrower MWD of the unstabilised m-LLDPE polymer does not broaden after the first extrusion pass but with increasing number of passes (pass 5) the m-LLDPE exhibited a broader MWD compared to the z-LLDPE, particularly at higher screw speeds (see figure 3.25). Furthermore, the MFR and GPC results suggest that the broadening of the MWD of the two unstabilised polymers is different; the m-LLDPE broadens and moves towards higher Mw polymer fractions, whereas, the z-LLDPE shifts towards the low Mw chains (see figures 3.26 & 3.30-3.31).
4. The compounding step (pass zero, Po) in the case of both m-LLDPE and z-LLDPE polymers (at 210°C/100rpm under nitrogen) has clearly shown that the addition of low concentrations of different antioxidants leads to a high extent of melt and colour stabilisation with the maximum change observed in MI, (relative to the virgin unstabilised PE), not exceeding 10% (see figure 4.6).

5. The chain breaking (CB) antioxidant activity of different classes of commercial stabilisers; Irganox HP136 (a lactone), Irganox E201 (Vitamin E), Irganox 1076 and Irgastab FS042 (hydroxylamine); used singly in m-LLDPE leads only to a high extent of melt stability, (i.e. no significant change in MI, see figure 4.8), with the latter giving lower stability (and more discolouration, see figure 4.8 & 4.9). Irganox HP 136 and Irganox E201 were used at particularly low concentration levels of 0.03% w/w. Other antioxidants such as the phosphite, Weston 399, and the R-HALS stabilisers; Tinuvin 765, Tinuvin 622LD and Chimassorb 119D offered a much lower level of melt stability (see figure 4.10). It is clear that AOs' which operate primarily as alkyl (R•) radical scavengers (e.g. Irganox HP136) are effective in inhibiting the thermal oxidative degradation of m-LLDPE in the melt, which occurs predominantly *via* cross-linking reactions (see figure 4.8). However, all the stabilised polymers (with single antioxidants) showed poor colour stability, particularly upon multiple extrusions (see figures 4.9 & 4.11). The antioxidants Irganox HP136 and Irganox E201 imparted the lowest levels of discolouration to the m-LLDPE during multiple extrusion (see figure 4.9), whilst the m-LLDPE polymer samples containing the R-HALS were the most highly discoloured (see figure 4.11).
6. From melt flow measurements of stabilised m-LLDPE and z-LLDPE polymer samples containing a 'traditional' Irganox 1076/Weston 399 stabiliser package and extruded at high temperatures (285°C) it was clear that increasing the concentrations of Weston 399 in the blends resulted in increasing melt and colour stability during multiple extrusions (see figures 5.17-5.21); thereby reflecting the increased levels of co-operative action of alkylperoxyl (ROO•) scavenging and hydroperoxide (ROOH) decomposition. The best Irganox 1076/Weston 399 blend combination was found to be a 1:4 wt ratio; and was found to be most effective in the Ziegler polymer (less so in m-LLDPE, under all extrusion conditions, see figures 5.20 & 5.21); thus reflecting the different oxidative degradation mechanisms of the two polymers.
7. Melt flow measurements of stabilised m-LLDPE and z-LLDPE polymers containing Vitamin E/ phosphite system (in a 1:2 ratio, s11, with a small concentration of TMP),

used at a fraction of the total concentration of the best Irganox 1076/Weston 399 system (s4, 1:4 ratio) led to a higher extent of melt and colour stability (under all processing conditions); reflecting the higher AO activity of Vitamin E/phosphite system (as compared to the Irganox 1076/phosphite system, see figures 5.27-5.33). Moreover, blends of Vitamin E in combination with the phosphite, Ultrinox 626 was shown to out-perform the activity of blends (in terms of melt and colour stability) of Vitamin E with Weston 399; thereby reflecting the strong peroxide decomposing and CB activity of U.626. The high level of synergism between Vitamin E and U.626 was shown previously [1] to result in the regeneration of Vitamin E (a feature unlikely to occur by the aryl phosphite, Weston 399). The addition of a small concentration of TMP to a Vitamin E/phosphite (e.g. Ultrinox 626) system improves the colour stability of multi-processed m-LLDPE and z-LLDPE polymer samples (see figure 5.54).

8. The addition of a commercial AO package based on Irganox HP136/Ultrinox 626 (XP-60, in 1:2.3 w/w ratio) to m-LLDPE was found to result in a high extent of melt stability with increasing processing severity (s33, 260°C/100rpm, see figure 5.36) which was attributed to the highly effective complementary chain breaking; donor (CB-D) and acceptor (CB-A) antioxidant action of Irganox HP136 (a lactone) with the peroxide decomposition (and additional CB-D) of the aryl hindered aromatic phosphite, Ultrinox 626. An equivalent (1:2.3 w/w) of Irganox HP136:Ultrinox 626 blend prepared 'in house' produced similar level of melt and colour stability (s34, see figure 5.36 and table 5.14). The blending of a range of different hindered phosphites used at the same phosphorus content (0.6%P) with the lactone Irganox HP136 (applied at a fixed ratio of 1:2.3), gave quite similar level of melt and colour stability; with the exception of the sterically unhindered phosphite, Weston 399, which gave slightly lower stabilising efficiency and produced polymer samples with intense yellowing (see figures 5.36 & 5.37). The best colour performance was produced by samples in which Irgafos P-EPQ is present but this stabiliser system is more expensive (see figure 5.38). The most cost-effective stabiliser additive package, exhibiting high melt and colour characteristics was shown to be based on a, a blend of Irganox HP136 and Ultrinox 626 (s34, see figures 5.36-5.38).



9. All the XP-490 based systems (Irganox 1076/Irganox HP136/phosphite in an approximate ratio of 1:2.3:3.3 w/w ratio, of a fixed 0.6% P content), used in the processing of m-LLDPE (260°C/100rpm) resulted in high melt stabilisation, comparable to both the XP-60 and Vitamin E based systems, but these were used at higher total AO concentrations (see figure 5.39). Moreover, there appeared to be no added benefit in having additional levels of Irganox 1076 (compared to XP-60) in XP-490 based systems to melt stability (see figure 5.41); indeed it led to more severe discolouration of the polymer (see figure 5.42). The melt and colour stability exhibited by all XP-490 combinations (with different phosphites) was similar, with the exception of Weston 399 where the colour performance was the worst (in combination with a high concentration of Irganox 1076/Irganox HP136), see figures 5.41 & 5.42.
10. All the Vitamin E/phosphite based systems (without any co-additives), used at a fraction of the total concentration of XP490 systems led to excellent levels of melt stability in m-LLDPE. The best vitamin E based system, in terms of melt and colour stability performance are the ones containing either the phosphite Doverphos S9228 (s46) or Ultrinox 626 (s44), see figures 5.51-5.53. However, the formulation containing the Doverphos S9228 (s46) is a more expensive one. Vitamin E antioxidant AO systems containing Weston 399 (at a concentration of 1330ppm) resulted in the highest discolouration (see figure 5.54). The addition of zinc stearate to Vitamin E/phosphite systems particularly in the case of the phosphite Weston 399 resulted in improved colour stability (see figure 5.53d).
11. Analysis of melt flow measurements and colour data of stabilised m-LLDPE polymers containing Irgastab FS042 (a hydroxylamine) in combination with a Vitamin E/phosphite system (s11) did not increase significantly the melt stability (during processing) but induced most severe discolouration (see figure 5.43 & 5.45). A similar finding was observed upon the addition of the hydroxylamine to a Irganox 1076/Weston 399 system (s4), see figures 5.46 & 5.48.

12. The blending of a small concentration of Irganox HP 136 (a lactone) with a Vitamin E/phosphite system (s11) did not increase significantly the extent of melt stability of m-LLDPE during processing, see figure 5.49. However, the colour stability of the extruded m-LLDPE polymer samples was found to be better compared to the performance of the same blend in the absence of the lactone, see figure 5.52b. This may have been due to the additional reactions of the lactone with some of the discolouring transformation products of Vitamin E, thus reducing their concentration and their adverse effect on the yellowing and/or possible reactions with traces of metal ions to prevent the formation of coloured phenoxyl complexes. The addition of different phosphites (at varying concentrations, keeping a fixed 0.6%P content) to an Irganox HP 136:Irganox E201 blend did not increase the level of melt stability but did effect the colour stability of the polymer to varying extents; with the Weston 399 giving the highest extent of discolouration, see figure 5.52c.
13. The addition of ZnSt to blends of Irganox HP136:Irganox E201:Weston 399 resulted in an improvement in the colour stability without affecting the melt stability significantly of m-LLDPE during processing (see figure 5.51 & 5.53d) . This increase in colour stability may have been due to the neutralisation of phosphorus acid (produced as a consequence of the hydrolytic instability of Weston 399) by ZnSt thereby giving stable colourless products.
14. Blending of various R-HALS with Irgastab FS042: Irganox 1076:Weston 399 did not increase the extent of melt stability of m-LLDPE significantly during processing (see figure 5.56). However their additions gave rise to increasing colour stability of resultant polymer samples (see figure 5.57).

## 6.2 Recommendations for Future Work

1. To investigate the nature of the transformation products formed from the different AOs' during extrusion and multi-pass extrusions in order to have a better understanding of the precise mechanism of action of different stabiliser systems and factors responsible for colour formation.

2. To investigate the actual (remaining) concentration of various AOs' after polymer processing and to compare this with the initial added concentration in the polymer. This can be achieved by chromatographic (e.g. HPLC) and spectroscopic methods.
3. To examine the structural changes in the stabilised polymers including determination of hydroperoxide concentration,  $>C=C<$  (concentration and type), chain branching and carbonyl containing impurities. This will help understand the changes in molecular structure and their effect on the mechanism of oxidative degradation.
4. In this work, the effect of different synergistic commercial antioxidant (AO) systems on the melt and colour stability of m-LLDPE was determined primarily under extrusion conditions of 260°C/100rpm. Further work may be carried out under different extrusion conditions in order to fully understand the underlying chemistry involved in the stabilisation of the m-LLDPE polymer at different temperatures and shear rates.
5. Migration of antioxidants is a major concern in applications involving polymers in direct contact with food and human environment. The migration behaviour of AOs' and their respective transformation products can be carried out in order to fully assess the suitability of various AOs'.
6. To determine the level of gel formed in stabilised m-LLDPE films (as in parts 4 and 9).
7. In this work the addition of the hydroxylamine imparted more colour to the m-LLDPE polymer both when used singly and in combination with other AOs'. Further work needs to be carried out to fully understand the reason for this.

8. During the course of this work, the colour stability offered by a vitamin E based system to m-LLDPE during processing was improved by the addition of a small concentration of a polyhydric alcohol, TMP. Further research may be carried out to determine the effect of a number of different polyhydric alcohols (i.e. DPE and TPE) in combination with other commercial antioxidant (AO) systems on the melt and colour stability of m-LLDPE during extrusion.
9. Effective stabilising packages, for readily oxidisable polymers such as polyolefins, may contain several expensive antioxidants, acting by different mechanisms. It is increasingly important in modern polymer-additive technology to develop cost-effective multi-component stabiliser packages. Hence the cost, an important consideration, must also be taken into account when developing effective stabiliser systems. The addition of small concentrations of solid/liquid AOs' was carried out during compounding step. Further work, may be carried out in order to determine the actual concentration of each AO in the polymer after compounding and multiple extrusion using chromatographic (e.g. HPLC) and possibly spectroscopic methods.
10. To assess the mechanical performance (i.e. tensile strength) of selected multi-processed stabilised m-LLDPE.

## REFERENCES

1. W. Kaminsky, "New Polymers by Metallocene catalysis", *Makromol. Chem. Phys.*, **197**, 3907-3945, (1996).
- 1a J. G. Cowie, Chapter 2: "Step Growth polymerisation", in *Polymers: chemistry & Physics of Modern Materials*, J. G. Cowie (Ed), Black Academic and Professional Publishers, (1996).
2. K. B. Sinclair and R.B. Wilson, "Metallocene Catalysis; a new revolution in olefin polymerisation", *Chemistry & Industry.*, 857-861, (1994).
3. H. Knuuttila, A. Lehtinen and H. Salminen, Chapter 16: "Metallocene catalyst technology in a Bimodal polymerisation Process" in *Metallocene-Based Polyolefins Volume 2.*, J. Scheirs and W. Kaminsky (Ed.), Wiley Series in Polymer Science Publishers, (2000).
4. K. Mehta, M.C. Chen and C.Y. Yin, Chapter 21: "Film applications for Metallocene-based Propylene polymers", in reference 3.
5. A. Montagna, J.C. Floyd, "Exxon Cites Breakthrough in Olefins Polymerisation", *Mod. Plast.*, **61**, (July 1991).
6. A. Montagna, J.C. Floyd, "Catalysts for the new polyolefin generation", *SRI International. Metallocenes*, **1**, (1993).
7. A. Montagna, J.C. Floyd, "Single site catalysts leading the revolution to new polyolefin products and processes", *Conference of Metcon.'93, Catalyst consultants*, Houston, Texas, USA (1993).
8. J.K. Rogers, "Exxon; full speed ahead on gas phase Metallocene Polyethylene", *Mod. Plast.*, **15**, (1993).
9. J.K. Rogers, "Exxon Expands line of Metallocene products", *Mod. Plast.*, **11** (1993).
10. D. Rotman, A. Wood, "Dow and Exxon jostle in race to bring Metallocene products to the market", *Chem. Week.*, Sept. 15<sup>th</sup> (1993).
11. T. Shimoura, M. Kohno, N. Inoue, T. Asanuma, R. Sugimoto, T. Iwatani, O. Uchida, S. Kimua, S. Harima, H. Zenkoh and E. Tanaka, "Recent advances in Olefin polymerisation", *Macromol. Symp.*, **101**, 289-299, (1996).
12. J.B.P Soares and A.E. Hamielec, "Metallocene / Aluminoxane catalysts for olefin polymerisation – a review", *Polymer Reaction Engineering*, **3** (2), 131-200, (1995).
13. K. Soga, T. Uozumi, S. Nakamura and T. Tomeri, "Structures of Polyethylene and copolymers of ethylene with 1-Octene and oligoethylene produced with the  $Cp_2ZrCl_2$  and  $[(C_5Me_4)SiMe_2N(t-Bu)]TiCl_2$  catalysts", *Macromol. Chem. Phys.*, **197**, 4237-4251, (1996).



14. J. Koivumaki and J.V. Seppala, " Copolymerisation of ethylene and 1-hexadecene with  $Cp_2ZrCl_2$ -methylaluminumoxane catalyst", *Polymer Communications*, **9** (34), 1958-1959, (1993).
15. J.C.W. Chien and T. Nozaki, "Ethylene-Hexene Copolymerisation by Heterogenous and Homogenous Catalysts and the 'Co-monomer effect'", *J. Polym.Sci.*, **31**, 227-237, (1993).
16. A. Todo and N. Kashiwala," Structure and properties of new olefin polymers", *Macromol. Symp*, **101**, 301-308, (1996).
17. H. Hocker, " Directed Polymer Synthesis for industrial applications", *Macromol. Sym.*, **101**, 1-9, (1996).
18. P. S. Subramanian and K.J.Chou, "Molecular modelling studies of the metallocene catalysed polymer reactions", *Trip.*, **10** (3), 324-329, (1995).
19. R. C. Portnoy and J. D. Domine, Chapter 22: "Medical Applications of Metallocene catalysed Polyolefins", in reference 3.
20. S. Betso, L.T. Kale and J.J. Hemphill, Chapter 23: "Constrained Geometry – catalysed polyolefins in durable and wire and cable applications", in reference 3.
21. G. A. Campbell and A. K. Babel, " Physical properties and processing conditions correlations of the LDPE/LLDPE tubular blown films", *Macromol. Symp.*, **101**, 199-206, (1996).
22. S.W. Shang and R.D. Kamla, " Influence of Processing conditions on the physical properties of LLDPE blown films", *J. Plastic. Film and Sheeting.*, **11**, 21-37, (1995).
23. S. P. Chum, C. I. Kao and G. Knight, Chapter 12: "Structure, properties and preparation of polyolefins produced by single site technology", in *Metallocene-Based Polyolefins Volume 1.*, J. Scheirs and W. Kaminsky (Ed.), Wiley Series in Polymer Science Publishers, (2000).
24. J. M. Carella and L. M. Quinzani, Chapter 17: "Rheological properties of metallocene catalysed polyolefins in the melt and comparison with conventional polyolefins", in reference 3.
25. C. Y. Cheng, Chapter 20: "Extrusion characteristics of metallocene based polyolefins", in reference 3.
26. D. C. Rohlffing and J. Janzen, Chapter 19: "Melt rheological characteristics of metallocene catalysed polyethylenes", in reference 3.
27. F.N. Cogswell, Chapter 1: "Introduction" in *Polymer Melt Rheology.*, Cogswell (Ed.), Woodhead Publishing, Cambridge, (1981).

28. A.B. Mathus and I.S. Bhardwari, Chapter 19: "Performance of Polyethylenes in relation to their molecular structure", in Handbook of Engineering Polymer Materials, N. P. Cheremisinoff (Ed.), Marcel Dekker, NY, (1997).
29. F.N. Cogswell, Chapter 1: "Physical features and flow", in reference 27.
30. S. S. Stivala, J. Kimura, and S. M. Gabbay, Chapter 3: "Thermal degradation and oxidative processes" in Degradation and Stabilisation of Polyolefins., N. Allen (Ed.), Elsevier Applied Science Publications; London, (1983).
31. T. J. Henman, Chapter 2: "Controlled Crosslinking and Degradation", in reference 30.
32. R. T. Johnston and E. J. Morrison, Chapter 39: "Thermal Scission and Cross-linking during Polyethylene Melt Processing", in Polymer Durability, R. Clough, N. Billingham and K.T. Gillen (Ed.), ACS, (1996).
33. H. Zweifel, Chapter 25: "Effect of stabilisation of Polypropylene during processing and its influence on long term behaviour under thermal stress", in reference 32.
34. D.H. Morton Jones, Chapter 2: "The physical basis of polymer processing", in Polymer Processing., D. Morton Jones (eds.), Chapman & Hall Publishing, London, (1995).
35. G. Scott and S. Al-Malaika, Chapter 6: "Thermal stabilisation of Polyolefins", in reference 30.
36. N. C. Billingham and P.D. Calvert, Chapter 1: "The Degradation and Stabilisation of Polyolefins- An Introduction", in reference 30.
37. N. C. Billingham, Chapter 4: "The physical chemistry of Polymer oxidation and Stabilisation", in Atmospheric Oxidation and antioxidants-2, G. Scott (Ed.), Elsevier Applied science Publications, London, (1985).
38. J.L. Bolland, "Kinetics of olefin oxidation", Q. Rev. (London), **3**, 1-21, (1949).
39. L. Bateman, "Olefin Oxidation", Q. Rev. (London), **8**, 147-167, (1954).
40. J.L. Bolland and P. Ten Have, "Kinetic studies in the chemistry of rubber and related materials", Trans. Faraday Soc., **43**, 201-210, (1947).
41. J. A. Howard, K. U. Ingold and M.S. Symonds, "Absolute rate constants for hydrocarbon oxidation. VIII. The reactions of cumylperoxy radicals", Can. J. Chem., **46**, 1017-1022, (1968).
42. G. Scott (Ed.), Chapter 4: "Antioxidants: Radical Chain-breaking Mechanism", in Atmospheric Oxidation and Antioxidants, Elsevier Publishing Company, Amsterdam, (1965).

43. J.A. Howard, W.J. Schwalm and K.U. Ingold, "Absolute Rate constants for Hydrocarbon Autoxidation" in Oxidation of Organic of Organic Compounds-I, Proceedings of the International Oxidation Symposium, San Francisco, California, 28 August-1 September 1967, Adv. Chem. Ser., R.F. Gould (Ed.), **75**, pp. 6-23, American Chemical Society, USA (1968). Adv.
44. G. Scott (ed), Chapter 1: "Autoxidation and antioxidants: historical perspective", in Atmospheric Oxidation and Antioxidants-1, Elsevier Science Publishers, Amsterdam, (1993).
45. M. Irving and F. Tudos, " Thermal oxidation of Polyethylene and Polypropylene effects of chemical structure and reaction conditions on the oxidation process", Prog. Polym. Sci., **15**, 217-262, (1990).
46. S. Al-Malaika, Chapter 2: " Autoxidation" in reference 44.
47. S. Al-Malaika and S. Issenhuth, "Oxidative Degradation Pathways of m-LLDPE melt extruded under different temperature extrusion conditions", unpublished work.
48. K. B. Chakraborty and G. Scott, "The effects of thermal processing on the thermal oxidative and Photo-oxidative stability of LDPE", Eur. Poly. J., **13**, 731-737, (1977).
49. G. Scott (ed.) Chapter 1: "Mechanism of Antioxidant Action", in Developments in Polymer Stabilisation - 4, Applied Science Publishers, London, (1981).
50. S. Al-Malaika, Chapter 6: "Reactive antioxidants for polymers", in Reactive Modifiers for Polymers, S. Al-Malaika (Ed.), Blackie Academic and Professional, Chapman and Hall Publishers, (1997).
51. S. Al-Malaika, Chapter 19: "Effects of antioxidants and stabilisers", in Comprehensive Polymer Science, G.C. Eastwood (Ed.), Pergamon Press Publishers, **6**, 539-578, New York (1989).
52. G. Scott, Chapter 4: "Antioxidants Chain Breaking" in reference 44.
53. H. Zweifel, " Stabilisation beyond the year 2000", Macromol.Symp., **115**, 181-201, (1997).
54. E.F.J. Duynstee, "Transformation of antioxidants in Polyolefin Systems", proc. 6<sup>th</sup> International Conference on advances in controlled degradation of polymers, Luzern, 1-4, (1984).
55. J. Scheirs, J. Pospisil, N.J. O'Connor and S.W. Bigger, Chapter 16 "Characterisation of Conversion products formed during the degradation of processing antioxidants", in Polymer durability. R. Clough, N. Billingham and K.T. Gillen (Eds), American Chemical Society, New York, (1996).

- 56 S. Al-Malaika, H. Ashley and S. Issenhuth, "The Antioxidant role of  $\alpha$ -tocopherol in Polymers. 1. The nature of Transformation products of  $\alpha$ -tocopherol formed during melt processing of LDPE", *J. Polymer. Science: Part A: Polymer Chemistry*, **32**, 3099-3113, (1994).
- 57 N. Grassie and G. Scott (Eds.), Chapter 5: "Antioxidants and Stabilisers", in *Polymer Degradation and Stabilisation*, Cambridge University and Press, Cambridge, (1985).
- 58 J. Pospisil and S. Nespurek, "Chain breaking stabilisers in polymers: the Current Status", *Polym. Degrad. Stab.*, **49**, 99-110, (1995).
- 59 J. Pospisil, "Chemical and Photochemical behaviour of phenolic antioxidants in polymer stabilisation": state of the art report, Part1", *Polym. Degrad. Stab.*, **40**, 217-232, (1993).
- 60 J. Pospisil, "Exploitation of the current knowledge of antioxidant mechanisms for efficient polymer stabilisation", *Polymers for advanced technologies*, **3**, 443-455, (1991).
- 61 S. Al-Malaika, "Mechanisms of Antioxidant action and stabilisation Technology- The Aston experience", *Polym. Deg. and Stab.*, **34**, 1-36, (1991).
- 62 J. Pospisil and S. Nespurek, "Highlights in Chemistry and Physics of Polymer stabilisation", *Macromol. Symp.*, **115**, 143-163, (1997).
- 63 D. Dilettao, P.J. Arpino, K. Nguyen and A. Bruchet, "Investigation of low mass oligomers and polymer additives from plastics. Part 2: Application to polyolefin soxhlet extracts", *J. High Resolution Chromatogr.*, **14**, 335-341 (1991).
- 64 D.W. Allen, M.R. Clench, A. Crowson and D.A. Leathard, "Characterisation of solvent extractable transformation products of high molecular weight hindered phenols in Polypropylene subjected to ionising radiation in air or therma ageing", *Polym.Deg.stab.*, **39**, 293-297, (1993).
- 65 D.W. Allen, M.R. Clench, A. Crowson, D.A. Leathard and R. Saklatvala, "Characterisation of electron beam generated transformation products of Irganox 1010 by particle beam liquid chromatography mass spectrometry with on line diode array detection", *J. Chromatogr.A.*, **679**, 285-297, (1994).
66. G.W. Burton and K.U. Ingold, "Vitamin E: Application of the Principles of Physical Organic Chemistry to the Exploration of structure and function", *Acc.Chem. Res.*, **19**, 194-201, (1986).
- 67 E. Niki, Y. Yamamoto, M. Takahashi, E. Komuro and Y. Miyama, "Inhibition of oxidation of Biomembranes by Tocopherol", *Ann.N.Y. Acad. Sci.*, **570**, 23-31, (1989).

- 68 V.L. frampton, W.A. Skinner, P. Cambour and P.S. Bailey, " $\alpha$ -Tocopurple, an Oxidation Product of  $\alpha$ -tocopherol", *J.Am.Chem.Soc.*, **82**, 4632-4634, (1960).
- 69 G.W. Burton, D.O. Foster, B. Perly, T.F. Slater, I.C.P. Smith and K.U. Ingold, "Biological Antioxidants", *Phil.Trans. R. Soc.Lond.*, **B311**, 565-578, (1985).
- 70 J. Gosh, J. Kenny "Vitamin E - A new choice for Polyolefin Film Stabilisation", in *Additives '99*, Executive Conference management, San San Francisco, March 22-24, (1999).
- 71 L.R.C. Barclay, M.R. Vinqvist, K. Mukai, S. Itoh and H. Morimoto, "Chain-breaking Phenolic Antioxidants: Steric and Electronic effects in Polyalkyl chromanols, Tocopherol nalogs, Hydroquinones and Superior antioxidants of the Polyalkylbenzochromanl and Naphtfuran Class", *J.Org.Chem.*, **58**, 7416-7420, (1993).
- 72 K. Mukai, K. Okabe and H. Hosose, "Synthesis and Stopped flow investigations of antioxidant activity of Tocopherols. Finding of new tocopherol derivatives having the highest antioxidant activity among phenolic antioxidants", *J. Org.Chem.*, **54**, 557-560, (1989).
- 73 G.W. Burton, T. Doba, E.J. Gabe, L. Hughes, F.L. Lee, L. Prasad and K.U. Ingold, "Autoxidation of Biological molecules. 4. Maximising the Antioxidant Activity of Phenols", *J.Am.Chem.Soc.*, **107**, 7053-7065, (1985).
- 74 S.Al-Malaika and S. Issenhuth, "The Antioxidant role of  $\alpha$ -tocopherol in Polymers. 3. The nature of Transformation products during Polyolefin Extrusion", *Polym.Deg.stab.*, **65**, 143, (1999).
- 75 S.Al-Malaika and S. Issenhuth, "The Antioxidant role of Vitamin E in Polymers – IV. Reaction products of dl  $\alpha$ -tocopherol with Lead Dioxides and with Polyolefins", *Polymer*, **42**, 2915-2939, (2001).
- 76 S.Al-Malaika and S. Issenhuth, "The Antioxidant role of Vitamin E in Polymers. V. Separation of stereoisomers and characteristics of other oxidation products of dl  $\alpha$ -tocopherol formed in Polyolefins during melt processing", *Polym.Deg.stab.*, **73**, 491, (2001).
- 77 S. Al-Malaika and G, Scott, Chapter 7: "Photostabilisation of Polyolefins", in reference 30.
- 78 P. Nesvadba and C. Krohnke, "A new class of highly active Phosphorus free processing stabilisers for polymers", in *Additives '97*, Executive Conference management, New Orleans, (1997).
- 79 J. R. Pauquet, " Technological advances in stabilisation of polyethylene films", *Plastics, Rubber and Composites processing and Applications.*, **27 (1)**, 19-24, (1998).
- 80 J. Kenny, " Further Applications for the use of Lactone Chemistry to improve the performance cost profile of traditional antioxidant Stabilisation systems",



- in ADDCON '99, Executive Conference Management, Prague, 27-28 October (1999).
81. M. Horton, D. Eisermann and D. Muller, "Productivity gains in BOPP film production through stabilisation with Lactone Technology", in ADDCON 2000, Executive Conference Management, Basel, Switzerland, (2000).
  82. D. Horsey, "Hydroxylamines, a new class of low colour stabilisers for polyolefins", in ADDCON '96, Executive Conference management, Houston, (1996).
  83. K. Schwetlick, Chapter 2: "Mechanisms of antioxidant action of Phosphite and Phosphonite Esters" in Mechanisms of Polymer Degradation and Stabilisation, Applied Science Publishers London, (1990).
  84. K. Schwetlick, T. Konig, C. Ruger, J. Pionteck and W.D. Habicher, "Chain-breaking antioxidant activity of Phosphite esters", Polym. Deg. Stab., **15**, 97-108, (1986).
  85. C. Neri, S. Constanzi, R. Riva, R. Farris and R. Colombo, "Mechanism of action of phosphites in Polyolefin stabilisation", Polym. Deg. Stab., **49**, 65-69, (1995).
  86. K. Schwetlick and W.D. Habicher, Chapter 23: "Action Mechanisms of Phosphite and Phosphonite Stabilisers", in reference 61.
  87. G.J. Klender, Chapter 26: "Fluorophosphonites as co-stabilisers in stabilisation of Polyolefins", in reference 32.
  88. J. Pospisil, "Chemical and Photochemical behaviour of phenolic antioxidants in polymer stabilisation": state of the art report, Part 2", Polym. Degrad. Stab., **39**, 103-115, (1993).
  89. G. Scott (ed.) Chapter 9: "Synergism and Antagonism", in reference 44.
  90. U. Daraz and S. Issenhuth, Unpublished Internal Report 5, Polymer Processing and Performance Research Unit, Aston University, June 1998.
  91. J. Schmeig, Exxon, Baytown, USA, (1999).
  92. S. Issenhuth, Unpublished Internal Reports, Polymer Processing and Performance Research Unit, Aston University, Birmingham, (1997-1999).
  93. R. McClean, Unpublished Internal Report, Polymer Processing and Performance Research Unit, Aston University, Birmingham, (1999).
  94. S. Mui, Unpublished Internal Report, Polymer Processing and Performance Research Unit, Aston University, Birmingham, (2000).
  95. J. G. Cowie, Chapter 1: "Introduction", in Polymers; Chemistry & Physics of Modern Materials, J. G. Cowie (Ed), Black Academic and Professional Publishers, (1996).

96. T. Asanuma, Y. Nishimori, M. Ito and T. Shiomura, "Syndiotactic polymerisation mechanism of  $\alpha$ -olefins using Metallocene catalysts", *Macromol. Chem. Rap. Comm.*, **14**, 315-322, (1993).
97. D. Fleming, "Polymer Rheology- A number science", *in Progress in rubber and Plastics technology*, **12**, (2), 74, (1996).
98. D. Kaylon, "Ultimate properties of Blown films of LLDPE resins", *Poly. Eng. and Sci.*, **28**, (24), (1988).
99. D. A. E. Chang and T. H. Kwack, "Rheology processing-property relationships in tubular blown film extrusion. 1. High pressure LDPE", *J. Polym. Sci.*, **28**, 3399-3418, (1983).
100. J. A. Brydson, Chapter 4: "Factors affecting viscous flow" in *Flow properties of Polymer Melts*, J. A. Brydson (Ed.) 2nd edition, Goodwin Publishers, London, (1981).
101. E. Epacher, J. Tolveth, C. Krohnke and B. Pukanszky, "Processing stability of high density polyethylene: effect of adsorbed and dissolved oxygen", *Polymer*, **41**, 8401-8408, (2000).
102. P. Agassant, L. Avenas, K. Sergent and C. Carreau, Chapter 4: "Polymer Extrusion", in *Polymer Processing; Principles and Modelling.*, P. Agassant (Ed.), Hanser Publishers, New York, (2000).
103. Y. Kim, C. Kim, J. Park, C. Lee and T. Min, "Morphological considerations on the mechanical properties of blown high density polyethylene films", *J. Applied Polymer. Science*, **63**, 289-299, (1997).
104. A. D. Channell and E. Q. Clutton, "The effects of short chain branching and molecular weight on the impact fracture toughness of polyethylene", *Polymer*, **33**, 4108-4112, (1992).
105. H. Hinksen, S. Moss, J.R. Pauquet and H. Zweifel, "Degradation of Polyolefins during melt Processing during melt processing", *Polym. Degrad. Stab.*, **34**, 279-293, (1991).
106. R. M. Patel, T. I. Butler, K. L. Walton and G. W. Knight, "Investigation of processing structure-properties relationships in Polyethylene blown films", *Polymer Engineering and Science.*, **34**, 1506-1514, (1994).
107. Y. Hong, S.J. Coombs, J.J. Cooper-White, M. E. Mackay, C. J. Hawker, E. Malmstrom and N. Rehnberg, "Film blowing of linear low density polyethylene blended with a novel hyperbranched polymer processing aid", *Polymer*, **41**, 7705-7713, (2000).
108. B. J. Qu and B. Ranby, "Photocross-linking of low density polyethylene II Structure and Morphology", *J. Applied Polymer. Science*, **48**, 711-719, (1993).

109. J. R. Pauquet, "Breakthrough Chemistry for Processing stabilisation of Polypropylene", *J. Pure Applied Chem.*, **36** (11), 1717-1730, (1999).
110. S. Al-Malaika and S. Issenhuth, Chapter 27: "Processing effects on Antioxidant transformation and solutions to the problem of Antioxidant Migration", in *Polymer Durability*, R. Clough, N. Billingham and K.T. Gillen (eds.), ACS, (1996).
111. S. Al-Malaika, C. Goodwin, D. Burdick and S. Issenhuth, "The Antioxidant role of  $\alpha$ -tocopherol in Polymers. 2. The melt stabilising effect in Polypropylene.", *Polym. Degrad. Stab.*, **64**, 145-156, (1998).
112. G. Scott, Chapter 2, in *Developments in Polymer Stabilisation - 7*, Applied Science Publishers, London, (1984).
113. S. Al-Malaika, W. Omikarede and G. Scott, "Mechanism of Antioxidant action: Transformation products of 2, 2, 6, 6-tetramethyl-4-hydroxypiperidinoxyl in polypropylene", *J. Applied Polymer Sci.*, **33**, 703, (1987).
114. J. Pospisil, S. Nespurek, Z. Osawa, S. Kuroda and W. Habicher, "Optimisation of Polymer stabilisation through a proper exploitation of stabiliser inherent chemical efficiency", in *ADDCON '98*, Executive Conference management, Prague, (1998).
115. J. Pospisil and S. Nespurek, "Stabilisation beyond the year 2000", *Macromol. Symp.*, **115**, 181-201, (1997).
116. J. Pospisil, Chapter 18: "Activity mechanisms of amines in polymer stabilisation", in reference 32.
117. V. Malatesta, C. Neri, G. Ranghino, L. Montanari and P. Fantucci, "Molecular mechanics and dynamic studies of Polysiloxane based hindered amine light stabilisers (HALS)", *Macromolecules*, **26**, 4287-4292, (1993).
118. I. Vulic, S. B. Samuels, A. H. Wagner and J. M. Eng, "New Breakthroughs in hindered amine light stabiliser performance", in *ADDCON '99*, Executive Conference management, Prague, (1999).
119. V.K. Gupta, Chapter 12: "Metallocene based polyolefin product characteristics", in *Handbook of Engineering Polymer Materials*, N. P. Cheremisinoff (Ed.), Marcel Dekker, NY, (1997).
120. F.N. Cogswell, Chapter 4: "Rheology and structure" in *Polymer Melt Rheology*, Cogswell (Ed.), Woodhead Publishing, Cambridge, (1981).
121. S. Al-Malaika, I. Plowright, P. Hurley and M. Khayat, unpublished work, (1999).
122. J. E. Kresta and J. J. Majer, "Interactions between remnants of Ziegler-Natta catalysts, Polyolefins and stabilisers during processing", *J. App. Poly. Sci.*, **13**, 478-480, (1969).

Missing page(s) from the bound copy

# Appendix 1



Table A1 The multiple extrusion characteristics of stabilised m-LLDPE samples containing single antioxidants; s14, s15 and s16 repeatedly processed at 260°C/100rpm under atmospheric conditions, P1, P3 and P5 in order to determine experimental error.

Formulation No.	Sample code	Screw Speed /rpm	Die Temp. /°C	Output rate/ kg.h <sup>-1</sup>	P/psi ±5%	l (A) ±0.5	Actual Melt Temp/ °C	ΔT <sup>1</sup>	P.C. <sup>2</sup>		Observ.	
									kW	kW.h /kg		
s-14 Irg. 1076	A	m-260-P1	100	260	4.8	1100	14.5	272	+12	1.77	0.37	Slight MF
		m-260-P3			4.8	1080	14.5	272	+12	1.77	0.37	Slight MF
		m-260-P5			4.8	1060	14.0	272	+12	1.70	0.36	Slight MF
	B	m-260-P1	100	260	4.8	1080	14.5	273	+13	1.77	0.37	Slight MF
		m-260-P3			4.8	1060	14.0	272	+12	1.70	0.36	Slight MF
		m-260-P5			4.8	1050	14.5	272	+12	1.77	0.37	Slight MF
	C	m-260-P1	100	260	4.8	1090	14.0	272	+12	1.70	0.36	Slight MF
		m-260-P3			4.8	1100	14.0	273	+13	1.70	0.36	Slight MF
		m-260-P5			4.8	1060	14.0	272	+12	1.70	0.36	Slight MF
s-15 Irg. HP136	A	m-260-P1	100	260	4.8	1030	14.5	274	+14	1.77	0.37	Slight MF
		m-260-P3			4.8	1010	14.0	274	+14	1.70	0.36	Slight MF
		m-260-P5			4.8	1050	14.0	274	+14	1.70	0.36	Slight MF
	B	m-260-P1	100	260	4.8	1020	14.0	273	+13	1.70	0.36	Slight MF
		m-260-P3			4.8	1050	14.0	273	+13	1.70	0.36	Slight MF
		m-260-P5			4.8	1030	14.5	273	+13	1.77	0.37	Slight MF
	C	m-260-P1	100	260	4.8	1090	14.0	272	+12	1.70	0.36	Slight MF
		m-260-P3			4.8	1100	14.0	273	+13	1.70	0.36	Slight MF
		m-260-P5			4.8	1060	14.0	272	+12	1.70	0.36	Slight MF
	D	m-260-P1	100	260	4.8	1090	14.0	272	+12	1.70	0.36	Slight MF
		m-260-P3			4.8	1080	14.5	273	+13	1.77	0.37	Slight MF
		m-260-P5			4.8	1060	14.0	272	+12	1.70	0.36	Slight MF
s-16 Irg. FS042	A	m-260-P1	100	260	4.8	1100	14.0	272	+12	1.70	0.36	Slight MF
		m-260-P3			4.8	1040	14.0	272	+12	1.70	0.36	Slight MF
		m-260-P5			4.8	980	14.0	272	+12	1.70	0.36	Slight MF
	B	m-260-P1	100	260	4.8	1020	14.5	274	+14	1.77	0.37	Slight MF
		m-260-P3			4.8	1090	14.0	272	+12	1.70	0.36	Slight MF
		m-260-P5			4.8	1070	14.5	273	+13	1.77	0.37	Slight MF
	C	m-260-P1	100	260	4.8	1100	14.0	272	+12	1.70	0.36	Slight MF
		m-260-P3			4.8	1090	14.0	273	+13	1.70	0.36	Slight MF
		m-260-P5			4.8	1090	14.5	272	+12	1.77	0.37	Slight MF
	D	m-260-P1	100	260	4.8	1070	14.0	272	+12	1.70	0.36	Slight MF
		m-260-P3			4.8	1060	14.0	273	+13	1.70	0.36	Slight MF
		m-260-P5			4.8	1080	14.5	272	+12	1.77	0.37	Slight MF

<sup>1</sup> ΔT is defined as the difference in melt and die temperature.

<sup>2</sup> P.C. is defined as the power consumption.

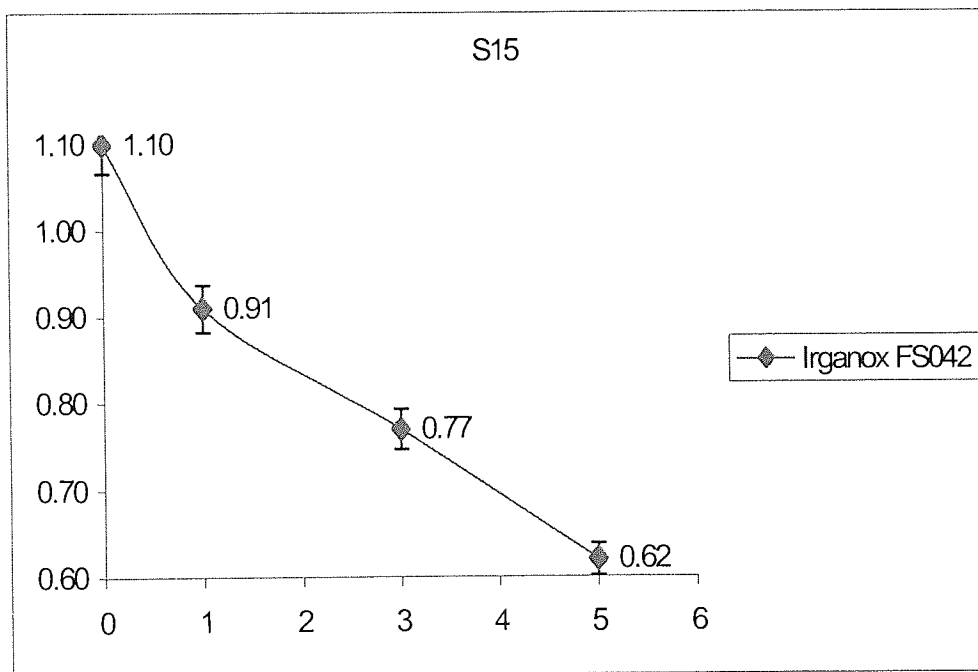
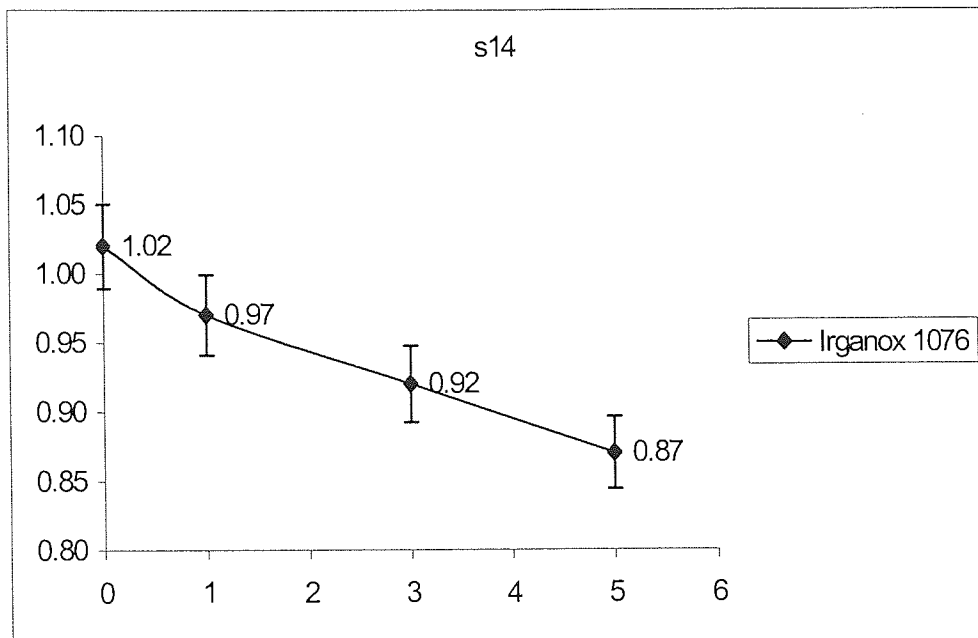


Figure A1. Experimental errors (determined from a number of processing repeats) of Po stabilised m-LLDPE stabilised; multi extruded at 260°C/100rpm under atmospheric conditions. Polymers are stabilised with 'new' batches of antioxidants (received from Exxon chemicals in May 2000), see table 4.2.

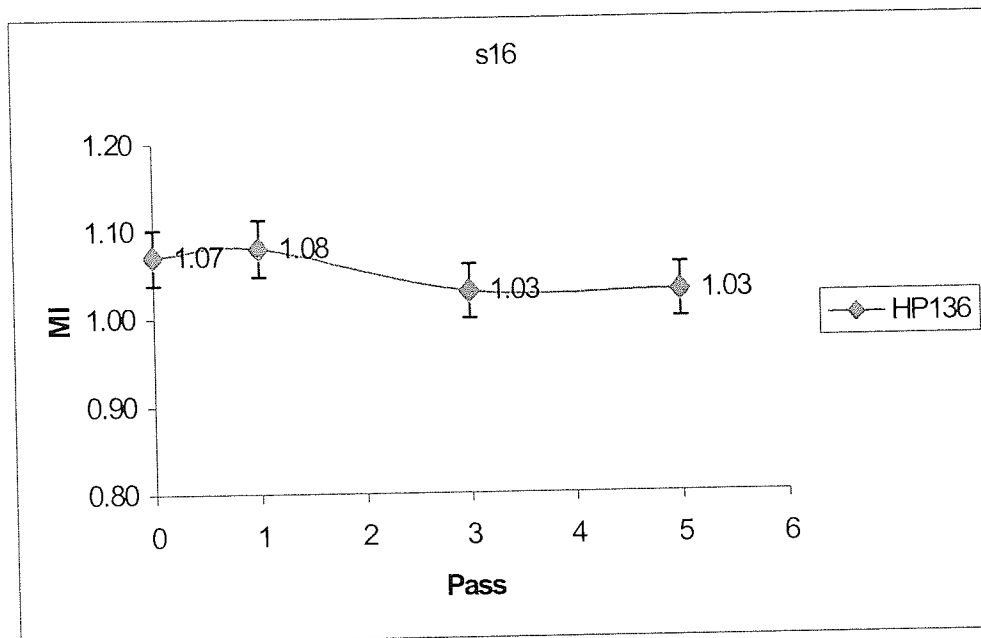


Figure A2. Experimental errors (determined from a number of processing repeats) of Po stabilised m-LLDPE stabilised; multi extruded at 260°C/100rpm under atmospheric conditions. Polymers are stabilised with 'new' batches of antioxidants (received from Exxon chemicals in May 2000), see table 4.2.

Table A2. Highlights the MI of Po stabilised m-LLDPE polymers, processed a number of times in order to determine errors in processing.

Sample	Passes	Number of Repeats				Average Mean (X) <sup>3</sup>	Standard Deviation <sup>4</sup>	% R.S.D <sup>5</sup>	Overall Processing error %	
		MI								
		1 <sup>6</sup>	2 <sup>7</sup>	3	4					
S14	0	1.02	1.10	1.11	-	1.08	0.05	5	3-5	
	1	0.97	1.05	1.06	-	1.03	0.05	5		
	3	0.92	0.97	0.97	-	0.95	0.03	3		
	5	0.87	0.92	0.88	-	0.89	0.03	3		
	Irg.1076	0	1.11	1.10	1.07	1.08	1.09	0.02		2
S16	1	1.09	0.91	0.88	0.86	0.90	0.02	2	2-5	
	3	0.83	0.77	0.80	0.80	0.80	0.03	4		
	5	0.68	0.62	0.62	0.63	0.64	0.03	5		
	Irg.FS042	0	1.05	1.07	1.10	-	1.07	0.03		2
	1	1.05	1.08	1.08	-	1.07	0.02	2		
S15	3	1.02	1.03	1.05	-	1.03	0.02	1	1-2	
	5	1.02	1.03	1.04	-	1.03	0.01	1		
	HP136	1	1.09	1.12	1.05	1.06	1.09	0.04		3
	3	-	1.09	1.06	1.05	1.07	0.02	2		
	5	-	1.08	1.03	1.06	1.06	1.06	0.04		3

<sup>3</sup> X= arithmetic mean =  $\sum Xi / N$  where Xi = numerical result of the i<sup>th</sup> run

<sup>4</sup> Standard deviation=  $S = [ \sum (Xi-X)^2 / N ]^{1/2}$

<sup>5</sup> RSD (%)= relative standard deviation =  $(S / X) \cdot 100\%$

<sup>6</sup> Using old antioxidants

<sup>7</sup> Processed using 'new' batch of antioxidants received from Exxon Chemicals in May 2000.

Table A3. The Experimental error measured from Three Individually Processed Samples Based on Statistics Method

Code*	MI	Mean (X)	Standard Deviation	RSD (%)	95% CL	Range
S16-1	0.91	0.88	0.02	2%	±0.05	0.88 +0.05
S16-2	0.88					
S16-3	0.86					

Thus the experimental error 2%, equates to ±0.05. Hence, if the average measured MI value; SAMPLE X-PASS 1 corresponds to 1.07, the experimental error will be 1.07±0.05. Thus, the experimental error % MI change (defined as MI sample- MIPo)/MI Po x 100) will be; 1.07±0.05 (range of 1.12 to 1.02) = ±5%



## Appendix 2

Table A1: Processing characteristics for Pass-zero stabilisation of m-LLDPE and z-LLDPE at different screw speeds (50 to 200rpm) at an extrusion temperature of 210°C (under nitrogen conditions, 4mm die) using stabilised formulations.

Processing characteristics of stabilised m-LLDPE, P <sub>0</sub>											
Formulation No. Irg.1076:Weston 399 [ppm]	Screw speed, rpm	T <sub>die</sub> , °C	Output Rate, kg.h <sup>-1</sup>	P, N/m <sup>2</sup>	I, A (±0.5)	actual T <sub>melt</sub> , °C (± 2)	ΔT <sup>1</sup>	Power		Observ.	
								Consumption kW	kW.h/kg		
S-1 500 : 1500	50	210	2.5	1000	14.5	214	+4	0.88	0.35	Uniform, MF	
	100	210	3.9	1150	12.5	231	+21	1.52	0.39	Melt fracture	
	150	210	6.6	1300	14.0	252	+42	2.56	0.39	Severe MF	
	200	-	-	-	-	-	-	-	-	-	
S-2 750: 1000	50	210	2.3	1000	14.0	213	+3	0.85	0.37	Uniform, MF	
	100	210	4.0	1100	13.0	230	+20	1.58	0.39	Melt fracture	
	150	210	6.0	1300	14.0	248	+38	2.56	0.40	Severe MF	
	200	210	5.9	1240	10.0	258	+48	2.44	0.41	Severe MF	
S-3 750: 2000	50	210	2.4	950	14.0	214	+4	0.85	0.35	Uniform, MF	
	100	210	4.0	1100	13.0	230	+20	1.58	0.39	Melt fracture	
	150	210	6.0	1350	13.0	249	+39	2.37	0.40	Severe MF	
	200	210	5.8	1250	10.0	267	+57	2.43	0.42	Severe MF	
Processing characteristics of stabilised z-LLDPE, P <sub>0</sub>											
S-1 500: 1500	50	210	3.1	800	14.0	211	+1	0.85	0.27	Uniform	
	100	210	4.7	850	12.0	220	+10	1.46	0.31	Uniform	
	150	210	6.7	950	12.0	229	+19	2.19	0.33	Slight MF	
	200	-	-	-	-	-	-	-	-	-	
S-2 750: 1000	50	210	3.1	800	14.0	213	+3	0.85	0.27	Uniform	
	100	210	4.6	850	14.0	219	+9	1.70	0.37	Uniform	
	150	210	6.5	900	13.0	234	+24	2.37	0.37	Slight MF	
	200	210	8.9	1050	14.0	240	+30	3.4	0.38	Slight MF	
S-3 750: 2000	50	210	3.1	750	14.0	212	+2	0.85	0.27	Uniform	
	100	210	4.3	800	13.0	220	+10	1.58	0.37	Uniform	
	150	210	6.1	950	13.0	233	+23	2.37	0.39	Slight MF	

<sup>1</sup> ΔT = T<sub>melt</sub> - T<sub>die</sub>

Table A2: The melt characteristics of Pass zero stabilised **m-LLDPE and z-LLDPE polymers**; based on s4 (Irganox 1076/W.399 system) processed at 210°C at varying screw speeds (50, 100, 150 and 200 rpm, under nitrogenous conditions on a Betol 30mm TSE with a 4mm die) with those of unstabilised virgin polymers.

Formulation [ppm]	Polymer	Screw Speed	Melt flow index /g/10min <sup>-1</sup>					
			MI	% MI <sup>1</sup> Change	HLMI	% HLMI <sup>2</sup> Change	MFR <sup>3</sup>	% MFR <sup>4</sup> change
Unstabilised	Virgin m-LLDPE	-	0.95	-	17	-	18	-
Unstabilised	m-LLDPE Pass 1	50	0.35	63	12	29	34	-89
S-1 500 : 1500	Metallocene	50	1.09	-15	18	-3	16	11
		100	1.06	-11	17	-1	16	11
		150	1.05	-10	17	-1	16	11
		200	-	-	-	-	-	-
S-2 750 : 1000		50	1.08	-14	17	+1	16	11
		100	1.05	-10	17	0	16	11
		150	1.08	-14	17	-1	16	11
		200	-	-	-	-	-	-
S-3 750 : 2000		50	1.02	-7	18	-4	17	6
		100	1.02	-7	17	-1	17	6
		150	1.07	-12	18	-4	17	6
		200	1.10	-16	18	-3	16	11
Unstabilised	Virgin z-LLDPE	-	0.97	-	32	-	33	-
Unstabilised	z-LLDPE Pass 1	50	0.77	21	29	9	38	-16
S-1 500 : 1500	Ziegler	50	1.03	-6	31	+2	31	6
		100	1.01	-4	30	+5	30	10
		150	0.98	-1	29	+9	30	10
		200	-	-	-	-	-	-
S-2 750 : 1000		50	1.09	-12	30	+7	27	18
		100	1.08	-11	31	+4	28	15
		150	1.03	-6	31	+4	30	10
		200	-	-	-	-	-	-
S-3 750 : 2000		50	1.05	-8	32	0	31	6
		100	1.02	-5	32	0	31	6
		150	0.99	-2	32	+2	32	3
		200	-	-	-	-	-	-

S-1

<sup>1</sup> MI<sub>0</sub> is defined as the MI of the virgin polymer : % MI change = (MI<sub>0</sub> - MI<sub>sample</sub>) / MI<sub>0</sub> \* 100

<sup>2</sup> % HLMI same as above except using HLMI.

<sup>3</sup> MFR = HLMI/LMI

<sup>4</sup> % MFR change = (HLMI<sub>0</sub> - HLMI<sub>sample</sub>) / HLMI<sub>0</sub> \* 100

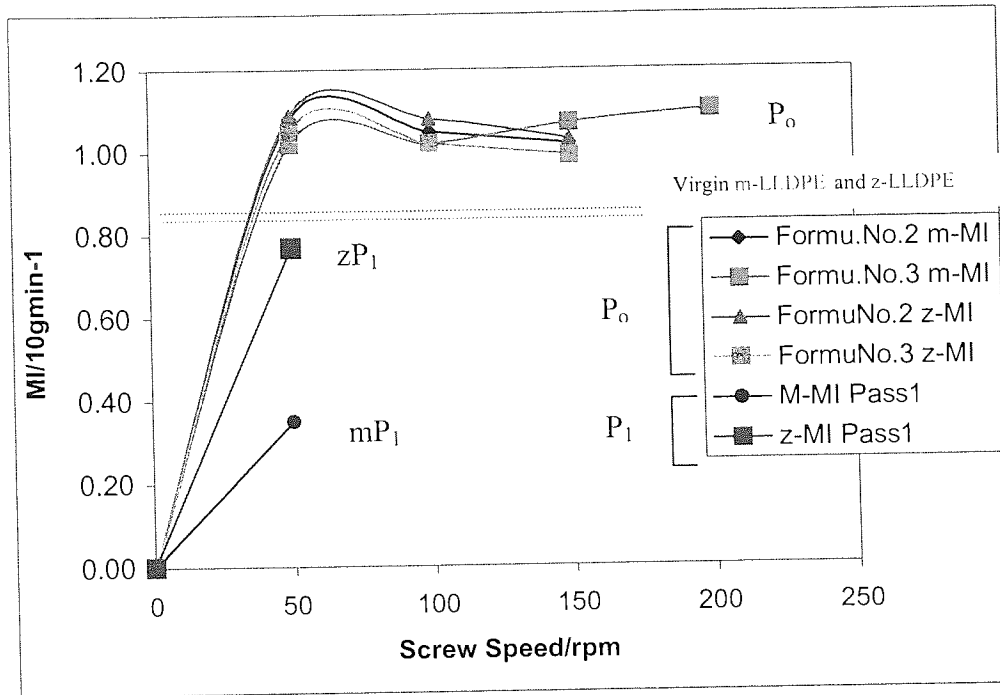


Figure A1. Effect of varying phosphite concentration on the MI of m-LLDPE and z-LLDPE polymer samples.

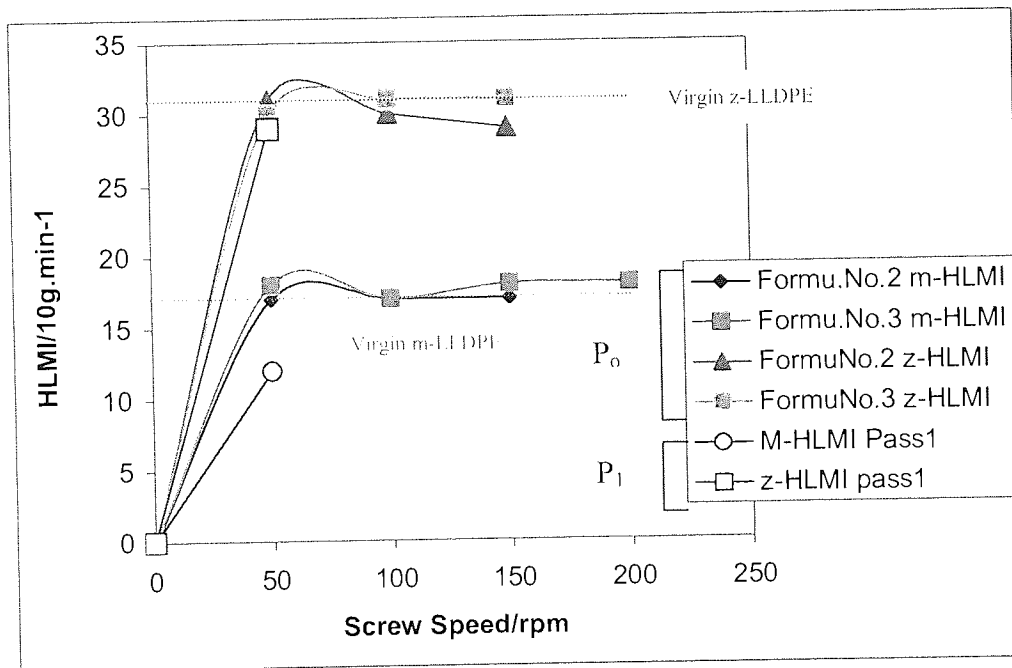


Figure A2. Effect of varying phosphite concentration on the HLMI of m-LLDPE and z-LLDPE polymer samples.

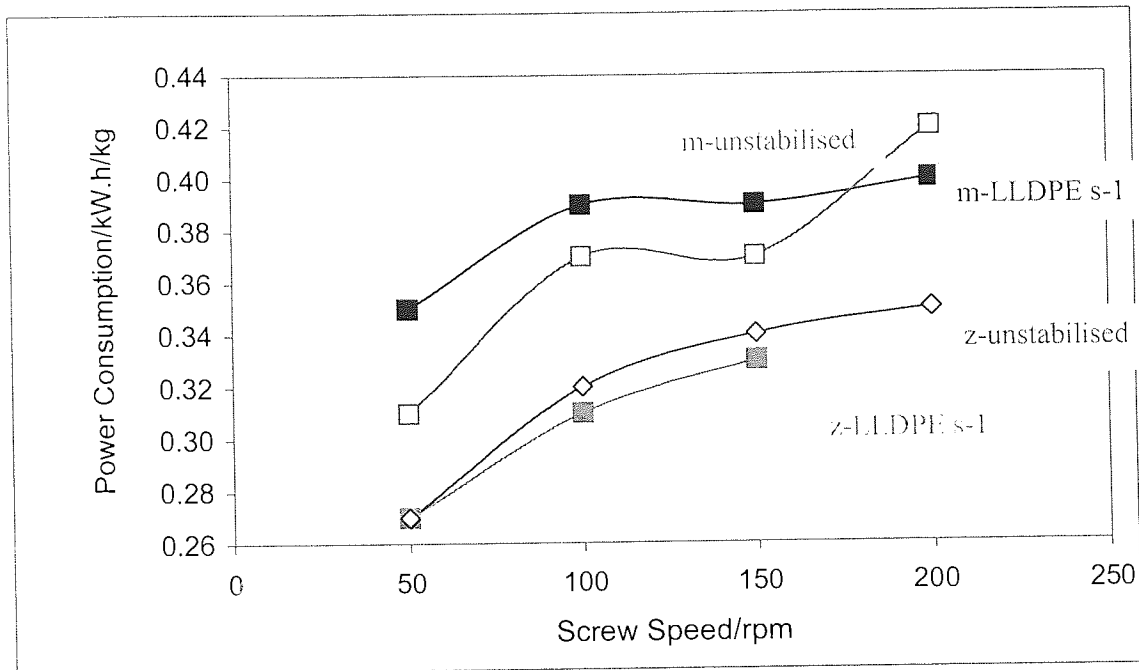


Figure A3. Change in Power consumption during twin screw extrusion ( $P_0$ , nitrogen) as a function of screw speed of stabilised m-LLDPE and z-LLDPE (formulation number 1, see table 5.1). Changes in unstabilised polymers extruded (atmospheric conditions, 210°C,  $P_1$ ) under similar conditions are shown for comparison.

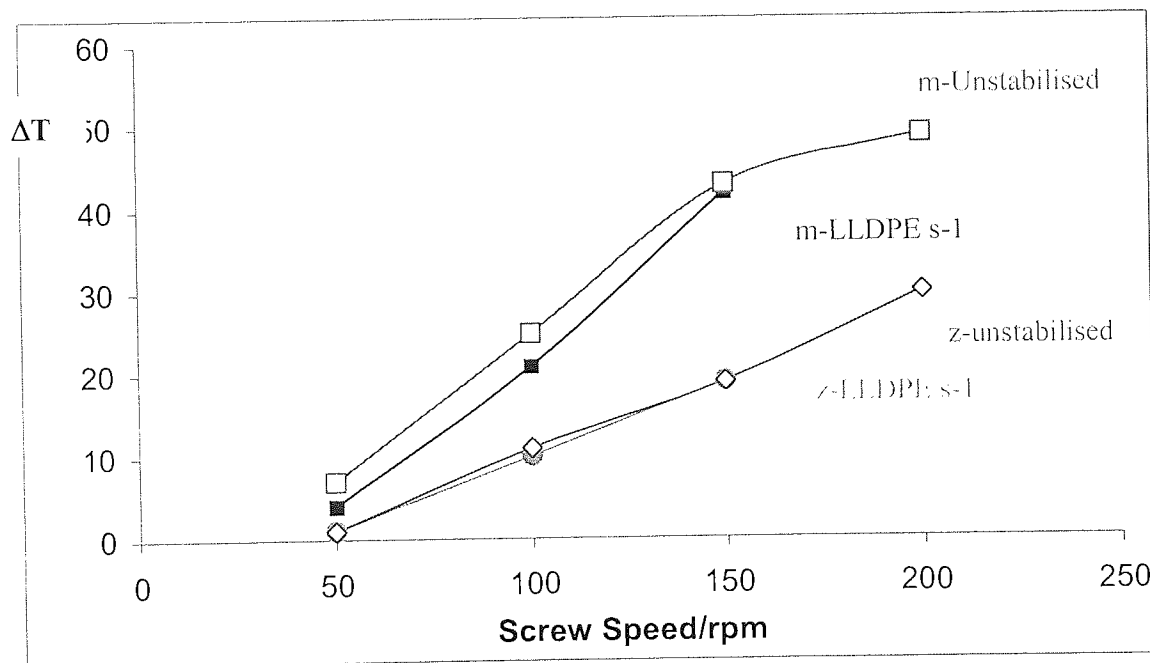


Figure A4: Difference between the actual PE melt and die temperature,  $\Delta T$ , during processing of stabilised ( $P_0$ , formulation number 1, nitrogen) and unstabilised ( $P_1$ , atmosphere) m-LLDPE and z-LLDPE samples.



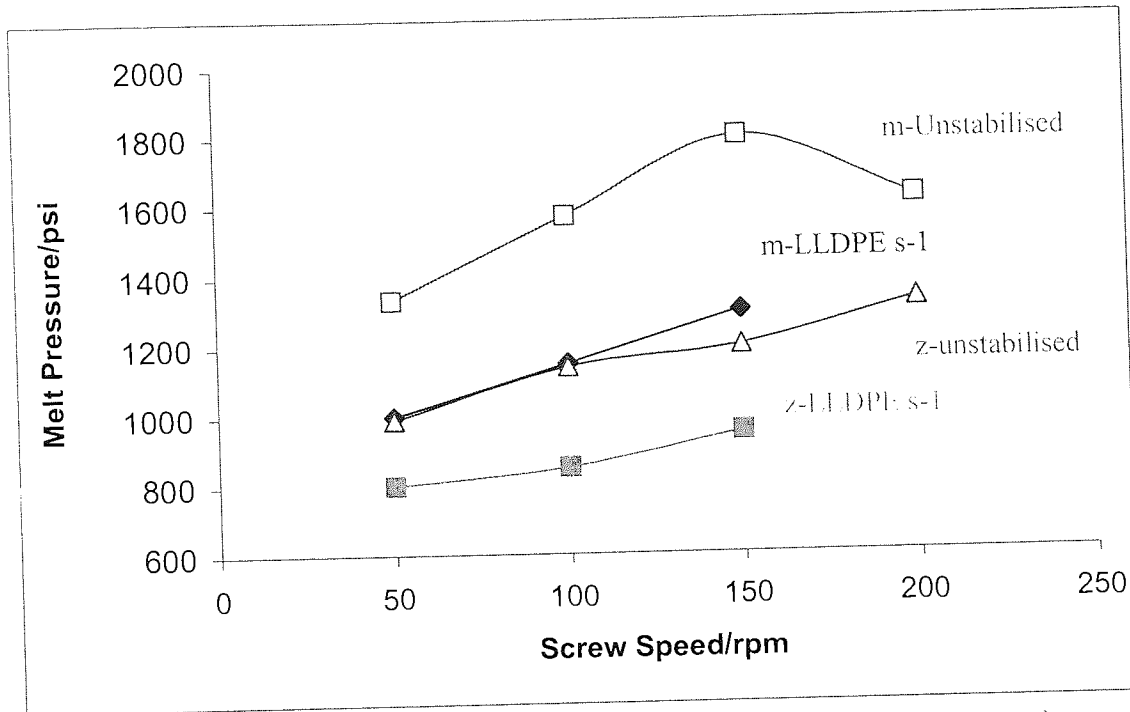


Figure A5: Change in melt pressure during twin screw extrusion ( $P_0$ , nitrogen) as a function of screw speed of stabilised m-LLDPE and z-LLDPE (formulation number 1, table 4.1). Change in unstabilised polymers extruded ( $P_1$ , atmospheric conditions, 210°C) under similar conditions are shown for comparison.

Table A.3: Processing characteristics for Po stabilised **m-LLDPE** and **z-LLDPE** samples containing single antioxidants and their combinations processed at 210°C/100rpm (under nitrogen conditions, 4mm single slit die).

Code All processed Under nitrogen	Screw speed, rpm	T <sub>die</sub> , °C	Output Rate, kg.h <sup>-1</sup>	P, N/m <sup>2</sup>	I, A (±0.5)	actual T <sub>melt</sub> , °C (± 2)	ΔT <sup>1</sup>	Power		Observ.
								Consumption		
								kW	kW.h/kg	
<b>Processing characteristics of stabilised z-LLDPE, P<sub>0</sub></b>										
<b>Two AO Based systems</b>										
<b>Synthetic Hindered Phenol : Phosphite</b>										
Virgin z-LLDPE	100	210	4.7	850	12.0	220	+10	1.46	0.31	Slight Melt fracture
S-1	100	210	4.7	900	12.0	222	+12	1.46	0.31	Slight Melt fracture
S-2	100	210	4.6	920	12.5	223	+13	1.52	0.34	Slight Melt fracture
S-3	100	210	4.7	900	12.0	221	+11	1.46	0.31	Slight Melt fracture
S-12	100	210	4.6	870	12.5	224	+14	1.52	0.33	Slight Melt fracture
S-4	100	210	4.7	920	13.0	223	+13	1.58	0.34	Slight Melt fracture
S-11	100	210	4.6	850	12.5	224	+14	1.52	0.33	Slight Melt fracture
<b>Processing characteristics of stabilised m-LLDPE, P<sub>0</sub></b>										
<b>Two AO Based systems</b>										
<b>Synthetic Hindered Phenol : Phosphite</b>										
Virgin m-LLDPE	100	210	4.0	1150	13.0	231	+21	1.58	0.39	Melt fracture
S-1	100	210	4.0	1260	13.0	233	+23	1.58	0.40	Severe Melt fracture
S-2	100	210	4.0	1250	13.5	232	+22	1.64	0.41	Severe Melt fracture
S-3	100	210	4.0	1280	13.0	231	+21	1.58	0.39	Severe Melt fracture
S-4	100	210	4.0	1250	13.0	233	+23	1.58	0.40	Severe Melt fracture
S-12	100	210	4.0	1300	13.5	233	+23	1.64	0.41	Severe Melt fracture
S-11	100	210	4.0	1250	13.5	233	+23	1.64	0.41	Severe Melt fracture
<b>Three AO Based systems</b>										
<b>Synthetic Hindered Phenol : Lactone : Phosphite</b>										
S-22	100	210	4.0	1260	13.0	233	+23	1.58	0.40	Severe Melt fracture
S-23	100	210	4.0	1250	13.5	232	+22	1.64	0.41	Severe Melt fracture
S-24	100	210	4.0	1280	13.0	231	+21	1.58	0.39	Severe Melt fracture
S-25	100	210	4.0	1260	13.0	233	+23	1.58	0.40	Severe Melt fracture

<sup>1</sup> ΔT = T<sub>melt</sub> - T<sub>die</sub>

Table A3 continued.....

<b>Processing characteristics of stabilised m-LLDPE, P<sub>0</sub></b>										
Code All processed Under nitrogen	Screw speed, rpm	T <sub>die</sub> , °C	Output Rate, kg.h <sup>-1</sup>	P, N/m <sup>2</sup>	I, A (±0.5)	actual T <sub>melt</sub> , °C (± 2)	ΔT <sup>1</sup>	Power Consumption		Observ.
								kW	kW.h/kg	
<b>Three AO Based systems</b>										
<b>Biological Hindered Phenol : Hydroxylamine: Phosphite</b>										
S-26	100	210	4.0	1250	13.5	232	+22	1.64	0.41	Severe Melt fracture
S-27	100	210	4.0	1280	13.0	231	+21	1.58	0.39	Severe Melt fracture
<b>Three AO Based systems</b>										
<b>Synthetic Hindered Phenol : Hydroxylamine: Phosphite</b>										
S-28	100	210	4.0	1250	13.5	232	+22	1.64	0.41	Severe Melt fracture
S-29	100	210	4.0	1280	13.0	231	+21	1.58	0.39	Severe Melt fracture
<b>Four AO Based systems</b>										
<b>Synthetic Hindered Phenol : Hydroxylamine: Phosphite : R-HALS</b>										
S-30	100	210	4.0	1250	13.5	232	+22	1.64	0.41	Severe Melt fracture
S-31	100	210	4.0	1280	13.0	231	+21	1.58	0.39	Severe Melt fracture
S-32	100	210	4.0	1250	13.5	232	+22	1.64	0.41	Severe Melt fracture
<b>XP-60 Two AO Based systems</b>										
<b>Lactone : Phosphite</b>										
S-33	100	210	4.0	1250	13.5	232	+22	1.64	0.41	Severe Melt fracture
S-34	100	210	4.0	1280	13.0	231	+21	1.58	0.39	Severe Melt fracture
S-35	100	210	4.0	1250	13.5	232	+22	1.64	0.41	Severe Melt fracture
S-36	100	210	4.0	1250	13.5	232	+22	1.64	0.41	Severe Melt fracture
S-37	100	210	4.0	1280	13.0	231	+21	1.58	0.39	Severe Melt fracture
<b>XP-490 Three AO Based systems</b>										
<b>Synthetic Hindered Phenol : Lactone : Phosphite</b>										
S-38	100	210	4.0	1260	13.0	232	+22	1.58	0.39	Severe Melt fracture
S-39	100	210	4.0	1270	13.0	231	+21	1.58	0.39	Severe Melt fracture
S-40	100	210	4.0	1260	13.0	232	+22	1.58	0.39	Severe Melt fracture
S-41	100	210	4.0	1260	13.0	233	+23	1.58	0.39	Severe Melt fracture
S-42	100	210	4.0	1230	13.5	233	+23	1.64	0.41	Severe Melt fracture

$$^1 \Delta T = T_{\text{melt}} - T_{\text{die}}$$

Table A3 continued.....

Processing characteristics of stabilised m-LLDPE, P <sub>0</sub>										
Code All processed Under nitrogen	Screw speed, rpm	T <sub>die</sub> , °C	Output Rate, kg.h <sup>-1</sup>	P, N/m <sup>2</sup>	I, A (±0.5)	actual T <sub>melt</sub> , °C (± 2)	ΔT <sup>1</sup>	Power		Observ.
								Consumption		
								kW	kW.h/kg	
Three AO Based systems Biological Hindered Phenol : Lactone : Phosphite										
S-43	100	210	4.0	1280	13.5	232	+22	1.64	0.41	Severe Melt fracture
S-44	100	210	4.0	1290	13.0	230	+20	1.58	0.39	Severe Melt fracture
S-45	100	210	4.0	1260	13.0	234	+24	1.58	0.39	Severe Melt fracture
S-46	100	210	4.0	1220	13.0	233	+23	1.58	0.39	Severe Melt fracture
S-47	100	210	4.0	1280	13.0	233	+23	1.58	0.39	Severe Melt fracture
S-48	100	210	4.0	1270	13.0	233	+23	1.58	0.39	Severe Melt fracture
S-49	100	210	4.0	1260	13.0	232	+22	1.58	0.39	Severe Melt fracture

<sup>1</sup> ΔT = T<sub>melt</sub> - T<sub>die</sub>

Table A4. Highlights of the extrusion characteristics of stabilised Po (extruded at 210°C, 100rpm under nitrogen using formulations s-1 to s-4, see table in table 1.1) and multipass extruded (with extrusion temperatures 210 to 285°C at 50rpm under atmospheric conditions, P1, P3 and P5) **m-LLDPE** polymer samples.

Formulation No.	Sample code	Screw Speed /rpm	Die Temp. /°C	Output rate/kg. h <sup>-1</sup>	P/ N/m <sup>2</sup>	I (A) ±0.5	Actual Melt Temp/ °C	ΔT <sup>1</sup>	P.C. <sup>2</sup>	
									kW	kW.h/ kg
Unstabilised	m-210-P1	50	210	2.7	1410	14.5	218	7	0.88	0.33
	m-210-P3			2.8	1450	13.5	218	7	0.82	0.29
	m-210-P5			2.8	1460	13.5	218	7	0.82	0.29
	m-285-P1	50	285	2.8	880	13.5	281	-4	0.82	0.29
	m-285-P3			2.9	875	14.0	281	-4	0.85	0.29
	m-285-P5			2.8	875	14.0	281	-4	0.85	0.30
<b>Two AO Based systems Synthetic Hindered Phenol : Phosphite</b>										
s-1	m-S1-210-P0	100	210	4	1260 ± 5	13.0	233	23	1.58	0.40
	m-S1-210-P1	50	210	2.7	1250 ± 5	15.0	214	4	0.91	0.34
	m-S1-210-P3			2.7	1250 ± 5	15.0	216	6	0.91	0.34
	m-S1-210-P5			2.7	1240 ± 5	15.0	217	7	0.91	0.34
	m-S1-285-P1	50	285	2.7	695 ± 5	14.0	279	-6	0.85	0.32
	m-S1-285-P3			2.7	680 ± 5	13.5	279	-6	0.82	0.30
	m-S1-285-P5			2.7	660 ± 5	13.5	281	-4	0.82	0.30
s-2	m-S2-210-P0	100	210	4	1250 ± 5	13.5	232	22	1.64	0.41
	m-S2-210-P1	50	210	2.7	1280 ± 5	15.0	212	2	0.91	0.34
	m-S2-210-P3			2.7	1280 ± 5	15.0	213	3	0.91	0.34
	m-S2-210-P5			2.7	1260 ± 5	15.0	213	3	0.91	0.34
	m-S2-285-P1	50	285	2.7	740 ± 5	14.0	285	0	0.85	0.32
	m-S2-285-P3			2.7	700 ± 5	14.0	285	0	0.85	0.32
	m-S2-285-P5			2.7	670 ± 5	13.5	285	0	0.82	0.30
s-3	m-S3-210-P0	100	210	4.1	1280 ± 5	13.0	231	21	1.58	0.39
	m-S3-210-P1	50	210	2.8	1265 ± 5	15.0	217	7	0.91	0.33
	m-S3-210-P3			2.8	1200 ± 5	15.0	217	7	0.91	0.33
	m-S3-210-P5			2.8	1200 ± 5	15.0	217	7	0.91	0.33
s-4	m-S4-210-P0	100	210	4	1280 ± 5	13.5	233	23	1.64	0.41
	m-S4-285-P1	50	285	2.7	700 ± 5	13.5	279	-6	0.82	0.30
	m-S4-285-P3			2.7	680 ± 5	13.5	281	-4	0.82	0.30
	m-S4-285-P5			2.7	670 ± 5	13.5	282	-3	0.82	0.30

<sup>1</sup> ΔT is defined as the difference in melt and die temperature.

<sup>2</sup> P.C. is defined as the power consumption.



Table A5. Highlights of the extrusion characteristics of stabilised Po (extruded at 210°C, 100rpm under nitrogen using formulations s-1 to s-4, see table in table 1.1) and multipass extruded (with extrusion temperatures 210 to 285°C at 50rpm under atmospheric conditions, P1, P3 and P5) **z-LLDPE** polymer samples.

Formulation No.	Sample code	Screw Speed /rpm	Die Temp. /°C	Output rate/kg. h <sup>-1</sup>	P/ N/m <sup>2</sup> ±10	I (A) ±0.5	Actual Melt Temp/ °C	ΔT <sup>3</sup>	P.C. <sup>4</sup>	
									kW	kW.h/ kg
Unstabilised	z-210-P1	50	210	3.2	1005	14.0	211	1	0.85	0.27
	z-210-P3			3.2	1000	14.0	211	1	0.85	0.27
	z-210-P5			3.2	935	14.5	211	1	0.88	0.28
	z-285-P1	50	285	3.2	575	12.5	277	-8	0.76	0.24
	z-285-P3			3.3	495	11.5	277	-8	0.70	0.21
	z-285-P5			3.4	480	11.5	277	-8	0.70	0.21
<b>Two AO Based systems Synthetic Hindered Phenol : Phosphite</b>										
s-1	z-S1-210-P1	50	210	3.1	850	14.0	213	3	0.85	0.27
	z-S1-210-P3			3.1	860	15.0	212	2	0.91	0.29
	z-S1-210-P5			3.1	860	15.0	212	2	0.91	0.29
	z-S1-285-P1	50	285	3.1	525	13.0	277	-8	0.79	0.26
	z-S1-285-P3			3.1	485	13.0	276	-9	0.79	0.26
	z-S1-285-P5			3.1	455	12.5	276	-9	0.76	0.25
s-2	z-S2-210-P1	50	210	3.1	860	15.0	212	2	0.91	0.29
	z-S2-210-P3			3.1	870	15.0	213	3	0.91	0.29
	z-S2-210-P5			3.1	880	15.0	213	3	0.91	0.29
	z-S2-285-P1	50	285	3.1	510	13.0	279	-6	0.79	0.26
	z-S2-285-P3			3.1	475	13.0	280	-5	0.79	0.26
	z-S2-285-P5			3.1	450	13.0	281	-4	0.79	0.26
s-3	z-S3-210-P1	50	210	3.1	850	15.0	213	3	0.91	0.29
	z-S3-210-P3			3.1	850	15.0	213	3	0.91	0.29
	z-S3-210-P5			3.1	850	15.0	213	3	0.91	0.29
s-4	z-S4-285-P1	50	285	3.1	500	13.5	279	-6	0.82	0.27
	z-S4-285-P3			3.1	470	13.5	279	-6	0.82	0.27
	z-S4-285-P5			3.1	460	12.5	279	-6	0.76	0.25

<sup>3</sup>ΔT is defined as the difference in melt and die temperature.

<sup>4</sup> P.C. is defined as the power consumption.

Table A6. Highlights the extrusion characteristics of stabilised Po (extruded at 210°C, 100rpm under nitrogen using formulations s-1 to s-12, see table in table 1.1) and multipass (with an extrusion temperatures 210 to 285°C at 50 to 200rpm under atmospheric conditions, P1, P3 and P5) **m-LLDPE** polymer samples.

Formulation No.	Sample Code	Screw Speed /rpm	Die Temp. °C	Output rate/kg.h <sup>-1</sup>	P/ N/m <sup>2</sup> ±10	I (A) ±0.5	Actual Melt Temp/ °C	ΔT <sup>5</sup>	PC <sup>6</sup>	
									kW	kW.h/kg
Unstabilised	m-210-P1	100	210	4.0	1575	12.0	235	+25	1.46	0.37
	m-285-P1	200	285	8.1	1250	12.5	311	+26	3.04	0.38
	m-285-P3			8.1	1000	12.0	311	+26	2.92	0.36
	m-285-P5			8.2	1000	12.5	311	+26	3.04	0.37
<b>Two AO Based systems Synthetic Hindered Phenol : Phosphite</b>										
s-12	m-S12-285-P1	50	285	2.7	690	13.5	279	-6	0.82	0.30
	m-S12-285-P3			2.7	660	13.5	280	-5	0.82	0.30
	m-S12-285-P5	200	285	2.7	640	13.5	279	-5	0.82	0.30
	m-S12-285-P1			7.9	980	13.0	311	+26	3.17	0.40
	m-S12-285-P3			7.9	900	12.5	310	+25	3.04	0.39
m-S12-285-P5	7.9	840	12.5	309	+24	3.04	0.39			
s-1	m-S1-285-P1	200	285	8.1	1000	12.5	313	+28	3.04	0.38
	m-S1-285-P3			8.1	850	12.0	313	+28	2.92	0.36
	m-S1-285-P5			8.1	860	12.0	313	+28	2.92	0.36
s-4	m-S4-285-P1	200	285	8.0	965	12.5	313	+28	3.04	0.38
	m-S4-285-P3			8.0	920	12.5	311	+26	3.04	0.38
	m-S4-285-P5			7.9	900	12.0	311	+26	2.92	0.37
s-2	m-S2-285-P1	50	285	2.7	740	14.0	285	0	0.85	0.32
	m-S2-285-P3			2.7	700	14.0	285	0	0.85	0.32
	m-S2-285-P5			2.7	670	13.5	285	0	0.82	0.30
s-11	m-S11-285-P1	50	285	2.7	650	13.0	277	-8	0.79	0.29
	m-S11-285-P3			2.7	650	13.0	278	-7	0.79	0.29
	m-S2-285-P5			2.7	650	13.0	278	-7	0.79	0.29

<sup>5</sup> ΔT is defined as the difference in melt and die temperature.

<sup>6</sup> P.C. is defined as the power consumption.

Table A7. Highlights the extrusion characteristics of stabilised Po (extruded at 210°C, 100rpm under nitrogen using formulations s-1 to s-12, see table in table 1.1) and multipass (with extrusion temperatures 210 to 285°C at 50 and 200rpm under atmospheric conditions, P1, P3 and P5) **z-LLDPE** polymer samples.

Formulation No.	Sample Code	Screw Speed /rpm	Die Temp. /°C	Output rate/kg.h <sup>-1</sup>	P/ N/m <sup>2</sup> ±10	I (A) ±0.5	Actual Melt Temp/ °C	ΔT <sup>7</sup>	PC <sup>8</sup>	
									kW	kW.h/kg
Unstabilised	z-210-P1	100	210	4.7	850	12.0	220	+10	1.46	0.31
	z-285-P1	200	285	8.7	810	11.5	295	+10	2.80	0.32
	z-285-P3			8.6	715	12.0	295	+10	2.92	0.34
	z-285-P5			8.8	620	12.0	295	+10	2.92	0.33
<b>Two AO Based systems Synthetic Hindered Phenol : Phosphite</b>										
s-12	z-S12-285-P1	50	285	3.1	520	12.5	277	-8	0.76	0.24
	z-S12-285-P3			3.1	400	12.5	277	-8	0.76	0.24
	z-S12-285-P5			3.1	350	12.0	274	-11	0.73	0.24
	z-S12-285-P1	200	285	8.7	650	12.5	298	+13	3.04	0.35
	z-S12-285-P3			8.7	610	11.5	295	+10	2.80	0.32
	z-S12-285-P5			8.7	560	11.0	295	+10	2.68	0.31
s-1	z-S1-285-P1	200	285	8.7	650	12.0	301	+16	2.92	0.33
	z-S1-285-P3			8.7	645	12.0	294	+9	2.92	0.33
	z-S1-285-P5			8.7	600	12.0	297	+12	2.92	0.33
s-4	z-S4-285-P1	200	285	8.0	650	12.0	294	+9	2.92	0.37
	z-S4-285-P3			7.4	580	11.5	301	+16	2.80	0.38
	z-S4-285-P5			7.4	560	11.5	300	+15	2.80	0.38
s-11	z-S11-285-P1	50	285	3.1	545	12.5	277	-8	0.76	0.24
	z-S11-285-P3			3.1	500	12.5	277	-8	0.76	0.24
	z-S2-285-P5			3.1	460	12.5	274	-11	0.76	0.24
	z-S11-285-P1	200	285	8.3	700	12.0	298	+13	2.92	0.35
	z-S11-285-P3			7.9	660	11.5	298	+13	2.80	0.35
	z-S11-285-P5			7.9	630	11.0	295	+10	2.67	0.34
s-2	z-S2-285-P1	50	285	3.1	510	13.0	279	-6	0.79	0.26
	z-S2-285-P3			3.1	475	13.0	280	-5	0.79	0.26
	z-S2-285-P5			3.1	450	13.0	281	-4	0.79	0.26

<sup>7</sup> ΔT is defined as the difference in melt and die temperature.

<sup>8</sup> P.C. is defined as the power consumption.

Table A8. The multiple extrusion characteristics of stabilised **m-LLDPE** samples containing combinations of antioxidants (see table 1.1) carried out at 260°C/100rpm under atmospheric conditions, P1, P3 and P5.

Formulation No.	Sample code	Screw Speed /rpm	Die Temp. /°C	Output rate/kg.h <sup>-1</sup>	P/ N/m <sup>2</sup> ±10	l (A) ±0.5	Actual Melt Temp/ °C	ΔT	P.C.	
									kW	kW.h/kg
<b>Unstabilised m-LLDPE Polymer</b>										
Unstabilised	m-260-P1	100	260	4.8	1090	14.0	273	+13	1.70	0.36
	m-260-P3			4.8	1080	14.0	273	+13	1.70	0.36
	m-260-P5			4.8	1020	14.0	273	+13	1.70	0.36
<b>Three AO Based systems; Synthetic Hindered Phenol : Lactone : Phosphite</b>										
s-23	m-260-P1	100	260	4.8	1000	14.0	272	+12	1.70	0.36
	m-260-P3			4.8	1050	14.0	273	+13	1.70	0.36
	m-260-P5			4.8	1020	14.0	273	+13	1.70	0.36
s-22	m-260-P1	100	260	4.8	1140	14.0	273	+13	1.70	0.36
	m-260-P3			4.8	1100	14.0	273	+13	1.70	0.36
	m-260-P5			4.8	1030	14.0	273	+13	1.70	0.36
s-23	m-260-P1	100	260	4.8	1000	14.0	272	+12	1.70	0.36
	m-260-P3			4.8	1050	14.0	273	+13	1.70	0.36
	m-260-P5			4.8	1020	14.0	273	+13	1.70	0.36
s-24	m-260-P1	100	260	4.8	1150	14.0	273	+13	1.70	0.36
	m-260-P3			4.8	1130	14.5	272	+12	1.77	0.37
	m-260-P5			4.8	1100	14.5	272	+12	1.77	0.37
s-25	m-260-P1	100	260	4.8	1020	14.0	274	+14	1.70	0.36
	m-260-P3			4.8	1020	14.0	273	+13	1.70	0.36
	m-260-P5			4.8	1000	14.0	273	+13	1.70	0.36
<b>Three AO Based systems; Biological Hindered Phenol : Hydroxylamine: phosphite</b>										
s-26	m-260-P1	100	260	4.8	1070	14.0	273	+13	1.70	0.36
	m-260-P3			4.8	1100	14.5	274	+14	1.77	0.37
	m-260-P5			4.8	1020	14.0	274	+14	1.70	0.36
s-27	m-260-P1	100	260	4.8	1030	14.5	274	+14	1.77	0.37
	m-260-P3			4.8	1060	14.0	273	+13	1.70	0.36
	m-260-P5			4.8	1050	14.0	273	+13	1.70	0.36
<b>Three AO Based systems Synthetic Hindered Phenol : Hydroxylamine: Phosphite</b>										
s-28	m-260-P1	100	260	4.8	1060	14.0	273	+13	1.70	0.36
	m-260-P3			4.8	1005	14.0	273	+13	1.70	0.36
	m-260-P5			4.8	1000	14.0	273	+13	1.70	0.36
s-29	m-260-P1	100	260	4.8	1000	14.0	274	+14	1.70	0.36
	m-260-P3			4.8	1000	13.5	271	+11	1.64	0.35
	m-260-P5			4.8	980	14.0	273	+13	1.70	0.36

Table A9. The multiple extrusion characteristics of stabilised m-LLDPE samples containing combinations of antioxidants (see table 1.1) carried out at 260°C/100rpm under atmospheric conditions, P1, P3 and P5.

Formulation No.	Sample code	Screw Speed /rpm	Die Temp. /°C	Output rate/kg.h <sup>-1</sup>	P/ N/m <sup>2</sup>	I (A) ±0.5	Actual Melt Temp/ °C	ΔT	PC	
									kW	kW.h/ kg
<b>Four AO Based systems</b>										
<b>Synthetic Hindered Phenol : Hydroxylamine: Phosphite : R-HALS</b>										
s-30	m-260-P1	100	260	4.8	1005	14.0	273	+13	1.70	0.36
	m-260-P3			4.8	1040	14.5	274	+14	1.77	0.37
	m-260-P5			4.8	1030	14.5	273	+13	1.77	0.37
s-31	m-260-P1	100	260	4.8	940	14.0	274	+14	1.70	0.36
	m-260-P3			4.8	1000	14.5	273	+13	1.77	0.37
	m-260-P5			4.8	970	14.5	273	+13	1.77	0.36
s-32	m-260-P1	100	260	4.8	1020	13.5	271	+11	1.64	0.35
	m-260-P3			4.8	1020	14.0	273	+13	1.70	0.36
	m-260-P5			4.8	1030	14.0	274	+14	1.70	0.36
<b>XP-60 Two AO Based systems</b>										
<b>Lactone : Phosphite</b>										
s-33	m-260-P1	100	260	4.8	1070	14.5	270	+10	1.77	0.37
	m-260-P3			4.8	1020	14.0	272	+12	1.70	0.36
	m-260-P5			4.8	1010	14.0	272	+12	1.70	0.36
s-34	m-260-P1	100	260	4.8	1090	14.0	273	+13	1.70	0.36
	m-260-P3			4.8	1070	14.0	272	+12	1.70	0.36
	m-260-P5			4.8	1060	14.0	273	+13	1.70	0.36
s-35	m-260-P1	100	260	4.8	1080	14.0	273	+13	1.70	0.36
	m-260-P3			4.8	1060	14.0	272	+12	1.70	0.36
	m-260-P5			4.8	1040	14.5	272	+12	1.77	0.37
s-36	m-260-P1	100	260	4.8	1040	14.0	273	+13	1.70	0.36
	m-260-P3			4.8	1030	14.0	273	+13	1.70	0.36
	m-260-P5			4.8	1030	14.0	272	+12	1.70	0.36
s-37	m-260-P1	100	260	4.8	1050	14.5	271	+11	1.77	0.37
	m-260-P3			4.8	1030	14.0	272	+12	1.70	0.36
	m-260-P5			4.8	1030	14.0	272	+12	1.70	0.36



Table A10. The multiple extrusion characteristics of stabilised m-LLDPE samples containing combinations of antioxidants (see table 1.1) carried out at 260°C/100rpm under atmospheric conditions, P1, P3 and P5.

Formulation No.	Sample code	Screw Speed /rpm	Die Temp. /°C	Output rate/kg.h <sup>-1</sup>	P/ N/m <sup>2</sup> ±10	I (A) ±0.5	Actual Melt Temp/ °C	ΔT	PC	
									kW	KW.h/kg
<b>XP-490 Three AO Based systems</b>										
<b>Synthetic Hindered Phenol : Lactone : Phosphite</b>										
s-38	m-260-P1	100	260	4.8	1030	14.0	272	+12	1.70	0.36
	m-260-P3			4.8	1020	14.0	271	+11	1.70	0.36
	m-260-P5			4.8	1050	14.0	272	+12	1.70	0.36
s-39	m-260-P1	100	260	4.8	1080	14.0	272	+12	1.70	0.36
	m-260-P3			4.8	1070	14.0	273	+13	1.70	0.36
	m-260-P5			4.8	1040	14.0	272	+12	1.70	0.36
s-40	m-260-P1	100	260	4.8	1030	14.0	273	+13	1.70	0.36
	m-260-P3			4.8	1020	14.0	273	+13	1.70	0.36
	m-260-P5			4.8	1080	14.0	273	+13	1.70	0.36
s-41	m-260-P1	100	260	4.8	1060	14.5	273	+13	1.77	0.37
	m-260-P3			4.8	1030	14.5	272	+12	1.77	0.37
	m-260-P5			4.8	1010	14.5	272	+12	1.77	0.37
s-42	m-260-P1	100	260	4.8	1030	14.5	273	+13	1.77	0.37
	m-260-P3			4.8	970	14.0	273	+13	1.70	0.36
	m-260-P5			4.8	980	14.0	273	+13	1.70	0.36

Table A11. The multiple extrusion characteristics of stabilised m-LLDPE samples containing combinations of antioxidants (see table 1.1) carried out at 260°C/100rpm under atmospheric conditions, P1, P3 and P5.

Formulation No.	Sample code	Screw Speed /rpm	Die Temp. /°C	Ouput rate/kg.h <sup>-1</sup>	P/ N/m <sup>2</sup> ±10	I (A) ±0.5	Actual Melt Temp/ °C	ΔT	PC	
									kW	kW.h/ kg
<b>Three AO Based systems</b>										
<b>Biological Hindered Phenol : Lactone : Phosphite</b>										
s-43	m-260-P1	100	260	4.8	1090	14.0	272	+12	1.70	0.36
	m-260-P3			4.8	1090	14.0	273	+13	1.70	0.36
	m-260-P5			4.8	1030	14.5	273	+13	1.77	0.37
s-44	m-260-P1	100	260	4.8	1010	14.0	271	+11	1.70	0.36
	m-260-P3			4.8	980	14.5	271	+11	1.77	0.37
	m-260-P5			4.8	990	14.5	271	+11	1.77	0.37
s-45	m-260-P1	100	260	4.8	980	14.0	274	+14	1.70	0.36
	m-260-P3			4.8	970	14.5	272	+12	1.77	0.37
	m-260-P5			4.8	970	14.5	272	+12	1.77	0.37
s-46	m-260-P1	100	260	4.8	980	14.0	272	+12	1.70	0.36
	m-260-P3			4.8	1030	14.0	271	+11	1.70	0.36
	m-260-P5			4.8	1060	14.0	271	+11	1.70	0.36
s-47	m-260-P1	100	260	4.8	1060	14.0	273	+13	1.70	0.36
	m-260-P3			4.8	1070	14.0	273	+13	1.70	0.36
	m-260-P5			4.8	1070	14.0	273	+13	1.70	0.36
s-48	m-260-P1	100	260	4.8	1060	14.0	273	+13	1.70	0.36
	m-260-P3			4.8	1090	14.0	273	+13	1.70	0.36
	m-260-P5			4.8	1080	14.0	273	+13	1.70	0.36
s-49	m-260-P1	100	260	4.8	980	14.0	271	+11	1.70	0.36
	m-260-P3			4.8	970	14.0	271	+11	1.70	0.36
	m-260-P5			4.8	910	14.0	272	+12	1.70	0.36

## **Appendix 3**

Table A1. The Experimental error measured from Three Individually Processed Samples Based on Statistics Method

Polymer	Degradation Cycle	Samples			Average <sup>1</sup> X	St.Dev <sup>2</sup>	% RSD <sup>3</sup>	Overall Processing Error
		A	B	C				
Virgin	5	35.3	35.6	35.4	35.4	0.15	4	4
m-LLDPE	15	36.1	36.2	36.2	36.2	0.06	2	
	25	36.4	36.6	36.5	36.5	0.12	3	

Thus the experimental error 4%, equates to  $\pm 0.04$ . Hence, if the average measured PI Max value; SAMPLE A-PASS Degradation Cycle 1 corresponds to 35.4, the experimental error will be  $35.4 \pm 0.4$ . Thus, the experimental error PL value will be;  $35.4 \pm 0.4$  (range of 35.8 to 35.0) =  $\pm 4\%$

<sup>1</sup> X= arithmetic mean =  $\sum X_i / N$  where  $X_i$  = numerical result of the  $i^{\text{th}}$  run

<sup>2</sup> Standard deviation=  $S = [ \sum (X_i - X)^2 / N ]^{1/2}$

<sup>3</sup> RSD (%)= relative standard deviation =  $(S / X) \cdot 100\%$